January 2023

“Blue” Hydrogen & Helium From Flare Gas Of The Bakken Formation Of The Williston Basin, North Dakota: A Novel Process

Martin R. Leipzig

Recommended Citation

Leipzig, Martin R., "“Blue” Hydrogen & Helium From Flare Gas Of The Bakken Formation Of The Williston Basin, North Dakota: A Novel Process" (2023). *Theses and Dissertations*. 5252.
https://commons.und.edu/theses/5252

“BLUE” HYDROGEN & HELIUM FROM FLARE GAS OF THE BAKKEN FORMATION OF THE WILLISTON BASIN, NORTH DAKOTA: A NOVEL PROCESS

by

Martin Robert Leipzig
Bachelor of Science, University of Wisconsin – Parkside, 1980
Master of Science, University of Wisconsin – Milwaukee, 1982

A Dissertation

Submitted to the Graduate Faculty

of the

University of North Dakota

In partial fulfilment of the requirements

for the degree of

Doctor of Philosophy

Grand Forks, North Dakota

May
2023

This dissertation, submitted by Martin R. Leipzig in partial fulfillment of the requirements for the Degree of Doctor of Philosophy from the Petroleum Engineering Department, University of North Dakota, has been read by the Faculty Advisory Committee under whom the work has been done and is hereby approved.

Dr. Hui Pu (Chairman)

Dr. Kegang Ling

Dr. Olusegun Tomomewo

Dr. Jon Maskaly

This dissertation is being submitted by the appointed advisory committee as having met all of the requirements of the School of Graduate Studies at the University of North Dakota and is hereby heartily approved.

Chris Nelson
Dean of the School of Graduate Studies

Date

PERMISSION

Title “Blue” hydrogen & helium from flare gas of the Bakken Formation of the Williston Basin, North Dakota: a novel process

Department Petroleum Engineering

Degree Doctor of Philosophy

In presenting this dissertation in fulfilment of the requirements for a graduate degree from the University of North Dakota, I agree that the library of this University shall make it freely available for inspection. I further agree that permission for extensive copying for scholarly purposes may be granted by the professor who supervised my dissertation work or, in his absence, by the Chairperson of the department or the Dean of the School of Graduate Studies. It is understood that any copying or publication or other use of this dissertation or part thereof for financial gain shall not be allowed without my written permission. It is also understood that due recognition shall be given to me and to the University of North Dakota in any scholarly use which may be made of any material in my dissertation.

Martin R. Leipzig
Date: April 18, 2023

TABLE OF CONTENTS

LIST OF FIGURES

LIST OF TABLES

ACKNOWLEDGMENTS

I wish to express my sincere appreciation to the members of my advisory Committee, particularly Dr. Vamegh Rasouli, and Dr. Minou Rabiei for their guidance and support during my time in the Doctoral program at the University of North Dakota.

Also wish to lavishly thank my wife, Stephanie A. Leipzig, for her putting up with me and 40^+ years of nomadic global oil and gas hunting to our semi-retirement in North Dakota; far from the peace and quiet of the Middle Eastern oil industry to the raucous hurly-burly of academia.

Dedicated to those who always had time to put up with an over-eager novice geologist:

Dr. Eugene I. Smith

Dr. Robert “Mac” West

Dr. Richard A. “RAP” Paull

Yes, you’re the ones responsible for all this…for which I thank you…

Also, a special thanks to the following Pink Floyd members whose past and present efforts provided a running soundtrack during the compilation and writing of this dissertation: David Gilmour, Nick Mason, Richard Wright, Roger Waters, Bob Klose, and Syd Barrett.

“If you think hiring a professional is expensive,

just wait until you hire an amateur.”

– Red Adair

ABSTRACT

Is it possible to curtail flaring in the Williston basin while simultaneously sequestering carbon dioxide, harvesting economic quantities of natural gas liquids, helium and other valuable products? Utilizing a novel approach described here, diatomic hydrogen and elemental helium, as well as other products, can be profitably extracted from the gas streams produced from horizontal, hydraulically-fractured Middle Bakken Member wells, in the Devonian-Mississippian Bakken Formation of the Williston Basin, North Dakota, USA.

However, there are two vastly different methods employed to extract these gasses. Hydrogen is harvested from the gas stream by physically reforming methane (CH_4) through the application of one or another of two-stage processes: “Autothermal Reformation + Water Gas Shift (WGS) reaction”, known as ATR; or “Steam Methane Reforming”, SMR. Both yield H_2, plus CO (carbon monoxide) in the first phase, and CO_2 (carbon dioxide) after the second. Elemental diatomic hydrogen (H_2) can be used in fuel cells to generate electricity or directly in certain internal combustion engines; primarily turbines, as primary fuel. The produced CO_2 can be captured (CCUS: Carbon Capture, Utilization and Sequestration) and injected downhole for both reservoir energy enhancement and CO_2 sequestration, or sold for industrial use because of its purity.

Helium, on the other hand, is inert and therefore it is unnecessary to expend the amount of energy required to reformat methane to liberate hydrogen. There are several methods commercially available to economically extract 99.995% pure helium from gas streams where the helium concentration can be as low as 0.010%.

The extraction of crude helium from natural gas requires three processing steps. The first step removes impurities through deamination, glycol absorption, nitrogen rejection, and desiccant adsorption, which remove CO_2, H_2O, N_2, and H_2S; a typical gas pre-treatment process. The second step removes high-molecular weight hydrocarbons (Natural Gas Liquids), if desired, while the third step is via cryogenics, which removes the final methane. The result is 75-90% pure helium. Final purification, before liquefaction, is accomplished via activated charcoal absorbers at liquid-nitrogen temperatures and high pressure, or pressure-swing adsorption (PSA) processes. Low-temperature adsorption can yield helium purities of 99.99 percent, while PSA processes recover helium at better than 99.9999 percent purity.

However, with the advent of selective zeolite or organometallic membranes, the cryogenic extraction of He from the CH_4 stream step can be eliminated. Heating the gas stream and passing it through selective semi-permeable membranes allow for the helium, with its much smaller size, and higher energy, pass while excluding the relatively massive CH_4 molecule. The helium can be isolated and purified via pressure swing adsorption (PSA) methods to achieve 99.999% purity. The heated methane can then be directly ported to a Steam Methane Reformer unit for extraction of hydrogen.

Both H_2 and He extraction procedures eliminate the need for gas flaring, as both yield salable products such as LNG and NGLs, and the opportunity to capture and sequester carbon dioxide (CO_2) from the produced gas stream. This extracted so-called “Blue Hydrogen” is slated for use in transportation via fuel cells or use in internal combustion engines and sells for approximately $3.00/MCF, depending on the cost of the feedstock natural gas. “Metallurgical helium” or “Grade-A Helium” (i.e., > 99.9999% pure), with myriad industrial and scientific uses, brings ~US$498/MCF (02-2023).

The cost of hydrogen vs. helium extraction is difficult to compare. Hydrogen production depends on the cost of natural gas as a feedstock, which is particularly variable. The cost of helium extraction depends on the volume of gas being processed, as most helium extraction units could handle 10-12 Bakken wells simultaneously. However, as a straight-up market product, helium revenue exceeds hydrogen by a factor of 100. Doing both coincidental from the same gas stream will enhance the revenue of each.

Extended Abstract

Is it possible to curtail flaring in the Williston basin while simultaneously sequestering carbon dioxide, harvesting economic quantities of natural gas liquids, helium and other valuable products? Utilizing a novel approach described here, diatomic hydrogen and elemental helium, as well as other products, can be profitably extracted from the gas streams produced from horizontal, hydraulically-fractured Middle Bakken Member wells, from the Devonian-Mississippian of the Williston Basin, North Dakota, USA.

By incorporating and utilizing the processes described below, the practice of flaring gas from the Bakken in the Williston Basin will cease to exist.

Additionally, with the sequential or simultaneous extraction of hydrogen and helium, carbon dioxide will be captured (CCUS), ready for sale or sequestering; hydrogen sulfide will be removed, as will be leftover methane, nitrogen, as well as other by-gasses. Extraction methods will necessarily yield products of high purity, generating LNG (Liquid Natural Gas – i.e., liquid pure methane (CH_4)), NGLs (Natural Gas Liquids – Ethane (C_2H_6), Propane (C_3H_8), Butane (C_4H_{10}), Pentane (C_5H_{12}), Pentane$^+$ (C_6H_{14}, etc.)), as well as H_2, He, CO_2,

N_2, and other saleable gases of very high purity. The selling of these can clearly offset the extra costs of hydrogen and helium extraction, and necessary cryogenic processing if liquification proves necessary.

There are two vastly different methods employed to extract hydrogen and helium. Hydrogen is harvested from the gas stream by physically reforming methane (CH_4) through the application of a two-stage process: either ATR (Autothermal Reforming plus Water Gas Shift reaction) or “Methane Steam Reforming”, both ‘Hot Processes’. They yield H_2, plus CO (carbon monoxide) in the first phase (ATR), and further hydrogen with high-purity CO_2 (carbon dioxide) after the second (SMR) and final stage. Diatomic hydrogen (H_2) is slated to be utilized in fuel cells to generate electricity, ostensibly for vehicles. There exists the great possibility of utilizing hydrogen as fuel for aviation in both piston-engine and turbine powered vehicles; as there is precedence for this today. High-purity CO_2 will also be captured and can be sold for analytical research; utilized in oilfield operations or injected downhole for both reservoir energy enhancement and CO_2 sequestration (CCUS).

Helium, on the other hand, is inert and therefore it is unnecessary to expend the amount of thermal energy needed to liberate hydrogen. It should be noted that both hydrogen and helium exist in atmospheric air is too low of concentration to make it viable to harvest them from liquified air. However, there are several methods commercially available to extract $99.995\%^{+}$ pure helium from gas streams where the helium concentration can be as low as 0.010%. These include the use of selectively semi-permeable membranes and Pressure Swing Adsorption. Cryogenic methods can also be employed.

Both the H_2 and He processes operate with modular ‘off the shelf’ technology, which is readily available in and for the Oil, as well as other industries. The novelty here is *the* *process* of sequential extraction of the gasses, as well as the gaseous by-products from flared surface gas, not the mechanics of the well-known, well-tested, and efficient extraction equipment.

Extraction of crude helium, a ‘Cold Process’, from natural gas requires three processing steps:

- The first step removes impurities through deamination, glycol absorption, iron-chelation, and desiccant adsorption, which remove such impurities as CO_2, H_2S, and H_2O; as in typical oilfield ‘gas pre-treatment’ processes.
- The second step removes high-molecular weight hydrocarbons via non-catalytic zeolite or membrane filters, beyond methane, i.e., ethane, propane, butane, pentane, hexane, heptane, etc.
- The third step utilizes selective (semi-permeable) non-catalytic membranes. which removes any final methane, and isolates helium. Finally, PSA or cryogenic methods can be employed to purify and liquify the helium.

The result is 75-90% pure helium. Final purification, before liquefaction, is accomplished via activated charcoal absorbers at liquid-nitrogen temperatures –130°F (–90°C) and high pressure, or through pressure-swing adsorption (PSA) processes. Low-temperature adsorption can yield helium purities of 99.99 percent, while PSA processes recover helium at better than 99.99999 percent purity. It is at this point the “Hot Process” for hydrogen and the “Cold Process” for helium intersect, that is, at the PSA point. Both gasses can go into the same processing sequence from here onwards.

Both H_2 and He extraction procedures eliminate the need for gas flaring, as it will utilize that gas completely as a feedstock. Both processes yield salable by-products such as

LNG and NGLs, sulfur, high-purity nitrogen, and the opportunity to capture, sell, and/or and sequester carbon dioxide (CO_2) from the produced gas stream. This extracted so-called "Blue Hydrogen", slated for use in transportation via fuel cells, or direct use as fuel in semi-modified piston or turbine engines, sells nominally for ~$3.00-7.50/MCF, depending on the cost of the feedstock natural gas. "Metallurgical helium" (i.e., >99.9999% pure), with myriad industrial uses, sells for (02-2023) ~US$485/MCF.

The cost of hydrogen vs. helium extraction from natural gas is difficult to compare. Hydrogen production depends on the cost of natural gas as a feedstock, which is particularly variable; though in the aforementioned scenario, using flare gas, the cost would be low (allowing for some OPEX from surface materials/facilities). The cost of helium extraction depends on the volume of gas being processed, as most helium extraction units (i.e., 'trains') could handle 10-12 Bakken wells simultaneously, depending on volume, pressure and continuality of flow. However, as a straight-up market product, helium revenue exceeds hydrogen by an order of magnitude.

Extracting both coincidentally from the same gas stream will enhance the revenue of each; while optimizing useful, saleable and profitable by-products, capturing and sequestering CO_2, and finally eliminating excess gas flaring from the Bakken in the Williston Basin.

CHAPTER 1

Hydrogen, Helium, CO_2 and the Bakken Formation

1.1 Introduction

When referring to the production of the Bakken Formation of the Williston Basin (Figure 1.1), what is usually reported is oil volumes, gas volumes, and the like. The gas of concern is 'natural gas', which is primarily methane (CH_4), with associated assorted additions (H_2S, CO_2, CO, etc.), and typically looked upon as a nuisance by-product of hydraulically-fractured horizontal Bakken oil production.

Given individual production units, i.e., one pad or a small collection of pads, the gas volumes are typically too low to allow for the economic recovery of the gas, with all the necessary and expensive surface equipment, pipelines, flowlines, compressors and the manpower to install, operate and maintain the systems (Figure 1.2); although there has been increases in gas being used for pressure maintenance through re-injection. However, with recent legislation in the Williston Basin (North Dakota Industrial Commission, 2020) oil operators must conform to established parameters concerning vented or flared gas, or oil production limits will be reduced (Aoun, et al, 2020). Although approximately 74% of Bakken wells flare less than 10% of their produced gas, overall, it still adds up to approximately 1 BCFGPD (billion cubic feet of gas per day) being flared throughout the basin.

Figure 1.1. The extent of the Bakken Formation in the Williston Basin. (SHSND-ND Studies).

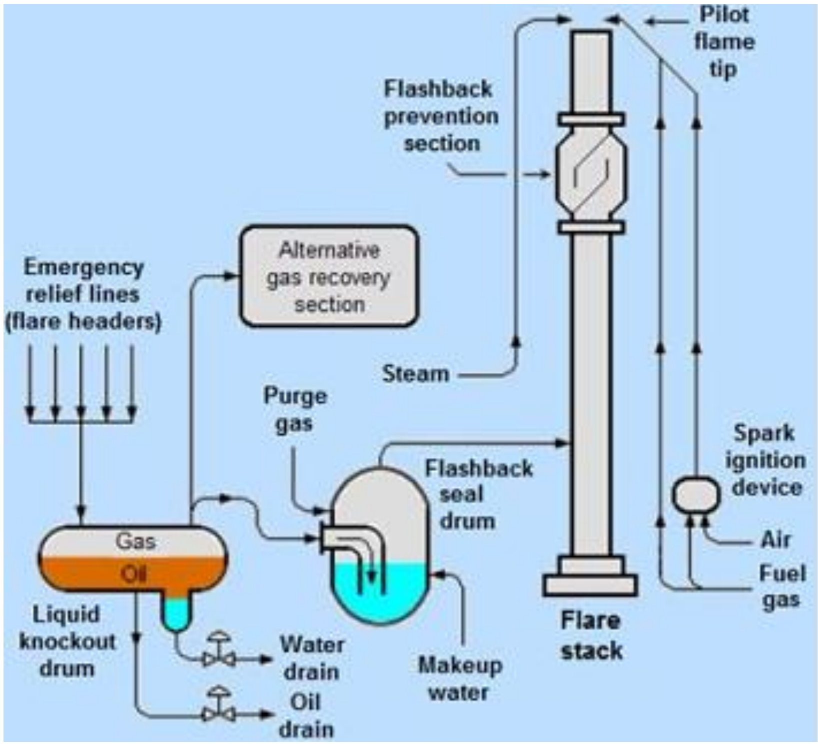

Figure 1.2. Overall flare stack system. After Emam, 2015.

Therefore, the gas is flared, which impacts the environmentally negatively and results in the loss of valuable commodities both from the effects on the local environment and the effects on local environmentalists, especially those with carbon control issues.

Herein lies a quandary: there exists a fuel source that through drilling, completion and production seems to be essentially worthless; in fact, worse than useless as more capital must be expended to dispose of these hydrocarbons. Though flaring is perhaps the most economic method of disposing of the gas, it is perhaps the worst environmentally, for its impact on public relations and governmental mandates to cease flaring by such-and-such date, all now passed. However, there now exists a possibility to turn this seeming liability into considerable positive cash flow.

Of course, it's a novel process, though one that in various incarnations is currently generating a positive cashflow for operators around the globe. It's not particularly cha inexpensive, it relies on some seemingly exotic hardware and methodologies, but it does possess at least five positive aspects rarely encountered in an industry as longstanding and cantankerous as the Oil Patch.

These are:

1. Reformation and capture of diatomic hydrogen, literally re-working CH_4 into H_2.
2. Capture and liquefaction of elemental helium, by various methods, such as Swing Pressure Adsorption, Cryogenics, *etc*.
3. Capture, and sequestration of carbon dioxide (CO_2 - CCUS) as a by-product of operations 1 and 2,
4. Isolation of both LNG (Liquified Natural Gas) and NGLs (Natural Gas Liquids) for sale and financial offset of the cost of helium and hydrogen extraction, and

5. Complete elimination of flaring from horizontal, hydraulically-fractured Bakken wells in the Williston Basin.

Item number 5 is free from the implementation of items #1, 2, and 3.

To date, simultaneous hydrogen and helium recovery both from a natural gas stream has not been attempted. Part of the reason is that hydrogen recovery is a “hot” technology, (literally from the use of superheated steam) as well as a media “Hot Topic” (Macpherson, 2021), while helium capture is a cryogenic, i.e., a cold, process; as hydrogen forms billions of compounds while helium does not, as it is a noble gas. It is proposed in this dissertation that there are processes that can extract, simultaneously, in the same processing sequence, both elemental hydrogen and helium. Carbon dioxide will be created and/or contained in either process, hot or cold, to be captured and available for sale, industry use or in-ground sequestration or storage.

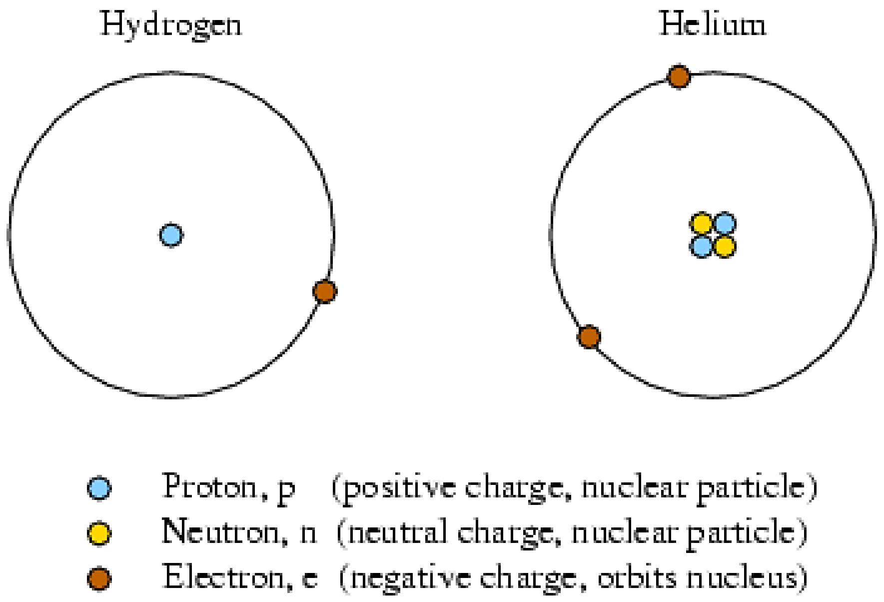

Figure 1.3. Hydrogen atom v. helium atom. Both are recoverable from Bakken flare gas. Woodgate, 1970.

Many people ask why we should bother with capturing both the admittedly small percentages of hydrogen, helium and carbon dioxide in Bakken, or other, natural gas streams derived from horizontal wells that are hydraulically fractured.

There are several reasons:

1. Mitsubishi and Bakken Energy and Mitsubishi Power announced their intent to acquire and convert a financially troubled synthetic natural gas plant in Beulah, North Dakota into the "largest producer of clean hydrogen in North America" — the first step in broader ambitions to establish North Dakota as a "world-class hydrogen hub" (Willis, 2021) (Figure 1.4).

Figure 1.4. New Clean-Hydrogen Hub in Beulah, North Dakota – to be developed by Mitsubishi Power and Bakken Energy. From Bakken Energy, 2021.

This so-called "Blue Hydrogen" will be used to power fuel-cell equipped vehicles, or use directly by particular internal combustion engines, both turbines and specially modified piston engines.

2. Helium is a non-renewable natural resource for which there are limited or no substitutes including for its use as an excipient in NASA spacecraft, certain types of nuclear reactors; providing low enough temperatures for superconducting magnets; enabling modern magnetic resonance imaging (MRI) technologies to operate; other cryogenic applications; and in other applications (Cai et al., 2012). Helium has myriad uses in modern heavy industry, to welding, fabrication, to provide an inert protective atmosphere for making fibre optics and semiconductors, to detect leaks, provide an inert atmosphere in oil field fluid sampling, *etc*. (Table 1.5).

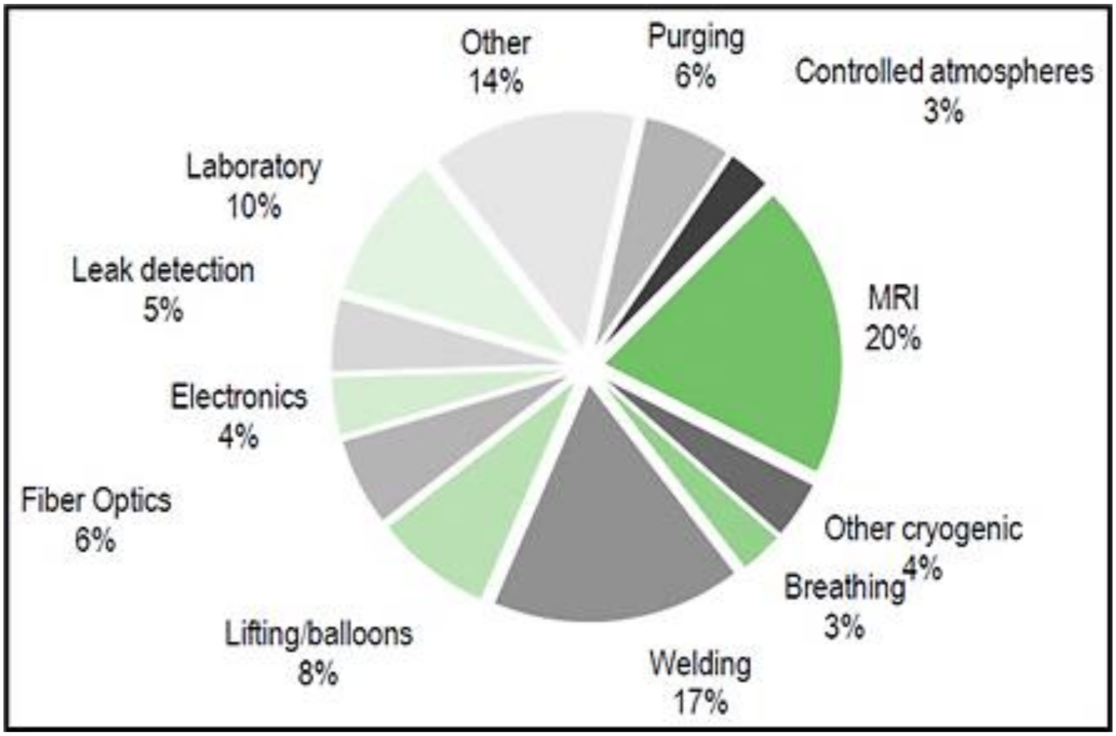

Figure 1.5. Helium uses in industry. Source: Edison Investment Research (Feb 2019)

99.999%-pure industrial helium also currently sells for US$*625/MCF* (Linde, Inc., 2023). By comparison, Henry Hub Gas (3/21/2023) which is predominantly methane, is selling for US$*2.09/MMCF* (Market Insider, 2023).

3. Carbon dioxide has been implicated in many local, regional and global environmental reviews as the main culprit in ‘global warming’; now more usually referred to as ‘climate change’. Carbon dioxide exists in the Earth’s atmosphere at a concentration of approximately 0.04 percent (400 parts per million) by volume (Lindsey, 2020). While water vapor, the verified champion and origin of climate change over periods of geological time, varies approximately 4.00%$^{\pm 0.5\%}$ (Blaettler, 2019). Be that as it may, there exist environmental, financial, governmental and public relations benefits in capturing and sequestering or selling carbon dioxide (CCU-CCUS) that will be produced from either the hydrogen reforming process or the membrane/cryogenic helium capture and concentration cycle (Figure 1.6).

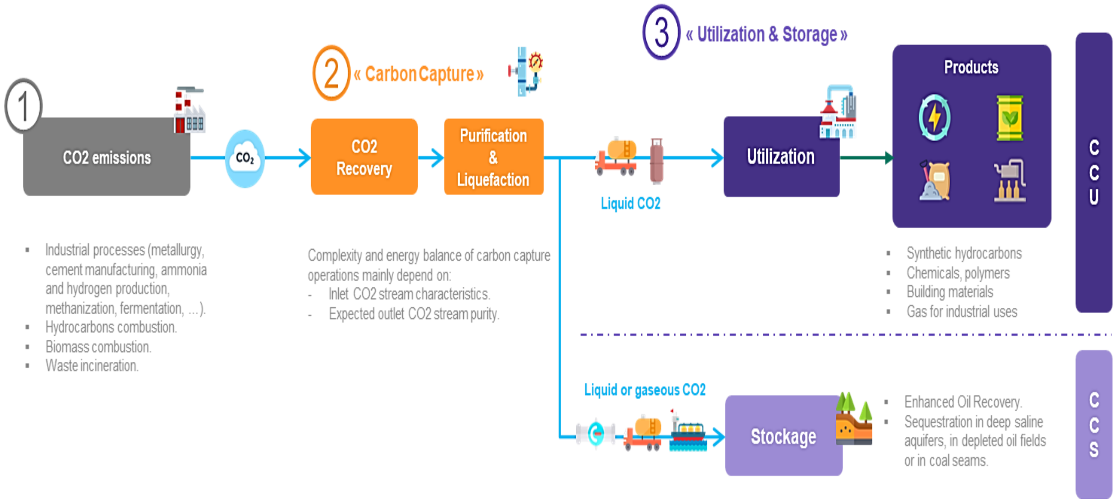

Figure 1.6. The CCUS Value Chain. From Alcimid, 2020.

4. The carbon dioxide captured in either the hot hydrogen or cold helium production streams can be used by the oil and gas extraction and drilling industry for mud conditioning with CO_2 to quickly and deliberately increase the density, viscosity and yield strength of the typically used water-in-oil based mud (Adebayo, et al, 2011).

5. The captured carbon dioxide can be added to the stimulation process to foam acids, ‘charge’ systems with additional chemical and mechanical energy, as well as lighten the column during hydraulic fracturing. It also has the benefit of creating a natural biocide when added to completion/stimulation fluids (SahleDemessie, et al, 2003) (Figure 1.7).

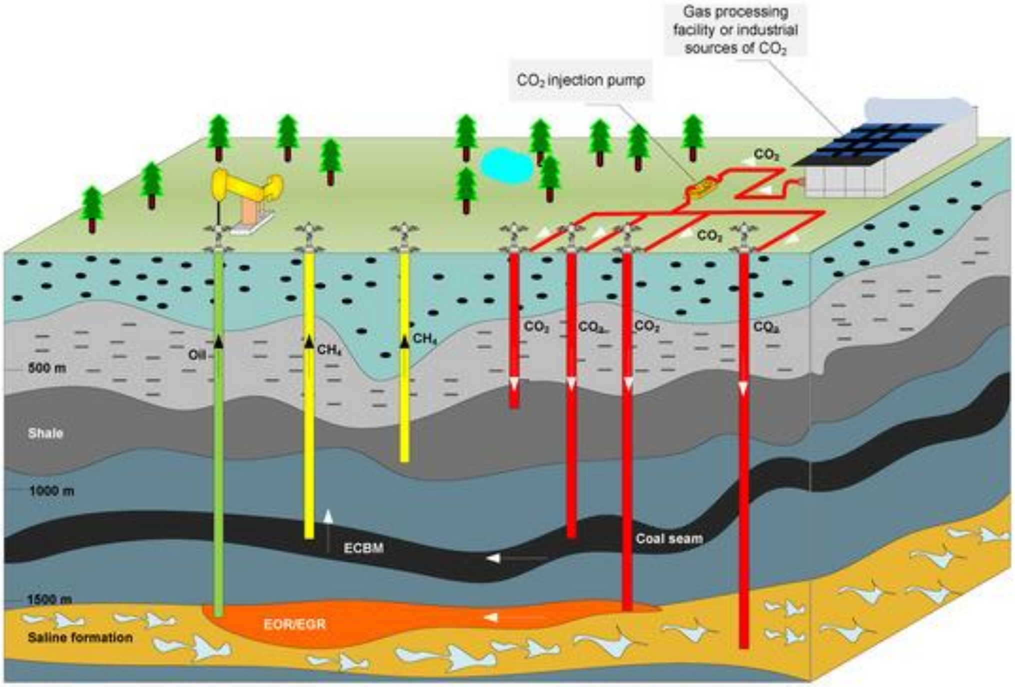

Figure 1.7. Carbon capture, utilization and storage (CCUS) technology-underground injection of CO_2. (From Novak, et al, 2019).

6. In all cases, the ‘free” CO_2, when utilized in drilling, completion or stimulation of Bakken horizontal wells, will be sequestered into the formation (Du, and Nojabaei, 2019). The CO_2 can also lower interfacial angles and promote positive wettability in Bakken and Bakken-type ultra-tight nanodarcy shale reservoirs (See Figure 1.7).
7. Finally, the processes of extracting helium or reforming Bakken gas to hydrogen will have a dramatic effect on oilfield operations. If enough operators can be convinced of the financial positives of the reforming and recovering these lightest elements, Bakken

gas flaring will cease and disappear. Besides the Public Relations goodwill and positive image presented to both the press and the public, environmentalists will be silenced as will their innumerable frivolous lawsuits. By removing flaring from the Williston Basin Bakken, not only will carbon capture and sequestration be rendered a moot question, but now revenue from the sale of hydrogen and helium, *et al*, instead of the political and economic expenses of flaring will be enjoyed by those progressive and forward-thinking oil and gas operators in the basin.

1.2 Hydrogen v. Helium

Hydrogen and helium are the two most primitive, and abundant, elements which exist in the universe (Figure 1.8).

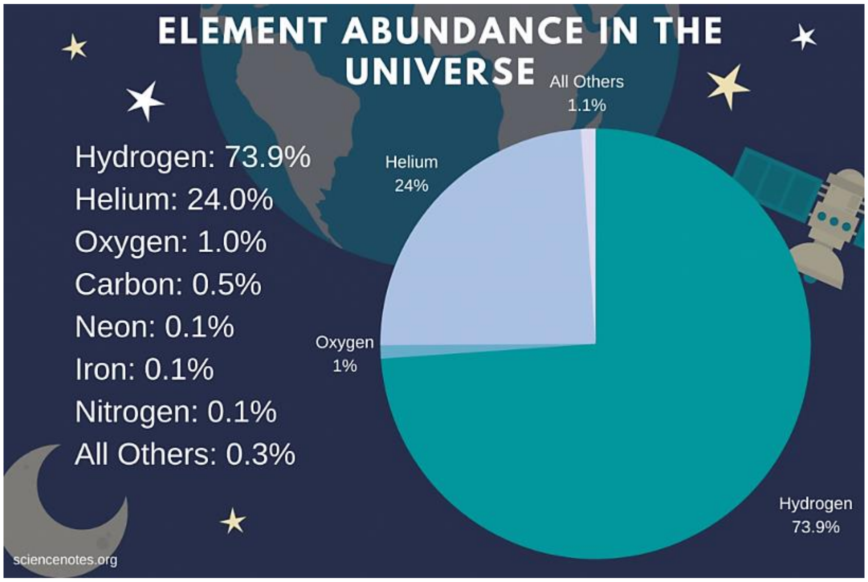

Figure 1.8. Element abundance in the universe. From Science Notes, 2020.

Approximately 380ka after the Big Bang (Klesman, 2019) some 13.4 GA, the universe was finally cool enough for elements to form, to where it was essentially filled with nothing but hydrogen and helium (Figure 1.9).

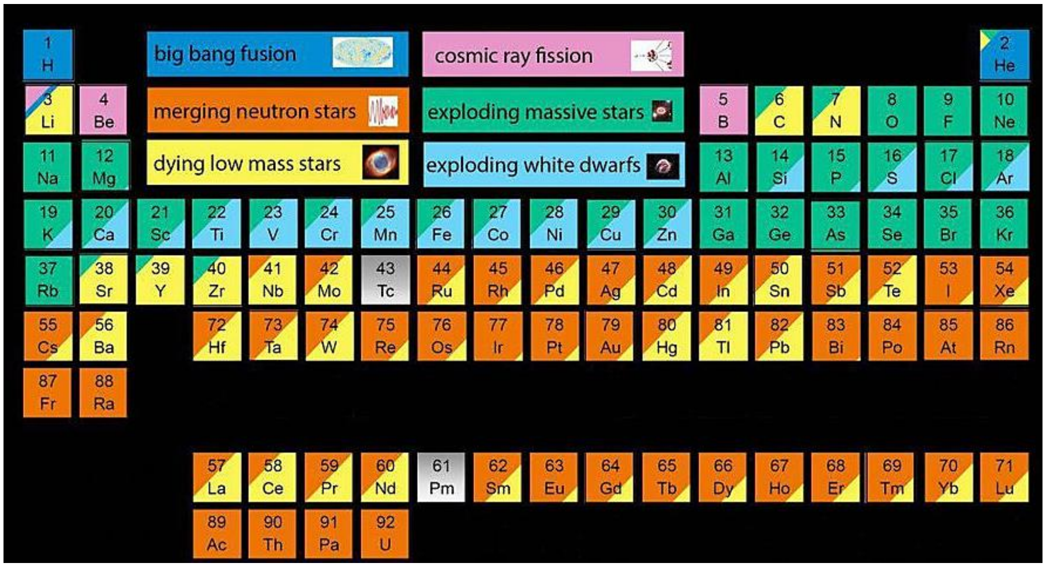

Figure 1.9. Nucleosynthesis of the Elements of the Periodic Table. From Johnson, 2020.

Hydrogen is the first member of the Periodic Table of the Elements (Mendeleev, 1869) and consists of one proton and one electron. Helium, second on the Periodical Table of the elements (Figure 1.9), consists of a nucleus of two protons and two neutrons surrounded by two electrons.

Hydrogen was discovered in the 16th century; however, it was referred to as flammable air or ‘phlogiston’. Lavoisier, in 1781, coined the term ‘hydrogène’, from when the English term is derived (American Chemical Society, 2015).

Hydrogen readily makes molecules, in fact, is present is all animal and vegetal tissue as well as ubiquitous in petroleum and petroleum products. It has three known isotopes: protium (hydrogen…+1), deuterium (+2), and tritium (+3).

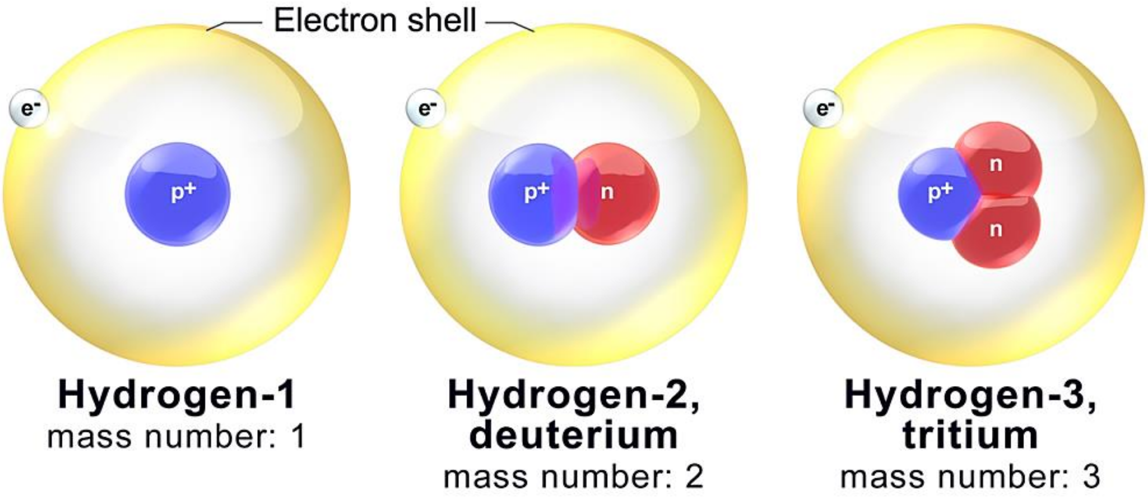

Figure 1.10. Hydrogen and its isotopes. From pedia.com

Helium was discovered first on the sun spectroscopically in 1868, then later on Earth in 1895 (Chodos, 2004). Helium, while being a noble gas which forms no natural molecules, does have six isotopes; however only ^{3}He and ^{4}He are stable (Figure 1.10).

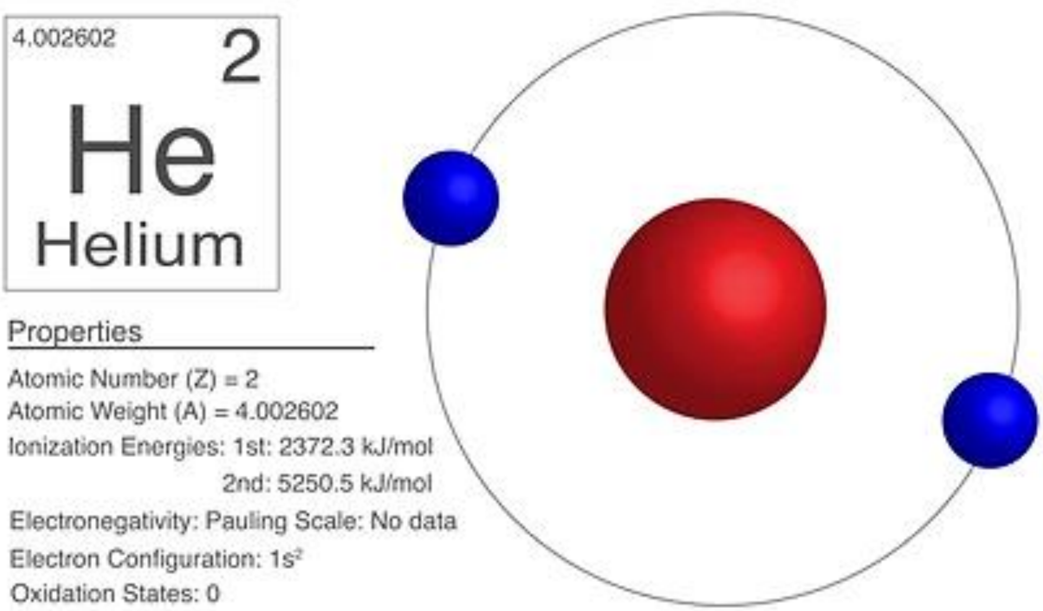

Atomic Number (Z) = 2
Atomic Weight (A) = 4.002602
Ionization Energies: 1st: 2372.3 kJ/mol
2nd: 5250.5 kJ/mol
Electronegativity: Pauling Scale: No data
Electron Configuration: $1s^2$
Oxidation States: 0

Figure 1.11. Properties of Helium. Courtesy of Shutterstock.com.

Hydrogen is the most abundant element in the universe, accounting for approximately 75 percent of normal matter. Helium accounts for about 25 percent of the atoms in the universe. However, on Earth, hydrogen it makes up only about 0.14 percent of Earth's crust by weight (Black, 2021). Helium is ever more elusive; being a noble gas, it forms no compounds, and is not primordial in nature, but the product of radioactive decay.

Both elemental hydrogen and helium are gasses at STP (Standard Temperature and Pressure), which makes them difficult to capture and retain, as they are so active and light, that they can escape Earth's gravity and bleed off into space. Hydrogen, being tied up in innumerable different compounds, requires considerable energy for its liberation, capture, purification and liquification for storage. Helium, inert and thus not involved in creating compounds, carries its own problems in capture, purification and liquification for storage. Both can escape most laboratory and industrial containers, even ones lined with PTFE (Polytetrafluoroethylene – Teflon), but superfluid helium can actually "climb walls" (Minkel, 2009) of containers due to its 'perfect flow', i.e., no measurable friction, when cooled to temperatures of 1K (-452 F^0 or -269 C^0).

Table 1.1. The differences between hydrogen and helium. From differencebetween.com. accessed 22 March, 2023.

Hydrogen vs Helium

More Information Online WWW.DIFFERENCEBETWEEN.COM

	Hydrogen	Helium
DEFINITION	Hydrogen, which is denoted as H, is the first and the smallest element in the periodic table	Helium is the second element in the periodic table, having the symbol He
ORBITALS	Has a half-filled s orbital	Has a fully filled s orbital
STABILITY	Less stable	More stable
INERTNESS	Reactive	Inert
COMPOUND FORMATION	Forms a wide variety of compounds	Does not form any compound
FLAMMABILITY	Extremely flammable	Not flammable
BOILING POINT	Higher compared to helium	Lower compared to hydrogen
ISOTOPES	Three	Seven

Even with suites of difficulties in dealing with the gasses in their elemental or diatomic forms, both hydrogen and helium possesses myriad uses in society today. Hydrogen, particularly "Blue Hydrogen" (that which is liberated from natural gas streams with associative carbon dioxide capture and sequestering) (Cloete, 2020) is being eyed particularly for fuel for vehicles; ranging from personal automobiles to long-haul trucks, both in fuel cells and as a green biogas. Currently, the price for 99.999% hydrogen is difficult to ascertain. Due to the vagaries of the costs of feedstock and types of liquification and storage required as well as location, hydrogen variously sells for between US$2.00-$5.00 *gge* (gallon of gasoline equivalent) or $1.80-$4.40/kg.

Helium, on the other hand, being non-flammable, non-reactive, and non-magnetic, has innumerable applications ranging from welding, to breathing mixtures, to inert gas for filling pressure vessels, to Magnetic Resonance Imaging (MRI).

Helium has had a long and disorderly price history since the establishment, and later sale of, the US National Helium Reserve. Since 1925, where the US controlled virtually all the world's industrial helium needs. Subsequently, the beginning of the US phasing out the Helium Reserve, helium prices have soared to over US$400/MCFG, and rising, in 2023 (Ashfield, and Kapadia, 2023).

Both hydrogen and helium exist is such small quantities in the atmosphere, that distillation of the gasses from liquifying air is immensely unprofitable. Also, hydrogen cannot be separated from the mixture of air as it is not present in the free diatomic state.

However, both hydrogen and helium can be obtained from natural gas streams; in this particular case, the Bakken of the Williston Basin of Montana and North Dakota. Unfortunately, the methodology of obtaining hydrogen by steam reforming of methane. i.e., "Blue Hydrogen", is seemingly diametrically opposite from the extraction of helium that is carried, unbonded, along with the natural gas stream. Steam reforming of hydrogen is a thermal process, while the isolation, purification and containment process of helium is cryogenic; which seems to impose insurmountable problems.

1.3 Objectives

If one were to follow the development of extracting, collecting, concentrating and storing hydrogen and helium for natural gas streams, there would appear to be a physical, or thermogenic, barrier from collecting the two dissimilar gasses simultaneously from a single gas stream.

The objective of this dissertation is to propose a modular methodology, based on existing “off the shelf” equipment that will not only allow for the simultaneous or consecutive capture of both hydrogen and helium from Bakken gas streams, but to also allow for carbon dioxide capture and sequestration (CCUS) which would lead to a huge reduction or elimination of flared gas from the Bakken in the Williston Basin.

The detailed objectives of this work can be summarized as followings:

1. Comprehensive review of existing literature on the reforming of natural gas (CH_4) through thermal aqueous methods, i.e., autothermal reforming plus water gas shift reaction, and steam methane reforming (SRM), to yield carbon monoxide (CO), carbon dioxide (CO_2) and hydrogen (H_2). This includes analytical models, lab experimental studies, numerical simulations and field observations.
2. Comprehensive review of existing literature on the mining of natural gas (CH_4) various methodologies (Pressure Swing Adsorption, selective catalytic and noncatalytic membranes, etc.) to yield 99.999% pure helium. This also includes analytical models, lab experimental studies, numerical simulations, and field observations.
3. Explicate and make recommendations on the positive and potential negative aspects of the differing methods of hydrogen reforming and helium extraction from Bakken gas streams.

4. Develop and demonstrate the efficacy of a simultaneous or sequential methodology for profitably extracting both hydrogen and helium from a single Bakken gas stream utilizing existing “off the shelf” technology and streamlined processes from wellhead through cryogenic storage.
5. Demonstrate how either thermal steam reforming of natural gas for hydrogen, or PSA extraction of helium from said gas, or combination of processes will yield carbon monoxide (CO), and carbon dioxide (CO_2) as part of the lighter element relinquishment from Bakken gas sourced from hydraulically-fractured horizontal wells, which can be captured.
6. Establish that CO_2 from lighter element extraction from Bakken gas streams can have positive impacts on operator’s financial ‘bottom lines’ through the use of said carbon dioxide in drilling, completion, and stimulation practices. Also validate that the use of carbon dioxide in such a manner will both contain and sequester the CO_2 in a deep, very low (nano-) permeability geological reservoirs for perpetuity.
7. Aid in eliminating Bakken-sourced natural gas flaring in the Williston Basin. Even with the relatively low cost of elemental hydrogen and the incrementally much higher value of helium in Bakken sourced gas stream, literally millions of dollars of potential product are wasted each year the flaring of this gas continues. Evidence that the additional costs of steam reforming methane to hydrogen, stripping helium from the gas stream and the cryogenic apparatus necessary for concentration and containment of these lightest of elements will be cost effective and have a very short pay-out period, particularly given the current escalating price of global helium.
8. Demonstrate to local operators the advantages of discontinuing Bakken gas flaring not only through the financial incentives of harvesting hydrogen, helium and CO_2, but the

heightened positive Public Relations and quelling of environmentalists over the fervent subject of air pollution, seeming oil industry nonchalance regarding flaring remediation, as well as flaring and public opinion over Bakken and Williston Basin oilfield operations in general.

1.4 Methodology

The methodologies that will be used to achieve the above objectives comprises of data inventory, extensive literature review, interviews with experts in all facets of the process, and analytical solutions.

These are briefly explained below.

- Define both "Blue Hydrogen" and the optimal method(s) for extracting said element from Middle Bakken-derived natural gas streams.
- Elucidate the primary method(s) for the optimal extraction, collection, refinement and containment of elemental helium from Middle Bakken-derived natural gas streams.
- Develop an optimal procedure, with attendant mechanical apparatus, that will allow for simultaneous or sequential extraction, collection and concentration of hydrogen, helium and carbon dioxide from Middle Bakken-sourced natural gas streams.
- Invite and encourage service companies and operators to share information and to take particular notice of the financial and public-relations boon of eliminating Bakken gas flaring through helium, hydrogen and carbon dioxide extraction.

1.5 Significance

The results of this research study will present manifold innovations including the following:

1. A unique, novel, and never before attempted, simultaneous, sequential straight-through process and methodology for the extraction of elemental hydrogen, helium and molecular carbon dioxide economically from Bakken-derived natural gas streams that would have been otherwise flared to the atmosphere.
2. Enhanced cash streams/flow for forward-thinking operators who would initially fund the development, acquisition, installation, operation and maintenance of the mechanical apparatus once pay-out through the sale of elemental hydrogen, helium and the tax benefits of capturing and sequestering carbon dioxide (“CO_2 credits”) had been achieved.
3. The elimination of flaring of Bakken natural gas in the Williston Basin.
4. The deep sequestering and/or utilization of carbon dioxide from said gas streams which would normally be released to the atmosphere.
5. The generation of positive Public Relations with local environmental activists, and an increase in esteem for the environment from both the local and regional government as well as the local populace.
6. Practical recommendations and suggestions that are proposed in this study can improve the drilling, completion, stimulation and operations in the Bakken of the Williston Basin which in turn can be of significant financial benefits for the companies.

1.6 Research Aims & Scope

1.6.1 Problem Statement

There is ~1 BCFGPD being flared in the Williston Basin, primarily composed of natural gas from the Bakken Formation. As flaring contributes to diverse environmental, political, geological, and public relations problems; there must be actions taken to alleviate these concerns while at the same time being both economic and profitable for operators to undertake remediation. This remediation program should be conservative, utilized proven technology, and be readily and economically available.

1.6.2 Research Hypothesis

Deeper critical-path understanding of how linear uniflow modular methodologies or techniques, based on existing “off the shelf” equipment to allow for simultaneous or consecutive capture of both hydrogen and helium from previously flared Bakken gas streams need to be examined for their efficacy, economy and utility.

1.6.3 Research Questions & Objectives

1. Can a novel liner-path gas treatment procedure, utilizing off-the-shelf technology, be employed to capture and monetize the currently flared Bakken natural gas?
2. Can a single unique program of flare gas capture, processing and transport aid in CCUS (Carbon Capture, Utilization and Sequestration) in the Williston Basin?
3. Can a novel, modularized process of flare gas capture, pre-treatment, NGL/helium extraction and providing feedstock for Steam Methane Reformatting be realized while monetizing the product stream and providing increased incentives for operators to abandon flaring in the Williston Basin, accept and implement the processes and procedures defined in this dissertation?

1.7 Dissertation Structure

This dissertation consists of nine total chapters.

Chapter 1 provides the background to the project and a very brief explanation of the elements and molecular compounds endemic to the study. It also contains the objectives of this study, the methodologies used, and the novelty of the processes defined herewith and the significance of this research.

Chapter 2 sets the topographic, geographic and geological stage through the definition of the Williston Basin, its extent, structural history, and general stratigraphy of the basin. Its distinctiveness and unique economic geologic history and stratigraphy is highlighted.

Chapter 3 focuses on the Late Devonian-Early Mississippian formation, the Bakken, with additional information on the petroleum geology of productive formations closely underlying or overlying the Bakken, and the development Bakken Total Petroleum System (TPS). The Bakken TPS includes the Bakken Formation, the upper parts of the subincumbant late Devonian Three Forks Formation, and parts of the superincumbent early Mississippian Lodgepole Formation.

Chapter 4 deals with the complex history and geological story of helium. Helium, being a noble gas and accessory to natural gas, forms no compounds yet is found in almost any gas accumulation of any size. Since its discovery in a Kansas, USA gas well in the 1930s, the gas has been both a novelty and a burden to the oil industry. However, as technology progressed, the scientific, academic, and commercial world could not exist as it does today without this unusual gas. The origins of helium have sparked debate since its discovery, but it basically is related to primary mantle exhalations and radioactive decay of Uranium/Thorium minerals.

Typically, there needs to be a thick, impervious regional seal to retain helium, due to its atomic and molecular activity so that major deposits of heliferous natural gas are restricted to Neoproterozoic-sourced gas under a regional evaporitic seal; thick, massively bedded carbonate-evaporite sequences or thick, massive Paleozoic euxinic black shales. Examples of each type are discussed, with the Bakken accumulation as a prime example of the latter.

Chapter 5 is concerned with hydrogen and its extraction from Bakken-derived gas streams. Primary extraction will focus on autothermal and steam reforming of methane. Steam methane reforming (SMR) is a process in which methane from natural gas is heated, with water steam, usually with a catalyst, to produce a mixture of carbon monoxide and hydrogen. Further application of SMR will generate additional hydrogen and carbon dioxide; the latter of which can be isolated for carbon capture and sequestration.

Chapter 6 examines helium and its extraction from the Bakken-derived gas streams. There are several different methods used in industry today to extract helium from natural gas. Primary among these is helium recovery by cryogenic fractionation, although there are myriad others. All must upgrade the helium to greater than 90% purity before liquefaction and transport. It is at this point in the process it seems most feasible to also extract hydrogen which has previously been reformed from Bakken methane.

Adsorption-based processes for helium recovery will also be examined. Adsorption-based processes are primarily used during the early pre-treatment process to remove water (H_2O), carbon dioxide (CO_2), hydrogen sulfide (H_2S) and other impurities from the feed natural gas. This process is also used for removing trace impurities of nitrogen (N_2) and methane (CH_4) during the purification process for helium (Tagliabue et al, 2009).

Also, the economic impact of the so-called “impurities” from the natural gas stream will be addressed, as well as the potential for generating Liquid Natural Gas (LNG) and other Natural Gas Liquids (NGLs) which can be sold to aid in offsetting the cost of helium extraction, liquification and storage.

Chapter 7 will address the novel simultaneous or sequential hybrid process and apparatus for the coeval extraction of elemental hydrogen, elemental helium, carbon dioxide, “impurities” such as nitrogen, hydrogen sulfide, and methane, potential for Liquid Natural Gas as well as Natural Gas Liquids and the financial impact of developing and operating such mechanics and the offsetting profits from the sale of the primary products.

Chapter 8 will deal with the intricacies of operating economics of Bakken flare gas capture and reformatting of the products attained either through mechanical or membrane means.

In Chapter 9, conclusions, and summary of the findings from this study will be presented along with recommendations for potential future investigations that can be carried out.

CHAPTER 2

The Williston Basin

2.1 The Williston Basin

The Williston Basin; North Dakota, and Montana, USA, and Saskatchewan and Manitoba, Canada (Figure 2.1), is a classic example of a large Phanerozoic-age interior cratonic sag basin.

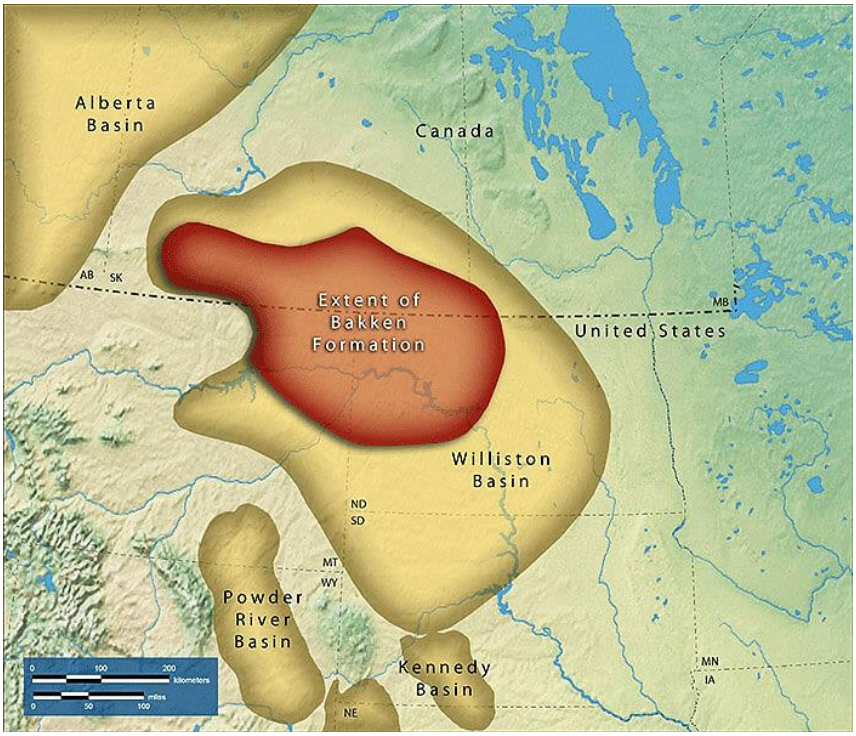

Figure 2.1. Location map of the Williston Basin and the limits of the Bakken Formation. From Williston Basin Petroleum Conference, 2021.

Located on the western periphery of the Phanerozoic North American craton, the Williston basin has undergone relatively mild deformation during Phanerozoic time. This deformation is primarily responsible from the reactivation of large Precambrian basement blocks of the Trans-Hudson Orogenic Belt, which has an age of approximately 1.8-19 GA (Gibson, 1995).

The Williston Basin is bound by the Alberta Basin to the north and west, the Powder River and smaller Kennedy Basins to the south and east. It is also bounded by the Precambrian Canadian Shield to the northeast (Figure 2.1).

2.2 Structural History

Structurally, the Williston Basin has a long history, which was probably initiated "Pre-Sauk" (Monroe, and Wicander, 1997) or in the Early-Middle Neoproterozoic. The initial tectonism was the result of the intrusion of an asymmetric probably granitic batholitic igneous body at depth. This resulted in radial extension in the central portion of the protobasin, and compressional to transpressional structural regimes at the peripheries. Cooling of this pluton or local erosion led to the initiation of basinal subsidence.

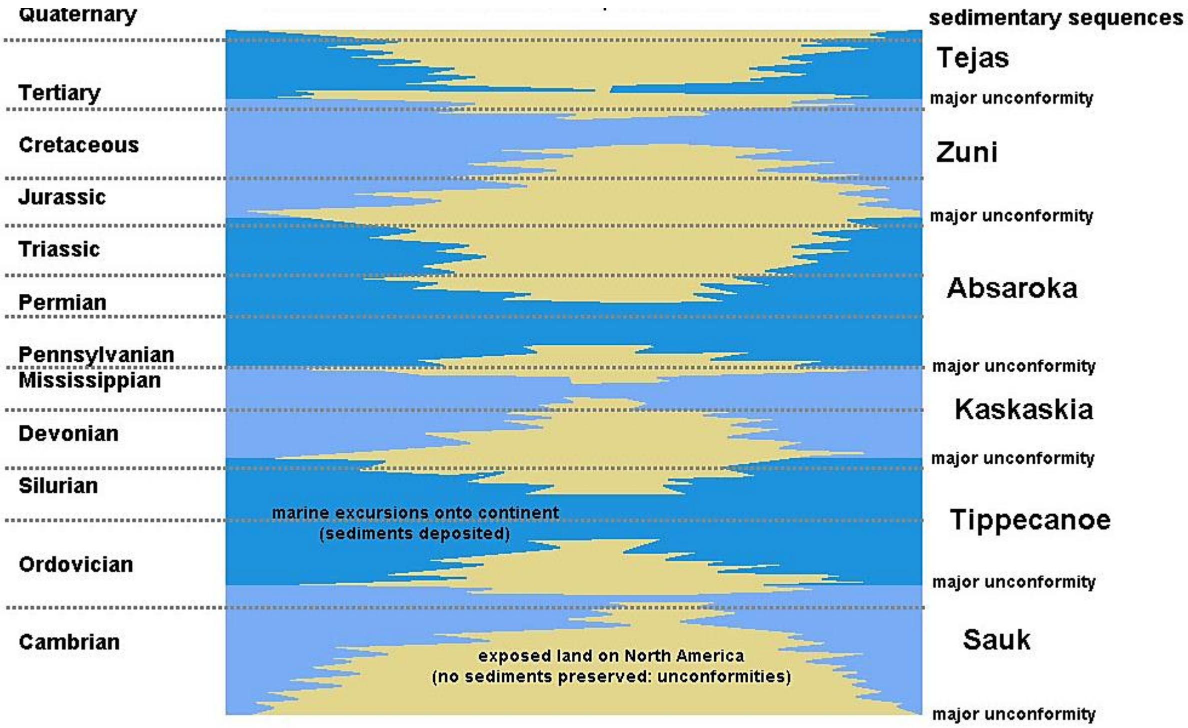

Figure 2.2. Sedimentary Sequences of North America. Bakken TPS is represented by Kaskaskia Sequence. From http://geologycafe.com/images/sloss.jpg, accessed 08-2021.

During the following “intracratonic” phase (Sauk-Absaroka) (Figure 2.2), the radial and peripheral structures were occasionally differentially reactivated, yielding structural inversion. The periods of reactivation were not related to global, but regional to local, tectonism. Excepting that of the Kaskaskia 1 (Devonian) period, when the entire region was tilted to the northwest.

The following “foreland” phase (Zuni-Tejas), the basin was subjugated by lateral forces of the Sevier and Laramide orogenies (Herrera, 2013). These orogenies left their own particular set of structural overprints on the Williston Basin; primarily in the NNW-SSE elliptical elongation of the basin and development of the predominant NE-SW/NW-SE fracturing and faulting patterns. Further results of these orogenic events were both the offset and rotation of pre-existing peripheral and radial tectonic structures (Redly, 1998) Figure 2.3

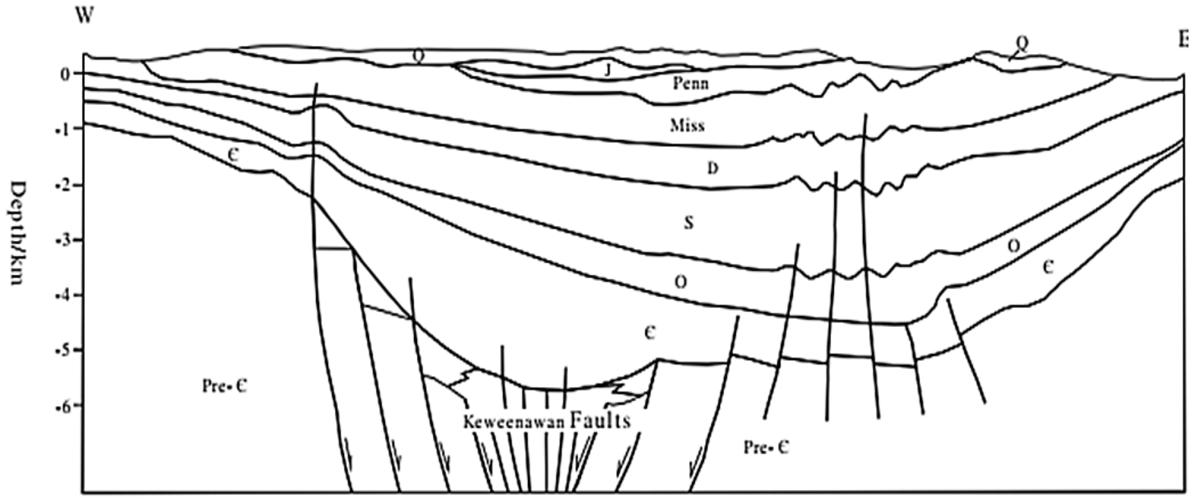

Figure 2.3. Geological profile (cross-section) of the Williston Basin, After Liu, et al, 2017.

Figure 2.3 denotes the ~16,000’ of Paleozoic, minor Mesozoic, and Quaternary fill of the Williston basin which resides upon the heavily fractured Upper Precambrian igneous-metamorphic basement. Reactivation and movements of these basement structures are responsible for the relatively low level of structuralization of the basin. Primarily vertical movements, coupled with dissociative periods of extension and transtension during localized orogenies (Antler, Acadian, etc.) led to the development of the Williston’s elongate sag-basin cross-section (Poole, et al, 1992).

2.3 Depositional History

Numerous continental-scale transgressions and regressions throughout the Paleozoic deposited the several thousands of feet of carbonate and clastic fill seen in the basin (Gibson, 1995). Subsidence and basin filling were most pronounced during the Ordovician, Silurian, and Devonian, when thick accumulations of carbonates were deposited. Subsidence continued into the Lower Carboniferous at a condensed scale and had largely ended by the Pennsylvanian.

Second and third order sequences can be delimited within the boundary of the basin through subsurface means. Several formations, such as the Bakken, do not crop out within or on the peripheries of the basin. They are totally contained within the Williston and only known through drilling, logging, and coring (Anna, et al, 2013).

Due to continental-scale tectonism beginning during the Lower Jurassic, subsidence returned during the Mesozoic. However, depositional sediment thicknesses were far less than during the Paleozoic. Near the terminal Cretaceous, tectonic activity of the Laramide Orogeny rejuvenated numerous Williston Basin basement structures that produced anticlines which today act as traps for oilfields (Redly, 1998).

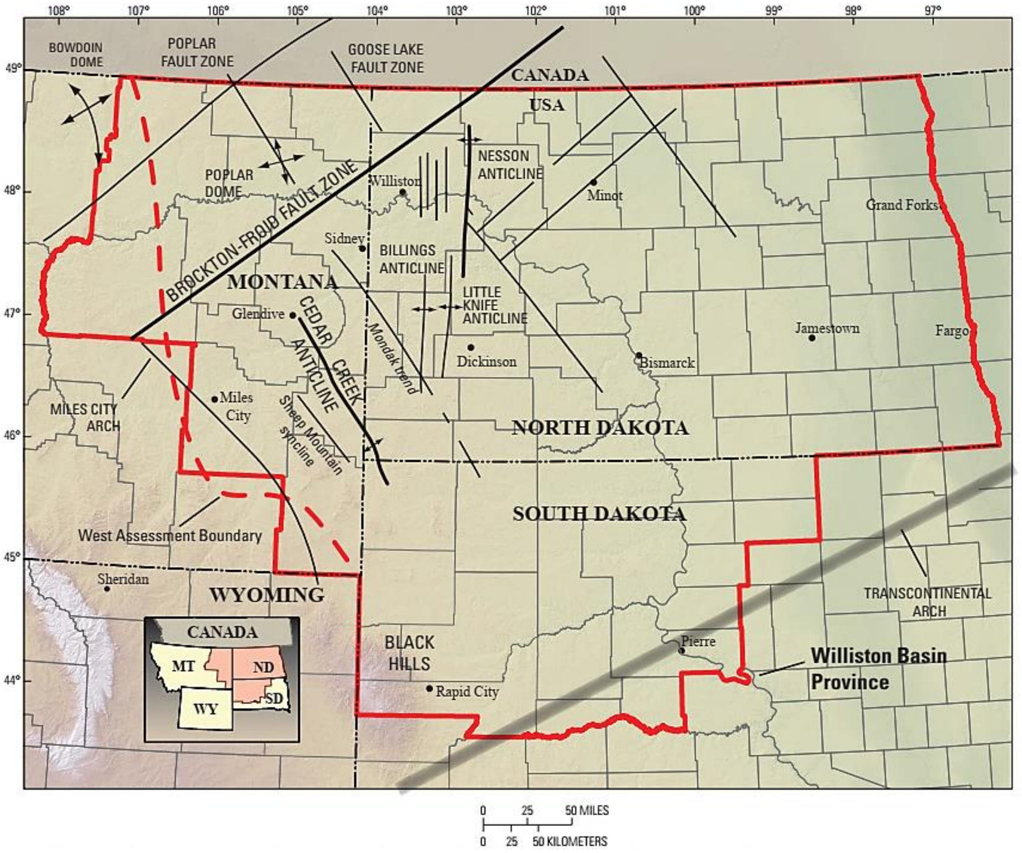

Figure 2.4. Location and physiographic feature of the Williston Basin area. Black lines not labeled are major lineaments or faults. Solid red line is province boundary. After Anna, et al, 2010.

2.4 Sedimentology and Stratigraphy

Sedimentary deposition in the Williston Basin area began in the Lower Cambrian with the deposition of the Deadwood Formation (Figure 2.5). The pattern of deposition in the Williston Basin is essentially described as carbonate deposition in the Paleozoic with clastic deposition in the Mesozoic and Cenozoic. As noted, the thickness of collective Phanerozoic strata in the Williston Basin is more than 16,000 ft in the basin center (Anna, et al, 2010).

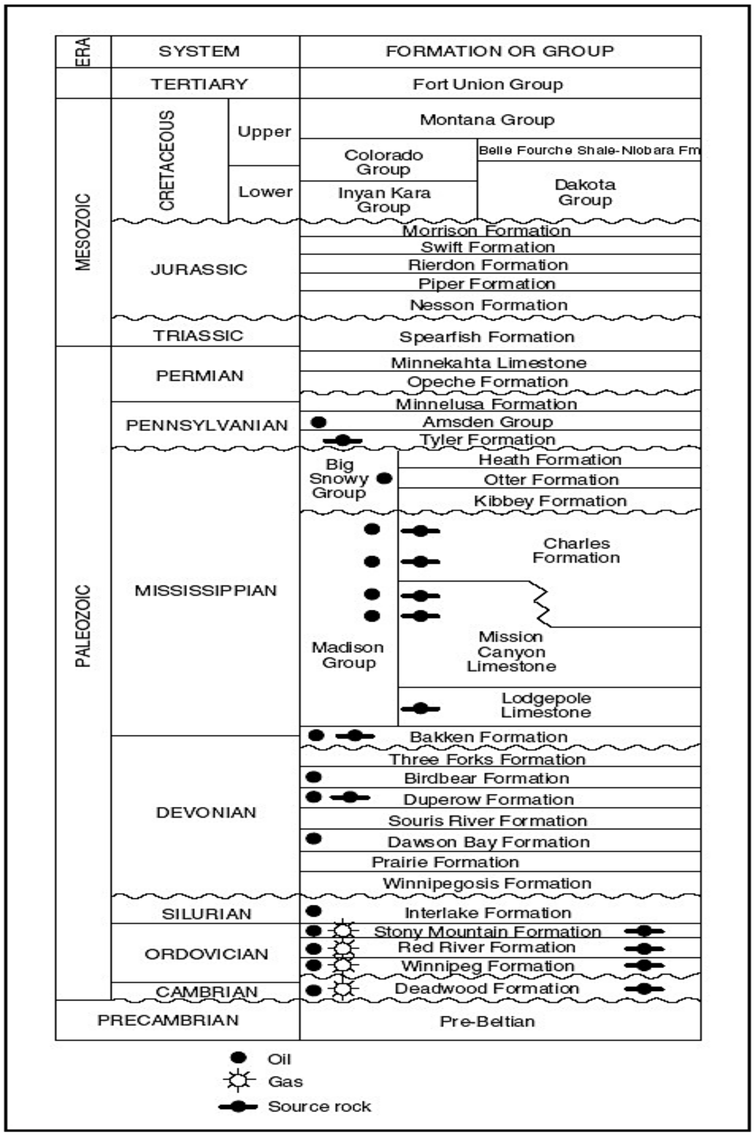

Figure 2.5. Stratigraphic column of the Williston Basin, Montana, and North Dakota, USA. From US Geological Survey, 2010.

CHAPTER 3

The Bakken Formation

3.1 Bakken Formation Defined

In the Williston Basin, the terminal Devonian and the earliest Mississippian is represented lithologically by the Bakken Formation. The formation is named after Henry Bakken, a farmer in Tioga, North Dakota (Universal Royalty Company, 2020), who owned the land where the formation was initially discovered while operators were drilling for oil.

The Bakken is an entirely subsurface formation, as it does not crop out anywhere within the Williston Basin or adjacent lands. However, considering the density of Middle Bakken and deeper oil and gas wells (>16,400), plus Upper Bakken tests, the formation is well represented from the subsurface by cuttings and cores.

Figure 3.1 shows the recent (2017) areal distribution of shale oil production from wells in the Bakken Formation and locations of these wells within the Williston Basin.

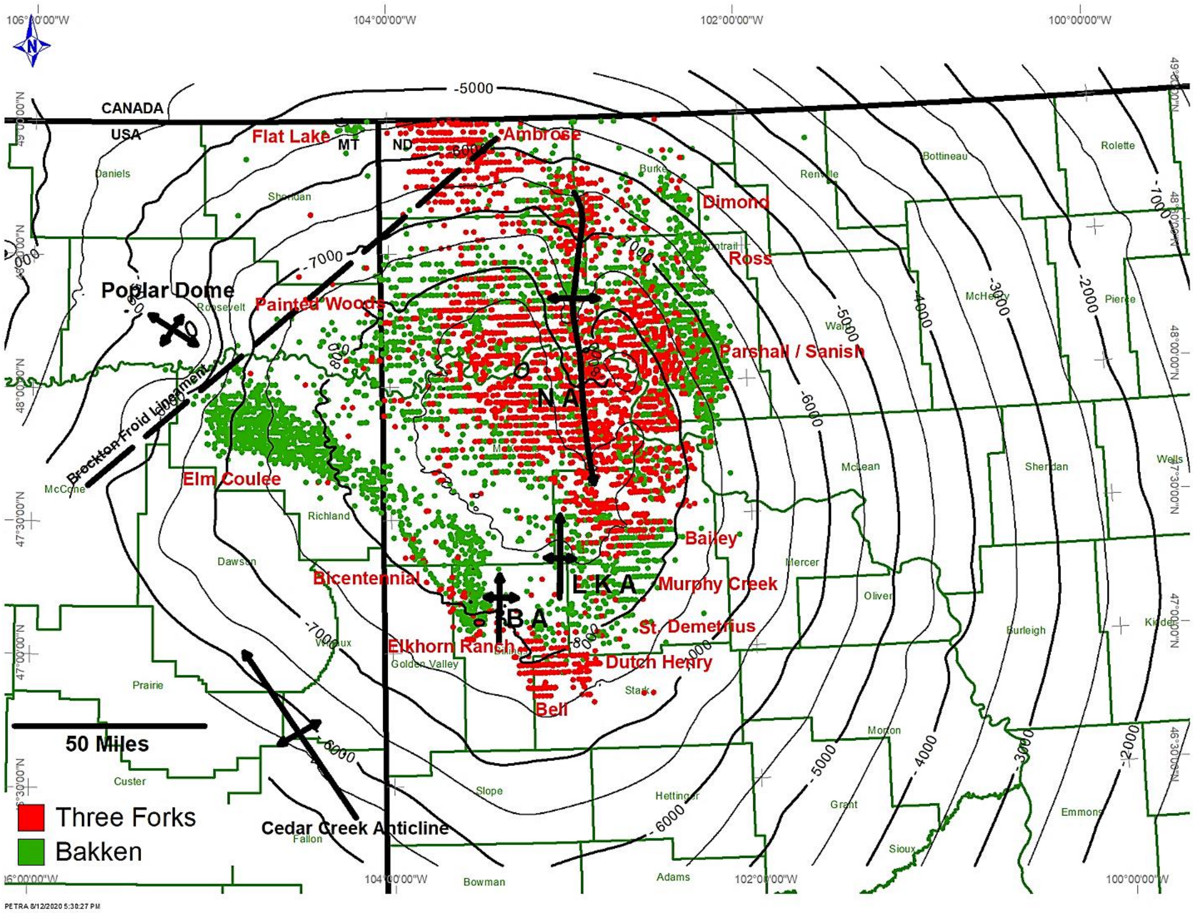

Figure 3.1. Location of Bakken TPS with well control, in excess of 16,500 wells. From Hamlin, et al, 2017.

The Bakken Formation is present throughout the Williston Basin in southern Saskatchewan and southwest Manitoba, Canada; as well as in Montana, and North Dakota in the United States (Figure 3.1). The formation is generally comprised of three distinct members (Figure 3.2): the lower shale, the middle dolomite, and an upper shale. The shales were deposited in relatively deep anoxic marine conditions, while the dolomite was deposited as a coastal carbonate bank in shallower, more well-oxygenated water. The middle dolomite member is the principal oil reservoir, although there is minor oil and gas production form the Upper and Lower Bakken. Both of these members of the Bakken are marine shales, which themselves are organic-rich.

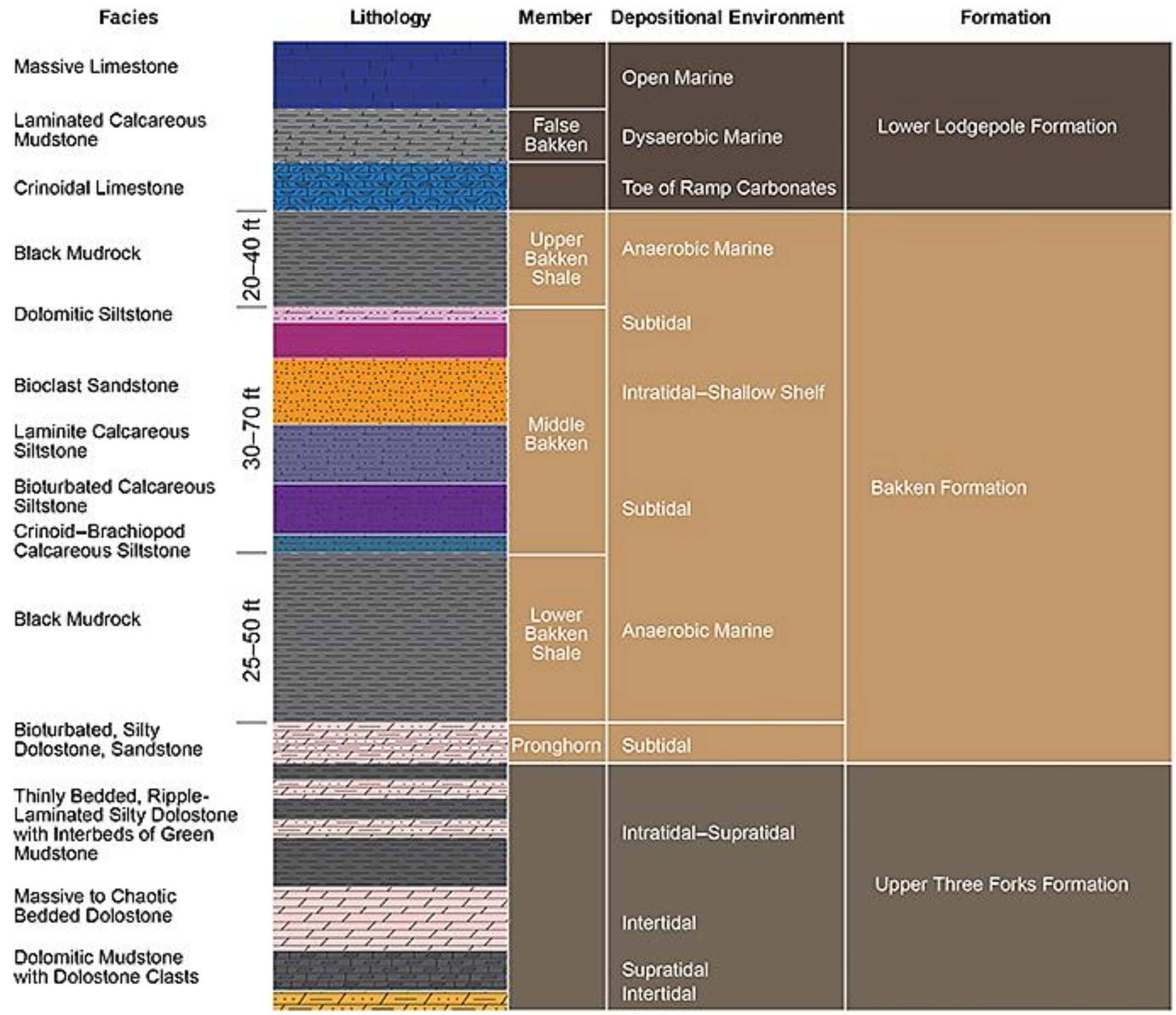

Figure 3.2. Stratigraphic column of the Bakken Petroleum System. Adapted from Sonnenberg, 2017.

3.2 Bakken TPS (Total Petroleum System)

The Bakken petroleum system includes the Bakken Formation, the upper parts of the subincumbant Three Forks Formation, and parts of the superincumbent Lodgepole Formation (Theloy, 2014). The Bakken Formation itself consists of the dolomitic Middle Bakken Member, which is the primary reservoir rock in the system. The superincumbent Upper Bakken shale is one source rock for the system as it is a high TOC black dolomitic mudstone-shale (Nordquist, 1953).

The subincumbant Lower Bakken is also considered a source rock in the system as it is also a high-TOC black dolomitic mudstone-shale. Underlying the Bakken Formation is the dolomitic Three Forks Formation which the upper section is considered the lowermost part of the Bakken Total Petroleum System (Figure 3.3).

The carbonate-rich Lodgepole Formation, superincumbent to the Bakken Formation, is considered to be the uppermost part of the Bakken petroleum system (Hamlin, 2017).

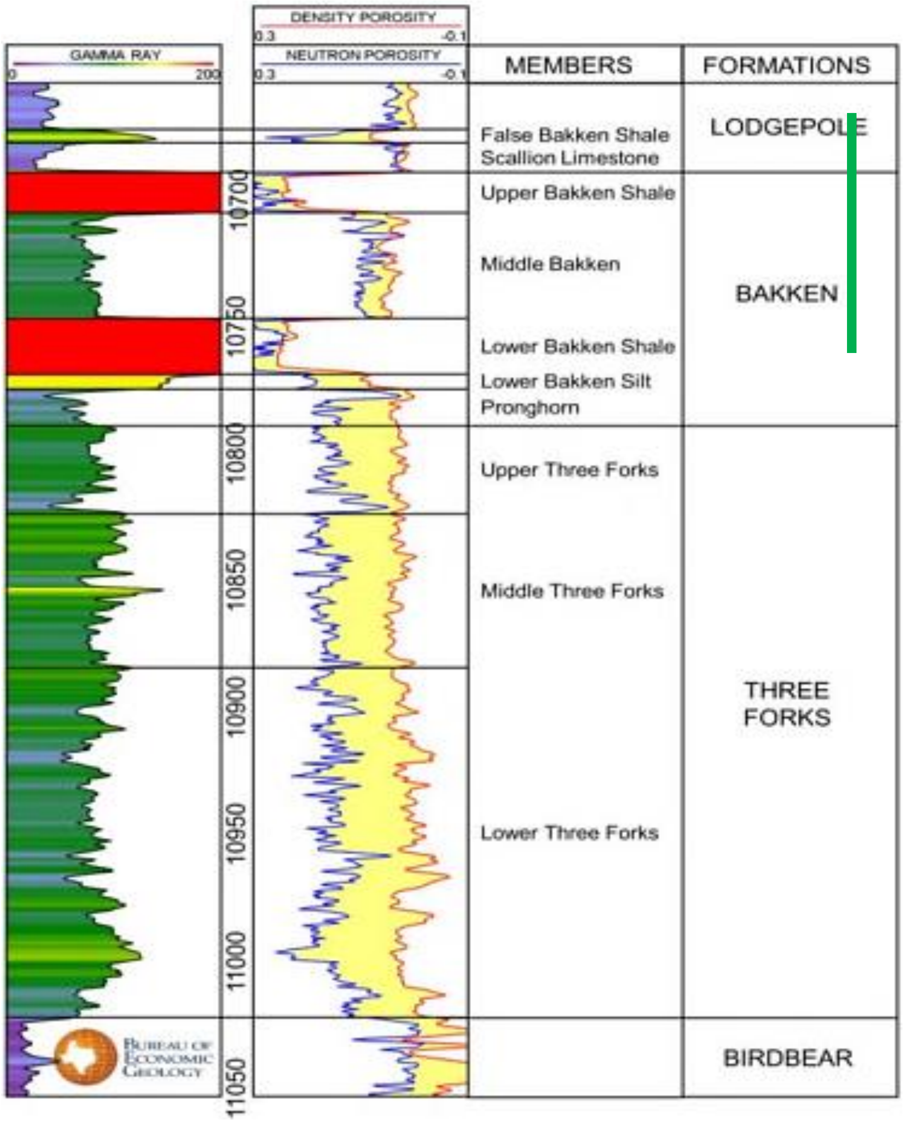

Figure 3.3. Petrological stratigraphy of the Bakken Petroleum System (green bar) noting typical gamma ray and porosity log responses with stratigraphic subdivisions.

Lower and Upper Bakken organic-rich shales cause high (off-scale) GR responses, which are shown in red. Well identification: XTO Energy, Jane Federal 11X-20, API 33-025-00794. From Hamlin, et al, 2017.

The Bakken petroleum system and adjacent formations are a part of Sloss' (1964) *Kaskaskia* North American sedimentary sequence (Figure 3.2). The basal Bakken rests unconformably upon the Three Forks Formation, apparently a result of the Antler/Acadian orogenies. However, for the remainder of the Bakken sequence, the formations are conformable.

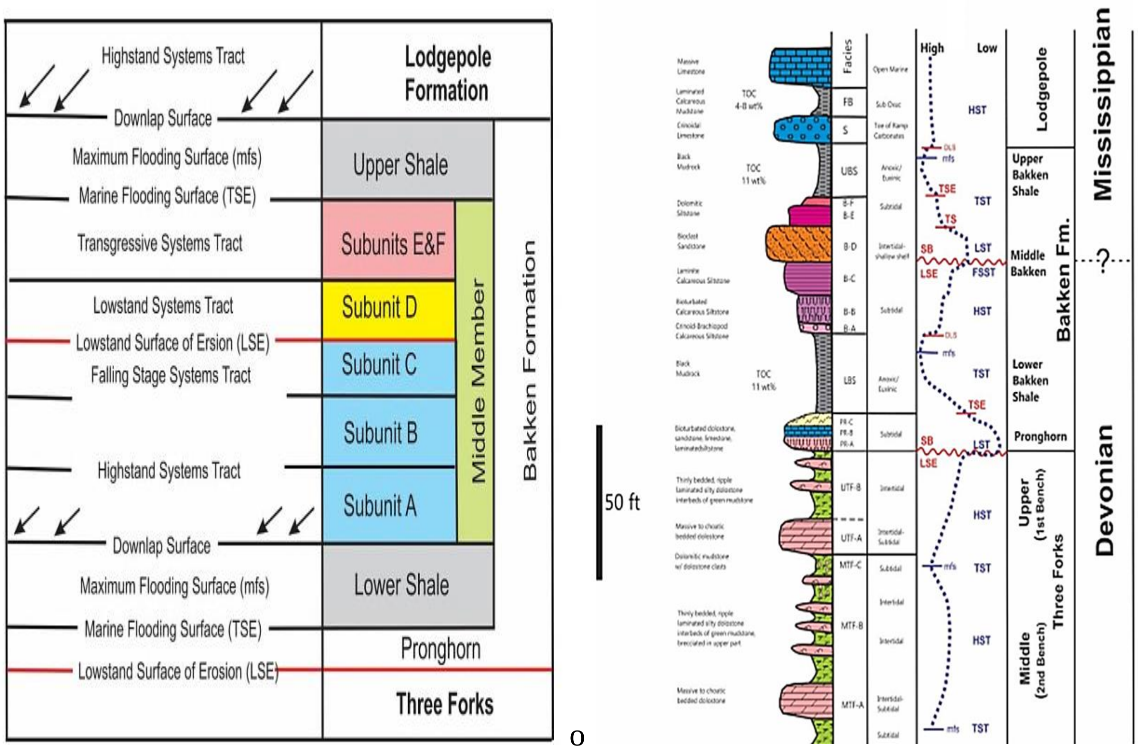

Figure 3.4. Sequence stratigraphy of the Bakken petroleum system. From Sonnenberg, 2017.

3.3 Sequence Stratigraphy

Beginning at the base of the Bakken Petroleum System, we first encounter the Upper Three Forks characterized by thinly-bedded, rippled and laminated silty dolostone and grey-green mudstone. The stratigraphic boundary between the Three Forks and the overlying Lower shale of the Bakken is a lowstand surface of erosion, the only unconformity noted in the Bakken petroleum system, as evidenced in the occasionally brecciated aspect of the uppermost Three Forks.

Proceeding upwards stratigraphically, some authors (Anna, et at, 2010, Sonnenberg, 2019; Theloy, 2014; etc.) make note of the lowermost Bakken unit, the Pronghorn. It is noted as being a unit comprised of bioturbated dolostones, sandstone, limestone and bioturbated siltstone. The top of this unit is a marine flooding surface, as evidenced by the voluminous bioturbation, which transitions to a maximum flooding surface, or deepest part of the depositional realm in the Bakken.

Here, the lower Bakken shale, a high-TOC (Total Organic Carbon) black shale was deposited, which is one of two major source rocks for the Bakken petroleum system. The next unit, the Middle Bakken, the reservoir member of the Bakken Petroleum System, consists of 5-6 subunits which through their bioturbated calcareous sandstones and siltstone record the drop from the lowermost subunit highstand systems tract through, stratigraphically upward, falling systems tracts to a lowstand of erosion near the middle of the Middle Bakken. The remainder of the Middle Bakken reservoir unit was deposited as dolomitic sandstones and siltstones of a deepening transgressive systems tract; bioturbated both top and bottom (Sesack, 2011).

From the Middle Bakken, the section transitions once again to the black high-TOC mudstones of the Upper Bakken. This is the second source rocks considered in the total Bakken Petroleum System. The end of Bakken deposition transitions from the maximum marine flooding surface of the Upper Bakken to a terminal downlap surface. This is transformed into a highstand systems tract and is represented by the crinoidal and massive limestones, as well as the intervening laminated calcareous mudstones of the overlying Lodgepole Formation. These mudstones of the Lodgepole can carry sufficient TOC to be source rocks, locally, for the Lodgepole Formation to be productive of oil and gas.

3.4 Depositional Environments

Beginning in the late Devonian Period, the Three Forks Formation was deposited in a relatively shallow, relatively warm, marine environment (Berwick and Hendricks, 2011). There is a widespread unconformity at the base of the Bakken and top of the Three Forks giving evidence to the basinwide regression at this time and the first-time continental deposition was noted in the Bakken petroleum system. A regional transgression occurred resulting in the deposition of the Bakken Formation from Late Devonian to Early Mississippian. Fossil assemblages indicate that this was in deep marine water with a stratified water column (LeFever, 1991).

The Bakken Shale indicates a transformation from highly oxidizing conditions during Three Forks time to highly anoxic conditions in lower Bakken time; an environment typified by a deep marine setting with a stratified water column. The anoxic conditions continued until middle Bakken as an influx of coarser clastics into the basin occurred. The middle reservoir facies of the Bakken have fauna and bedding features indicative of a normal shallow marine depositional environment.

This clastic middle member is usually interpreted as a significant drop in sea level associated with massive sediment influx. High-energy, highly oxygenated near-shore tidal basins and lower shoreface depositional regimes are represented in the middle member. The upper Bakken shale indicates a return to anoxic conditions, as noted by the presence of pyrite, high concentrations of organic matter derived from marine algae and bacteria, with few benthic fossils, followed by highly oxidizing water conditions once again during the Lodgepole time (Jin and Sonnenberg, 2013).

3.5 Source Rocks/Reservoir Rocks

The source rocks of the Bakken petroleum system are the Lower and Upper Bakken shales, which have exceptionally high organic matter content. The Middle Bakken is the primary reservoir unit. The laminated sandstone/siltstone zones of the Middle Bakken form the best reservoir facies in the Bakken petroleum system (Jin, et al, 2015).

The Upper Three Forks, which is a moderately important reservoir interval within the basin, is made up of silty to sandy dolostone and laminated green mudstone. In each case, the reservoirs are closely adjacent to source beds, and migration of oil has been minimal. The Lodgepole and Upper and Lower Bakken shales are rich in organic matter, but the reservoirs in each case possess low porosity and permeability. (Hamlin, et al 2017).

3.6 Diagenetic History

Sandstones and siltstones of the Bakken Petroleum system typically consists of fine-grained to very fine grained, matrix-rich rocks composed of quartz, minor feldspar, and variable rock fragments; the grain size varies wildly from very fine grained to into the medium sand range. Framework grains are well-rounded to rounded, however, in some samples, the finer grained material is subrounded to subangular. Generally, the sandstones are moderately well to well sorted but poorly sorted and poorly rounded. Frosting is noted in a small percentage of the grains (Alcoser, et al, 2012).

Given the history of transgressions and regressions withing the boundaries of the Williston Basin, there are sequences of diagenetic events seen in the rocks of the Bakken petroleum system. From youngest to oldest these are:

- mechanical and chemical compaction,
- calcite cementation,
- dolomitization,
- pyrite cementation,
- microcrystalline quartz cementation,
- syntaxial calcite overgrowth,
- quartz overgrowth,
- K-Feldspar overgrowth,
- dolomite dissolution,
- feldspar dissolution,
- dedolomitization,
- anhydrite cementation and
- hydrocarbon migration (after Ayhan, 2016).

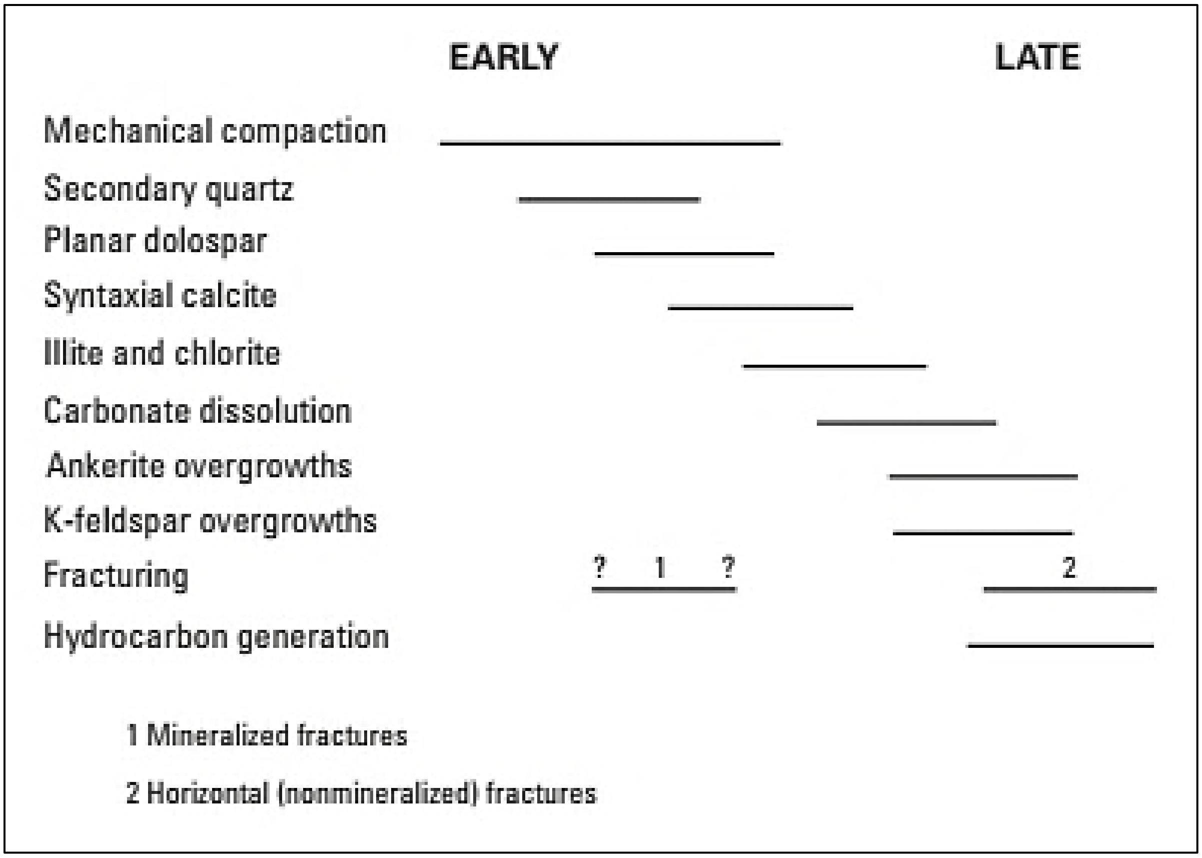

Figure 3.5. Chart noting post-depositional events observed in sandstones and siltstones of the Bakken Formation. After Pitman, 2001.

Diagenesis can be assigned as either early or late in the Bakken. Most early diagenetic events include physical compaction leading to late lithifications, deposition of secondary minerals such as quartz and dolostone, as well clay minerals such as illite and smectite (Mba, et al, 2010).

Later diagenetic events include dissolution of carbonates, Fe-rich carbonate and K-feldspar overgrowths, which continued until a perhaps a two-phase series of fracturing events yielded to hydrocarbon generation and migration. Oil migrating into the reservoir rock displaced residual water from the matrix pores and prevented further diagenetic alteration from taking place in the sandstones and siltstones (Butler, et al, 2019).

Most diagenetic events began soon after burial and ends when oil entered the reservoirs in the Late Cretaceous. It is noteworthy that there are no significant variations in authigenic mineral type related to changes in depositional facies across the basin. In addition, the paragenetic sequence remains relatively constant with no major changes in diagenesis relative to variations in thermal maturity or burial depth (Pitman, et al, 2001).

3.7 Oil and Gas Production

North Dakota is currently producing 1,113,000 BOPD and 2,750 MMCFGPD (August 2021). The Bakken is responsible for more than 92% of these volumes.

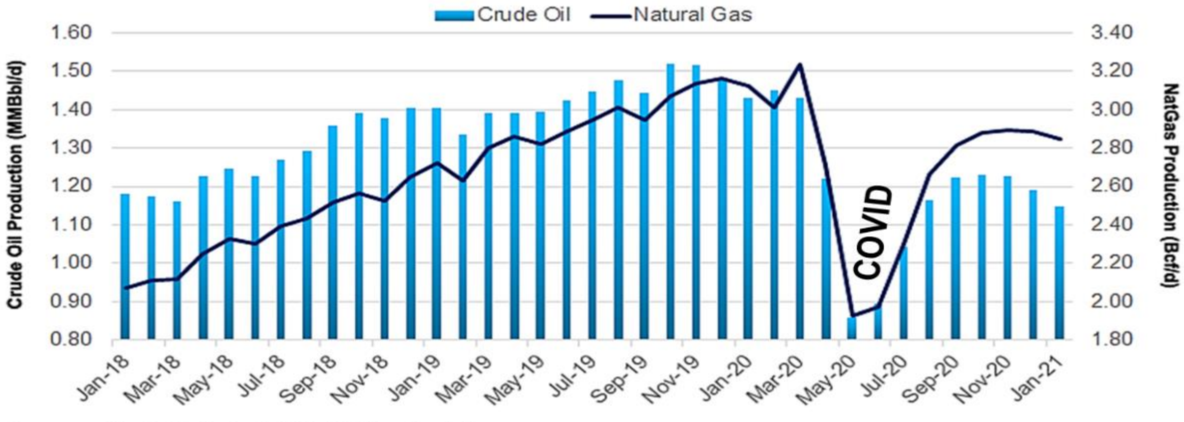

Source: North Dakota DMR. NGI calculations

Figure 3.6. Monthly North Dakota Crude Oil and Natural Gas Production. Source: North Dakota DMR, NGI Calculations.

CHAPTER 4

The Geology of Helium

4.1 The Discovery of Helium in Natural Gas

A unique incident occurred in Dexter, KS in May of 1903. That, in and of itself, was a newsworthy event (McCool, 1905). That it had to do with the budding oil and gas industry and would have global repercussions, made it even more newsworthy.

A gas well, drilled by the Gas Oil and Developing Company, became a "howling gasser" as it was described in the news of the day, when it blew in producing over 9 MMSCFG/D from 560' TD.

It seemed like "a bird's nest on the ground" quipped one Erasmus Cook of nearby Burden, KS (Anonymous, 1903).

There was much excitement in the town and people gathered, eager to see and hear the gas stream ignited, but the flame used to ignite the new-found gas discovery was quickly extinguished. A second try was made to ignite the gas; it too failed. People quickly lost interest in this gas well that produced so much gas that wouldn't burn (American Chemical Society National Historic Chemical Landmarks, 2000).

Interested, the Kansas state geologist Erasmus Haworth sampled the gas and sent it to David F. McFarland at the Chemistry Department of the University of Kansas. McFarland published the results of the analysis in 1903 (Haworth and McFarland, 1903) and of other natural gas accumulations from the Midwest in 1907 (Cady, and McFarland, 1907).

The non-flammable gas sampled at Dexter was mainly nitrogen (82.7 percent) with some methane present (16.85 percent). The third most abundant component was helium at 1.84 percent. Of the other wells tested only the nearby Greenwell well at Dexter was of similar composition with 1.64 percent helium (Cady and McFarland, 1907).

Commercial production of helium comes from natural gas, as extraction from the atmosphere is uneconomic. There are two basic types of commercial helium deposits: natural gas produced primarily for the hydrocarbon content, typically containing less than 3 percent helium; and gas with little or no hydrocarbons, produced solely for the helium, which typically makes up between 5 and 10 percent helium. Natural gas where helium is only a secondary by-product which contains a lower percentage of helium, has historically and ironically, supplied the most helium (Gluyas, 2020).

4.2 Geospatial Diversity of Helium

Most geologists know that the majority of helium in natural gas derives from radioactive decay of uranium and thorium, either from radioactive black shales, or granitoid igneous and metamorphic basement rock. Granite and related rocks tend to contain more uranium and thorium than other rock types. However, some contend that the helium is largely primordial, emanating from primary mantle exhalations (Bräuer, *et al*, 2016).

Unusual geological conditions are typically necessary for the development of commercial concentrations of helium in natural gas. A direct correlation between the exploration solely for natural gas does not always align with exploration for highly mobile gases such as helium (Energy Weekly News, 2018).

Helium accumulations are occasionally found in structural closures overlying bedrock highs, much the same as for natural gas. Faults, fractures, and igneous intrusives are regarded by some workers as important pathways for helium to migrate upward into the overlying sedimentary section (Grall, *et al*, 2018). In deep-seated Meso- and Neoproterozoic sections, this is not so much the case.

There must be some sort of impermeable regional seal, particularly if the closure areas are highly compartmentalized. Nonporous caprock such as halite, anhydrite or bedded, cyclic evaporites are more effective in trapping helium and preventing further upward migration (Grunau, 1981). This is the typical situation for the large Meso- to Neoproterozoic accumulations in Eastern Siberia, China, Oman, and Australia.

The atomic radius of helium is so small, about ½ the size of a typical methane (CH_4) molecule, that shale, which is effective in trapping methane, *might* allow the helium to migrate upward through the shale pores. That is, if those pores are not previously occupied by oil, gas or water; and the permeability of the rocks are measured in nanodarcies. This is the presumed genesis of helium deposits which occur mostly in Paleozoic rocks (Pathak, 2018).

High helium content of natural gas is often accompanied by high contents of nitrogen and carbon dioxide; though rarely with hydrogen sulfide (H_2S). The percentage of nitrogen is usually 10 to 20 times that of helium, so that natural gas with 5 percent or more helium may have little to no methane (Broadhead, 2018).

A representative sample coming from the Shittim #1 well in Tasmania, for instance, has 4.8 percent helium, 80.6 percent nitrogen, 0.7 percent carbon dioxide, but only 10 percent methane (Bacon, *et al*, 1996). In such cases, the gas is produced solely for its helium content (Burrett, 1997).

In other wells, such as some in Indonesia, the CO_2 gas content may reach up to 70% from the total gas composition in some fields. This has become a serious threat for an economic development of the CO_2 gas field (Lahuri, *et al*, 2018). Such a volume of CO_2, which needs to be handled closed-loop to prevent atmospheric venting hinders the concentration of the CH_4 and He in the LNG (Liquid Natural Gas) extraction and concentration process (Price and Mahaley, 2013).

Similar wells in the Middle East, and the Russian Far East, with high N_2, CO_2 and moderate H_2S contents, as well as marginally economical helium concentrations (Xu, *et al*, 2019) are doubly vexed. Apart from having to remove the nitrogen and carbon dioxide via a closed loop system, the hydrogen sulfide, a pernicious and deadly gas, must also be removed before liquification of the remaining methane and helium can commence (Lang, *et al*, 2017). These wells must be monitored continually as they walk that very fine line between profitability and loss (Daly, 2005).

Most of the helium that is removed from natural gas is thought to form from radioactive decay of uranium and thorium in granitoid rocks of Earth's continental crust (Keller, and Rowe, 2017). As a very light gas, it is buoyant and seeks to move upward as soon as it forms.

The richest helium accumulations are found where three conditions exist:

1. granitoid basement rocks are rich in uranium and thorium;
2. the basement rocks are fractured and faulted to provide escape paths for the helium; and,
3. porous sedimentary rocks above the basement faults are capped by an impermeable seal of halite, anhydrite, or tight shale (Speight, 2018).

When all three of these conditions are met, helium might accumulate in porous sedimentary rock layer (Sears, 2015) below an interregional seal.

Helium has the smallest atomic radius of any element, about 0.2 nanometers. So, when it forms and starts moving upward, it can fit through very small pore spaces within the rocks (Cecconi, and Easow, 2017).

Halite and anhydrite are seemingly the only sedimentary rocks that can block the upward migration of helium atoms (King, 2016). Shales that have their pore spaces plugged with abundant organic materials (kerogen), or gas or water sometimes serve as an effective barrier and form helium-rich reservoirs.

Helium-bearing natural gas deposits of the United States (Figure 4.1):

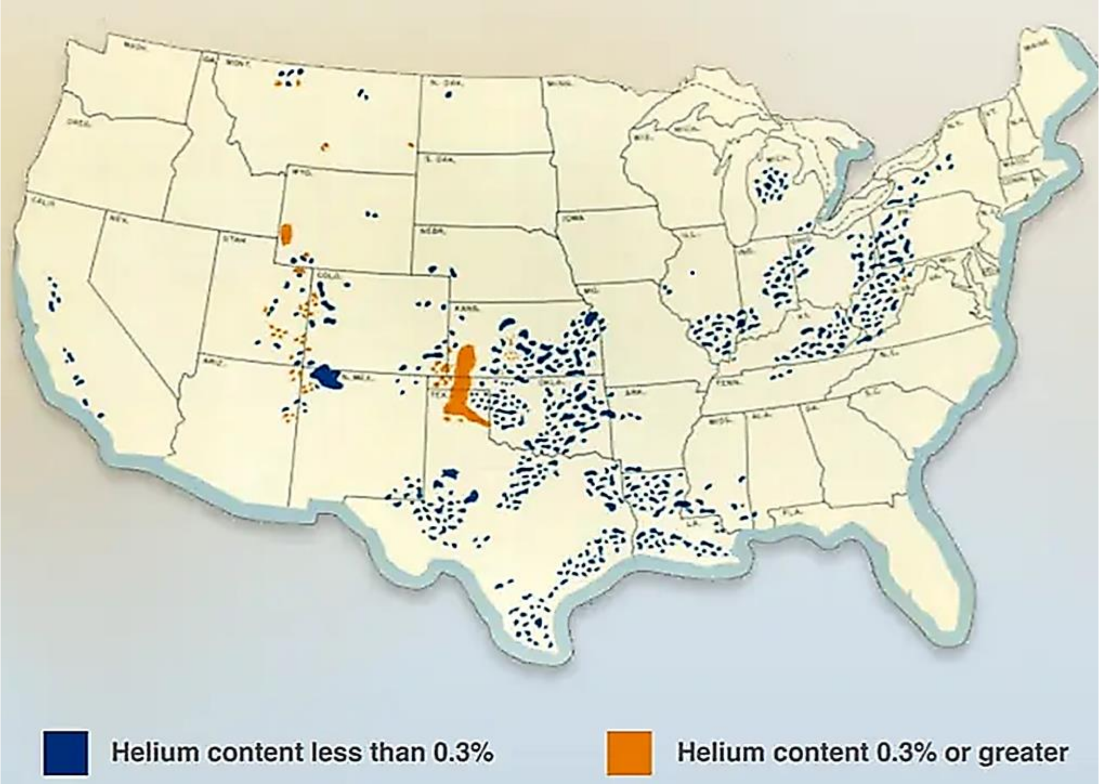

Figure 4.1. A map of major gas fields in the U.S. showing those that contain an economically viable concentration of helium and those that do not. Image source: American Physical Society, Materials Research Society, American Chemical Society

The natural gas produced from these fields contains between 0.3% to over 7% helium. The majority of natural gas fields in the US and internationally usually possess a helium concentration of less than 0.02%. Some regions, like the Holbrook Basin of the US and Officer-Otway Basin of Australia report helium volumes exceeding 10%vol.

4.3 Global Occurrence of Helium

The United States continues to lead the world in helium production (Figure 4.2 and Table 4.1)

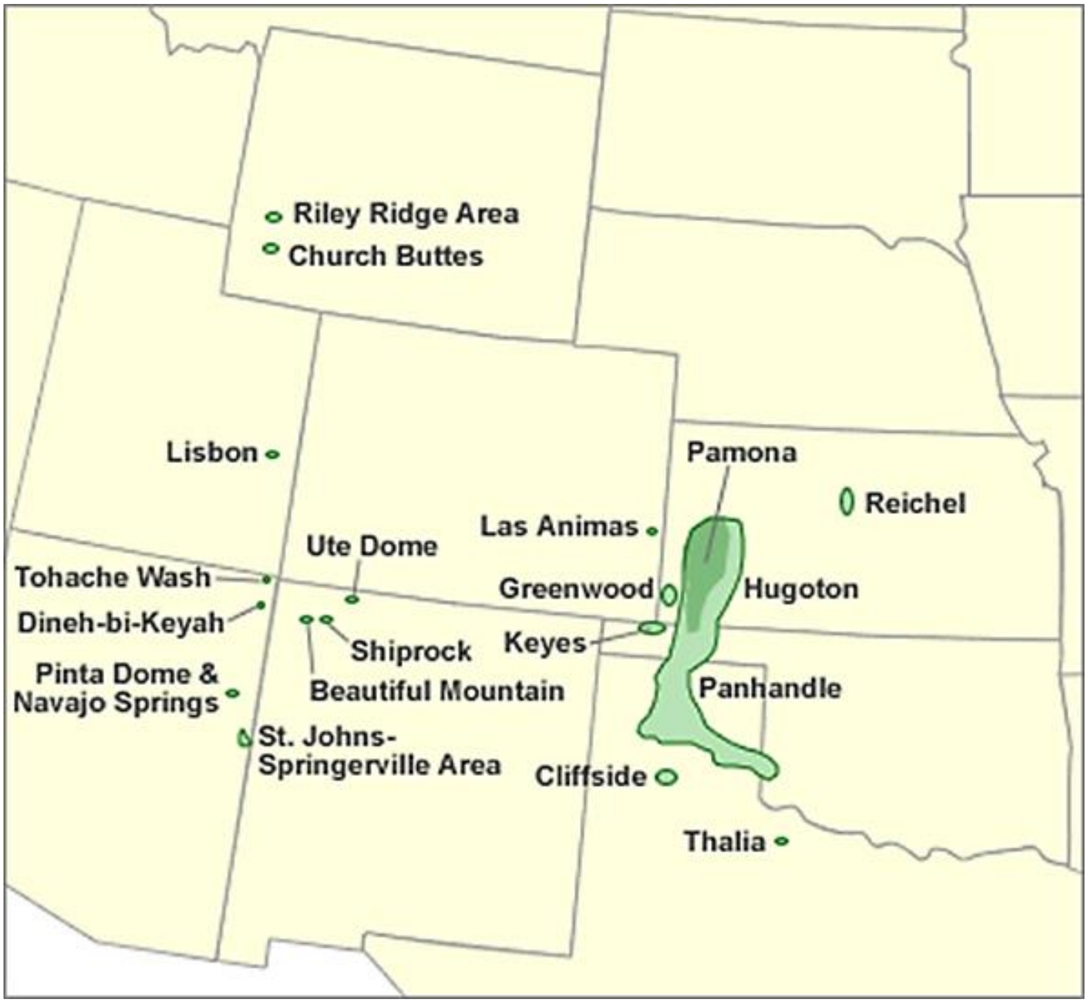

Figure 4.2. Location of major helium-rich gas fields in the United States. Image by Geology.com.

Table 4.1. Age, reservoir and helium concentration, helium-rich gas fields in the United States. From Ward and Pierce, 1973.

State	Field	Formation	Age	Percent Helium
Arizona	Dineh-bi-Keyah	McKracken Sandstone	Pennsylvanian, Devonian	4.8-5.6
Arizona	Pinta Dome	Coconino Sandstone	Permian	5.6-9.8
Colorado	Model Dome	Lyons Sandstone	Permian	6.7-8.3
Kansas	Greenwood	Topeka Limestone, Kansas City Group	Pennsylvanian	0.4-0.7
Kansas	Otis-Albert	Reagan Sandstone	Cambrian	1.2-2.3
Kansas	Ryersee	Chase group	Permian	1.0-1.9
Kansas, Oklahoma, Texas	Hugoton	Various	Permian	3.0-1.9
New Mexico	Hogback	Hermosa Formation	Pennsylvanian	1.4-8.0
New Mexico	Rattlesnake	Leadville/Ouray Limestone	Mississippian/Devonian	7.5-8.0
Oklahoma	Keyes	Morrow (Keyes) Sandstone	Pennsylvanian	0.3-2.7
Texas	Cliffside	Various	Permian	1.7-1.8
Texas	Panhandle	Various	Permian	0.1-2.20
Texas	Petrolia	Cisco Sandstone	Pennsylvanian	0.65-1.14
Utah	Harley Dome	Entrada Sandstone	Jurassic	7
Wyoming	Riley Ridge	Madison Limestone	Mississippian	5.5-9.1

As of December 31, 2006, the total helium reserves and resources of the United States were estimated to be 20.6 billion cubic meters (744 billion cubic feet). This includes 4.25 billion cubic meters (153 billion cubic feet) of measured reserves, 5.33 billion cubic meters (192 billion cubic feet) of probable resources, 5.93 billion cubic meters (214 billion cubic feet) of possible resources, and 5.11 billion cubic meters (184 billion cubic feet) of speculative resources. Measured reserves include 670 million cubic meters (24.2 billion cubic feet) of helium stored in the Cliffside Field Government Reserve and 65 million cubic meters (2.3 billion cubic feet) of helium contained in Cliffside Field native gas (Anderson, 2018).

The Cliffside (Texas), Hugoton (Kansas, Oklahoma, and Texas), Panhandle West (Texas), Panoma (Kansas), and Tip Top Field of Sublette County and Riley Ridge (Wyoming) Fields are the depleting fields from which most U.S.-produced helium is extracted. These fields contained an estimated 3.9 billion cubic meters (140 billion cubic feet) of helium (USGS, 2021).

The United States represents 21 percent of the world's known helium reserves. It produces 71 percent of the world's helium and is the single largest consumer of helium. Helium resources of the world, exclusive of the United States, were estimated to be about 31.3 billion cubic meters (USGS, 2021) (Figure 4.3).

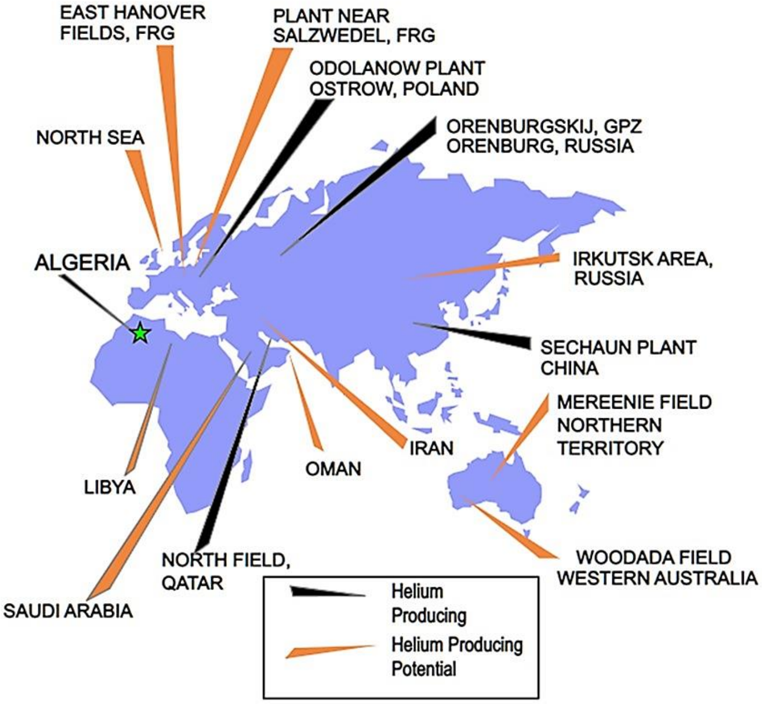

Figure 4.3. Producing and potential helium field areas, exclusive of the Americas. From Air Liquide.

Helium resources of the world, exclusive of the United States, were estimated to be about 31.3 billion cubic meters (1.13 trillion cubic feet). The locations and volumes of the major deposits, in billion cubic meters, are Qatar, 10.1; Algeria, 8.2; Russia, 6.8; Canada, 2.0; and China, 1.1.

Helium produced in Algeria, Poland and Russia is sold almost exclusively into European markets, and helium produced in Qatar is sold exclusively into Asian markets. These countries combined own 79 percent of the worldwide helium reserves yet produce only 29 percent of the world's helium (Sönnichsen, 2021).

4.4 Geological Sources of Helium

4.4.1 Helium Accumulation in Precambrian (Neoproterozoic) Sequences

Helium has been noted to exist in virtually all natural gas accumulations and in economic quantities in numerous diverse geological settings (Handley, and Miller, 1992).

The accumulations that produce economic quantities of helium can be broken down into three categories:

1. Mesoproterozoic to Neoproterozoic sourced gas fields under thick, regional evaporitic seals:
    a. Eastern Siberian Platform
    b. Sichuan Basin, China
    c. South Oman Salt Basin, Sultanate of Oman,
    d. Amadeus Basin, Centralia Superbasin, Australia.

2. Thick Paleozoic euxinic black shales or stable platformal build-ups of cyclic carbonate-evaporite series:
    a. Khuff Group, North Field uplift, offshore Qatar,
    b. genet

3. Paleozoic deep-marine anoxic black shales, typically thick with mixed clastics and carbonate zones, as well as local radioactive ‘hot’ shales:
    a. Black River and Trenton, Michigan Basin, and
    b. Bakken, Manitoba and Saskatchewan, Canada

Infracambrian sedimentary basins are a major source of hydrocarbons and helium in many parts of the world, including Russia, China, Oman and Australia; to name but a few. While some of this helium has an ultimate mantle source, much of the helium in sedimentary basins is purportedly derived from radioactive decay of uranium and thorium from intrusive Hadean-Archean basement igneous and metamorphic rocks, from the reservoir formations themselves, or primary mantle exhalations (Buttitta, et al, 2020).

4.4.1.1 *Helium accumulation in Eastern Siberia, Russia (4)*

Perhaps the best known and certainly the world’s largest accumulations are helium sourced from Meso-Neoproterozoic, or earlier, rocks, trapped by Infracambrian-Cambrian regional seals. This is where the gas migrates in much the ssame way as hydrocarbons, only to be trapped beneath thick, impermeable strata.

Prominent among these types of helium accumulations sealed by a regional Vendian-Cambrian (“Infracambrian”) Usolian evaporite sequence, as in Eastern Siberia at Yurubchen-

Tokohomo Field Complex (Rapatskaya, et al, 2020) (Figure 4.4). This field is also the world's record holder for oldest source rocks (1.60-1.11 BYA: Riphean) that support an economic field.

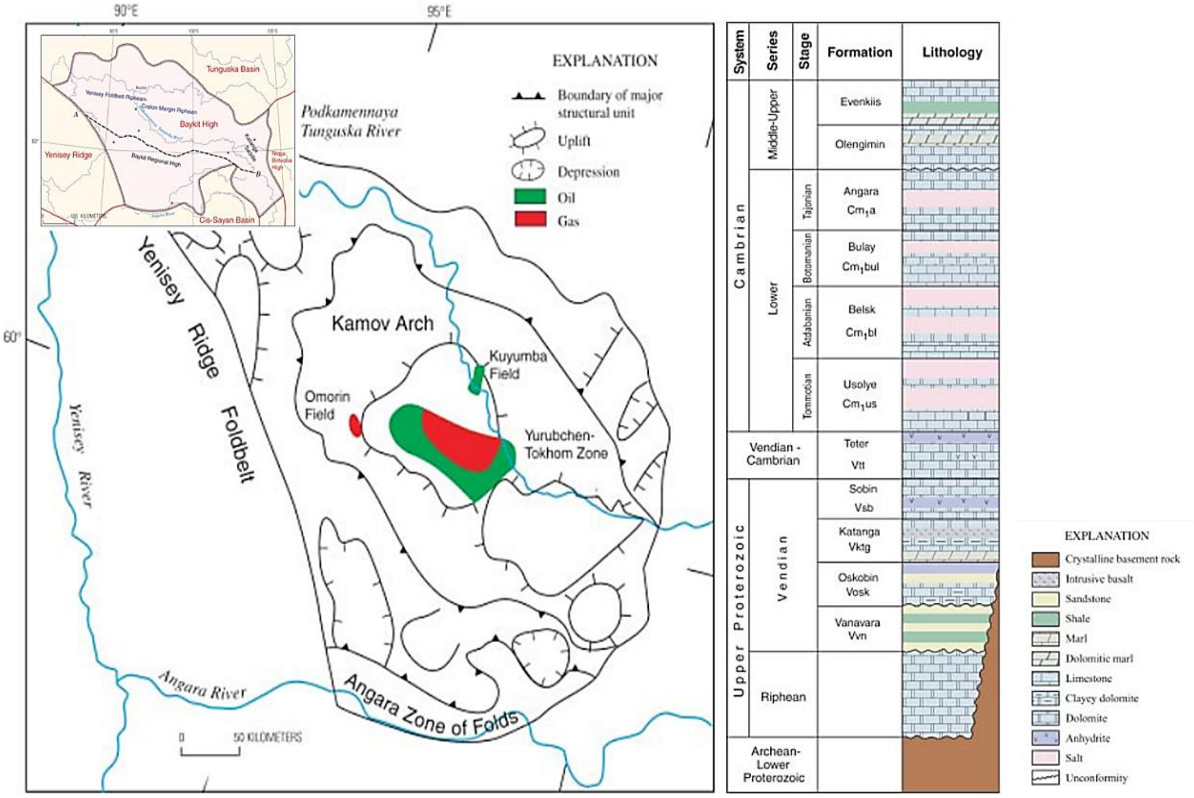

Figure 4.4. Location map of the Baykit regional high, home to the Yurubchen-Tokhomo Field Complex (left), and the stratigraphic column of the Meso-Neoproterozoic Riphean-Vendian-Cambrian sequence of the fields. Adapted from Ulmishek, 2001.

The composition of the Cambrian *Usolie* Formation, its near zero horizontal or vertical permeability, and its screening properties allows it to serve as a most reliable impervious seal that ensures the retention of helium reserves. Rock salt (massive halite) is characterized by low-to-zero porosity, plasticity, high density, low hydraulic conductivity, as well as by very low helium diffusivity (Rapatskaya, et al, 2020).

In far Eastern Siberia, on the Lena-Angara Step, the gas from the mixed carbonate and clastic reservoirs of Kovykta Field contains 0.26-0.66% helium (Howard, *et al*, 2012), which is reckoned as 37–42% of Russia’s total helium reserves, (Poussenkova, 2007) Figure 4.5.

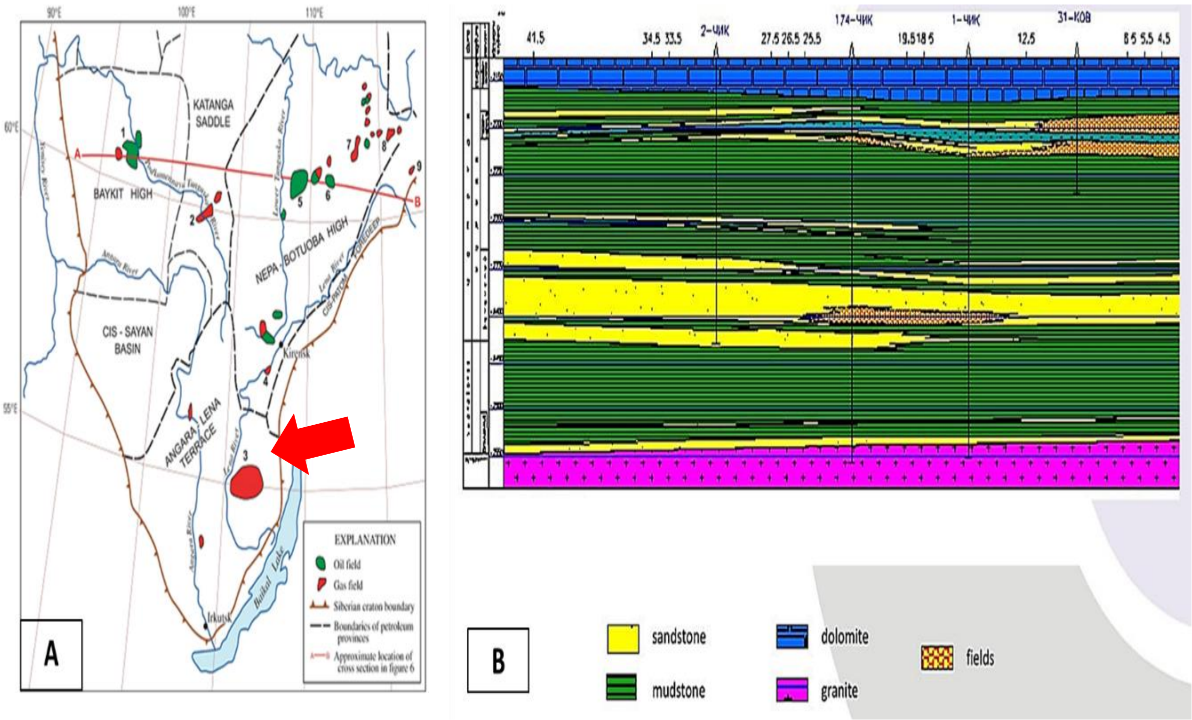

Figure 4.5. A. Oil and gas of the Southern Siberian craton, Field 3 (red arrow) = Kovykta Gas Field. From Ulmishek, 2001. B. Geological cross-section of Kovykta Field from basement through Neoproterozoic to Paleozoic. From Trudy Sibirskogo NauchnoIssledovatelskogo Instituta, Geologii, Geofiziki i Mineralnogo Sirya (SNIGGIMS) (Siberian Scientific Research Institute for Geology, Geophysics and Mineral Resources).

Principal reserves of the field are in Vendian clastic reservoirs of the lower Mota Formation and its stratigraphic equivalents (commonly called the ‘Nepa-Tira sequence’). Anhydritic sections of the Vendian Chora Formation form the regional seal draped over fault-block and anticlinal traps. Gas of the Kovykta field contains more methane (91–93 percent), less heavy hydrocarbon gases (3.5–4.5 percent ethane, butane, propane, etc.), and a higher relative concentration of helium (0.36–0.66 percent) (Moiseev, *et al*, 2007).

4.4.1.2 *Helium accumulation in Weiyuan Field, Sichuan Basin, China*

The Weiyuan gas field lies to the south of Chengdu, the capital of Sichuan Province in southwestern China (Figure 4.6).

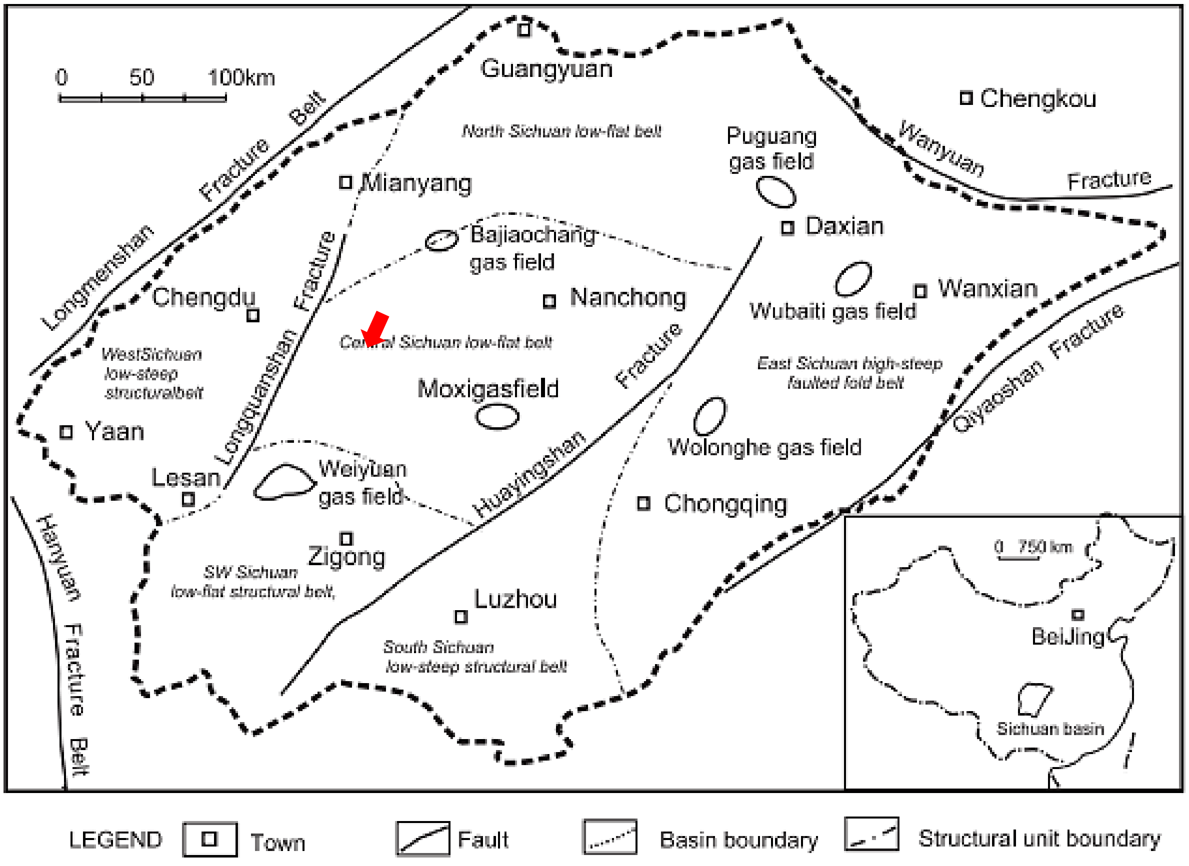

Figure 4.6. Location of Weiyuan Field, Sichuan Basin, China (red arrow). From Wei, et al, 2008.

The Weiyuan structure is a large domal feature located on the Weiyuan-Longnusi anticlinal belt (Figure 4.6).

Sichuan Basin, Weiyuan Field, central China, (Montages 1 & 1A)

Weiyuan, the oldest gas field in China, is a rare Oriental example of a giant Neoproterozoic gas field. It is located in southwestern Sichuan Basin, a large (180,000 km^2) intermontane basin in southwestern China. In August 1965, a daily gas flow of 741,000m^3

was obtained from the production test in the Wei-2 field discovery well, confirming the Sinian Dengying gas pools. Thus far, 107 wells have been drilled to the Neoproterozoic Sinian strata in the Weiyuan gas field.

The Weiyuan gas field, as noted, is the earliest discovered giant gas field in China. It was developed on the Leshan-Longnvsi Paleozoic paleo-high, with gases being derived from the Lower Cambrian Jiulaodong Formation and trapped in the Sinian Dengying Formation (Bao, 1988; Xu et al., 1989).

About 670m of Upper Sinian rocks were deposited as the Doushantuo and Dengying formations. The Doushantuo Formation is composed of 11–16m of supratidal anhydrite-bearing dolomite, sandstone and variegated mudstones. The Dengying Formation, 648–654m in thickness, forms the main reservoir in the Weiyuan field.

About 900m of Cambrian rocks were deposited, which can be divided into three formations. The Lower Cambrian Jiulaodong Formation contains 500m of open marine mudstones and shales. The top part is mainly composed of fine sandstones and siltstones intercalated with shales, while the middle-lower parts are mainly black shales. The black shales account for two-thirds of the sedimentary column, thus forming both the source rock and caprock for gas pools in the Sinian Dengying Formation. The field has proven in place gas reserve of 40 billion cubic meters (bcm) or 1.41 trillion cubic feet (tcf) in reservoirs of the Dengying.

Sichuan Basin, Weiyuan Field, central China, (Montage 1)

Country: China
Geological region: Sichuan Basin
Field(s): Weiyuan
Reservoir age(s): Sinian (Neoproterozoic)
Gas/Helium EUR: 1412 BCF/79 BCF

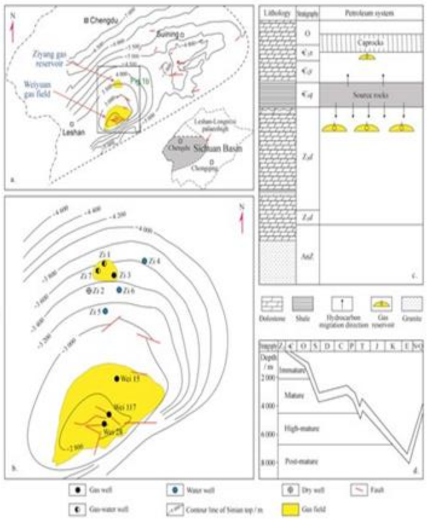

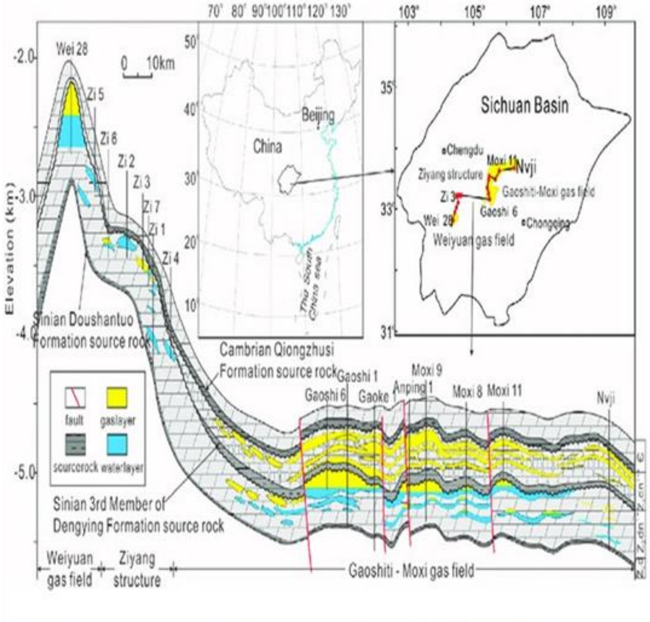

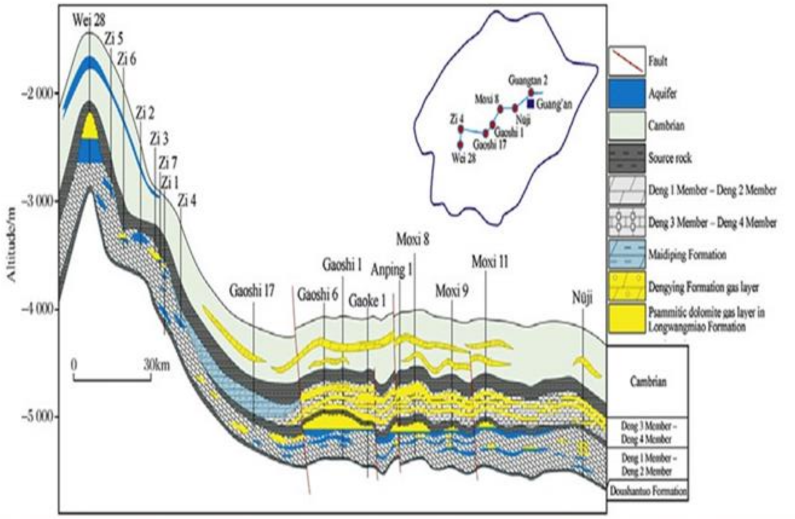

Country	Region	Field	N2%	CO2%	He%	CH4%	N2/He	Reservoir age	Average depth ft. (m)	Reservoir thickness ft. (m)	Reservoir area mi^2 (km^2)	Porosity (%)	Sw (%)	Permeability (mD)	Age of pore water	Gas, recoverable BCFG (BCM)	Helium BCFG (BCM)	Economic or non-economic?
China	Sichuan Basin	Weiyuan	10.00	4.30	0.21	83.00	47.62	Sinian - Dengying	9580 (2921)	295 (90)	100 (261)	Low: 3, High: 14	39.00	80-240	Sinian	1412 (73.72)	79 (4)	Economic

Sichuan Basin, Weiyuan Field, central China, (Montage 1A)

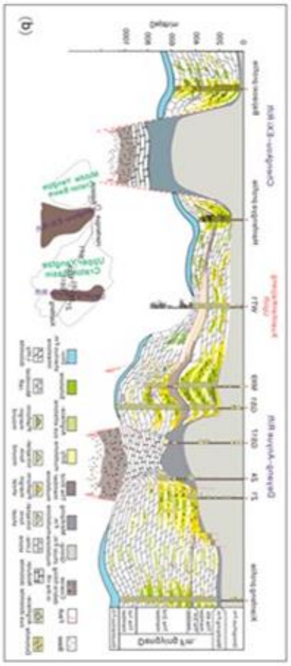

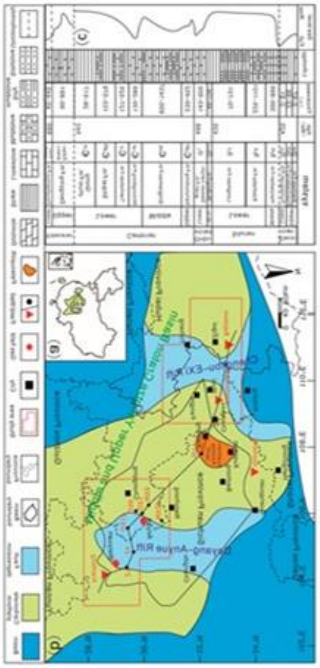

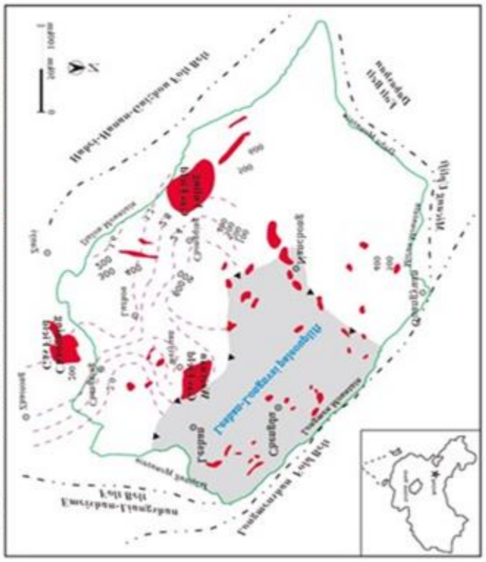

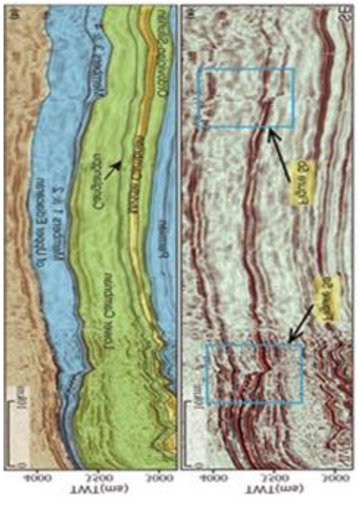

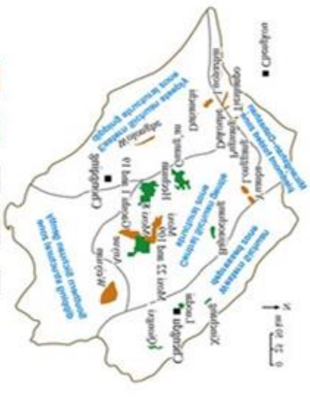

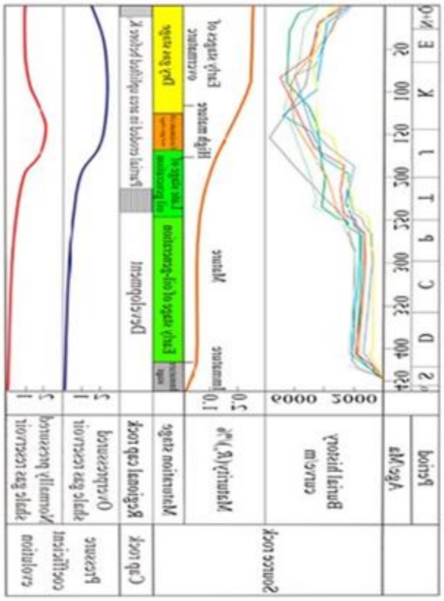

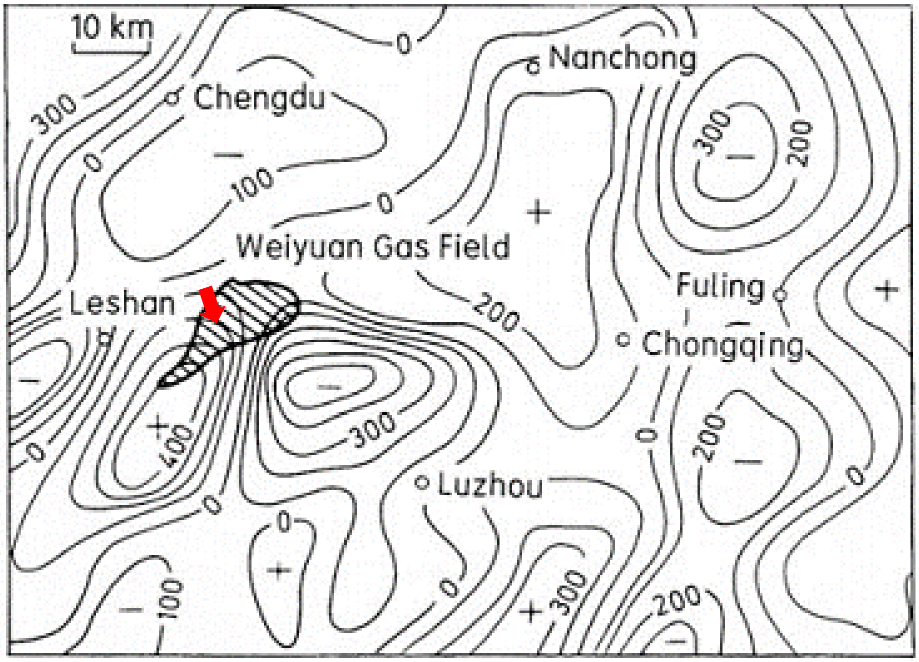

Figure 4.7. Structure contour map on the top of the Lower Sinian (Precambrian) System in the Sichuan Basin. Weiyuan Fields at red arrow. C.I. = 100m. From Yongchang, et al, 1992.

The main reservoir horizon in the Weiyuan gas field occurs within the 650-m-thick, Late Sinian dolomites which unconformably overlie the Early Sinian Emei Mountain granite. The upper part of the Sinian Series has been subdivided into four units. The basal unit (ZI) of dolomitic siltstone (11-14 m) is called the Labagang Group. The overlying units (Z2 to Z4) comprise the Dengying Group which consists mostly of laminated dolostone containing a large variety of fossil cyanobacteria and algae (Cao and Yaosong, 1983).

The Dengying Group forms the main hydrocarbon reservoir (Figure 4.8, A and B).

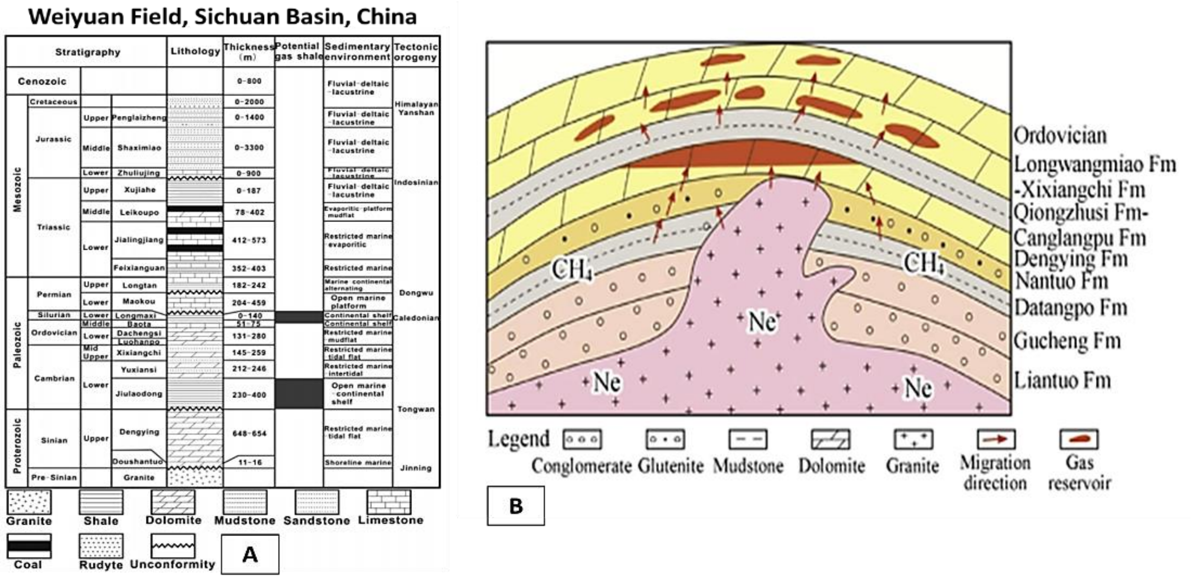

Figure 4.8. (A) Schematic diagram showing the stratigraphy of the Weiyuan Field area, sedimentary environments and tectonic events. After Zhou, et al, 2014. (B) Accumulation model of the gas reservoirs with high helium content in the Weiyuan Field area. After Zhang, et al, 2015.

Porosity is vuggy and interconnected by fracture systems. The seal to this gas reservoir is provided by Early Cambrian mudrocks (Yongchang, *et al*, 1992).

In the Sichuan Basin, data shows that the basement consists of a set of igneous rocks and metamorphic rocks several thousands to ten thousand meters thick, including crystalline basement and sedimentary basement. Archean-Early Proterozoic Kangding Group acts as deep crystalline basement through Zhongtiao Movement (1700 - 1900 Ma); Middle Proterozoic-Late Proterozoic Ebian Group-Banxi Group acts as basin folded basement through Jinning Movement (780 - 1700 Ma), which is mainly composed of sedimentary rocks, which, in some areas, has transited into epi-metamorphic rocks due to the metamorphism and metasomatism of late stage orogenesis (Zhang, *et al*, 2015).

It is thought by Chinese geologists that the hydrocarbon gas in the natural gas of this area is dominantly sourced from the argillaceous source rocks of Presinian, Sinian and

Cambrian. The helium in the natural gas would then be dominantly sourced from the helium released from Uranium and Thorium decay in intrusive granite (Huquan, *et al*, 2005). Therefore, intrusive granite in Presinian is the “helium source rock”.

When helium generated by “helium source rock” and the hydrocarbon gas generated by normal organic source rocks enter Sinian, Cambrian and Ordovician reservoirs at the same time, high-helium gas reservoirs would come into being.

4.4.1.3 *Helium accumulations in South Oman Salt Basin*

Helium was discovered in the *Greater Birba* area at Budour NE Field within the ‘Carbonate Stringer’ section of the Ara Carbonates (Infracambrian) A4C unit in the South Oman Salt Basin of the Sultanate of Oman (Figure 4.9) in 2010.

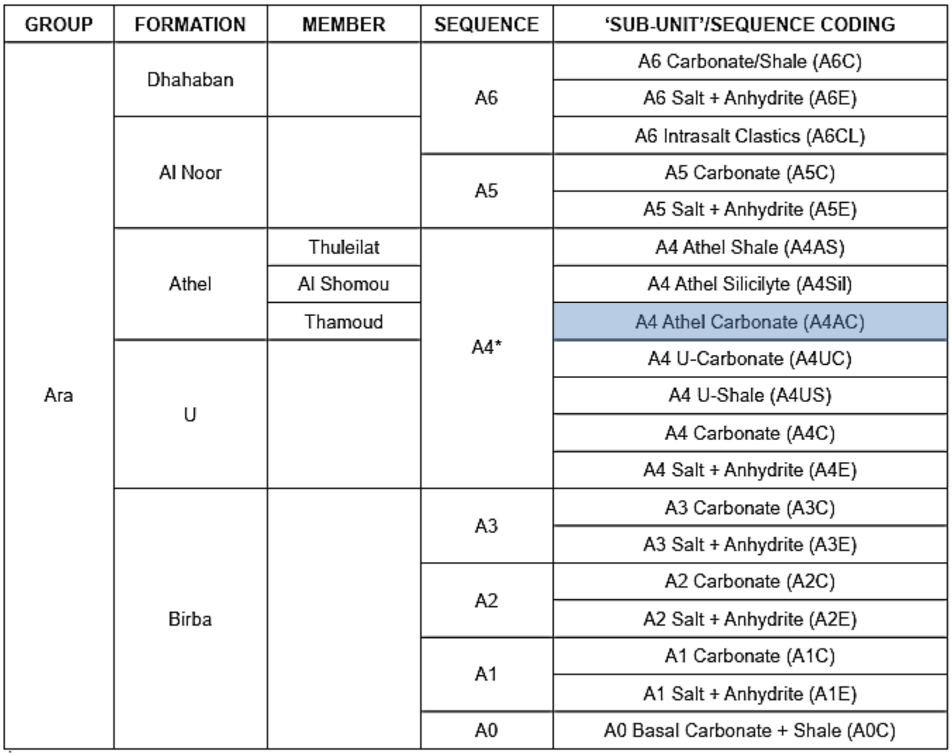

GROUP	FORMATION	MEMBER	SEQUENCE	‘SUB-UNIT’/SEQUENCE CODING
Ara	Dhahaban		A6	A6 Carbonate/Shale (A6C)
				A6 Salt + Anhydrite (A6E)
	Al Noor			A6 Intrasalt Clastics (A6CL)
			A5	A5 Carbonate (A5C)
				A5 Salt + Anhydrite (A5E)
	Athel	Thuleilat	A4*	A4 Athel Shale (A4AS)
		Al Shomou		A4 Athel Silicilyte (A4Sil)
		Thamoud		A4 Athel Carbonate (A4AC)
	U			A4 U-Carbonate (A4UC)
				A4 U-Shale (A4US)
				A4 Carbonate (A4C)
				A4 Salt + Anhydrite (A4E)
	Birba		A3	A3 Carbonate (A3C)
				A3 Salt + Anhydrite (A3E)
			A2	A2 Carbonate (A2C)
				A2 Salt + Anhydrite (A2E)
			A1	A1 Carbonate (A1C)
				A1 Salt + Anhydrite (A1E)
			A0	A0 Basal Carbonate + Shale (A0C)

Figure 4.9. Ara Group stratigraphy in the South Oman Salt Basin of the Sultanate of Oman, after Hughes Clarke, 1988. Ediacaran-Cambrian boundary of $541^{\pm}$ MYA found at top of A4C Carbonate (blue box).

Oil was first discovered in the Greater Birba area of the South Oman Salt Basin by the well Nassir-l, which was drilled in 1976 to test a presumed pre-salt carbonate build up in the Buah (middle Huqf platformal carbonate of Neoproterozoic age) (Figure 4.10) (Bowring, *et al*, 2007).

This then proved to be a 74m thick dolomite ‘stringer’ or ‘carbonate slab’, which tested ~960 m^3/d of 23 API gravity oil. Based on seismic interpretation, several stringers were recognized over an area in excess of 300 km^2.

Budour and Budour NE., Harweel Area, South Oman Salt Basin, the Sultanate of Oman (Montages 2 & 2A)

Intrasalt carbonate slabs of the Ediacaran–Cambrian Ara Group comprise a substantial reservoir element of the intrasalt “carbonate stringer” play in Oman, in which slabs of dolomitic carbonates are encased in salt at depths of 3 to 7 km (1.9 to 4.3 mi). These reservoirs are typically over-pressured, encased in and sealed effectively by thick Ara evaporites and contain sour oil and gas. They are effectively self-sourced. They have been a focus for exploration since the late 1950s. The discovery in 1976 of commercial oil in these “stringers” opened up the Ara play. Budour and Budour NE. fields, discovered in 2005, were the first to be tested and where it was conclusively proven that economic quantities of helium exist within these unusual reservoirs.

Since these carbonate slabs commonly contain intervals rich in organic matter, stringers may form a self-charging petroleum system encased in salt, and such reservoirs can yield more than 6,000 b/d of oil in production tests, particularly as the reservoirs are highly overpressured Grotzinger, and Al-Rawahi, 2014).

The Ara Carbonate Stringer play is unusual, although valuable, due to its ubiquitous hydrocarbon charge from mature high-quality (Type I/II) source rocks within the carbonate ‘stringers’, and the excellent sealing properties of the thick Ara salts that encase the ‘stringer’ carbonates, with hydrocarbon bearing reservoirs being typically highly overpressured.

Reserves for the Budour area are carried as 952 BCFG and 20.3 BCF helium. However, even with the apparent scarcity of helium in international markets and the price commanded by the gas, the Sultanate has done nothing to capture this resource. It is rather preferred to flare or vent the gas rather than reap the today ~US$400/MCF price.

Budour and Budour NE., Harweel Area, South Oman Salt Basin, the Sultanate of Oman (Montage 2)

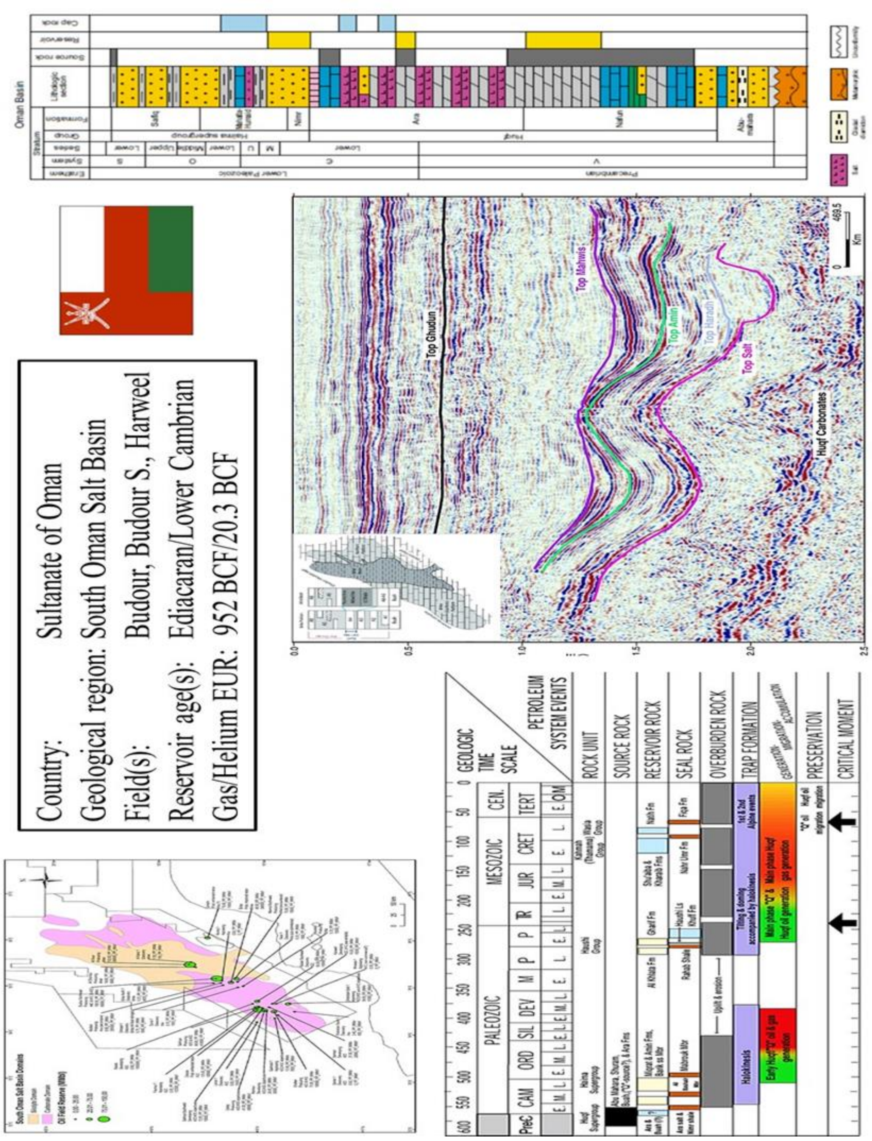

Country: Sultanate of Oman
Geological region: South Oman Salt Basin
Field(s): Budour, Budour S., Harweel
Reservoir age(s): Ediacaran/Lower Cambrian
Gas/Helium EUR: 952 BCF/20.3 BCF

Country	Region	Field	N_2%	CO_2%	He%	CH_4%	N_2/He	Reservoir age	Average depth ft. (m)	Reservoir thickness ft. (m)	Reservoir area mi^2 (km^2)	Porosity (%)	Sw (%)	Permeability (mD)	Age of pore water	Well type	Cost (US$)	Gas, recoverable BCFG (BCM)	Helium BCFG (BCM)	Economic or non-economic?
Oman	SOSB - Budour	Budour 2-A	1.00	3.72	0.39	81.00	2.56	PC/C - Ara Carbonates - A4C	1.9 to 4.3 mi (3-7 km)	262 (80)	90 (233)	Low: 2, High: 8	22.00	<120	530 +/- 2.5 MYA. Latest PC to Lower Cambrian	3,100m vertical	US$8,100,000	952 (27)	20.3 (10.5)	?

Budour and Budour NE., Harweel Area, South Oman Salt Basin, the Sultanate of Oman (Montage 2a)

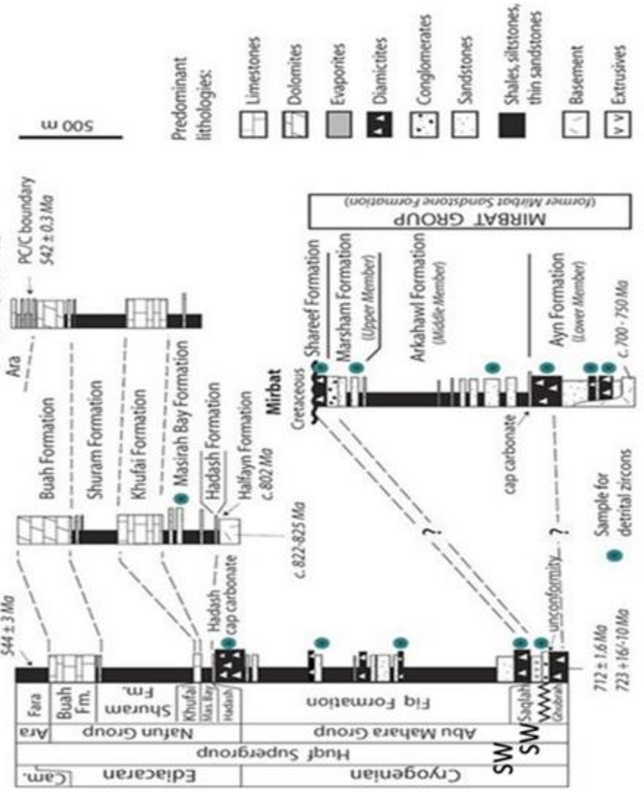

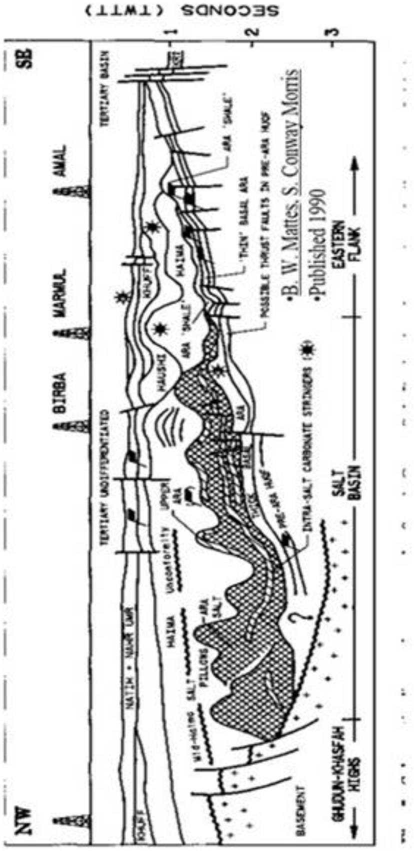

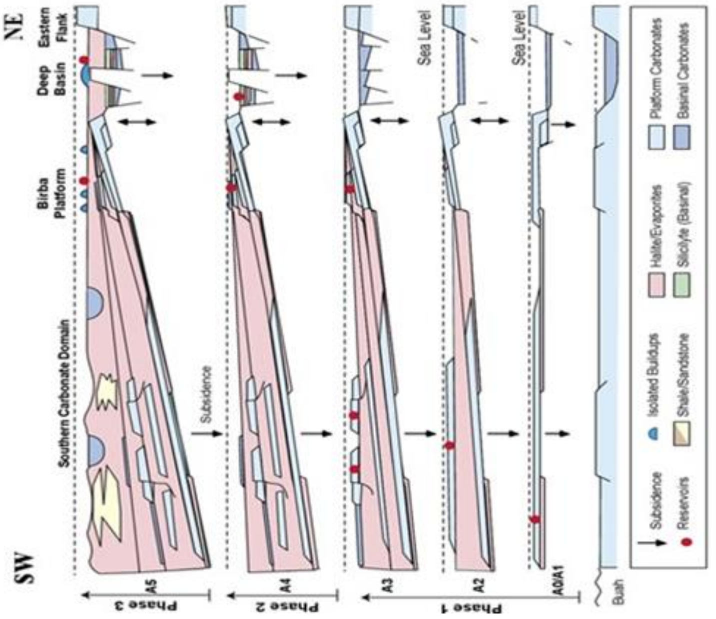

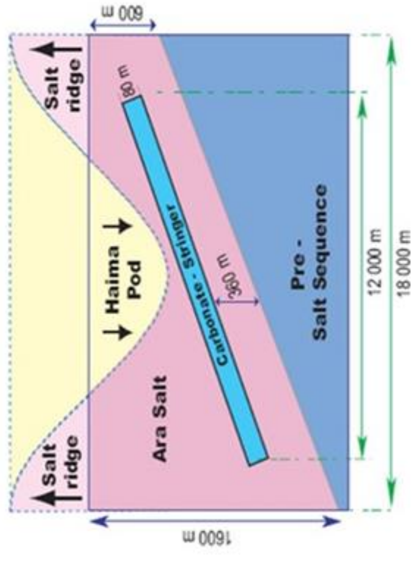

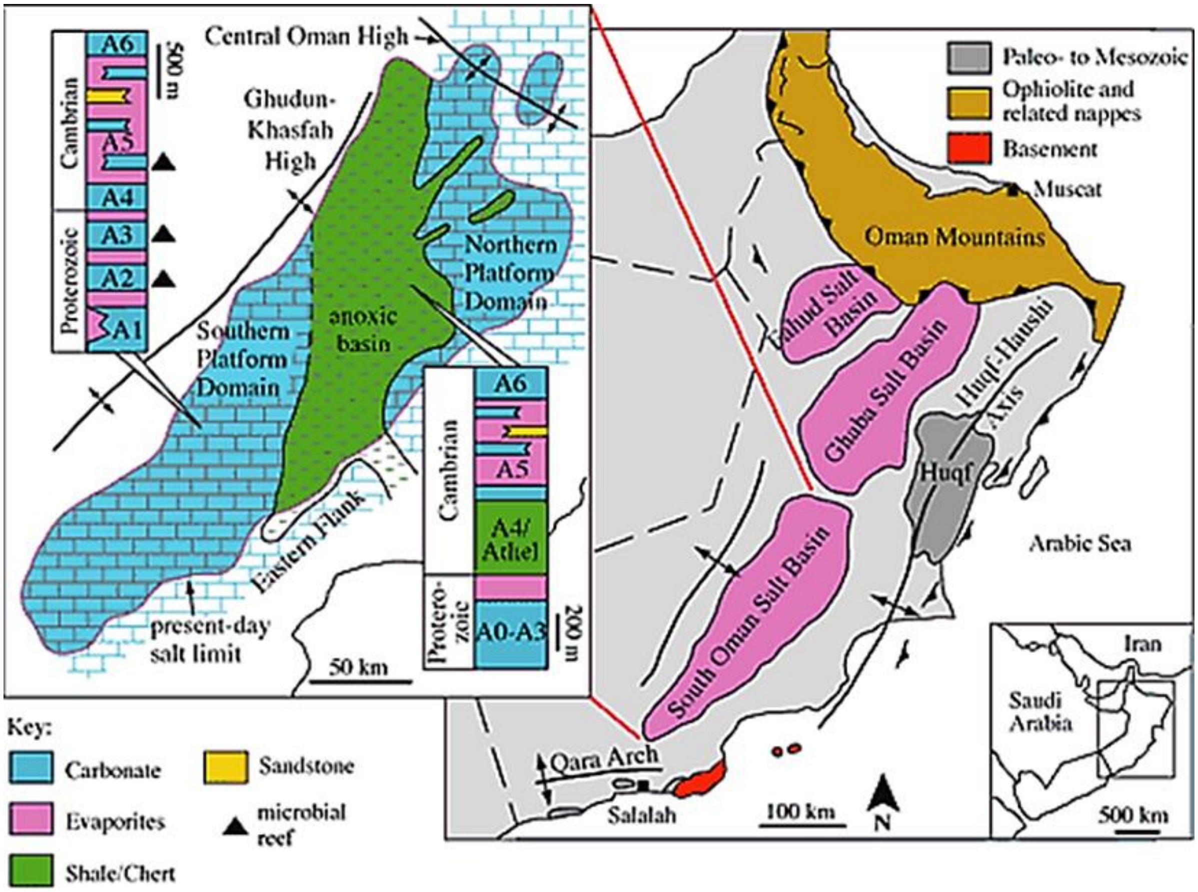

Figure 4.10. Maps of Oman and the South Oman Salt Basin. The South Oman Salt Basin is subdivided into two platform domains, separated by a deep, probably anoxic basin.

The Ara evaporite-carbonate sequences are labelled A1 to A6. Carbonate slabs or stringers are found in the blue areas, silicilytes are found in the green. Map after Loosveld et al. (1996).

In 1978, well BB-l was proposed to test a closed structure 7 km to the north and down dip of the Nassir accumulation (Figure 4.11). Three dolomite stringers were discovered by well BB 1 near the base of the Ara Salt. The top stringer (so-called ‘A4C’, which contains the Precambrian-Cambrian chronoboundary: ~541 MA) produced 1,440 m^3/d of oil with an API gravity of 28^0 (AI-Ghammari, 2006).

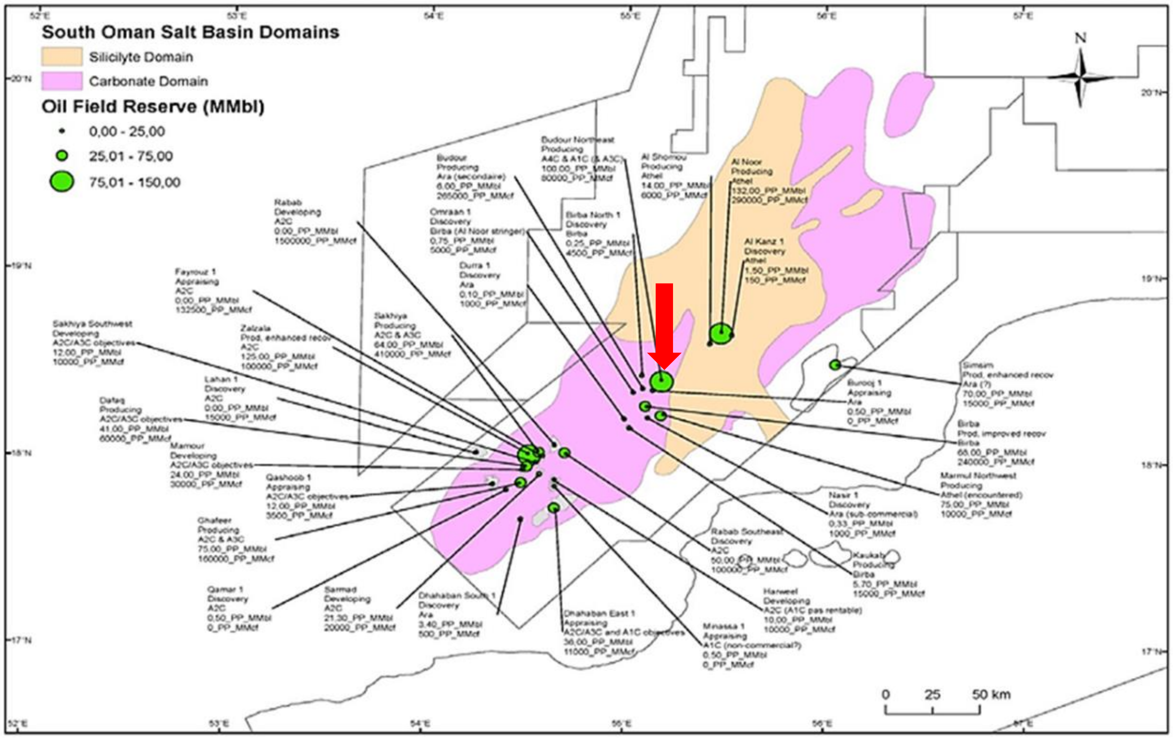

Figure 4.11. South Oman Salt Basin Domains, Carbonate and Silicilyte. Budour Field at red arrow. After Despinois, 2018

The discovery of gas, condensate, and helium at the Budour Northeast field was revealed by Budour NE-2, a well drilled in 2007 to follow up the field's original discovery well, Budour NE-1. It consists of a reservoir lying below the one tapped by the Budour NE-1. When tested, Budour NE-2 produced as much as 5,800 barrels of relatively heavy, sour oil per day (Rigzone.com, 2008) with over 2,000 BOPD of heavily saline water.

The Ara Group is dominated by a cyclic arrangement of evaporites (mainly halite, common anhydrite, rarely sylvite) and carbonates (mostly dolomites), with associated siliciclastic and rare interbedded volcanic ash beds (Al-Ghammari, 2006). The carbonates often 'float' isolated in the salt (hence the term 'stringers'), they can attain considerable thickness (50–200 m) and can be traced (on seismic sections) over large areas within the salt. The carbonates are of (restricted) marine origin and have been deposited on platform, rimmed shelf or carbonate-ramp settings (Forbes, et al, 2010).

This is an unusual, some would argue unique, setting for the accumulation of helium, as the reservoir rocks are totally encased within the relatively impervious Ara Evaporites. Indeed, there are still ongoing questions of the genesis and emplacement of hydrocarbons in both the carbonate stringers and the silicilytes (Allen, 2007). Consensus to date is that the hydrocarbons are self-charged from the carbonates, which would explain the overpressured situation found as well as the high H_2S, CO_2 and N_2 values.

Evidently, helium was emplaced before the isolation of the carbonates or silicilytes before encasement and migration into the Ara Salt. This would point to a source from the igneous-metamorphic basement of Oman, which is a relatively young assemblage of Neoproterozoic rocks formed from a northeast-trending mélange of accretionary wedge, ophiolitic, magmatic arc, and microcontinental terranes that plated onto the southeast periphery of the East Arabian Craton during the Pan African Orogeny. Geochronology suggests that the main phase of accretion and associated igneous activity was completed in Oman at around 800 MA (Mercolli, *et al.*, 2006; Allen, 2007; Bowring et al., 2007).

4.4.1.4 ***Helium occurrences in the Neoproterozoic of the Amadeus basin, Australia***

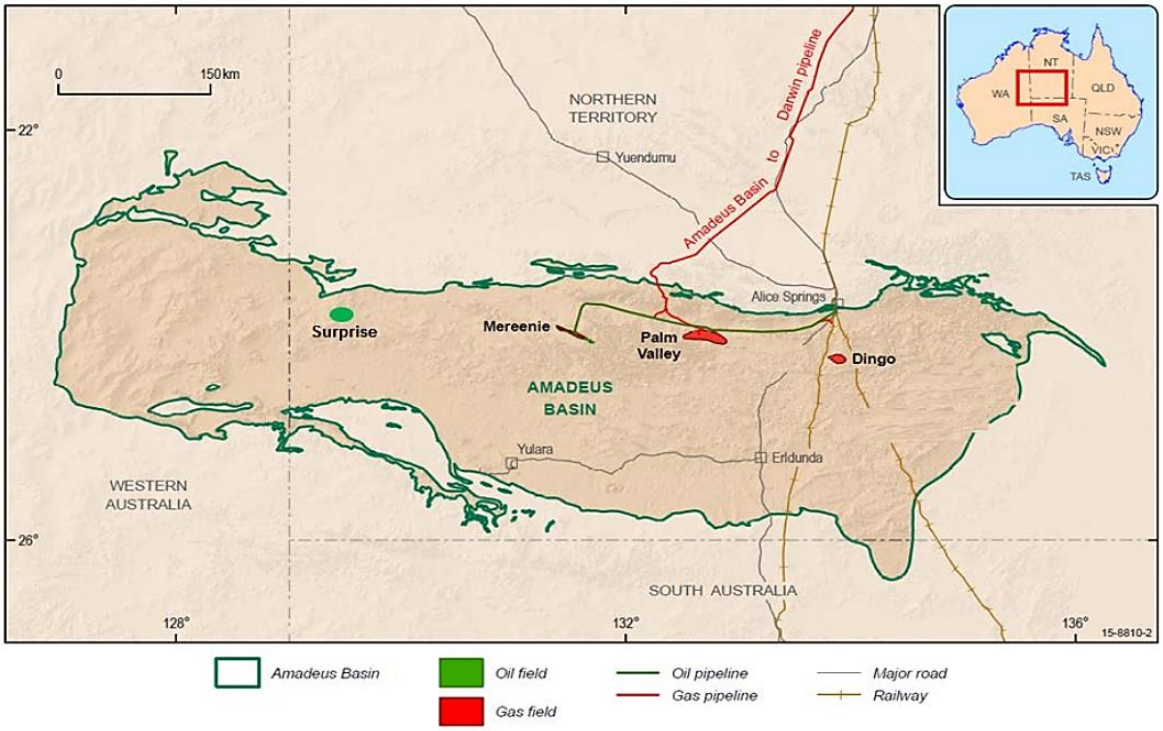

Figure 4.12. Location map of Amadeus Basin, part of the Centralia Superbasin, Central Australia. From *Carr, et al*, 2015.

The Amadeus Basin (Wells, *et al.*, 1970; Preiss, *et al.*, 1978; Edgoose, 2013) is an east-west trending belt of folded Neoproterozoic–Paleozoic rocks in central Australia. The Western Australia succession is mostly of Neoproterozoic to Cambrian age (Figure 4.12) (Carr, *et al.*, 2016).

It overlies Paleo- to Mesoproterozoic metamorphic, sedimentary and igneous basement domains of the Arunta Orogen, exposed to the north, and Musgrave region (Musgrave Province and overlying Warakurna Large Igneous Province and Bentley Basin) to the south (Carr, *et al*, 2016). The current southern and northern boundaries of the basin are of tectonic origin, created during basement uplift of the Ediacaran to early Cambrian Petermann Orogeny and the mid-late Paleozoic Alice Springs Orogeny (Haines, and Allen, 2019).

Petroleum exploration in the Amadeus Basin has been restricted to the more accessible NT portion of the basin (Figure 4.13). Early exploration targeted surface anticlines, with later exploration focusing more on seismically defined targets. Exploration drilling commenced in 1963 with Ooraminna-1, (Konecki, 1967) which flowed gas to surface from a Neoproterozoic reservoir.

The first commercial discoveries followed in 1964 (Mereenie Oil and Gas Field) and 1965 (Palm Valley Gas Field). Later commercial discoveries include the Dingo Gas Field, originally discovered in 1981, that commenced production via a pipeline to Alice Springs in December 2015 (Haines, and Allen, 2019).

The Dingo Gas Field represents the first commercialization of Neoproterozoic hydrocarbons in Australia. The Surprise Oil Field, the most westerly in the NT, was discovered in 2010. The field commercially produced oil from Ordovician reservoirs for over a year, but is not in production currently. The Mereenie, Palm Valley and Surprise fields are all related to the semi-regional Ordovician Larapintine Petroleum Supersystem (Haines, 2020).

Despite a focus on the Larapintine Petroleum Supersystem, the Neoproterozoic has remained attractive to explorers. Apart from the Dingo Gas Field, where data suggests the potential for 2.4 Tcf gas and 493 Bcf helium, (Black, 2017) there have been significant gas flows from Ooraminna-1 and -2, Orange-1 and -2, and two subsalt wells Magee-1 and Mount Kitty-1, detailed below. Minor oil shows have also been reported from the Neoproterozoic at several levels, including a probable paleo-oil column in the Wallara Formation in Finke-1 (Figure 4.13) (Marshall et al., 2007).

Mount Kitty region, South Amadeus Basin, Central Australia, (Montages 3 & 3A)

The Mt Kitty test well resides in the heavily faulted and folded structure of the southern Amadeus Basin, approximately 220 km southwest of Alice Springs in central Australia (Palmer and Ambrose, 2012). The well was drilled in 2014 to a TD of 2,295 m. (7529 ft.). It is one of the two tests that were drilled to evaluate the subsalt section (below the two thick salt accumulations of the Neoproterozoic Gillen Member of the Bitter Springs Formation) in the entire region.

The well was drilled to test the possibilities of a reservoir existing beneath the evaporite seal of the Gillen Salt, that being the Neoproterozoic Heavitree Formation, a primarily siliciclastic unit of sands and shales. The formation, which consists of pale-tan or white quartzose sandstone interbedded with rare occurrences of laminated mudstones and conglomeratic intervals, was deposited in at least four depositional sequences (Lindsay, 1999).

The original primary target at Mt Kitty -1 was the Heavitree Quartzite, while helium/gas charged fractured basement was a secondary target, however, as a result of pinch-out the Heavitree Quartzite was absent. The paleo-high appears scalped of this unit which now presents as a downdip ‘halo’ or ring play. The exact vertical extent of mobile inert basement gases into granitoid basement remains uncertain as is the nature of fracture distribution in the structure (Palmer and Ambrose, 2012).

Analysis of well data indicates the gas flows emanated from fractured granitoid rocks of the Musgrave Province, with high helium contents (6-12% v/v) derived from a radiogenic basement. Progress reports from the operator (Santos) indicate a flow test at 2144 m produced 500 Mcfd before declining to 70 Mcfd after ten minutes. A second test at 2156 m produced 530 Mcfd, decreasing to 420 Mcfd after 18 minutes.

Mount Kitty region, South Amadeus Basin, Central Australia, (Montage 3)

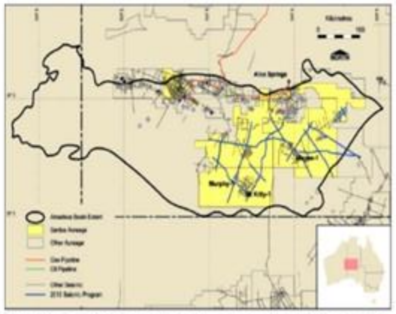

Figure 1. Amadeus Basin map highlighting Santos acreage, regional seismic lines acquired in 2013 AMSAN seismic survey and key well locations.

Country:	Australia
Geological region:	Southern Amadeus Basin
Field(s):	Mt. Kitty
Reservoir age(s):	Neoproterozoic
Gas/Helium EUR:	883 BCFG/3.8 BCFG

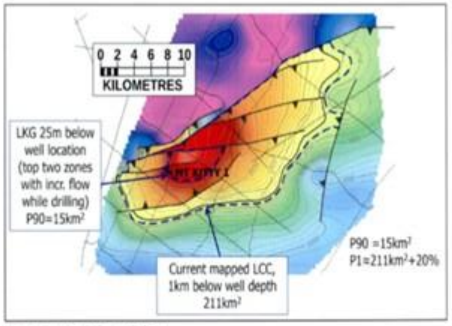

Figure 2 - Basement Depth Structure Map (mSS)

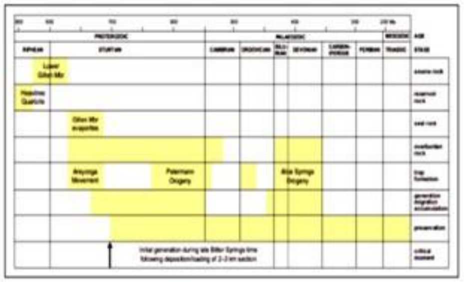

Figure 8. Events chart for the Gillen Member petroleum system (Young and Ambrose, 2007)

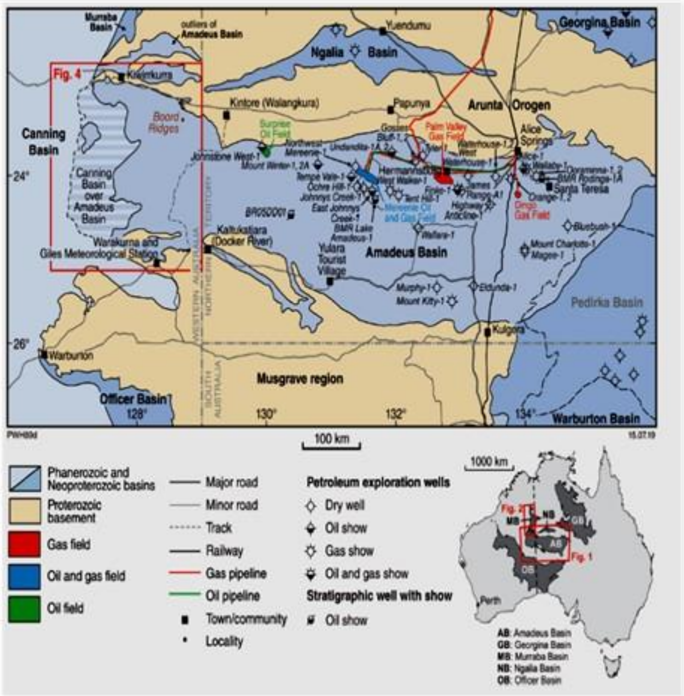

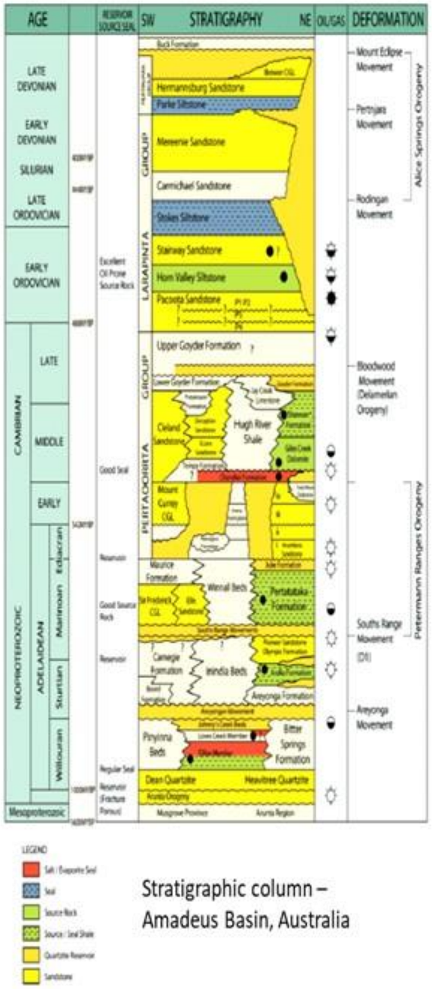

Stratigraphic column – Amadeus Basin, Australia

Country	Region	Field	N2%	CO2%	He%	CH4%	N2/He	Reservoir age	Average depth ft. (m)	Reservoir thickness ft. (m)	Reservoir area mi^2 (km^2)	Porosity (%)	Sw (%)	Permeability (mD)	Age of pore water	Gas, recoverable BCFG (BCM)	Helium BCFG (BCM)	Economic or non-economic?
Australia	Southern Amadeus	Mt. Kitty	70.33	0.21	6.60	10.22	10.66	Neoproteozoic - Heavitree Quartzite	7530 (2295)	27.4 (8.5)	15.75(40.75)	Fracture	0.00	Fracture	Neoproterozoic	883 (25)	3.8 (1.34)	Non-Economic (Facilities $)

Mount Kitty region, South Amadeus Basin, Central Australia, (Montage 3A)

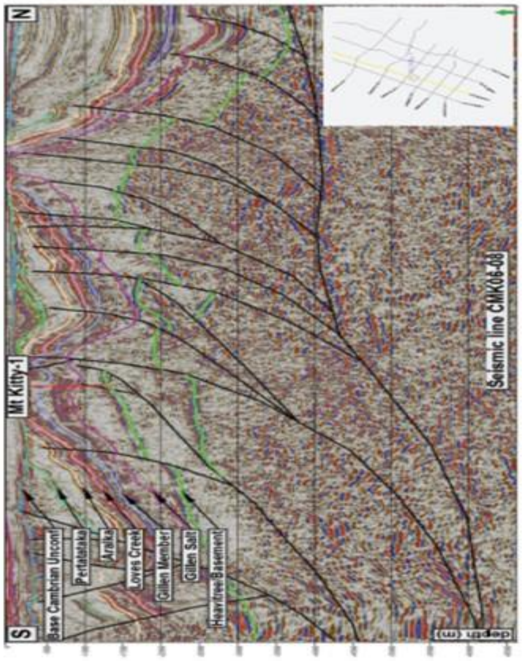

Figure 4. Dip line CMK06-08 across Mt Kitty Prospect with annotations of mapped horizons and faults (green – top Heavitree horizon).

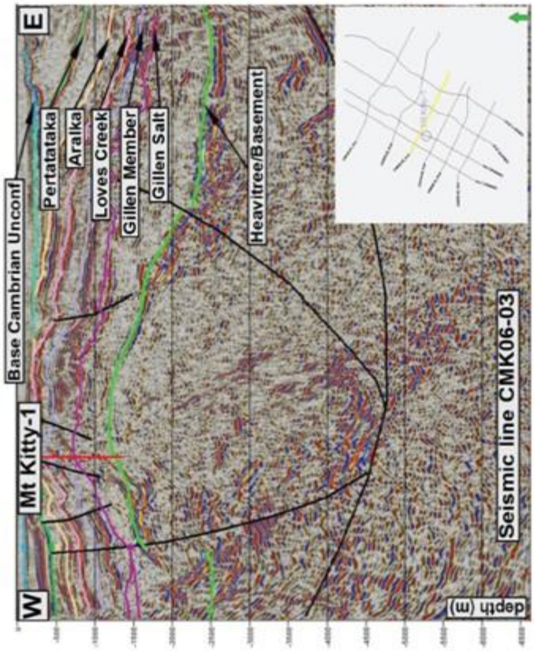

Figure 5. Strike line CMK06-03 across Mt Kitty Prospect with annotations of mapped horizons and faults (green – top Heavitree horizon).

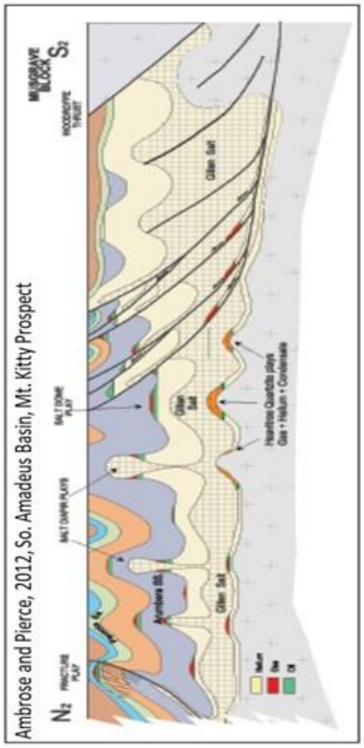

Figure 10. Structural styles and hydrocarbon play types in the southern Amadeus Basin, highlighting structures of the Petermann Ranges Orogeny (Ambrose, 2006b).

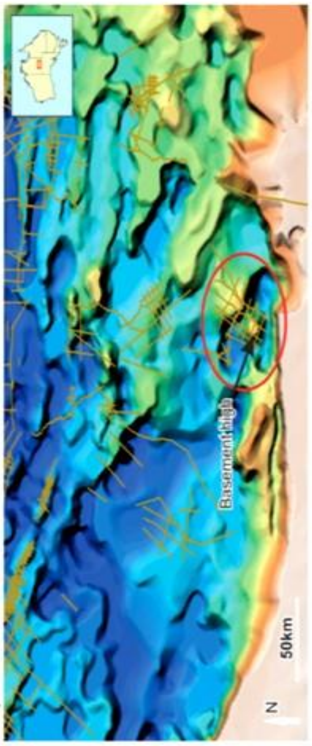

Figure 3. SEEBASE™ depth-to-basement model over the southern Amadeus Basin. The southern and western parts of the basin exhibit basin highs believed to

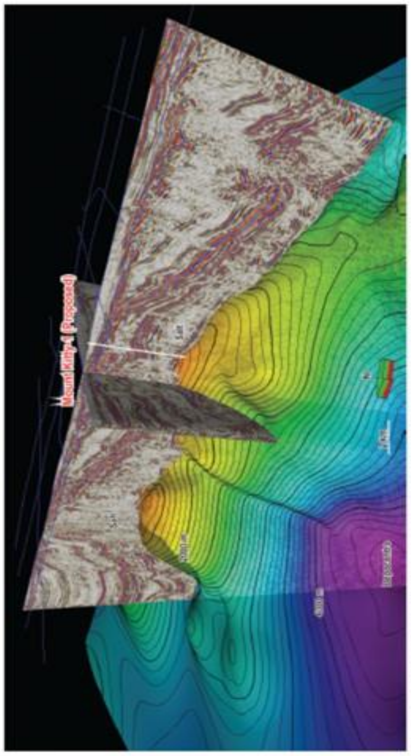

Figure 11. 3D view of the anticlinal structure mapped at Mt Kitty (Heavitree horizon, mTVDSS) and proposed Mt Kitty-1 location.

The only two NT petroleum exploration wells, Magee-1 (Wakelin-King, 1994) and Mount Kitty-1, have penetrated below Gillen Formation salt, both to basement. Both wells were technical successes with gas flows to surface from beneath the salt seal (Pironon, and Grishina, 1995) demonstrating the existence of a subsalt hydrocarbon source, and the viability of this proposed hydrocarbon system (Plummer, 2015).

In the case of Mount Kitty-1, there was no subsalt sandstone unit (no Heavitree Formation or equivalent) and the gas flowed from fractured granitic basement (Clarke et al., 2014; Debacker *et al.,* 2016).

In Magee-1, gas flowed from a thin sandstone (4.5 m gross, 3.6 m net pay) interpreted as unusually thin Heavitree Formation, possibly thinned over a nascent basement high (Wakelin-King, 1994). It is possible that the Heavitree Formation is entirely missing and the thin sandstone is a basal component to the Gillen Formation (Haines, and Allen, 2019).

The reservoir is overlain by 20m of bitumen-stained black shale, interpreted as lower Gillen Formation, which is presumably the source of the hydrocarbons. In both wells the gas had very high helium contents of 6.2% in Magee-1 (Wakelin-King, 1994; Clarke *et al.,* 2014) and an impressive 9% in Mount Kitty-1 (Debacker, *et al.,* 2016; Boreham, *et al.*, 2018; McInnes, *et al.,* 2017). The unusual Mount Kitty-1 gas composition (9% He, 61% N_2, 13% CH_4, 4% C_2H_6 and 11% H_2) includes one of the highest recorded helium concentrations for any well on Earth (McInnes, *et al.,* 2017).

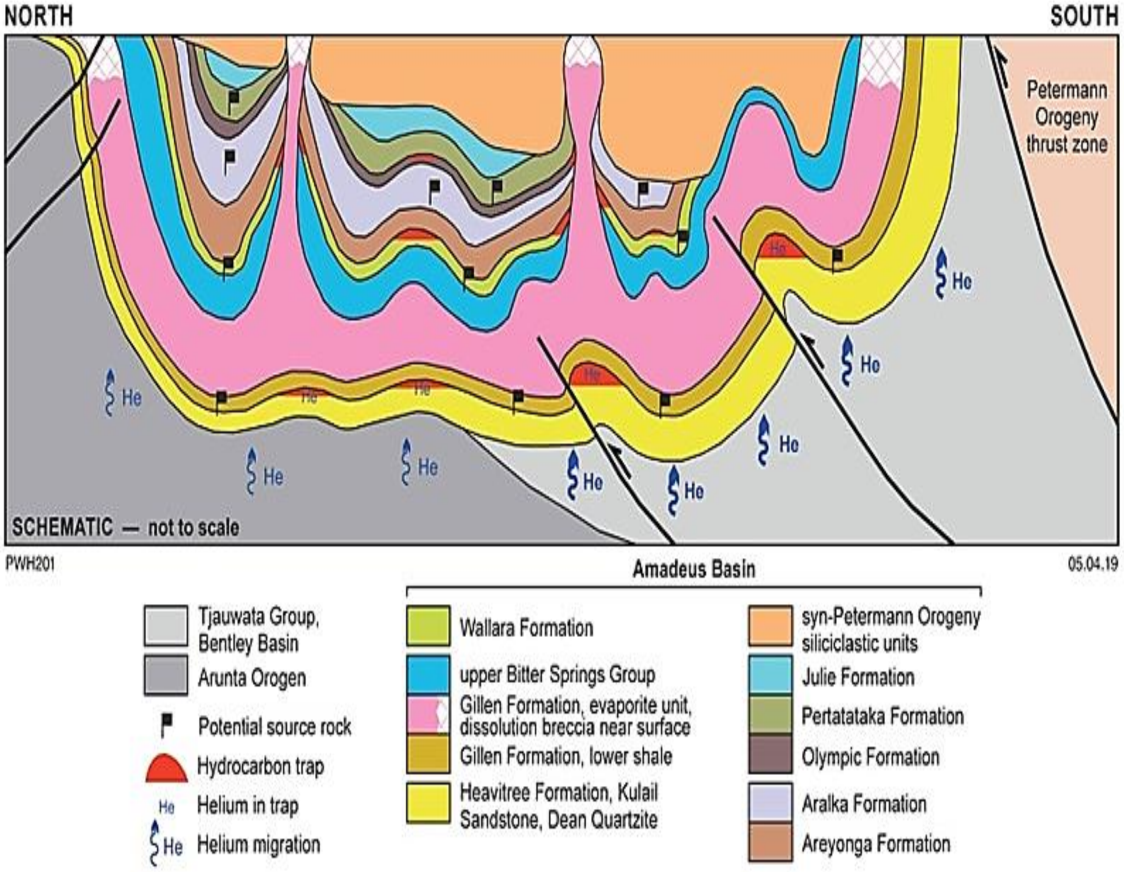

Figure 4.13. Schematic N-S cross section through the Western Australian Amadeus Basin showing potential source rock units and hypothetical plays.

Helium migrating from the igneous-metamorphic basement as well as from the immature siliciclastic rocks and volcanics of the Tjauwata Group, is captured along with hydrocarbons sourced from subsalt shales (Haines and Allen, 2019).

It could also be speculated that the rocks of the Bentley Basin, inferred to underlie the southern WA Amadeus Basin, could provide an equal or more efficient source of helium-bearing fluids than granites or other crystalline basement rocks of the Arunta Orogen in the north (Ambrose, et al, 2012). Crystalline rocks will typically require faults and fractures to assist migration for helium-bearing fluids (Boreham et al., 2018).

The thick pile of mineralogically immature siliciclastic rocks of the upper Bentley Basin (Figure 4.14) derived directly from such crystalline rocks, might be a more efficient source of helium if there is preserved porosity and associated formation fluids (Palmer, and Ambrose, 2012). Radiometric surveys over outcropping Bentley Basin along the southern margin of the Amadeus Basin demonstrate the radiogenic nature of these rocks (Haines, and Allen, 2019).

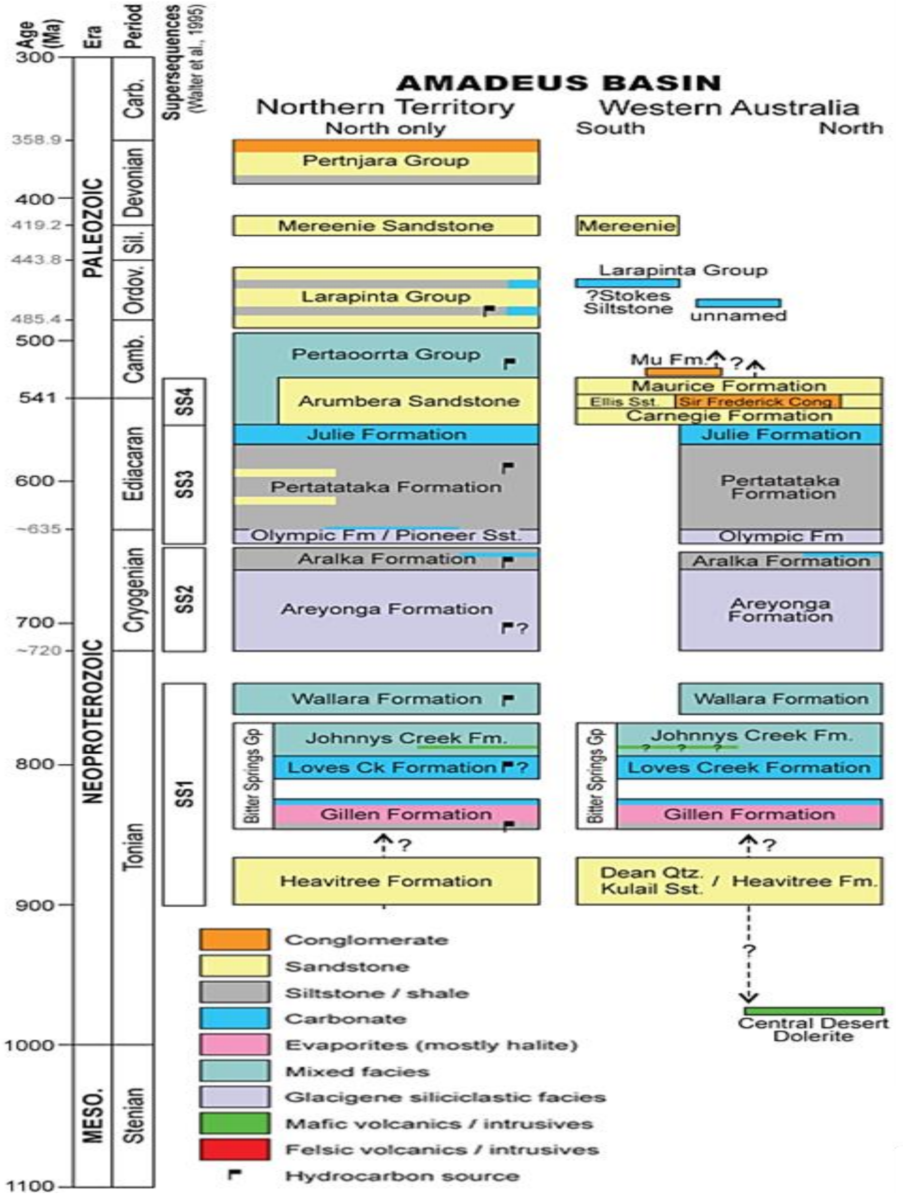

Figure 4.14. Simplified stratigraphy of the Amadeus Basin in The Northwest Territories and Western Australia. Modified from Haines, and Allen, 2019.

4.4.2 Helium from Thick Paleozoic Carbonate-Evaporite Packages: The Khuff Group, North Field Dome, Offshore Qatar, and South Pars Field, Offshore Iran

In Qatar, the Khuff Formation is only recognized in the subsurface at depths between 8,300 ft. and 11,900 ft. subsea and ranges in thickness from about 1,600 ft. to 2,600 ft.

Gas in commercial quantities was first discovered in Dukhan, North West Dome and Bull Hanine Fields (Sugden, 1975) (Figure 4.15), in the Arab Series of Mesozoic carbonates. Khuff production from the vast North Field began to come online in the late 1990s.

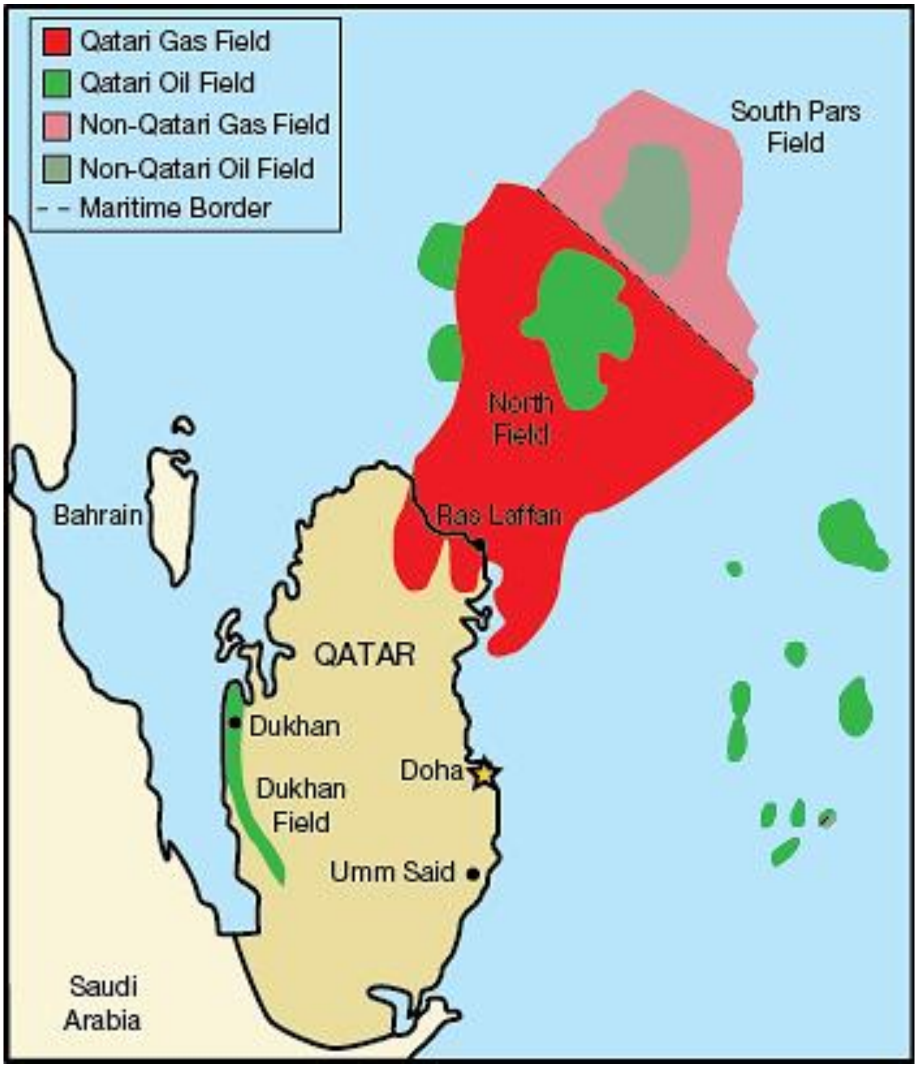

Figure 4.15. Location of Qatar’s North Field and Iran’s South Pars Field, exploiting the thick Permotriassic Khuff Formation. From Alfadala and El-Halwagi, 2017.

Although the North Field Khuff gas contains only a trace amount of helium, estimated at 0.04%, the immense size of the reservoir (~1,500 TCFG with associated condensate) means that the helium available is expected to be enough to meet world demand for the next 30 years. And *if* both Qatar's helium plants were operating at full capacity, Qatargas could supply approximately 25% of the world's total helium production (Qatargas Operating Company Limited, 2021) based on current consumption.

The Khuff is made up of five cycles of carbonate-evaporite deposits and is probably one of the more complex carbonate reservoirs in the Middle East (van Buchem, et al, 2014). This heterogeneity is considered to be the most significant geological uncertainty likely to affect sustainable field production performance and it is therefore very important that the factors affecting it are fully understood (Bishlawy, 1985).

The complexity is a result of changing sedimentary conditions and variations in diagenesis, with relatively high rates of deposition in environments oscillating between shallow intertidal and open marine. The formation was first deposited as a carbonate platform during the mid-Permian, but the climate gradually became warmer and more arid, resulting in the deposition of evaporates and dolomitization of the carbonates (Whitson and Kuntadi, 2005).

The Permian Khuff formation containing gas condensate is wide-spread in the Middle East, with major deposits in Qatar, Iran, Saudi Arabia, Bahrain, and Abu Dhabi. North Field (NF) in Qatar and South Pars (SP) in Iran are a common source of supply (NF-SP) at approximately 9,000 ft subsea, with initial reservoir pressure about ~5,300 psia and a bottomhole temperature of 220°F (Sugden and Standring, 1975).

The Khuff Formation is described as a fine-to-coarse crystalline dolomite with some interbeds of limestone and anhydrite (Al-Siddiqi, and Dawe, 1999). There are four major non-communicating Khuff geological units, generally numbered from top to bottom K1, K2, K3 and K4. A layer of anhydrite caps K2, a layer of mudstone and anhydrite separates K2 and K3, and a layer of anhydrite separates K3 and K4 (Figure 4.16) (Alsharhan and Nairn, 1997).

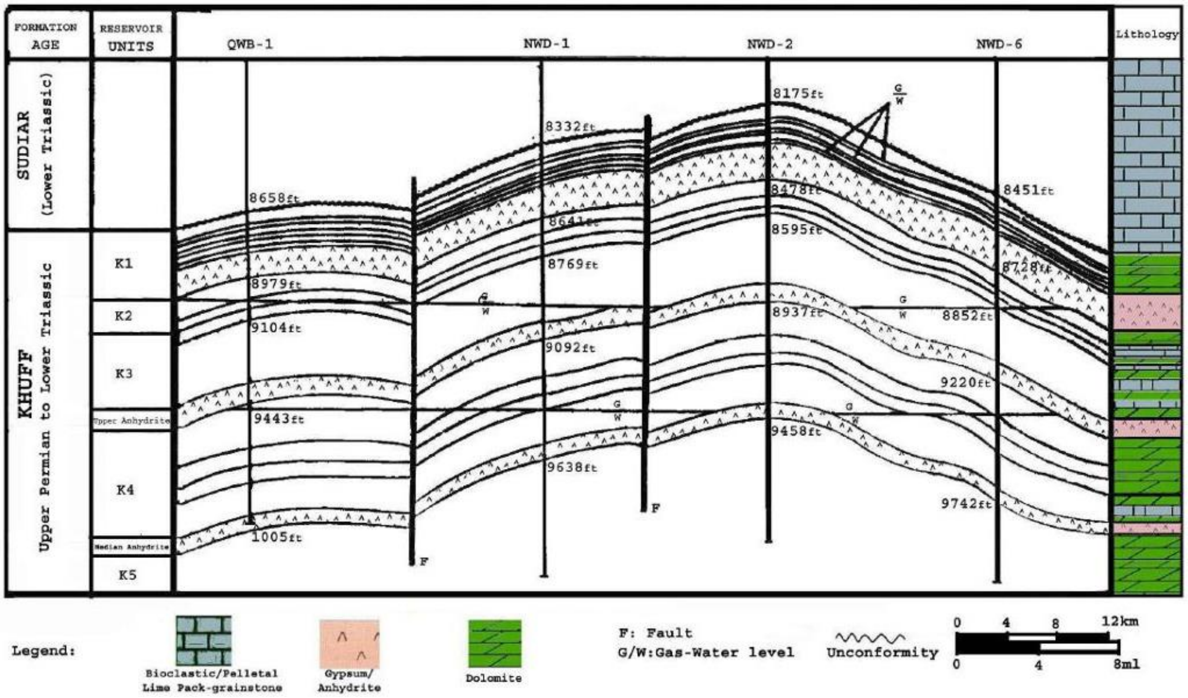

Figure 4.16. Cross-section through the North Field.

Five megacycles are recognized in the Upper Khuff carbonate reservoir, the youngest two of which are possibly Triassic. The oldest cycle (K5) consists of tight, slightly argillaceous dolomites and occasional interbedded anhydrite, terminated by the thick Median Anhydrite. Each of the succeeding four cycles (K1-4) can be broken down into fining-up subcycles with similar lithologies. (From Alsharhan and Nairn, 1997)

Important geological features of the Khuff are high-permeability, low-thickness layers consisting primarily of vugs and fractures, located in some or all Khuff units (Poppelreiter, 2013). These zones apparently have significant areal extent, and contribute the majority of production in any given well.

While Qatar's natural gas has only 0.04 percent helium, along with H_2S, CO_2 and N_2, the country produces so much natural gas that even with the extra costs and steps necessary to remove the gas stream adjuncts (Andrieu, et al, 2006), it has the revenue from the accumulated helium by-product for a considerable second gas income stream (Alfadala and El-Halwagi, 2017) that could possibly eclipse the value of the methane produced.

4.4.2.1 *Helium accumulations in thick Paleozoic euxinic black shales: The Mancos Shale of the Western United States*

In order to provide a proof-of-concept, a case study was undertaken in the Uinta basin of eastern Utah and Piceance basin of north-western Colorado (McDowell, et al, 2017). These basins produce nearly three percent of the total natural gas in the United States and also contribute appreciable amounts of helium from various geologic formations. The helium system is identified by its source rock, reservoir, trap, seal, and migration pathway.

Two helium systems are identified and tentatively called the Uncompahgre and Uinta systems; named after their interpreted source rock intervals (Lillis, et al., 2003). The helium gas, as well as nitrogen and carbon dioxide, are believed to have migrated through basinal brine systems until trapped in conventional petroleum traps. These gases are found primarily in the Entrada, Morrison, Dakota, Frontier, and Prairie Canyon Member of the Mancos formations (Norton, and Groat, 2003. (Figure 4.17).

The Mancos Shale provides a basin-wide seal for both helium systems and prevents significant stratigraphically upward leakage to the younger Mesaverde, Wasatch, and Green River gas-productive intervals. A common risk segment (CRS) approach was utilized and areas of low, moderate, or high risk were mapped for the occurrence of pools with potentially significant helium content (McDowell, Milkov, and Anderson, 2017).

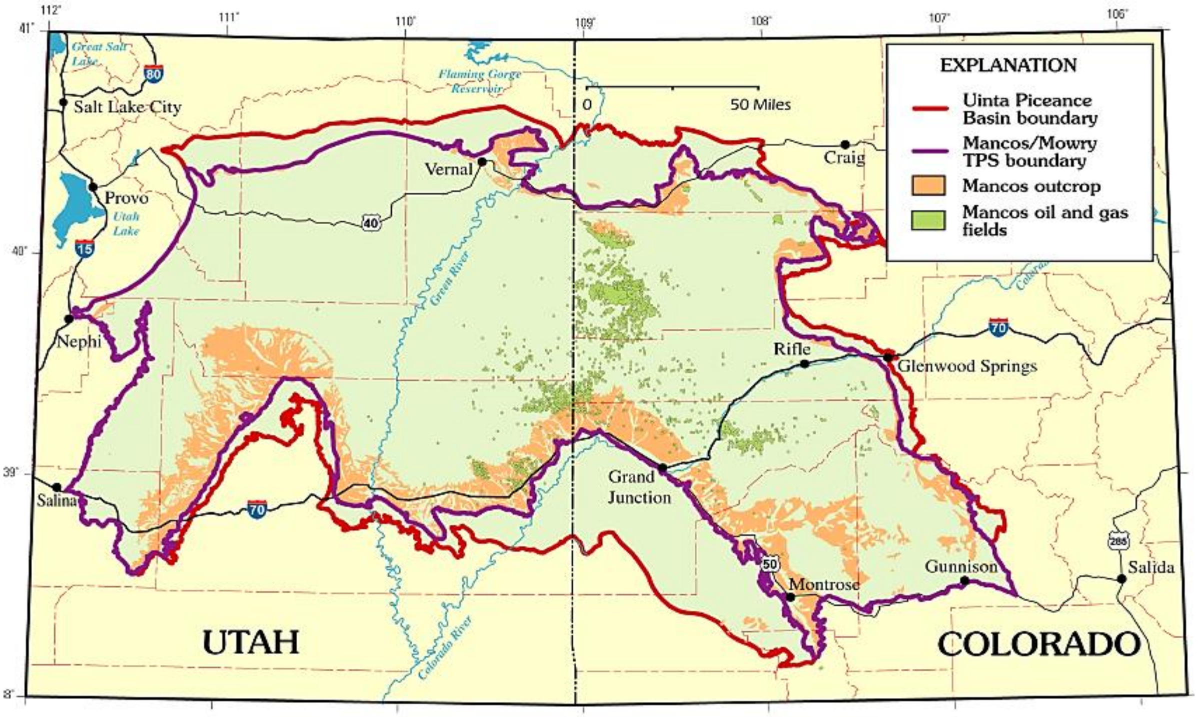

Figure 4.17. Location map of the Mancos Shale outcrops and oil and gas fields, Utah and Colorado, US, Source: USGS Uinta-Piceance Assessment Team, 2002.

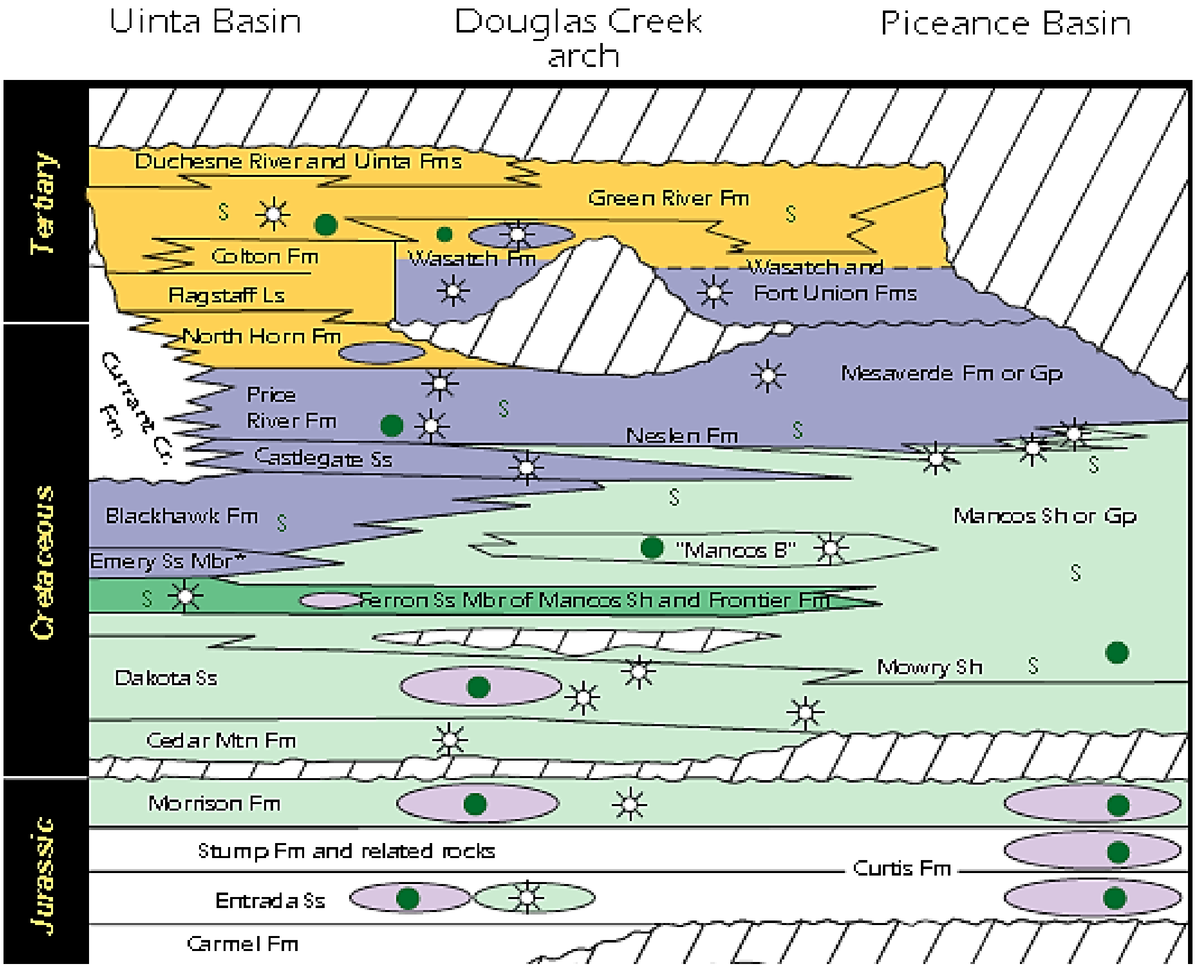

Figure 4.18. Stratigraphic column showing the relationship of the Mancos and Mowry shales.

Uinta Piceance Basin stratigraphic column. Orange is the Green River System, dark purple is the Mesaverde System, dark green is the Ferron/Wasatch Plateau System, light green is the Mancos/Mowry System, and light purple is the Phosphoria System. Green circles represent significant oil production, open star-circles represent significant gas production, “S”s represent source rocks: USGS Uinta-Piceance Assessment Team, 2002.

A concentration of helium found in the gas stream of 0.3% or more is considered a potential helium source. Concentrations over 7.0% helium are rare yet have been discovered and documented in the gas stream of wells drilled in east-central Utah (Wiseman and Eckels, 2019).

Helium accumulates as the radioactive decay product of uranium and thorium. Joints in formations at depth may provide pathways for helium microseepage to the surface. Under ideal circumstances, the buoyant decay products of igneous or crystalline basement rocks can travel up fractures and faults to porous reservoirs sealed by impermeable salt layers or thick shale deposits (Sorkhabi and Tsuji, 2005).

In eastern and south-eastern Utah, helium is often found in reservoirs below the thick Paradox Formation salt or below the thick Mancos Shale. While many helium-prospective regions exist, very few natural gas fields contain enough to justify a helium recovery process (Editors, 2013). Helium shows in Utah range from trace amounts up to 7.5%, with the highest concentrations on the crest of the Harley Dome structure (Herndon, 2013), east-central Utah, from the Entrada Sandstone reservoir at a depth of 965 feet.

Although many resources have been documented since the early twentieth century, recent renewed interest of several helium exploration companies has brought attention back to the helium potential of Utah. Such attention has motivated the compilation of a verifiable database of economic helium analyses from 12 helium-prospective fields, 89 wells and one gas plant (Anderson, 2018).

With several high-percentage helium plays and natural gas wells with associated helium concentrations at or above the so-called 0.3% economic threshold, Utah deserves the consideration of those interested in exploring for and producing helium (Wiseman and Eckels, 2020).

4.4.2.1.1 *Black River and Trenton, Michigan Basin*

Formation of the intracratonic Michigan Basin initiated with late Precambrian mid-continental rifting and crustal extension (Van Schmus, 1992), followed by deposition of more than 4.5 km of sandstones, carbonates, shales, and evaporites from the Cambrian to Jurassic (Dorr and Eschman, 1970).

The sedimentary succession begins with 17 m of basal Cambrian sandstone on granitic gneiss of the Precambrian shield. The overlying Ordovician Black River Group comprises peritidal lithographic limestones, which grade upward into the Trenton Group argillaceous shelf limestones (Patchen, *et al*, 2004).

Basin deepening during the Late Ordovician Taconic Orogeny resulted in the deposition of more than 200 m of Ordovician shale in the basin. Restricted circulation during Silurian to Devonian time produced ~200 m of interlayered shale, carbonate, and evaporite units (Gbadeyan, and Dix, 2013) (Figure 4.19).

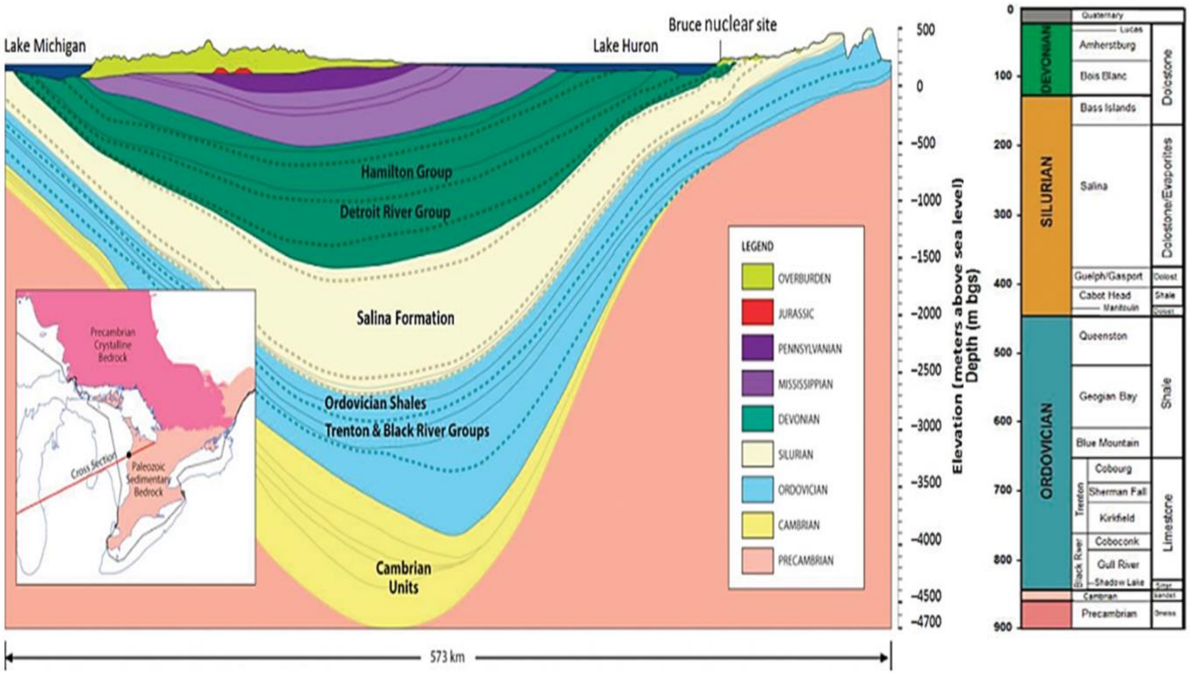

Figure 4.19. Michigan Basin bedrock stratigraphy. Section length 573 km. Modified from Clark, et al., 2013.

Authigenic helium that has been accumulating in an aquiclude for more than 260 MA is found to be isolated from underlying allochthonous, He-enriched helium that originated from the rifted base of the Michigan Basin and the Canadian Shield (Clark, et al., 2013).

Low-permeability, sedimentary rocks such as those found in the lower Paleozoic of the Michigan Basin have increasingly become a global focus for a wide range of environmental and geoscience studies, including nuclear waste management (Russell and Gale, 1982; Hendry, *et al.*, 2015), CO_2 sequestration (Shafeen *et al.*, 2004; Benson and Cole, 2008), helium concentration and extraction (Petts, *et al.*, 2017), and gas extraction from shale (Arthur and Cole, 2014). In the cases of CO_2 sequestration and extraction of gas with hydraulic fracturing, the low-permeability rocks play a critical role in limiting the upward migration of fluids that are injected or displaced.

Much like the thick, impervious evaporite sequences that trap Meso-Neoproterozoic helium around the world (Russia, Oman, China, etc.), here thick, Paleozoic limestones, the Trenton and Black River, which is subincumbant, are regional seals (Budai and Wilson, 1991). The Trenton Limestone is more grain-rich than the Black River Limestone. Crinoid, bryozoan, mollusk, and trilobite debris are common. In completely dolomitized sections, the presence of crinoid ghosts and gastropod-moldic porosity indicate similar lithologies.

There is no evidence of lateral sedimentary facies changes in the Trenton Limestone. The Trenton Limestone is interpreted to have been deposited on a low-angle planar carbonate ramp under shallow water open-marine conditions (Fara and Keith 1989) (Figure 4.20).

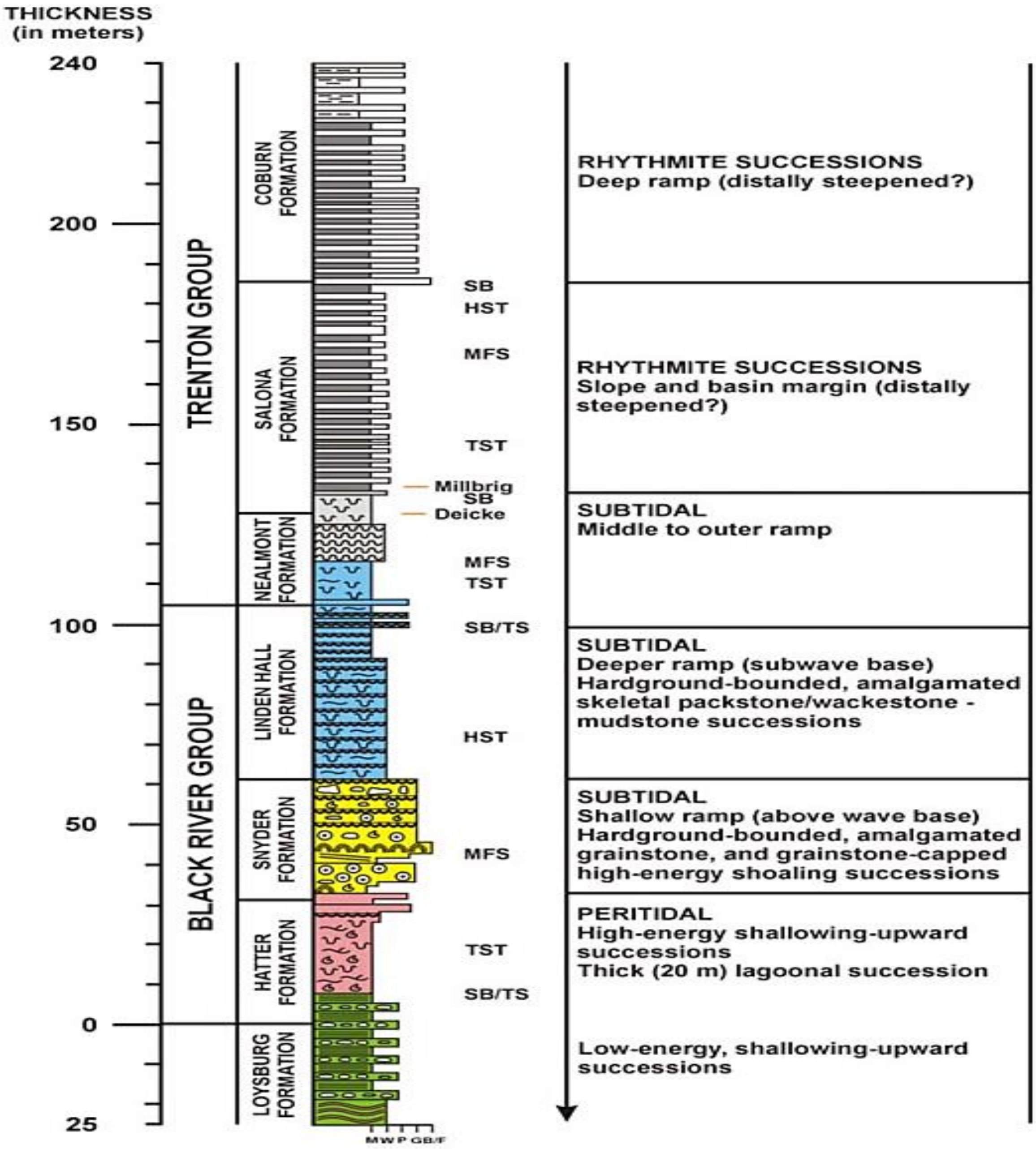

Figure 4.20. Measured section for the Black River and Trenton Groups the vertical stacking pattern of carbonate facies.

SB/TS – combined sequence boundary/transgressive surface. TST – transgressive systems tract. MFS – maximum flooding surface. HST – highstand systems tract. Modified from Patchen, *et al.*, 2004, The Trenton and Black River Formations of the Michigan Basin have been diagenetically altered by a complex sequence of events related to both the stratigraphic and structural history of the basin (Speight, 2016). The physical distribution and chemical composition of dolomite in the Trenton and Black River Formations are variable and suggest multiple episodes of dolomitization (Budai and Wilson, 1991), with overprints based on the sequence stratigraphy and rhythmic deposition of the units.

The Trenton and Black River Limestones are dolomitized extensively with the proportion of dolomite decreasing to the south and southeast. Planar and nonplanar dolomite replacement textures and rhombic and saddle void-filling dolomite cements are present (Williams, 2020). Three stages of dolomitization, involving different fluids, are inferred on the basis of petrographic and geochemical characteristics of the dolomites (Chan, et al., 2000).

These is extensive diagenetic alteration of both Trenton and Black River limestones which has occurred in fracture-controlled hydrocarbon reservoirs. Within reservoirs several stages of dolomitization were followed by carbonate and sulfate cementation, and sulfide mineralization (Dorr and Eschman, 1970).

It is this multi-episodic dolomitization and the overall diagenetic history of the Trenton and Black River carbonates which reduced their permeability. It was reduced to the point as to be a barrier to the migration of Cambrian-sourced hydrocarbons, but also helium sourced from the Precambrian igneous and metamorphic bedrock (Petts, *et al*, 2017).

4.4.2.2 *Bakken Formation, Williston Basin, Manitoba and Saskatchewan, Canada*

The Williston Basin in southwestern Manitoba is geologically well positioned for economic helium deposits within its sedimentary strata (Nicolas, 2016). A search of oil and gas well files identified 80 wells with recorded helium occurrences. Of those occurrences, six wells had helium values above the economic cut-off of 0.30% He with ranges from 0.30 to 2.00 mol % He. (Gage, and Driskill, 2019).

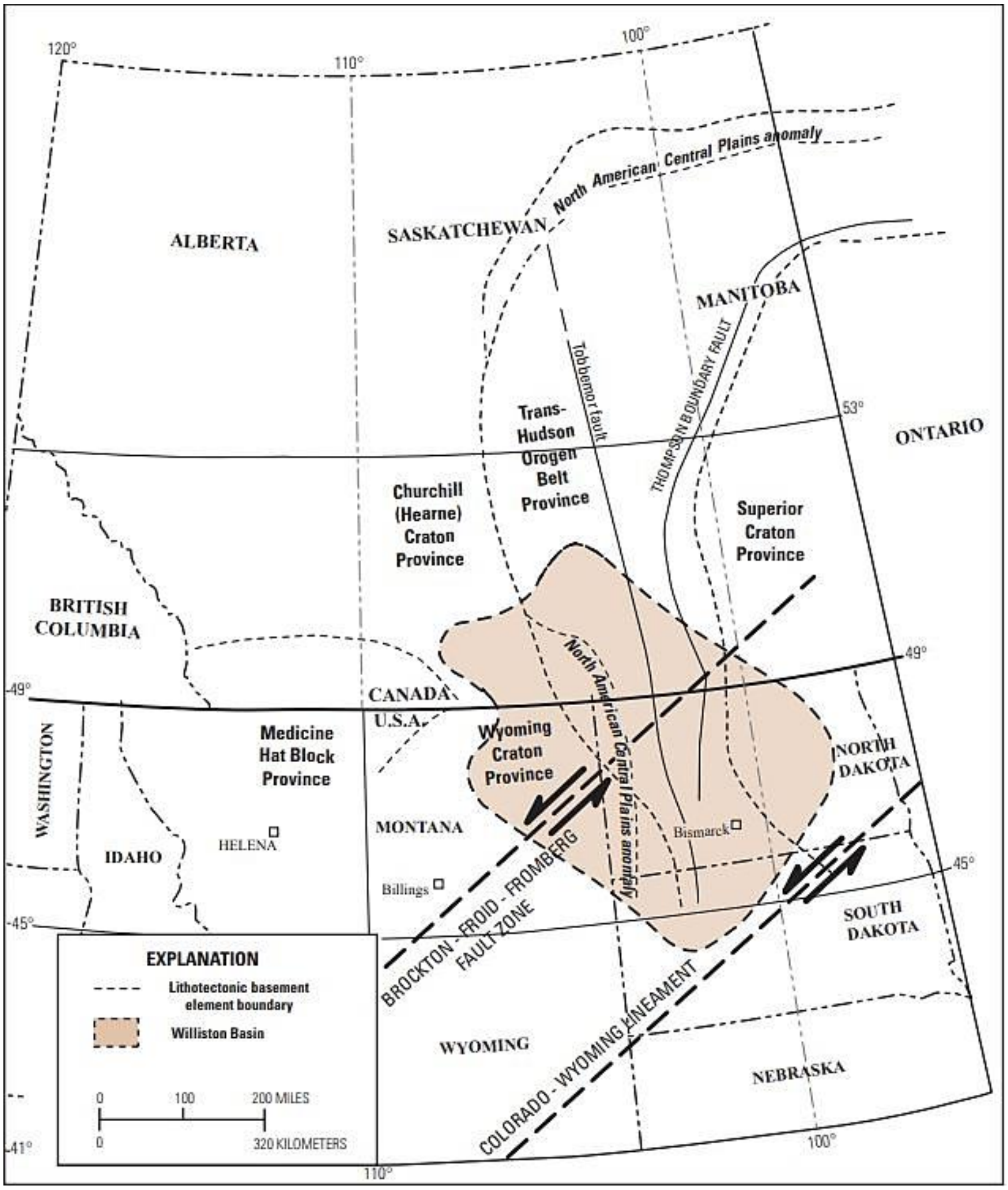

Figure 4.21. Areal extent and structural elements of the Williston Basin, Saskatchewan and Manitoba, Canada, Montana and North Dakota, USA. From Anna, et al, 2010.

In 1964, Sproule noted the Devonian Duperow Formation, below the Bakken, Threeforks and Birdbear (Figure 4.22), produces in the Beaverlodge Field, near the north end of the Nesson

Anticline, in North Dakota. Oil shows have also been reported in several wells in western Saskatchewan. It is of interest to note that significant amounts of helium have been obtained from tests of the Duperow in Saskatchewan, and there appears to be no reason why there should not be helium reservoirs in the Duperow in Manitoba (Sproule, 1964), or in the American Williston Basin.

Table 4.2. Gas analyses of 75 Williston Basin wells in North Dakota.

					HE	CO2	N2	CH4
NO. 8	46.8663918	-103.41	SCORIA	BILLINGS	0.10	1.00	0.50	77.00
HERMAN MAY NO. 1	46.8742321	-103.3	WILDCAT	BILLINGS	0.01	1.90	1.30	48.40
FED. NO. 8-24	47.1052688	-103.42	BIG STICK W	BILLINGS	0.01	4.00	0.70	45.60
VOLENSKY NO. 1	46.9901189	-103.09	UNNAMED	BILLINGS	0.04	0.90	0.90	76.30
FED. NO. 1-28	47.0867348	-103.35	TREE TOP	BILLINGS	0.05	2.30	1.00	46.10
YOURK NO. 1	47.2136322	-103.23	WHITETAIL	BILLINGS	0.05	1.10	0.90	84.30
FED. NO. 6-2	47.3257871	-103.54	ROUGH RIDER	BILLINGS	0.01	0.70	0.90	64.30
CENEX FED. NO. 34-4	47.1397978	-103.61	ROOSEVELT	BILLINGS	0.01	0.50	0.60	56.50
PICKETT FARM			PICKETT FARM	BOTTINEAU	0.10	0.20	29.10	70.00
ARNOLD NERMYR A. NO. 2	48.7756134	-100.94	NEWBURG	BOTTINEAU	0.04		26.00	11.80
ROLLIN STAIRS TR-2 NO. 4	48.7574219	-100.88	NEWBURG	BOTTINEAU	0.06		17.60	27.60
NO. 1	46.0392828	-103.88	CEDAR CREEK	BOWMAN	0.04	0.10	9.50	87.10
NO. 1	46.0392828	-103.88	CEDAR CREEK	BOWMAN	0.20	0.30	42.40	45.50
NO. 1	46.0392828	-103.88	CEDAR CREEK	BOWMAN	0.30	0.10	6.60	92.10
NO. 1	46.0392828	-103.88	CEDAR CREEK	BOWMAN	0.05	0.30	4.70	94.60
RINGSTAD NO. 1	46.1117309	-103.94	LITTLE MISSOURI	BOWMAN	0.04	0.10	5.50	93.80
GAS DEVELOPMENT CO. NO. 38	46.1176891	-104.04	CEDAR CREEK	BOWMAN	0.05		3.20	96.30
BATTERY NO. 3			RIVAL	BURKE	0.02	2.60	1.70	68.00
C. S. STAALESON NO. 1	48.8884331	-102.52	LIGNITE	BURKE	0.01	0.50	1.30	46.60
H. HERMANSON NO. 1-B	48.8598557	-102.58	BLACK SLOUGH	BURKE	0.03	2.40	3.20	65.90
HOLTE-BANK OF ND NO. 1	48.7331234	-102.93	STONEVIEW	BURKE	0.37	0.80	46.80	43.10
SKACHENKO NO. A-1	47.4388872	-102.83	JIM CREEK	DUNN	0.01	0.50	0.80	55.70
FREDERICK SKACHENKO NO. A-1	47.2573257	-103.01	LITTLE KNIFE	DUNN	0.05	2.90	0.30	27.80
KNUTSON-WERRE 34 NO. 1	47.597991	-102.91	BEAR CREEK	DUNN	0.03	0.90	0.90	74.40
BULLINGER NO. 1-30	47.0868543	-102.9	RUSSIAN CREEK	DUNN	0.04	0.80	0.60	84.20
SIGNALNESS NO. 1	47.8419082	-102.94		MCKENZIE	0.02	2.90	0.90	65.30
UNIT NO. 3	47.970365	-102.93	CLEAR CREEK	MCKENZIE	0.04			
ANTELOPE UNIT E NO. 1	48.035619	-102.8	ANTELOPE	MCKENZIE	0.02	0.70	5.00	56.70
ANTELOPE UNIT C NO. 1	48.0211064	-102.79	ANTELOPE	MCKENZIE	0.02	0.90	0.90	69.60
SILURIAN UNIT 5 NO. 1	48.1148308	-102.89	CHARLSON	MCKENZIE	0.05	0.60	3.00	75.40
CROWFLY NO. 17-10	47.9847722	-103.76	MARLEY	MCKENZIE	0.01	0.50	0.30	62.10
MORK NO. 1	47.7378782	-103.38	CHERRY CREEK	MCKENZIE	0.03	1.40	0.20	75.70
M. L. SLAATEN UNIT NO. 1	48.0833201	-102.93	CHARLSON	MCKENZIE	0.06	1.50	98.00	0.40
MILDRED BANCROFT NO. 1	48.0085959	-102.76	ANTELOPE	MCKENZIE	0.02	0.70	1.90	70.30
E-518, E. BRENNA TR-1 NO. 1	48.0117973	-102.79	ANTELOPE	MCKENZIE	0.01	2.50	2.20	54.00
UNIT NO. 3	47.9647764	-102.94	CLEAR CREEK	MCKENZIE	0.06	3.00	96.00	0.50
UNIT NO. 3	47.9647764	-102.94	CLEAR CREEK	MCKENZIE	0.06	3.70	95.80	0.40
PETERSON NO. 1	47.7419015	-103.33	CHERRY CREEK	MCKENZIE	0.03	1.50	0.40	83.00
CHARLSON DEEP UNIT NO. 2	48.1077768	-102.89	CHARLSON	MCKENZIE	0.07	1.50	2.70	73.50
STATE-ROGNESS NO. 1	47.7162066	-103.46	ELLSWORTH	MCKENZIE	0.03	1.30	0.50	73.00
EIDE 35-11 NO. 1	47.6801008	-103.32	JUNIPER	MCKENZIE	0.02	1.20	2.60	74.10
IVERSON NO. A-1	47.9332944	-103.79	ELK	MCKENZIE	0.02	1.10	1.60	63.60
BURNING-MINE BUTTE NO. 4-33	47.5790447	-103.68	BURNING MINE	MCKENZIE	0.02	0.60		69.90
ROY MOEN NO. 1	47.7739361	-103.45	TIMBER CREEK	MCKENZIE	0.02	0.20	0.50	92.60
FELLANO NO. A-1	47.8063446	-103.34	TOBACCO GARDEN	MCKENZIE	0.02	1.00	0.50	80.80
OSCAR JONSRUD NO. 1	47.9324336	-103	EDGE	MCKENZIE	0.03	1.30	5.60	71.30
FEDERAL STORM NO. 13-6	47.4048995	-103.35	BIECEGAL CREEK	MCKENZIE	0.04	1.60	1.10	77.70
OSCAR JONSRUD NO. 1	47.9324336	-103	EDGE	MCKENZIE	0.01	0.80		62.00
RIGGS NO. 10-31	47.8516012	-102.88	BLUE BUTTES	MCKENZIE	0.01	0.90		70.90
L.M. STENEHJEM NO. 2	47.9164826	-103.46	POE	MCKENZIE	0.03	0.80	0.60	81.60
SOVIG NO. 44-31	47.8497815	-103.52	SPRING CREEK	MCKENZIE	0.03	0.90	0.40	74.60
MCKEEN NO. 30-23	48.0429277	-102.82	ANTELOPE DEEP	MCKENZIE	0.04	0.70	3.10	80.60
CONOCO-NELSON NO. 41-7	47.6584557	-103.46	BUFFALO WALLOW	MCKENZIE	0.04	1.30	3.50	81.60
BRENNA-LACEY NO. 1-32	48.0185589	-102.78	ANTELOPE	MCKENZIE	0.17	5.46	11.65	79.90
MOTT NO. 32-3	48.9766655	-101.94	NEWPORTE	RENVILLE	0.07	0.70	45.30	28.40
LARSON NO. 23X-9	48.9565972	-101.97	NEWPORTE	RENVILLE	0.17	0.10	67.00	20.30
DUERRE NO. 43-5	48.9707123	-101.98	NEWPORTE	RENVILLE	0.17	0.60	74.40	15.70
OGRE NO. 1-24-1C	46.8419896	-102.36	RICHARDTON	STARK	0.09	1.10	2.10	90.70
IVERSON NO. 1	48.2713589	-102.95	BEAVER LODGE	WILLIAMS	0.07		5.60	79.40
CLARENCE IVERSON NO. 1	48.2713589	-102.95	BEAVER LODGE	WILLIAMS	0.01	0.60	1.30	70.00
B-122	48.43771	-102.94	TIOGA	WILLIAMS	0.03			
1-210 BATTERY			CAPA	WILLIAMS	0.02	2.00	2.00	66.10
BLDU I-315	48.3284193	-102.94	BEAVER LODGE	WILLIAMS	0.01	0.30	0.10	58.70
BLSU D-408	48.2795582	-102.98	BEAVER LODGE	WILLIAMS	0.09	0.50	5.30	80.60
ZIMMERMAN NO. 10-1	47.9946266	-103.98	BUFORD	WILLIAMS	0.04	0.60	1.00	60.00
BLOU NO. 8	48.27779	-102.98	BEAVER LODGE	WILLIAMS	0.13	0.14	6.00	79.75
BLOU NO. 1	48.2801754	-102.98	BEAVER LODGE	WILLIAMS	0.20	2.90	12.80	78.60
BLOU NO. 1	48.2801754	-102.98	BEAVER LODGE	WILLIAMS	0.13	1.90	6.40	78.70
BLMU O-25	48.329324	-102.93	BEAVER LODGE	WILLIAMS	0.02	1.80	1.20	61.70
SLETTE-STANGELAND NCT 1 NO.1	48.080264	-103.49	WILLOW CREEK	WILLIAMS	0.03	0.60	0.70	72.30
TIOGA MADISON UNIT NO. D-132	48.4721459	-102.92	TIOGA	WILLIAMS	0.05	1.20	97.60	1.00
TEMPLE NO. 30-16	48.3897415	-103.13	RAY	WILLIAMS	0.01	0.87		47.36
ASTRID ONGSTAD 14-22	48.4249931	-102.92	TIOGA	WILLIAMS	0.46	2.86	70.31	24.83

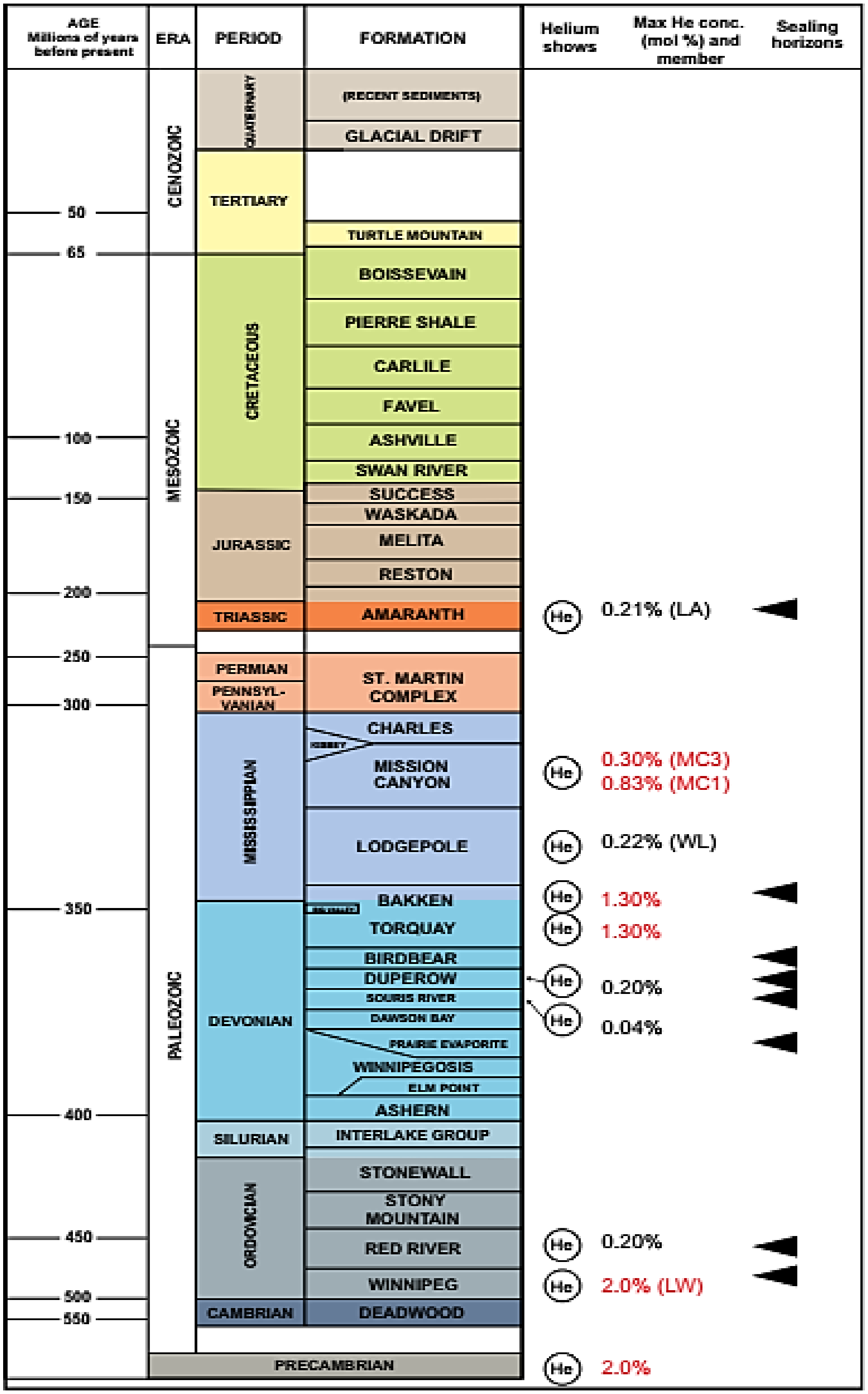

Figure 4.22. Stratigraphic column of the Williston Basin, Manitoba Canada, showing high helium values. From Nicholas, 2018.

Some of the highest helium values came from the Middle Bakken Member to Torquay Formation interval. The source of this helium is thought to be the basement Precambrian rocks and radioactive (high gamma-ray or ‘hot’) shales of the Upper Bakken Member (Jiang and Li, 2002).

The best prospects for economic helium deposits are within the Middle Bakken Member to Torquay Formation interval where the Middle Bakken Member sandstone is thick and the Upper Bakken Member shale has a strong gamma-ray (‘hot’) signature (Nicolas, 2018).

Saskatchewan currently is experiencing renewed interest in potential helium production due to increasing commodity prices (Speer and Stroeder, 2021). Helium was reported in gas analyses from wells in southwestern Saskatchewan as early as the 1950s, with anomalous values of helium up to 2.00%. Helium was produced in the early 1970s from four wells and recently three wells have produced in Saskatchewan, with another 13 wells that have recently been drilled for helium targets (Yurkowski, 2016).

With the mounting interest in helium, a study was initiated to better understand the generation, accumulation and geological setting of helium resources. This included an examination of 5,532 analyses from 4,240 wells analyses in Ministry of the Energy and Resources well files from southern Saskatchewan (Yurkowski, 2016), which identified anomalous helium concentrations in stratigraphic intervals ranging from the Cambrian to the Cretaceous.

Of these, it was found that, 17 wells have helium values of greater than 1%, with the most shows concentrated in southwestern Saskatchewan (Figure 4.23).

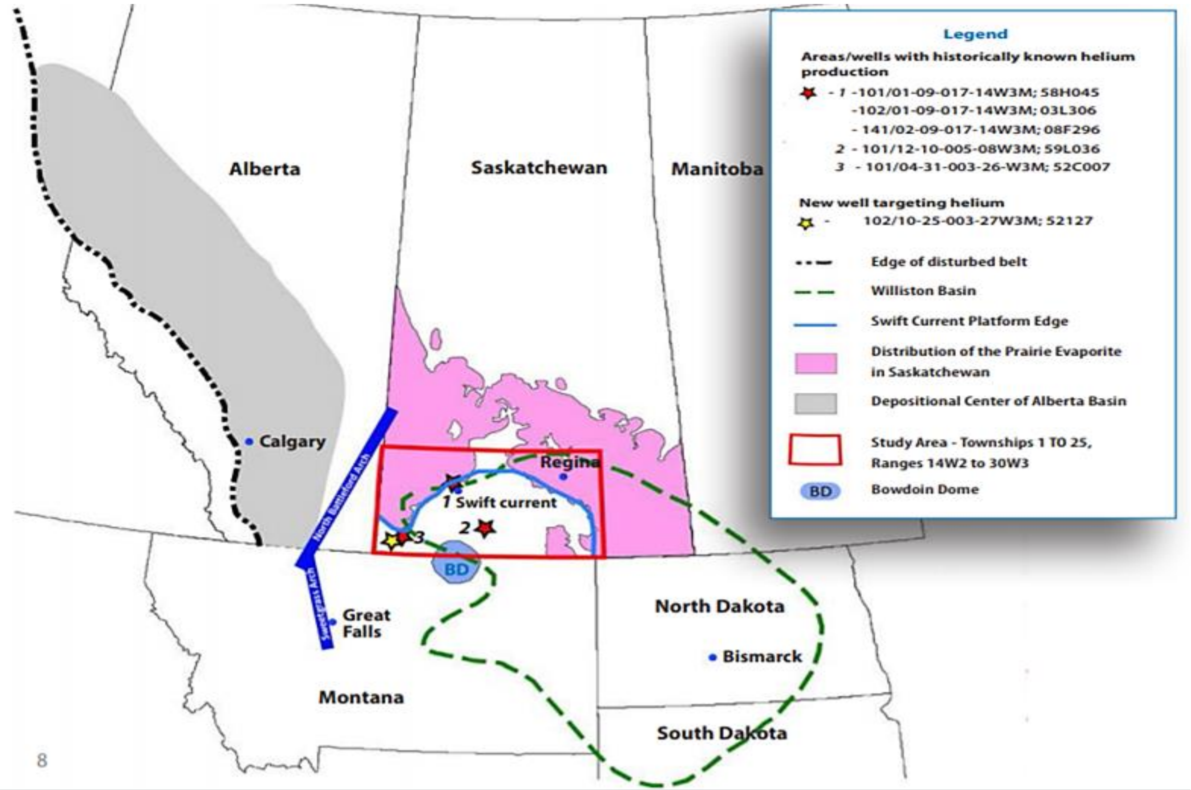

Figure 4.23. The areal location of the Williston Basin and Saskatchewan wells with high helium values. From Yurkowski, 2016.

Understanding the source, migration and trapping of the helium is critical in understanding where the economic accumulations occur. Although the physical processes required to trap economic amounts of helium are similar to hydrocarbon natural gas traps, it requires a more robust seal for its reservoir (Figure 4.24) (Burwash and Cumming, 1974).

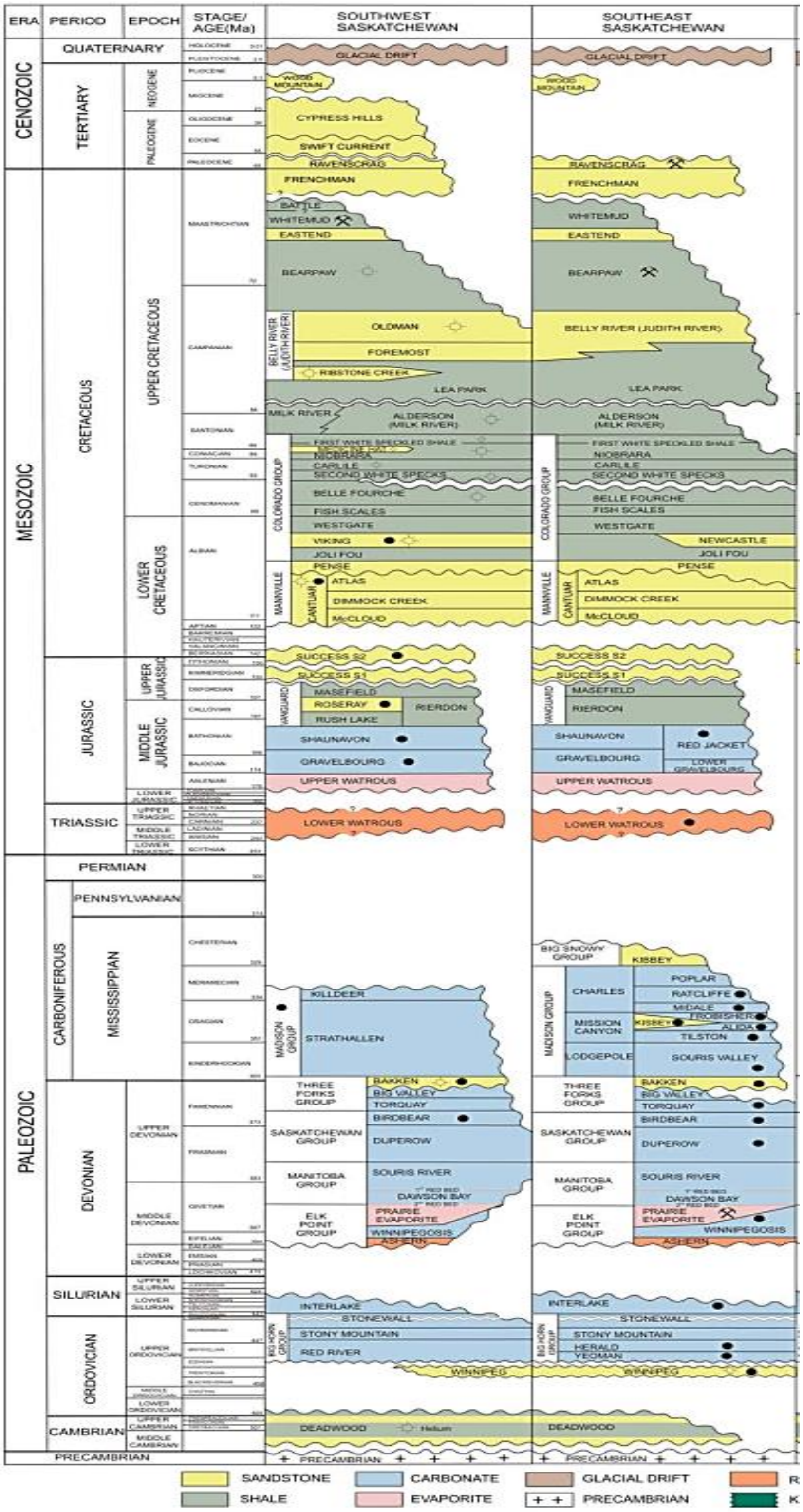

Figure 4.24. Saskatchewan's stratigraphic correlation chart (from Saskatchewan Ministry of the Economy, 2014).

Helium has been reported in gas analyses from stratigraphic intervals spanning the Cambrian to Cretaceous in the southwestern Saskatchewan Williston Basin.

The two likely models for the development of helium plays in southern Saskatchewan are: 1) generation of helium by radioactive decay of uranium and thorium in Precambrian granitic basement rocks; migration along fracture/fault systems developed throughout the Phanerozoic (Burwash, et al, 1994) by the numerous tectonic elements in this part of the province (e.g. the Great Falls Tectonic Zone); and pooling/entrapment in sediments draping structural highs with effective seals (Lee, 1963); and 2) generation of helium by radioactive decay of uranium and thorium naturally occurring in the shales of the lower Paleozoic rocks with migration into stagnant pore water, partitioning of the helium from the water into gas, and pooling/entrapment as noted above (Yurkowski, 2016).

With the interest building, and companies drilling, over the potential of large helium reserves in the Williston Basin in Manitoba and Saskatchewan (Zinchuk, 2018) in the Bakken and adjacent formations. Saskatchewan is home to numerous primary helium shows of greater than 1 percent throughout the southern portions of the province. In particular, helium has been produced in southwestern Saskatchewan from 1963 to 1977 (Yurkowski, 2016) and from 2014 to the present day.

4.4.3 Helium in the Williston Basin, North Dakota

From Manitoba to Saskatchewan's Williston Basin, helium has been noted since its discovery in southwestern Saskatchewan in 1952, with production occurring from four wells during the years of 1963 to 1977 (Yurkowski, 2016).

Helium production resumed in the region in 2014 due to the rapid grow in helium prices from the sale of the US Federal Helium Reserve. Recent reporting of gas analysis from wells in southwestern Saskatchewan suggests the Deadwood Formation and other lower Paleozoic formations tend to have the highest helium concentrations (Lutey, 2021), as expected, but economic amounts occur in the Bakken and underlying Torquay.

Natural gases with high concentrations of helium appear to also be associated with high concentrations of nitrogen. A U.S. Bureau of Mines study of 10,074 gas samples representing 6,445 reservoirs from 35 states (Tongish, 1980) found that the samples with the highest helium concentrations came from reservoirs which contained high concentrations of nitrogen (Nesheim and Kruger, 2019) (Figure 4.25).

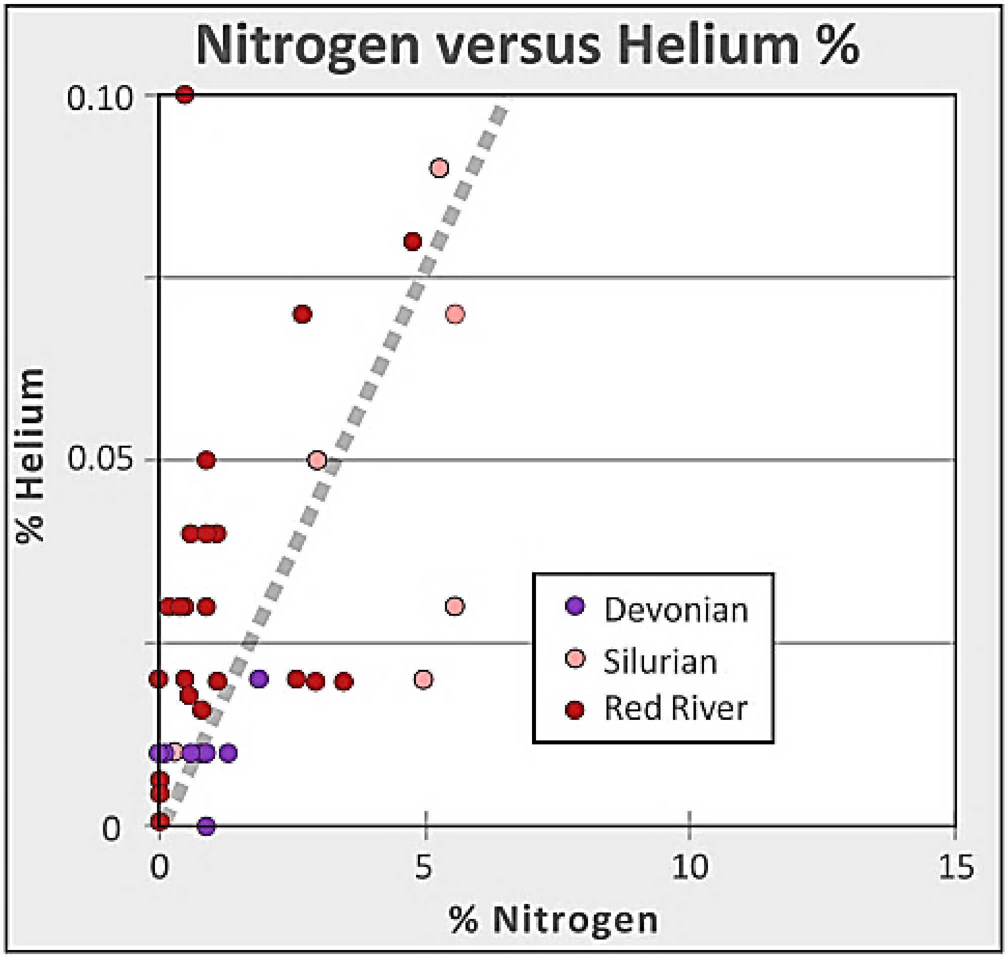

Figure 4.25. Nitrogen v. Helium in North Dakota, Williston Basin. Data from the BLM gas analysis database.

A model proposed by Yurkowski (2016) for the occurrences of helium within the Williston Basin consists of the following three components:

1. helium generation through the radioactive decay of uranium and thorium in Precambrian granitic rocks, Figure 4.26,
2. migration along fracture and/or fault systems, and
3. entrapment along structural highs (Burwash, et al, 1994).

The Williston Basin is underlain by varying types of igneous and metamorphic basement rocks (Figure 4.26), which range from mafic to felsic in composition (Sims et al., 1991).

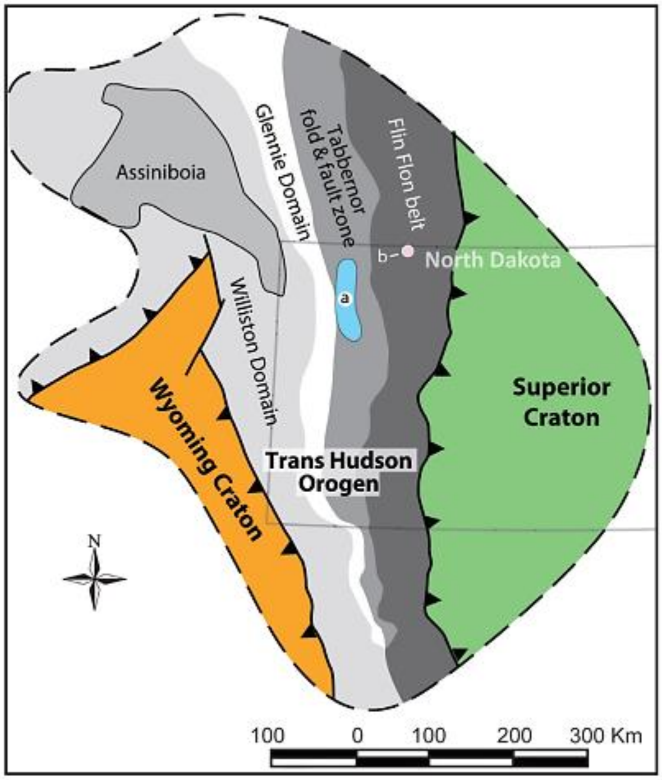

Figure 4.26. Precambrian basement terrane map for the Williston Basin. a = Nesson-Antelope trend; b = Newporte structure, potential Astrobleme. Modified from Bader, 2019; and Nesheim and Kruger, 2019.

Basement-rooted faulting exists in the basin, particularly along the western margins, (Gerhard, et al., 1987) and the north-eastern margins of the basin. Each of these previously mapped faults may create migration pathways for helium from the Precambrian basement rocks into the overlying sedimentary formations (Nesheim and Kruger, 2019).

Substantial amounts of helium may have unknowingly been produced already from at least one well in North Dakota. Amerada Hess's Pederson #14-22, the northernmost well tested along the Nesson anticline, (Figure 4.23) had a nitrogen measurement of 27.7% of the total gas in the Black Island Formation.

The Black Island went on to produce over 8 BCF of gas (Nesheim and Kruger, 2019). In addition, the upper Deadwood was perforated, flow tested, and yielded 1,300 MCF gas per day with 65.6% nitrogen. Applying the nitrogen-helium plot in Figure 4.25, the 27.7% nitrogen value correlates with 0.2% helium.

Assuming this helium value, the 8.1 BCF of Black Island gas cumulatively produced from the Pederson #14-22 would have contained ~16,000 MCF of helium, which is worth $6.40 million at a recent helium price of ~$400/MCF (Peterson, 2019).

All criteria necessary for helium accumulation within the Williston Basin of North Dakota are obviously met:

1. Precambrian igneous-metamorphic basement.
2. Fault, fractures and joint sets to allow vertical migration of helium, and,
3. Entrapment in structural highs.

How does this affect the potential of economic amounts of helium in the Williston in the Bakken?

The above criteria are all met in conventional reservoirs of Paleozoic age, but how does that apply to the unconventional Bakken Formation?

The distribution and transport of noble gases in sedimentary basins, noticeably helium, are controlled by the evolution of the sedimentary unit structure (thickness, porosity, and permeability), fluid flux from the crystalline basement into the base of the sediments and groundwater recharge events (Klasner, and King, 1986). Characterizing the migration history of sedimentary fluids and any basement fluid flux are crucial for environmental projects such as carbon sequestration and nuclear waste repositories. These are also significant elements that contribute to the emerging topics of hydrogen and helium exploration (Cheng, et al, 2019).

As helium generation from basement igneous-metamorphic rocks is more or less continuous over geological time, the highly impermeable Bakken, as it acts as source and reservoir for natural gas, would do the same for upwardly-migrating helium (Kringstad, et al, 2020).

In the stratigraphy of the Williston Basin, the Bakken is one of the few thick predominantly shale packages. The Ordovician Roughlock is relatively thin, and not as laterally extensive (McCoy, 1952) as the Bakken Group. The Devonian Prairie Formation, consisting of evaporites, siltstones, and anhydrite lenses is discontinuous across the basin, due to differential accumulation of salt during deposition, and differential removal of salt by dissolution post-deposition (Oglesby, 1988).

The proportion of helium in pore spaces which is in solution, is dependent on the partial pressure of the helium. The total pressure in the pores is generally fixed by the overburden pressure, which would mean that the partial pressure of helium is reliant on the quantities of other gases present (Gherabati, et al, 2019). This could explain why N_2 has often been cited as a ‘carrier’ (Newton and Round, 1961) gas. The timing of trap formation is key for helium systems, especially for fields which contain high levels of N_2.

Since helium and petroleum gases can occupy the same trap, the main variable which determines whether helium is still present after a significant amount of geological time is the stability of the trapping structure (Li, et al, 2019). Most of hypotheses for helium entrapment are based on the same principles as petroleum entrapment, except with greater attention paid to the pore throat radius of sealing rocks due to the small atomic radii cross-section of helium owing to its potential propensity for microseepage (Danabalan, 2017).

While evaporite deposits always make the best reservoir seals because of their lack of pores and ductility, it may be possible that shale could also suffice since helium is never naturally the primary gas in a reservoir and would therefore be in an admixture with other gases (N_2, CO_2 or CH_4)(S. Khatibi, et al, 2018).

In a natural system helium would be dependent on the partial pressures of the other gases in the reservoir for mobility since the total pressure in reservoir pores is generally fixed by the overburden pressure. Therefore, hypothetically, as long as the reservoir pressure does not exceed capillary entry pressures in the caprock, helium should remain in the trap along with the other gases and would only begin to leak if the trap was breached (Danabalan, 2017).

One other possible source for helium in the Bakken is exsolution in the presence of an existing gas phase beneath caprock/degassing of oversaturated connate water and /or direct input into a trap of a free gas phase (Ayhan, 2016). This would require a viable trap to be in place enabling a helium-rich gas accumulation to form either from the emplacement of a free gas phase or from exsolution from connate water. The microporosity found in shales could satisfy these requirements (Abba, *et al.,* 2018).

There is also the possibility of in-situ generation of helium in the nanopore systems of an organic-rich shale (Bhattacharya, and Carr, 2016). There is a growing body of evidence that gas situated within the pores of nanoporous materials may not have the same equation of state (pressure, volume, and temperature, PVT) properties as macroscopic free gas (Dobbin, 1968).

However, there is limited experimental measurement of in-situ fluid properties for gases taken up by nanoporous shales (Chakraborty, *et al*, 2020). Given the proclivity of helium in shale reservoirs, helium cannot be discounted. The underlying mechanism for gas densification could potentially be explained by adsorption, although further experimentation will be required for a definitive answer. Whatever helium is present in the shales is usually thought to be of crustal origin, as is evidenced by helium isotopes, while, in contrast, conventional reservoirs may have helium of magmatic origin (Milkov and Etope, 2019).

Even where helium generated by decay of nearby radioactive elements is caught in the same trap as hydrocarbon gas, the share of helium in the total volume of trapped gasses is extremely low (Brown, 2010). Still, it could be economic to separate and produce even extremely lean helium content (as low as 0.03% He, or even 0.015% He), if the natural gas were to be used to produce liquefied natural gas (LNG) (National Research Council, 2010; Waltenberg, 2013; Brennan *et al.,* 2017).

Thus far, reports of such low levels of helium content in natural gas that has been produced directly from hydrocarbon source rocks by hydraulic fracturing are not available (Clarke, *et al.,* 2013). Increasing use of this ‘‘shale gas’’ to produce LNG is “not likely” to result in any significant additions to helium resources (Anderson, 2017), although further study and practice is required to come up with definitive results. Until that time, given the economics and apparent ready availability of shale gas helium, one cannot discount this possibility out of hand.

One further possibility for enriched helium concentration in the Bakken is that naturally occurring radiogenic ^{4}He is present in high concentration in most shales. During rock deformation, accumulated helium could be released as fractures and fissures are created and new transport pathways are created (Bauer, Gardner, and Heath, 2016). Helium released during deformation is observable at the laboratory scale and the release is tightly coupled to the shale deformation (Mba, and Prasad, 2010). These first measurements of dynamic helium release from rocks undergoing deformation show that helium provides information on the evolution of microstructure as a function of changes in stress and strain (Bauer, et al, 2016).

Until this point, the recovery of helium from shale reservoirs has centered on shale gas, for reasons that both hydrocarbon natural gas and helium are gases. However, there is a growing corpus of evidence that helium can also reside in the liquid phase of the naturally occurring hydrocarbons extracted from shale reservoirs; i.e., helium from shale oil (Milkov and Etope, 2019).

Early work in Russia regarding the solubility of monatomic gases and nitrogen in hydrocarbons (Eremina, 1950) lead to the idea that helium, as well as other noble monatomic gasses, can be sequestered in the liquid phase of a hydrocarbon reservoir as well as in the gaseous phase. Indeed, there were even suggestions that helium could be stored, as well as transported, in the mobile waters of those aquifers which were hydrocarbon reservoir-drive mechanisms.

Decades later, work was being done, again in Russia, on the solubility of helium, carbon dioxide and nitrogen in hydrocarbon fuels. The work of Logvinyuk, Makarenkov, Malyshev and Panchenkov (1970) noted that solubility depends very little on the temperature, although the solubility of carbon dioxide does increase considerably with a reduction in temperature. Further, they noted that the solubility of gases in petroleum products increases in the following order: He-N_2-CO_2 (Logvinyuk, Makarenkov, Malyshev, and Panchenkov, 1970).

Further to this work, the solubility of the noble gases He, Ne, Ar, Kr and Xe were measured in two typical crude oils at temperatures of 25–100°C by Kharaka and Specht (1988). Here, results showed that the solubility of He and Ne in both oils is approximately the same; solubility then increases with atomic mass, with the solubility of Xe at 25°C being two orders of magnitude higher than that of He, but it did provide more data on the solubility and possible exsolution of helium in crude oil (Kharaka and Specht, 1988).

CHAPTER 5

Extraction of Hydrogen from Bakken-Sourced Methane Gas

5.1 Hydrogen: Methane Reforming, Purification, Liquefaction

Relatively recently (3 June, 2021) Mitsubishi and Bakken Energy announced their intentions to develop a "Blue Hydrogen" hub in Beulah, North Dakota (Standard and Poors, 2021), for creating diatomic hydrogen (H_2) from methane (CH_4). Hydrogen gas can be produced from hydrocarbon fuels through three basic technologies: (i) steam reforming (SR), (ii) partial oxidation (POX), and (iii) autothermal reforming (ATR) (Figure 5.1).

These technologies produce a great deal of carbon monoxide (CO) along with Synfuel. Thus, in a subsequent step, one or more chemical reactors are used to largely convert carbon *monoxide* (CO) into carbon *dioxide* (CO_2) via the water-gas shift (WGS) process (together known as SMR: Steam Methane Reformation), preferential oxidation (PrOx) or various methanation reactions (Baltrusaitis, and Luyben, 2015).

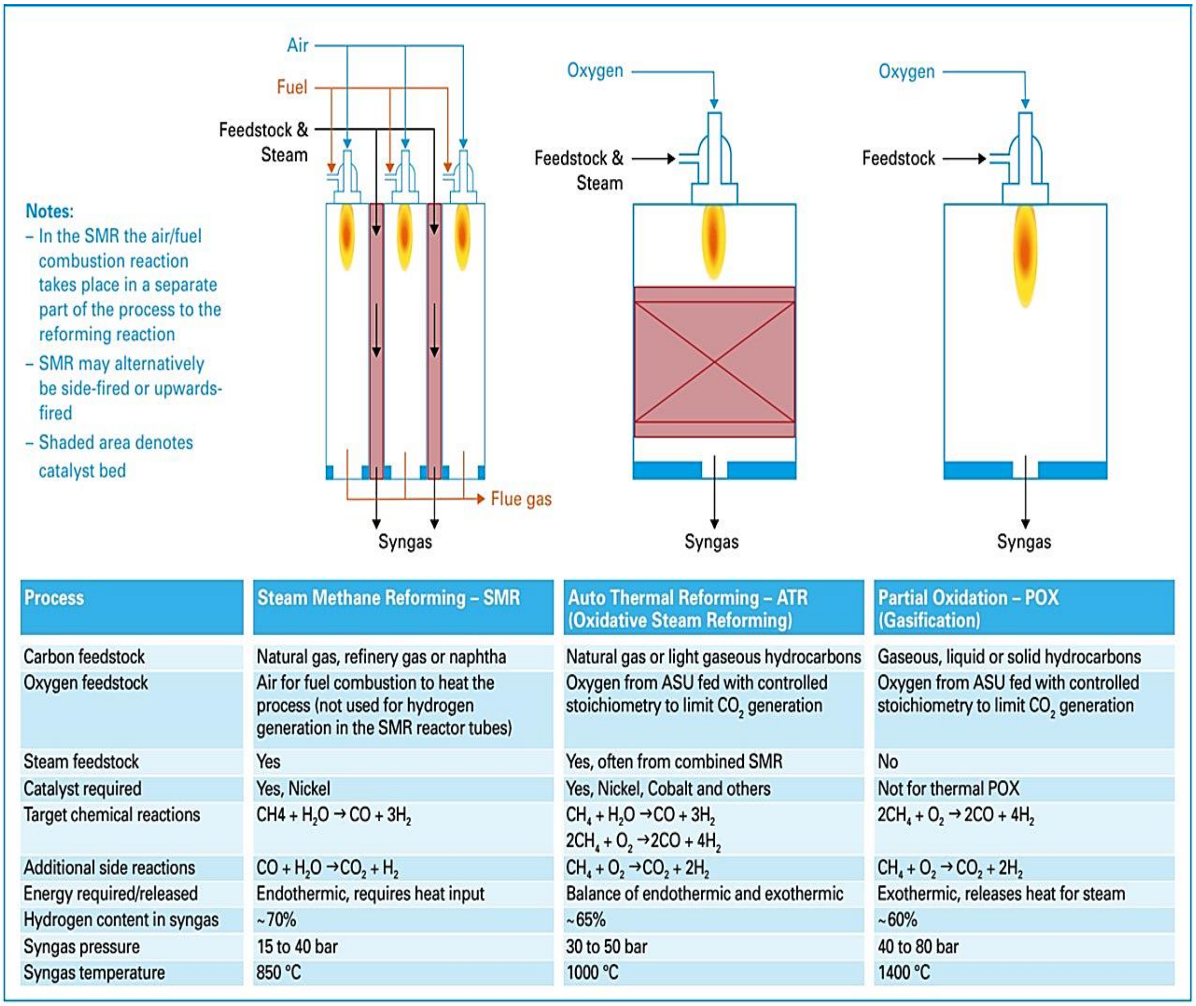

Notes:

- In the SMR the air/fuel combustion reaction takes place in a separate part of the process to the reforming reaction
- SMR may alternatively be side-fired or upwards-fired
- Shaded area denotes catalyst bed

Process	Steam Methane Reforming – SMR	Auto Thermal Reforming – ATR (Oxidative Steam Reforming)	Partial Oxidation – POX (Gasification)
Carbon feedstock	Natural gas, refinery gas or naphtha	Natural gas or light gaseous hydrocarbons	Gaseous, liquid or solid hydrocarbons
Oxygen feedstock	Air for fuel combustion to heat the process (not used for hydrogen generation in the SMR reactor tubes)	Oxygen from ASU fed with controlled stoichiometry to limit CO_2 generation	Oxygen from ASU fed with controlled stoichiometry to limit CO_2 generation
Steam feedstock	Yes	Yes, often from combined SMR	No
Catalyst required	Yes, Nickel	Yes, Nickel, Cobalt and others	Not for thermal POX
Target chemical reactions	$CH4 + H_2O \rightarrow CO + 3H_2$	$CH_4 + H_2O \rightarrow CO + 3H_2$ $2CH_4 + O_2 \rightarrow 2CO + 4H_2$	$2CH_4 + O_2 \rightarrow 2CO + 4H_2$
Additional side reactions	$CO + H_2O \rightarrow CO_2 + H_2$	$CH_4 + O_2 \rightarrow CO_2 + 2H_2$	$CH_4 + O_2 \rightarrow CO_2 + 2H_2$
Energy required/released	Endothermic, requires heat input	Balance of endothermic and exothermic	Exothermic, releases heat for steam
Hydrogen content in syngas	~70%	~65%	~60%
Syngas pressure	15 to 40 bar	30 to 50 bar	40 to 80 bar
Syngas temperature	850 °C	1000 °C	1400 °C

Figure 5.1. SMR vs. ATR vs. POX. From SbH4 Consulting, 2021.

Table 5.1. The key results of different reforming techniques. From Ayad, et al, 2018.

Composition	ATR Technique		POX Technique		SMR Technique	
	Mole flow (Kmol/hr)	Mole percent %	Mole flow (Kmol/hr)	Mole percent %	Mole flow (Kmol/hr)	Mole percent %
H_2	5 032	57.2	6 058	65.66	4 932	59.7
CO	2 516	28.6	3 131	33.93	1 670	20.2
CH_4	457	5.3	-	-	1 429	17.3
CO_2	166	1.9	-	-	33	0.4
O_2	-	-	1	0.01	-	-
H_2O	579	6.6	7	0.08	164	2
N_2	30	0.4	30	0.32	30	0.4
Total Flow	8 780	100	9 227	100	8 258	100

The above table notes the typical efficiencies of each of the three main reforming techniques. The Hydrogen Hub in Beulah, ND has chosen SMR (Steam Methane Reformatting) due to its relative efficiency given its lower overall cost and lack of dedicated oxygen supply (Bakken Energy, 2021).

Hydrogen Color

"Blue Hydrogen" is purported to be one type of 'greener' (i.e., more environmentally 'friendly') sources of hydrogen out of 9 differing polychromatic models:

Figure 5.2. The varying different 'colors' of hydrogen production. From H_2 Bulletin.

The so-called 'colors of hydrogen' (Nationalgrid, 2021) are based primarily on the power source used to generate the hydrogen, the process utilized, and whether carbon dioxide is captured and sequestered or released to the atmosphere.

The nine types polychromatic hydrogen are as follows:

Black or brown hydrogen is generated from coal. The black and brown colors refer to the type anthracite or bituminous (black) and lignite (brown) coal. The gasification of coal is the method used to produce hydrogen. However, it is a very polluting process; as CO_2 and carbon monoxide are produced as by-products and released to the atmosphere and not captured or sequestered. For some, it is equivalent to a circular argument (Figure 5.3).

Figure 5.3. Coal liquefaction to oil solidification. From Harris and Bailey, 1977.

Blue hydrogen is sourced from fossil fuel, primarily through coal gasification and from reforming of methane from natural gas streams. However, CO_2 is captured and stored underground (carbon sequestration) or otherwise sequestered. Companies are also trying to utilize the captured carbon called carbon capture, utilization and storage (CCUS). Utilization is not essential to qualify for blue hydrogen. As no CO_2 is emitted, the blue hydrogen production process is categorized as carbon neutral. Reforming of methane via steam will be the process of note in this paper as it is being planned for use in the Williston Basin using Bakken-sourced natural gas.

Gray hydrogen is produced from fossil fuel and commonly uses steam methane reforming (SMR) method. During this process, CO_2 is produced and continually released to the atmosphere, rather than captured or used.

Green hydrogen is produced through the electrolysis of water by using renewable electricity; biomass, windfarm, etc. It is called green is that there are no CO_2 emissions during the production process. Water electrolysis is a process which uses electricity to decompose water into molecular hydrogen gas and oxygen; which is constrained by the inherent inefficiency and expense of electrolysis.

Pink hydrogen is generated through electrolysis of water by using electricity produced from a nuclear power plant.

Purple hydrogen is made though using nuclear power and heat through combined thermochemical electrolytic splitting of water.

Red hydrogen is produced through the high-temperature catalytic splitting of water using nuclear power thermal as an energy source.

Turquoise hydrogen can be extracted by using the thermal splitting of methane via methane pyrolysis. The process, though at the experimental stage, remove the carbon in a solid form (Dry Ice) instead of CO_2 gas.

White hydrogen refers to naturally occurring hydrogen.

(Modified from “Hydrogen colors codes”, https://www.h2bulletin.com/knowledge/hydrogen-colours-codes/, accessed 8-2021).

"Blue Hydrogen" which generates diatomic hydrogen (H_2) derived from natural gas through the process of steam methane reforming (SMR) and/or Autothermal Reformation plus the WGS (Water Gas Shift) reaction, are the processes which will be discussed in-depth in this work.

SMR

Steam methane reforming (SMR) Figure 5.4, is a process in which methane from natural gas is heated, with steam, usually with a catalyst, to produce a mixture of carbon monoxide and hydrogen used in organic synthesis and as a fuel. SMR is the most widely used process for the generation of hydrogen (Air Liquide Engineering & Construction, 2021).

In SMR, methane reacts with steam under 3-25 bar pressure (1 bar = 14.5 psi) in the presence of a metallic catalyst to produce hydrogen, carbon monoxide, and carbon dioxide. Steam reforming reaction is endothermic (US Department of Energy, 2019), i.e., heat must be supplied to the process for the reaction to proceed.

In a "water-gas shift reaction," (Callaghan, 2006) a continuation of the SMR process which primarily produces hydrogen and carbon monoxide, the carbon monoxide and steam are again reacted using a catalyst, typically nickel or platinum, to produce carbon dioxide and additional hydrogen (Faheem, et al, 2021).

In a final process step called "pressure-swing adsorption," or PSA, carbon dioxide and other impurities are removed from the gas stream, leaving essentially pure hydrogen (Shi, et al, 2018). In lieu of PSA, selective membranes can be utilized to eliminate contaminants and leave the yield with near pure hydrogen (Figure 5.4). Steam reforming can also be used to produce hydrogen from other fuels, such as ethanol, propane, or even gasoline.

Steam-Methane Endothermic Reforming Reaction

$$CH_4 + H_2O \text{ (+heat)} \rightarrow CO + 3H_2$$

Water-Gas Shift Reaction

$$CO + H_2O \rightarrow CO_2 + H_2 \text{ (+ small amount of heat}^{\uparrow}\text{).}$$

This occurs while generating 1 kg. high purity H_2, SMR will also generate ~7 kg CO_2 (Soltani, et al, 2014).

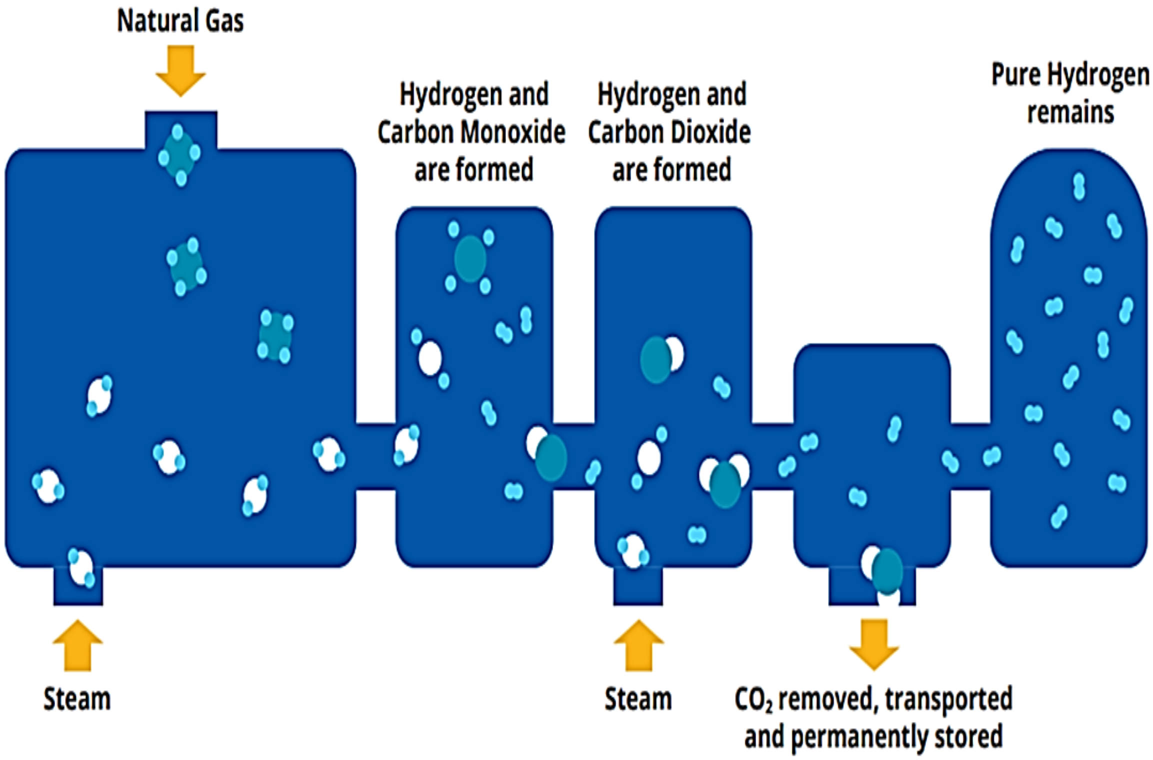

Figure 5.4. Schematic of Steam Methane Reforming. From Takahashi, et al, 2021.

5.1.1 Detailed Process Description: Steam Methane Reforming (adapted from Soltani, et al, 2014; Vergis, 2007; Janssen, 2018; and Arzamendi et al, 2013, et al)

Large-scale catalytic steam reformation of natural gas is the most common, and the least expensive method of producing hydrogen commercially available today. Nearly 50% of the world's hydrogen is produced via steam methane reformation (Velazquez and Dodds, 2017). On average, natural gas is approximately 95% methane, with the balance being higher hydrocarbons (ethane, propane, butane, heptane, etc.) and other low-quantity contaminants, such as H_2S, N_2, and CO_2.

SMR is widely used, especially in the United States, to provide high purity hydrogen to the chemical, petrochemical, and refining industries. It also has the added benefit of enabling the capture, storage and eventual sequestration of large volumes of carbon dioxide (CO_2) as a by-product (Collodi, et al, 2017).

Steam Methane Reforming or Reformatting is a multi-stage process that incorporates feedstock gas pre-treatment (deamination, dehydration, etc.); catalytic reforming; high temperature water–gas shift; low temperature water–gas shift; purification; and compression/liquefaction (Himmelstein, 2021). Descriptions of each major component technology are based on Figure 5.5.

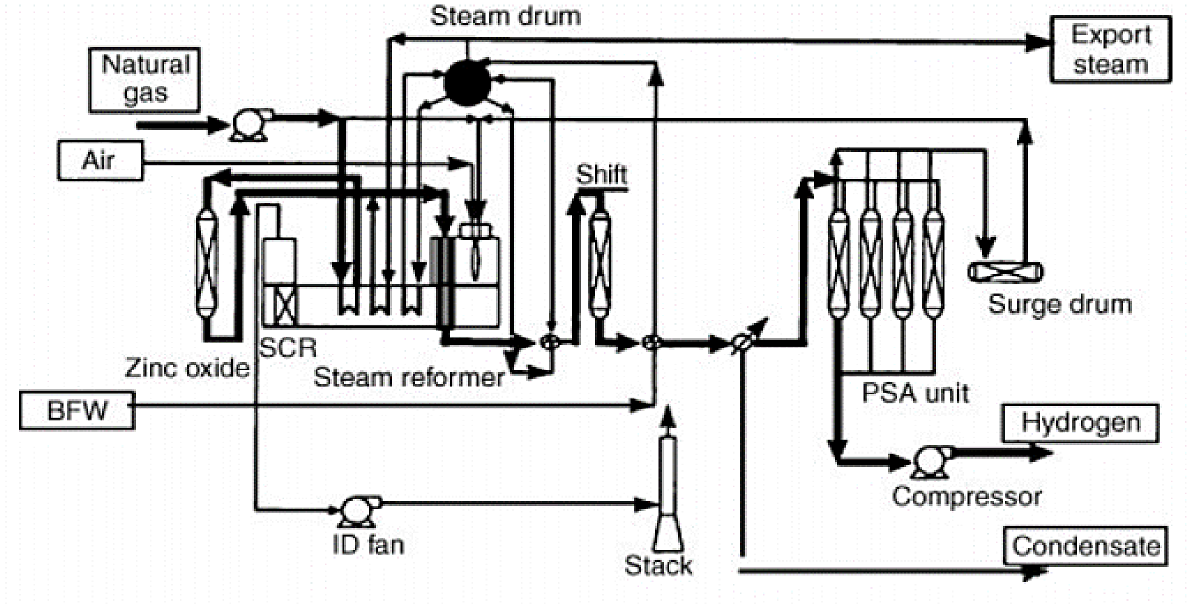

Figure 5.5. Simplified Block Diagram of an SMR system. From Vergis, 2007.

- Feedstock: The natural gas to be used must be cleaned and compressed before it undergoes reformation. Gas feed pre-treatment is generally required, since untreated natural gas nearly always contains sulfur, iron and other undesirable compounds (Currence, Rapavi, and Clifford, 2015). Pre-treatment and handling of compressed natural gas is easier and cheaper than that required for coal, biomass, or any other solid carbonaceous matter used in gasification (Himmelstein, 2021).
- Purification (Desulfurization): After the feed is compressed, natural gas undergoes desulfurization to remove traces of sulfur from the gas by removal or amelioration of primarily hydrogen sulfide (H_2S). Desulfurization of the feed gas, which is usually carried out utilizing a bed of zinc oxide (Song, et al, 2021), is needed since sulfur can poison the reformer catalyst. Iron chelation or scrubbers must also be employed as the

iron can plate off the internals of the stage, causing restrictions, unstable pressure regimes, and significantly reduced pass through (Shi, et al, 2018).

- Selective Catalytic Reduction (SCR): Low NOx burner technology is typically not able to meet strict pipeline and environmental regulations alone and therefore, new SMRs also require the addition of an SCR unit to the stack (O'Leary, et al, 2004). Here liquid ammonia is vaporized and injected into the flue gas, which passes over a hexahedral or honeycomb-shaped vanadium or titanium oxide (V_2O_5 - TiO_2: Rutile-Brookite) catalyst.

The ammonia reacts with NOx in the presence of oxygen to form nitrogen and water vapor. By varying the ammonia injection rate, NOx is controlled to the desired level.

- Reformation: After pre-treatment, the feed gas is mixed with steam at an appropriate steam-to-carbon mole ratio of ~3, to prevent the production of solid carbon or coke, which can build up on the catalyst and plug the reactor tubes. The catalytic steam reforming reaction (CSRR) takes place at pressures of approximately 3-25 bar (Othmer, 1998) and relatively high temperatures (650-900°C). The reformation is heightened by high temperature and steam; however, it is reduced by higher pressure. Advancements in reformer technology (i.e., high pressure catalyst tubes) will allow for reliable hydrogen production even at higher operating pressures (Price, and Mahaley, 2013).

$$CH_4 + H_2O\ (g) \leftrightarrow CO + 3H_2\ (\Delta H = {}^{+}206\ \text{kJ/mol}\ CH_4)\ (2\text{-}1)$$

The catalysts, typically nickel based, are packed into tubes and the heat needed for reaction shown above is provided externally by combustion of additional natural feed or purge gas. Environmental controls appreciably add to the upfront capital and operating costs of a hydrogen production facility. The SMR process is a more environmentally acceptable process of producing hydrogen than gasification (Naterer, Jaber, and Dincer, 2010).

Low NOx burners utilize multi-staged fuel combustion and flue gas recirculation to minimize NOx production. (Staged fuel combustion involves introducing the fuels at different locations to create two or more combustion zones (Pfaff, and Kather, 2009)). Tail gas from the Pressure Swing Adsorption (PSA) (Gomes and Yee, 2002) unit provides bulk of the heat input to the furnace, with natural gas (methane) for startup and control.

Once the reformer is heated, the unit can operate with 100% PSA fuel. The basic layout has the convection section and the stack mount on top, with a process gas waste heat boiler located underneath. A steam drum is typically mounted on top of the reformer (Tugnoli, et al, 2008).

- Shift: The synthesis gas mixture ("syngas" is a mixture of hydrogen and CO after the first stage of reforming (Go, et al, 2009)) is sent to the high and low temperature shift reactors, where additional hydrogen is produced via the water–gas shift reaction:

$$CO + H_2O\ (g) \leftrightarrow CO_2 + H_2\ (\Delta H = -41\ kJ/mol\ CO)\ (2\text{-}2)$$

The reaction in equation 2-2 is favored by lower temperatures as opposed to the reformer reaction (Reddy, and Smirniotis, 2015).

To offset the slower reaction dynamics at lower temperatures, solid Co-Mo catalysts are used. To take advantage of the higher temperatures generated, a two-stage water-gas shift reaction is generally used, with the high temperature stage operating at ~ 400°C and the low temperature stage at ~ 250°C (Ozcan, H., and Dincer, I., 2015).

The exit gas contains primarily H_2, and also CO_2, H_2O and small amounts of CO, methane and higher hydrocarbons unless these have been mitigated through multi-stage pre-treatment. Since residual CO leaving the primary shift converter is recovered in the PSA unit as reformer fuel, the gain in plant efficiency if a second stage of shift is added is less when compared to the increase in equipment cost (Collodi, et al, 2017). The costs involved for the shift reactions are high, but lower when compared to the same process taking place in gasification. This can be attributed to the higher amounts of steam required to shift the larger amounts of CO generated for an equivalent amount of hydrogen (Garbarino, et al, 2020).

- Pressure swing adsorption (PSA): After cooling the raw gas and separation of process condensate, a PSA unit is used to purify the raw H_2 (Shi, et al, 2018). They function at about 20 bar and reach molecular H_2 separation efficiencies in the range 85–90%. It is the most common process used in large scale multi- systems, where very high purity hydrogen (99.999%) at ~ 30 bar is the desired product (James, et al, 2016).

  The adsorbent used is a mixture of activated carbon and zeolites which removes all of the contaminants from the hydrogen product in a single step (Lopes, et al, 2009). With adjustments to the PSA operation, one can also produce a very high purity CO_2 stream (Bains, et al, 2017) for sequestration or for sale (CCUS), in addition to the hydrogen stream, however the purity of the hydrogen might suffer slightly (Okken, PA, 1992). Tail gas from the PSA unit can be once again used as reformer fuel (Reddy, and Smirniotis, 2015).

- Compression: Following the PSA purification step, hydrogen gas is compressed to ~60 bar and sent to steam generators as shown in the Figure 1.2.1.3 (Wu, and Kuo, 2015).
- Thermal recovery: Heat recovery apparatus include mixed feed (gas and steam) preheat, feed-gas preheat, steam generation, and steam superheating (Pashchenko, 2019). The

reformer furnace process outlet is cooled in a waste heat boiler by a heat exchanger with recirculating feed-water to produce steam. This steam can be exported to a nearby refinery or petrochemical facility for process needs and/or converted into electricity (Pashchenko, 2020).

5.2 Autothermal Reforming (ATR)

Autothermal reforming (ATR) utilizes both oxygen (O_2) and carbon dioxide (CO_2) or steam (SMR: see § 5.2) in a reaction with methane (CH_4) to form syngas, a combination of hydrogen (H_2), carbon monoxide (CO) and carbon dioxide (CO_2) (Ortiz, et al, 2011).

Autothermal reforming combines the steam reforming reaction and fuel oxidation into a single unit, the exothermic oxidation providing the heat for the endothermic reforming process. ATR yields higher H_2 production than partial oxidation (POX) and faster start-up and response times than steam reforming (SMR) (Chen, et al, 2010). The reaction occurs within a single chamber where the methane feedstock is only partially oxidized. The reaction is exothermic due to this oxidation.

When Autothermal Reforming utilizes uses carbon dioxide, the H_2:CO ratio produced is 1:1; when Autothermal Reforming uses steam, the H_2:CO ratio produced is 2.5:1. (Ghoneim, et al, 2016).

The reactions can be described in the following equations, with using CO_2:

$$2\,CH_4 + O_2 + CO_2 \rightarrow 3\,H_2 + 3\,CO + H_2O \text{ [Syngas]}$$

And using steam:

$$4\,CH_4 + O_2 + 2\,H_2O \rightarrow 10\,H_2 + 4\,CO$$

The outlet temperature of the syngas is between 950–1,100°C and outlet pressure can be as high as 100 bar.

The primary difference between Steam Methane Reforming (SMR) and Autothermal Reforming (ATR) is that SMR uses only air for combustion as a heat source to create steam, while ATR uses purified oxygen. The advantage of ATR is that the H_2:CO can be varied, which can be useful for producing specialty products. By adding the Water Gas Shift (WGS) reaction with ATR, you have SMR equivalence (Baltrusaitis, andd Luyben, 2015).

However, SMR can be run in conjunction after ATR to eliminate excess carbon monoxide and provide for a higher degree of carbon capture, usage and sequestration (CCUS).

5.2.1 Detailed Process Description

Autothermal reforming (ATR) is the combination of POX and SMR in one reactor. Methane is partially oxidized in a combustion zone, while superheated steam is injected in a SMR zone. Hence, both the POX and the SMR reactions are simultaneously active (SBH4.de, 2021). This concept also requires a metallic element (ruthenium, rhodium, palladium, osmium, and iridium) or nickel-based catalyst bed in the steam reforming section of the reactor. The primary advantages of this systemic process are that the exothermic POX reaction is expended by the endothermic SMR reaction (Xu, et al, 2017). This creates a closed system, impounded from an external heat supply. Secondarily, since the oxidation occurs within the reaction chamber, flue gas is not produced, thus so reducing the instance of local emissions.

The autothermal reforming (ATR) process for hydrogen production saves substantial exothermic energy for the reforming reaction as compared with endothermic steam methane reforming (SMR). Nevertheless, it requires a supply of purified oxygen, for which a cryogenic air separation unit (ASU) is needed (Pfaff and Kather, 2009). This processing need hinders the adoption of ATR over SMR in industrial applications because of both the high capital and operating costs (Kim, et al, 2021). However, when used in sequence, SMR can be added to run in conjunction with ATR to both lower costs of pure O_2 and eliminate CO in favor of CO_2 (Baltrusaitis, and Luyben, 2015).

ATR combines the effects of both the endothermic steam reforming and the exothermic partial oxidation by feeding the fuel together with the oxidant (air fed or oxygen fed) and steam over a catalyst in a fixed bed reactor (Halabi, et al, 2008).

In the autothermal reforming process, the organic feedstock (e.g., natural gas) and steam (and sometimes carbon dioxide) are mixed directly with oxygen and air in the reformer. The reformer itself comprises a refractory-lined vessel which contains the catalyst, together with an injector located at the top of the vessel (Speight, 2015). Partial oxidation reactions occur in a region of the reactor referred to as the combustion zone. It is the mixture from this zone which then flows through a catalyst bed where the actual reforming reactions occur. Heat generated in the combustion zone from partial oxidation reactions is utilized in the reforming zone, so that in the ideal case, it is possible that the autothermal reforming process can exhibit heat balance (Loukou, 2017).

When the autothermal reformer uses carbon dioxide, the H_2:CO ratio produced is 1:1; when the autothermal reformer uses steam, the H_2:CO ratio produced is 2.5:1 (Swee Leong, 2003). The reactions can be described in the following equations, using CO_2:

$$2CH_4 + O_2 + CO_2 \rightarrow 3H_2 + 3CO + H_2O + \text{heat}$$

Using steam:

$$4CH_4 + O_2 + 2H_2O \rightarrow 10H_2 + 4CO$$

Here, the Water Gas Shift (WGS) reaction is required to convert CO into CO_2:

$CO + H2O \rightarrow H_2 + CO_2$.

5.3 ATR v. SMR

The difference between SMR and ATR is how heat is provided to activate the endothermic steam reforming reaction. In SMR, the catalyst is contained in tubes that are heated by an external burner. In ATR, a portion of the natural gas is burned to raise the temperature of the process gas before it contacts the catalyst (Myers, et al, 2002).

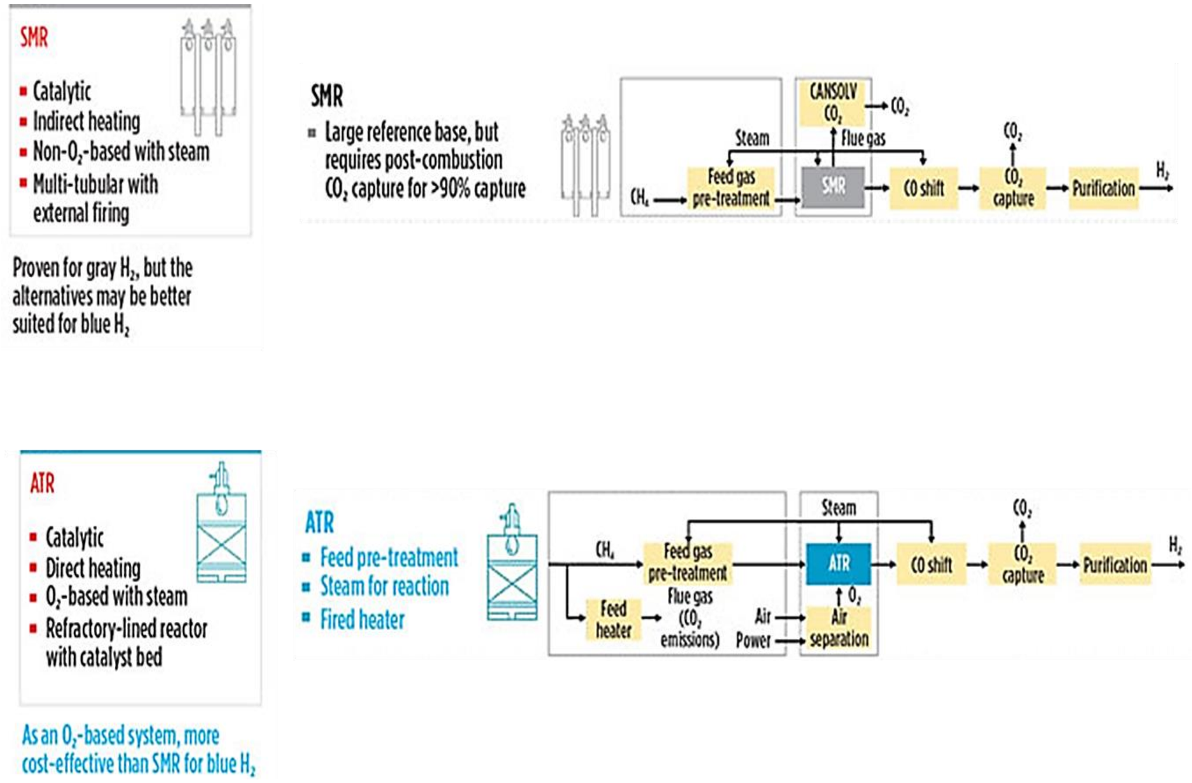

Figure 5.6. ATR v. SMR process schematic comparison.

The ATR process will produce a *syngas* (Synthetic Natural Gas) with very favorable H_2- to - CO ratio for downstream usage in chemical synthesis. The ratio should be ~2 for Fischer – Tropsch liquids (ammonia) or methyl alcohol synthesis (Exterran, 2015).

ATR has the advantages of not requiring external heat and being simpler and less expensive than SR of methane (Kalamaras, 2013), but requires the water gas shift (WGS) reaction for CO removal and its conversion to H_2.

ATR requires pure oxygen in high volumes, the cost of such an air liquification/ differentiation plant is not inconsiderable (Armor, 2005).

Autothermal reforming (ATR), steam is added in the catalytic partial oxidation process. ATR is a combination of both steam reforming (endothermic) and partial oxidation (exothermic) reactions (Chen, et al, 2021).

ATR has lower energy requirements to compensate for the effects of endothermic reactions, (steam reforming) and exothermic reactions (partial oxidation) (Chen, et al, 2021).

Another significant advantage of ATR over SR process is that it can be shut down and started very rapidly, while producing a larger amount of hydrogen (Kalamaras, and Efstathiou, 2013).

ATR presents low specific consumption, and there is effective control over the H_2/CO ratio by adjusting the feed rates of oxygen and steam (Cai, et al. 2006) and as an operational bonus, ATR is a soot-free operation.

- Limitations
    - Must use a clean, light hydrocarbon feed.
    - Expense of oxygen; air or LOX plant.
    - Limitation in H2 pressure.
    - Limitation in exit temperature.
    - Excess steam production.
    - Requires WGS for CO to CO2 conversion with hydrogen.
    - Needs waste heat boiler to limit Bouduard carbon formation* (Velazquez, and Dodds, 2017).

*When a gas rich in CO is cooled to the point where the activity of carbon exceeds one, the Boudouard reaction can take place. Carbon monoxide then tends to disproportionate into carbon dioxide and graphite, which forms soot.

The following are the advantages of using the autothermal reforming process: (1) compact in design, hence less associated footprint, (2) low investment, (3) economy of scale, (4) flexible operation – short startup periods and fast load changes, and (5) soot-free operation (Speight, 2014).

Steam methane reforming has its own advantages and disadvantages:

- SMR already incorporates the WGS reaction, thus reducing CO for H_2 and CO_2 (Faheem, et al, 2021).
- Recovery of the heat from the combustion products can be implemented in order to improve the efficiency of the overall process (Jadhao and Thombare, 2013).
- The deposition of carbon via the Boudouard reaction can be an acute problem with the use of nickel-based catalysts in the primary reformer (Bain, et al, 2017).
- A major challenge in steam reforming development is the energy intensive nature of the process due to the high endothermic character of the reactions (Yancheshmeh, et al, 2016).
- Conventional steam reforming plants operate at pressures between 200 and 600 psi with outlet temperatures in the range of 815 to 925 °C. However, analyses have shown that even though it is more costly to initially construct, a well-designed SMR can produce hydrogen more cost-effectively than an ATR in smaller applications (BNP Media, 2004).

- Limitations:
  - Carbon formation at low steam; carbon ratio.
  - Higher hydrogen pressure limits CH_4 conversion.
  - High CH_4 conversion requires high temperature.
  - Excess steam production.
  - Cooling by waste heat boiler to limit Bouduard carbon formation (Pashchenko, 2019).
  - Low NOx levels required in stack gas (White, et al, 2009).

5.4 Combined Reforming

Combined reforming incorporates the combination of both steam reforming and autothermal reforming. In such a configuration, the hydrocarbon (e.g., methane) is first only partially converted, under relatively mild conditions, to synthesis gas in a relatively small steam reformer (Dybkjær, and Aasberg-Petersen, 2016).

The off-gas stream from the steam reformer is then sent to an oxygen-fired secondary reactor, the autothermal reforming reactor. Here, the unreacted methane is converted to Syngas by partial oxidation followed by a steam reforming (York, et al, 2003).

Another configuration requires the hydrocarbon feed to be split into two streams which are then fed in parallel to the steam reforming and autothermal reactors (Oh, and Song, 2018).

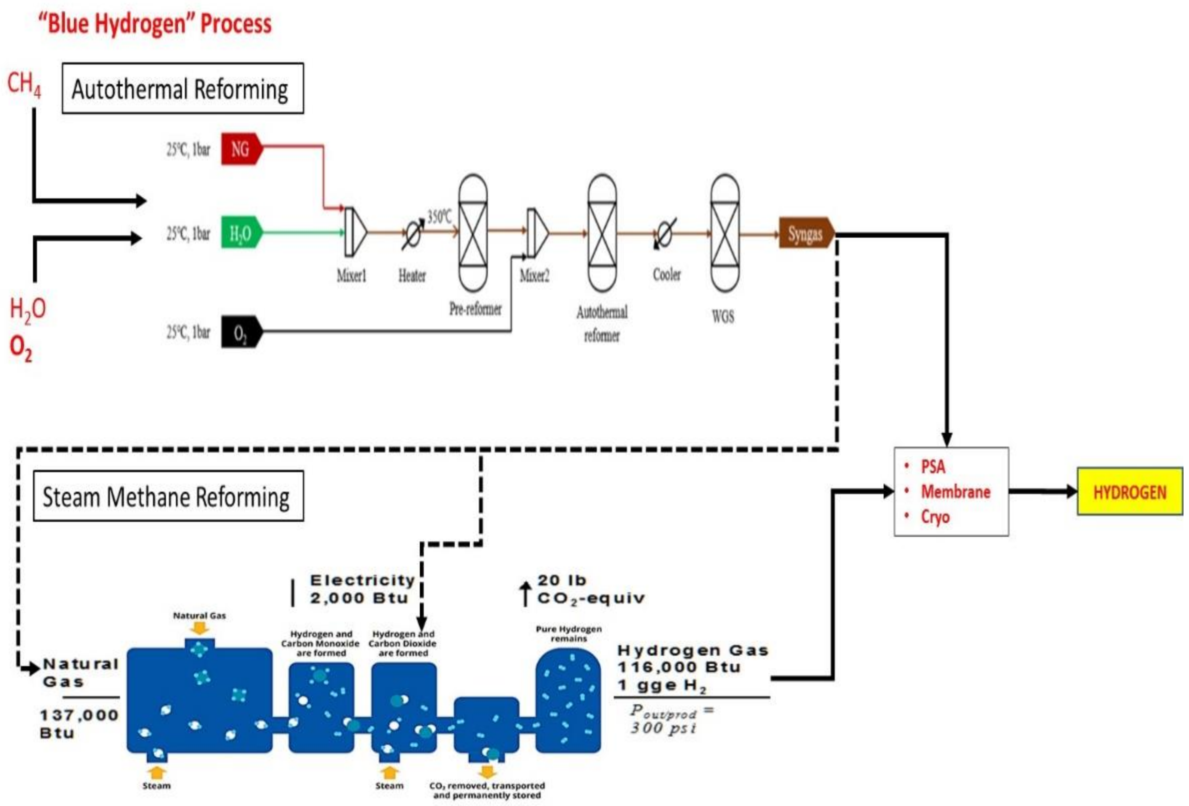

Figure 5.7. Conceptual combined ATR-SMR methane-hydrogen reformer. The final conversion of hydrocarbons is carried out mainly through steam reforming and WGS reactions.

Process

Beginning with Autothermal reforming (ATR), which uses purified oxygen from an on-site liquid air or LOX plant, with carbon dioxide or water steam in a reaction with a methane feedstock heated and compressed to form syngas. Syngas is an intermediate feedstock mixture consisting primarily of hydrogen, carbon monoxide, and carbon dioxide (Aasberg-Petersen, et al, 2011). Syngas can be further processed to create Synthetic Natural Gas, or ammonia and methanol (or methyl alcohol) (Trop and Goricanec, 2016). From this point, for hydrogen production, the Syngas requires undergoing WGS (Water Gas shift) via SMR (Figure 5.8).

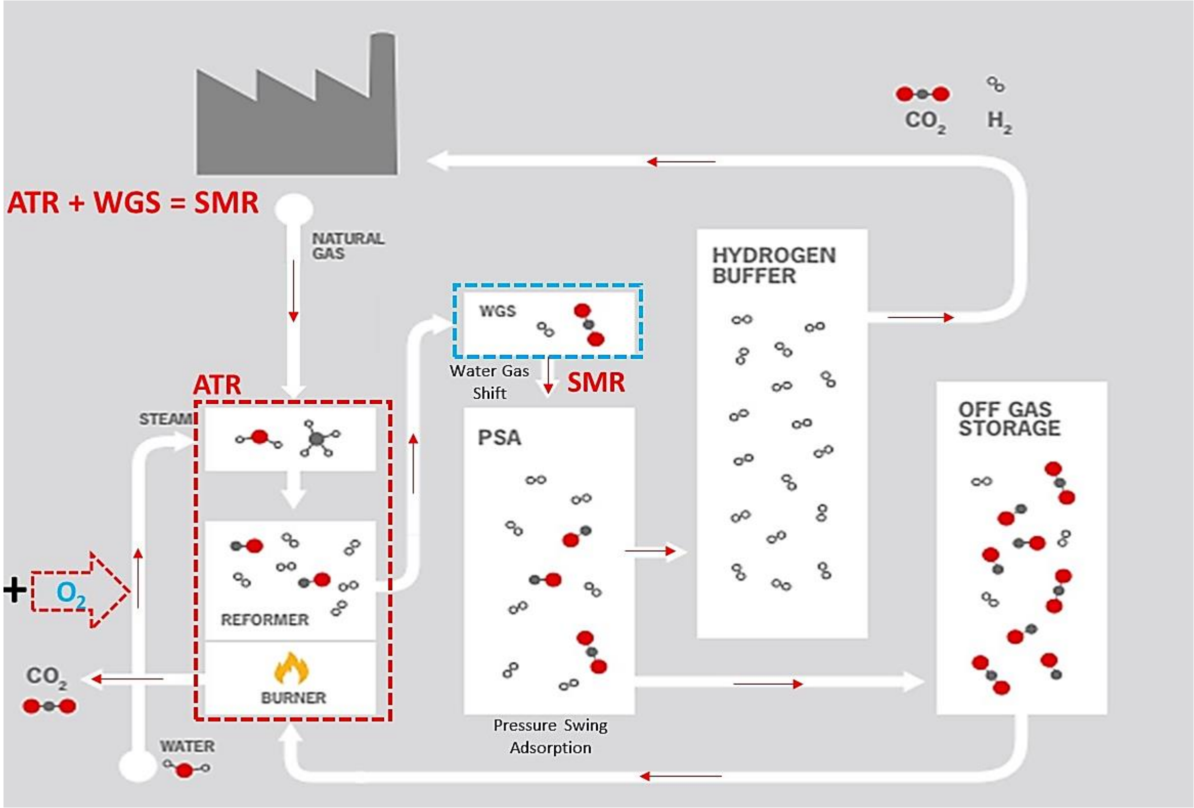

Figure 5.8. Schematic illustrating that ATR + WGS = SMR. Note: ATR (in red box) requires dedicated oxygen input (red arrow).

Steam reforming (SR), typically referred to as steam methane reforming (SMR) uses an external source of hot gas (heated from feedstock) to heat tubes where a catalytic reaction takes place that converts steam and lighter hydrocarbons such as methane, biogas or refinery feedstock into hydrogen and carbon monoxide (Syngas) (Nguyen. and Clausen, 2018).

Syngas reacts further via the WGS reaction ($CO + H_2O \rightleftharpoons CO_2 + H_2$) to produce more hydrogen and carbon dioxide, and less carbon monoxide, in the reactor. From there the hydrogen undergoes SPA (swing pressure adsorption (Marcoberardino, et al, 2018)) for concentration and purification, while CO_2 is extracted via an amine plant or dedicated membranes for CCUS (Novak Mavar, et al, 2019).

Both ATR and SMR are catalytic reactions; using nickel or platinum group metals as catalysts.

The main difference between SMR and ATR is that SMR only uses oxygen via air for combustion as a heat source to create steam, while ATR directly combusts oxygen (Salkuyeh, Saville, and MacLean, 2017).

Advantages of combined ATR and SMR:

- According to the best fit solution, the process is available as a standalone technology or as ‘Combined Reforming’ with Steam Methane Reformer.
- Syngas is adjustable to downstream usage offering a wide field of applications.
- Syngas components can be separated into diatomic hydrogen, carbon monoxide and carbon dioxide; where hydrogen can be purified and liquified and CO_2 extracted for CCUS (Mahant, Linga, and Kumar, 2021).
- High-pressure steam can be generated. (After Linde Engineering, 2021).

CHAPTER 6

Helium: Extraction, Purification, Liquefaction

6.1 Occurrences of Helium

Virtually all natural gas produced contains some amount of helium (Cook, 1979); however, this incredibly useful gas is rarely tested for in normal well evaluations (Danabalan, et al, 2021).

Helium, being a noble gas, is inert, forms no compounds or molecules as it is totally non-reactive (Grandinetti, 2018). Therefore, it found associated with natural gas much in the same manner natural gas is collected into porous reservoirs with impermeable regional seals.

Where the natural gas originates from organic matter subjected to eons of high temperatures and pressures, it is thought that most helium is generated through the radioactive decay (alpha decay) of the heavy isotopes of Uranium (Anderson, 1998); specifically, Uranium-238, Uranium-235, and Thorium-232. Uranium-238 is the most common isotope, constituting 99.275% of all uranium in the earth’s crust (Grynia, and Griffin, 2017).

Typical rocks that contain large amounts of Uranium and Thorium are basement igneous and metamorphic rocks, and to a lesser extent, black, organic-rich shales. Therefore, Meso- and Neoproterozoic sources of natural gas will typically have higher helium contents than rocks of a younger age (Priyatkina, et al, 2016).

For instance, the Precambrian-sourced Kovykta Field in Eastern Siberia, RSFSR has a helium content of over 3.0% (Ghori, et al, 2009). Contrastingly, North Field (Permocarboniferous), the world's largest non-associated gas field, has a helium content of less than 0.04% (Manning, 2008), but it is still profitable to extract the Helium because of the enormous amount of gas and gas liquids produced from the field daily.

However, once the helium is generated in the source rocks, it behaves much like any other subsurface gas. It must migrate along fracture and/or faults systems, to be entrapped along structural highs. Unlike methane and other natural gasses, helium because of its small atomic size, can escape from most normal reservoirs, unless they have a thick and impermeable regional seal (Shipton, et al, 2004).

These seals, such as the Ediacaran-Cambrian Usolian salt of Eastern Siberia, the Ara Salt of the South Oman Salt Basin of the Sultanate of Oman, and the Bitter Springs Group in the Officer Basin of Australia, are documented to be sufficient to hold helium for millions, if not billions, of years.

Table 6.1. Helium concentrations from various world gas fields. * = Neoproterozoic source.

Location	Field site	Concentration, vol%
United States		
Wyoming	Tip Top Field	0.4–0.8
San Juan, New Mexico	Beautiful Mountain	4.05
North Slope, Alaska	South Barroweast	2.54
Young, Texas	Young Regular	1.17
Grant, Kansas	Hugoton (Compressor station)	1.90
US Mid Continental Rift System	Forest City Basin, KS	1.50
Canada		
Alberta	Worsley	0.53
Ontario	Norfolk	0.36
The Netherlands	Groningen	0.05
The Netherlands	De Wijk	0.05
Poland	Ostrów	0.40
North Sea, British Sector	Indefatigable	0.05
West Germany Niedersachsen	Apeldorn	0.12
Russia	Urengoi	0.06
Russia	Orenburg	0.20
Russia-Eastern Siberia	Srednebotuobinsk*	0.40
Russia-Eastern Siberia	Kovykta*	0.56
Orange Free State	O.F.S. Goldfields	2.91
Algeria	Hassi R Mel	0.19
Australia	NWT, Pal Valley	0.21
Australia	Amadeus Basin	0.01
Australia	Amadeus Basin, Magee*	6.30
India	Baghewala-1*	0.05
China	Weiyuan Basin*	0.40
Oman	Budour, South Oman Salt Basin*	0.35
Pakistan Salt Range	Karampur*	1.00
Tasmania	Shittim*	1.26

As can be seen from Table 6.1, much of the higher concentration of helium originates with gas fields sourced by rocks of Neoproterozoic age. Perhaps it is due to much 'richer' source rocks (i.e., basement rocks enriched with uranium and thorium), or simply a matter of having been structurally quiescent and impermeable for millions to billions of years (Kontorovich, et al, 1988).

Exploration for helium is much the same as exploration for natural gas, indeed, the vast majority of helium is discovered inadvertently, only if the gas from the field is assayed and helium is not utilized as a carrier gas in some of the openhole sampling or logging procedure (Maione, 2004). There have been several attempts at guidelines in helium exploration, such as the apparent synchronicity between elevated nitrogen levels and high helium levels in a reservoir; presumably that the nitrogen and helium share a similar source rock (Danabalan, et al, 2021).

However, the origin of nitrogen at depth has not been shown to correlate directly with the radiogenic origin of helium. They are almost always sound together, often with carbon dioxide as well, but straightforward discussions of origins remain problematic and argumentative (Jenden, and Kaplan, 1989). Various postulates have been presented, such as the thermal metamorphism of bituminous carbonates which could generate both nitrogen and carbon dioxide. This mechanism has been postulated for the Beaverhill Lake formation of Alberta and Saskatchewan (Hitchon, 1963).

However the helium was generated, migrated and was stored within a reservoir; there are many steps that must be taken to extract and isolate the element from the natural gas and other non-hydrocarbon gasses.

Most typically, a natural gas discovery will also, besides methane (CH_4), contain carbon dioxide (CO_2), hydrogen sulfide (H_2S), water (H_2O), nitrogen (N_2), neon (Ne), argon (Ar), along with heavy metals such as cadmium (Cd), arsenic (As), chromium (Cr), thallium (Tl), lead (Pb), mercury (Hg), nickel (Ni), vanadium (Va), as well as organometallic compounds such as: $(CH_3)_2Hg$, diethylmercury, and the methylmercury (II) cation, CH_3Hg^+ (Elschenbroich, 2016).

These organometallic compounds are particularly pernicious, as they possess the proclivity of poisoning catalysts in petroleum processing.

6.2 Extraction and Treatment of Helium from Natural Gas

Regardless of the source, age, volume or provenance of the natural gas stream that is to be processed for helium extraction, there are similarities that must be addressed in each situation.

Virtually every natural gas stream will contain other noble gasses, potentially deleterious and dangerous compounds (CO_2, H_2S, etc.), metals and organometallic compounds as well as nitrogen, and natural gas liquids (Hosseini, 2009; Hosseini and Najari, 2016). Each of these must be isolated, treated and removed from the stream to leave the elemental helium so that it alone can be further processed and purified (See Figure 6.1).

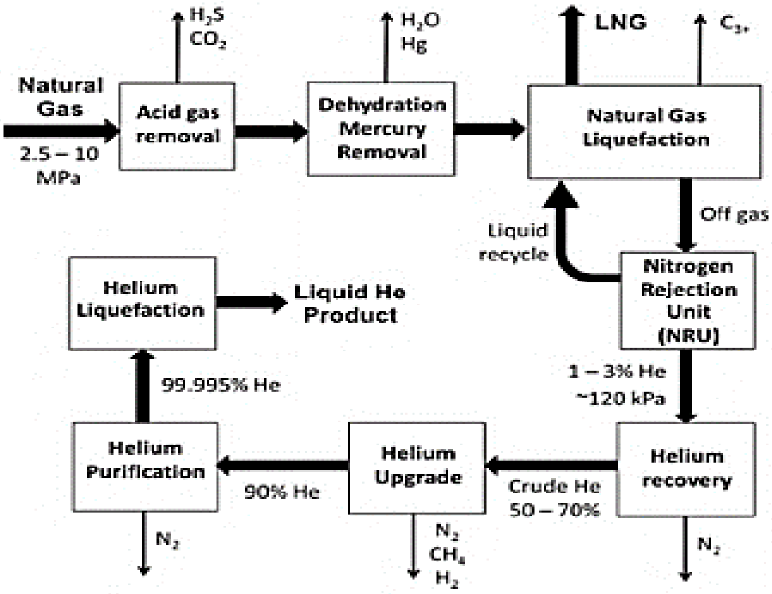

Figure 6.1. Schematic representation of a typical helium recovery process from natural gas (Soleimany et al, 2017).

Fortunately, these additional elements and compounds have vastly different physical properties. See Table 6.2.

Table 6.2. Physical properties of helium and other gasses found in natural gas. From Grynia, and Griffin, 2017.

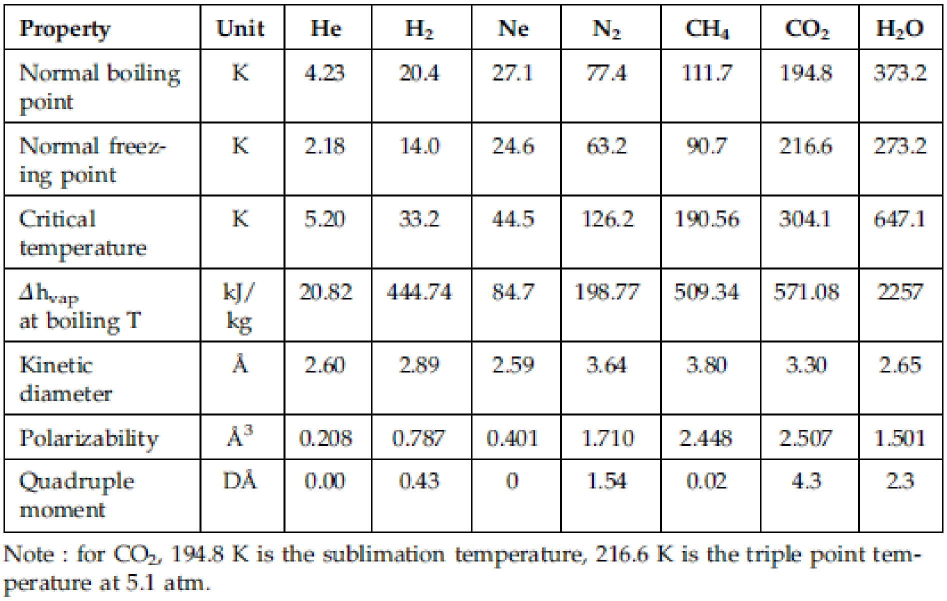

Property	Unit	He	H_2	Ne	N_2	CH_4	CO_2	H_2O
Normal boiling point	K	4.23	20.4	27.1	77.4	111.7	194.8	373.2
Normal freezing point	K	2.18	14.0	24.6	63.2	90.7	216.6	273.2
Critical temperature	K	5.20	33.2	44.5	126.2	190.56	304.1	647.1
Δh_{vap} at boiling T	kJ/kg	20.82	444.74	84.7	198.77	509.34	571.08	2257
Kinetic diameter	Å	2.60	2.89	2.59	3.64	3.80	3.30	2.65
Polarizability	$Å^3$	0.208	0.787	0.401	1.710	2.448	2.507	1.501
Quadruple moment	DÅ	0.00	0.43	0	1.54	0.02	4.3	2.3

Note : for CO_2, 194.8 K is the sublimation temperature, 216.6 K is the triple point temperature at 5.1 atm.

Exploiting these differing physical properties, it is possible through a number of different processes to remove the other constituents from the gas stream, concentrate and sell them to help offset the sometimes-expensive processes that lead to “Industrially Pure” or 99.99999% pure helium (Saberimoghaddam, and Khebri, 2018).

In recent years, there has been the move away from more expensive cryogenic practices in favor of selective membranes (Kita, et al, 2008). In fact, economically, selective membranes can work profitably with lower helium concentrations, i.e., <0.02%, whereas cryogenic methods would be prohibitively expensive, bulky, and energy profligate (Hamedi, et al, 2019).

Alternately, the use of pressure swing adsorption (PSA) apparatus is a bridge method between membranes and full cryogenic processes (Shi, et al, 2018). In fact, PSA can be used as a precursor method before or after membranes (for concentration and purification in the latter) or before cryogenic methods to somewhat reduce the necessity of full-on cryogenic processes (Sazali, 2020).

6.2.1 Comparisons and Contrasts of Each System Follow

6.2.1.1 *Membranes: are non-catalytic*

Gas separation by membranes rely upon two properties; those of permeability and selectivity (Sunarso, et al, 2017). Selectivity refers to the ability of a specific membrane to allow or deny passage of a certain size of molecule while permeability refers to the flow rate of a particular gas component multiplied by the membrane thickness and normalized by the membrane area and the pressure difference (Scholes, and Ghosh, 2017). Different materials can be utilized to construct such selective membranes, which range from polymer to natural zeolite to silicate and hybrids (combinations of the aforementioned) (Park, et al, 2017).

Whatever the composition, they all exhibit the same set of properties that make them, in the last few decades, more attractive due to their low operating cost, moderate initial costs, absence of moving parts, that the process does not involve a phase change, and overall small physical footprint (Scholes, and Ghosh, 2016). Further, membranes have such a low operating cost, that it has lowered the point at which helium extraction is profitable.

As little as 0.005%vol of helium can now be processed profitably (Chaudhuri, et al, 2019). Membranes rely on relative permeation rates for separation, so that helium can still be profitably extracted from a gas stream containing species other than CH_4 (Figure 6.2).

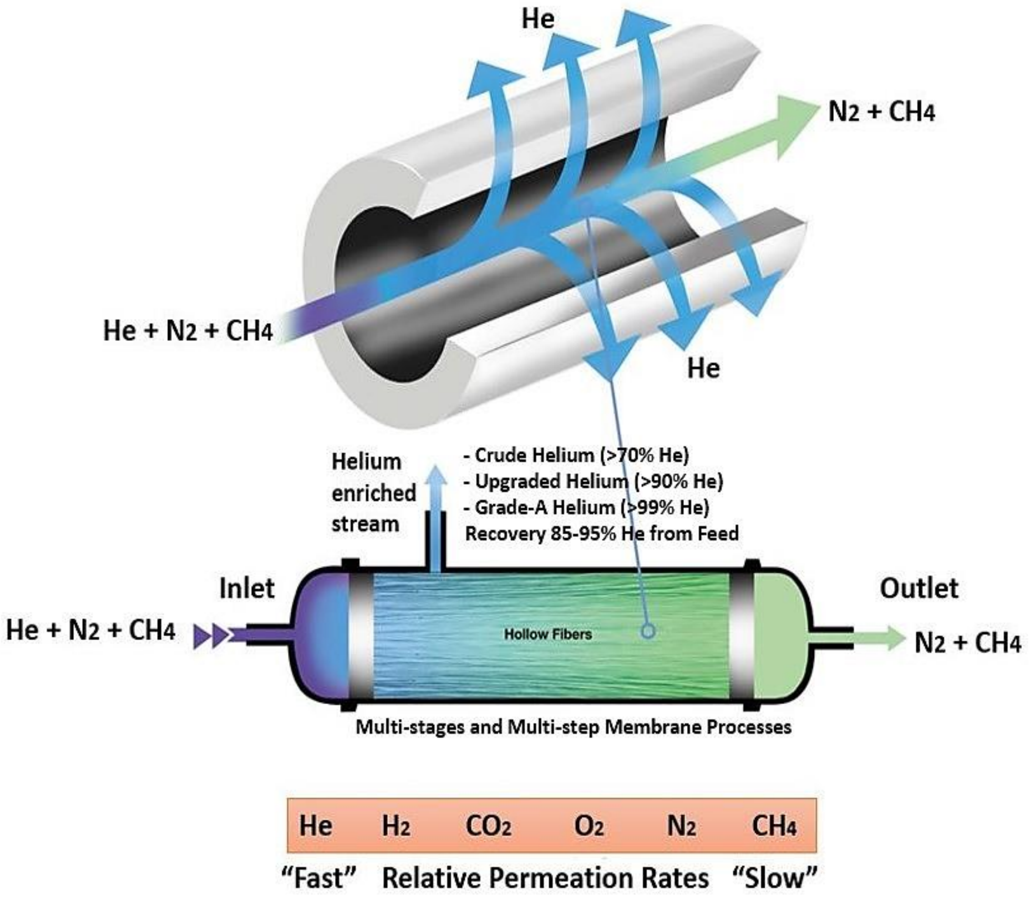

Figure 6.2. Membrane extraction of helium from multi-species gas stream. From Worrell, 2019.

Since the membranes are under pressure and run continually, extraction of the helium, especially through stages, can reach 99.9999% at high recovery factors. However, this is only for multistage processing; initial single-phase extraction will typically only yield helium with a purity of ~70%, though with high recovery factors (Haider, et al, 2019).

6.2.1.1.1 *PSA: pressure swing adsorption*

It is a non-catalytic, non-cryogenic cyclic adsorption process used to separate gas species from a mixture of gases, under pressure, corresponding to the species' molecular characteristics and affinity for a particular adsorbent material. It operates at near-ambient temperature which is expressively different than cryogenic distillation commonly used to separate gases (Pearson and Gupta, 2005). Selective adsorbent materials (e.g., zeolite, activated carbon, silica gel, alumina, synthetic resins, etc.) are used as trapping material, preferentially adsorbing the target gas species at high pressure. The process then swings to low pressure to desorb the adsorbed gas (Figure 6.3).

$$4\ \mathrm{CH4} + \mathrm{O2} + 2\ \mathrm{H2O} \rightarrow 10\ \mathrm{H2} + 4\ \mathrm{CO}$$

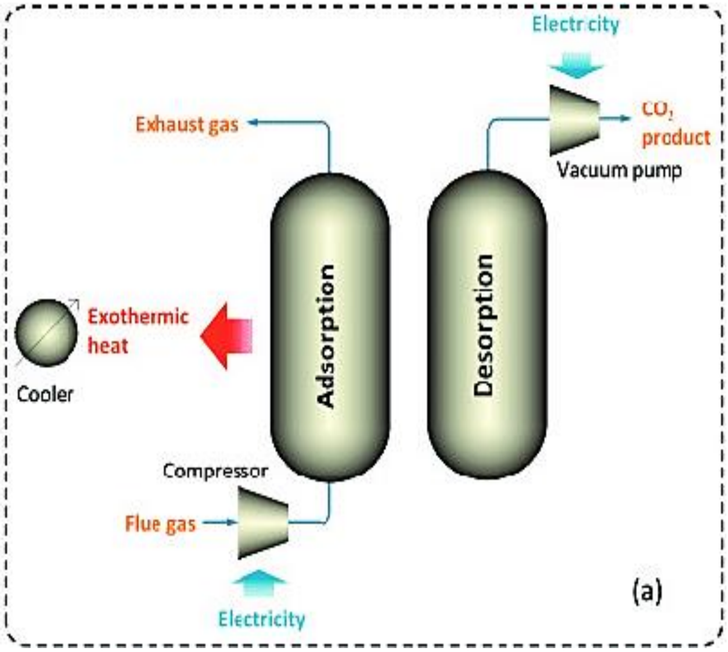

Figure 6.3. Energy and material flow of the conventional PSA process. From Song, et al, 2014.

Typically, several phases of adsorption/desorption are required to obtain helium of required purity (Sunarso, et al, 2016). In each of the successive stages, the adsorptive material is different than the former; by possessing a higher affinity for helium and lower adsorptive affinity for other non-helium species. However, in each stage, helium is lost in the desorptive stage, so overall efficiency is near 60% (Das, et al, 2012).

6.2.1.2 *Cryogenic: referring to a process of helium extraction which require extreme low temperatures*

In cryogenic technologies, separation is achieved at temperatures below -65 ºC where cryogenic separations can accomplish up to 90% helium recovery and purities exceeding 99.9999%. Cryogenic processes are divided into two groups: multi-flash cycles and high-pressure distillation column processes (Victory, Miles and Oelfke, 2009).

As can be seen in Figure 6.4, cryogenic extraction requires much more in the line of equipment and physical floorspace.

Figure 6.4. Equipment and footprint of a typical cryogenic helium extraction unit. Courtesy http://www.fuhaicryo.com/.

Cryogenic processes for helium extraction and purification fall into two categories: multi-stage flash cycles and high-pressure distillation column processes. In the multi-stage the pressure of the gas stream feed, which contains the dissolved helium and minor dissolved N_2, is reduced in a series of flash vessels (See Figure 6.4, item 3). In each flash stage, the helium will be vaporized along with the N_2. The helium content of the crude helium product will depend on the feed’s He concentration, as well as the available pressure drop and resulting temperature change (Rufford, et al, 2014).

In high-pressure distillation column processes, recovering the helium from the natural gas stream by conventional cryogenic distillation methods is expensive and energy intensive. The four basic cryogenic distillation processes used for helium extraction from NG are multi-stage flash separators, the single-column heat-pumped process, the double-column process, and the dual-column cycle (Agrawal et al. 2003).

As helium liquefies at 4.4 K (-268.75 °C), most of the helium liquefiers are Claude-cycle based (Singh, et al, 2017). The "Claude Cycle" is a process for liquefying gasses on a commercial basis. Gas under pressure is used as the working substance in a piston engine, where it does external work and cools adiabatically (Soleimany, et al, 2017). This cooled gas is fed to a counter-current heat exchanger, where it reduces the temperature of the next intake of high-pressure air. The same gas is re-compressed and used again, and after several cycles eventually liquefies. Figure 6.5.

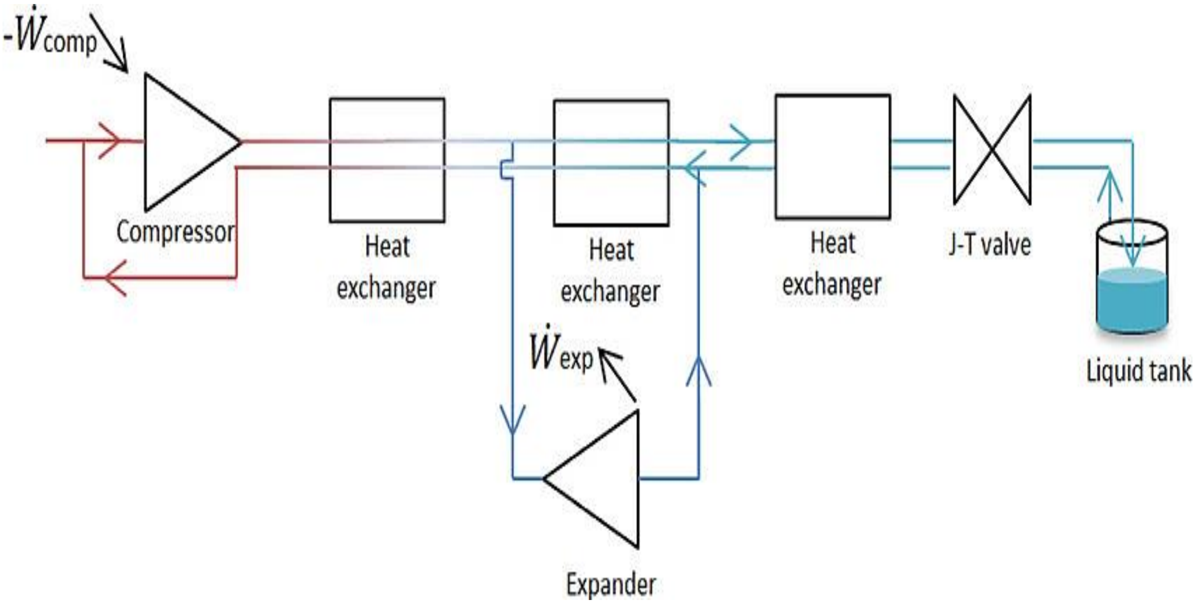

Figure 6.5. Illustrating the Claude Cycle in high pressure cryogenic distillation. From Damak, et al, 2019.

In extracting helium, after an indeterminate number of circulations of helium, the impure helium is fed to the purifier unit. By cooling down the impure gas with cold high-pressure gas impurities, nitrogen and traces of other gases condensate and freeze out. The purified gas is fed into the cold box high pressure-inlet side (Berdais, Wilhelm, and Ungricht, 2008). By warming up the purifier will be regenerated, whereby the removed undesirable gases are discharged and eliminated. When temperature of helium goes to 8-10 K, a JT (Joule-Thomson) valve opens (Figure 6.6), which rapidly allows the gas to expand. By passing through the valve, the helium liquefies and is stored in the main system Dewar (Ansari, et al, 2017).

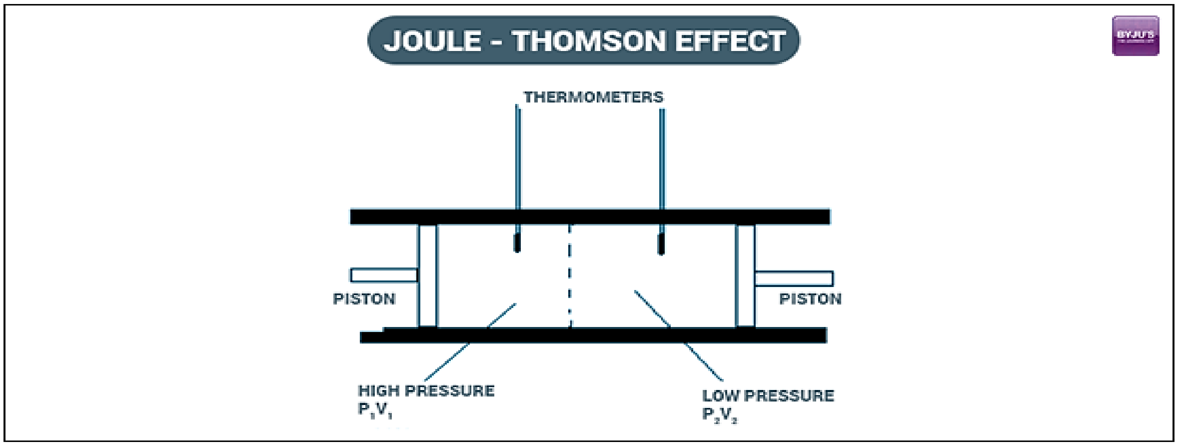

Figure 6.6. A Joule-Thompson valve, allowing the transformation of temperature, pressure and volume in a cryogenic stream. From Winterbone, and Turan, 2015.

6.2.1.3 *Gas processing procedures*

In any case; membrane, PSA and/or cryogenic, there are a set of prescribed practices typically necessary for a helium extraction and purification process (Soleimany *et al*, 2017):

1. Natural gas processing/pre-treatment (removal of hydrogen sulfide, carbon dioxide, water and heavy metals);

2. Natural gas refrigeration (removal of heavier hydrocarbons if any) and liquefaction (production of liquefied natural gas (optional));
3. Nitrogen rejection (removal of nitrogen) / helium recovery from natural gas;
4. Helium upgrading;
5. Helium purification; and
6. Helium liquefaction.

Pre-treatment can be accomplished by a self-contained skid-mounted gas pre-treatment unit. The unit include an amine plant, glycol dehydration, gas sweetening (if persistent H_2S is problematic), and a nitrogen rejection unit. This will enable the retention of the most methane, helium and other aproblematic gasses in the gas stream, while addressing the difficulties of CO_2, H_2O, N_2, H_2S, heavy metals and organometallic compounds.

If extraction of Natural Gas Liquids and/or LNG are desired, an optional module, after Nitrogen Rejection, consisting of a primary turboexpander and demethanizier, are required (Al-Kaabi, 2014); along with modular concept attendant compression and heating. From this, the gas flow would go through a fractionation train (deethanizer, debutanizer, depropanizer, etc.) to a sweetening unit consisting of a Merox processor, Sulfrex processor and appropriate molecular sieves (Keller, 2012). This would then yield gaseous or liquid (if sent through Pressure Swing and/or Cryogenic Apparatus) ethane, propane, butane and pentanes$^+$ (natural gasoline) (Mehrpooya, et al, 2014).

The remaining pass-through from the Nitrogen Rejection Unit and the NGL apparatus would be heated (Scholes, 2018), compressed and sent onward to helium recovery. Here, semipermeable membranes (zeolitic, silicious, or inorganic hybrid) extract the helium selectively. This ‘permeate’ can be sent off for further processing (upgrading, purification and liquefaction: SPA or Cryogenic) while the remaining ‘retentate’ will be pressurized and heated high-purity methane (Crawford, et al, 2010).

In the case presented here, for full clarity, this retentate will then be sent off to a Steam Methane Reformer unit. In a two-part closed-loop system, high volume water steam will react with the methane to produced diatomic hydrogen and carbon monoxide (Baltrusaitis, and Luyben, 2015). Running the retentate through the system a second time yields further hydrogen and carbon dioxide (approximately 20 pounds CO_2/MCF of hydrogen). Thus, per 1 million standard cubic feet (SCF) of hydrogen produced from methane, 250,000 SCF of CO_2 will be produced (Ayodele, et al, 2021). However, this CO_2 will be of very high purity and can be sold for oilfield activities (hydraulic fracturing, activating acids, etc.) or other industrial activities; or captured, stored and/or sequestered (Collodi, et al, 2017).

CHAPTER 7

Hybrid H_2-He Extraction System

In this paper, it is proposed, for the first time to create a novel hybrid linear, closed-loop system for the processing of Bakken Formation natural gas which is currently being flared.

Processing this gas would recover several saleable products, most notably elemental helium and diatomic hydrogen from gas that was previously being flared. The process is non-cryogenic i.e., below the temperature of liquid nitrogen; (− 196 °C [− 320 °F]) at least to the point of refining, purifying and compressing the hydrogen and helium.

7.1 The Modular Concept

The process consists of three (or four, as one is optional) substages or modules (Figure 7.1):

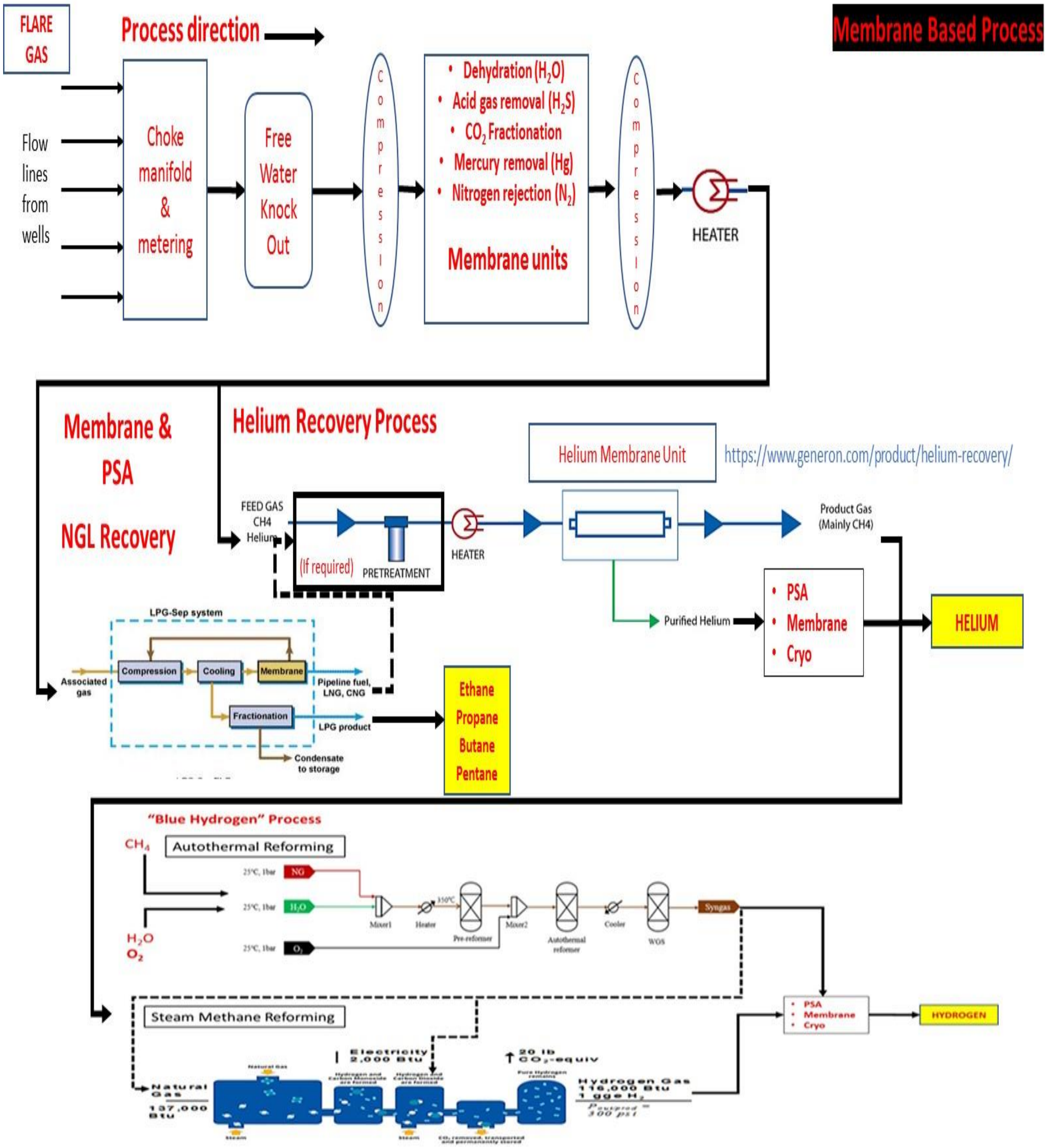

Figure 7.1. The modular construction of a hybrid H_2-He extraction process.

1. Gas gathering, metering, initial dewatering (FWKO), compression and treatment utilizing a skid-mounted natural gas pre-treatment membrane array.
2. If desired, NGLs (Natural Gas Liquids) can be extracted here via continuous membranes. NGLs include ethane, propane, butane, pentane, etc.

3. Helium extraction by selective membrane filters.
4. Hydrogen extraction by ATR (Autothermal Reforming) and WGS, potentially with SMR (Steam Methane Reforming).

However, it has been determined that the process can be even more simplified via combining Modules 1 and 2 through the employment of selective gas membranes; virtually identical to those proposed for helium extraction in Module 3.

See Figure 7.2. for a detailed schematic of the process.

Besides the isolation of up to eight different saleable products derived from gas that was previously destined to be flared, the process also allows for carbon capture, utilization and storage, or CCUS, as high-purity CO_2 will be isolated from two distinct nodes in the pathway:

1. Amine plant or selective gas membranes, during natural gas pre-treatment, and
2. Steam Methane Reforming which generates both CO and CO_2 during the reforming of CH_4 and the extraction of H_2.

7.1.1 The “Mechanical System”

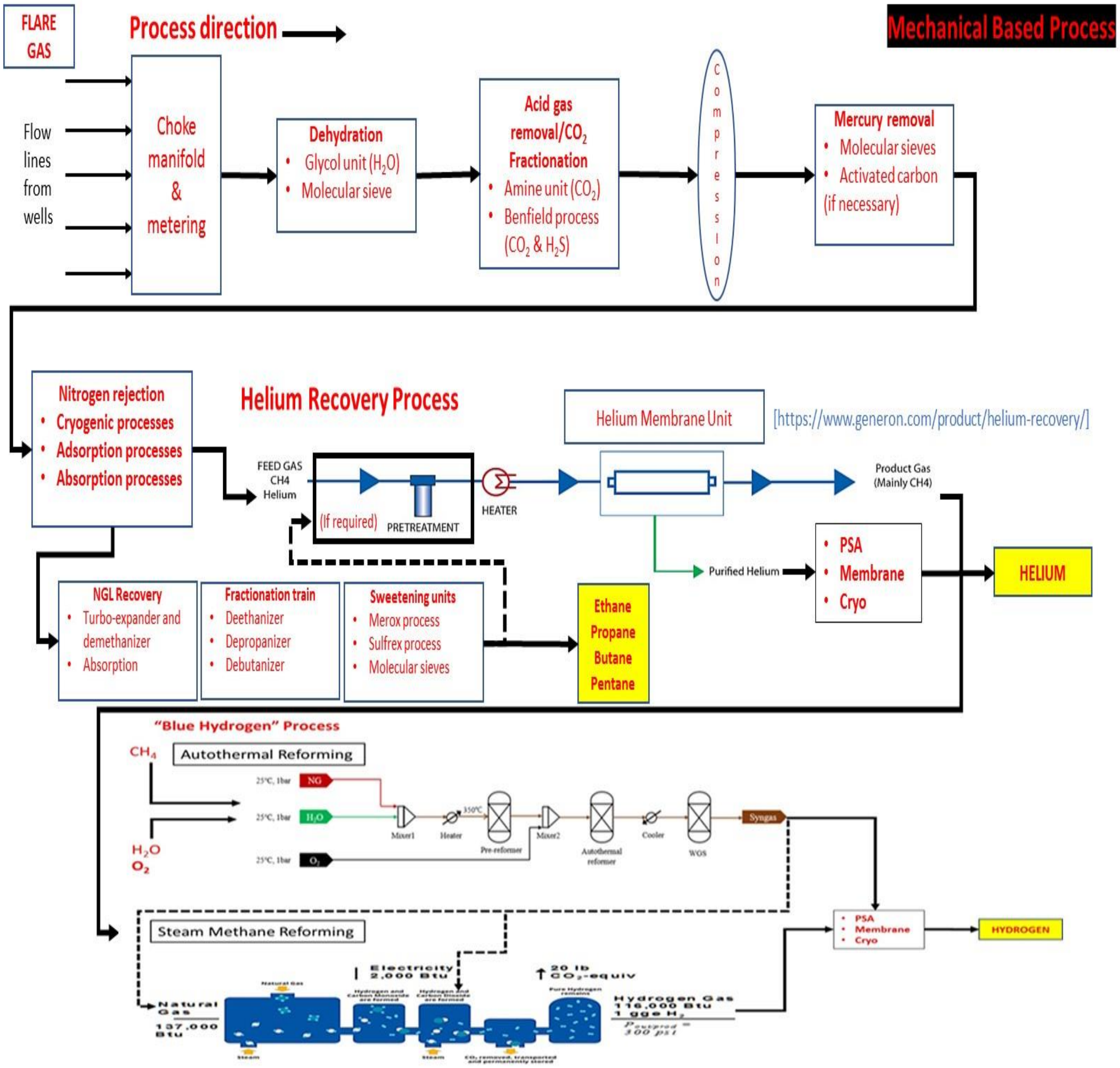

Figure 7.2. Full field schematic for extraction of “Blue Hydrogen” and helium from Bakken flared gas via mechanical means.

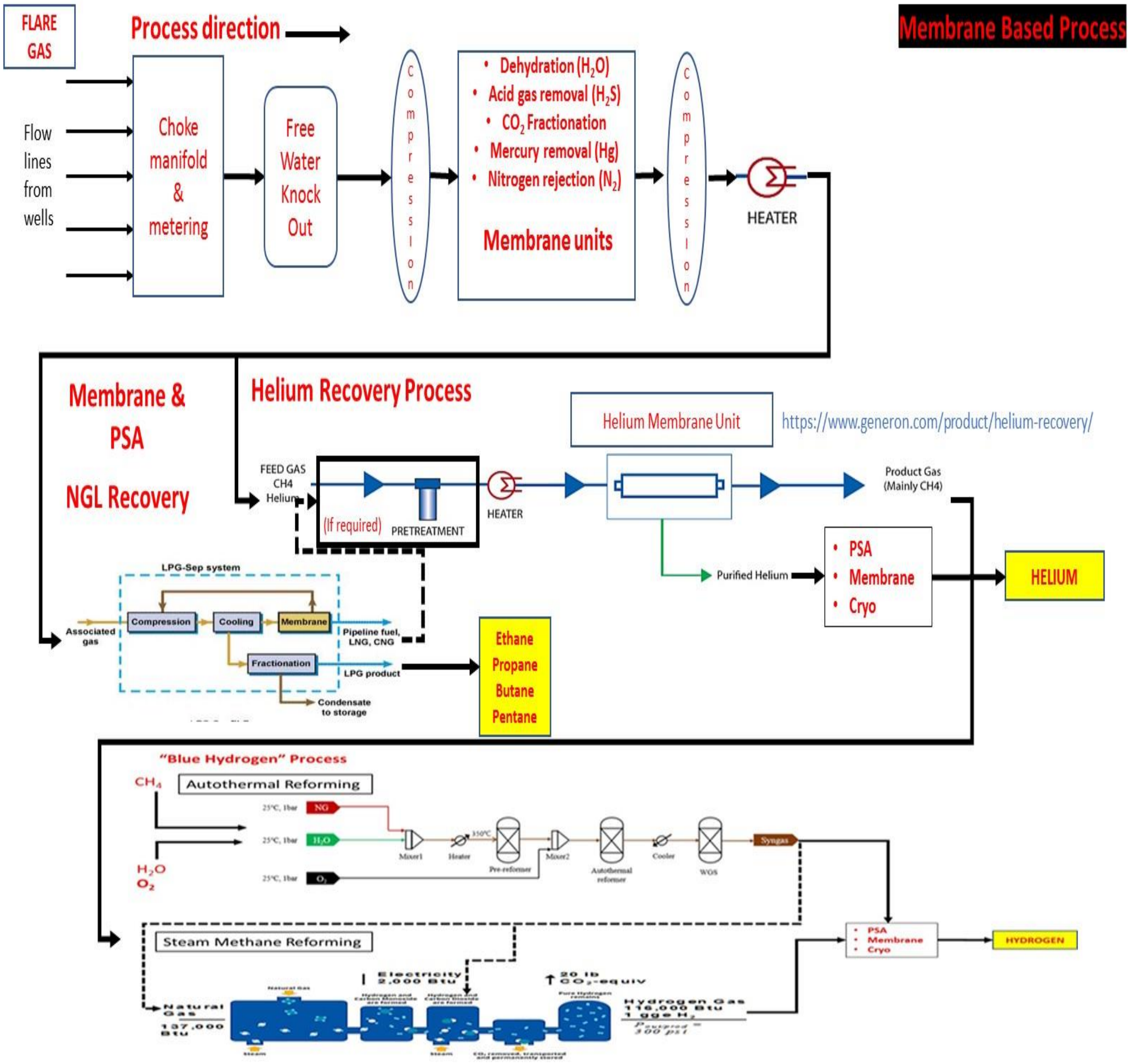

Figure 7.3. Full field schematic for extraction of "Blue Hydrogen" and helium from Bakken flared gas via selective molecular membranes.

Both linear hybrid systems schematically pictured above utilizes no novel or experimental technologies. The complete process can be attained through the use of "off the shelf" technology.

The novelties here are the use of previously flared Bakken gas to derive a number of saleable products, the linear or "straight through" closed-loop feed system, the utilization of non-cryogenic apparatus to isolate both helium and hydrogen, and the flexibility to add other sub-units for additional saleable products recovery. Each of the technologies noted in every sub-unit are proven technologies that have been in use in the oil industry for decades. However, this is the first time they have been linked in unison, to provide a straight-through feed path.

Figure 7.4. 'Typical' Bakken Field surface activities. Note multiple wells on pump and central flare. From Cameron, 2021.

In the figure above are gas-collecting piping and metering from each of the pumps. These are tied in together at a surface header and then all gas contributions are sent to the flare unit. This is where the new hybrid system proposed here would begin (Figure 7.4).

Instead of sending the gas to the flare unit, the combined gas would be sent from collection and metering surface choke manifold header to a free water knockout (Figure

7.5). Here is the first step in processing and pre-treating the gas for extraction of saleable products (Dengel, 2020).

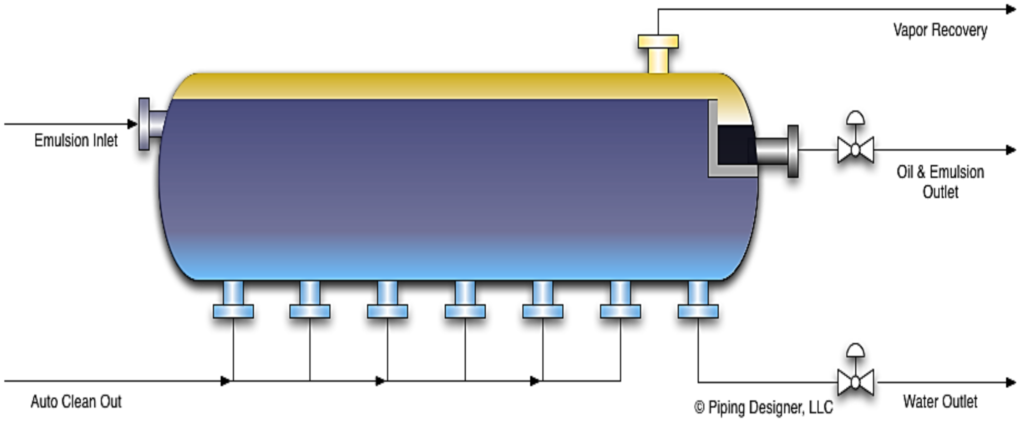

Figure 7.5. Schematic of a free water knockout vessel. From Piping Designer, 2021.

The dehydrated gas, which still contains some small degree of water, will now undergo compression before it is piped to Natural Gas Pre-treatment (Song, et al, 2021). This skid-mounted unit is made up of several different devices, all designed to eliminate anything other than methane and helium from the flow stream before it is introduced to the helium extraction membranes in the next step (Figure 7.6).

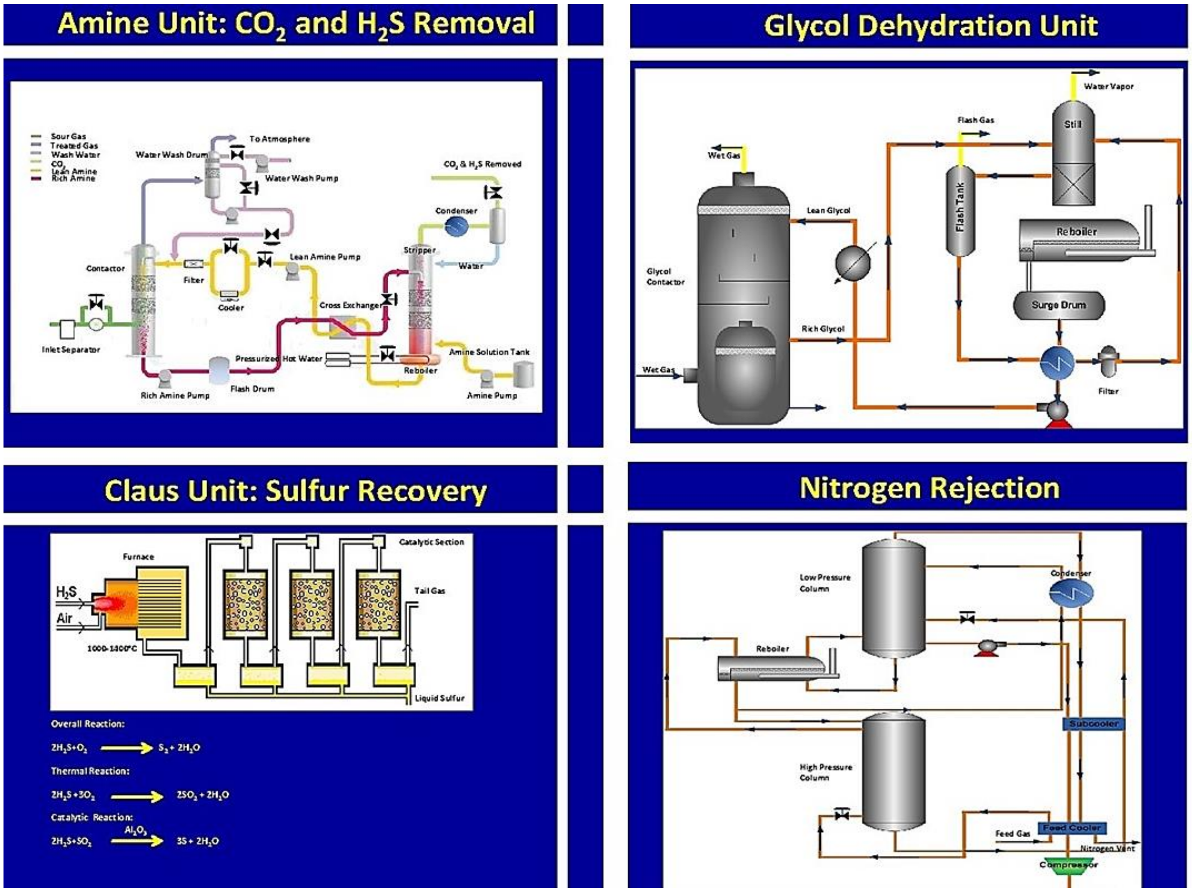

Amine Unit: CO_2 and H_2S Removal

Glycol Dehydration Unit

Claus Unit: Sulfur Recovery

Nitrogen Rejection

Overall Reaction:

$2H_2S + O_2 \longrightarrow S_2 + 2H_2O$

Thermal Reaction:

$2H_2S + 3O_2 \longrightarrow 2SO_2 + 2H_2O$

Catalytic Reaction:

$2H_2S + SO_2 \xrightarrow{Al_2O_3} 3S + 2H_2O$

Figure 7.6. Methodology and mechanisms of removing natural gas stream contaminants: Amine plant, Glycol Dehydrator, Gas Sweetening, and Nitrogen Rejection. Can be done either mechanically or with selective membranes.

However, there is an optional process, that which captures NGLs (Natural Gas Liquids such as ethane, propane, butane, and the like). Although an optional sub-treatment, it will also be described later as it generates much in the line of more saleable products.

Continuing, the gas will first be introduced to an amine plant (Rao, and Rubin, 2002). The amine plant treats and removes carbon dioxide (CO_2) and hydrogen sulfide (H_2S) from the gas stream. The process is known as gas sweetening or acid gas removal, using various alkanolamines, commonly referred to as amines. Some of the more usual amines used in the decarbonizing-desulfiding process are:

- DGA® Agent (DIGLYCOLAMINE)® A primary amine that is used in natural gas treatment applications requiring stringent outlet gas specifications, applications where oxygen (O_2) is present and low-pressure applications. DGA® Agent and DIGLYCOLAMINE® are registered trademarks of the Huntsman Corporation (Alper, 1990).
- MDEA (Methyldiethanolamine): A tertiary amine designed to have a higher affinity for H_2S than CO_2 which allows some CO_2 “slip” while retaining heightened H_2S removal capabilities.
- DEA (Diethanolamine): A secondary amine that, like DGA® can be used in applications with stringent outlet specifications. It is often used in conjunction with MDEA to help remove some of the CO_2 that would otherwise “slip” (TransTexTreating, 2021).

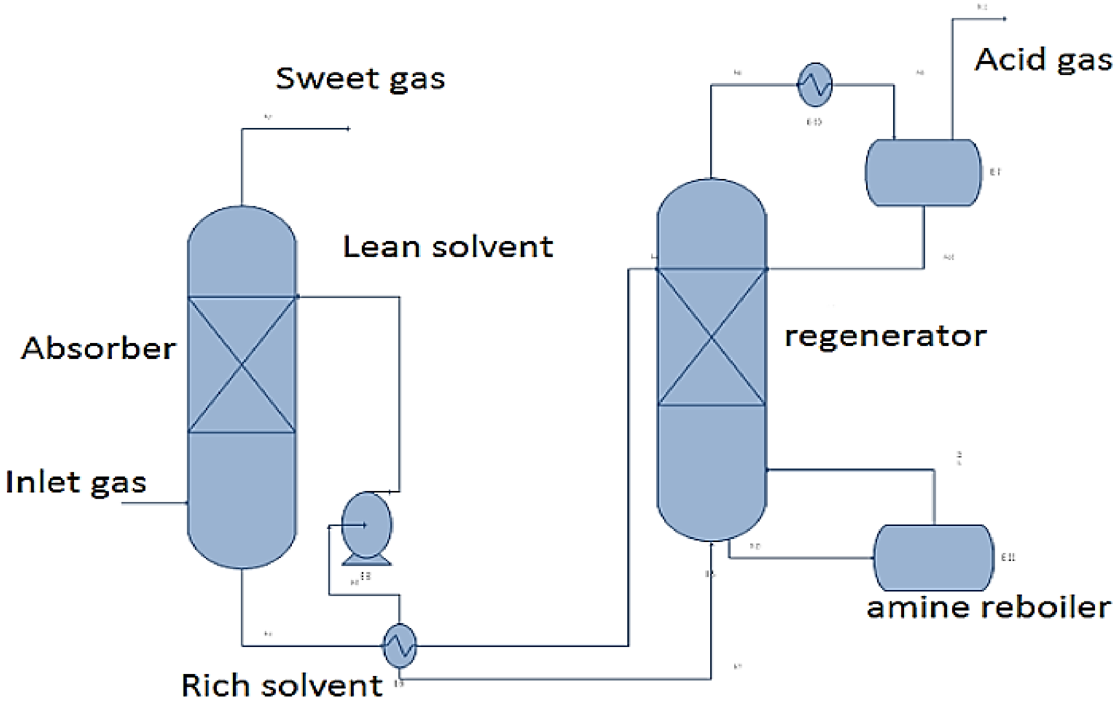

Figure 7.7. Schematic of natural gas flow directions through an amine plant. From Abdulrahman, et al, 2015.

The amine plant delivers both a high purity CO_2 from the gas stream, as well as elemental sulfur from the removal of the H_2S. If further gas sweetening is required, there is a separate module on the skid for further gas sweetening, However, the CO_2 and sulfur here are the first of several saleable products derived by the processes being explained. Elemental sulfur is currently selling for ~$40.00/metric ton. However, the H_2S content of the Bakken gas is quite low (0.39%) (Kringstad, et al, 2020), so while the sulfur could be sold, it will take some time before marketable quantities are achieved (Abdulrahman, et al, 2015).

However, with concentrations of carbon dioxide (CO_2) in excess of ~1.00%, (Kringstad, et al, 2020), and the inherent purity of the gas from deamination, this high-purity gas could be captured and either geologically sequestered, or sold to oil and gas operators for use in EOR (Enhanced Oil Recovery) operations (foaming acid, CO_2 fracturing, etc.). In either case, CO_2 that would have gone up the flare stack is now contained and can be put to good use, at a good price, as well as going into geological storage.

Also, Steam Methane Reforming (SMR) also produces a hot, highly pure stream of CO_2 in its operations, and is a second location in the proposed processing sequence where carbon dioxide can be captured and sequestered or sold and utilized.

The next step in the gas processing train is the glycol unit or glycol dehydrator (Figure 7.8).

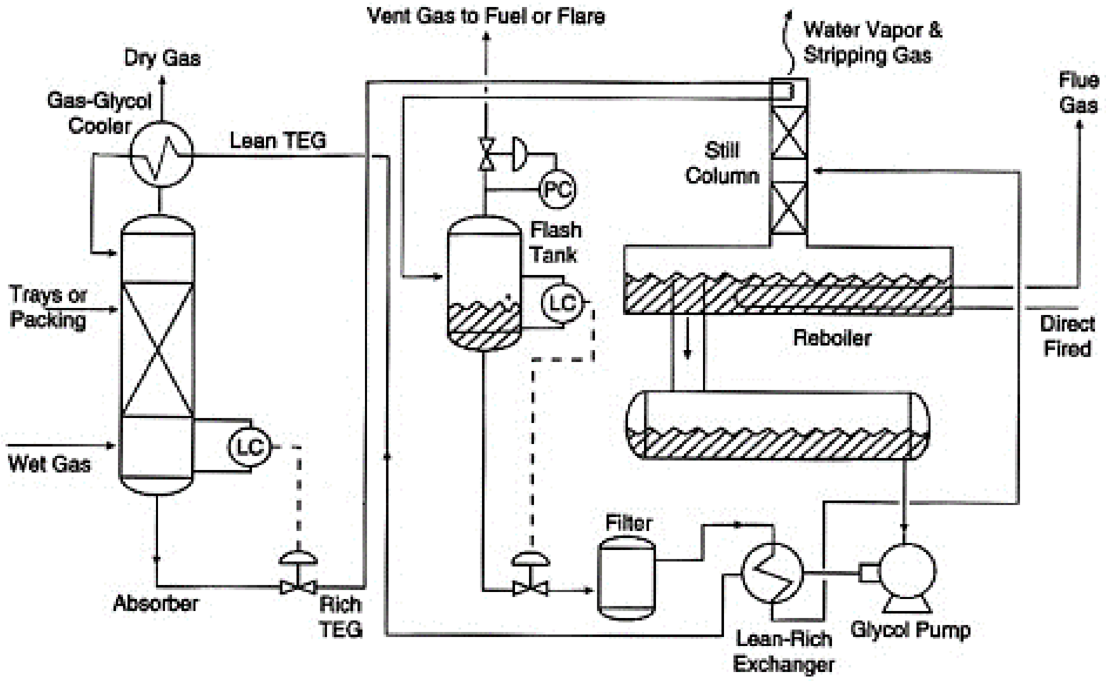

Figure 7.8. Schematic diagram of a glycol dehydrator unit. From Campbell, 1998.

The most desirable dehydrating agents that can be used for industrial dehydration purposes would possess the ensuing vital properties:

- High water absorption efficiency;
- High decomposition temperature;
- Low vaporization losses;
- Easy and economical for water to be separated and regenerated;
- Be non-corrosive and non-toxic to the system (Campbell, 1998).

Glycols such as ethylene glycol (EG), diethylene glycol (DEG), triethylene glycol (TEG), and tetraethylene glycol (T4EG) fall into this category.

Table 7.1. Properties of Ethylene Glycol, Diethylene Glycol, and Triethylene Glycol. From Speight, 2016.

	Ethylene Glycol	Diethylene Glycol	Triethylene Glycol
Chemical formula	$C_2H_6O_2$	$C_4H_{10}O_3$	$C_6H_{14}O_4$
Acronym molar mass	MEG 62.07 g mol^{-1}	DEG 106.12 g/mol	TEG 150.17 g mol^{-1}
Appearance	Clear, colorless liquid	Colorless liquid	Colorless liquid
Density	1.1132 g/cm^3	1.118 g/cm^3	1.1255 g/cm^3
Melting point	− 12.9 C (8.8 F)	− 10.45 C (13.19 F)	− 7 C (19 F)
Boiling point	197.3 C (387.1 F)	244 C (471 F)	285 C (545 F)
Solubility in water	Miscible	Miscible	Miscible

In Figure 7.8 we see distinctions between “Dry gas” and “Wet gas” as well as “Lean” and “Rich” TEG (in this case, triethylene glycol). “Dry” and “Wet” gas refers to the amount of water carried in the gas stream as does “Lean” and “Rich” glycol, referring to the dehydrant being lean or rich with water (Liu, et al, 2015).

Previously in the process train, immediately after gathering and exit of the combined gas streams from the choke header manifold, the gas stream was passed through a free water knock out (FWKO). This was imperative to avoid the necessity of three-phase separation at this level in the gas processing sequence. As the gas stream enters the dehydrator, it goes through a two-phase separator so that liquid can be isolated from the gas stream (Brown, 2005).

The gas leaving the separator from the top contains a small amount of water vapor despite the mist eliminator on top of the separator. This still “wet” gas then enters the bottom of the glycol gas absorber, flows upwards through the packed tower with the mist eliminator to eliminate any entrained glycol droplets from the gas stream, and exits on the top of the absorber as dry gas. The dry gas then flows through an atmospheric glycol cooler to cool the hot regenerated glycol before the glycol enters the absorber (Xiuli and Economides, 2009).

The desiccated lean glycol, flows down the tower, absorbs water from the up-flowing gas mixture, and exits at the bottom of the absorber as rich glycol. This rich glycol then flows through a reflux condenser at the top of the still column, and enters a flash tank where most of the entrained, soluble, and volatile components are vaporized. After leaving the flash tank, the rich glycol flows through the glycol filters and the rich-lean glycol exchanger, where it exchanges heat with the hot lean glycol (Ranjbar, et al, 2015).

The rich glycol then enters the glycol regenerator unit that contains the still column and reboiler, where the water is removed by simple one-stage distillation, and the glycol concentration is augmented to meet the lean glycol requirement. For processes requiring gas with very low water dew points, a stripping vapor will most likely be needed to aid the regeneration process (Hernandez-Valencia, et al, 1992).

The amount of water excluded here at this stage will be considerably less than that from the FWKO. Upon the regeneration of the rich glycol to lean glycol, the water that was absorbed in the contactor is released in the regenerator, and was typically vented into the atmosphere. Regrettably, the glycol not only absorbs water, it also physically absorbs some hydrocarbons and acid gas; even after the amine treatment, some sulfide members may remain in the gas stream (Rao, and Rubin, 2002).

However, the absorptivity of paraffinic hydrocarbons, such as methane, ethane, etc. is not great. Though aromatic hydrocarbons such as benzene, toluene, ethylbenzene, and xylene (BTEX) are more easily absorbed (Rezazadeh, et al, 2012). These vapors are considered carcinogenic by the 1990 amendments to the Clean Air Act in the US, and all contribute to atmospheric pollution (Fisher, et al., 1995). Further processing of these must be accomplished before any water vapor can be released into the environment. These vapors are collected after condensation from the glycol reboiler in forced-air coolers, whereby they are burned in the glycol reboiler firebox to reduce fuel gas consumption and to achieve an overall minimum destruction efficiency of 99.7% (Sivals, 1995).

At this point, the gas stream exits the glycol unit essentially as dry gas with very low CO_2 and H_2S content, though still carrying an unknown quantity of mercaptans (or *thiols*). If still there remains these compounds in values deemed excessive for further processes (a variable depending on source gas concentrations), gas sweetening may be necessary (Alper, 1990).

Natural gas can be termed ‘sweet gas’ if it contains only minute trace quantities of H_2S, mercaptans and CO_2. Sweet gas in its pure form is non-corrosive, requires little further pre-refining.

Gas sweetening can be achieved by any one of several measures. Those most common are:

- Amine Process (described previously)
  - DEA (Diethanol Amine)
  - DGA (Diglycolamine)
  - DIPA (Di-isopropanol Amine)
  - MDEA (Methylethanol Amine)
  - MEA (Monoethanol Amine)
  - Mixed Amines
- Physical Solvents (Absorption)

  - Fluor Solvent (propylene carbonate is used primarily for removal of CO_2 from high pressure gas streams, (Coker, 2010)).
  - Selexol (DOW process: a physical solvent, unlike amine-based acid gas removal solvents that rely on a chemical reaction with the acid gases. It is dimethyl ether of polyethylene glycol. (Fahim, et al, 2010.))
- Combination of Chemical and Physical Solvents
  - SULFINOL-D (Sulfolane + DIPA)
  - SULFINOL-M (Sulfolane + MDEA) (Angaji, et al, 2013).

The Sulfinol process was developed in the early 1960s. The solvent consists of an aqueous amine and sulfolane. The process is used for the removal of hydrogen sulfide, carbonyl sulfide, mercaptan (thiol) derivatives, other organic sulfur compounds and all or part of the carbon dioxide load in gas stream (Speight, J., 2019).

- Other Methods
  - Molecular Sieve
  - Locat
  - Sulferox (After Deyin, 2021).

At this point in time, given the Bakken gas assays and the apparent lack of appreciable volumes of mercaptans and the relatively low volumes of H_2S and CO_2 (Gherabati, et al, 2019), it is not envisioned that additional gas sweetening will be required. However, as the gas processing sequence being described had been designed to utilize ‘off the shelf’ materials and technology, since most skid-mounted gas pre-treatment platforms will include gas sweetening, it was included here as a possibility.

At this point there is a processing decision that needs to be made. Will the gas stream be processed for Natural Gas Liquids (NGLs)? If so, there are differing schools of thought from where the gas stream should be diverted to the module of Natural Gas Liquids recovery.

For instance, Figure 7.9 (Tobin, et al, 2006) shows a schematic representation of gas processing where the offtake for the Natural Gas Liquids occurs immediately after the Nitrogen Rejection Unit.

Expanding on this idea (Ghorbani, et al, 2016) Figure 7.10, adds cryogenics to the process and mixed refrigerant cycles to the gas stream to achieve extraction of the NGLs. As the process being described in this paper has to go through both proof of concept and a pilot project, with the additional costs of cryogenics, it does not justify the refrigerant cycles at this time.

Finally, in Figure 7.11, there is shown the process whereby NGLs are extracted before passing the gas stream to the Nitrogen Rejection Unit.

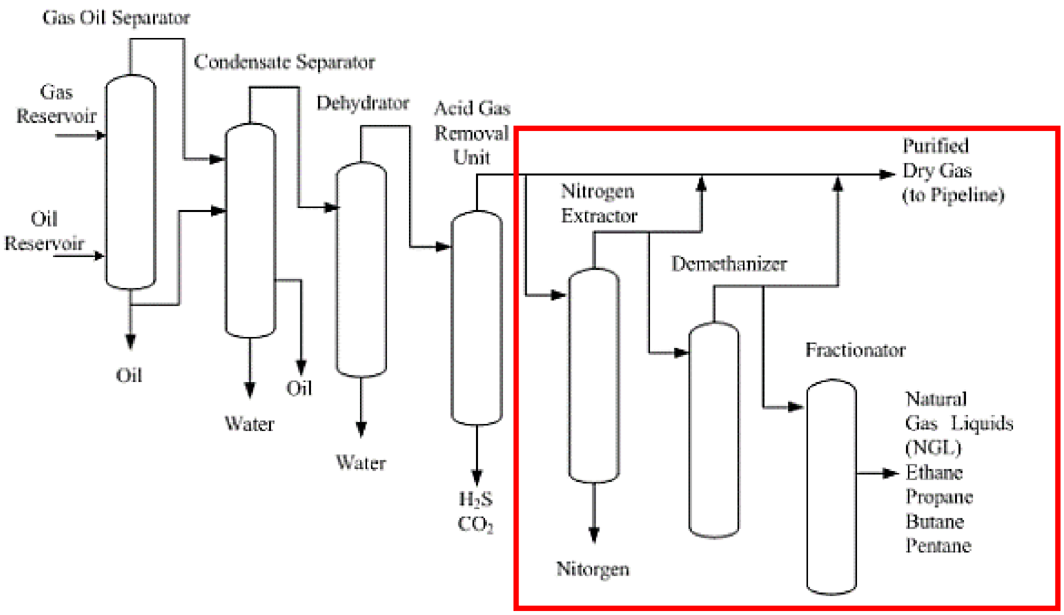

Figure 7.9. Schematic representation of a gas processing plant (Tobin, et al, 2006), showing offtake for NGLs from Nitrogen Rejection Unit (red box).

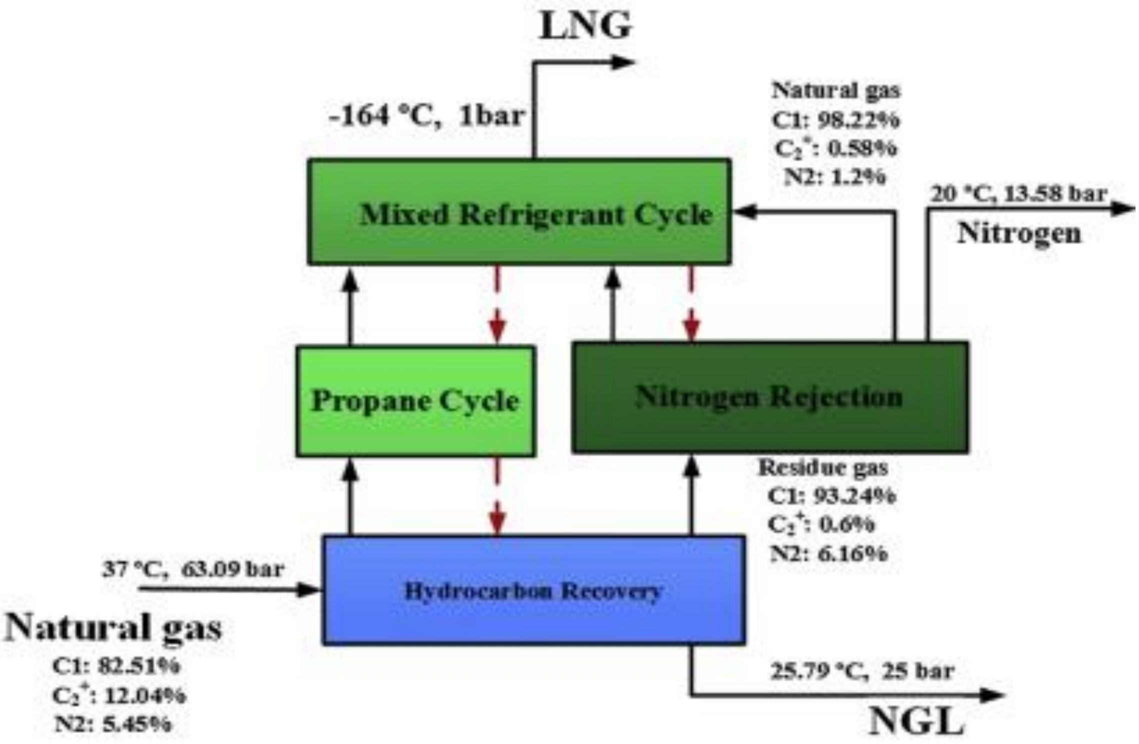

Figure 7.10. A new integrated cryogenic process from Ghorbani, et al, 2016, utilizing refrigerant units after the Nitrogen Rejection Unit.

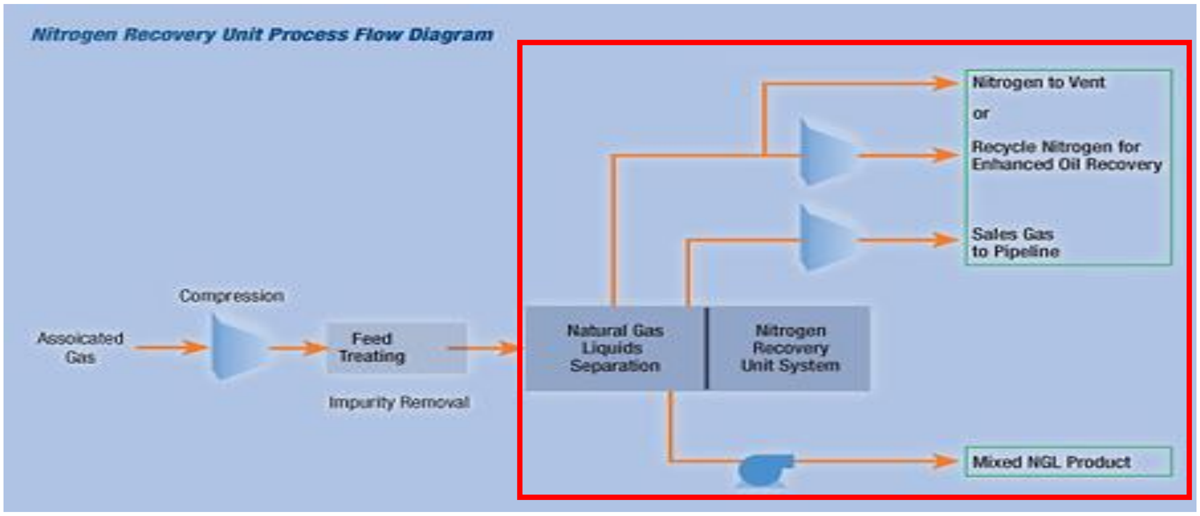

Figure 7.11. Schematic of gas purification system with NGL recovery directly before Nitrogen Rejection (red box). From Air Products, 2020.

As the entire gas processing sequence being described in this paper is being done so for the first time, straightforwardness and coherency dictate that simplicity of design should be paramount (Hernandez-Valencia, et al, 1992). Therefore, the entire process of Natural Gas Liquids, Liquid Natural Gas and fractionation will be considered as a separate and distinct module, completely optional, but sourced *from* the Nitrogen Rejection Unit.

The objective of Nitrogen Rejection is to remove nitrogen from feed residue gas to produce a treated stream with minimal nitrogen and an improved lower heating value (LHV) specification. The optimum Nitrogen Rejection process is highly dependent on the nitrogen content in the feed gas stream. Additionally, if recoverable quantities of helium exist in the gas stream, helium recovery can be integrated into the Nitrogen Rejection Unit (NRU) (Scholes, and Ghosh, 2017).

Nitrogen Rejection is a distillation process utilizing the different volatilities of methane rich residue gas (boiling point of [-161.5°C @ 1 atm]) and nitrogen (boiling point of [-195.8°C @ 1 atm]) to achieve separation. Depending on the composition of the feed gas, either a single column or double column (similar to Air Separation) Nitrogen Rejection fractionation system is used (Figure 7.12) (Spatolisano and Pellegrini, 2021).

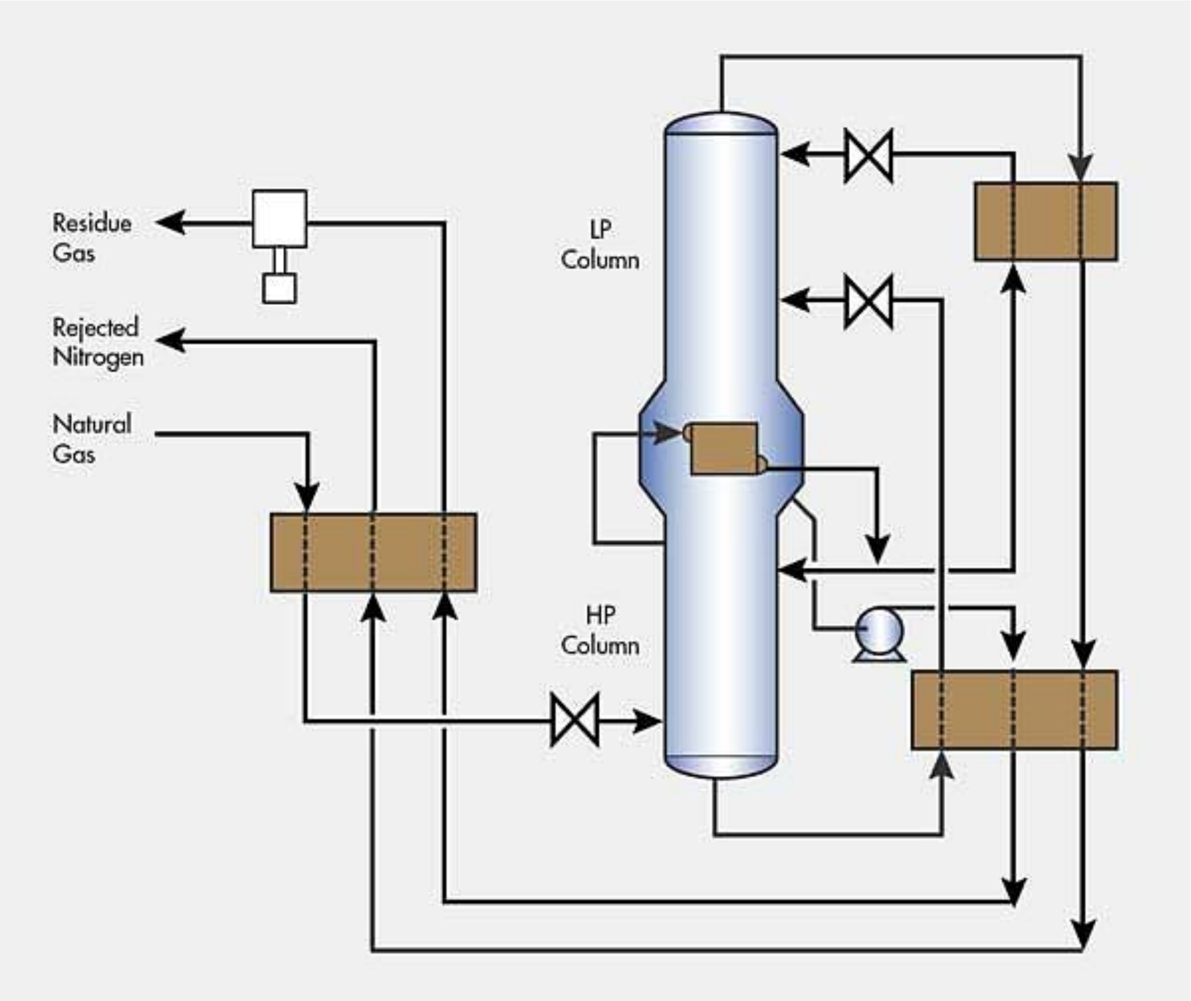

Figure 7.12. A double column style nitrogen rejection unit. From Hall, 2003. If NGLs were to be extracted, the ‘residue gas’ stream would be split between NGLs and helium extraction.

Nitrogen rejection units (NRUs) in gas processing are used to remove inert components from the gas to meet consumer standards. In a Nitrogen Rejection Unit, natural gas containing nitrogen is partially condensed (Knapik, Kosowski, and Stopa, 2018).

Methane and nitrogen are then separated in a system composed of one to three distillation columns depending on the feedstock composition and pressure and desired output.

Typically, the extracted nitrogen and a small amount of methane was vented to the atmosphere as waste or residual gas (Kuo, Wang, and Chen, 2012).

However, with environmental laws in place today governing oilfield wastes and by-products, there are better options. Refining the nitrogen to remove any contaminant and cooling the result would yield high purity liquid nitrogen, a very saleable commodity. At $US2.00/liter, the small price of retro-refining the first pass through an NRU would be covered and pay-out time would be short. Instead of expelling methane and nitrogen freely to the atmosphere, the so-called greenhouse gas methane and rejected nitrogen can be re-tasked as a saleable commodity.

The remaining gas stream, >99% methane, was then routed to sales or next processing phase; in this case, helium extraction membranes.

However, the residue gas stream here can also be mined for Natural Gas Liquids (NGLs), as noted earlier. As stated previously, there's no real consensus on where the gas stream is tapped for NGLs, so for streamlined and straightforward schematic modelling, if NGLs were to be tapped, it would be at this juncture (Ghorbani, et al, 2016).

Figure 7.13 shows the processes of extracting NGLs from the 'residue' gas generated by a Nitrogen Rejection Unit.

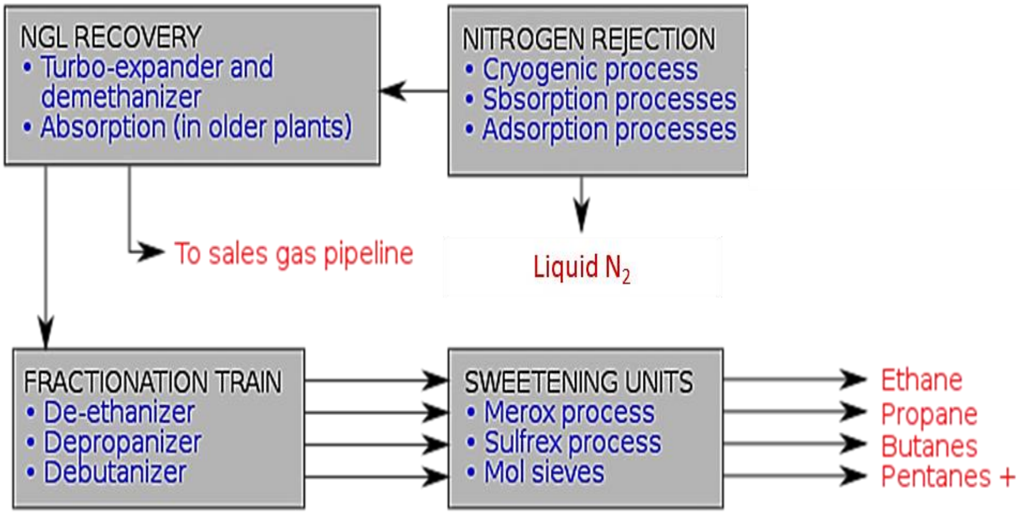

Figure 7.13. Process schematic of "residue gas" from Nitrogen Rejection Unit to Natural Gas Liquid fractionation and sweetening. From Wikimedia.com Creative Commons.

In an entirely optional step, the gas stream emerging from the Nitrogen Rejection Unit can be 'mined' for the Natural Gas Liquids, such as ethane, propane, etc., before liquifying the remainder as LNG (Liquified Natural Gas) (Ghorbani, and Amidpour, 2021).

Nitrogen rejection has been an economically viable option for decades, but historically only at flowrates in excess of 100 MMSCFD. With improved technology and increased natural gas prices over the past twenty years that rate has been reduced to as low as 5 MMSCFD (Hall, 2016), which makes it especially attractive to operators in shale plays whose product is mostly oil with relatively small volumes of associated gas (Joshi, et al, n.d.).

The process of extracting NGLs from a gas stream produced by a Nitrogen Rejection Unit is a multi-step procedure. The extraction of the NGLs mechanically typically involves a turboexpander and a low-temperature distillation column (called a demethanizer) shown in Figure 7.13 (Roy, et al, 2019). The inlet gas to the demethanizer is first cooled to about −51 °C in a heat exchanger (noted as a 'cold box'), which partially condenses the inlet gas. The resultant gas–liquid mixture is then separated into a gas stream and a liquid stream. The gas stream from the gas–liquid separator enters the turboexpander, where it undergoes an isentropic expansion (Bloch, and Soares, 2001) from an absolute pressure of 6.2 to 2.1 MPa that lowers the gas stream temperature from about −51 °C to about −91 °C as it enters the demethanizer (Figure 7.14).

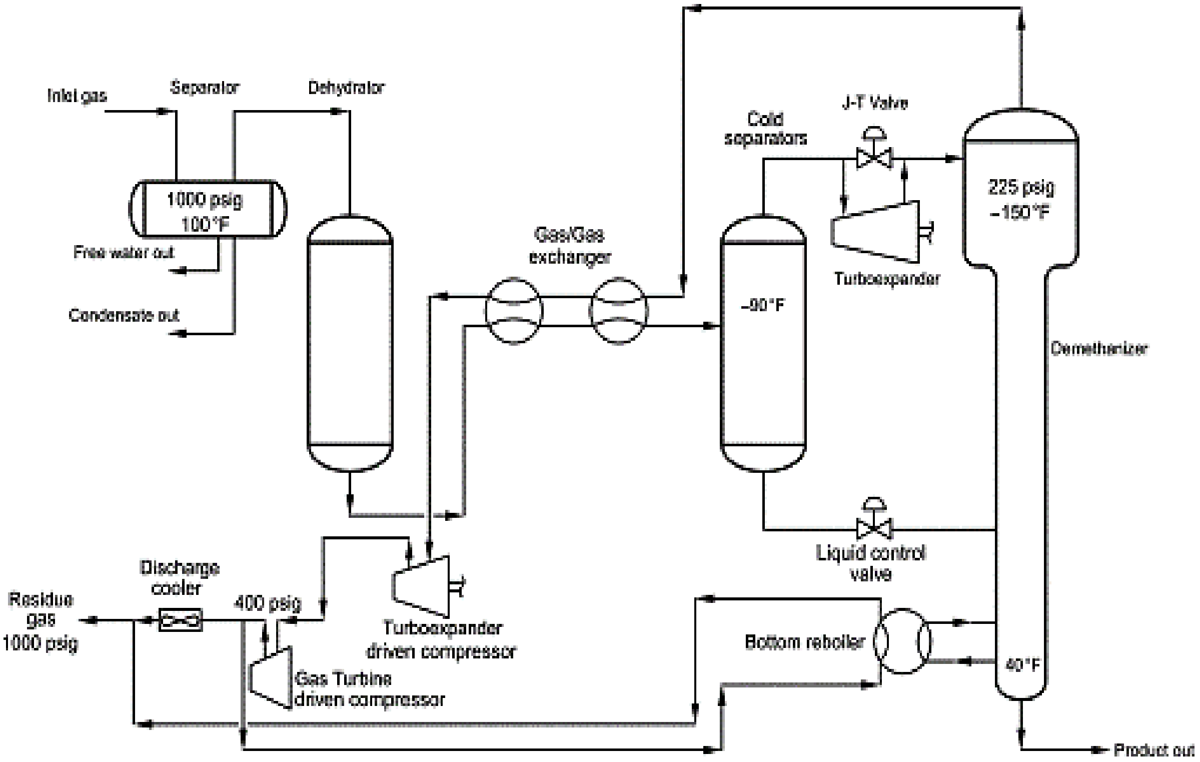

Figure 7.14. Schematic of Natural Gas Liquids recovery first stage: Turbo-expansion and demethanization. From Stewart, 2014.

Dry gas exits the molecular sieve section and is cooled by a gas/gas exchanger and demethanizer reboiler, after which it flows to a cold separator. Liquid from the lower section of the cold separator feeds midway into the demethanizer tower, which separates the methane from the liquids. The cooled gas and condensed liquid flow into the demethanizer tower where the gas rises and the liquid descends. The liquid product exits the bottom of the tower to be further processed as required. The cold residual gas exits the top of the tower and flows through the sub-cooler and into the gas/gas heat exchanger. Warm gas exiting the gas/gas exchanger flows to the suction side of the booster compressor and then to residue compression (Exterran, 2015).

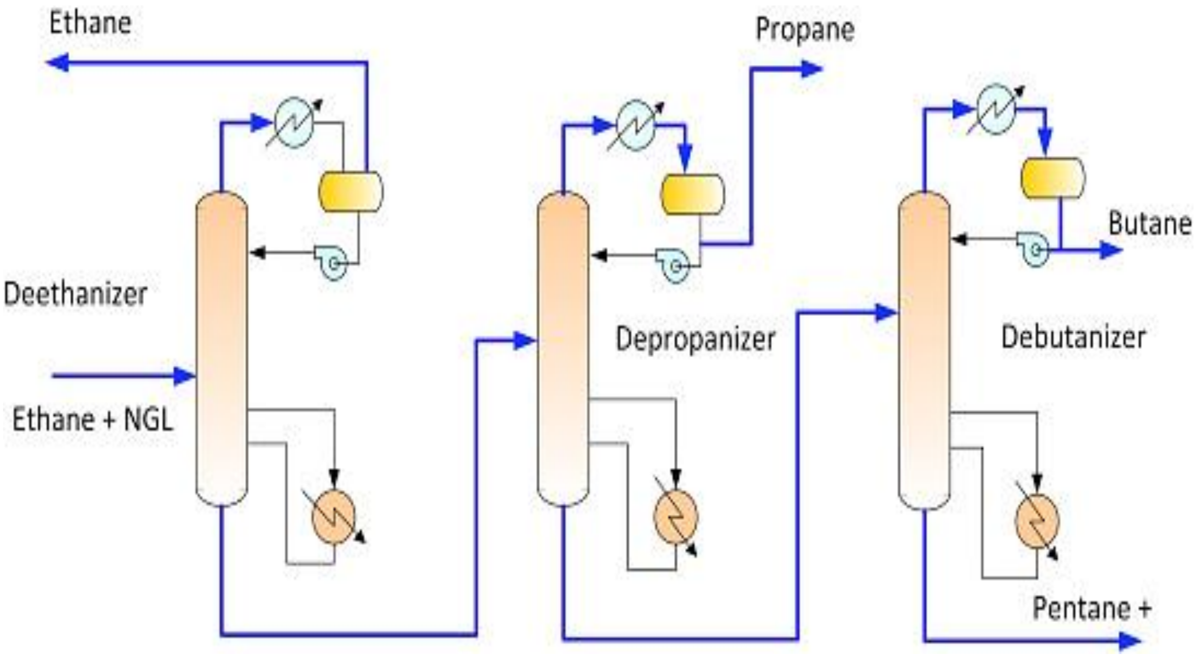

Figure 7.15. Fractionation train, Natural Gas Liquids recovery stream. From Mokhatab, et al, 2013.

The next step in the process is the fractionation of the various natural gas liquids. This is accomplished by a “Fractionation Train” which, in essence, is a series of heater/treater units which boil off and collect one particular member of the NGL content before flowing the residuals to the next heater/treater to extract the member with the next highest boiling point (Abdel-Aal, et al, 2015).

The train is essentially a series of distillation units (i.e., ‘stills’) interconnected from that which extracts the lowest carbon number member (typically ethane, C_2H_6) followed by the next member, propane (C_3H_8), then butane (C_4H_{10}), and pentane (C_5H_{12}). Although most fractionation trains stop with pentane, there is no reason, other than economic, that this series cannot be extended (Figure 7.16) to include the isomeric ("iso-") and normal extracts of butane and pentane, but to continue through "natural gasoline" heptane$^+$ and condensates.

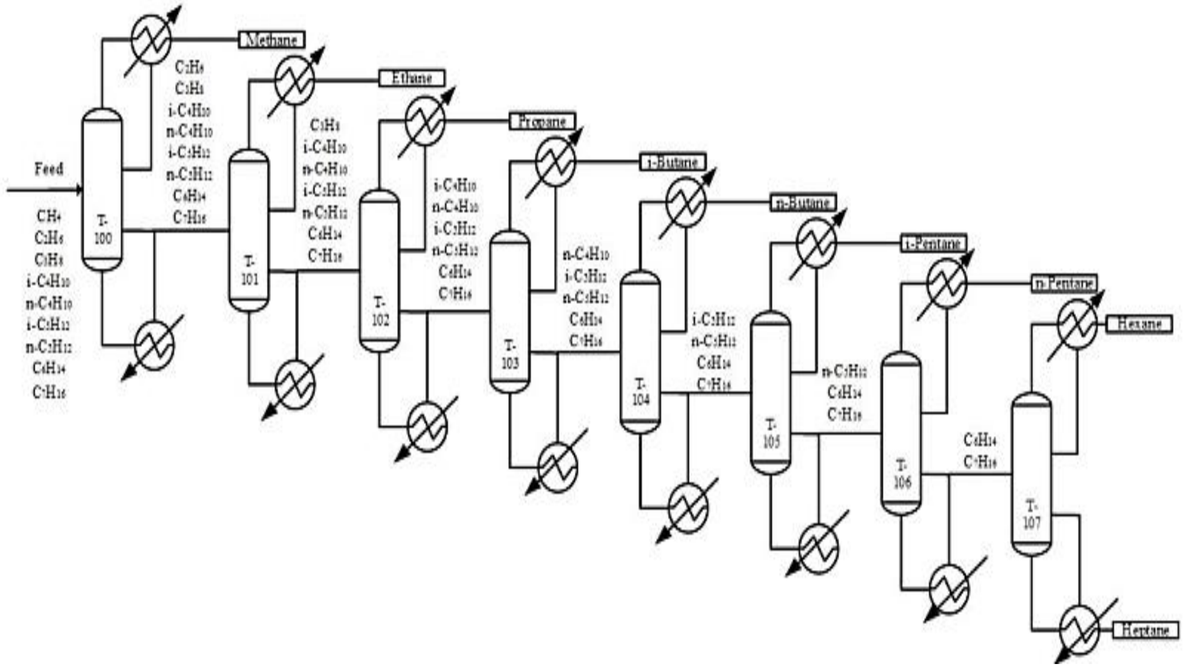

Figure 7.16. Continuous fractionation unit. From Rahimi, et al, 2015.

Once fractionate, the NGLs go through a process referred to as "Sweetening", typically via a Merox or Sulfrex process (Deyin, 2021). "Merox" or 'mercaptan oxidation' is the removal of mercaptans (aka 'thiol', which are extraordinarily noisome sulfur compounds of the generalized formula R-SH, where R represents an alkyl or other organic substituent and -SH is the thiol group; examples include *Methanethiol* – CH_3SH, *Ethanethiol* – C_2H_5SH and *Butanethiol* – C_4H_9SH) from the flow stream. It requires an alkaline environment, which is created by adding caustic or alternatively ammonia to the feed, and passing the mixture over a series of catalysts in a reactor. The mercaptans are converted to hydrocarbon disulfides, which are then washed out in various filter beds (Sadeghbeigi, 2020).

The Sulfrex (or *Sulferox*) process used in NGL sweetening units employs a caustic soda solution to extract the mercaptans from the propane and butane cuts respectively (Figure 7.17).

After extraction of mercaptans and separation from the organic phase, the exhaust caustic solution streams coming from the two units are collected and fed to caustic regeneration unit, where they are regenerated by a catalytic oxidation using air (Zarei, et al, 2012).

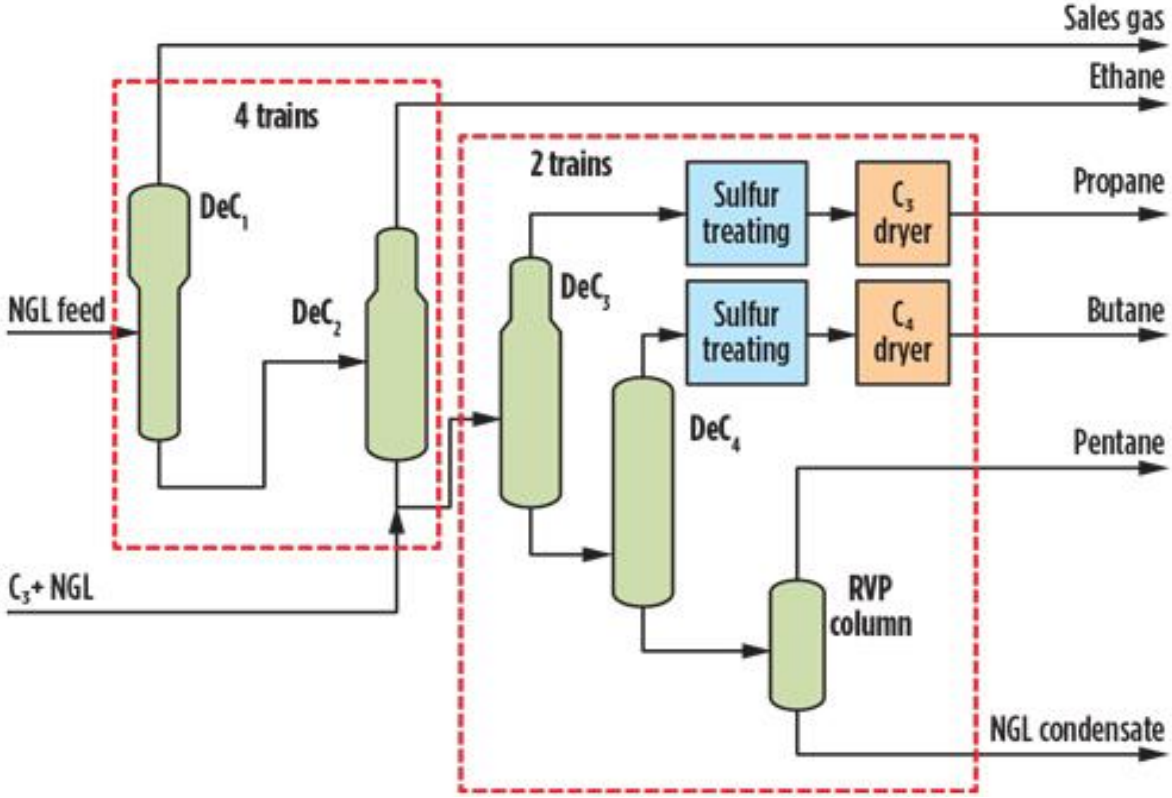

Figure 7.17. Sweetening units through fractionation to sales. From Rithauddeen, et al, 2021.

Although an entirely optional set of processes, the economic return from certain basins indicates that the cost of recovery and treatment of NGLs are outweighed by the return on investment. Part of the allure of membranes is that they are a low-cost adjunct to the gas treatment phase, have no moving parts, and represent very little capital, making the NGL option more attractive (Mills, and Antoine, 2021).

In the following figure (Keller, 2012), various lower 48 oil and gas basins are noted as are their typical GPM (gallons of NGLs per 1000 CFG). Although the range is rather variable, most oil shale plays, Bakken included, are rather 'rich' as compared with conventional plays. This has a potential positive impact on the economics of extracting NGLs from the gasses produced in these fields.

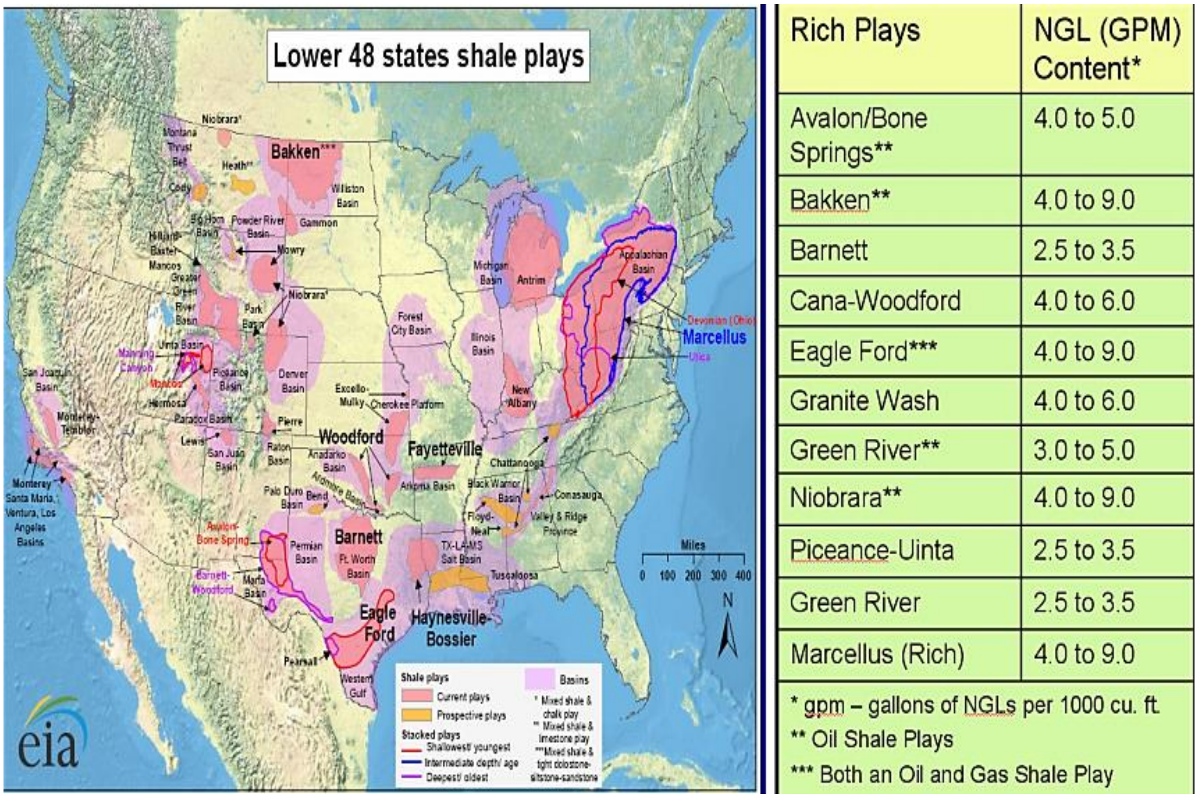

Rich Plays	NGL (GPM) Content*
Avalon/Bone Springs**	4.0 to 5.0
Bakken**	4.0 to 9.0
Barnett	2.5 to 3.5
Cana-Woodford	4.0 to 6.0
Eagle Ford***	4.0 to 9.0
Granite Wash	4.0 to 6.0
Green River**	3.0 to 5.0
Niobrara**	4.0 to 9.0
Piceance-Uinta	2.5 to 3.5
Green River	2.5 to 3.5
Marcellus (Rich)	4.0 to 9.0

* gpm – gallons of NGLs per 1000 cu. ft
** Oil Shale Plays
*** Both an Oil and Gas Shale Play

Figure 7.18. Natural gas liquids, processing economics. Note the GPM content for the Bakken. From Keller, 2012.

The overall economics of NGLs are varied and complicated. Since 2008 and the upsurge in oil shale plays (i.e., those with nanodarcy reservoir rock that are produced through horizontal wells that are multiply and/or massively hydraulically fractured), the production of NGLs have outstripped demand and for the first time, the US engaged in net export of these products (Figure 7.19).

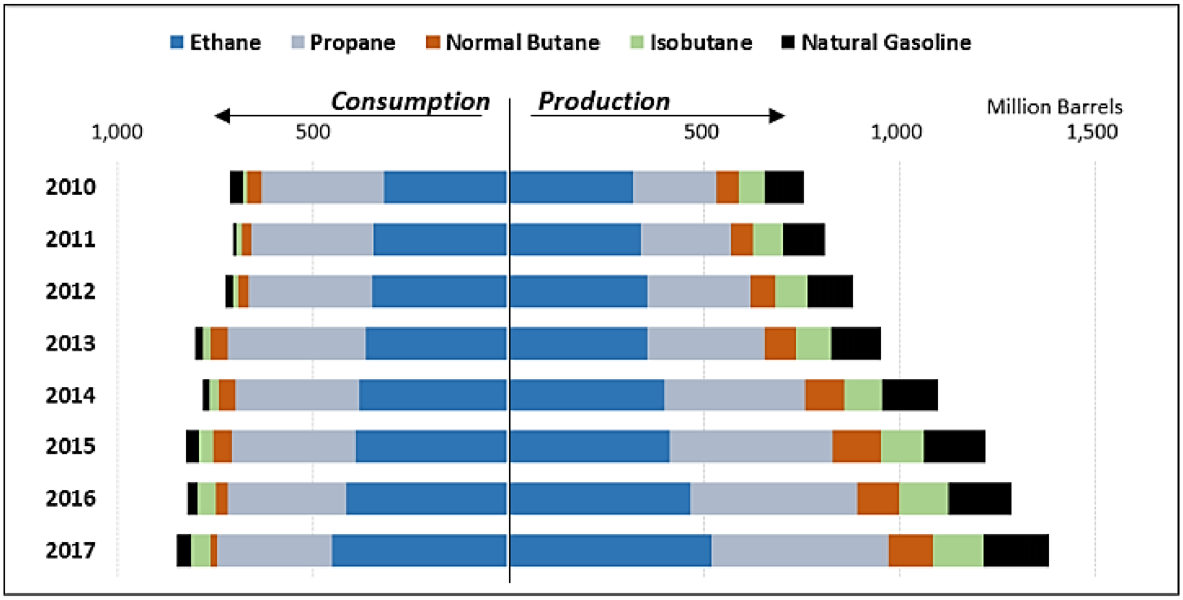

Figure 7.19. US Production and consumption of NGLs, 2010-2017. From U.S. Energy Information Administration, 2018.

Since 2008, the higher prices received for NGLs have caused a divergence from that of natural gas and created new markets. These markets moved away from the usual markets in the Gulf Coast and shifted to the US Interior and Northwest, toward the basins which have higher NGL values. As production costs decreased, technology improved, and production values increased (US EIA, 2018), Figure 7.20.

As the international competitiveness of U.S. NGLs has risen and as U.S. production has exceeded domestic demand, companies have increasingly looked to world markets. Over the years, demand for NGLs has remained mostly flat, even declining in some years. Without increasing demand in the United States, companies have increased their exports of NGLs (Rogers and He, 2020).

In the same time frame—2008 to 2017—U.S. imports of NGLs have fallen by over 30%. As a whole, the United States imports far fewer NGLs than it exports. In 2017 the United States exported over five times as many barrels of NGLs as it imported (Keller, 2012).

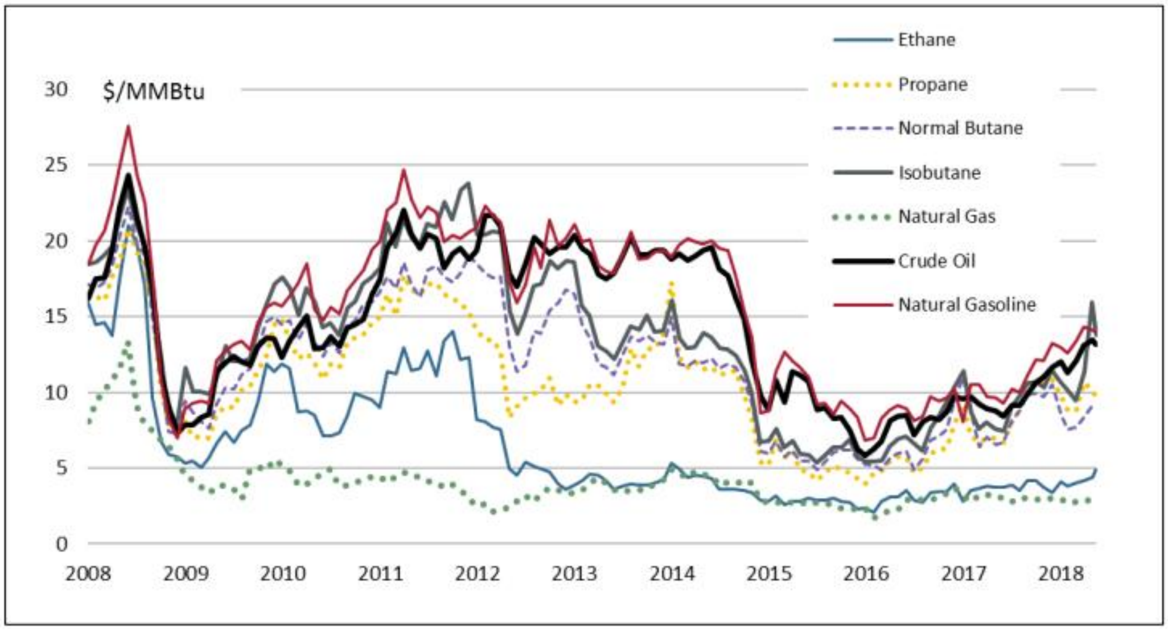

Figure 7.20. NGL prices by year, 2008-2018, compared to Crude Oil and Natural Gas Prices. From U.S. Energy Information Administration, 2018.

Of course, oversupply has led to a decrease in prices, and the influence during 2020-2022 of the global Covid-19 pandemics, lead to both decreased global demand for NGLs, caused disruptions, decreased production of NGLs and decreased revenue.

A global oil price war erupted and has raised the situation to extraordinary proportions. Oil prices have plummeted, tearing down the historical price relationships in the energy and chemical markets, including NGLs (Rogers and He, 2020).

NGL prices are influenced by many other non-oil factors including but not limited to natural gas, naphtha, basic chemicals (including ethylene and propylene) balances and prices, and waterborne freight rates (Rogers, and He, 2020).

The oil price war shock does not affect all NGLs (ethane, propane, butane, natural gasoline) prices to the same degree, nor at the same time. In fact, reversals in pricing for NGLs can occur if the supply of natural gas suddenly becomes impinged.

Typically, the costs of extraction of NGLs from sources like the unconventional Bakken would be profitable, however, with the vagaries of supply, demand, the impact of COVID-19 and its variants, one is only able to take a ‘wait and see’ attitude until the pandemic lifts.

However, pandemic-accelerated environmental, social, and governance (ESG) issues add another layer of complexity and will shrink the pool of available capital until *the industry makes the necessary investments to end flaring,* venting, and leakage along the entire value chain (Joseph, et al, 2020).

Moving from the optional extraction of NGLs, we now turn to the primary function of the proposed process, the extraction, purification and liquification of helium from Bakken-sourced flare gas.

7.1.2 Membrane Gas Separation

In opposition to the previously noted mechanical means of gas treatment, selective semi-permeable membranes offer a coast-advantaged and simpler method of separating and treating adjunct to the flare gas stream (Figure 7.21).

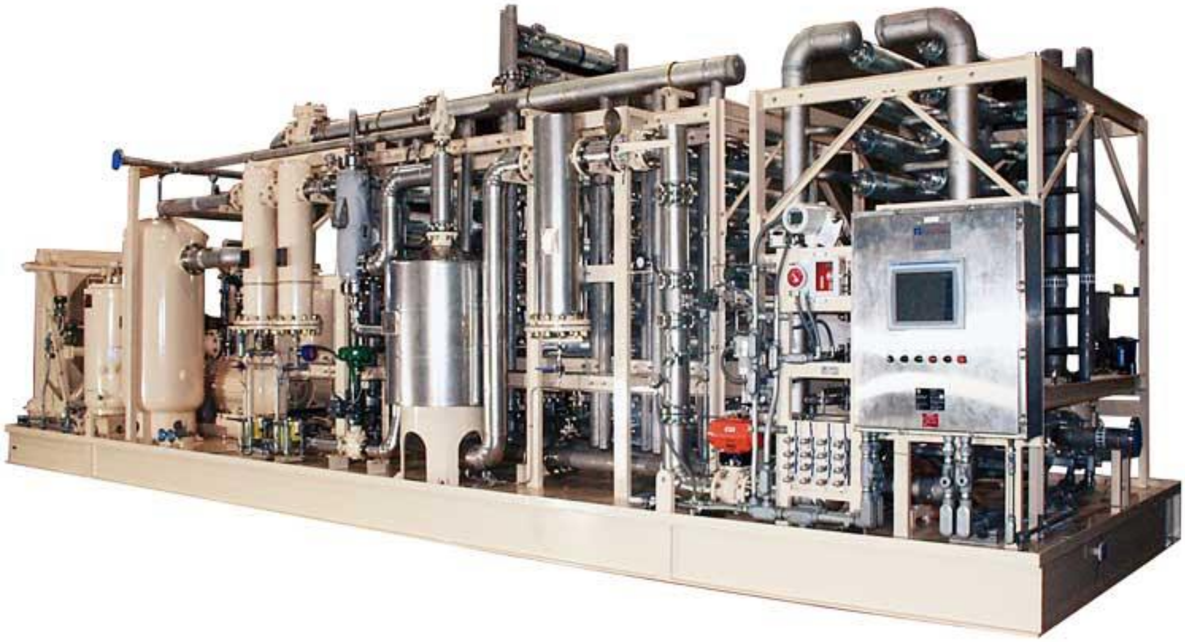

Figure 7.21. Integrated Gas Treatment and NGL membrane plant. Courtesy of Generon, Inc., 2021.

Membranes offer a series of size-selective semi-permeable membranes that differentiate on different molecules of a gas stream strictly by physical molecular size. These membranes are non-catalytic, have no moving parts, other than the fore and aft compressors necessary to keep the gas stream in motion, have near zero in consumables, require little maintenance, and require little in up keep other than changing out membrane particulars annually.

The unit seen above encompasses Module 1, gas treatment, and Module 2, HGL extraction, in one skid-mounted unit. As a part of the novel flow-through process described herein, this has the bonus of removing the “optional” from extracting Natural Gas Liquids. There is very low cost in taking the gas stream from the gas treatment side of the unit and passing it directly through to NGL extraction, see Figure 7.22.

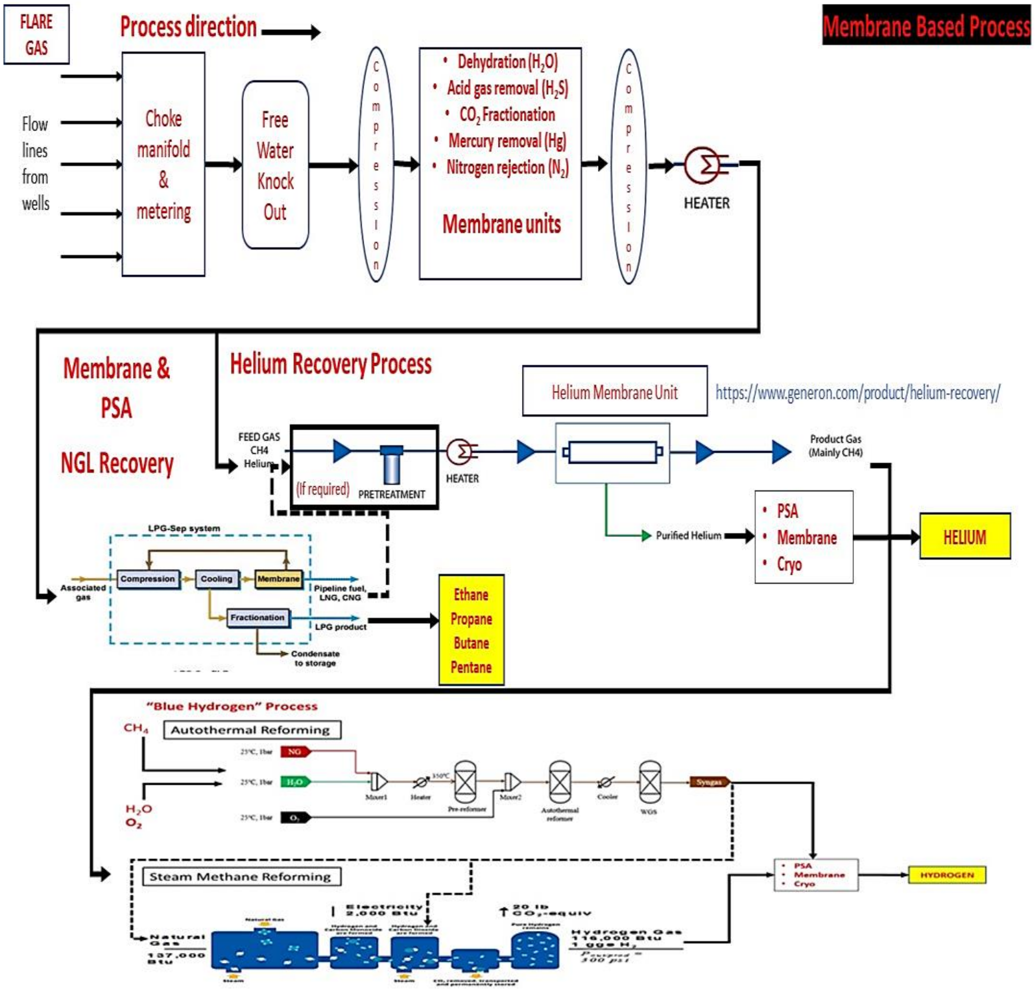

Figure 7.22. Membrane based process flow. Note that Gas treatment and NGL recovery are combined before helium extraction.

7.1.2.1 *Modules 1 and 2 combined*

Membrane gas separation (MGS) is a pressure-driven process that represents only a small fraction of myriad potential applications in refineries, the oil, gas and chemical industries. The first inception of this technology was in the middle 1960's (Stern, et al, 1965). Since ˜1980, when the serial production of commercial polymeric membranes was implemented, membrane gas separation has rapidly become a competitive separation technology (Bernardo, et al, 2009).

Being non-cryogenic, non-catalytic and with no consumables, they are therefore much less expensive, they have triggered an upsurge in both the use of membranes for helium extraction, but actually lowered the inherent volume of helium in natural gas which was thought to be an unchallengeable economic limit. Previously set at approximately 0.03% vol (National Research Council, 2000), the inexpensive to own and fairly simple to operate membranes have reduced that figure to less than 0.01% vol (Das, et al, 2012).

Membranes for gas separation is a proven technology, and one of the simpler processes to occur in recent years. Essentially a ‘pass through’ technology, it has no moving parts, physically a small ‘footprint’, and relies on the activity, volume and pressure of the gas stream and its constituents to operate effectively. These attributes, along with the fact that they are not cryogenic, along with low operating costs, makes the upsurge in the use of membranes for gas separation so extraordinary over the last 2-3 decades (Rezakazemi, Sadrzadeh, and Matsuura, 2018).

7.1.2.2 ***Helium Extraction via membrane***

As noted, the membrane helium recovery systems are a simple, pass through, ‘off the shelf’ piece of technology. As seen in Figure 7.23, the unit has no moving parts as the only pieces of the system are the gas feed lines, potentially a compressor, and a heater.

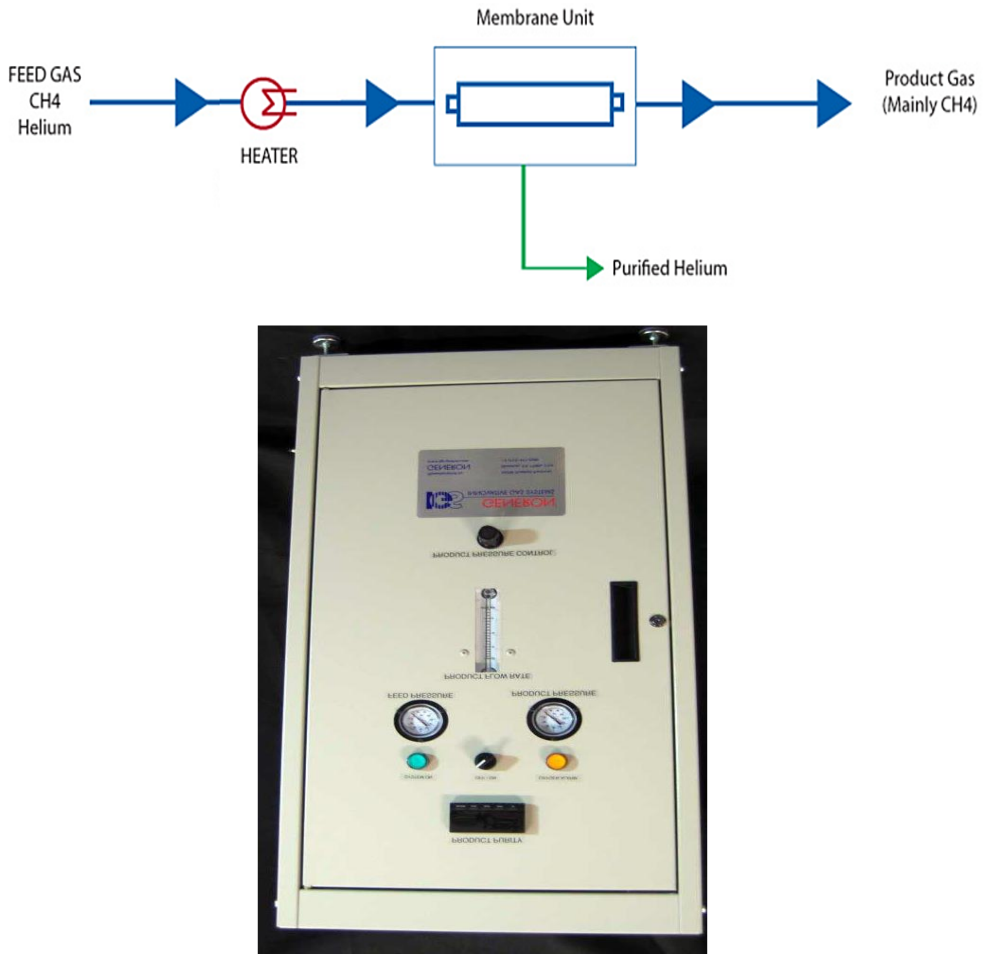

Figure 7.23. The Selective Membrane Helium Recovery System Diagram and device. From Generon.com, 2020.

Gas separation properties of membranes, as there exist myriad different types of membranes, rely upon several factors. These are:

- the material (permeability, separation factors),
- the membrane structure and thickness (permeance),
- the membrane configuration (e.g., flat, hollow fiber, etc.) and
- the module and system design.

Depending on the gasses which are to be separated, there are a number of different materials from which they can be constructed. Five different membrane types, i.e., polymer, silica, zeolite, metal-organic framework, and mixed matrix metal-organic framework membranes. (Sunarso, et al, 2016) are usually recognized:

- Polymeric membranes,
- Silica membranes,
- Zeolite membranes,
- Metal organic framework, and
- Mixed matrix metal-organic framework membranes

Polymeric (or polymer) membranes are the earliest variety of membranes which were devised for CO_2/natural gas separation (Dai, et al, 2021). Examples include polyamide or cellulose acetate, polyvinyl-allyl-dimethylsilane (PVADMS), dimethyl silicon rubber, poly(4-methyl-2-pentyne), polydimethylsiloxane (PDMS), poly[1-(trimethylsilyl)-1-propyne] (PTMSP), etc. (Iulianelli, and Drioli, 2020).

They have been proven to be incredibly efficient and inexpensive to operate, especially where such a light atom as helium is being filter extracted from a methane stream.

Other types of membranes have been utilized for selective gas separation, such as inorganic membranes (i.e., silica and zeolite). These have a number of advantages over catalytic or polymeric membranes, for example their ability to withstand harsher conditions such as high temperatures and corrosive gases (Mottern, et al, 2008).

Silica membranes are prepared in an acidic environment yielding ultrathin films atop an asymmetric substrate structure. This is also encompassed by macroporous support and numerous mesoporous interlayers (Sunarso, et al, 2017). Silica membranes also enable thermally-activated diffusion and operation at high temperature, i.e., ~600–800 °C, over which silica matrix starts to densify and delaminate. These advantages are offset by the relatively complicated procedures, time consuming synthesis and low reproducibility (Wackerlig, and Schirhagl, 2016).

Zeolite offers numerous advantages as gas separation membranes, such as the accrued information in its synthesis, relatively easy preparation technique, option to modify its chemical compositions via cation exchange, and relatively high thermal and chemical stability due to the Al_2O_3 content in a SiO_2-Al_2O_3-based compound (Caro, et al, 2000). SiO_4 and AlO_4 are the building blocks of zeolites. The three-dimensional zeolite framework is formed from the corner-shared tetrahedra and contains channels, channel intersections and 0.2 to 1 nm-width cages. A large number of zeolite frameworks have been developed as well documented in the works of the Structure Commission of the International Zeolite Association (Meier, et al, 1996).

Zeolite nonetheless has better thermal stability in a gas steam presence than non-doped amorphous silica, alumina, titania or zirconia membranes due to its crystalline structure. Phase transformation of a crystalline zeolite into thermodynamically more stable dense phases starts usually at high temperatures, i.e., above 1000^0C. As such, zeolite structure is stable below 1000^0C (Caro, et al, 2000).

However, given the relatively large pore-size of most zeolites, that condition does not favor molecular sieving behavior for small gases such as He and H_2 (Duke, et al, 2008). The major commercial direction on zeolite membrane development is to attempt post-synthesis procedures, which accounts for extra expense in collecting the smaller gas species.

Metal organic framework membranes (MOF), a relatively new species of what are now classified with the inorganic membrane clan, provide high selectivity, mostly due to the fact that the framework morphology can be specially designed to enable helium diffusivity while hindering other gases permeation (Asaeda, and Yamasaki, 2001), particularly methane.

Metal-organic framework membranes (MOFs) are crystalline or cryptocrystalline materials with structural cellblocks of ions or clusters of ions bridged by organic linkers to form one-, two-, or three-dimensional structures. This class of materials is also called ‘coordination polymers’ or ‘coordination networks’ (Zaręba, 2017). The primary advantage of MOFs relative to polymers or zeolites is the possibility to control the pore aperture, framework chemistry, surface area and pore volume (Pimentel, et al, 2014). They are relatively new and currently one of the more expensive choices in membrane gas separation technology.

- Mixed matrix metal-organic framework membranes.

Polymer-based membranes containing MOFs as additives or fillers, are defined as mixed-matrix membranes (MMMs). These semi-permeable membranes have been developed within the last decade. In contrast to pure polymeric membranes, these hybrid membranes display improved gas permeabilities and selectivity as the porosity of MOFs can be precisely tuned (Zornoza, et al, 2013) during construction. This method permits uniting the advantages of the organic polymers processability and respectable discriminatory adsorption and diffusion properties from MOFs (Tanh, et al, 2012).

Besides the physical composition of the membrane, the physical form of the membrane is also important. The variances of solid, perforated or hollow fiber membranes predicate which gas combination will respond most optimally to the form of the membrane (Peretti, et al, 2005).

For instance, recently hollow-fiber technology (HFT) (Figure 7.4) for the recovery of helium from natural gas or nitrogen rich gases has increased dramatically. Hollow fiber membranes provide the most highly efficient means of selectively separating gases due to the ultrahigh surface area available for gas permeation per unit volume (Dai, et al, 2021).

In a raw gas feed stream primarily consisting of methane and other hydrocarbons, nitrogen, and helium; helium's very simple atomic structure allows it to selectively permeate and enrich in concentration much faster than the other components (Scholes, and Ghosh, 2017).

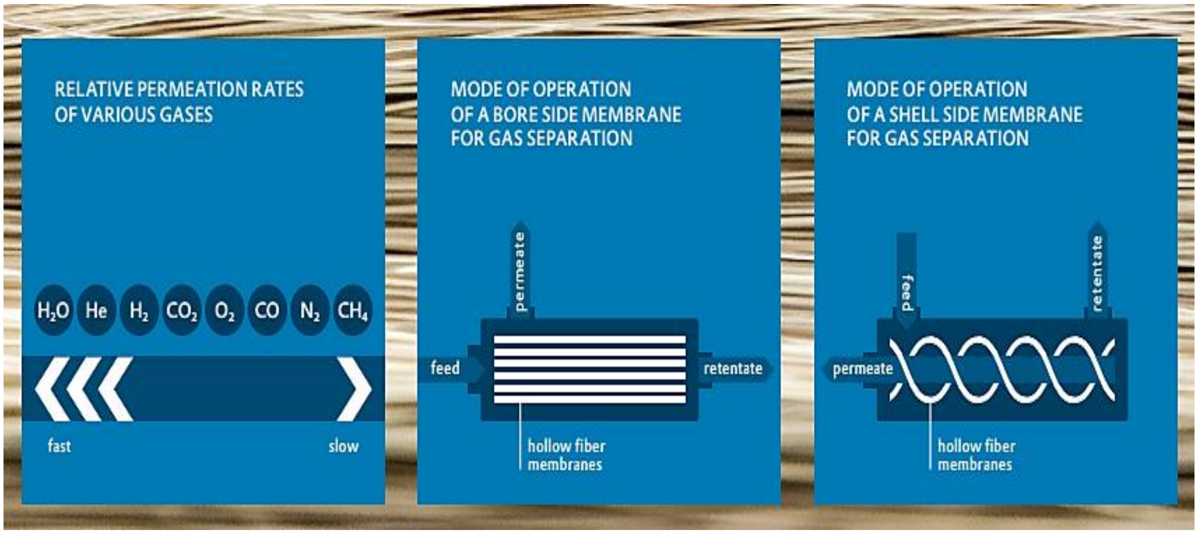

Figure 7.24. Helium selective hollow-fiber membrane operation. From Evonik, 2021.

When a natural gas stream containing helium is fed at pressure to a hollow fiber membrane, helium is selectively concentrated in the permeate stream, leaving a helium-depleted methane-rich stream as the retentate (residue) stream (Blamey, et al, 2016).

Depending on the compression, volume, operating pressure and concentration of one gas to another, this is accomplished quite rapidly, sometimes in the matter of seconds. This type of facilitated selective permeability has allowed the economic concentration of helium in a natural gas stream to fall an order of magnitude in the last decade (Evonik, 2021).

Immediately after gas treatment and NGL extraction, the cleaned, heated and compressed gas stream would go into the next section of membranes, that for helium extraction. Helium extract happens extraordinarily quickly due to the molecular activity of helium, its small atomic size and the large size differential between helium atoms (He) and methane molecules (CH_4) (Denning, et al, 2019).

Exiting the membrane suite would be a clean, heated and compressed stream of nearly pure methane. In the next step, methane reforming for hydrogen via Autothermal Reforming (ATR) or Steam Methane Reforming (SMR), the common feedstock is the clean, compressed, nearly pure gas stream (Baltrusaitis, and Luyben, 2015).

7.1.2.3 ***Autothermal Reforming and Steam Methane Reformation***

Autothermal reforming (ATR) utilizes both oxygen (O_2) and carbon dioxide (CO_2) or steam (SMR: see § 5.2) in a reaction with methane (CH_4) to form Syngas, a combination of hydrogen (H_2), carbon monoxide (CO) (Jack, et al, 2019).

Autothermal reforming combines the steam reforming reaction and fuel oxidation into a single unit, the exothermic oxidation providing the heat for the endothermic reforming process. ATR yields higher H_2 production than partial oxidation (POX) and faster start-up and response times than steam reforming (SMR) (Oh, et al, 2018). The reaction occurs within a single chamber where the methane feedstock is only partially oxidized. The reaction is exothermic due to this oxidation. When Autothermal Reforming utilizes uses carbon dioxide, the H_2:CO ratio produced is 1:1; when Autothermal Reforming steam the H_2:CO ratio produced is 2.5:1 (Faheem, Tanveer, Abbas, and Maqbool, 2021).

The reactions can be described in the following equations, with using CO_2:

$$2\ CH_4 + O_2 + CO_2 \rightarrow 3\ H_2 + 3\ CO + H_2O\ \text{[Syngas]}$$

The outlet temperature of the syngas is between 950–1,100°C and outlet pressure can be as high as 100 bar (Azimi, et al, 2013).

The primary difference between Steam Methane Reforming (SMR) and Autothermal Reforming (ATR) is that SMR uses only air for combustion as a heat source to create steam, while ATR uses purified oxygen. The advantage of ATR is that the H_2:CO can be varied, which can be useful for producing specialty products (Noureldin, et al, 2015).

However, SMR can be run in conjunction after ATR to eliminate excess carbon monoxide and provide for a higher degree of carbon capture, usage and sequestration (CCUS).

Steam Methane Reforming (SMR) is the one process used today globally to extract over 50% of the world’s industrial hydrogen (GTI, 2021). Known colloquially as “Blue hydrogen”, is separates itself form other hydrogen generating schemes by being based on natural gas and having at the outcome not only high-purity hydrogen, but large amounts of carbon dioxide (CO_2) which can be captured, stored, sequestered or sold.

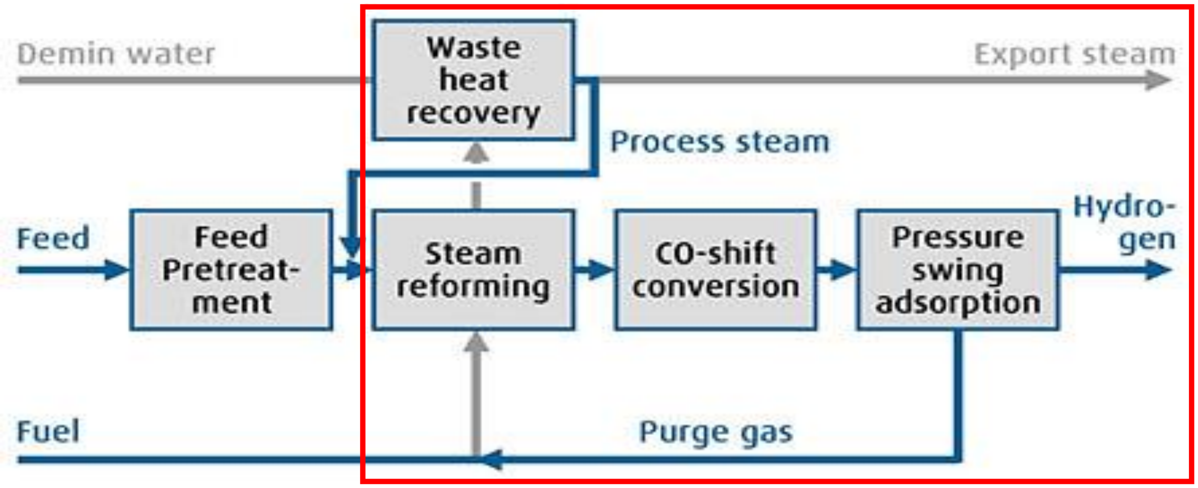

Figure 7.25. Stream Methane Reformer schematic (red box). Feed pretreatment described earlier. From Costa, 2021.

The schematic form of the steam methane reforming pathway in Figure 7.25 notes, like other processes described here within, is modular. In the modular schematic, the feed pre-treatment would be handled by the various devices of Module 1 “Gas Pretreatment”. This includes removal by an amine plant, gas sweetening, dehydration by a glycol dehydrator and nitrogen exclusion by a dedicated nitrogen rejection unit.

Steam reforming of CH_4 into 2 molecules of H_2 and one of CO would be next, fueled by a small amount of the gas stream saved from the flares. This gas would fire the boilers and produce the necessary 700°C–1,000°C steam at 3-25 bar (42 – 350 psig). Here a metal catalyst (platinum, palladium, etc.) is required to produce hydrogen, carbon monoxide, and a relatively small amount, at this stage, of carbon dioxide. Since steam reforming is endothermic, heat must be supplied to the process for the reaction to proceed (Figure 7.26)

Steam-methane reforming reaction[1]

$CH_4 + H_2O \text{ (+ heat)} \rightarrow CO + 3H_2$

Water-gas shift reaction[2]

$CO + H_2O \rightarrow CO_2 + H_2 \text{ (+ small amount of heat)}$

Figure 7.26. Steam-methane reforming reaction, and 2. Water-gas shift reaction. From Office of Energy Efficiency and Renewable Energy, 2021.

Successively, in what is called the "water-gas shift reaction," the carbon monoxide and high temperature, high pressure steam is reacted via a metal catalyst to produce carbon dioxide and more hydrogen. In a final process step called "pressure-swing adsorption", (PSA) carbon dioxide and other impurities are removed from the gas stream, leaving essentially pure hydrogen. The process produces approximately 8 and 12 kg of CO_2 per kilogram of hydrogen (Grande, 2012). However, this CO_2 is of high purity and can be captured, stored, sequestered or sold.

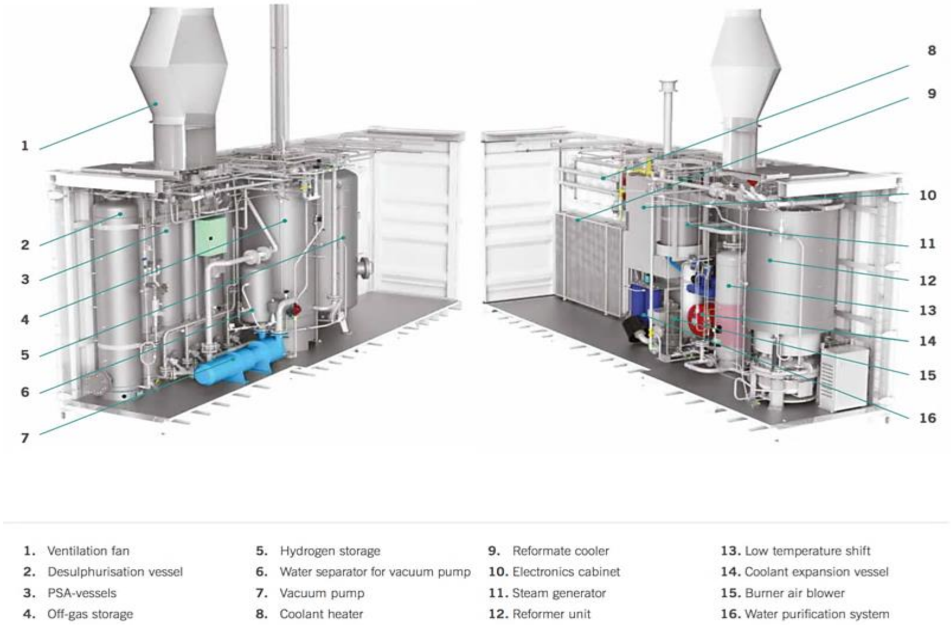

Figure 7.27. Conceptual design of a steam methane reformer plant. From Fuel Cells, Hydrogen, Hydrogen Production, 2016.

As seen in Figure 7.27, a steam methane reformer unit does appear to be more complex than either natural gas pre-treatment or helium extraction via membranes, it can be broken down into simpler sub-units (Wishart, 2019).

Disregarding, for the time, compression, various pumps, heaters and treaters; the process can be simplified as seen in Figure 7.28.

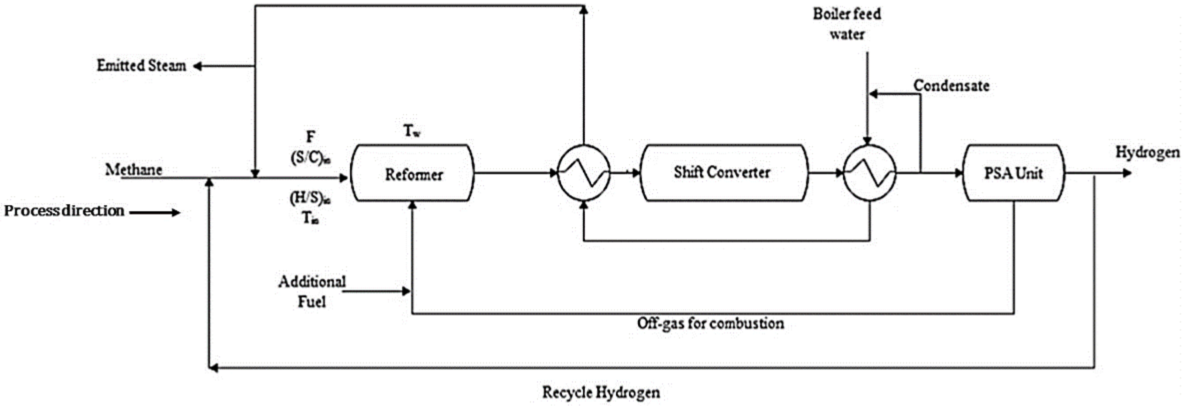

Figure 7.28. Simplified diagram for steam methane reforming. From Sinaei Nobandegani, et al, 2016.

However, this process chain includes hydrogen purification and liquification. To break down the process to its simplest and most explicatory, see Figure 7.29.

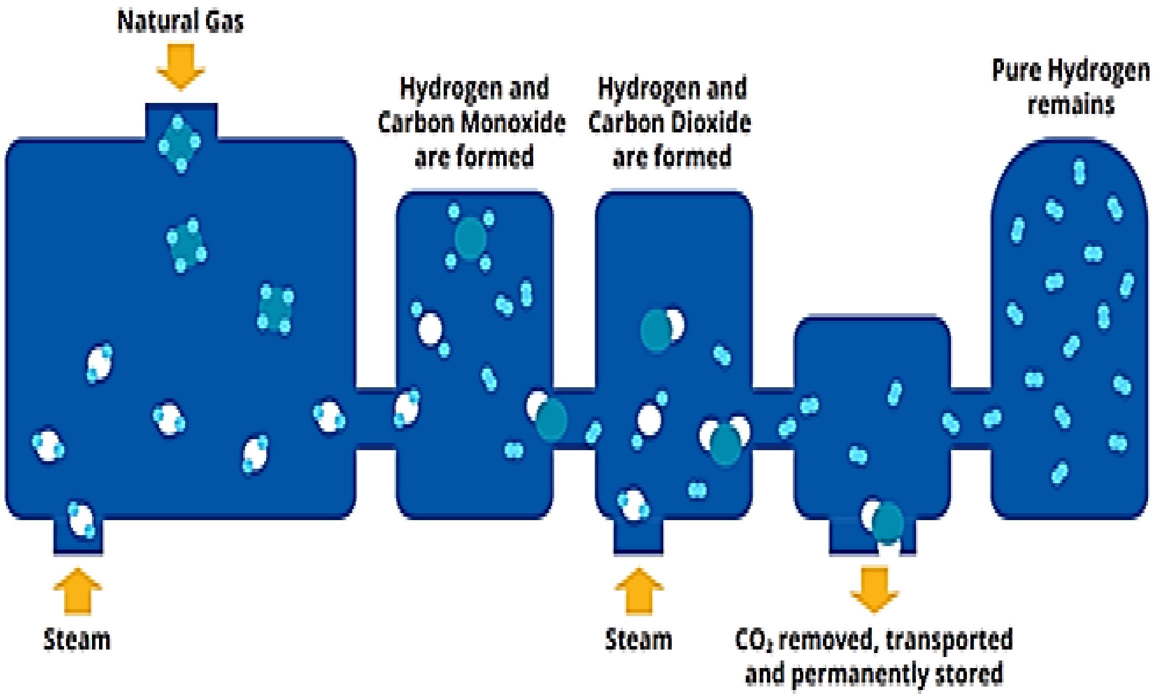

Figure 7.29. Steam Methane Reforming process. From Costa, 2021.

Here we have a straight-through, as opposed to the actual closed-loop system. Both types exist, however, the closed-loop system predominates in industry today. In either form, though, they each possess almost equal efficiency (Collodi, et al, 2017).

For the sake of discussion, we'll concentration on the straight-through system noted in Figure 7.29.

Phase one requires the heated, high purity methane stream to be introduced to the reformer chamber. Here, superheated water steam, at a temperature of 700°C–1,000°C steam at 3-25 bar (42 – 350 psig) is presented from a supercritical steamer. The high temperatures promote reactions between the methane stream and water to capture as much hydrogen as practical from the process. At these elevated temperatures, the high-purity methane (CH_4) reacts with steam (H_2O) to produce hydrogen (H_2) and carbon monoxide

(CO) by physically removing the hydrogens from the methane molecule (Palmer, et al, 2021).

The presence of a nickel, platinum or palladium catalyst increases the process rate and aids in retaining as much hydrogen as achievable, Figure 7.30. The hydrogen-carbon monoxide mixture exits the reformer via the cold outlet manifold. Carbon monoxide may be harmful if released into the environment (Bakey, 2015). However, it does have a plethora of industrial uses; such as in metal fabrication, electronics and in the creation of certain pharmaceuticals (Linde Air, 2012). However, here it is kept in the reaction chain as the steam/hydrogen/CO enters into the next section of the SMR apparatus, the Shift Converter. Being a closed system, the CO at this point is not extracted from the continuing process (Cinti, et al, 2016).

The next phase of the process moves the steam/CO/hydrogen to the Water Gas Shift Reactor (WGS Reactor) or Shift Converter (Martınez-Merino, et al, 2103). To utilize the produced carbon monoxide and produce additional hydrogen, carbon monoxide from the reforming reaction enters the water gas shift reactor. This reactor is filled with water and includes an iron chrome-based catalyst which causes steam (H_2O) to catalytically break down into oxygen (O_2) and hydrogen (H_2). Hydrogen is captured while oxygen unites with the carbon monoxide (CO) from the reforming reaction to produce carbon dioxide (CO_2) (Bakey, 2015). The carbon dioxide here produced is of exceptionally high purity and can be captured for CCUS; i.e., stored, sequestered, or sold. Approximately 7 kg. of CO_2 is produced with every single kg of diatomic hydrogen (H_2).

Gas Purification – Pressure Swing Absorption (PSA) is the next part of the SMR process. However, the gas mixture exiting the WGS Reactor is not pure hydrogen, and needs to be further refined to meet pipeline and fuel conditions. Although there are numerous manners in which to purify hydrogen, utilizing pressure swing absorption (PSA) is the most common in industry (Grande, 2012).

The gas mixture enters the purifier, where explicit absorptive materials entrap impurities at elevated pressures. Purified hydrogen is then pumped out of the vessel. Finally, the vessel is completely de-pressurized to release trapped contaminants (Deusner, et al, 2012.)

PSA is also used for the removal of high purity carbon dioxide, remnant methane, residual carbon monoxide, and any remaining water from the diatomic hydrogen. Overall, steam methane reforming (SMR) has high hydrogen yield efficiency (~74-78%) and is estimated to produce hydrogen at a cost of around $1.8 /kg (Velazquez Abad, and Dodds, 2017), depending on the cost of the feedstock.

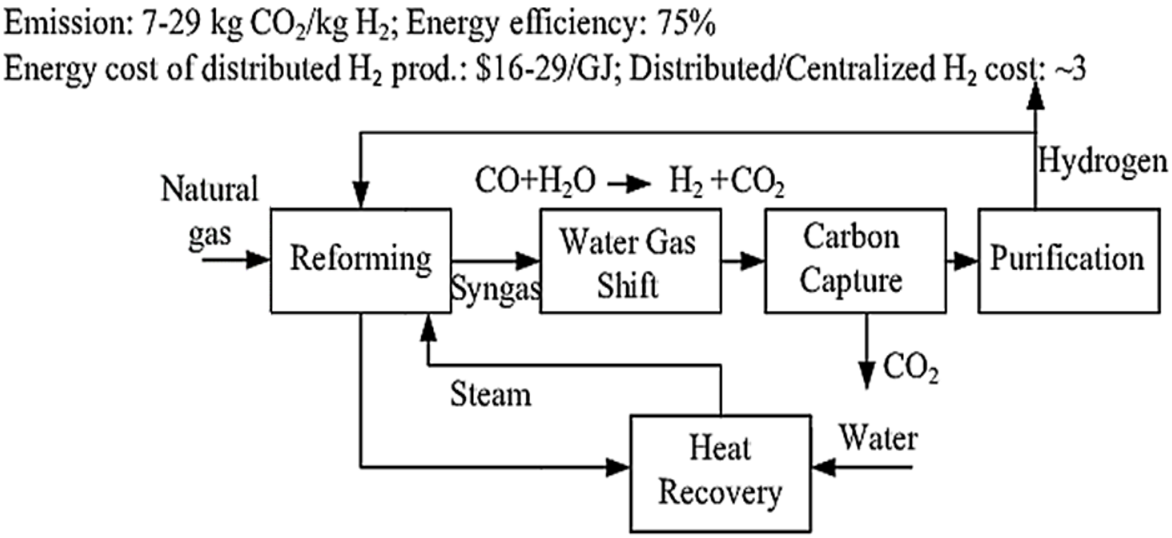

Figure 7.30. Hydrogen production by steam reforming of natural gas, showing CO-CO_2 train and carbon capture. From Demirel, 2015.

It has also been suggested that elemental carbon ('carbon black') could also be obtained from the SMR process. For reference's sake, carbon black currently sells for ~$1.35/kg (US$1,365/metric ton). However, as noted by Dagle, et al, (2017), thermal decomposition of natural gas is currently used in the carbon black industry to produce carbon black for use in tires, certain road paving treatments, and electrical equipment; but natural gas as the feedstock has been largely replaced by heavy oil fractions from crude oil processing. Further, most carbon black today is created through methane pyrolysis, also known as 'turquoise hydrogen'; where all the carbon content in the methane is captured in solid form (elemental carbon – 'char') rather than as carbon dioxide. The high reaction temperature (>1000^{o}C) required for methane conversion contributes greatly to process inefficiencies, limits the choice of materials of construction, causes steam pressure build-up and loss of catalytic active sites due to carbon fouling (Bartholomew, 2001), which are all problematic. It adversely impacts catalyst life, and exacerbates heat losses, increasing costs and lessening profits.

In summary, by utilizing the original gas stream water, from the FWKO or glycol dehydrator from Module 1, and using a small percentage of the gas stream for fuel, the operating costs of the SRM stream are practically nil. However, if ATR is to be used, either alone or in conjunction with SMR, the cost of a liquid air or standalone oxygen plant must be taken into consideration (Noelker, and Johanning, 2010).

There is, of course, compression to ensure the reformer and water-gas shift are within operating parameters, but with heating and water being obtained as part of the procedure, the operating costs will be very low. With the creation of ~7 Kg of CO_2 with every kilogram of hydrogen (Day, et al, 2005) (Figure 7.30), this high purity product can be captured, stored, sequestered or sold. If sold, perhaps to the Food and Beverage or Oil Industry, the returns can be used to offset any costs of purification and liquification of the hydrogen, making this an eminently economical process to produce liquid hydrogen.

CHAPTER 8

Economics

8.1 The Unusual Economics of Helium

The economics of helium as it applies to geological and engineering projects is daunting. For years it was thought that a simple rule of thumb, such as “if the concentration of Helium in the gas stream exceeds *x.xx*%, then it will be economic to extract”.

That no longer holds true, if it ever had.

8.1.1 Hotelling

The fundamental principle of the economic theory of non-renewable resources was first derived by Harry Hotelling in 1931. This principle is often called the ‘‘Hotelling Rule’’, and it is typically represented by some form of the following equation (Dasgupta and Heal 1979; Devarajan and Fisher 1981).

$$P_{(t)} = P0e^{rt} \text{ (Equation 8.1)}$$

In Eq. 8.1, P(t) is the (settlement) price of one unit of the resource in period *t*, P0 is the initial price (at t = 0), and *r* is the rate of interest. In another interpretation, the Hotelling Rule theorizes that the owners of non-renewable (and non-fungible) resources will only produce basic commodities if in doing so it can yield more than could be earned from available monetary instruments, such as U.S. Treasury Bonds or other similar interest-bearing securities. Hotelling’s work (1931) noted that the price of an exhaustible resource *must* grow. Hotelling's Theory defines the price or yield at which the owner of a non-renewable resource will extract and sell it, rather than leave it and wait, Figure 8.1.

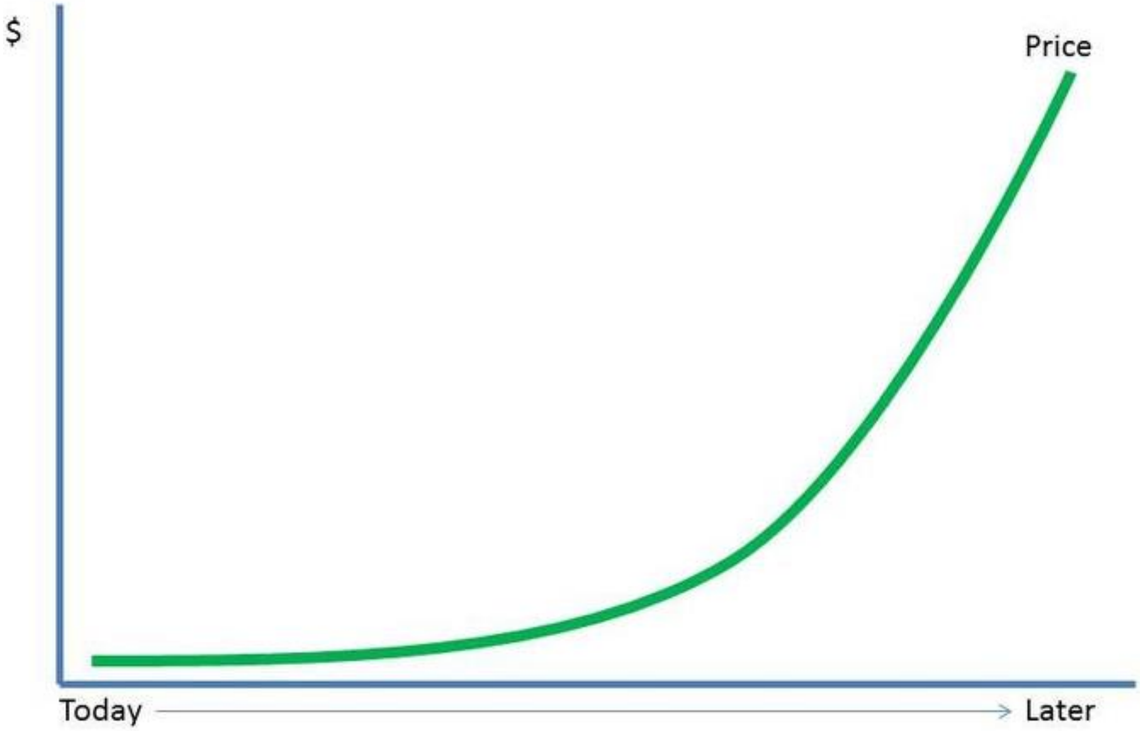

Figure 8.1. Hotelling's Price Path for a non-renewable, exhaustible resource with completely known stock, no discoveries possible, no alternatives, no recycling, private ownership and constant costs of extraction. From Haab, 2013.

Hotelling (1931) also studied the market structures of 'monopoly' and 'oligopoly'. He was able to demonstrate that a monopolist would tend to extract the resource at a lower rate than a competitive firm (Devarajan and Fisher 1981), which is a situation not reflected in the economy of helium today.

Although global helium production is not controlled by a cartel, *per se*, the relatively few firms producing this exhaustible resource could still be considered a more-or-less effective oligopoly (Cai et al., 2010).

From the late 1930s to 1960, the U.S. Bureau of Mines (USBM) was the only major producer of helium in the world (U.S. Government Accountability Office 2015), and fewer than five global producers have controlled the helium market since 1990 (Kornbluth 2015, 2017c).

For these later decades, the price of global helium had been controlled by the US Federal Government. Around 40 percent of the world's helium supply had been stored in the U.S. Federal Helium Reserve in Amarillo, TX. The reserve is kept in an enormous natural underground reservoir connected to nearby helium refining facilities as well as several natural gas fields via pipeline (Morgan, 2000).

Centered on the mid-continent of the US, its major helium field was Hugoton in Kansas, Oklahoma and Texas. The US government also had created an underground helium storage at Cliffside Field in Texas (Holland, and Emerson, 1979), along with surface infrastructure to support both the gathering, cleansing, purification, and injection of the helium.

The U.S. Congress decided to privatize the federal helium program in 1996, requiring that their entire helium supply be sold off by 2015. The goal was to recoup the \$1.30$^+$ billion that the government spent accumulating helium by selling their helium supply at a constant rate.

It was assumed that by the time the federal reserve had sold off most of its helium, new sources of helium would become available. What happened was that not nearly as much helium was produced by the private industry as the US Congress thought, which led to a diminishing supplies and spiking prices situation, Figure 8.2.

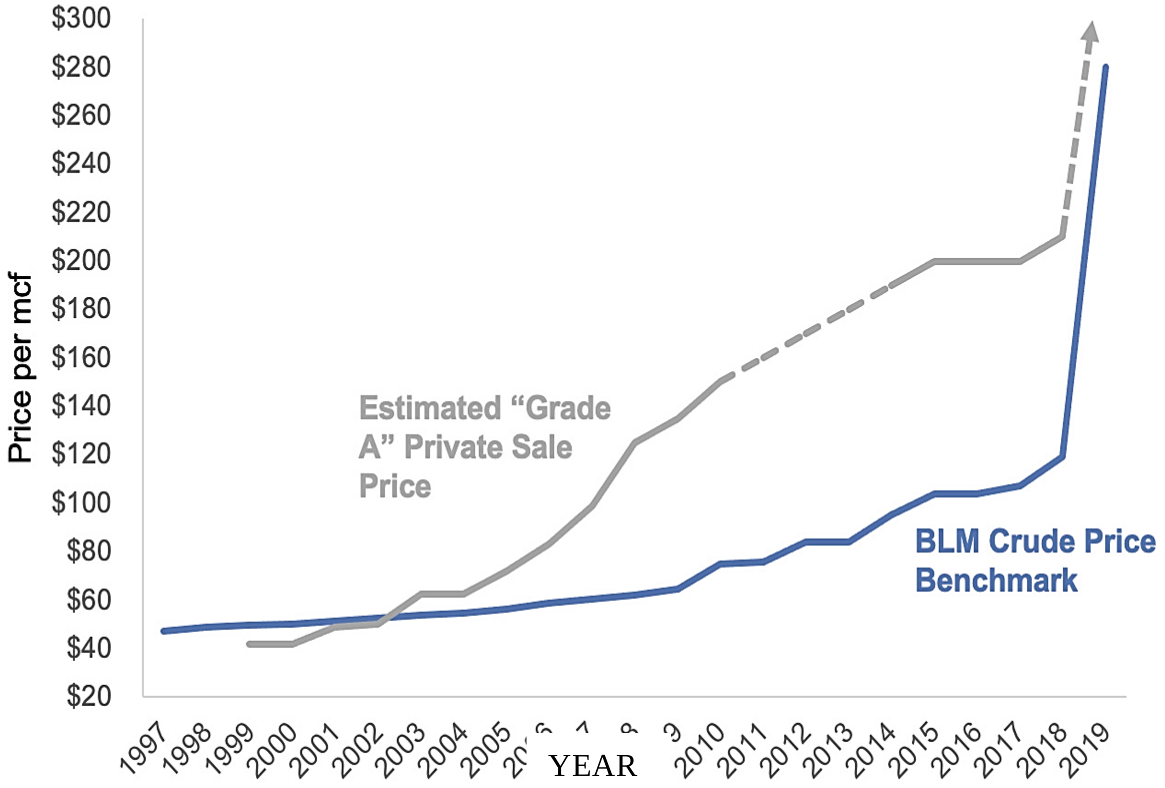

Figure 8.2. Historical US BLM and Private Helium Prices. Courtesy U.S. Bureau of Land Management.

By 2013, Congress realized it needed to change course. It delayed the final sell-off date by another 10 years and instead of selling off the federal helium supply at a fixed price, they would *auction* it off piecemeal. The idea was to help increase competition and to stabilize the market price. Unfortunately, this law may appear to have done the exact opposite (Anderson, 2017).

The steadily decreasing supply and the global increase in demand also caused the price of helium to go up by a staggering 400 percent in the past decade alone.

Furthermore, as a result of the Helium Stewardship Act passed in 2013, roughly 10 percent of the BLM's (Bureau of Land Management) helium was sold through auction in 2014-2019. Out of the 13 companies that sold refined helium at the time, only four had refineries connected to the federal helium reserve, which reminds one of a helium oligarchy.

This meant that the other nine companies had to work out a deal with one of the four refiners in order to process it. But because those helium sales went through auction, they went to the highest bidder, which resulted in two of the refiners buying it all, completely shutting out the other nine (A. Winchester, personal communication, March 2, 2023). Basically, the competition has decreased drastically, which contributed to a sharp monopolistic spike in costs. Foreshadowing by Hotelling in the early 1930s seems prescient.

Now, the Federal Helium Reserve has discontinued the sale of crude helium to private industry, with the remaining stockpile earmarked for Federal contract holders and users only. The BLM held its final crude helium auction in 2019, with the price rising 135%, from US$119/Mcf a year earlier to US$280/Mcf.

Market pricing for helium is difficult to discern. It is not a traded commodity, and both short- and long-term pricing is normally based on confidential contracts. It’s a niche market that suffers from a lack of detailed analysis due in large part to the availability of its closely held data (Wright, 2021).

At this time (~2013), international growth in helium exploration and production was thought to be growing enough to replace that which was to be lost by the closing of the BLM Federal Helium reserve.

Table 8.1. Worldwide proven and potential Helium reserves and contained helium by region by country.

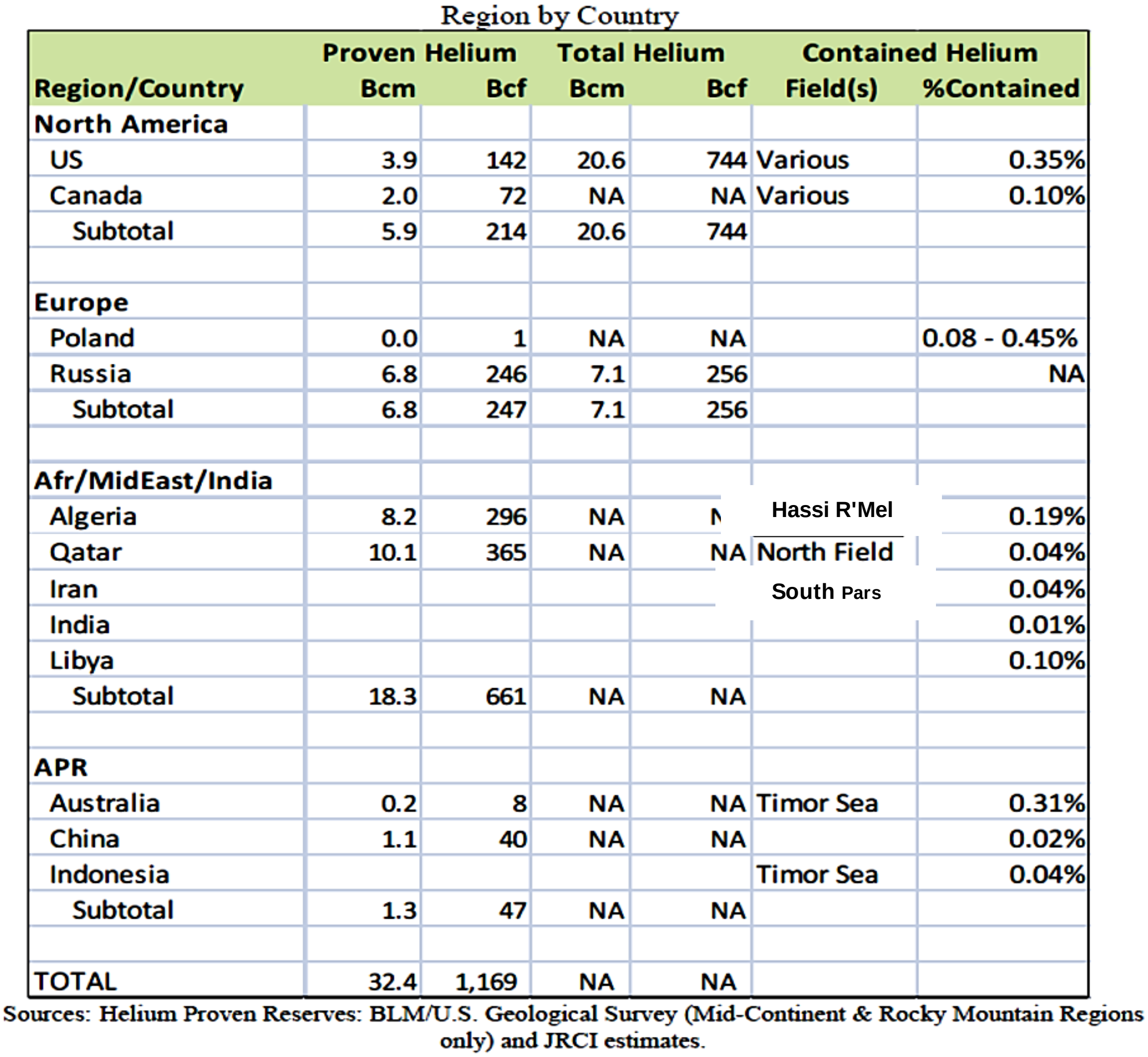

Region by Country

	Proven Helium		Total Helium		Contained Helium	
Region/Country	**Bcm**	**Bcf**	**Bcm**	**Bcf**	**Field(s)**	**%Contained**
North America						
US	3.9	142	20.6	744	Various	0.35%
Canada	2.0	72	NA	NA	Various	0.10%
Subtotal	5.9	214	20.6	744		
Europe						
Poland	0.0	1	NA	NA		0.08 - 0.45%
Russia	6.8	246	7.1	256		NA
Subtotal	6.8	247	7.1	256		
Afr/MidEast/India						
Algeria	8.2	296	NA	N	Hassi R'Mel	0.19%
Qatar	10.1	365	NA	NA	North Field	0.04%
Iran					South Pars	0.04%
India						0.01%
Libya						0.10%
Subtotal	18.3	661	NA	NA		
APR						
Australia	0.2	8	NA	NA	Timor Sea	0.31%
China	1.1	40	NA	NA		0.02%
Indonesia					Timor Sea	0.04%
Subtotal	1.3	47	NA	NA		
TOTAL	32.4	1,169	NA	NA		

Sources: Helium Proven Reserves: BLM/U.S. Geological Survey (Mid-Continent & Rocky Mountain Regions only) and JRCI estimates.

Of these countries, Russia, Canada, Qatar, Australia, and Algeria were thought to be the largest suppliers of helium, both bulk and refined, for the foreseeable future. However, along with the worldwide effects of the COVID-19 flu (https://www.rockymountainair.com/blog/pandemic-effect-on-global-helium-market/) from 2020-2023 delivering essentially a global Force Majeure across the international board, there were other unforeseen disruptions and lags that abounded in the helium supply worldwide:

- Qatar: 2017-2022: sanctions by GCC countries.
    - https://www.bbc.com/news/world-middle-east-55538792
    - http://www.gasprocessingnews.com/news/qatar-closes-helium-plants-amid-rift-with-arab-powers.aspx
- Russia: January, 2022: Amur helium plant fire.
    - https://www.reuters.com/business/energy/russias-amur-gas-plant-says-unit-caught-fire-2022-01-05/
- Russia: International helium suppliers depart Russia after war in Ukraine, and Amur Plant fire.
    - https://www.euronews.com/next/2022/06/22/ukraine-crisis-linde-russia-sibur
- Australia: Mt. Kitty prospect, in the southern Amadeus about 200 km south southwest of Alice Springs. Skyrocketing infrastucture costs and relatively lackluster exploration results.
    - https://geoscience.nt.gov.au/gemis/ntgsjspui/handle/1/83965
- Algeria: 1991-2003: Forced to shut down its helium operations because of soaring natural gas demand in Europe.
    - https://cen.acs.org/business/specialty-chemicals/War-Ukraine-makes-helium-shortage-more-dire/100/i10
- United States: One of the leading contributors of helium supply shutdown happened due to a leak in mid-January 2021 at the Cliffside crude helium enrichment plant in Texas. The leak led to an unplanned shutdown in 2021, followed by a four-month outage of the plant in 2022, and extended and expensive remediation.

    - https://www.blm.gov/sites/default/files/docs/2022-06/20220601%202000%20Cliffside%20Gas%20Plant%20Status%20Report.pdf
- Canada: Only begun drilling specifically for helium in 2021, after declaration of a provincial Helium Development Plan.
    - https://www.reuters.com/business/energy/canadas-saskatchewan-province-gets-lift-record-helium-activity-2022-01-18/
    - https://www.saskatchewan.ca/government/news-and-media/2021/november/15/government-of-saskatchewan-launches-helium-action-plan

The Russia-Ukraine war quashed the chances of global economic recovery from the COVID-19 pandemic, at least in the short term. The war between these two countries has led to economic sanctions on multiple countries, a surge in commodity prices, and supply chain disruptions, fueling inflation across goods and services and affecting many markets across the globe.

However, it is estimated that the global helium market size will still grow from $4.45 billion in 2022 to $5.63 billion in 2023 at a compound annual growth rate (CAGR) of 12.9%. (https://www.thebusinessresearchcompany.com/report/helium-global-market-report).

At this current point in time, the Federal Helium Reserve only sells to federal users. As such, the apparent lack of market has caused four of the largest helium suppliers in the past to shut in or curtail much of their helium supply.

Accidents and Force Majeure seem to be the describing terms when forecasting or even divining the cost of helium today. War and sanctions in Russia disrupt both supply and demand.

However, besides the upswing in Saskatchewan helium exploration and production, many companies in the US have set their sights solidly on exclusive exploration for and production of helium in the Western US. Desert Mountain Energy, Four Corners Helium, North American Helium, et al, are exploring in Arizona, New Mexico, Colorado, Utah, Wyoming, and Montana; specifically for helium (Halford, 2018). However, these are admittedly small companies and will take some time for them to be adding to the helium supply.

This still leaves the question of pricing for helium for use in forecasting the viability and profitability of projects.

Helium in a non-fungible commodity. It cannot be exchanged for hydrogen or other Noble gasses because it possesses unique fit-for-purpose characteristics. For instance, it is wholly non-reactive, non-flammable and does not form compounds. Contrast that with hydrogen, which is very reactive, flammable and forms literally billions of molecules, i.e., organic chemistry.

Further, there is only a embryonic spot market for helium. Unlike other more transparent commodities, helium is not presently traded on the spot market and a visible price per MCF [one thousand cubic feet] is not available.

South African natural gas and helium producer Renergen has signed a $25 million forward sale agreement with US company Argonon Helium, which is intended to bring price transparency to the currently murky helium market. (https://www.renergen.co.za/renergen-announces-forward-sale-helium-agreement-to-commence-tradeable-helium-spot-market/).

Therefore, without a spot or futures market for helium, the market pricing for gas is difficult to ascertain as it is not a traded commodity and pricing is normally based on long-term, confidential contracts. This results in opaque pricing given there are only a few key suppliers and industrial gas buyers. (https://mineralrightspodcast.com/mrp-155-helium-royalties-at-all-time-high/).

Based on research and personal communications with personnel in the Helium industry, the following has been ascertained regarding actual pricing of both Crude and Grade-A helium to date, with estimates for the next two years: (Dr. J.E, Fitzgerald, personal communication, February 19, 2023; Dr. Arkady Efimov, personal communication, Feb. 03, 2032, Mr. Robert Cook, personal communication, February 16, 2023; Mr. John Hoey, personal communication, February 12, 2023).

Table 8.2. Crude and refined Helium prices from 2015-2025 (est.).

HELIUM PRICES (/MCFG)		
Year	Crude	Grade-A
2015	$92.00	$106.00
2016	$110.00	$138.00
2017	$118.00	$147.00
2018	$135.00	$179.00
2019	$280.00	$301.00
2020	$320.00	$326.00
2021	$337.00	$358.00
2022	$340.00	$505.00
2023	$498.00	$625.00
2024	$575.00	$800.00
2025	$640.00	$965.00
		Estimate

Now as each grade commands its own particular price, the price of your "average" grade helium has been racing upwards at a frantic pace. It is often difficult to establish a price that could be used in scoping studies or to make a determination if the helium possesses enough value to extract. There exists a continuum of prices from crude helium, through the six (or nine) grades to Grade-A (99.99999%) helium.

As of this writing (02-2023), Henry Hub Natural Gas is bringing US$1.92/MMBTU /MMCF. “Raw (unrefined- crude) helium” today commands approximately $400/MCFG (~150 times the value of natural gas), while “Grade A helium” delivers $625/MCFG, or over 230 times the value of the hydrocarbons.

Referring to the included “Scoping Study” for Bakken flare gas-derived helium, conducted by the Chemical Engineering Department of UND, we find:

Table 8.3. Bakken helium plant annual income.

Flow rate				**Gas constant**		**Gas price**	**Helium income/year**
ft^3/hr	*	hr/year	*	R	*	$/mcf	
2,440		8,760		0.95		400	$10,112,228.64

Based on 25,000 MCF/yr., which is 21,240,000 cubic feet raw Helium per year, due to utilizing “R”, the gas constant, or 21MMCFHeG/Y (21 Million Cubic Feet of Helium Gas per Year), this translates to $27,704/day, or $10,112,228.64/year, based on 2-6 well pads (12 wells equivalent gas) and US$400/MCF helium. The flow rate of raw flare gas at 2,440 ft^3/hour is equivalent to 69,600 lbs/hr (37.178 MCFGPD)* and will send the treated associated gas product to a downstream plant for further processing.

Gas pre-treatment/helium separator modules can be specially designed and custom-built for approximately $5M to handle 25MMCF of raw gas. Therefore, a good pad could pay-out in less than half a year.

Looked at another way, the feedstock for Bakken-derived hydrogen is free. It is basically a waste product and therefore of consideration only for disposal rather than retail.

**69,600 lbs/hr = 25.82 SCF/minute * 60 * 24 = 37,178.38 SCFPD or 37.178 MCFGPD*

In 2022, according to the EIA, the amount of gas flared/vented was 76,332 MMCF (76.3 BCFG). It is noted through sample and survey that Bakken gas contains, on average, 0.03% helium. So there exists ~2.3 BCF helium that could be obtained through helium capture and concentrating. Given the price of crude helium at 03-2023 of US$400/MCF, the total revenue from this captured helium would be 2,300,000MCF * $400 = US$920,000,000.00; assuming, of course, no losses and 100% conversion.

Although this project notes that there are upwards of 10 different products that can be had from the capture of Williston Basin flare gas, the majority of the importance has been given to helium. In fact, there are times that it appears that the other saleable products are forgotten and the project stands or falls based on the economics derived from helium only. This is not the actual case, though.

A previous incarnation of this dissertation was written less than 10 months ago when crude helium was bringing approximately US$152/MCF on the world market. At the time of this editing, crude helium is commanding over US$400/MCF, and rapidly headed upward, as outlined in the vagaries of helium pricing noted previously.

The present cost of a simple portable He extraction unit varies from $750,000 (US) to $5,000,000 (US) (Tedesco, 2022). With that one-time cost, the value of He is significantly greater than the value of the CH_4 which at the time of writing is US$1.92/MMCF, Henry Hub. A 12-well pad producing 25,000 MCF Helium/year could easily pay the higher cost out in less than 6 months.

Also, in the USA, only Arizona and Utah, and Saskatchewan and Alberta in Canada, levy royalties on helium at the state, or provincial level. Private mineral owners only receive a royalty from the sale of helium if it is specified in the lease; which is typically not the case.

There is a monetary incentive for the operator when the government does not accrue dividends from helium exploration or production and mineral owners can be assuaged with small royalties on a commodity that has much higher growth potential.

The Economics of Bakken Flare Gas recovery and product extraction

The following table notes the parameters of the composition of Bakken Flare Gas and the volumes utilized in the attached Scoping Study in determining the size and cost of the required helium extraction apparatus.

Table 8.4. Bakken Scoping Study economic parameters.

Field	**Flare Gas/day (MCF)**	**Total # wells**	**Contribution/well (avg.) MCF**
Bakken Scoping Study	37.18	12	3.1
He content (vol %)	**MCFG/Year 99.99% He**	**Price He/MCF**	**Helium gross value/year**
0.2	25,000	$400.00	$10,000,000.00
Methane CH4	**Ethane C2H6**	**Propane C3H8**	**Butane C4H10**
0.58	0.2	0.11	0.025
Pentane C5H12	**Liquid Nitrogen**	**Carbon Dioxide**	
0.08	0.0003	0.01	*Percentage*

This table notes the parameters of the *total* Bakken contribution to Williston Field flared gas on an annual basis.

Table 8.5. Total Bakken economic parameters.

Field	**Flare Gas/day (MCF)**	**Total # wells**	**Contribution/well (avg.) MCF**
Total Bakken	1,150,000.00	14,981	76.76
He content (vol %)	**MCFG/Year 99.99% He**	**Price He/MCF**	**Helium gross value/year**
0.2	619,032	$400.00	$247,612,800.00
Methane CH4	**Ethane C2H6**	**Propane C3H8**	**Butane C4H10**
4,440,506	15,312,086	8,421,648	3,828,020

Pentane C5H12	**Liquid Nitrogen**	**Carbon Dioxide**	
12,249,670	2,067,132	765,604	*MCF/Annum*

Table 8.6 is a table of comparative natural gas, helium and NGLs in ten world helium fields. For comparison’s sake, Australia (Mt. Kitty), Oman and Tasmania do not currently export helium, for various reasons. The remaining seven countries are/were net helium exporters, depending on current global events.

Table 8.6. Economic parameters of global helium-producing fields

Country	**Field/ region**	**EUR - Gas-BCF**	**N2 %**	**CO2 %**	**HE %**	**H2S %**	**Methane CH4 %**	**Ethane C2H6 %**	**Propane C3H8 %**	**Butane C4H10 %**	**Pentane C5H12 %**	**Sulfur**	**Fed. CIT% (Commercial Income Tax)**
Russia	Yurubchen-Tokhomo	73,000	6	0.8	0.4	1.56	88	0.73	0.245	0.124	0.511	0.529	32
Australia	Mt. Kitty	883	79.62	3.3	6.6	0.45	7.29	0.7	0.5	0.1	0.1	0.12	30
Canada	Williston Basin	6	97	0.5	2	0	0.5	0	0	0	0	0	15
China	Sichuan Basin	520	2.94	4.3	0.2	5.13	83	3.31	0.97	0.49	0.015	0.003	25
Oman	South Oman Salt Basin	952	3.5	3.72	0.39	3.2	81	4.3	2.02	1.01	1.014	0.009	17
Qatar	North Dome	1.8E+07	3.55	1.76	0.04	0.55	84.99	5.524	2.008	0.059	0.147	Trace	35
Tasmania	Shittim	8	75.5	0.6	1.26	0.01	21	2.12	Trace	Trace	Trace	Trace	30
US	Mid Continent Rift System	25	20	43	1.5	9.5	26	Trace	Trace	Trace	Trace	Trace	21
US	Hugoton - KS, CO,	76	14.62	0.24	0.44	0	72.59	6.5	3	1	0.8	0.075	21
US	Dineh-bi-Keyah, AZ	6	78.7	11.1	4.39	0	3.4	0.5	0.2	0.2	0	0	21

Table 8.7. NGL commodity prices (03-2023)

Methane Price	**Ethane Price**	**Propane Price**	**Butane Price**	**Pentane Price**	**Liquid Nitrogen**	**Carbon Dioxide**
$1.97/MMcf	**$6.22/BBL**	**$28.71/BBL**	**$43.06/BBL**	**$55.74/BBL**	**$318/BBL**	**$60.16/BBL**

Table 8.7 notes the most current (03/2023) Natural Gas Liquids prices in the United States. Also included are the latest prices for high-purity liquid nitrogen and carbon dioxide.

8.2 Economic Analysis

Economic analysis of the process as described should be fairly straightforward. The cost of the feedstock is zero; or near enough to be discounted, as it is currently a waste product which can now be captured and capitalized upon.

The costs of materials depend upon whether they are purchased used or new, or are leased, or leased for sale (Miller and Upton, 1976). The cost for process fuel is nil as it is aimed to take a small portion of the captured natural gas stream after nitrogen rejection to use as fuel for the system. Water for the boilers of the Steam Methane Reformer (I.e., Hydrogen Hub) would come from the Free Water Knock Out and the glycol dehydrator seen in Module 1.

Consumable costs should be low, as apart from compressors, the process has virtually no moving parts. In fact, module 3 (helium membrane capture) has neither catalysts nor moving parts so the only costs are in buying, refurbishing, or rentals and insurance (Haider, at al, 2019).

Environmental and manpower concerns are most definitely difficult to determine, particularly at this point. North Dakota's climate is typical of a continental climate with cold winters and warm-hot summers. This will certainly impact the efficiency of the process, but until a pilot plant is built, *in situ*, in the Williston Basin, it will be maximally difficult to forecast the effects of climate on the process (Turner, 1989).

This planned process is admittedly complex, but it has the benefit of relying on 'off the shelf' technology which is proven by decades of use and experience in the oilfield. Therefore, manpower, once the process is installed and operating, should be a relatively minor expense (Lee, 1963). It will probably rank along the costs of manpower for oil wells that require pumping and gauging.

There are some numbers we can use to get an idea of the return from the sale of the marketable products generated by this process (03-2023 prices):

1. Hydrogen US$7.39/kg
2. Helium US$400/MCFG
3. High purity CO_2 US$60.16/BBL
4. High purity liquid N_2 US$318.00/BBL
5. LNG US$29.74/MMBTU
6. NGLs
    a. Ethane US$6.22/BBL
    b. Propane US$28.71/BBL
    c. Butane US$43.06/BBL
    d. Pentane$^+$ US$59.74/BBL

These are the results from day one of operations. These products, ready for sale, will be extracted and delivered to offset the costs of operations, manpower, whatever consumables arise and normal operational wear and tear on equipment.

One product of special note is, of course, helium. The price for Grade-A helium is hovering around the US$600/MCFG price (Q1/2023) mark. This is over 300 times the price received from the natural gas produced (US$1.97/MMCFG) by the Bakken when it is gathered, dehydrated, and shipped to market.

There are numerous aspects of hydrogen as an alternative fuel that makes economic forecasting at this point nearly irresolvable. Items such as:

- Taxes at the federal, state, and local levels.

- Tax incentives for reducing flaring.

North Dakota's very recent Senate Bill 2328 created a state tax credit of up to $6,000 per well for companies that implement a *flare mitigation strategy,* as a means of spurring innovative solutions to North Dakota's rising volumes of produced gas. Potential solutions include devices such as the recently introduced EcoVapor ZerO2 Tower (Renee, 2021) (Figure 8.3.) This tower scrubs raw natural gas to make it pipeline ready. It's precisely the same as Module 1, but we take it further to extract multiple sellable NGL products.

Figure 8.3. EcoVapor's ZerO2 unit. A BOG, tank and truck loadout vapor recovery system. From EcoVapor, 2021.

- Tax incentives for alternative clean fuels.
- Subsidies for alternative fuels.

- Production costs (price of feedstock in non-Williston examples).
- Transportation costs.
- Storage costs.
- Infrastructure development.
- Gas or liquid hydrogen.
- Used as fuel for fuel cells or turbine/piston engines.
- Offset due to carbon capture/storage/sequestration.

Offset due to vagaries of price of marketable products.

Scoping Studies

In order to better be able to address the construction, implementation and operation of the processes noted here, it was decided that groups of Chemical Engineering students would undertake, with the supervision of the author, studies of what would be necessary, and what the necessary costs would be to build systems to:

1. Strip helium from the captured Bakken Flare Gas and,
2. Extract Natural Gas Liquids for that same gas stream.

So, during the Spring Semester of 2022, two teams of Chemical Engineering students under the primary direction of Dr. W. Seames, examined both the potential and economic feasibility of the processes described here in this dissertation.

One group undertook (1.) the proposal to fund the separation of mixed associated Bakken-derived gasses while the other (2.) investigated the proposal to fund a helium separation plant. Their methodologies, results and determination of the economic validity of the two processes are detailed here:

(1.) Scoping study report for the proposal to fund the separation of mixed associated Bakken derived gases.

Nik Dirkson, Michelle Nieves, Figueroa, Paul VanDruff - University of North Dakota

May 5, 2022

A scoping study report detailing the recommended process for the separation of mixed Bakken-derived associated gases was undertaken. The recommended process uses five distillation columns, an absorber, and absorber regenerator to separate the mixed associated gas into six product streams: methane and lighter, ethane, propane, butanes (isobutane and normal butane), pentane and heavier, and one waste stream of hydrogen sulfide [H_2S]. The process is designed to process 60 MMscfd of associated gas recovered from Bakken-derived gas gathering stations in North Dakota.

The overall process production is projected to reach purities of 90% by volume for methane [CH_4], 95% by volume for ethane [C_2H_6], 90% by volume for propane [C_3H_8], 95% by volume for isobutane [$i\text{-}C_4H_{10}$], 94% by volume for normal butane [$n\text{-}C_4H_{10}$] with a by-product pentane [C_5H_{12}] stream less than 1% by volume of the butane components. Additionally, a hydrogen sulfide [H_2S] stream of 95% purity will be produced which will be sold as a by-product to be further processed into sulfuric acid or elemental sulfur.

The report encompasses input/output diagrams, block flow diagrams, process flow diagrams, and detailed descriptions of each process area. Additionally, a raw material/product list, utility requirements list, major equipment list, and a safety and environmental impact statement were added to support the recommended process description.

The total capital investment for this project is \$31 million and has a net present value (NPV) of \$370 million at an 18% hurdle rate. The discounted cash flow rate of return (DCFROF) is 110%.

The project is expected to take 33 months to commission and has a potential lifetime of 20 years.

The next best alternative uses of an absorber column with pentane [C_5H_{12}] as a sorbent, to recirculate the pentane [C_5H_{12}] and heavier hydrocarbon stream, followed by five distillation columns to complete the remaining separations.

The selected process was chosen due to its ability to ensure the desired product purities while minimizing utility requirements. It provides an efficient way to separate mixed associated gas while reducing the need for flaring which in turn will reduce the emissions associated with the practice.

Budget Brief - Proposal to Fund

Title: Separation of Mixed Associated Bakken-Derived Gases

Funding Request: \$31,000,000

Project Duration: 33 months*

Proposal: The proposed project uses distillation to separate associated gas into its constituent components of methane, ethane, propane, butanes, pentanes and heavier. All product streams are anticipated to achieve a minimum purity of 90%. The waste stream containing hydrogen sulfide is removed using an absorber/scrubbing system with methyl diethanolamine (MDEA) as the sorbent material.

Present Situation: The Bakken-derived associated gas is collected from twelve well-heads at an average of 60 MMSCF/day. These gases are either flared into the atmosphere, cleaned, and sold as natural gas, or are used on-site to run pumping equipment. This project proposes to separate the associated gas and sell the products on the open commodities market.

Qualitative Justification: The associated gas recovery project recommended will allow for the recovery and purification of oil-well gas that is currently flared, vented, or recovered less efficiently. By improving the efficiency of the process and recovering gas that is currently flared or vented, less product is wasted. Furthermore, the reduction of methane and CO_2 into the atmosphere greatly reduces the greenhouse gasses that are attributed to global warming.

Quantitative Justification: This project is estimated to have an NPV of $370,000,000 at a hurdle rate of 18% and a DCFROR of 110% over the 20-year life of the project. The project is projected to be economically viable.

Alternative: The best alternative is similar to the chosen path, with many of its operations involving component separation using distillation. The primary difference is the use of an absorber on the feed stream to the unit. Pentane is recycled from a downstream distillation column and used as a sponge oil to remove heavier components. This is a functional option; however, more equipment is required and similar energy is needed to complete the process. Additional expenses for initial equipment and added maintenance removed this as an option.

Hazards: The projects NPV is dependent on the fixed capital investment and the market price for each material stream. A 40% increase in the FCI while holding everything else constant would lower the NPV to $350 million and result in an 87% DCFROR. A 40% decrease in product prices while holding everything else constant would lower the NPV to

$120 million and result in a 57% DCFROR. Finally, in the very unlikely event that commodity prices sell at the historical low during the life of the project while holding everything else constant, the NPV would lower to $ -15 million and result in a 12% DCFROR which is lower than the 18% hurdle rate. Electricity prices were not considered during the analysis due to the limited impact they have on project economics. The more likely event to consider is where commodity prices come in lower by 40% as discussed above.

(2.) Scoping Study for the Proposal to Fund a Helium Separation Plant

Lindsey Malina, Dominick Van Ess, Zach Greniger, Brandon Bush – University of North Dakota, April 1, 2022

TITLE: Scoping Study for the Proposal to Fund a Helium Separation Plant Enclosed is a scoping study proposing a process to remove helium from an associated gas stream. It is recommended to fund the recommended process, a gas membrane system followed by pressure swing adsorption. The project is set to recover 88.3% of the helium found in the associated gas with a targeted purity of 99.99% by volume. The process would have a total inlet flow rate of *69,600 lbs./hr.* associated gas and will return the treated associated gas to the gas plant.

The report details the recommended process along with an alternative process. The report includes input/output diagrams, block flow diagrams, and process flow diagrams. In addition, a preliminary schedule, major equipment list, raw materials requirements, utility requirements, products list, consumable chemical requirements, economic assessment, economic hazards analysis, and safety and environmental impact statements are included.

The recommended process uses a system of membranes followed by pressure swing adsorption (PSA) steps. The project calls for a total capital investment of $1.7 million ±$0.6 million and an NPV@18% of $6.0 million ± $2.4 million. The project has a lifespan of 20 years and an operating factor of 95%. The discounted cash flow rate of return (DCFROR) for the recommended process is 34%. The preliminary project duration is calculated to be 30 months.

The next best alternative project utilizes cryogenic distillation followed by both a nitrogen rejection unit and a helium rejection unit. The project would have a total capital investment of $18.0 million and an NPV@18% of -$3.1 million ± $1.2 million. This project also has a lifespan of 20 years and an operating factor of 95%. Due to the largely negative NPV@18%, the alternative has a DCFROR of 3%.

An incremental economic analysis was conducted, showing that the recommended process has a higher NPV@18%. The incremental NPV@18% is calculated to be $20 million. Economics was the primary basis for the selection of the recommended process followed by operability and safety.

Budget Brief - Proposal to Fund

Title: Proposal to Fund a Helium Separation Plant

Funding Request: $3,100,000

Project Duration: 30 months*

Proposal: The proposed project is a bolt on to an associated gas plant that will extract helium gas from a methane gas stream using a system of gas membranes and pressure swing adsorption units. The project is set to achieve 88.3% helium recovery at a purity of 99.99% by volume. The proposed process will have the capacity to process gas from a total of twelve oil well heads from the Bakken formation. The treated associated gas will then return to the gas plant.

Present Situation: The methane gas produced by a proposed associated gas plant in New Town, ND. They are planning to flare this gas. One of the gases found in the stream is helium. There is currently a domestic supply shortage for helium with no large plants planned to compensate.

Qualitative Justification: The recommended project will allow previously wasted methane gas to have a sellable helium product recovered.

Quantitative Justification: The recommended project is anticipated to have an

NPV@18% of $14 million ± $5.6 million over a 20-year lifespan. It has a DCFROR of 67%. The project is projected to be economically viable.

Alternative: The alternative project utilizes cryogenic distillation followed by a nitrogen and helium rejection unit. It is projected to have a 99.1% helium recovery at a purity of 99% by volume. The alternative process also produces a byproduct of nitrogen gas at a recovery of 95.5% and a purity of 95.3%. The process has a TCI of $18 million ±$7.2 million and an NPV@18% of -$3.1million ± $1.2 million during its 20-year lifespan. The

DCFROR for the alternative process is 14%. The calculated incremental NPV@18% is $18 million. Due to the greater amount of equipment, the alternative process will always have a higher FCI. The recommended process was chosen based on economics.

Hazards: The project economics are contingent upon the market value of helium. The NPV@ 18% decreases to -$2.2 million ± $0.8 million with a decrease in the price of helium to a 2014 low value. The breakeven price of helium for the process is $110/MCF. This results in the price of helium being the most significant economic hazard. A 12% risk was calculated from the sensitivity analysis conducted. This risk is not significant enough to halt furthering the project, but great enough a further market study should be done on the projection of helium gas pricing.

8.3 Bakken Oil and Gas Production

During the time this dissertation was written, there have been several innovations regarding mechanical methods vs. membranes. So much so, in fact, that the main process for extracting salable products from captured Bakken flare gas has changed its focus from a process dominated by mechanicals, i.e., those devices requiring external fuel, that possess rotating/reciprocating parts, require continuous maintenance, etc., to one dominated by very low maintenance membrane extraction. The chief driver of this was economics.

Further, the main hydrogen generation pathway has shifted from Steam Methane Reforming (SMR) to Autothermal Reforming (ATR). However, without steam reforming (SR), ATR generates only Synfuel; a mixture of carbon monoxide (CO) and hydrogen (Cheekatamarla and Lane, 2005). It appears that a combination of both ATR and SMR will be utilized in the final Hydrogen Hub build. The chief driver of this was economics; however, with the cost of a dedicated oxygen plant for ATR (Romano, et al, 2011) and SMR feedstock being free via reclaimed flare gas, the question of economics for Module 4 remains unanswered.

However, with either process, there are several key issues that affect the project's economics. Primary amongst these are volumes, flowrates and pressures of the flare gas derived from Bakken horizontal wells. It is expected for these values to vary widely. For the proof-of-concept project, 5 MMCFGPD at 800 PSIG and 70^0F were assumed; based on Bakken production numbers of varying vintages. As membranes are readily linearly scaleable, once it is determined the membrane necessity for these numbers, the project can be scaled down to a workable size.

Securing documented values from operators, the EERC (Energy and Environmental Research Center, 2021) or North Dakota Geologic Survey has been somewhat problematical. Given there are over 19,000 wells in the Williston Basin, many operators, large and small, ownerships seem to change almost on a daily basis. Plus, with the disquietude over flaring as it is an environmentally and politically charged issue, is an Augean Task. The data exists but assembling any relatively recent data is near impossible. Adding to this the 2020-2021 COVID pandemic and disruption to work schedules across the oil industry (de Vries, Erumban, and van Ark, 2021), from drillers to operators to governmental agencies, the problem is only exacerbated.

Colloquially, it’s noted that some 3 BCF of non-associated gas per day are generated in the Williston Basin and of that, currently (10/2021), ~0.7 BCFGPD is being flared. However, there is a significant, though unmetered, amount of gas that is simply vented to the atmosphere.

We now have data (EERC, 2020) that notes, on average, new Bakken completions have and IP (Initial Potential) of 2,500 BOPD. The GOR (Gas-Oil Ratio) of these wells is 1.87 Mcf of gas per barrel of oil (Oil and Gas 360, 2017). Nonetheless, these numbers give us, at best, an approximation of the values needed to create a robust economic model and return meaningful results.

However, new production figures from the North Dakota Industrial Commission, Oil and Gas Division (2021) have arrived that allow enough documented referential data with which to perform a more detailed and data-driven analysis.

Yet, currently available are but few oil and gas assays for crudes and gas originating from the Bakken in the Williston Basin (Figure 8.4 and Table 8.8.):

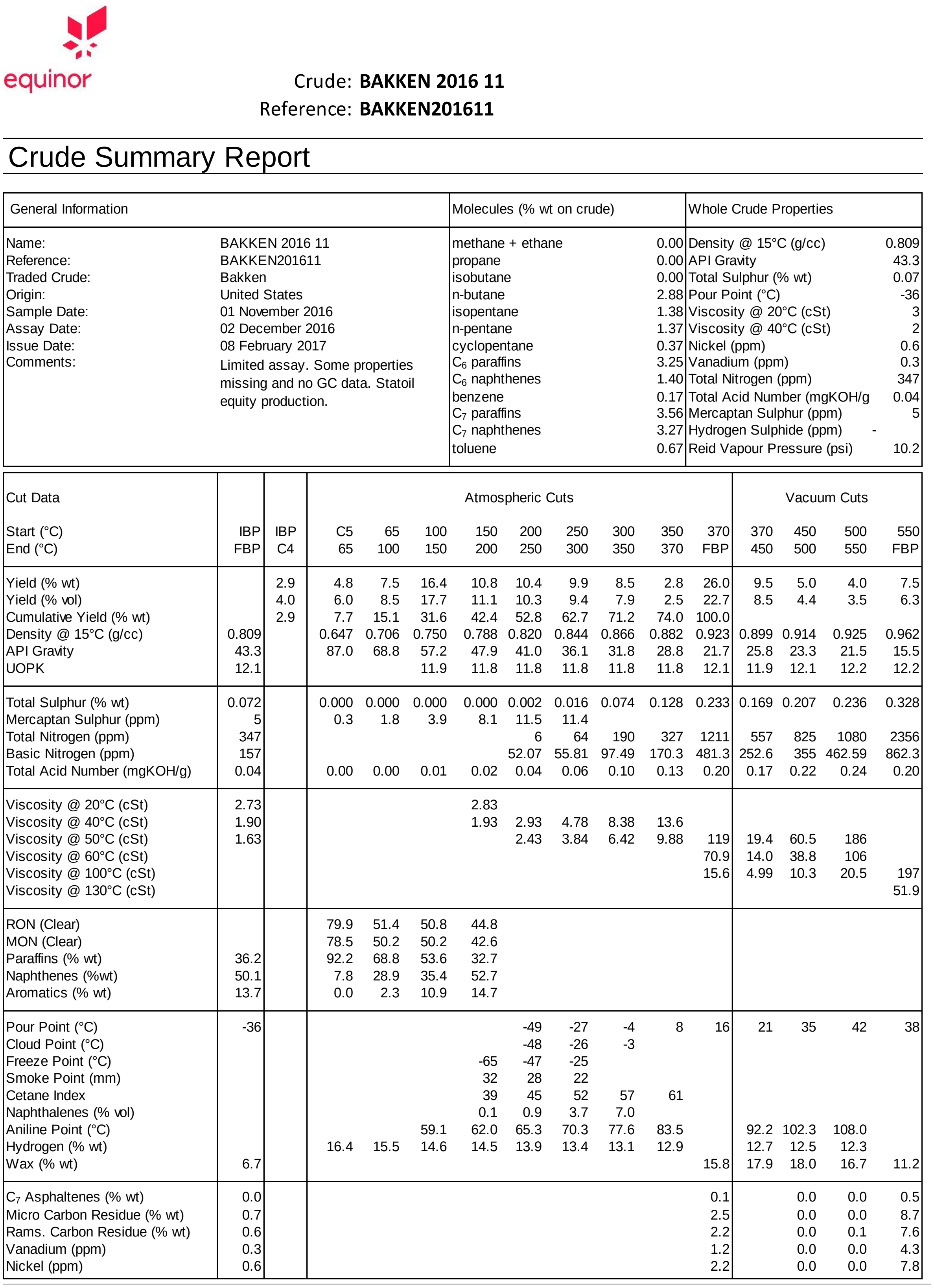

equinor

Crude: **BAKKEN 2016 11**
Reference: **BAKKEN201611**

Crude Summary Report

General Information		Molecules (% wt on crude)		Whole Crude Properties	
Name:	BAKKEN 2016 11	methane + ethane	0.00	Density @ 15°C (g/cc)	0.809
Reference:	BAKKEN201611	propane	0.00	API Gravity	43.3
Traded Crude:	Bakken	isobutane	0.00	Total Sulphur (% wt)	0.07
Origin:	United States	n-butane	2.88	Pour Point (°C)	-36
Sample Date:	01 November 2016	isopentane	1.38	Viscosity @ 20°C (cSt)	3
Assay Date:	02 December 2016	n-pentane	1.37	Viscosity @ 40°C (cSt)	2
Issue Date:	08 February 2017	cyclopentane	0.37	Nickel (ppm)	0.6
Comments:	Limited assay. Some properties missing and no GC data. Statoil equity production.	C_6 paraffins	3.25	Vanadium (ppm)	0.3
		C_6 naphthenes	1.40	Total Nitrogen (ppm)	347
		benzene	0.17	Total Acid Number (mgKOH/g	0.04
		C_7 paraffins	3.56	Mercaptan Sulphur (ppm)	5
		C_7 naphthenes	3.27	Hydrogen Sulphide (ppm)	-
		toluene	0.67	Reid Vapour Pressure (psi)	10.2

Cut Data			Atmospheric Cuts									Vacuum Cuts			
Start (°C)	IBP	IBP	C5	65	100	150	200	250	300	350	370	370	450	500	550
End (°C)	FBP	C4	65	100	150	200	250	300	350	370	FBP	450	500	550	FBP
Yield (% wt)		2.9	4.8	7.5	16.4	10.8	10.4	9.9	8.5	2.8	26.0	9.5	5.0	4.0	7.5
Yield (% vol)		4.0	6.0	8.5	17.7	11.1	10.3	9.4	7.9	2.5	22.7	8.5	4.4	3.5	6.3
Cumulative Yield (% wt)		2.9	7.7	15.1	31.6	42.4	52.8	62.7	71.2	74.0	100.0				
Density @ 15°C (g/cc)	0.809		0.647	0.706	0.750	0.788	0.820	0.844	0.866	0.882	0.923	0.899	0.914	0.925	0.962
API Gravity	43.3		87.0	68.8	57.2	47.9	41.0	36.1	31.8	28.8	21.7	25.8	23.3	21.5	15.5
UOPK	12.1				11.9	11.8	11.8	11.8	11.8	11.8	12.1	11.9	12.1	12.2	12.2
Total Sulphur (% wt)	0.072		0.000	0.000	0.000	0.000	0.002	0.016	0.074	0.128	0.233	0.169	0.207	0.236	0.328
Mercaptan Sulphur (ppm)	5		0.3	1.8	3.9	8.1	11.5	11.4							
Total Nitrogen (ppm)	347						6	64	190	327	1211	557	825	1080	2356
Basic Nitrogen (ppm)	157						52.07	55.81	97.49	170.3	481.3	252.6	355	462.59	862.3
Total Acid Number (mgKOH/g)	0.04		0.00	0.00	0.01	0.02	0.04	0.06	0.10	0.13	0.20	0.17	0.22	0.24	0.20
Viscosity @ 20°C (cSt)	2.73					2.83									
Viscosity @ 40°C (cSt)	1.90					1.93	2.93	4.78	8.38	13.6					
Viscosity @ 50°C (cSt)	1.63						2.43	3.84	6.42	9.88	119	19.4	60.5	186	
Viscosity @ 60°C (cSt)											70.9	14.0	38.8	106	
Viscosity @ 100°C (cSt)											15.6	4.99	10.3	20.5	197
Viscosity @ 130°C (cSt)															51.9
RON (Clear)			79.9	51.4	50.8	44.8									
MON (Clear)			78.5	50.2	50.2	42.6									
Paraffins (% wt)	36.2		92.2	68.8	53.6	32.7									
Naphthenes (%wt)	50.1		7.8	28.9	35.4	52.7									
Aromatics (% wt)	13.7		0.0	2.3	10.9	14.7									
Pour Point (°C)	-36						-49	-27	-4	8	16	21	35	42	38
Cloud Point (°C)							-48	-26	-3						
Freeze Point (°C)						-65	-47	-25							
Smoke Point (mm)						32	28	22							
Cetane Index						39	45	52	57	61					
Naphthalenes (% vol)						0.1	0.9	3.7	7.0						
Aniline Point (°C)					59.1	62.0	65.3	70.3	77.6	83.5		92.2	102.3	108.0	
Hydrogen (% wt)			16.4	15.5	14.6	14.5	13.9	13.4	13.1	12.9		12.7	12.5	12.3	
Wax (% wt)	6.7										15.8	17.9	18.0	16.7	11.2
C_7 Asphaltenes (% wt)	0.0										0.1		0.0	0.0	0.5
Micro Carbon Residue (% wt)	0.7										2.5		0.0	0.0	8.7
Rams. Carbon Residue (% wt)	0.6										2.2		0.0	0.1	7.6
Vanadium (ppm)	0.3										1.2		0.0	0.0	4.3
Nickel (ppm)	0.6										2.2		0.0	0.0	7.8

Figure 8.4. A typical Bakken oil assay. From Equinor, 2017.

Table 8.8. Typical Bakken gas assay.

	Temperature deg F	**75**
	Pressure, psa	UNKNOWN
	Mass flow lb/hr	UNKNOWN
	Avg. mol. Wt.	UNKNOWN
	Flowrate MMCFGPD	UNKNOWN
	Nitrogen	0.027
C1	Methane	0.58
C2	Ethane	0.2
C3	Propane	0.11
C4	i-Butane	0.025
C4	n-Butane	0.025
C5	i-Pentane	0.08
C5	n-Pentane	0.08
C6	n-Hexane	0.054
C7	n-Heptane	0.00001
C8	n-Octane	0.000001
C9	n-Nonane	0.00000025
C10	n-Decane	0
	Carbon Dioxide	0.01
	Hydrogen sulfide	0.0039
	Water	0.0000004

However, the recently delivered Bakken production, on a per-well basis through August of 2021 from the North Dakota Industrial Commission (NDIC), Oil and Gas Division (2021) allows data gaps to be somewhat filled.

This data noted that the current (08-2021) 15,552 Williston Basin Bakken completions flared 6,380,036 MCFG in the month of August 2021; or approximately 410 MCFG/well/month, with a range from 0 to 36,196 MCFG.

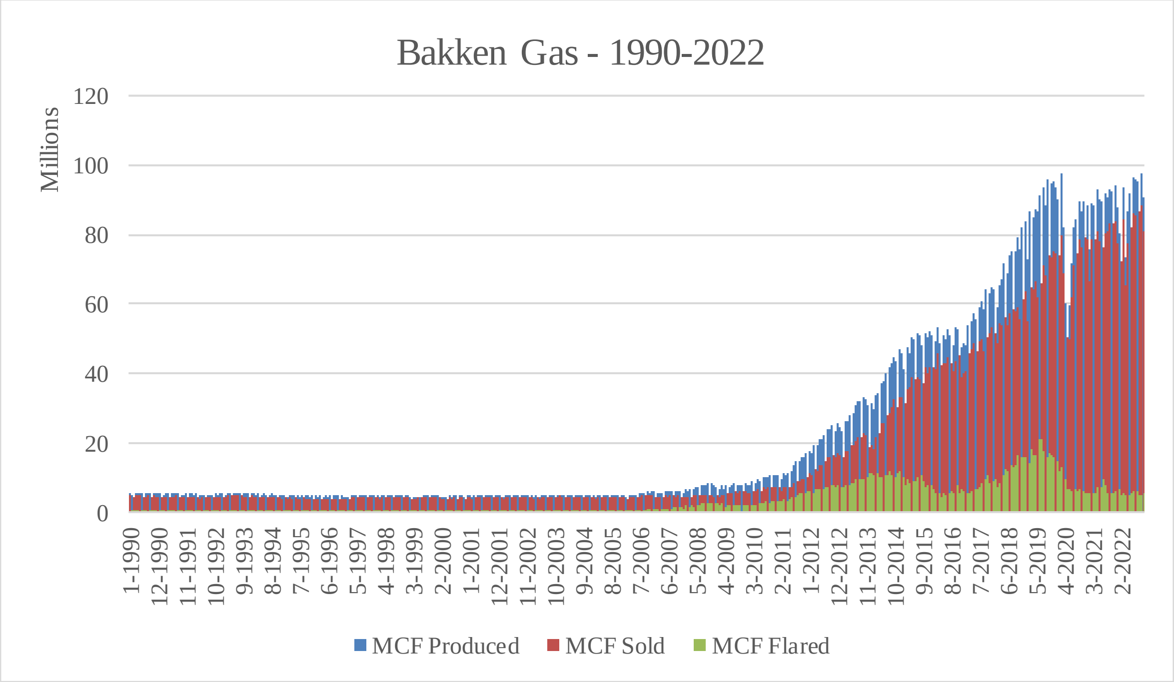

Figure 8.5. Disposition of produced Bakken Gas, 1990-2022

This equates to some 205,807.6 MCFG *per day* flared from the Bakken during the month of August, 2021.

Given Henry Hub statistics for August, 2021 of US$4.20/MMBTU * 0.9756 (constant) = US$4.10/MCFG. This compares to a loss through flaring of Williston Basin Bakken gas of USD $843,300.81 per day, USD $26,142,325.11 per month, USD $313,707,901.33 per year; or one-third of a billion US dollars (Table 8.9).

Table 8.9. Williston Bakken wells and flaring data, August 2021. Data from NDIC.

Williston Basin: Bakken Reservoir	August, 2021	Revenue Lost to Flaring
Number Operators Flaring Gas	50	
Total wells	15,532	
No. Flaring wells	9,531	
Average Henry Hub August 2021 price (MCF)	$4.10	
Gas flared/day (MCF)	205,808	$843,300.81

Williston Basin: Bakken Reservoir	August, 2021	Revenue Lost to Flaring
Gas flared/mo. (MCF)	6,380,036	$26,142,325.11
Gas flared/year (MCF)	76,560,432	$313,707,901.33

Incorporating these figures into an economic analysis used for stand-alone wells, if we take the 12-well contribution of 25,000 MCF helium/year and include the additional (NGLs) products, we can generate a putative cash flow for the life of the project. Here, we assume oil at US$75/bbl, Helium at US$400/MCF, and NGLs at US$45/bbl, we take the further assumptions as (Note: The 12 wells refer to the flare gas from 2 6-well Bakken pads, rather than individual wells):

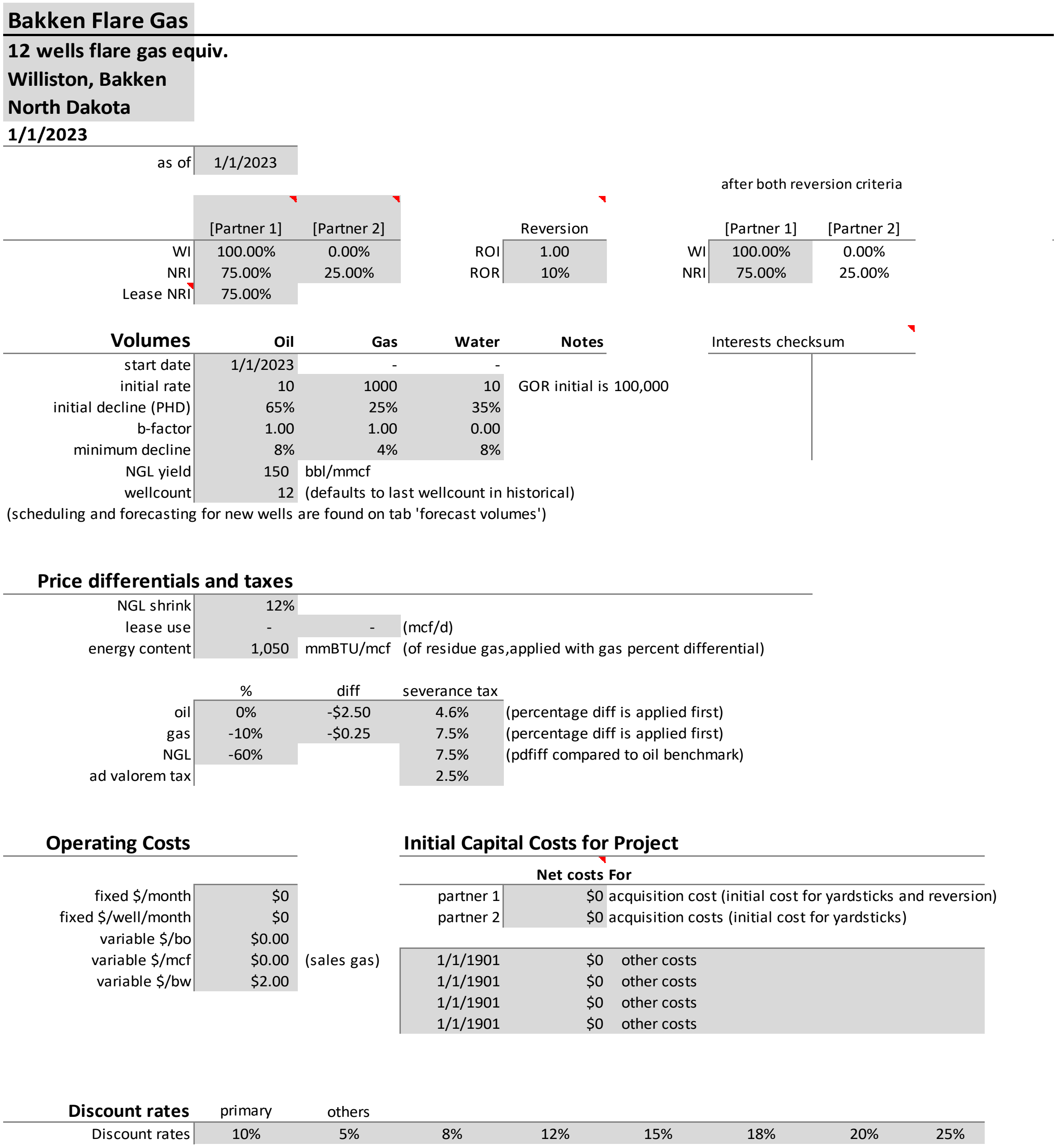

Bakken Flare Gas

12 wells flare gas equiv.
Williston, Bakken
North Dakota
1/1/2023

as of 1/1/2023

after both reversion criteria

	[Partner 1]	[Partner 2]		Reversion		[Partner 1]	[Partner 2]
WI	100.00%	0.00%	ROI	1.00	WI	100.00%	0.00%
NRI	75.00%	25.00%	ROR	10%	NRI	75.00%	25.00%
Lease NRI	75.00%						

Interests checksum

Volumes	**Oil**	**Gas**	**Water**	**Notes**
start date	1/1/2023	-	-	
initial rate	10	1000	10	GOR initial is 100,000
initial decline (PHD)	65%	25%	35%	
b-factor	1.00	1.00	0.00	
minimum decline	8%	4%	8%	
NGL yield	150	bbl/mmcf		
wellcount	12	(defaults to last wellcount in historical)		

(scheduling and forecasting for new wells are found on tab 'forecast volumes')

Price differentials and taxes

NGL shrink	12%		
lease use	-	-	(mcf/d)
energy content	1,050	mmBTU/mcf	(of residue gas,applied with gas percent differential)

	%	diff	severance tax	
oil	0%	-$2.50	4.6%	(percentage diff is applied first)
gas	-10%	-$0.25	7.5%	(percentage diff is applied first)
NGL	-60%		7.5%	(pdfiff compared to oil benchmark)
ad valorem tax			2.5%	

Operating Costs

fixed $/month	$0	
fixed $/well/month	$0	
variable $/bo	$0.00	
variable $/mcf	$0.00	(sales gas)
variable $/bw	$2.00	

Initial Capital Costs for Project

	Net costs For	
partner 1	$0	acquisition cost (initial cost for yardsticks and reversion)
partner 2	$0	acquisition costs (initial cost for yardsticks)
1/1/1901	$0	other costs
1/1/1901	$0	other costs
1/1/1901	$0	other costs
1/1/1901	$0	other costs

Discount rates	primary	others						
Discount rates	10%	5%	8%	12%	15%	18%	20%	25%

Figure 8.6. Bakken helium cash-flow production assumptions.

Table 8.10. Bakken cash flow output Table 1.

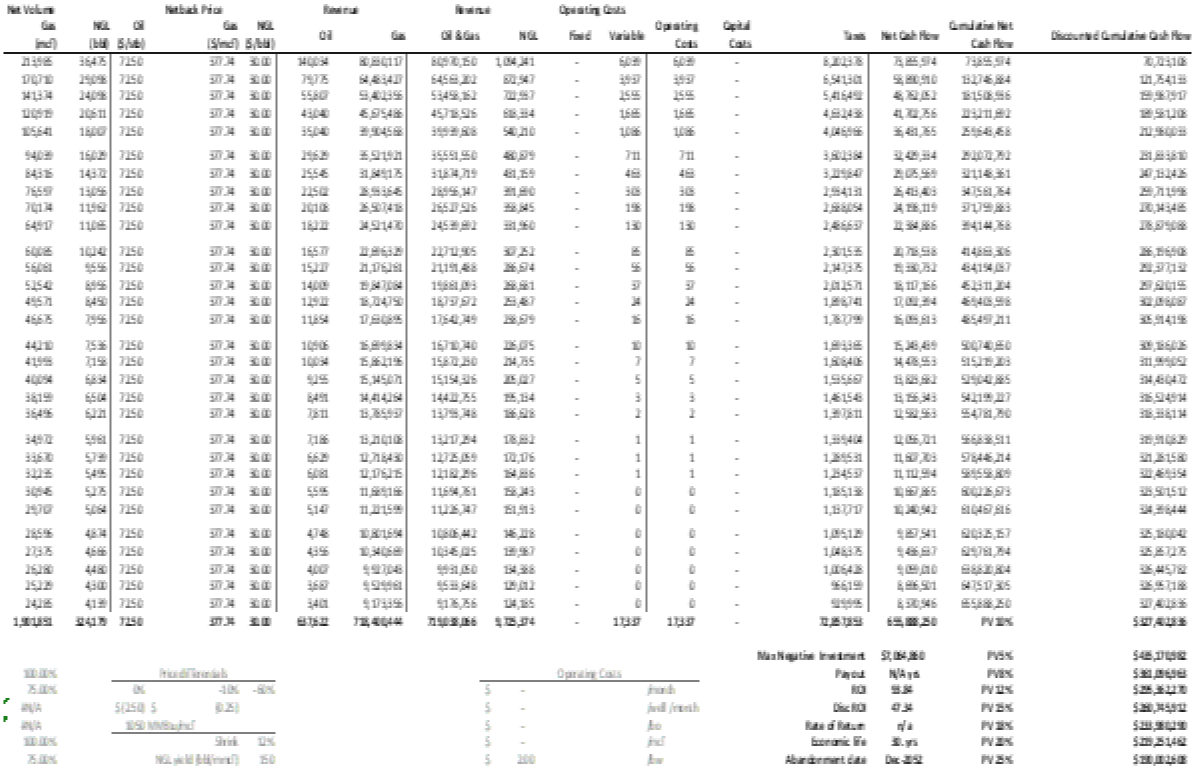

Above is the Bakken cashflow based on the assumptions from the Scoping Studies and the values for produced oil, gas, helium and NGLs. Figure 8.7, below, denotes the cash flow of the project for 17 years.

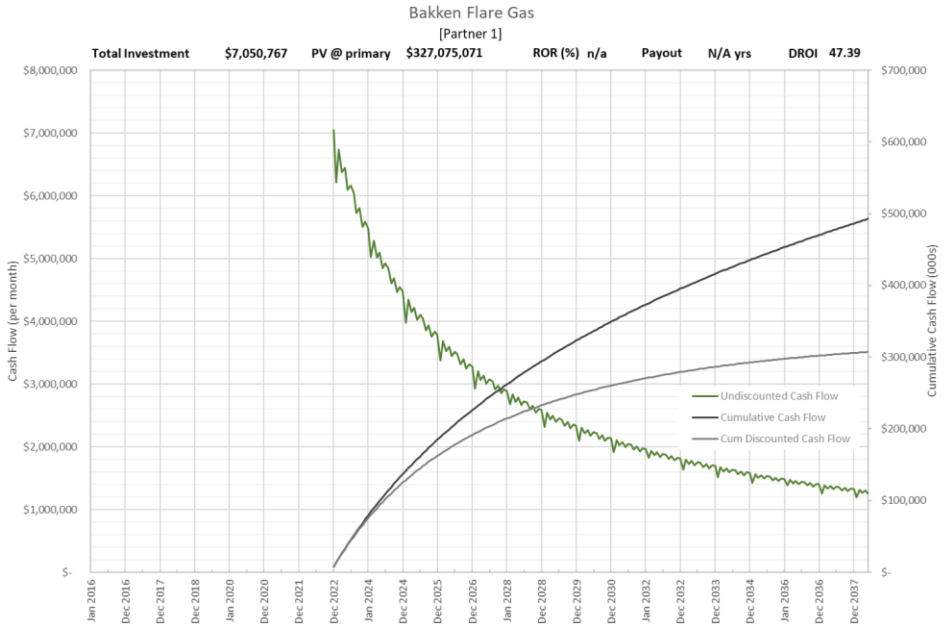

Figure 8.7. Undiscounted, Cumulative and Cumulative Discounted cash flow for helium extraction from Bakken flare gas, 2023-2037.

Table 8.11. Bakken project cashflow (continuation of Table 8.10) Operating costs and capital costs omitted to reconcile net income by adjusting for non-cash expenses, changes in working capital, and capital expenditures.

Netback Price Gas ($/mcf)	NGL ($/bbl)	Revenue Oil & Gas	NGL	Operating Costs	Capital Costs	Taxes	Net Cash Flow	Cumulative Net Cash Flow	Discounted Cumulative Cash Flow
377.74	30.00	26,990,050	364,747	-	-	2,734,126	24,620,671	24,620,671	23,576,299
377.74	30.00	21,521,067	290,982	-	-	2,180,434	19,631,616	44,252,287	40,587,781
377.74	30.00	17,819,387	240,979	-	-	1,805,497	16,254,869	60,507,156	53,333,045
377.74	30.00	15,239,509	206,111	-	-	1,544,146	13,901,474	74,408,630	63,197,870
377.74	30.00	13,313,203	180,070	-	-	1,348,989	12,144,284	86,552,914	70,997,711
377.74	30.00	11,850,517	160,293	-	-	1,200,795	10,810,015	97,362,929	77,282,442
377.74	30.00	10,624,906	143,720	-	-	1,076,616	9,692,011	107,054,939	82,382,062
377.74	30.00	9,652,049	130,563	-	-	978,044	8,804,569	115,859,508	86,575,301
377.74	30.00	8,842,509	119,615	-	-	896,018	8,066,106	123,925,614	90,052,492
377.74	30.00	8,179,897	110,653	-	-	828,879	7,461,672	131,387,286	92,964,376
377.74	30.00	7,570,968	102,417	-	-	767,178	6,906,208	138,293,493	95,403,660
377.74	30.00	7,063,829	95,558	-	-	715,792	6,443,596	144,737,089	97,463,740
377.74	30.00	6,620,364	89,560	-	-	670,857	6,039,068	150,776,157	99,211,418
377.74	30.00	6,245,891	84,496	-	-	632,914	5,697,473	156,473,629	100,704,064
377.74	30.00	5,880,916	79,560	-	-	595,933	5,364,543	161,838,172	101,976,103
377.74	30.00	5,570,247	75,358	-	-	564,455	5,081,150	166,919,322	103,066,713
377.74	30.00	5,290,743	71,578	-	-	536,135	4,826,186	171,745,509	104,004,389
377.74	30.00	5,051,442	68,342	-	-	511,889	4,607,895	176,353,404	104,814,862
377.74	30.00	4,807,585	65,045	-	-	487,181	4,385,449	180,738,853	105,513,010
377.74	30.00	4,597,916	62,209	-	-	465,937	4,194,188	184,933,041	106,117,410
377.74	30.00	4,405,765	59,611	-	-	446,468	4,018,907	188,951,949	106,641,648
377.74	30.00	4,241,686	57,392	-	-	429,844	3,869,235	192,821,183	107,098,565
377.74	30.00	4,060,765	54,945	-	-	411,512	3,704,198	196,525,382	107,494,490
377.74	30.00	3,898,254	52,748	-	-	395,046	3,555,955	200,081,337	107,838,542
377.74	30.00	3,742,249	50,638	-	-	379,239	3,413,648	203,494,984	108,137,520
377.74	30.00	3,602,147	48,743	-	-	365,043	3,285,847	206,780,831	108,398,053
377.74	30.00	3,448,342	46,662	-	-	349,458	3,145,546	209,926,377	108,623,797
377.74	30.00	3,310,350	44,796	-	-	335,476	3,019,670	212,946,047	108,819,966
377.74	30.00	3,177,883	43,004	-	-	322,053	2,898,834	215,844,881	108,990,434
377.74	30.00	3,058,919	41,395	-	-	309,998	2,790,315	218,635,196	109,138,984
377.74	**30.00**	**239,679,355**	**3,241,791**	**-**	**-**	**24,285,951**	**218,635,196**	**PV 10%**	**$109,138,984**
						Initial Investment	**$0**	**PV 5%**	**$145,062,157**
						Payout	**N/A yrs**	**PV 8%**	**$120,370,507**
						ROI	**n/a**	**PV 12%**	**$98,458,583**
						Disc ROI	**n/a**	**PV 15%**	**$86,919,561**
						Rate of Return	**n/a**	**PV 18%**	**$77,997,474**
						Economic life	**30. yrs**	**PV 20%**	**$73,087,734**
						Abandonment date	**Dec-2052**	**PV 25%**	**$63,337,824**

Price differentials		
	-10%	-60%
$	(0.25)	
MMBtu/mcf		
	Shrink	12%
	NGL yield (bbl/mmcf)	150

Operating Costs		
$	-	/month
$	-	/well /month
$	-	/bo
$	-	/mcf
$	2.00	/bw

Based on the various costs provided by products in this simulation, it can be seen that with the helium percentage present in the Bakken reclaimed-flare stream, the financials can be shown to be always positive. Even with the Scoping Study, which used as a baseline US$152/MCF helium, coming up potentially risky, the new projections at US$400/MCF helium note that the cash flow for this project is positive, and in fact, very attractive. Also note, this does not include the price accrued for the pure CH_4 stream to be sold to the Hydrogen Hub.

Considering the 10 fields that were referred to previously, with the exception of Mt. Kitty in Australia, which was deemed 'non-economic' for the size of the build necessary to move gas and helium some 1,000 km from field to the nearest population center; Oman, who has never acted on a helium initiative, even though the percentages found in their subsalt reservoirs are world class and Tasmania's Shittim well, which had superior helium percentages, but lack the overall necessary footage of reservoir to allow it to produce enough to fund a helium plant; the remaining seven are exceptionally economic. In fact, helium producers such as Linde and American Gas Producers, and helium 'market analysts' such as Mordor Intelligence and Fortune Business Insights all agree that the helium market will do nothing but grow (at a CAGR (compound annual growth rate) between 5-12%), and that North America will dominate the market.

In fact, as the price of crude helium continues to escalate, 'unconventional' sources of helium, such as riftogenic helium in Tanzania, helium in groundwater in India, and volcanogenic helium in South Africa, all existing in percentages less than 0.01%, are being sought after as now economic.

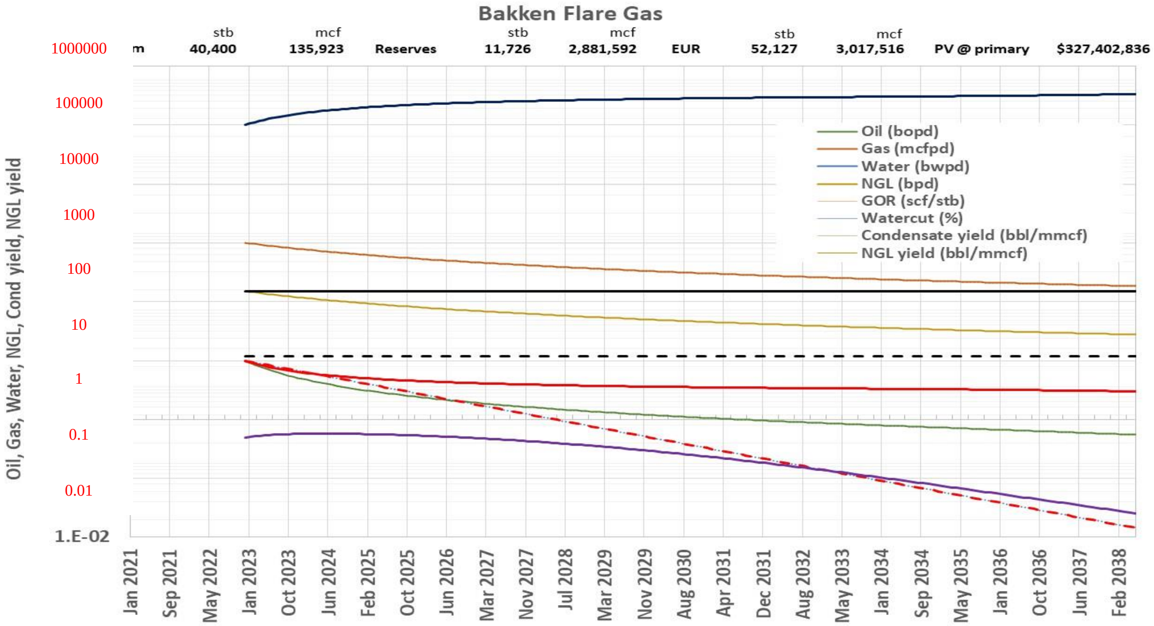

Figure 8.8. Bakken Flare Gas rate/time graph.

The above Flare Gas rate chart notes the flatness of production of the various commodities noted in the proposal over time. Water, which appears to be increasing over time, will be dealt with at the surface before pre-treatment, and should not be thought of as being produced in the traditional per well sense. Helium here is noted under ‘gas’.

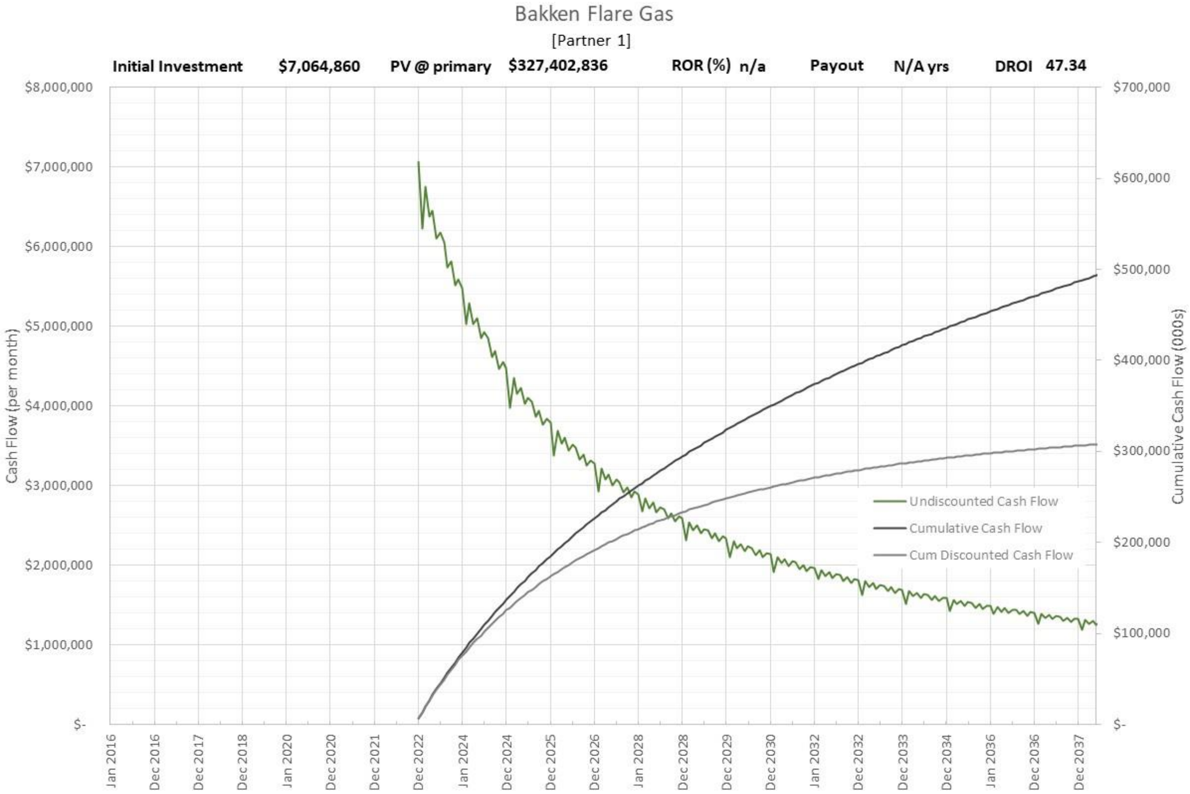

Figure 8.9. Bakken cash flow chart.

The flow chart for the cash flow of a combined helium-NGL project from Bakken flare gas notes the strongly positive cash flow from inception of the project; where cumulative cash flow is near US$500,000,000 in a scant 15 years, and a DROI of over 47. Remembering there will be no lease costs, rentals, royalties nor bonuses paid for collecting and processing the Bakken Flare gas, and as helium, and NGL, prices rise, as is the conclusion of those currently embroiled in the helium market, this can only mean a stronger cash flow can be realized from previously wasted and environmentally-hostile materials.

Genetic Classification of Helium Accumulations

Through investigation of the varied types of global helium accumulations with natural gas, it has been noted that certain patterns emerge. These patterns are based primarily on the geological composition of the seal and trap which both contain and retain elemental helium, but are also representative of a complex of depositionally related facies originating in the same environment and mostly as the effect of a single primary process.

Utilizing this type of depositional hierarchy, nine distinct groups of natural gas/helium accumulations are noted. Much like natural gas accumulations worldwide, the high helium content fields range from classical reservoir with impervious regional evaporitic seals, to self-sealing massive shales and carbonates, mixed reservoir type fields and finally, surface manifestations.

1. Carbonates/clastics sealed below Neoproterozoic-Cambrian evaporite sequences:
   a. Russia – Eastern Siberia
   b. China – Sichuan Basin
   c. Oman – South Oman Salt Basin
   d. Australia – Amadeus Basin
   e. Australia – Officer Basin
   f. Brazil – São Francisco Basin

2. In massive, tight sandstones:
    a. Dongsheng – Ordos Basin, China
    b. Hetianhe – Tarim Basin, China

3. Under and within massive black shales:
    a. US – Trenton
    b. US – Black Earth
    c. Russia – Bazhenov

4. Sealed by Permian-Mesozoic carbonates and evaporites:
    a. Algeria – Hassi R'Mel
    b. Mauritania – Taoudenni Basin
    c. USA – Anadarko Basin
    d. USA – Williston Basin - Bakken

5. Panhandle-Hugoton type: Hydrocarbons from adjacent high He/N_2 basin and from low He/N_2 mixed-water reservoirs:
    a. US – Hugoton
    b. US – Keyes
    c. US – Las Animas
    d. US – Fain
    e. US – Panhandle West
    f. US – Panoma

6. 4-Corners – Colorado Plateau type: Precambrian source rocks high U/Th, overlain by thousands of feet of faulted, low-permeability Paleozoic-Mesozoic sedimentary rocks:
    a. US – Ratherford
    b. US – Tocito Dome
    c. US – Navajo Springs
    d. US – Pinta Dome,
    e. US – Dineh-Bi-Keyah

7. Within massive carbonate/evaporite sequences:
    a. Paleozoic –
        - Qatar/Iran – Khuff – North Field, South Pars Field
        - Changqing Field – China
        - Mancos Shale, Western United States

8. Exhalations-Surface seeps:
    a. Tanzania – Riftogenic
    b. South Africa – Volcanogenic
    c. Himalayan India – Aqueous Geothermal

Economics of low, medium and high percentage Helium gas streams

Three fields were chosen as representative for comparison and contrast of various economic factors. These are: The Bakken of the Williston Basin, North Field of Qatar and Yurubchen Field in the Krasnoyarsk Krai of East Siberia.

Yurubchen-Tokhomo Field Complex, Eastern Siberian Platform, Russia RSFSR (Montages 4 & 4A)

The Yurubchen–Tokhomo zone (YuTZ) of oil-and-gas accumulation, as it is known in Russia, is located on the southwestern margins of the North Asian Craton (Kuznetsova, and Varnavsky, 2018). It is located on the western margin of the Eastern Siberian Platform (North Asian Craton) within the Kama arch of the Baikit anteclise (~anticline). The field complex was discovered in 1980.

The field complex is unique as it contains oil, gas and condensate obtained from the oldest commercial source rocks in the world, from the Meso- to Neoproterozoic age Riphean, some 1.1-1.6 BYA (Montage-1). It also produces oil, gas and condensate from the younger Vendian (~Ediacaran) series, some 650 to 543 MYA (Mel'nikov,, et al, 2008). The entire series is overlain by the Lower Cambrian Usolian salt, which acts as an impermeable barrier to vertical or lateral migration.

The Riphean section in the zone is represented by alternating clay-dolomite and dolomite members. The age of deposits in the zone is from 1000 to 1600 Ma. The zone occupies an area of about 16,000 km^2 and is faulted into several hydrodynamically secure blocks. Both the Riphean and Vendian deposits are oil-, helium and gas-bearing in the zone. The main Riphean pool is of the horizon *P1*. The reservoir type is cavernous-fractured in the pool. The height of oil interval is about 40 m; that of gas cap is about 90 m (Kontorovich, and Izosimova, 1997).

The main reservoirs of the field complex are estimated to contain 73 TCFG (73,000 BCFG) with a helium content of approximately 0.4% vol, which yields roughly 4,052 BCF helium which can be exploited.

Montage 4. Yurubchen-Tokhomo Field

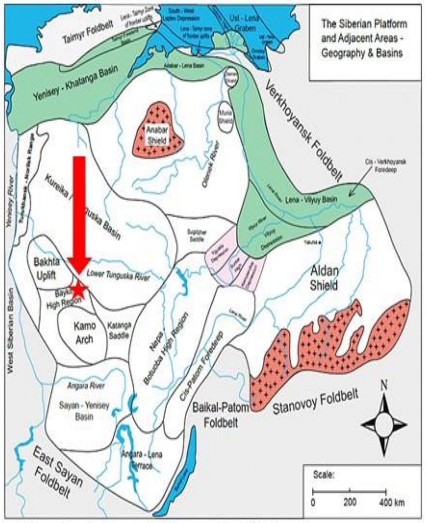

Geology Today, Volume: 37, Issue: 1, Pages: 18-22, First published: 26 January 2021, DOI: (10.1111/gto.12337)

Country:	Russia
Geological region:	Eastern Siberian Platform
Field(s):	Yurubchen-Tokhomo complex
Reservoir age(s):	Neoproterozoic Riphean & Vendian
Gas/Helium EUR:	16 TCF/2.8 TCF

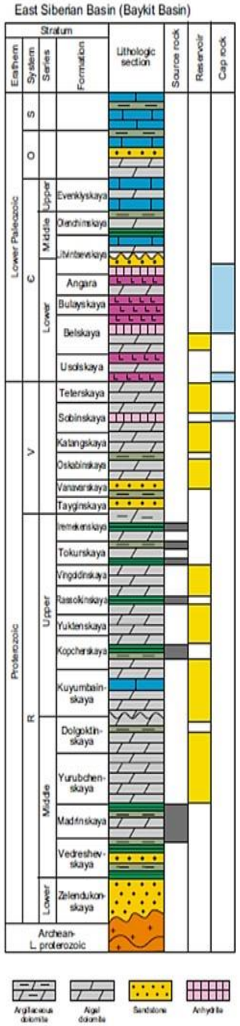

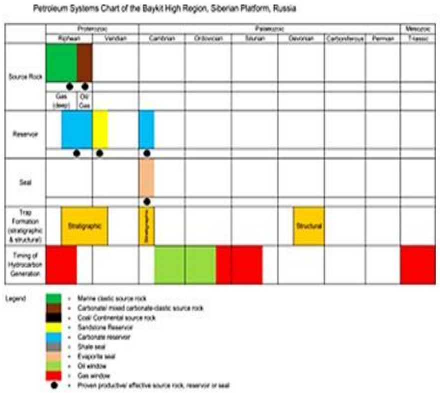

Petroleum Systems Chart of the Nepa-Botuoba High Region, Siberian Platform, Russia

Geology Today, Volume: 37, Issue: 1, Pages: 18-22, First published: 26 January 2021, DOI: (10.1111/gto.12337)

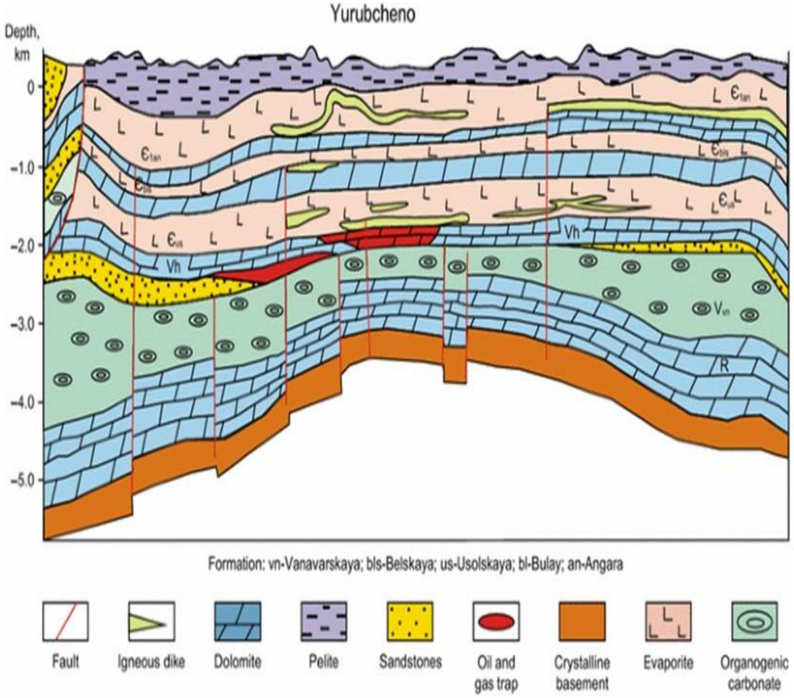

Formation: vn-Vanavarskaya; bls-Belskaya; us-Usolskaya; bl-Bulay; an-Angara

Country	Region	Field	N_2%	CO_2%	He%	CH_4%	N_2/He	Reservoir age	Average depth ft. (m)	Reservoir thickness ft. (m)	Reservoir area mi^2 (km^2)	Porosity (%)	Sw (%)	Permeability (mD)	Age of pore water	Well type	Cost (US$)	Gas, recoverable BCFG (BCM)	Helium BCFG (BCM)	Economic or non-economic?
Russia	Eastern Siberian Platform	Yurubchen-Tokhomo	7.80	0.23	0.18	83.00	42.62	Riphean	9850 (3,000)	410-426 (125-130)	3861 (10000)	Primary: 1-2%, 2'ndary: 15-20%	10.00	750-800	Riphean 1.35 BYA	3,500m vertical	US$4,500,000	73700 (2087)	4090 (115)	Economic

Montage 4A. Yurubchen-Tokhomo Field.

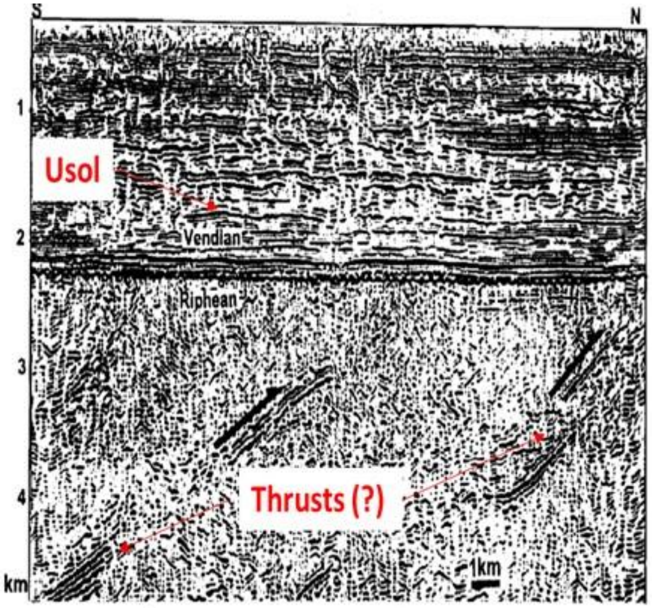

Depth-converted seismic line through the Yurubchen-Takhom field showing the Riphean-Vendian unconformity and the presence of interpreted thrust faults in the deeper Riphean section. Usolian (Lower Cambrian) evaporites at ~1.8 km.

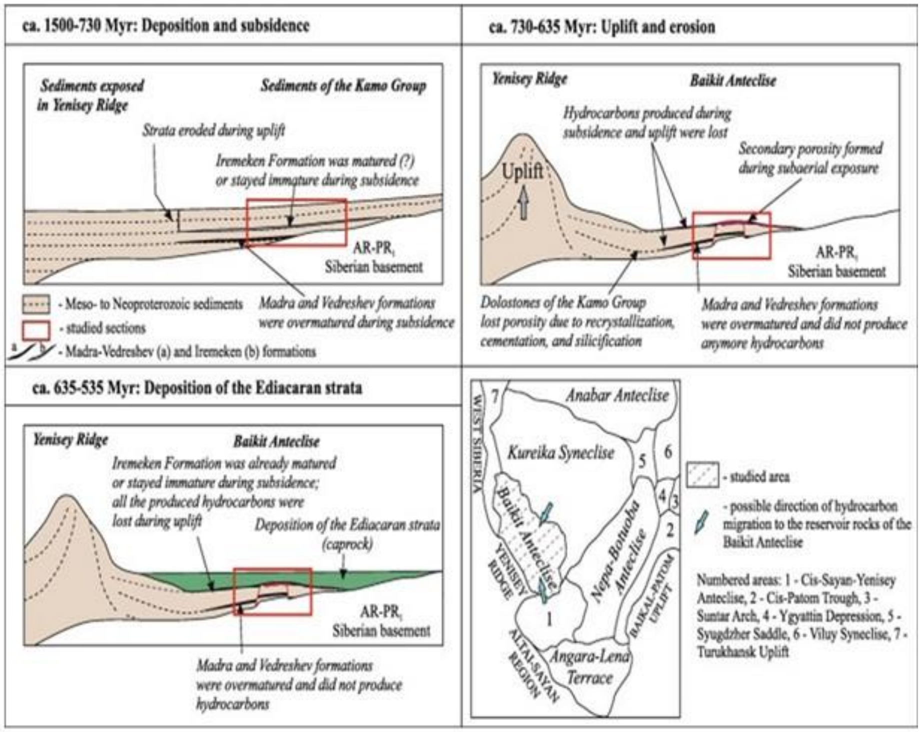

Uralmash 3D-76 Rig

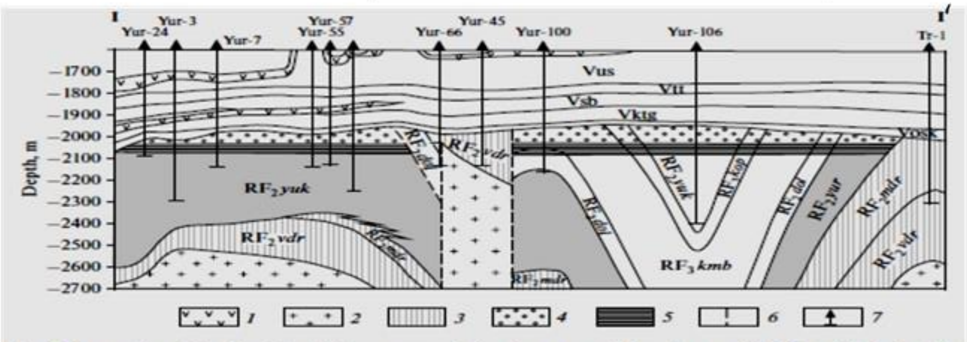

Fig. 4. Deep section of the Yurubchen–Tokhomo zone of oil-and gas accumulation along profile I–I (modified after [9]). (*1*) Dolerites; (*2*) granite gneisses and granites of the crystalline basement; (*3*) impermeable clayey and carbonate–clayey sequences of the Madra and Vedreshev sequences; (*4*) permeable gas-saturated sequences; (*5*) oil-saturated sequences—intervals of the sub-Vendian weathering crust; (*6*) faults; (*7*) oil-and gas prospecting holes.

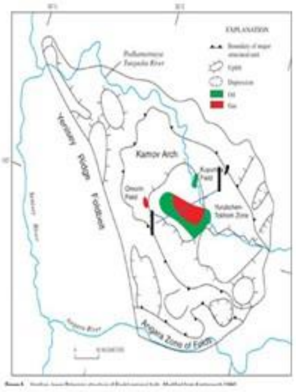

North “Dome” Field, Qatar and South Pars Field, Iran, (Montages 5 & 5A)

The Qatari North “Dome” and Iranian South Pars Fields form the largest known accumulation of non-associated gas on the planet. This field covers an area of more than 6000 square kilometres which is nearly half the size of the Qatari peninsula. North field and South Pars fields overlie the broad Qatar arch, which subdivides the Khuff depositional basin, into two basins located north west and south east of the arch.

Organic-rich mudstones of the Lower Silurian Qusaiba Member of the Qalibah Formation and equivalent rocks in the Arabian Peninsula are the source of oil and gas for this most prolific petroleum-generating systems in the Middle East region. As is typical for this sector of the Middle East, these Lower Silurian organic-rich shales are the main source for hydrocarbons in Qatar and southern Iran (Aali, et al., 2006), and attain thickness in excess of 400m with unusually high TOC.

North Field reservoir which is a part of Permian Khuff formation mainly consists of mixture of dolomite and limestone and has 4 geological layers (stratigraphically): K4, K3, K2 and K1. These gas reservoirs are found at shallow depth in the Khuff, usually between 2470 and 2830 m below sea level (Al-Marri and Al-Bader, 1989).

The North Field contains only a trace amount of helium estimated at 0.04%. However, due to the enormous size of this reservoir the total contained helium is thought to be 360^{+} billion cubic feet, enough to supply the world demand for the next 30 years. At this low concentration helium extraction would generally not be economically viable. However, a fortunate side effect of the existing LNG process is to concentrate the helium tenfold. Qatar has gone from producing zero helium in 1997 to producing over 1/3 of the world’s helium, both crude and grade-A, today.

North “Dome” Field, Qatar and South Pars Field, Iran, (Montage 5)

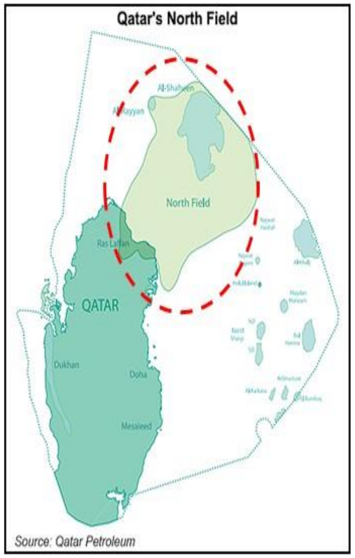

Source: Qatar Petroleum

Country: Qatar
Geological region: North Dome
Field(s): North
Reservoir age(s): Permocarboniferous Khuff
Gas/Helium EUR: 1000 TCFG/360$^+$ BCF

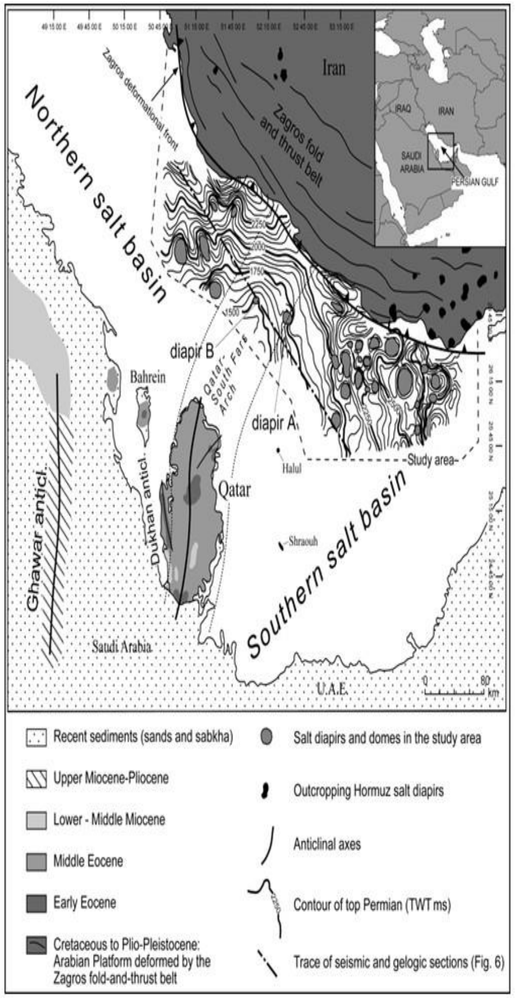

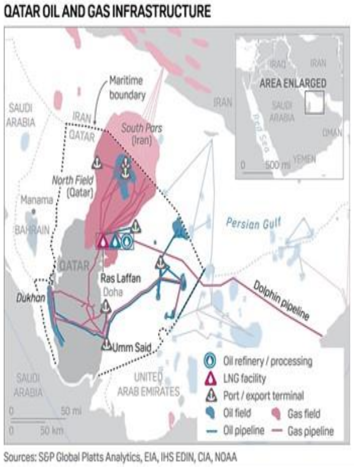

Sources: S&P Global Platts Analytics, EIA, IHS EDIN, CIA, NOAA

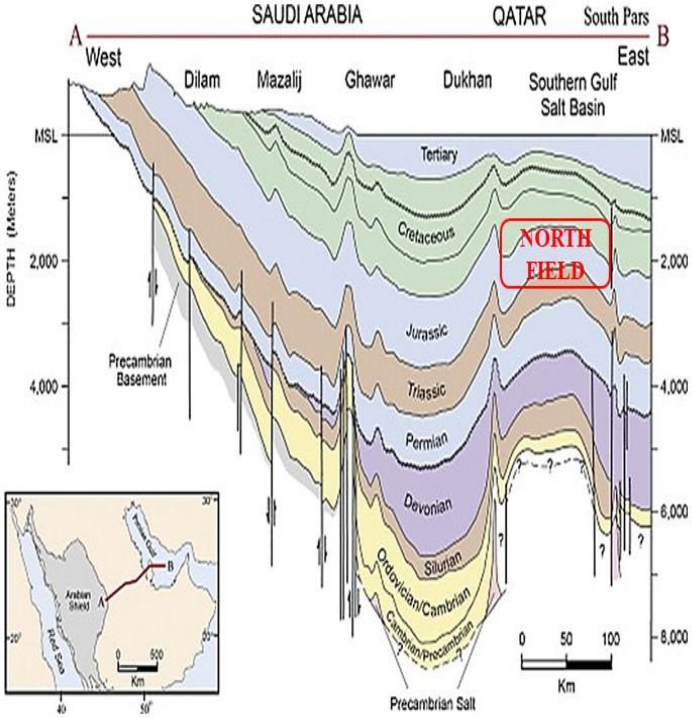

Country	Region	Field	N_2%	CO_2%	He%	CH_4%	N_2/He	Reservoir age	Average depth ft. (m)	Reservoir thickness ft. (m)	Reservoir area mi^2 (km^2)	Porosity (%)	Sw (%)	Permeability (mD)	Age of pore water	Well type	Cost (US$)	Gas, recoverable BCFG (BCM)	Helium BCFG (BCM)	Economic or non-economic?
Qatar	Qatar Dome	North/Pars Field	3.35	1.76	0.05	83.27	68.37	Khuff	10000	1431'	6000 km^2	Low: 1, High: 27	18.00	3-120	Permocarboniferous	9,000 ft with a sail angle up to 70º	US$17,000,000 (Est)	1,800,000 BCFG	360 BCF (10.2)	Economic

North “Dome” Field, Qatar and South Pars Field, Iran, (Montage 5A)

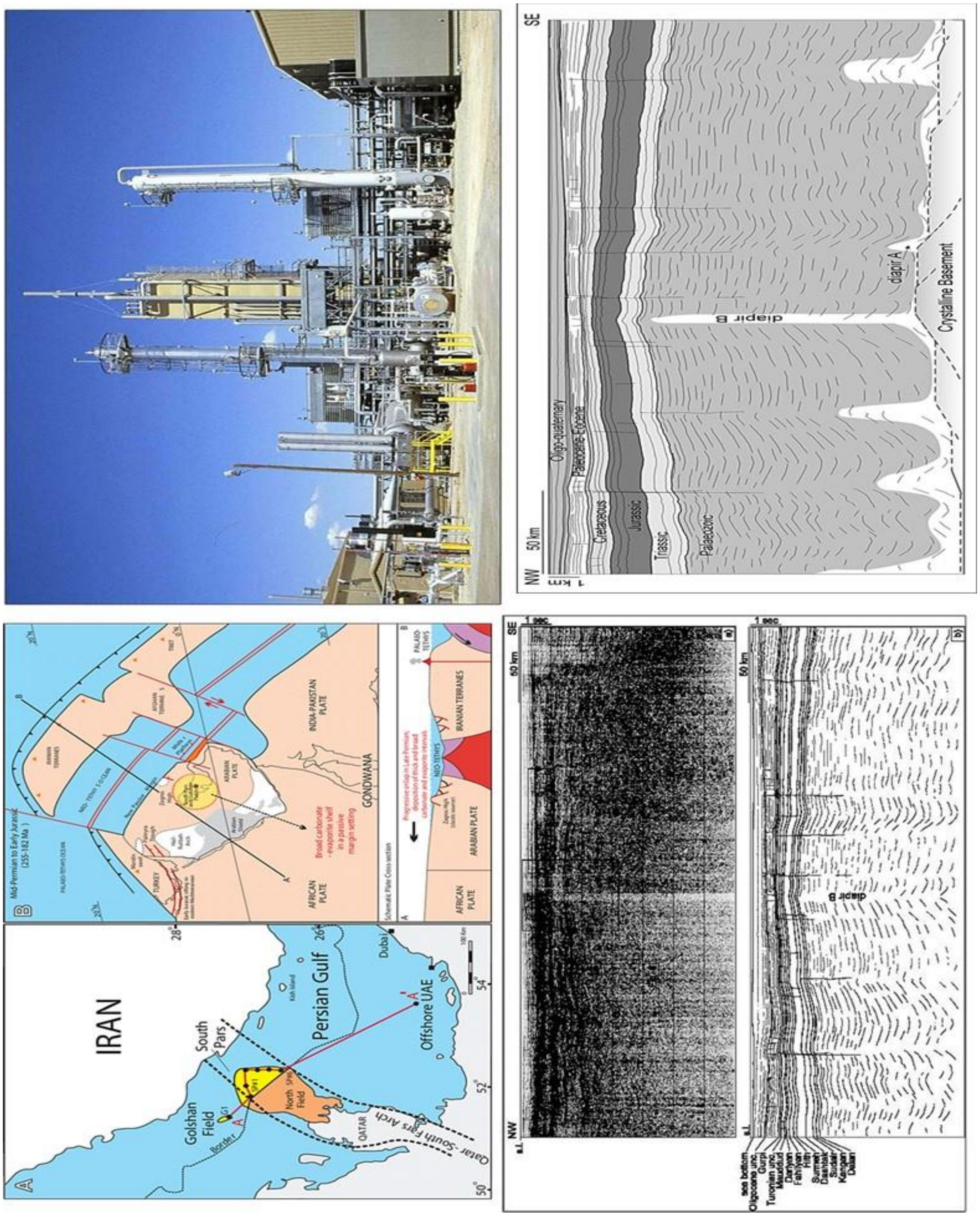

Bakken-sourced flare gas, Williston Basin, North Dakota., (Montages 6 & 6A)

The Bakken Formation is a rock unit from the Late Devonian to Early Mississippian age occupying about 200,000 square miles (520,000 km^2) of the subsurface of the Williston Basin, underlying parts of Montana, North Dakota, Saskatchewan and Manitoba.

The Bakken consists of three members: lower shale, middle dolomite, and upper shale. The upper and lower shales were deposited in relatively deep anoxic marine conditions, and the central dolomite was deposited as a coastal carbonate bank during a time of shallower, well-oxygenated water. The middle dolomite member is the principal oil reservoir, roughly 3 km below the surface. Both the upper and lower shale members are organic-rich marine shale and source the middle reservoir zone.

The great increases in oil and gas production due to the inclusion of horizontal drilling and massive hydraulic fracturing have exceeded the area's pipeline capacity to transport hydrocarbons to markets. Additionally, there is only one refinery in the area. As a result, the oil and gas prices received have been much lower than the normal North American index prices of West Texas Intermediate for oil and Henry Hub for gas (Anonymous, 2012).

Therefore, a large proportion of the associated gas has been flared. This has been decreasing in the last few years, but according to the North Dakota Geological Survey, there is still an average of 1 BCF/D flared in the Williston Basin, with the majority of that gas coming from the Bakken Formation. This gas has a helium concentration of 0.03-0.07%v/v, (Nicolas, 2016, and Cheng, et al, 2108) can be extracted economically given the use of passive selective membranes and a cost for crude helium over US$498/MCFG. In fact, the gas gathered and previously flared from 12 Bakken wells can support from the first year a helium extraction facility economically at a price of $US30MM. Payout occurs within the first year of operation.

Bakken-sourced flare gas, Williston Basin, North Dakota., (Montage 6).

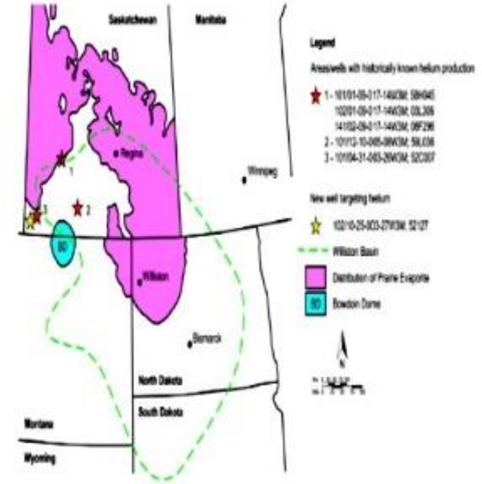

Figure 9. Regional map showing the extent of the Williston Basin and Prairie evaporite in relations to state and provincial borders as well as commercial helium production wells in southwestern Saskatchewan. Modified from Yurkowski (2016).

Trace amounts of helium appear to be present in the majority of oil and gas productive reservoirs within North Dakota.

The highest helium concentrations are found within the older, deeper Cambrian-Ordovician rock units.

Positive nitrogen-helium correlations occur within the Cambrian and Ordovician formations and possibly in the overlying Silurian and Devonian rock units as well.

Elevated nitrogen and helium concentrations occur within Cambrian and Ordovician formations most commonly along the Nesson and Antelope anticlines, as well as the Deadwood Formation (Cambrian) within the Newporte structure area.

Late Ordovician-Early Silurian anhydrite beds and/or the salt-dominated Prairie Formation may form the upper seal for basement-originated helium gas migration.

Country:	USA
Geological region:	Williston Basin
Field(s):	Bakken
Reservoir age(s):	Devonian-Mississippian
Gas/Helium EUR:	Economic

In 1952, helium concentrations were discovered in southwestern Saskatchewan. Production from four wells took place from 1963 to 1977, and resumed again in 2014. The Deadwood Formation, and other Lower Paleozoic formations, had the highest concentration. The helium originated through natural radioactive decay of uranium and thorium in Precambrian granitic basement rocks, or Lower Paleozoic shales.

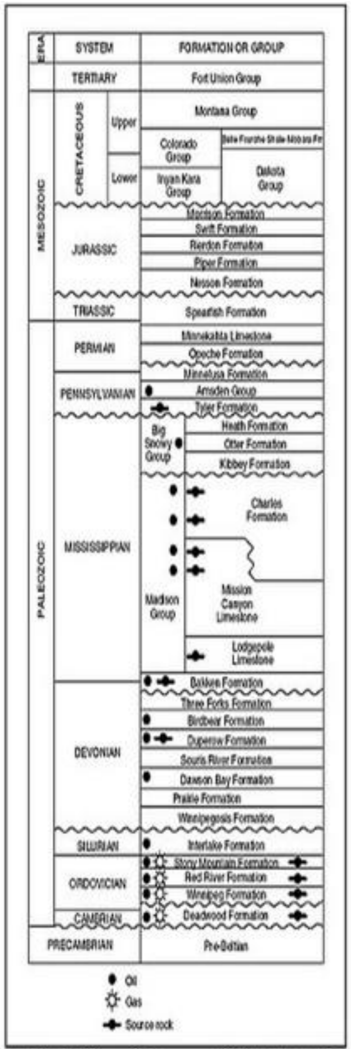

Country	Region	Field	N_2%	CO_2%	He%	CH_4%	N_2/He	Reservoir age	Average depth ft. (m)	Reservoir thickness ft. (m)	Reservoir area mi^2 (km^2)	Porosity (%)	Sw (%)	Permeability (mD)	Age of pore water	Well type	Cost (US$)	Gas, recoverable BCFG (BCM)	Helium BCFG (BCM)	Economic or non-economic?
USA	Williston Basin - Bakken	Flare Gas	0.70	2.70	0.60	96.00	1.17	Devonian-Mississippian	N/A	N/A	25,000 acres	N/A	N/A	N/A	Devonian-Mississippian	N/A	N/A	N/A	N/A	Economic by Scoping Report

Bakken-sourced flare gas, Williston Basin, North Dakota., (Montage 6A)

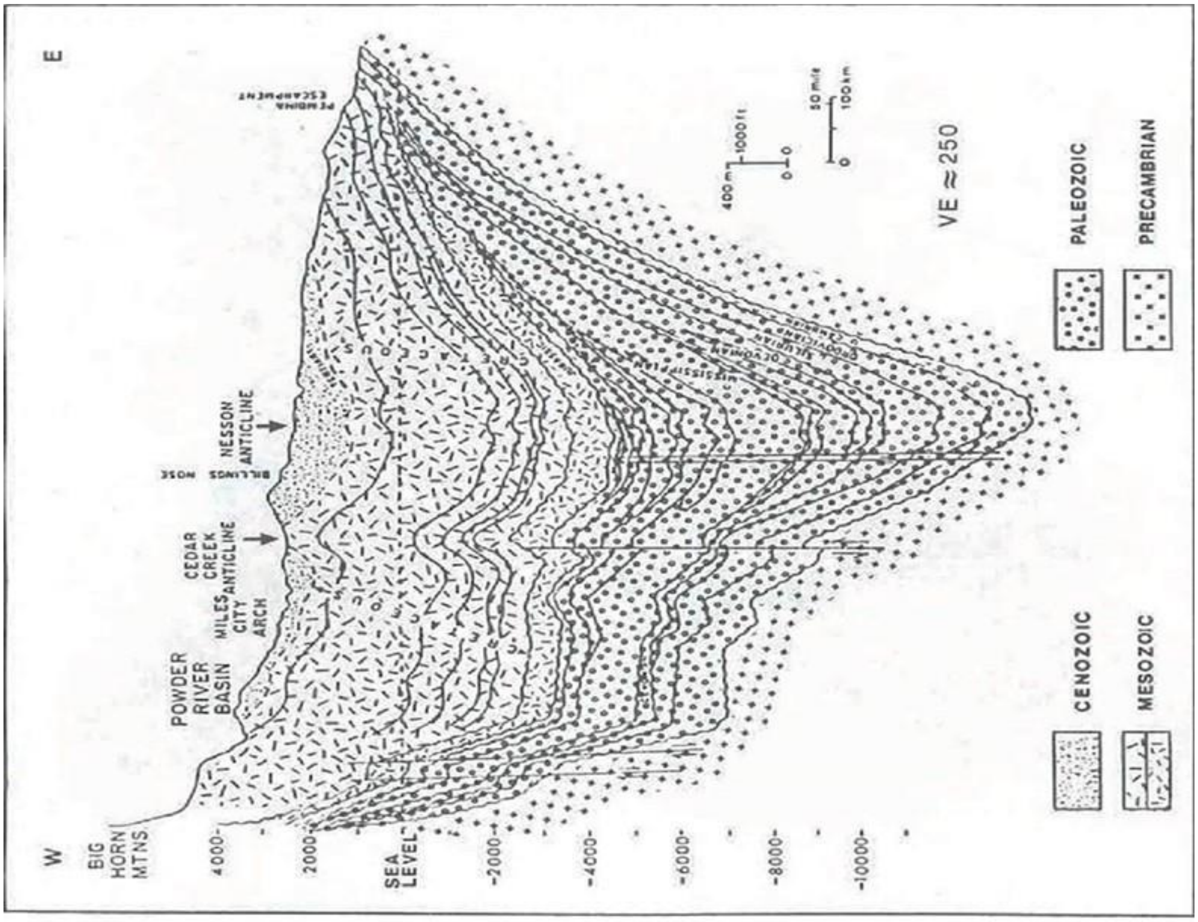

The choices may seem odd, due to their geographical (North Dakota, the Middle East and Eastern Siberia), geological (Bakken: Devonian-Mississippian, North Field: Permocarboniferous and Yurubchen Field: Riphean, Vendian and Ediacaran), sedimentary (Bakken: shales, dolostones, siltstones, sandstones, and minor occurrences of anhydrite, North Field: massive dolomitic carbonates and evaporites, and Yurubchen: and structural (Bakken: intercratonic basin, North Field: intercratonic dome, and Yurubchen: intercratonic margin of the North Asian Craton) differences. However, they all are productive (or potentially productive in the case of the Bakken) of great volumes of helium, have long, multi-decade production histories, and a relatively low number of long-established operators.

Taking the Scoping Study for a Bakken helium plant, we see that we're assuming the Bakken plant will handle 25,000 MCF annually of crude helium. Utilizing the same ratio for North and Yurubchen Fields, we come up with 8.17 million MCF Helium for North Field per year and 11.0 million MCF He for Yurubchen. Gross revenue (at 100% recovery) would be $26 Million for the Bakken, $8.3 billion for North Field and nearly $10 billion for Yurubchen Field. This simple economic outlook does not include recovery factors, processing losses, transport losses and the like, but are kept simple to demonstrate that with the value of crude helium at US$400/MCF, even low-volume, low-helium concentration fields can be remarkably profitable, Table 8.13

Table 8.12. /MCF on three different fields.

Field	Raw Gas MMCFPD	Raw Gas MMCFG/Yr	He %	He/year MCF	US$/MCF He	Gross Revenue (US$/YR)	NPV@18%	Operating costs
Bakken	490	180,000	0.2	25,000	$400.00	$10,000,000.00	$26,006,318.86	$3,580,000.00
North Field	560	204,400	0.04	8,176,000	$400.00	$3,270,400,000.00	$8,266,478,179.78	$1,170,803,200.00
Yurubchen	76	27,740	0.4	11,096,000	$400.00	$4,438,400,000.00	$9,935,440,888.10	$1,588,947,200.00

Bakken – 12 wells equivalent (2 -6 well pads)

Time Since Evaluation Year	**Helium MCF/yr**	**Helium price $/MCFG**	**Revenue (He* price)**	**Operating Costs (0.385 of revenue)**	**Gross Profit (=h12-I12)**	**Depreciation**	***Overall Taxable Profit*** **(=j12-k12)**	**Federal Taxes (US = 21%) (=J12*0.21)**	**Net Profit (=l12-m12)**	***Present Value @ HR & Evaluation Date***
1	25000	400	$10,000,000	$3,850,000	$6,150,000	$0	$6,150,000	$1,291,500	$4,858,500	$4,117,373
2	25000	400	$10,000,000	$3,850,000	$6,150,000	$0	$6,150,000	$1,291,500	$4,858,500	$3,489,299
3	25000	400	$10,000,000	$3,850,000	$6,150,000	$0	$6,150,000	$1,291,500	$4,858,500	$2,957,033
4	25000	400	$10,000,000	$3,850,000	$6,150,000	$0	$6,150,000	$1,291,500	$4,858,500	$2,505,960
5	25000	400	$10,000,000	$3,850,000	$6,150,000	$0	$6,150,000	$1,291,500	$4,858,500	$2,123,695
6	25000	400	$10,000,000	$3,850,000	$6,150,000	$0	$6,150,000	$1,291,500	$4,858,500	$1,799,742
7	25000	400	$10,000,000	$3,850,000	$6,150,000	$0	$6,150,000	$1,291,500	$4,858,500	$1,525,205
8	25000	400	$10,000,000	$3,850,000	$6,150,000	$0	$6,150,000	$1,291,500	$4,858,500	$1,292,546
9	25000	400	$10,000,000	$3,850,000	$6,150,000	$0	$6,150,000	$1,291,500	$4,858,500	$1,095,378
10	25000	400	$10,000,000	$3,850,000	$6,150,000	$0	$6,150,000	$1,291,500	$4,858,500	$928,287
11	25000	400	$10,000,000	$3,850,000	$6,150,000	$0	$6,150,000	$1,291,500	$4,858,500	$786,684
12	25000	400	$10,000,000	$3,850,000	$6,150,000	$0	$6,150,000	$1,291,500	$4,858,500	$666,681
13	25000	400	$10,000,000	$3,850,000	$6,150,000	$0	$6,150,000	$1,291,500	$4,858,500	$564,984
14	25000	400	$10,000,000	$3,850,000	$6,150,000	$0	$6,150,000	$1,291,500	$4,858,500	$478,800
15	25000	400	$10,000,000	$3,850,000	$6,150,000	$0	$6,150,000	$1,291,500	$4,858,500	$405,763
16	25000	400	$10,000,000	$3,850,000	$6,150,000	$0	$6,150,000	$1,291,500	$4,858,500	$343,867
17	25000	400	$10,000,000	$3,850,000	$6,150,000	$0	$6,150,000	$1,291,500	$4,858,500	$291,412
18	25000	400	$10,000,000	$3,850,000	$6,150,000	$0	$6,150,000	$1,291,500	$4,858,500	$246,960
19	25000	400	$10,000,000	$3,850,000	$6,150,000	$0	$6,150,000	$1,291,500	$4,858,500	$209,288
20	25000	400	$10,000,000	$3,850,000	$6,150,000	$0	$6,150,000	$1,291,500	$4,858,500	$177,363
Basis Date				Evaluation Date		Hurdle Rate	0.18		NPV@18% =	$26,006,319

North Field – 36 wells

Time Since Evaluation Year	Helium MCF/yr	Helium price $/MCFG	Revenue (He* price)	Operating Costs (0.385 of revenue)	Gross Profit (=h12-I12)	Depreciation	*Overall Taxable Profit*	Federal Taxes (Qatar= 35%) (=J12*0.21)	Net Profit (=l12-m12)	*Present Value @ HR & Evaluation Date*
1	8176000	400	$3,270,400,000	$1,259,104,000	$2,011,296,000	$0	$2,011,296,000	$703,953,600	$1,307,342,400	$1,107,917,288
2	8176000	400	$3,270,400,000	$1,259,104,000	$2,011,296,000	$0	$2,011,296,000	$422,372,160	$1,588,923,840	$1,141,140,362
3	8176000	400	$3,270,400,000	$1,259,104,000	$2,011,296,000	$0	$2,011,296,000	$422,372,160	$1,588,923,840	$967,068,103
4	8176000	400	$3,270,400,000	$1,259,104,000	$2,011,296,000	$0	$2,011,296,000	$422,372,160	$1,588,923,840	$819,549,240
5	8176000	400	$3,270,400,000	$1,259,104,000	$2,011,296,000	$0	$2,011,296,000	$422,372,160	$1,588,923,840	$694,533,254
6	8176000	400	$3,270,400,000	$1,259,104,000	$2,011,296,000	$0	$2,011,296,000	$422,372,160	$1,588,923,840	$588,587,504
7	8176000	400	$3,270,400,000	$1,259,104,000	$2,011,296,000	$0	$2,011,296,000	$422,372,160	$1,588,923,840	$498,802,969
8	8176000	400	$3,270,400,000	$1,259,104,000	$2,011,296,000	$0	$2,011,296,000	$422,372,160	$1,588,923,840	$422,714,381
9	8176000	400	$3,270,400,000	$1,259,104,000	$2,011,296,000	$0	$2,011,296,000	$422,372,160	$1,588,923,840	$358,232,526
10	8176000	400	$3,270,400,000	$1,259,104,000	$2,011,296,000	$0	$2,011,296,000	$422,372,160	$1,588,923,840	$303,586,886
11	8176000	400	$3,270,400,000	$1,259,104,000	$2,011,296,000	$0	$2,011,296,000	$422,372,160	$1,588,923,840	$257,277,022
12	8176000	400	$3,270,400,000	$1,259,104,000	$2,011,296,000	$0	$2,011,296,000	$422,372,160	$1,588,923,840	$218,031,375
13	8176000	400	$3,270,400,000	$1,259,104,000	$2,011,296,000	$0	$2,011,296,000	$422,372,160	$1,588,923,840	$184,772,352
14	8176000	400	$3,270,400,000	$1,259,104,000	$2,011,296,000	$0	$2,011,296,000	$422,372,160	$1,588,923,840	$156,586,739
15	8176000	400	$3,270,400,000	$1,259,104,000	$2,011,296,000	$0	$2,011,296,000	$422,372,160	$1,588,923,840	$132,700,626
16	8176000	400	$3,270,400,000	$1,259,104,000	$2,011,296,000	$0	$2,011,296,000	$422,372,160	$1,588,923,840	$112,458,158
17	8176000	400	$3,270,400,000	$1,259,104,000	$2,011,296,000	$0	$2,011,296,000	$422,372,160	$1,588,923,840	$95,303,523
18	8176000	400	$3,270,400,000	$1,259,104,000	$2,011,296,000	$0	$2,011,296,000	$422,372,160	$1,588,923,840	$80,765,698
19	8176000	400	$3,270,400,000	$1,259,104,000	$2,011,296,000	$0	$2,011,296,000	$422,372,160	$1,588,923,840	$68,445,507
20	8176000	400	$3,270,400,000	$1,259,104,000	$2,011,296,000	$0	$2,011,296,000	$422,372,160	$1,588,923,840	$58,004,667
Basis Date				Evaluation Date		Hurdle Rate	0.18		NPV@18% =	$8,266,478,180

Yurubchen Field – 44 wells

Time Since Evaluation Year	Helium MCF/yr	Helium price $/MCFG	Revenue (He* price)	Operating Costs (0.385 of revenue)	Gross Profit (=h12-I12)	Depreciation	*Overall Taxable Profit*	Federal Taxes (Russia = 32%) (=J12*0.21)	Net Profit (=l12-m12)	*Present Value @ HR & Evaluation Date*
1	11096000	400	$4,438,400,000	$1,708,784,000	$2,729,616,000	$0	$2,729,616,000	$873,477,120	$1,856,138,880	$1,572,999,051
2	11096000	400	$4,438,400,000	$1,708,784,000	$2,729,616,000	$0	$2,729,616,000	$873,477,120	$1,856,138,880	$1,333,050,043
3	11096000	400	$4,438,400,000	$1,708,784,000	$2,729,616,000	$0	$2,729,616,000	$873,477,120	$1,856,138,880	$1,129,703,426
4	11096000	400	$4,438,400,000	$1,708,784,000	$2,729,616,000	$0	$2,729,616,000	$873,477,120	$1,856,138,880	$957,375,785
5	11096000	400	$4,438,400,000	$1,708,784,000	$2,729,616,000	$0	$2,729,616,000	$873,477,120	$1,856,138,880	$811,335,411
6	11096000	400	$4,438,400,000	$1,708,784,000	$2,729,616,000	$0	$2,729,616,000	$873,477,120	$1,856,138,880	$687,572,382
7	11096000	400	$4,438,400,000	$1,708,784,000	$2,729,616,000	$0	$2,729,616,000	$873,477,120	$1,856,138,880	$582,688,460
8	11096000	400	$4,438,400,000	$1,708,784,000	$2,729,616,000	$0	$2,729,616,000	$873,477,120	$1,856,138,880	$493,803,779
9	11096000	400	$4,438,400,000	$1,708,784,000	$2,729,616,000	$0	$2,729,616,000	$873,477,120	$1,856,138,880	$418,477,779
10	11096000	400	$4,438,400,000	$1,708,784,000	$2,729,616,000	$0	$2,729,616,000	$873,477,120	$1,856,138,880	$354,642,186
11	11096000	400	$4,438,400,000	$1,708,784,000	$2,729,616,000	$0	$2,729,616,000	$873,477,120	$1,856,138,880	$300,544,225
12	11096000	400	$4,438,400,000	$1,708,784,000	$2,729,616,000	$0	$2,729,616,000	$873,477,120	$1,856,138,880	$254,698,496
13	11096000	400	$4,438,400,000	$1,708,784,000	$2,729,616,000	$0	$2,729,616,000	$873,477,120	$1,856,138,880	$215,846,183
14	11096000	400	$4,438,400,000	$1,708,784,000	$2,729,616,000	$0	$2,729,616,000	$873,477,120	$1,856,138,880	$182,920,494
15	11096000	400	$4,438,400,000	$1,708,784,000	$2,729,616,000	$0	$2,729,616,000	$873,477,120	$1,856,138,880	$155,017,368
16	11096000	400	$4,438,400,000	$1,708,784,000	$2,729,616,000	$0	$2,729,616,000	$873,477,120	$1,856,138,880	$131,370,651
17	11096000	400	$4,438,400,000	$1,708,784,000	$2,729,616,000	$0	$2,729,616,000	$873,477,120	$1,856,138,880	$111,331,060
18	11096000	400	$4,438,400,000	$1,708,784,000	$2,729,616,000	$0	$2,729,616,000	$873,477,120	$1,856,138,880	$94,348,356
19	11096000	400	$4,438,400,000	$1,708,784,000	$2,729,616,000	$0	$2,729,616,000	$873,477,120	$1,856,138,880	$79,956,234
20	11096000	400	$4,438,400,000	$1,708,784,000	$2,729,616,000	$0	$2,729,616,000	$873,477,120	$1,856,138,880	$67,759,520
Basis Date				Evaluation Date		Hurdle Rate	0.18		NPV@18% =	$9,935,440,888

In fact, given the US$3.85 MM cost of the helium separation and concentration plant for the Bakken, the NPV notes that the figure (US$4.117 MM) would be paid out in less than one year. Given that the price of helium has not decreased in the last decade and has always risen, it just makes the case stronger for helium capture and concentration from the Bakken. However, this does not address the similar situation found in the NGL scoping study, where that would only add further revenue for a joint NGL-Helium-H_2 feedstock stream to be captured from gas being now flared from the Bakken, Table 8.13.

Table 8.13. Cash Flow Worksheet Bakken NGL plant. NPV@HR: $370 MM, DCFROR = 110%

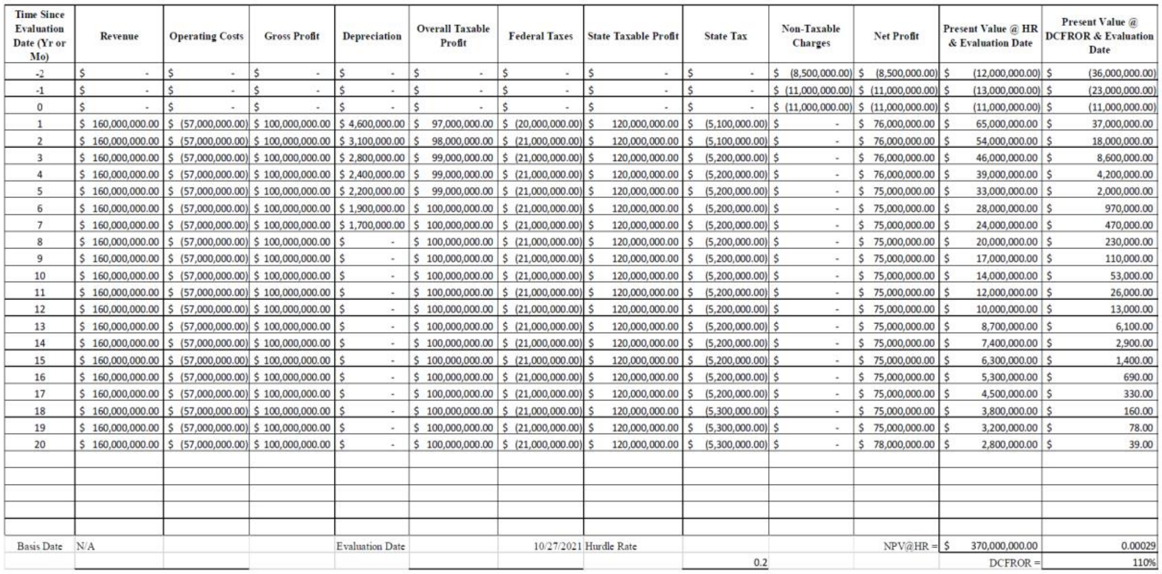

Time Since Evaluation Date (Yr or Mo)	Revenue	Operating Costs	Gross Profit	Depreciation	Overall Taxable Profit	Federal Taxes	State Taxable Profit	State Tax	Non-Taxable Charges	Net Profit	Present Value @ HR & Evaluation Date	Present Value @ DCFROR & Evaluation Date
-2	$ -	$ -	$ -	$ -	$ -	$ -	$ -	$ -	$ (8,500,000.00)	$ (8,500,000.00)	$ (12,000,000.00)	$ (36,000,000.00)
-1	$ -	$ -	$ -	$ -	$ -	$ -	$ -	$ -	$ (11,000,000.00)	$ (11,000,000.00)	$ (13,000,000.00)	$ (23,000,000.00)
0	$ -	$ -	$ -	$ -	$ -	$ -	$ -	$ -	$ (11,000,000.00)	$ (11,000,000.00)	$ (11,000,000.00)	$ (11,000,000.00)
1	$ 160,000,000.00	$ (57,000,000.00)	$ 100,000,000.00	$ 4,600,000.00	$ 97,000,000.00	$ (20,000,000.00)	$ 120,000,000.00	$ (5,100,000.00)	$ -	$ 76,000,000.00	$ 65,000,000.00	$ 37,000,000.00
2	$ 160,000,000.00	$ (57,000,000.00)	$ 100,000,000.00	$ 3,100,000.00	$ 98,000,000.00	$ (21,000,000.00)	$ 120,000,000.00	$ (5,100,000.00)	$ -	$ 76,000,000.00	$ 54,000,000.00	$ 18,000,000.00
3	$ 160,000,000.00	$ (57,000,000.00)	$ 100,000,000.00	$ 2,800,000.00	$ 99,000,000.00	$ (21,000,000.00)	$ 120,000,000.00	$ (5,200,000.00)	$ -	$ 76,000,000.00	$ 46,000,000.00	$ 8,600,000.00
4	$ 160,000,000.00	$ (57,000,000.00)	$ 100,000,000.00	$ 2,400,000.00	$ 99,000,000.00	$ (21,000,000.00)	$ 120,000,000.00	$ (5,200,000.00)	$ -	$ 76,000,000.00	$ 39,000,000.00	$ 4,200,000.00
5	$ 160,000,000.00	$ (57,000,000.00)	$ 100,000,000.00	$ 2,200,000.00	$ 99,000,000.00	$ (21,000,000.00)	$ 120,000,000.00	$ (5,200,000.00)	$ -	$ 75,000,000.00	$ 33,000,000.00	$ 2,000,000.00
6	$ 160,000,000.00	$ (57,000,000.00)	$ 100,000,000.00	$ 1,900,000.00	$ 100,000,000.00	$ (21,000,000.00)	$ 120,000,000.00	$ (5,200,000.00)	$ -	$ 75,000,000.00	$ 28,000,000.00	$ 970,000.00
7	$ 160,000,000.00	$ (57,000,000.00)	$ 100,000,000.00	$ 1,700,000.00	$ 100,000,000.00	$ (21,000,000.00)	$ 120,000,000.00	$ (5,200,000.00)	$ -	$ 75,000,000.00	$ 24,000,000.00	$ 470,000.00
8	$ 160,000,000.00	$ (57,000,000.00)	$ 100,000,000.00	$ -	$ 100,000,000.00	$ (21,000,000.00)	$ 120,000,000.00	$ (5,200,000.00)	$ -	$ 75,000,000.00	$ 20,000,000.00	$ 230,000.00
9	$ 160,000,000.00	$ (57,000,000.00)	$ 100,000,000.00	$ -	$ 100,000,000.00	$ (21,000,000.00)	$ 120,000,000.00	$ (5,200,000.00)	$ -	$ 75,000,000.00	$ 17,000,000.00	$ 110,000.00
10	$ 160,000,000.00	$ (57,000,000.00)	$ 100,000,000.00	$ -	$ 100,000,000.00	$ (21,000,000.00)	$ 120,000,000.00	$ (5,200,000.00)	$ -	$ 75,000,000.00	$ 14,000,000.00	$ 53,000.00
11	$ 160,000,000.00	$ (57,000,000.00)	$ 100,000,000.00	$ -	$ 100,000,000.00	$ (21,000,000.00)	$ 120,000,000.00	$ (5,200,000.00)	$ -	$ 75,000,000.00	$ 12,000,000.00	$ 26,000.00
12	$ 160,000,000.00	$ (57,000,000.00)	$ 100,000,000.00	$ -	$ 100,000,000.00	$ (21,000,000.00)	$ 120,000,000.00	$ (5,200,000.00)	$ -	$ 75,000,000.00	$ 10,000,000.00	$ 13,000.00
13	$ 160,000,000.00	$ (57,000,000.00)	$ 100,000,000.00	$ -	$ 100,000,000.00	$ (21,000,000.00)	$ 120,000,000.00	$ (5,200,000.00)	$ -	$ 75,000,000.00	$ 8,700,000.00	$ 6,100.00
14	$ 160,000,000.00	$ (57,000,000.00)	$ 100,000,000.00	$ -	$ 100,000,000.00	$ (21,000,000.00)	$ 120,000,000.00	$ (5,200,000.00)	$ -	$ 75,000,000.00	$ 7,400,000.00	$ 2,900.00
15	$ 160,000,000.00	$ (57,000,000.00)	$ 100,000,000.00	$ -	$ 100,000,000.00	$ (21,000,000.00)	$ 120,000,000.00	$ (5,200,000.00)	$ -	$ 75,000,000.00	$ 6,300,000.00	$ 1,400.00
16	$ 160,000,000.00	$ (57,000,000.00)	$ 100,000,000.00	$ -	$ 100,000,000.00	$ (21,000,000.00)	$ 120,000,000.00	$ (5,200,000.00)	$ -	$ 75,000,000.00	$ 5,300,000.00	$ 690.00
17	$ 160,000,000.00	$ (57,000,000.00)	$ 100,000,000.00	$ -	$ 100,000,000.00	$ (21,000,000.00)	$ 120,000,000.00	$ (5,200,000.00)	$ -	$ 75,000,000.00	$ 4,500,000.00	$ 330.00
18	$ 160,000,000.00	$ (57,000,000.00)	$ 100,000,000.00	$ -	$ 100,000,000.00	$ (21,000,000.00)	$ 120,000,000.00	$ (5,300,000.00)	$ -	$ 75,000,000.00	$ 3,800,000.00	$ 160.00
19	$ 160,000,000.00	$ (57,000,000.00)	$ 100,000,000.00	$ -	$ 100,000,000.00	$ (21,000,000.00)	$ 120,000,000.00	$ (5,300,000.00)	$ -	$ 75,000,000.00	$ 3,200,000.00	$ 78.00
20	$ 160,000,000.00	$ (57,000,000.00)	$ 100,000,000.00	$ -	$ 100,000,000.00	$ (21,000,000.00)	$ 120,000,000.00	$ (5,300,000.00)	$ -	$ 78,000,000.00	$ 2,800,000.00	$ 39.00
Basis Date	N/A			Evaluation Date		10/27/2021	Hurdle Rate			NPV@HR =	$ 370,000,000.00	0.00029
								0.2			DCFROR =	110%

8.4 Comparison of Bakken Gas with Qatar Gas

When examining the helium and gas production harvested from Bakken Flare gas, it is much reminiscent of the situation in Qatar during the 1990s; this is only the price for the produced gas independent of the extraction of products from the main gas stream. When North Field was first being developed in the early 1990s, there were only two NGL plants in the entire country, one for Dukhan Field on the western border and the other for North Field to the north and west (Al-Maslamani, 2008). Although only barely stripping out NGLs for export, there were extraordinary problems, not to mention a lack of global market for these products (Metz, 1993). There were also logistical, production and technological problems of dealing with their chosen fractionation methods, that is cryogenic, in a very hot desert Middle Eastern country (Tamvakis, 2013).

However, with both Western oil and service companies, and the Qatari government realizing the need for foreign expertise, the drilling rate increased as did the production rate of gas. From 1990 to 2020, the annual production of gas, primarily from the North Field, increased from 16.5 to over 175 BCM per year (Sönnichsen, 2021). Concomitant with that, there are now 14 ‘super-gas trains’ whereby Qatar now sells LPG, primarily to Japan, as strictly liquid methane; while the trains extract for sale ethane, propane, butane, decane, decane^{+}, sulfur, helium and petrochemical feedstocks; all told, some 77 million tons of natural gas *products* in 2020 (Qatargas, 2021).

Such is the case in North Dakota. The flared gas in calculations is only capturing the Henry Hub price of methane; excluding all NGLs, helium, sulfur, CO_2, N_2, and in the case of the newly being developed Hydrogen Hub in North Dakota, liquid hydrogen.

However, unlike Qatar, in North Dakota, the feedstock natural gas is free, actually being captured gas that was destined to be wasted through flaring. As noted by Allison and Mandler (2018), plastics, agricultural fertilizers, synthetic fibers, pharmaceuticals, and detergents are potentially a few of the non-fuel by-products of natural gas processing.

Apart from providing clean fuel for the aviation industry (hydrogen), and gaseous hydrogen for fuel cells, carbon black can be extracted for use by the automotive industry, and polyethylene wrapping has great utility in the commercial foodstuffs industry (People’s

Gas, 2020). These are but a few of myriad potential additional products that can be gleaned from the membrane-driven process from captured flare gas to commercial products.

8.5 Steps in the Design, Commissioning and Implementation of Oil/Gas Projects

Given the complexities of construction projects in the oilfield, particularly ones as novel as the one described within, and the quantity of steps necessary to realize such a project through to initial operations:

- Planning/design
- Pre-construction
- Procurement
- Project execution
- Construction
- Post-construction
- Pre-commissioning
- Commissioning
- Implementation
- Operations
- Maintenance
- Remote monitoring
- Technical support

This would require a dedicated series of economists from several subdisciplines; such as construction, exterior design, execution, etc. Such a degree of exaction is unfortunately well beyond the scope of this dissertation; but recognized as necessary before embarking on such a project.

There are numerous methods used in the oil and gas industry today to divine the economics and risks of various projects. Monte-Carlo simulations, Project-Risk Analysis, Sensitivity Analysis, Upstream vs. Midstream Modeling, and EPA economic impact analysis (Fitch, 2019) are all methodologies that incorporate certain aspects of the projects described here within, but still lack rigor, robustness and certain facets of production to make comparisons logical.

However, as noted in Van Hull (2021), “to optimize the economic analysis, a more sophisticated processing model is needed that goes deeper than a simple frac spread to combine *measurement, quantity, quality and value (MQQV) factors* in assessing processing plant economics and answering such questions as whether ethane recovery or rejection would be more profitable for a given plant”.

Determining when NGL extraction will make money, and what factors go into calculating the economic uplift from processing a particular inlet gas stream at a given plant, is where the MQQV approach comes in. The first step in the MQQV approach (Lavenant, 2021) is defining the quantity or volume of liquid per volume of gas, the energy content per volume of gas, or the energy content per volume of liquids for all of the NGLs, expressed as:

- Gallons of liquids per Mcf of gas (GPM).
- Btus per cubic foot of gas.
- Btus per gallon of NGLs.

Another deviation form ‘normal economics’ are that the cost of the feedstock from the produce is essentially zero, so that producer and processor agreements are not required; as the plants will be optimized to accept any and all potential Bakken flare gas. Nor are pipeline minimum volume commitments relevant, as the flare gas to clean fuels plants will be built to be able to handle the estimated growth in drilling and concomitant oil and gas production in the Williston from the Bakken for decades to come (Brandt, et al, 2016).

However, using a modeling paradigm that includes measurement, quantity, quality and value considerations brings greater clarity to processing economics for improved decision making (Choi, 1993).

Although, even given this more robust version of economical modeling, it metaphorically is putting the ‘cart before the horse’. We still must ascertain primary values such as detailed flow volumes, molecular weight, flare gas chemistry, flow pressures, etc., and take these into account when designing the necessary size and magnitude of necessary surface facilities.

As the first deliverable of this project is a scaled-down ‘proof of concept’ model from the captured flare gas through clean hydrogen fuel; can numbers be derived from this physical model which will allow for better design of the following ‘Pilot Plant’ step in the field, to the ultimate field-wide Blue Hydrogen program.

It is only with these preliminary figures from the proof-of-concept that any meaningful economics other than gross field-wide approximations can be determined.

CHAPTER 9

Conclusions and Recommendations

9.1 Study Conclusions

9.1.1 *Can a novel liner-path gas treatment procedure, utilizing off-the-shelf technology, be employed to capture and monetize the currently flared Bakken natural gas?*

Yes. Utilizing a modularized approach of gas collection, pre-treatment, NGL extraction, helium extraction and condensation with concomitant methane feedstock for Steam Methane Reformatting, heretofore wasted Bakken flare gas can be economically converted into many salable products, the least of which is Grade-A helium valued at US$400/MCF. Not only will this drastically reduce the carbon footprint of oilfield activities in the Williston Basin, it will decrease light and particulate pollution, cut down on NOx and SOx emissions, and provide salable products such as ethane, butane, propane and pentane, and liquid nitrogen where none existed previously.

9.1.2 *Can a single unique program of flare gas capture, processing and transport aid in CCUS (Carbon Capture, Utilization and Sequestration) in the Williston Basin?*

Yes. Part of the linear, straight-run module system is the selective isolation and deamination of the raw natural gas feedstock. The carbon dioxide will be sequestered from the natural gas feedstock via chemical reactions in a contactor tower by combining weak carbonic acids with a water solution of a weak base, namely, an alkanolamine. The purified and sweetened CO_2 will then undergo Pressure Swing Adsorption, dropping the temperature to where the CO_2 becomes purified and liquid, ready for bulk sale.

9.1.3 *Can a novel, modularized process of flare gas capture, pre-treatment, NGL/helium extraction and providing feedstock for Steam Methane Reformatting be realized while monetizing the product stream and providing increased incentives for operators to abandon flaring in the Williston Basin, accept and implement the processes and procedures defined in this dissertation?*

Yes. Particularly, since the global price of helium has increased 300% in the last 5 years, and shows no signs of reversing that trend, simple non-mechanical selective membranes, without moving parts, can be utilized to exclude helium from a captured and pre-treated flare gas stream. Economics show that at 25,000 MCF helium per year, the size of the envisioned test plant, the plant would be paid out in less than one year. That is just concerning the revenue of the helium plant, and not including the revenue from the NGL plant, nor the value of the purified methane stream as feedstock for the Hydrogen Hub plant being built in Beulah, North Dakota. It also does not include the additional revenue for operators who no longer have to pay state fines for exceeding the ever-constricting field gas flaring restrictions.

9.1.4 *Given the vagaries and vicissitudes of helium pricing on a global scale, can new helium extraction projects be conducted economically, even if the percentage of helium in the gas stream is below X.xx% (some pre-determined rule-of-thumb value)?*

Yes. Helium prices have been held down artificially by the United States government through their Helium National Reserve for decades. Now, along with COVID-19, fires and a shooting war in Russia, sanctions on Qatar, a heightened call for Algerian natural gas supplies and the *de facto* establishment of an oligarchy when it comes to helium pricing, those helium prices have done nothing over the last two decades but increase. This situation is not forecast by economists nor oil men to change for the long foreseeable future; virtually all forecasts predict rising Helium prices for at least 2-3 decades. Given the evolution of crude helium prices from US$152 to over US$400 in the last year, even non-traditional projects like riftogenic helium in Tanzania, aqueous geothermal helium in India, and volcanogenic helium in Africa, with their classically low “uneconomic” helium rates of ~0.01%, are now being pursued with renewed vigor.

Helium gas is a non-fungible commodity. There are simply no substitutes for the gas in certain critical aerospace, manufacturing and scientific applications. This, along with the perceived shortages of the gas in the previous decade (there was enough gas, but just not at the inexpensive prices to which consumers were used) has driven market demand. Now that the US government is handing down the mantle of being the world’s helium producer, market forces have emerged. These are primarily the five largest specialty gas companies in the world which are determined to fill consumer demand but also pass along taxes, storage charges and transportation charges in the price of the commodity.

With the previous suppliers of helium engaged elsewhere, it will be decades before anything like a free market economy finally catches up to helium. Until then, it is reminiscent of the 1849 California Gold Rush, where anyone with access to crude helium in however small of volumes are scrambling to bring their product to market.

As such, the millions of dollars in NGLs along with the hundreds of millions of dollars of helium being flared or vented in the Williston Basin present for the savvy operator a situation where the helium and NGLs are being donated freely to the atmosphere. Capturing these gases for processing and sale noting a company’s commitment to the environment only doubles the value of Public Relations to a company and their commitment to HSE, as well as to their shareholders.

9.2 Potential Earnings from Extracted Bakken Gas Products

If implementation of this or a modified version of the processes described within are implemented and the remaining flaring of Bakken gas in the Williston Basin is ceased, there would be the elimination of over 7.6 million tons of CO_2, 444 million tons of CH_4 and 2.99 million tons of H_2S being released into the atmosphere (Table 9.1) per year.

Table 9.1. Amounts of noxious materials eliminated per year from the atmosphere if Bakken gas flaring were completely ceased.

Bakken Gas flared per year:		**76,560,432**	**765,604,326.44**
Bakken constituent	**Percentage**	**MCF**	**TONS**
Nitrogen	0.0270	2,067,131.66	20,671,316.64
Methane	0.5800	44,405,050.56	444,050,505.60
Ethane	0.2000	15,312,086.40	153,120,864.00
Propane	0.1100	8,241,647.52	84,216,475.20
i-Butane	0.0250	1,914,010.80	19,140,108.00
n-Butane	0.0250	1,914,010.80	19,140,108.00
i-Pentane	0.0800	6,124,834.56	61,248,345.60
n-Pentane	0.0800	6,124,834.56	61,248,345.60
n-Hexane	0.0540	4,134,263.33	41,342,633.287
n-Heptane	0.0000	765.60	7,656.04
n-Octane	0.0000	76.56	765.60
n-Nonane	0.0000	19.14	191.40
Carbon Dioxide	0.0100	765,604.32	7,656,043.20
Hydrogen Sulfide	0.0039	298,585.68	2,985,856.85
Water	0.001	30.62	360.24

Further, there would be substantial, but at present unquantified reductions of CO, NO_x (Nitrogen oxides) and SO_x (Sulfur oxides) as well.

On the economic side, given the vagaries and volatility of hydrocarbons and associated by-products markets, it is difficult to extract the income possible, per year, by cessation of Bakken flaring at January 2023 rates.

However, for some of the major products, an estimation can be made (Table 9.2).

Table 9.2. Values of the 4 most common products and by-products of the proposed process stream, on a per year basis, from the processing of Bakken flare gas.

Hydrogen	56,654,720	MCF	$ 141,636,799.20
Helium	1,148,406	MCF	$ 459,362,400.00
Nitrogen	2,067,132	MCF	$ 31,006,974.96
Carbon Dioxide	765,604	MCF	$ 3,362,534.17
Total (per year)			$ 635,368,708.33

This does not include the income potential for Natural Gas Liquids (NGLs) such as ethane, propane, butane, or pentane, nor the price potential for sulfur and other saleable by-products; high purity Liquid Nitrogen, for instance.

Even absent the considerable income possible NGLs, it is clear that by harvesting Bakken flare gas from the Williston Basin instead of allowing it to escape up a flare tower, over one half of a billion US dollars in product could be realized. This is a low estimate, as the amount procured for the extracted NGLs would definitely contribute another sizeable dollar amount (Guilford, et al, 2011).

9.3 Proof of Concept

With those caveats in mind, the progression from this point is toward a 'proof-of-concept' small-scale version of the membrane-based process; utilizing captured Bakken-sourced flare gas and processing it through a scaled-down version of the described process.

Given the scalability of membrane units, these will pose no problem in acquisition and inauguration. Scaled down ATR-SMR (Autothermal Reforming - Steam Methane Reforming) plants exist (GTI, 2021) and the manufacturers (Air Liquide Engineering and Construction, 2021; Price and PlugPower, 2016, for example) of these have been contacted.

In either case, there exists room at the University of North Dakota's Drilling and Completion Laboratory ("DRACOLA") for the physical construction and testing of such a preliminary project.

After success of the proof of concept, a field-based Pilot Plant would be the logical next step. Incorporating several actual flowing and flaring Bakken wells or pads, this part of the project would capture the gas and subject it to a full-scale version of the membrane-based plant envisioned in this document. Engineering and economic questions, though many, would be answered by a plant of this size, giving final recommendation for the next logical step.

The final step would be a full-sized full-field production plant. Given the number of unknowns at this point, there are many different possibilities for the collection, helium extraction and SMR plant location.

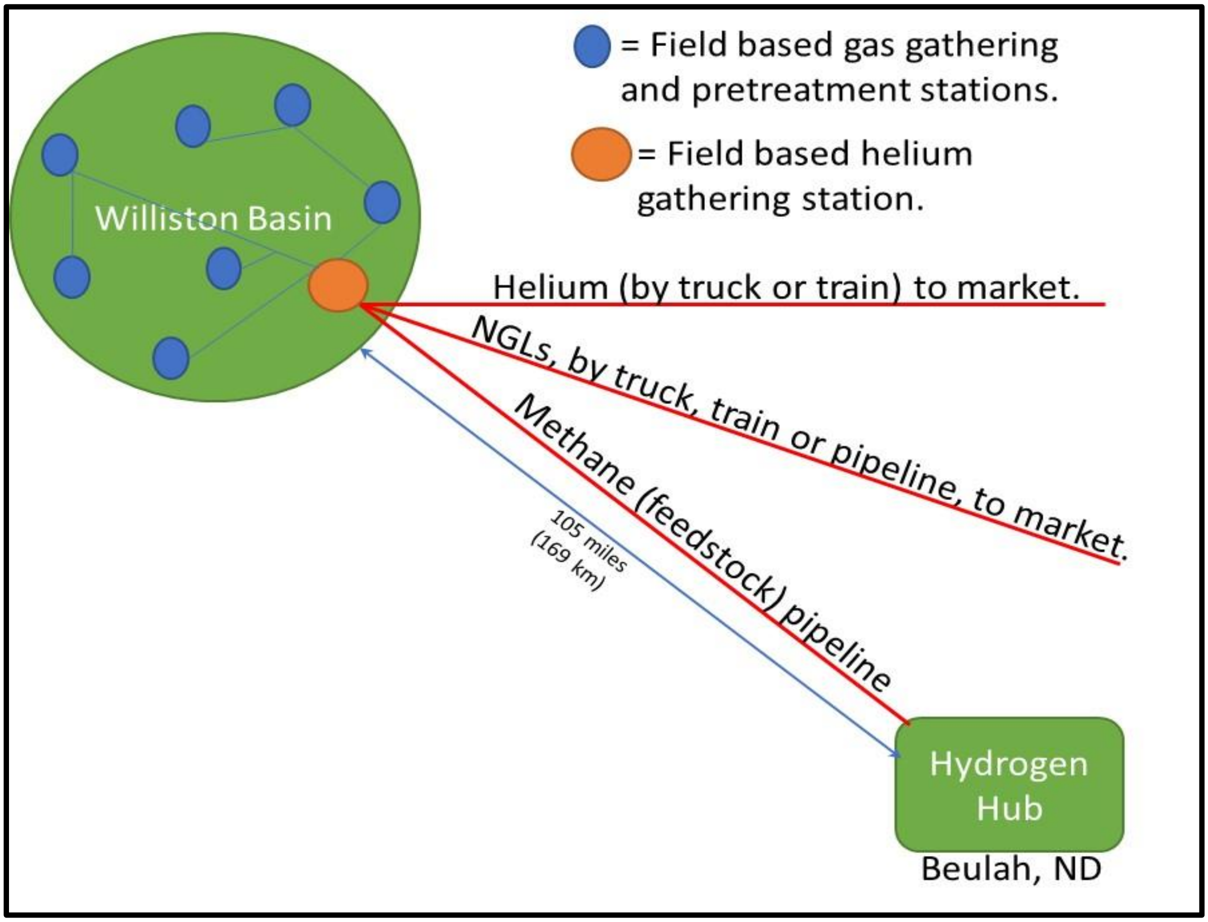

Figure 9.1. One concept of development of Williston Basin NGLs, helium and methane via field-based extraction, and piping of methane feedstock to hydrogen hub in Beulah, ND. Given plasticity of the process, pipeline could ship raw materials to Hydrogen Hub where NGLs and He could be extracted before passing the methane feedstock to the SMR plant.

It could either be entirely field-based, with products trucked or delivered to market via pipeline; or it could have the ATR/SMR portion closer to the final market destination such as the one being built in Beulah, North Dakota, where the heated and compressed CH_4 from the field helium extraction module delivered to the remote ATR-SMR hydrogen plant 105 miles via insulated subsurface pipeline.

That is, of course, only one in an entire gamut of possibilities for future work; but these will have to be addressed if the project continues.

Flaring vs. flare-gas capture: The principal issues & remediations.

Objections to flaring:

1. **Geological –** loss of reservoir energy *and* saleable products (Chowdhury, et al, 2014; Cao, 2014; Loe and Ladehaug, 2012).
2. **Environmental –**releasing large volumes of "greenhouse gases" like methane and carbon dioxide (CO_2) and health-harming volatile organic compounds (VOCs), leading to acid rain, mud, etc. (Shahab-Deljoo, et al, 2023; Franklin, et al, 2019; Ikpeze, et al, 2016; Friedrichs, and Inderwildi, 2013).
3. **Aesthetic –** It's unsightly, ruining the rural ambiance of the Williston Basin for those who live/work/visit there (Wells, 2013; Davis, 2016.)
4. **Political –** lack of key economic incentives to capture and use gas; it is not "economically feasible" to market the gas, distance to markets, etc. (Willyard, 2019; Beebeejaun, 2019, Rabe, et al, 2020).
5. **Operational -** a lack of gas gathering lines or close-in surface processing facilities (Alkaim, and Al_Janabi, 2020; Soltanieh, et al, 2016; Buzco-Guven, and Harriss, 2010).
6. **Economic –** "Unfeasible and costly" to collect and process flared gas; or volumes of gas 'insignificant' and therefore uneconomic to remediate (Romsom, and McPhail, 2021; Emam, 2015).

Keys to flare-gas capture and processing:

- **Geological –** Methane captured for potential re-injection or feedstock; numerous saleable products recovered (Aoun, A.E., Rasouli, V. and Khetib, Y., 2023; Stiglbauer, 2015; Gadhamshetty, et al, 2015; Aoun, A.E., Pu, H., Khetib, Y. and Ameur, M.C.B., 2023).
- **Environmental –** N_2, CO, CO_2, NOx, SOx, and VOCs captured and sequestered from the environment; no longer a threat of acid rain nor an outsized "carbon footprint" (Environmental Defense Fund, 2021; Ravindran, Ruffer, and Sneary, 2016).
- **Aesthetic –** Flaring ceased, returning some of the rural ambiance of the Williston Basin for those who live, work, or visit there (Ikpeze, O.V., Osaro, E. and Ikpeze, N.G., 2016; Mjachina, et al, 2018).
- **Political –** Federal: US Department of Energy providing up to 20 grants/year (~$7MM) to investigate flaring cessation methods. State: North Dakota offers financial incentives to operators who reduce or cease flaring; as opposed to fines for non-compliance (U.S. Environmental Protection Agency, 2021; Rabe, Kaliban, and Englehart, 2020; Ehrman, 2014; Beacom, 2015; Lade, and Rudik, 2020).
- **Operational –** Small scale, small diameter surface gathering lines are inexpensive and can service many wells/pad or pads/surface gathering systems (Wilcox, 2019; International Energy Agency, 2021).
- **Economic –** Government grants offset costs of R&D and implementation, as do governmental incentives. Prices garnered from the recovered He, H_2, CO_2, N_2, S, and CH_4 more than offset implementation costs (Romsom, and McPhail, 2021; Maung, et al, 2012; Hamid, et al, 2020; Thomas, 2017).

For every objection to flare gas capture and refining, there exist economical and practical remedies. These rely upon heavily field-tested "off the shelf" technologies; be they mechanical or membrane based. The process outlined as the modular "Hybrid Approach" of utilizing both mechanical and membrane technology in concert attempts to take advantage of the "best of both worlds". Initial gathering, water removal, and primary compression before gas pre-treatment is a tested and proven economical mechanical technology, as is pre-treatment for the initial removal of CO_2, H_2S, S, Hg (if present) and CO. Once through pre-treatment, the economics will decide on the nature of Natural Gas Liquid extraction, it could be either mechanical or membrane. Both are proven technologies, but final decision would remain on certain field-centric parameters (volumes, need for additional compression, nitrogen rejection, availabilities, etc.). Then helium extraction would be 100% membrane technology, as it's completely automated, has no moving parts, is readily available, environmentally friendly and is nearly infinitely scalable through additional membrane units or larger ID membrane inserts, yielding 99.999% pure Helium. From this process, the remainder is a 99.99% pure CH_4 (methane) feedstock stream, already heated and compressed, for use in Steam Methane Reformation (SMR) hydrogen generation at the Bakken Energy/Mitsubishi Power Americas Inc. Hydrogen Hub in Beulah, North Dakota.

Further Work

1. Sourcing materials for building the 'proof of concept' small-scale model in the UND Drilling and Completions lab.
2. Sourcing economists, economic data, and economic trials for:
    a. Planning/design

   b. Pre-construction
   c. Procurement
   d. Project execution
   e. Construction
   f. Post-construction
   g. Pre-commissioning
   h. Commissioning,
   i. Implementation
   j. Operation
   k. Maintenance
   l. Remote monitoring
   m. Technical support

3. Sourcing Bakken flared gas in quantities sufficient to support a “proof of concept” small- scale project.
4. Pilot plant
5. Full-field plant and trials.

APPENDIX 1

Advantages of Utilizing Bakken Flare Gas for Hydrogen and Helium Extraction

1. Elimination of Bakken flaring in the Williston Basin.
2. Drastic reduction of Bakken oilfield activities “Carbon Footprint” via CCUS.
3. Carbon dioxide can be sold, utilized in oilfield operations, stored and/or sequestered.
4. Gas extraction leads to numerous saleable products (03-2023 prices):

a.	Hydrogen	US\$5.39/kg
b.	Helium	US\$400^{+}/MCFG
c.	Sulfur	US\$40/ton
d.	High purity CO_2	US\$60.16/Bbl
e.	High purity liquid N_2	US\$318.21/Bbl
f.	LNG	US\$9/MMBTU
g.	NGLs	
i.	Ethane US	\$6.22/Bbl
ii.	Propane US	\$28.71/Bbl
iii.	Butane US	\$43.06/Bbl
iv.	Pentane^{+} US	\$55.74/Bbl

5. Hydrogen uses:
   a. Fuel cells to generate electricity,

   b. Clean fuel for modified piston engines,
   c. Clean fuel for turbine engines: trains, aircraft, etc.

6. Helium uses:
   a. Magnetic Resonance Imaging (MRI)
   b. Welding
   c. Cryogenics
   d. Pressure/Purge Systems
   e. Controlled atmospheres
   f. Breathing mixtures
   g. Leak detection
   h. Semiconductors and fiber optics

7. Flare gas to helium *and* hydrogen pathway never before attempted
8. Potential partnerships with UND PE:
   a. Bakken Oil and Gas Operating companies

      i. Continental Resources
      ii. Hess
      iii. Oxy (Occidental Oil)

   b. Aviation – airlines and aircraft providers

      i. Boeing
      ii. Airbus
      iii. Cessna

    c. Oilfield Service Companies
    d. Agricultural sectors
        i. Corn
        ii. Soybeans
    e. Mechanical/Automotive sectors
    f. Brewers/Distillers
    g. Fuel providers

9. Would provide local source uninterruptable feedstock for Mitsubishi-Bakken Energy H_2 Hub.

APPENDIX 2

Glossary of Terminology

Glossary of Terminology Related to Flare Gas Treatment and Recovery

Amine plant: Amine treating is a type of gas sweetening that refers to a group of processes that utilize solvents to remove acid gases, H_2S (Hydrogen Sulfide) and CO_2 (Carbon Dioxide), from process streams. It is commonly used in refineries and gas plants to improve safety, prevent corrosion and meet environmental regulations. A typical Amine Unit consists of an absorber (contactor) and regenerator (stripper) along with their ancillary equipment. A process gas stream is first passed through the absorber, where H_2S and CO_2 are removed by the “lean” solvent. The now “rich” solvent is sent to the regenerator where the acid gases are removed and either sent to flare or a Sulfur Recovery Unit (SRU).

Butane: An alkane with the formula C_4H_{10}. Butane is a gas at room temperature and atmospheric pressure. Butane is a highly flammable, colorless, easily liquefied gas that quickly vaporizes at room temperature.

Butane Splitter: An n-butane/isobutane splitter is operated by compressing the isobutane overhead to increase its condensing temperature, using the compressed overhead to heat bottoms in a reboiler, which is operated to condense the overhead and cooling the condensed overhead to a temperature no lower than the temperature on the top tray of the splitter and no higher than 20° F. above the temperature on the top tray, whereby the throughput of the splitter is increased by 10 to 20%.

Carbon Capture, Use, and Storage (CCUS): Carbon capture, use, and storage (CCUS) is the process of capturing carbon dioxide (CO_2) emissions from fossil power generation and industrial processes for storage deep underground or re-use.

Cryogenics: The branches of engineering that involve the study of very low temperatures, how to produce them, and how materials behave at those temperatures.

Debutanizer: A type of fractional distillation column used to recover light gases (C1-C4) and Liquefied Petroleum Gas (LPG) from the overhead distillate before producing light naphtha during the refining process. Distillation is the process of heating a liquid to vapor and condensing the vapors back to liquid in order to separate or purify the liquid. The main equipment of this process consists of a distillation column, reboiler and condenser. The debutanizer condenser condenses the overhead vapor and the debutanizer overhead pressure control valves controls the overhead system.

Deethanizer: A continuously operated distillation column used for the removal of ethane as distillate from a mixed feed of light hydrocarbons. Any methane also leaves the top of the column along with the ethane while heavier components leave the bottom.

Demethanizer: the natural gas processing unit that separates methane rich residue gas from the heavier hydrocarbons (e.g., ethane, propane, butane, pentane-plus) in the feed natural gas stream.

Depropanizer: The fractionating column in a natural gasoline plant in which propane and lighter components are removed overhead. The gas stream remaining is depropanized.

Ethane: an organic chemical compound with chemical formula C_2H_6. At standard temperature and pressure, ethane is a colorless, odorless gas. Like many hydrocarbons, ethane is isolated on an industrial scale from natural gas and as a petrochemical by-product of petroleum refining.

Flare: A tall stack equipped with burners used as a safety device at wellheads, refining facilities, gas processing plants, and chemical plants. Flares are used for the combustion and disposal of combustible gases. The gases are piped to a remote, usually elevated, location and burned in an open flame in the open air using a specially designed burner tip, auxiliary fuel, and steam or air. Combustible gases are flared most often due to emergency relief, overpressure, process upsets, startups, shutdowns, and other operational safety reasons. Natural gas that is uneconomical for sale is also flared. Often natural gas is flared as a result of the unavailability of a method for transporting such gas to markets. (Source: U.S. Energy Information Administration 2019)

Free Water Knockout (FWKO): Free water is water produced with crude oil that is not emulsified. Free water will generally settle out of the oil emulsion mixture if given time. A free water knockout (commonly abbreviated as FWKO) is an oil and gas production vessel that separates the produced oil emulsion into its various elements.

Gas compression: Gas compression is done to increase the pressure of the gas; this is accompanied by change of state of the gas which means change in temperature and volume of a quanta of gas going under compression. If the pressure of gas is raised from P1 to P2, the compression ratio for this process is defined as, P1/P2. The physical state of gas will undergo change depending on the process, whether it is isothermal, adiabatic or typically polytropic.

Gas flaring (effects of): Gas flaring can potentially introduce toxic pollutants such as sulfur dioxide (SO_2) into the atmosphere. This has been claimed by some to lead to environmental problems such as acid rain, as well as the generation of greenhouse gases which contribute to a supposed global climate change.

Gas sweetening unit: Gas sweetening is a process that has to be executed to remove hydrogen sulphide (H_2S) from natural gasses. Gas sweetening is sometimes referred to as amine treating. Amine treating can be used in refineries, petrochemical plants, natural gas processing plants and other industries. In oil refineries or chemical processing plants it is more referred to as gas sweetening. This is because they result in a product which no longer has the sour and foul odors of H_2S. As amine treating does not recover the sulphur in elemental form it must be followed by a sulphur recovery step.

"Global warming" vs. Climate change: Global warming generally refers to the supposed 'observed' warming of the planet due to human-caused (anthropogenic) greenhouse gas emissions. Climate change generally refers to all of the various natural geologically long-term changes in our climate; including precipitation, temperature, and global wind patterns.

Glycol dehydrator: any device in which a liquid glycol absorbent (including, ethylene glycol, diethylene glycol, or triethylene glycol) directly contacts a natural gas stream and absorbs water. A unit used to remove minute water particles from natural gas if dehydration was not attained using separators. A glycol dehydrator unit is usually composed of an absorber and a reboiler. The wet gas enters at the bottom of the absorber. As the wet gas percolates upward, it releases its water into the glycol solution and dry gas is obtained at the top of the absorber. When the glycol solution becomes saturated with water, the glycol solution is pumped through a reboiler, also called a re-concentrator, which boils the glycol-water mixture and separates the glycol from the water. After separation, the glycol can return to the absorber to contact additional wet gas.

Greenhouse gas: A greenhouse gas is a gas that absorbs and emits radiant energy within the thermal infrared range, causing the greenhouse effect. The primary greenhouse gases in Earth's atmosphere are water vapor, carbon dioxide, methane, nitrous oxide, and ozone.

Helium Extraction from Natural Gas: For the extraction of helium, all other impurities and contaminants must be removed in accordance with industry standards. The process of extracting and producing liquefied helium from natural gas consist of up to seven steps:

- Natural gas processing/pre-treatment (removal of hydrogen sulphide, carbon dioxide, water and heavy metals);
- Natural gas refrigeration (removal of heavier hydrocarbons if any) and liquefaction (production of liquefied natural gas);
- Nitrogen rejection (removal of nitrogen);
- Helium recovery from natural gas; via membranes, PSA, or cryogenics;
- Helium upgrading;
- Helium purification; and
- Helium liquefaction.

Liquid Natural Gas: Liquefied natural gas (LNG) is natural gas that has been cooled to a liquid state (liquefied), at about -260° Fahrenheit, for shipping and storage. The volume of natural gas in its liquid state is about 600 times smaller than its volume in its gaseous state in a natural gas pipeline.

Membrane gas separation: Gas mixtures can be effectively separated by synthetic membranes made from polymers such as polyamide or cellulose acetate, or from natural or synthetic ceramic materials. Membrane materials have expanded into the realm of silica, zeolites, metal-organic frameworks, and perovskites due to their strong thermal and chemical resistance as well as high tunability (ability to be modified and functionalized), leading to increased permeability and selectivity. Membranes can be used for separating gas mixtures where they act as a permeable barrier through which different compounds move across at different rates or not move at all. The membranes can be nanoporous, polymer, etc. and the gas molecules penetrate according to their size, diffusivity, or solubility.

Merox process: A proprietary technology that selectively sweetens petroleum products by oxidizing the foul-smelling mercaptans into the sweeter disulfides which remain in the product, leaving the total sulfur content the same.

Methane: The principal constituent of natural gas; the simplest hydrocarbon molecule, containing one carbon atom and four hydrogen atoms.

Molecular sieve: A material with pores (very small holes - nanopores) of uniform size. These pore diameters are similar in size to small molecules, and thus large molecules cannot enter or be adsorbed, while smaller molecules can. As a mixture of molecules migrate through the stationary bed of porous, semi-solid substance referred to as a sieve (or matrix), the components of highest molecular weight (which are unable to pass into the molecular pores) leave the bed first, followed by successively smaller molecules.

Natural gas liquids (NGL): Natural gas liquids (NGL) are components of natural gas that are separated from the gas state in the form of liquids. This separation occurs in a field facility or a gas processing plant through absorption, condensation, or other methods.

There are several types of natural gas liquids and many different applications for NGL products.

Natural Gas Liquids plant: An NGL plant consists of a series of fractionators whose purpose is to separate a mixture of light hydrocarbons into various pure products. The NGL Plant typically consists of a demethanizer, a deethanizer, a depropanizer, a debutanizer, and, typically, a butane splitter. Other arrangements of columns are possible for NGL Plants and also parallel columns may be present for higher plant processing capacity.

Natural gas processing: Consists of separating all of the various hydrocarbons and fluids from the pure natural gas, to produce what is known as ‘pipeline quality’ dry natural gas. Major transportation pipelines usually impose restrictions on the make-up of the natural gas that is allowed into the pipeline.

Nitrogen Rejection Unit: A nitrogen rejection unit (NRU) selectively removes nitrogen from a gas. The name can be applied to any system that removes nitrogen from natural gas.

Pressure swing adsorption (PSA): is a technique used to separate some gas species from a mixture of gases (typically air) under pressure according to the species’ molecular characteristics and affinity for an adsorbent material. It operates at near-ambient temperature and significantly differs from the cryogenic distillation commonly used to separate gases. Selective adsorbent materials (e.g., zeolites, (aka molecular sieves), activated carbon, etc.) are used as trapping material, preferentially adsorbing the target gas species at high pressure. The process then swings to low pressure to desorb the adsorbed gas.

Processing plant: A facility designed to separate or process hydrocarbons through chemical, physical or physical-chemical procedures in order to produce marketable hydrocarbons and other (e.g., sulphur) products.

Propane: a three-carbon alkane with the molecular formula C_3H_8. It is a gas at standard temperature and pressure, but compressible to a transportable liquid.

Steam methane reforming (SMR): Most hydrogen produced today in the United States is made via steam-methane reforming, a mature production process in which high-temperature steam (700°C–1,000°C) is used to produce hydrogen from a methane source, such as natural gas. In steam-methane reforming, methane reacts with steam under 3–25 bar (43.5 - 362.5 psi) pressure in the presence of a catalyst to produce hydrogen, carbon monoxide, and carbon dioxide. Steam reforming is endothermic—that is, heat must be supplied to the process for the reaction to proceed. Subsequently, in what is called the “water-gas shift (WGS) reaction,” the carbon monoxide and steam are reacted using a catalyst to produce carbon dioxide and more hydrogen. In a final process step called “pressure-swing adsorption,” carbon dioxide and other impurities are removed from the gas stream, leaving essentially pure hydrogen.

The Colors of Hydrogen: There are different ‘kinds’ of hydrogen. The diverse methods of producing the gas emit dissimilar amounts of CO_2. Depending on the production methods, hydrogen can be green, turquoise, blue or grey. For hydrogen to support climate targets, it is essential that it be generated in a climate-neutral manner, without causing additional CO_2 emissions.

- **Black (Brown) hydrogen**: Black or brown hydrogen is produced from coal. The black and brown colors refer to the type bituminous (black) and lignite (brown) coal. The gasification of coal is a method used to produce hydrogen. However, it is a very polluting process, and CO_2 and carbon monoxide are produced as by-products and released to the atmosphere.

- **Blue hydrogen:** blue hydrogen is produced by what is known as natural gas steam reforming, meaning the separation of natural gas into hydrogen and CO_2. The CO_2 is not released into the atmosphere afterwards but is directly stored (CCUS = carbon capture, use, and storage).
- **Green hydrogen**: green hydrogen is produced by the electrolysis of water, meaning the breakdown of water molecules into the two individual elements hydrogen and oxygen. Only electricity from renewable energies is used. This way no CO_2 is produced, making the generated hydrogen climate neutral.
- **Grey hydrogen**: grey hydrogen is obtained by steam reforming fossil fuels such as coal or natural gas without CCUS.
- **Pink hydrogen:** pink hydrogen is generated through electrolysis of water by using electricity from a nuclear power plant.
- **Purple hydrogen**: purple hydrogen is made though using nuclear power and heat through combined chemo thermal electrolysis splitting of water.
- **Red hydrogen**: red hydrogen is produced through the high-temperature catalytic splitting of water using nuclear power thermal as an energy source.
- **Turquoise hydrogen:** turquoise hydrogen is created when natural gas is broken down with the help of methane pyrolysis into hydrogen and solid carbon.
- **White hydrogen**: white hydrogen refers to naturally occurring hydrogen. Needless to say, it’s rather rare.

Turboexpander: Also referred to as a turbo-expander or an expansion turbine, is a centrifugal or axial flow turbine through which a high-pressure gas is expanded to produce work that is often used to drive a compressor. Because work is extracted from the expanding high-pressure gas, the expansion is approximated by an isentropic process and the low-pressure exhaust gas from the turbine is at a very low temperature, −150 °C or less depending upon the operating pressure and gas properties

APPENDIX 3

Helium recovery from Bakken Flare Gas: Economic Model

Objective: The project is set to recover 88.3% of the helium found in the associated gas with a targeted purity of 99.99% by volume. The process would have a total inlet flow rate of 69,600 lbs./hr. (37.18 MCFGPD) associated gas.

Process: The recommended process uses a system of passive selective membranes followed by pressure swing adsorption (PSA) steps. The project calls for a total capital investment of $1.7 million ± $0.6 million and an NPV@18% of $6.0 million ± $2.4 million. The project has a lifespan of 20 years and an operating factor of 95%. The discounted cash flow rate of return (DCFROR) for the recommended process is 34%. Funding Request: $3,100,000.00

Table A3.1. Comparison of Bakken Helium Plant v. other world helium plants.

AD = Canadian Dollars, QAR = Qatari Rials, AUD = Australian Dollars, USD = United States Dollars

PLANT	YEAR	Project cost	Project cost (M$USD)	Capacity (tons/ annum)	Capacity (MCF/annum)	$USD/ MCF He
Skikda	2003	87M USD	87,000,000	2,824	545,904	159
Qatar, He-1	2005	115M USD	115,000,000	3,106	600,417	192
Darwin	2009	50M AUD	33,300,000	913	176,491	189
Qatar, He-2	2013	1000M QAR	274,800,000	6,529	1,262,112	218
Doe Canyon	2015	134M USD	134,000,000	1,082	209,160	641
Mankota	2016	12M CAD	8,900,000	188	18,171	490
Ningxia	2020	5.7M USD	5,700,000	20	3,866	1,474
Qatar, He-3	2020	600M QAR	164,800,000	2,000	386,617	426
Battle Creek	2021	32M CAD	23,700,000	275	36,342	652
Bakken	2023	3.1M USD	3,100,000	130	25,000	124

McElroy, L., G. Xiao, R. Weh, and E. F. May, 2022, A case study of helium recovery from Australian natural gas: Case Studies in Chemical and Environmental Engineering, v. 5, no. January, p. 100200, doi:10.1016/j.cscee.2022.100200.

Comparing nine relatively recent helium plants around the world (Table A3.1), it can be shown that the processes elucidated in this dissertation are the most attractive economically, even when contrasted with such voluminous plants as the ones noted in Qatar. This is due to the fact that the proposed Bakken Plant in the Williston Basin capitalizes upon a free source of gas, i.e., gas that was to be flared, as well as the novel use of passive, selective membranes for helium extraction. Only two of the other plants shown here utilize membrane technology, Mankota and Battle Creek, but this is tasked for sorting wellhead natural gas and nitrogen, as well as helium. The remainder of the plants utilize distillation of LNG (liquid natural gas, CH_4) end-flash gas using auto-refrigeration.

Given parameters for the Williston Basin Bakken Plant are:

- Price of Helium: USD$400/MCF (Price Crude He., 03/2023)
- Plant output of Helium: 25,000 MCF/Yr.
- Operating costs: 0.385 of revenue

Table A3.2. Product List for Recommended Process

Description	**Amount**	**Units**
Helium Product	**30.3**	**lbs/hr**
Components		
Helium	30.3	lb/hr
Methane	Trace	lb/hr
Nitrogen	Trace	lb/hr
Ethane	0	lb/hr

Methane Product	**69,600**	**lbs/hr**
Components		
Methane	67300	lb/hr
Ethane	1930	lb/hr
Nitrogen	360	lb/hr
Helium	3.95	lb/hr

Table A3.3. Revenue for Bakken Helium Plant

BAKKEN			Revenue (He* price)	Operating Costs (0.385 of revenue)	Gross Profit (=h12-I12)	Depreciation	*Overall*	Federal Taxes (US = 21%) (=J12*0.21)	Net Profit (=l12-m12)	*Present Value*
Evaluation	Helium	Helium price					*Taxable*			*@ HR &*
Year	MCF/yr	$/MCFG					*Profit*			*Evaluation Date*
							(=j12-k12)			
1	25000	400	$10,000,000	$3,850,000	$6,150,000	$0	$6,150,000	$1,291,500	$4,858,500	$4,117,373
2	25000	400	$10,000,000	$3,850,000	$6,150,000	$0	$6,150,000	$1,291,500	$4,858,500	$3,489,299
3	25000	400	$10,000,000	$3,850,000	$6,150,000	$0	$6,150,000	$1,291,500	$4,858,500	$2,957,033
4	25000	400	$10,000,000	$3,850,000	$6,150,000	$0	$6,150,000	$1,291,500	$4,858,500	$2,505,960
5	25000	400	$10,000,000	$3,850,000	$6,150,000	$0	$6,150,000	$1,291,500	$4,858,500	$2,123,695
6	25000	400	$10,000,000	$3,850,000	$6,150,000	$0	$6,150,000	$1,291,500	$4,858,500	$1,799,742
7	25000	400	$10,000,000	$3,850,000	$6,150,000	$0	$6,150,000	$1,291,500	$4,858,500	$1,525,205
8	25000	400	$10,000,000	$3,850,000	$6,150,000	$0	$6,150,000	$1,291,500	$4,858,500	$1,292,546
9	25000	400	$10,000,000	$3,850,000	$6,150,000	$0	$6,150,000	$1,291,500	$4,858,500	$1,095,378
10	25000	400	$10,000,000	$3,850,000	$6,150,000	$0	$6,150,000	$1,291,500	$4,858,500	$928,287
11	25000	400	$10,000,000	$3,850,000	$6,150,000	$0	$6,150,000	$1,291,500	$4,858,500	$786,684
12	25000	400	$10,000,000	$3,850,000	$6,150,000	$0	$6,150,000	$1,291,500	$4,858,500	$666,681
13	25000	400	$10,000,000	$3,850,000	$6,150,000	$0	$6,150,000	$1,291,500	$4,858,500	$564,984
14	25000	400	$10,000,000	$3,850,000	$6,150,000	$0	$6,150,000	$1,291,500	$4,858,500	$478,800
15	25000	400	$10,000,000	$3,850,000	$6,150,000	$0	$6,150,000	$1,291,500	$4,858,500	$405,763
16	25000	400	$10,000,000	$3,850,000	$6,150,000	$0	$6,150,000	$1,291,500	$4,858,500	$343,867
17	25000	400	$10,000,000	$3,850,000	$6,150,000	$0	$6,150,000	$1,291,500	$4,858,500	$291,412
18	25000	400	$10,000,000	$3,850,000	$6,150,000	$0	$6,150,000	$1,291,500	$4,858,500	$246,960
19	25000	400	$10,000,000	$3,850,000	$6,150,000	$0	$6,150,000	$1,291,500	$4,858,500	$209,288
20	25000	400	$10,000,000	$3,850,000	$6,150,000	$0	$6,150,000	$1,291,500	$4,858,500	$177,363
Basis Date				Evaluation Date		Hurdle Rate	0.18		NPV@18% =	$26,006,319

Once the Helium has been isolated from the methane stream, which is destined for use to create Hydrogen via Steam Methane Reformation (SMR) at the North Dakota Hydrogen Hub in Beulah, ND, the helium has to be shipped to market.

If it is desired to extract the Helium near the Hydrogen Hub, the treated (de-watered, deaminated, sweetened and denitrogenized) but not de-heliumed gas stream, could be transported via pipeline. The 4.5” ID pipeline length would be approximately 110 miles (177 Km) from Williston to Beulah, ND, at a cost of USD$5,067,055.

Economics of Helium transport

1. Costs for 110 mile 4.5” ID pipeline: Cost (dia, length) = [8,417(dia) + 7,324] (length) + 95,000 where (dia) is in inches, (length) is in miles, and cost is in dollars.

[8,417(4.5) + 7,324] (110) + 95,000 = $5,067,055

Parker, N., n.d., Using Natural Gas Transmission Pipeline Costs to Estimate Hydrogen Pipeline Costs: Institute of Transportation Studies, v. 1, no. 1, p. 85.

Or, if the helium was to be extracted in the field, it could be shipped to market via overland trucking, or by railway. Breakdowns for transport are as follows:

2. Cost for trucking:
    a. Bulk liquid: Iso containers: USD$350/MCF
    b. Bulk gas: Tube trailers: USD$225/MCF
    c. Packaged: Gas HP containers: USD$160/MCF
    d. Packaged: Liquid Dewars: USD$275/MCF

J. R. Campbell & Associates, I., 2013, Determination of Fair Market Value Pricing of Crude Helium Final Report: 94 p.

3. Cost for railroad transport:
    a. UNNO 1046: Helium, compressed - An inert gas. Lighter than air:
        i. Rail tank car unit cost: USD$1,584
        ii. Overall Cost per Ton Mile: USD$0.064
        iii. Cost per MCFG: USD$0.64
    b. UNNO 1963: Helium, refrigerated liquid - Liquefied inert gas and lighter than air.
        i. Rail tank car unit cost: USD$1,584
        ii. Overall Cost per Ton Mile: USD$0.097
        iii. Cost per MCFG: USD$0.97

Hermiyanty, Wandira Ayu Bertin, D. S., 2017, Risk Assessment of Surface Transport of Liquid Natural Gas and other Gasses: Journal of Chemical Information and Modeling, v. 8, no. 9, p. 1–58.

Conclusion

It is estimably economic to extract from Bakken flare gas elemental helium by selective passive membranes and condensation by Pressure Swing Adsorption as noted in this dissertation. Given the current price of crude helium at USD$400 and its estimation to rise by approximately USD$$100^{+}$/annum for the foreseeable future, the project will become even more attractive to operators in the Williston Basin, especially since it will lead to a reduction or cessation of flaring; something politically much desired.

However, although helium alone would carry the project economics, there are numerous other materials that will be isolated and concentrated for sale. These include:

1. High purity CO2	US$60.16/BBL
2. High purity liquid N2	US$318.00/BBL
3. LNG (Methane)	US$29.74/MMBTU
4. NGLs	
a. Ethane	US$6.22/BBL
b. Propane	US$28.71/BBL
c. Butane	US$43.06/BBL
d. Pentane+	US$59.74/BBL

Of particular note is the question of CO_2 capture, a very hot topic in both the environmental and industrial sectors. This high-purity commodity can be sold in many markets, from fabrication to food, though use in the oil industry would seem the most logical.

Carbon dioxide has myriad uses in the oilfield, from an additive in hydraulic fracturing, to adding chemical and mechanical energy to acids, to EOR (Enhanced Oil Recovery) by enhancing reservoir pressure through CO_2 flooding, to its use as a cement additive used for reducing the weight of certain oilfield cements.

In every case, the CO_2 is injected downhole, never to return; as it is sequestered.

Capturing and forever isolating CO_2, plus generating seven further saleable products from an erstwhile oilfield waste product seems a sound scientific, economic, and environmental process.

Bakken gas process schematics

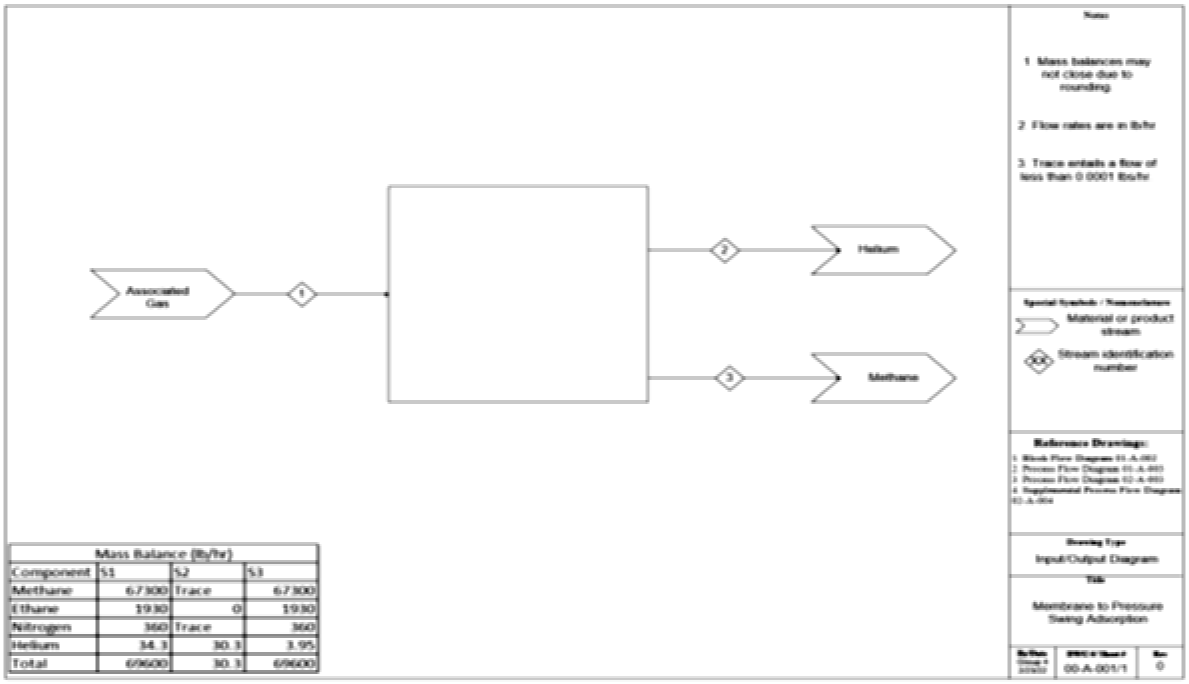

Mass Balance (lb/hr)

Component	S1	S2	S3
Methane	67300	Trace	67300
Ethane	1930	0	1930
Nitrogen	360	Trace	360
Helium	34.3	30.3	3.95
Total	69600	30.3	69600

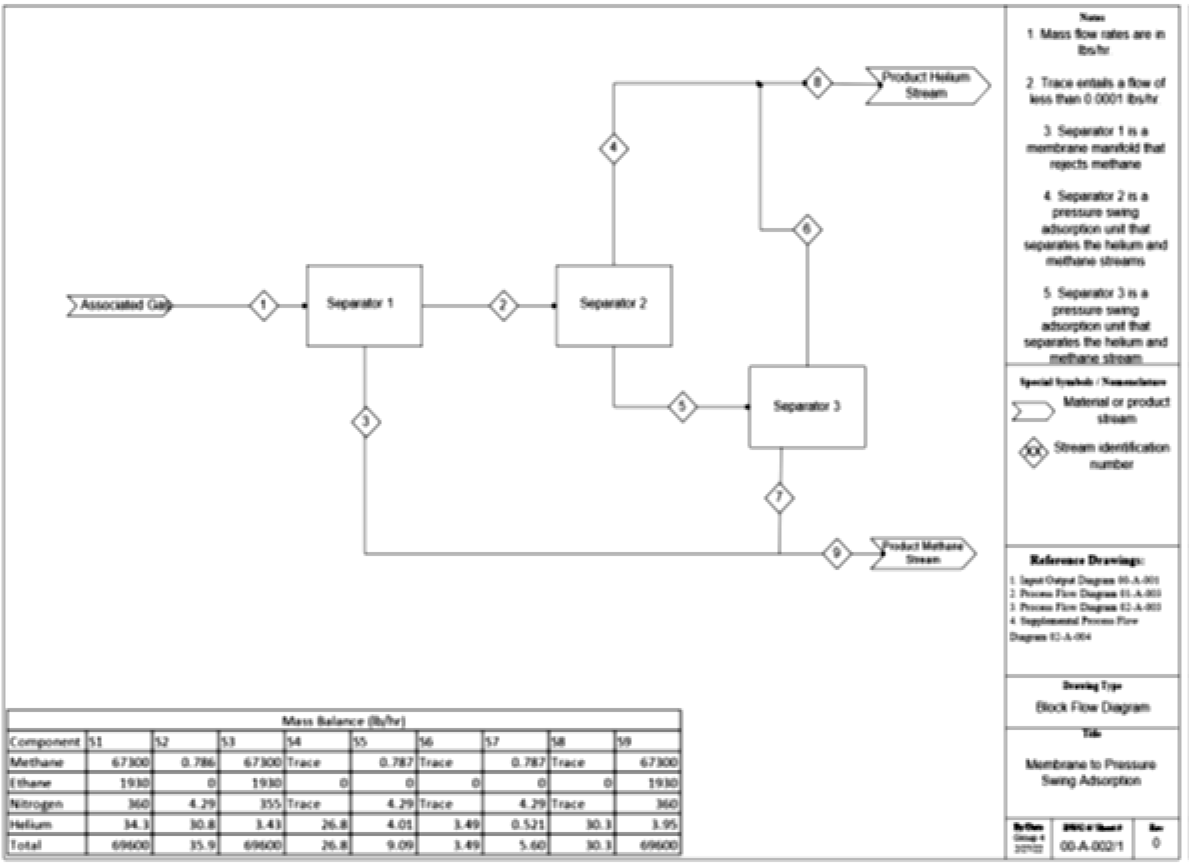

Notes

1. Mass flow rates are in lbs/hr

2. Trace entails a flow of less than 0.0001 lbs/hr

3. Separator 1 is a membrane manifold that rejects methane

4. Separator 2 is a pressure swing adsorption unit that separates the helium and methane streams

5. Separator 3 is a pressure swing adsorption unit that separates the helium and methane stream

Reference Drawings:

1. Input Output Diagram 00-A-001
2. Process Flow Diagram 01-A-003
3. Process Flow Diagram 02-A-003
4. Supplemental Process Flow Diagram 02-A-004

Drawing Type

Block Flow Diagram

Title

Membrane to Pressure Swing Adsorption

Mass Balance (lb/hr)

Component	S1	S2	S3	S4	S5	S6	S7	S8	S9
Methane	67300	0.786	67300	Trace	0.787	Trace	0.787	Trace	67300
Ethane	1930	0	1930	0	0	0	0	0	1930
Nitrogen	360	4.29	355	Trace	4.29	Trace	4.29	Trace	360
Helium	34.3	30.8	3.43	26.8	4.01	3.49	0.521	30.3	3.95
Total	69600	35.9	69600	26.8	9.09	3.49	5.60	30.3	69600

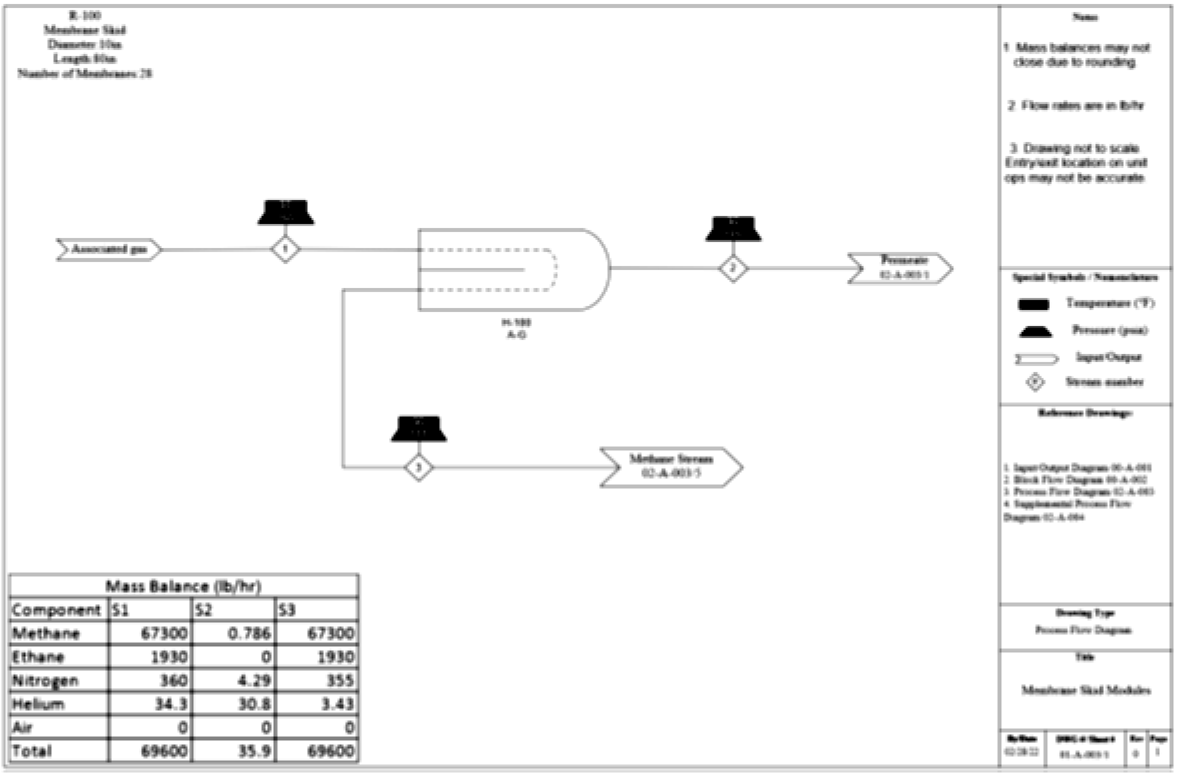

Notes

1. Mass balances may not close due to rounding

2. Flow rates are in lb/hr

3. Drawing not to scale. Entry/exit location on unit ops may not be accurate

Reference Drawings:

1. Input Output Diagram 00-A-001
2. Block Flow Diagram 00-A-002
3. Process Flow Diagram 02-A-003
4. Supplemental Process Flow Diagram 02-A-004

Drawing Type

Process Flow Diagram

Title

Membrane Skid Modules

Mass Balance (lb/hr)

Component	S1	S2	S3
Methane	67300	0.786	67300
Ethane	1930	0	1930
Nitrogen	360	4.29	355
Helium	34.3	30.8	3.43
Air	0	0	0
Total	69600	35.9	69600

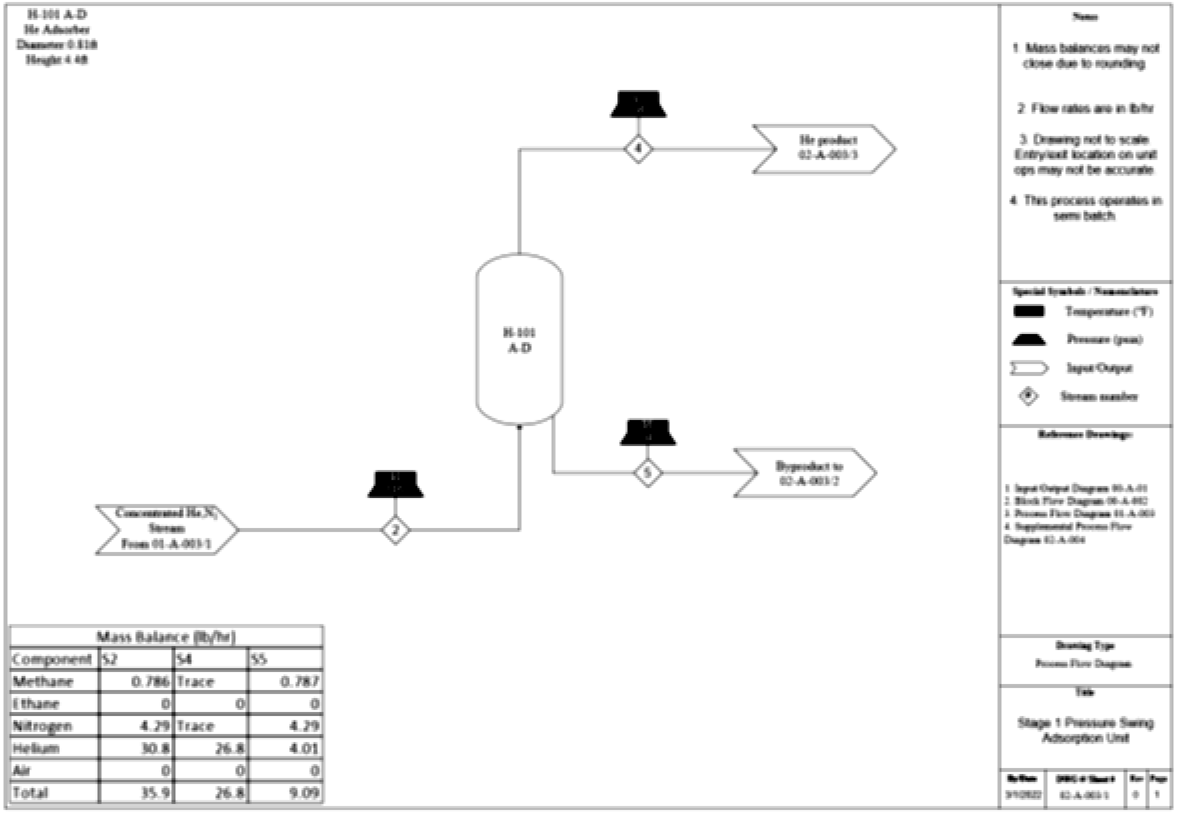

Mass Balance (lb/hr)			
Component	S2	S4	S5
Methane	0.786	Trace	0.787
Ethane	0	0	0
Nitrogen	4.29	Trace	4.29
Helium	30.8	26.8	4.01
Air	0	0	0
Total	35.9	26.8	9.09

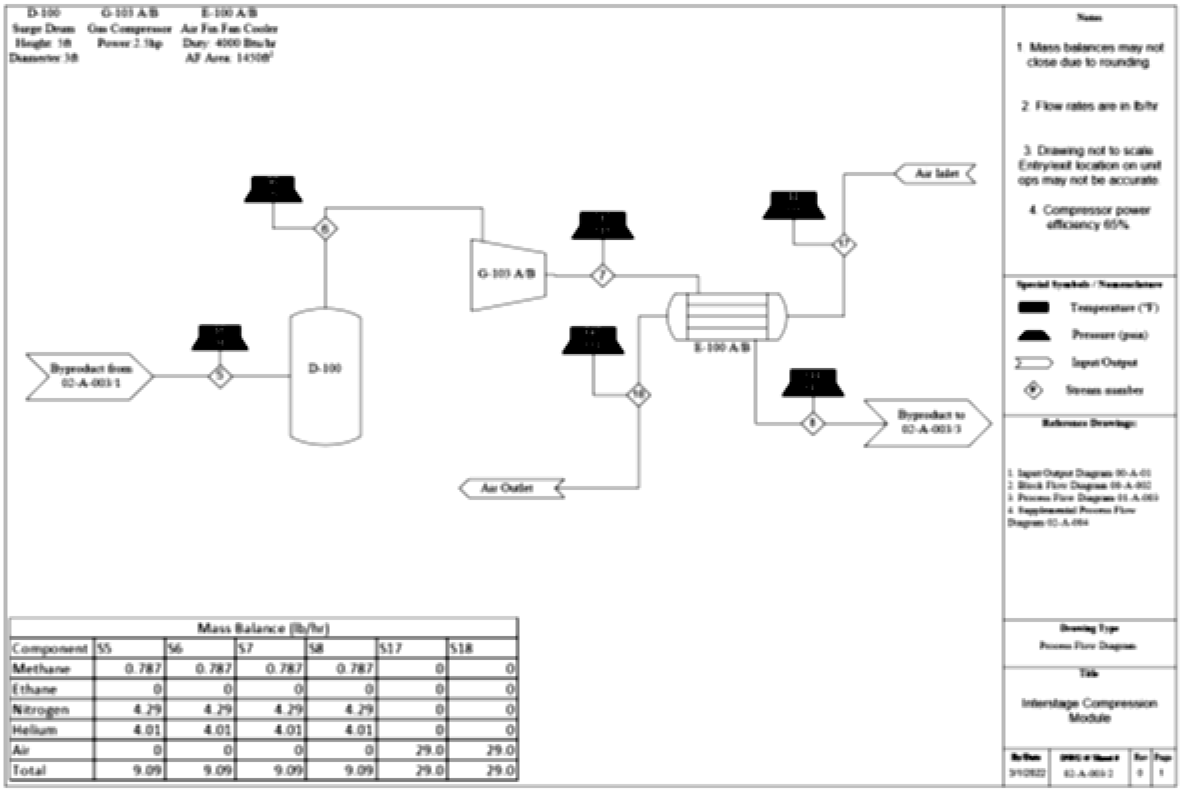

Mass Balance (lb/hr)						
Component	S5	S6	S7	S8	S17	S18
Methane	0.787	0.787	0.787	0.787	0	0
Ethane	0	0	0	0	0	0
Nitrogen	4.29	4.29	4.29	4.29	0	0
Helium	4.01	4.01	4.01	4.01	0	0
Air	0	0	0	0	29.0	29.0
Total	9.09	9.09	9.09	9.09	29.0	29.0

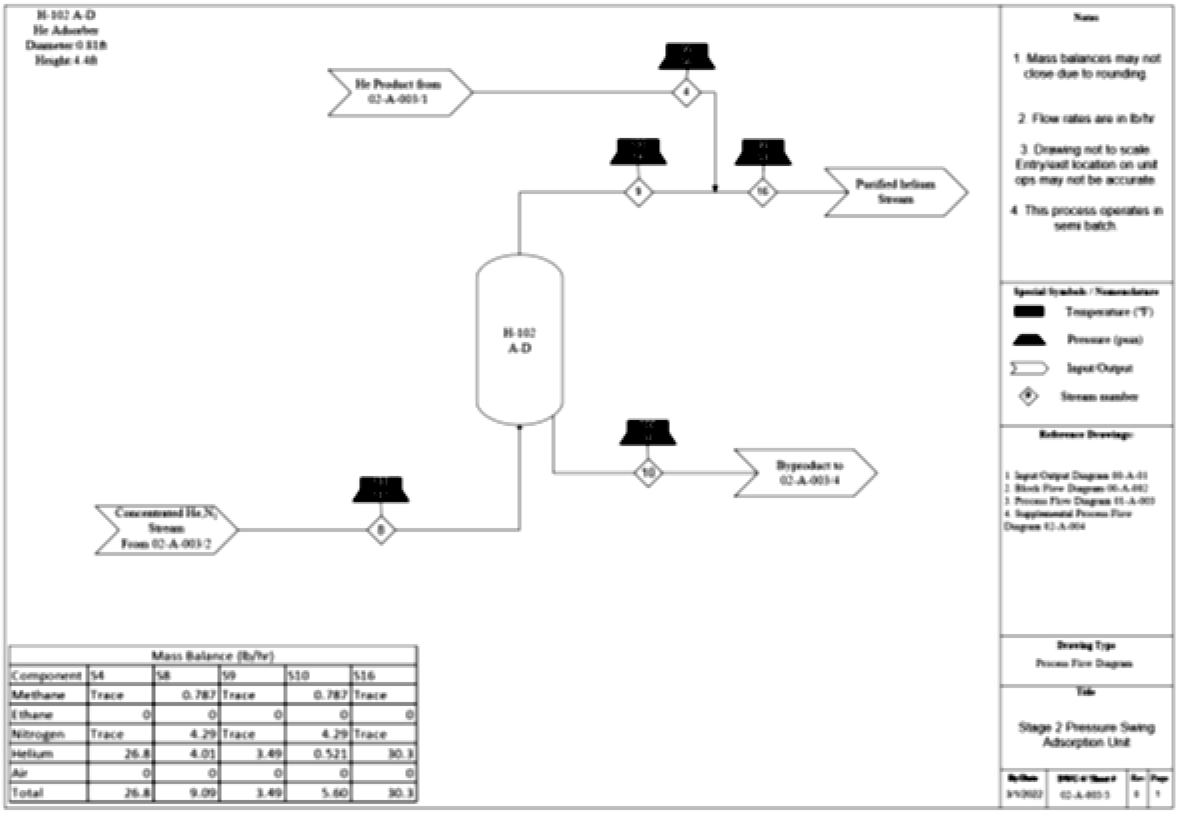

Mass Balance (lb/hr)					
Component	S4	S8	S9	S10	S16
Methane	Trace	0.787	Trace	0.787	Trace
Ethane	0	0	0	0	0
Nitrogen	Trace	4.29	Trace	4.29	Trace
Helium	26.8	4.01	3.49	0.521	30.3
Air	0	0	0	0	0
Total	26.8	9.09	3.49	5.60	30.3

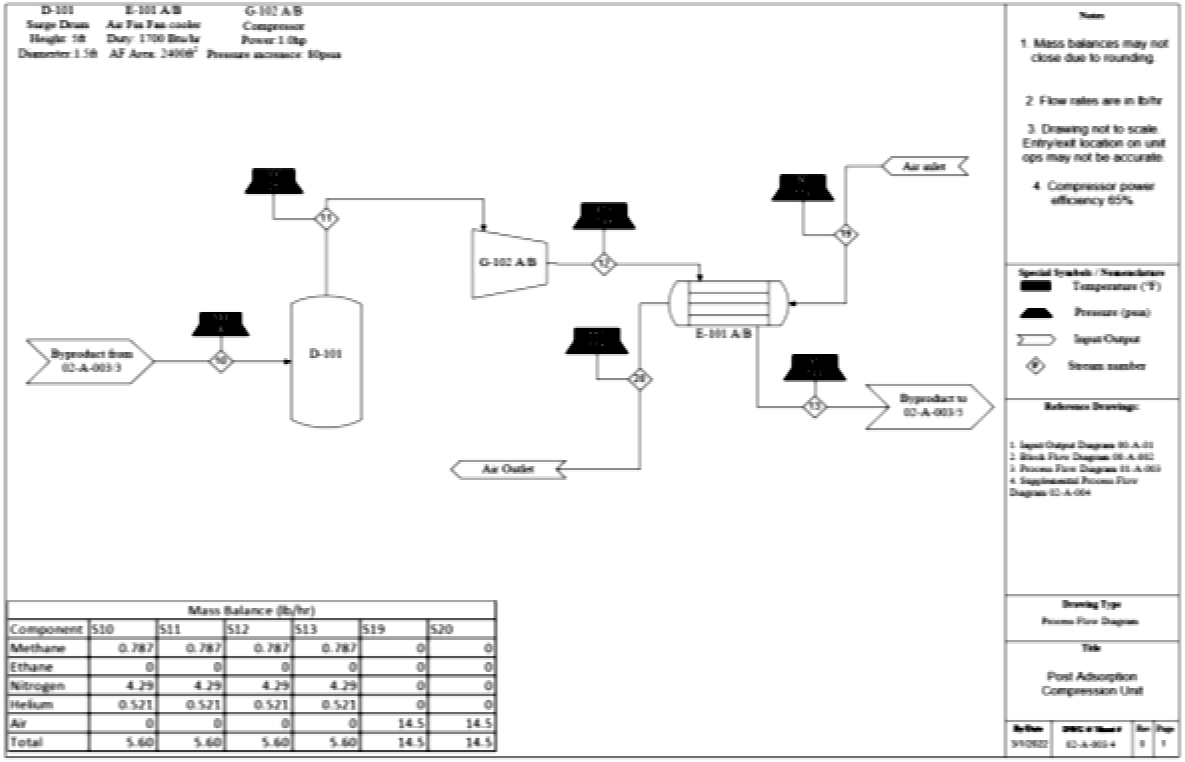

Mass Balance (lb/hr)						
Component	S10	S11	S12	S13	S19	S20
Methane	0.787	0.787	0.787	0.787	0	0
Ethane	0	0	0	0	0	0
Nitrogen	4.29	4.29	4.29	4.29	0	0
Helium	0.521	0.521	0.521	0.521	0	0
Air	0	0	0	0	14.5	14.5
Total	5.60	5.60	5.60	5.60	14.5	14.5

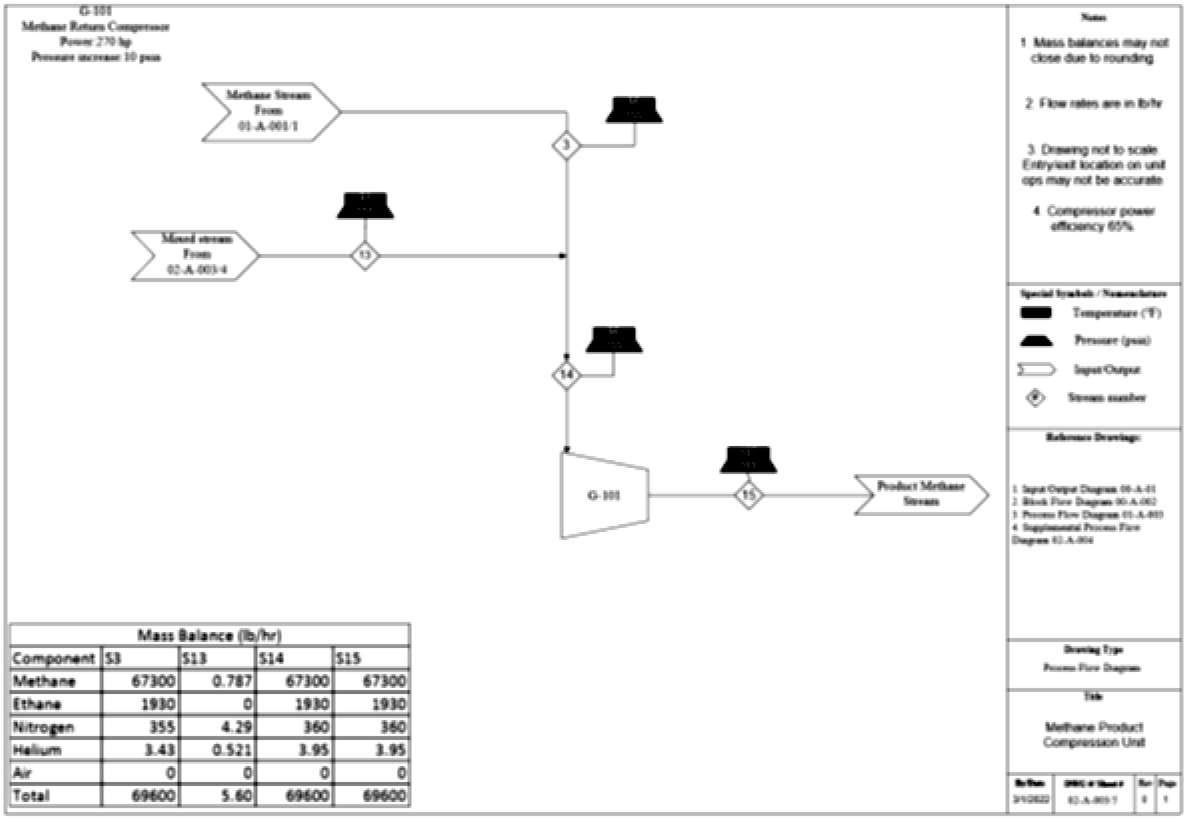

Mass Balance (lb/hr)				
Component	S3	S13	S14	S15
Methane	67300	0.787	67300	67300
Ethane	1930	0	1930	1930
Nitrogen	355	4.29	360	360
Helium	3.43	0.521	3.95	3.95
Air	0	0	0	0
Total	69600	5.60	69600	69600

Notes

1. Mass balances may not close due to rounding
2. Flow rates are in lb/hr
3. Drawing not to scale Entry/exit location on unit ops may not be accurate
4. Compressor power efficiency 65%

Reference Drawings

1 Input/Output Diagram 00-A-01
2 Block Flow Diagram 00-A-002
3 Process Flow Diagram 01-A-003
4 Supplemental Process Flow Diagram 02-A-004

Drawing Type

Process Flow Diagram

Title

Methane Product Compression Unit

By/Date	DWG # Sheet #	Rev	Page
3/1/2022	02-A-003-[illegible]	0	1

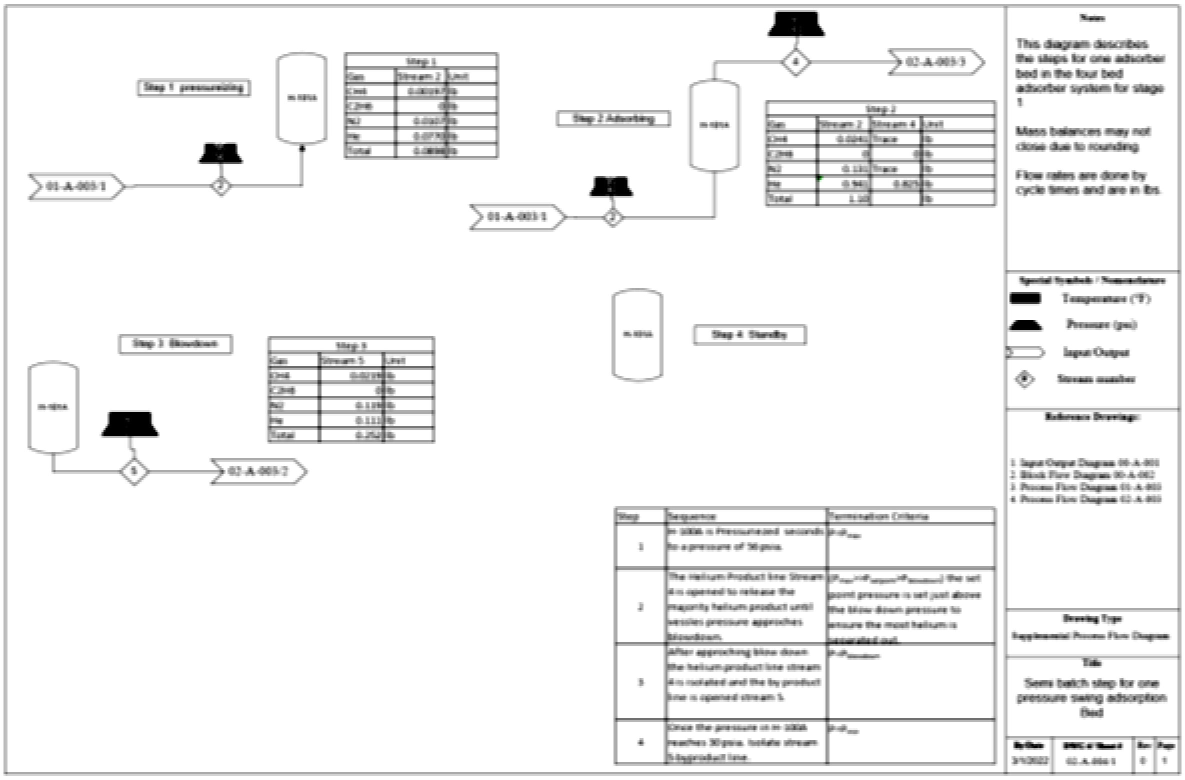

Step 1		
Gas	Stream 2	Unit
CH4	0.00197	lb
C2H6	0	lb
N2	0.0107	lb
He	0.0770	lb
Total	0.0898	lb

Step 2			
Gas	Stream 2	Stream 4	Unit
CH4	0.0241	Trace	lb
C2H6	0	0	lb
N2	0.131	Trace	lb
He	0.941	0.825	lb
Total	1.10		lb

Step 3		
Gas	Stream 5	Unit
CH4	0.0219	lb
C2H6	0	lb
N2	0.119	lb
He	0.111	lb
Total	0.252	lb

Step	Sequence	Termination Criteria
1	H-100A is Pressurized seconds to a pressure of 56psia.	$P=P_{max}$
2	The Helium Product line Stream 4 is opened to release the majority helium product until vessles pressure approches blowdown.	$(P_{max}>=P_{setpoint}>=P_{blowdown})$ the set point pressure is set just above the blow down pressure to ensure the most helium is separated out.
3	After approaching blow down the helium product line stream 4 is isolated and the by product line is opened stream 5.	$P=P_{blowdown}$
4	Once the pressure in H-100A reaches 30psia. Isolate stream 5 byproduct line.	$P=P_{min}$

Notes

This diagram describes the steps for one adsorber bed in the four bed adsorber system for stage 1

Mass balances may not close due to rounding

Flow rates are done by cycle times and are in lbs.

Reference Drawings

1 Input Output Diagram 00-A-001
2 Block Flow Diagram 00-A-002
3 Process Flow Diagram 01-A-003
4 Process Flow Diagram 02-A-003

Drawing Type

Supplemental Process Flow Diagram

Title

Semi batch step for one pressure swing adsorption Bed

By/Date	DWG # Sheet #	Rev	Page
3/1/2022	02-A-004-1	0	1

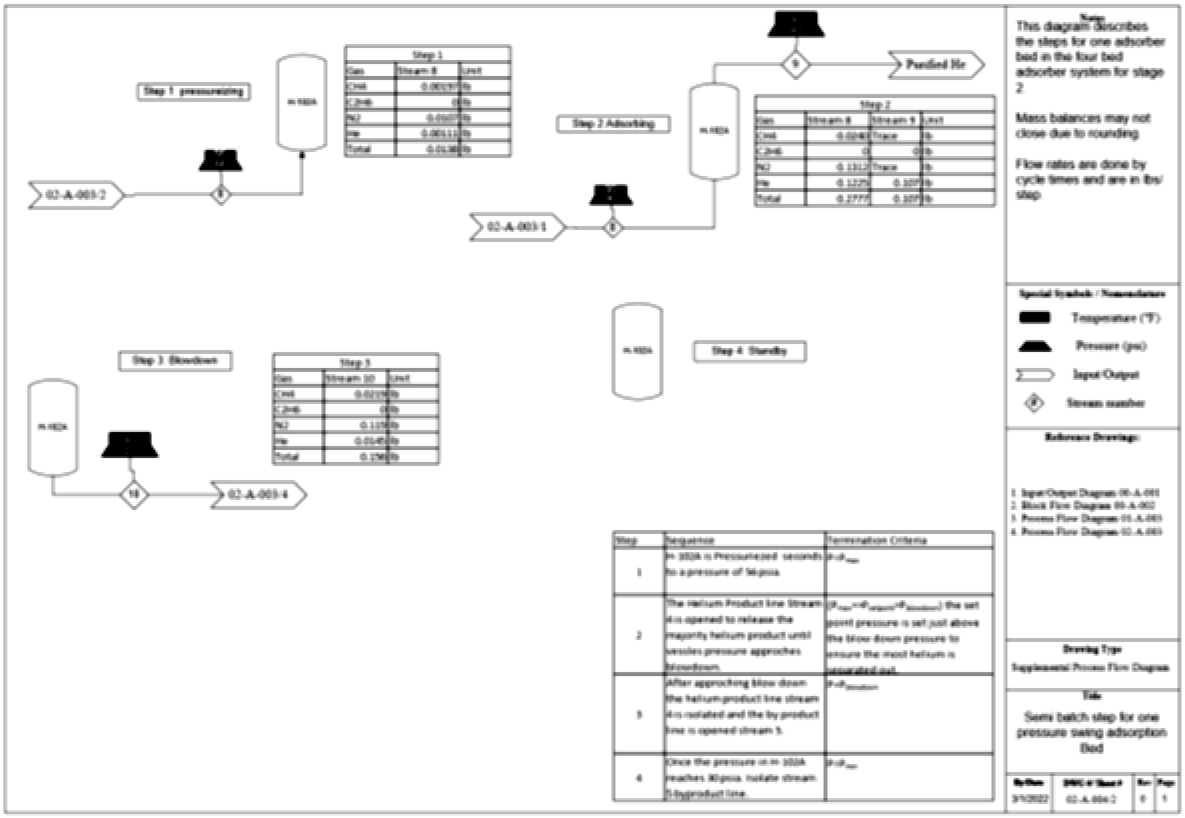

Step 1		
Gas	Stream 8	Unit
CH4	0.00197	lb
C2H6	0	lb
N2	0.0107	lb
He	0.00111	lb
Total	0.0138	lb

Step 2			
Gas	Stream 8	Stream 9	Unit
CH4	0.0240	Trace	lb
C2H6	0	0	lb
N2	0.1312	Trace	lb
He	0.1225	0.107	lb
Total	0.2777	0.107	lb

Step 3		
Gas	Stream 10	Unit
CH4	0.0219	lb
C2H6	0	lb
N2	0.1158	lb
He	0.0145	lb
Total	0.156	lb

Step	Sequence	Termination Criteria
1	H-102A is Pressurized seconds to a pressure of 56psia.	$P=P_{max}$
2	The Helium Product line Stream 4 is opened to release the majority helium product until vessles pressure approaches blowdown.	$(P_{max}>=P_{setpoint}>P_{blowdown})$ the set point pressure is set just above the blow down pressure to ensure the most helium is separated out.
3	After approching blow down the helium product line stream 4 is isolated and the by product line is opened stream 5.	$P=P_{blowdown}$
4	Once the pressure in H-102A reaches 30psia. Isolate stream 5 byproduct line.	$P=P_{min}$

Notes

This diagram describes the steps for one adsorber bed in the four bed adsorber system for stage 2

Mass balances may not close due to rounding

Flow rates are done by cycle times and are in lbs/step

Special Symbols / Nomenclature

▬	Temperature (°F)
▲	Pressure (psi)
⊐	Input/Output
◇	Stream number

Reference Drawings:

1. Input/Output Diagram 00-A-001
2. Block Flow Diagram 00-A-002
3. Process Flow Diagram 01-A-003
4. Process Flow Diagram 02-A-003

Drawing Type

Supplemental Process Flow Diagram

Title

Semi batch step for one pressure swing adsorption Bed

By/Date	DWG # / Sheet #	Rev	Page
3/1/2022	02-A-004-2	0	1

REFERENCES CITED

Aasberg-Petersen, K., Dybkjær, I., Ovesen, C.V., Schjødt, N.C., Sehested, J. and Thomsen, S.G., 2011, Natural gas to synthesis gas–catalysts and catalytic processes. Journal of Natural gas science and engineering, 3(2), pp.423-459.

Abdel-Aal, H.K. and Alsahlawi, M.A. eds., 2013, Petroleum economics and engineering. CRC Press.

Abdel-Aal, H.K., Aggour, M.A. and Fahim, M.A., 2015, Petroleum and gas field processing. CRC press.

Abdulrahman, Ribwar & Kamal, Ibtisam & Ali, Jagar, 2015, Natural Gas Desulfurization Process by MEA Amine: The preferable Engineering Design Procedure. International Journal of Engineering Trends and Technology. 25 10.14445/22315381/IJETT-V28P242.

Adams, C.W., 1990. Jace and Moore-Jonson fields. In: Sonnenberg, S.A., Shannon, L.T., Rader, K., von Drehle, W.F., Martin, G.W. (Eds.), Morrow Sandstones. Rocky Mountain Association of Geologist, pp. 157 - 161.

Adams, D.C., and G.R. Keller, 1994, Possible Extension of the Mid-Continent Rift in West Texas and Eastern New Mexico, Canadian Journal of Earth Science, v. 31, p. 709-720.

Adams, D.C., and K.C. Miller, 1995, Evidence for Late Middle Proterozoic Extension in the Precambrian Basement Beneath the Permian Basin: Tectonics, v. 14, p. 1263-1272

Adams, J.G., Gonzales, D., Darrah, T., 2015. Application of Noble Gas Isotopic Signatures at McElmo Dome-DOE Canyon Field to Investigate CO_2 Source and System Characterization. American Association of Petroleum Geologists. Search and Discovery 41711.

Addicks, S., 2015, Membrane Technology: A Method of Gas Separation: Texas Christian University, 31 p.

Adebayo, Thomas A, Balogun Omotola, Igweze Augusta, Harrison Oluwaseyi, 2011, Alteration of oil-based drilling mud properties due to contact with CO_2 gas kick during drilling, Asian Transactions on Engineering (ATE ISSN: 2221-4267) Volume 01, Issue 04

Ader, M., Boudou, J.P., Javoy, M., Goffe, B., Daniels, E., 1998. Isotope study on organic nitrogen of Westphalian anthracites from the Western Middlefield of Pennsylvania (U.S.A.) and from the Bramsche Massif (Germany). Org. Geochem. 29, 315 - 323.

Agrawal, R., Herron, D.M., Rowles, and Kinard, GE, 2003, Cryogenic Technology, Kirk-Othmer Encyclopedia of Chemical Technology, Volume 8, John Wiley & Sons, Hoboken, NJ,

Ahlbrandt, T.S., Charpentier, R.R., Klett, T.R., Schmoker, J.W., Schenk, C.J. and Ulmishek, G.F., 2005, Global Resource Estimates from Total Petroleum Systems: AAPG Memoir 86 (No. 86). AAPG.

Ahmed, T., 2006. Reservoir Engineering Handbook. Elsevier, p. 1360.

Air Liquide Engineering & Construction, 2021, Steam Methane Reforming - Hydrogen Production: Producing hydrogen through SMR, p. 1.

Air Liquide, 2021. Nitrogen Rejection Unit | Air Liquide. engineering-airliquide.com .

Air Products, 2020, Enhanced Oil and Gas Recovery: 300 p., From: http://www.airproducts.ca/industries/Energy/Enhanced-Oil-and-Gas-Recovery-Technology.aspx, Accessed 09-2021.

Airbus, 2021, ZeroE: ZEROe - Hydrogen – Airbus, p. 11–13. From https://www.airbus.com/innovation/zero-emission/hydrogen/zeroe.html, accessed 10-2021.

Alberta Geological Survey, 2020. Helium Concentrations from Natural Gas Analysis Tests in Alberta (Tabular Data, Tab-Delimited Format). https://ags.aer.ca/publication/dig-2020-0033.

Alcimid, 2020, CCUS technology: CO_2 as a resource or a waste? Alcimid Log Book, no. March, p. 1–5.

Alcoser, L., Ovalle, A., and M. Parsons, 2012, The Bakken: Utilizing a Petroleum System Based Analysis to Optimally Exploit One of the World's Largest Oil Deposits." Paper presented at the SPE Hydrocarbon Economics and Evaluation Symposium, Calgary, Alberta, Canada, September 2012. doi: https://doi.org/10.2118/158918-MS

Alders, M., Winterhalder, D., and Wessling, M., 2017, Helium recovery using membrane processes, Separation and Purification Technology, 189, 2017, 433-440.

Alekseev S.V., Alekseeva L.P., Gladkov A.S. et al., Deep-seated brines of the kimberlite pipe Udachnaya (In Russ.), Geodinamika i tektonofizika, 2018, no. 9(4), pp. 1235–1253.

Al-Kaabi, S.M., 2014, Utilizing Integrated Natural Gas Liquids (NGL) and Nitrogen Rejection unit (NRU) technology in Qatar on the Barzan Gas Project. In International Petroleum Technology Conference. OnePetro.

Alkaim, A.F. and Al_Janabi, S., 2020, Multi objectives optimization to gas flaring reduction from oil production. In Big Data and Networks Technologies 3 (pp. 117-139). Springer International Publishing.

Allen, P.A., Allen, J.R., 2013. Basin Analysis: Principles and Application to Petroleum Play Assessment. John Wiley & Sons, p. 619.

Allen, W.E., 1978a. Pinta dome springs. In: Fassett, J.E., Thomaidis, N.D., Matheny, M.L. (Eds.), Oil and Gas Fields of the Four Corners Area, vol. I. Four Corners Geological Society, pp. 85 - 89.

Allen, W.E., 1978b, Navajo Springs (Helium), in Fassett, J.E., ed., Oil and gas fields of the Four Corners area, v. 1: Four Corners Geological Society, p. 80-84.

Allison, E., and B. Mandler, 2018, Non-Fuel Products of Oil and Gas: American Geoscience Institute, p. 24–27.

Al-Maslamani, M.J., 2008, Assessment of atmospheric emissions due to anthropogenic activities in the state of Qatar (Doctoral dissertation, Brunel University Institute for the Environment PhD Theses).

Alper, E., 1990, Kinetics of reactions of carbon dioxide with diglycolamine and morpholine. The Chemical Engineering Journal, 44(2), pp.107-111.

Alqaheem, Y., A. Alomair, M. Vinoba, and A. Pérez, 2017, Polymeric Gas-Separation Membranes for Petroleum Refining: International Journal of Polymer Science, v. 2017, doi:10.1155/2017/4250927.

Alsharhan, A.S., Nairn, A.E.M., 1997. Sedimentary Basins and Petroleum Geology of the Middle East, first ed. Elsevier, Amsterdam, p. 843.

Al-Siddiqi, A., Dawe, R.A., 1999, Qatar's oil and gas fields: a review. J. Petrol. Geol. 22 (4), 417436.

Ambrose, G.J., Heough, J.P., Shortt, T., 2012, Ooraminna-2, a gas discovery in the Neoproterozoic pioneer sandstone, eastern Amadeus Basin. In: Central Australian Basins Symposium III. Petroleum Exploration Society of Australia, Alice Springs, NT, 9 p.

Ambrose, W.A., Cutright, B.L., 2017. Living on the Moon: Lessons of Mars. American Association of Petroleum Geologists. Search and Discovery Article #70279, 24 p.

American Chemical Society, 2015, The Chemical Revolution of Antoine-Laurent Lavoisier: Académie des Sciences de l'Institut de France in Paris, France, p. 14.

Anderson, C.C., Hinson, H.H., 1951. Helium-bearing Natural Gases of the United States. USGS Bull., p. 486

Anderson, D.L., 1998, The helium paradoxes. Proceedings of the National Academy of Sciences, 95(9), pp.4822-4827.

Anderson, E.C., 1959. Carbon Dioxide in New Mexico, 1959, New Mexico Bureau of Mines and Mineral Resources, Circular 43, 13 p.

Anderson, R.R. (ed.), 1990, The Amoco M.G. Eischeid #1 Deep Petroleum Test, Carroll County, Iowa, Preliminary Investigation: Iowa Department of Natural Resources, Special Report Series No. 2, 186 p.

Anderson, Steven, 2017, Economics, Helium, and the U.S. Federal Helium Reserve: Summary and Outlook. Natural Resources Research. 27. 10.1007/s11053-07-9359-y.

Anderson, S. T., 2018, Economics, Helium, and the U.S. Federal Helium Reserve: Summary and Outlook: Natural Resources Research, v. 27, no. 4, p. 455–477, doi:10.1007/s11053-017-9359-y.

Andrews, J.N., 1985. The isotopic composition of radiogenic helium and its use to study groundwater movement in confined aquifers. Chem. Geol. 49 (1 - 3), 339 - 351.

Andrieu, F., Tsevery, J.-M., Schmitt, N., Peyron, J.-M., Blanc, S., Pareja, T. and Cognard, M., 2006, The Ras Laffan Helium Purification Unit; Air Liquide Advanced technologies, URL: https://engineering.airliquide.com/qatar-start-worlds-largest-helium-unit

Angaji, M.T., Ghanbarabadi, H. and Gohari, F.K.Z., 2013, Optimizations of Sulfolane concentration in propose Sulfinol-M solvent instead of MDEA solvent in the refineries of Sarakhs. Journal of Natural Gas Science and Engineering, 15, pp.22-26.

Anna, L. O., R. Pollastro, and S. B. Gaswirth, 2010, Williston Basin Province — Stratigraphic and Structural Framework to a Geologic Assessment of Undiscovered Oil and Gas Resources: Assessment of Undiscovered Oil and Gas Resources of the Williston Basin Province of North Dakota, Montana, and South Dakota, 2010, p. Chapter 2/7.

Anonymous, 2000, The Impact of Selling the Federal Helium Reserve: 98 p., doi:10.17226/9860.

Anonymous, 2019, Hydrogen Compared with Other Fuels: Hydrogen Data Book, p. 7.

Anonymous, 2019, Process Technologies for Helium Recovery from Natural Gas: A Review: EPCM Holdings, p. 5.

Anonymous, 2020, Fuel Gas Conditioning - Membrane Technology and Research: 1–6 p.

Ansari, N.A., Goyal, M., Chakravarty, A., Menon, R.S., Jadhav, M., Rane, T., Nair, S.R., Kumar, J., Kumar, N., Bharti, S.K. and Chakravarty, A., 2017, February. Development of helium refrigeration/liquefaction system at BARC, India. In IOP Conference Series: Materials Science and Engineering (Vol. 171, No. 1, p. 012007). IOP Publishing.

AOGCC well files, 2022, Arizona Oil and Gas Conservation Commission, GIS Maps, azogc.az.gov

Aoun, A.E., Pu, H., Khetib, Y. and Ameur, M.C.B., 2023, Natural gas flaring status in the Bakken shale play and potential remedial solutions. Fuel, 342, p.127807.

Aoun, A.E., Rasouli, V. and Khetib, Y., 2023, Assessment of Advanced Technologies to Capture Gas Flaring in North Dakota. Arabian Journal for Science and Engineering, pp.1-19.

Aoun, Ala Eddine and Pu, Hui and Khetib, Youcef, Natural Gas Flaring Status in the Bakken Shale Play and Potential Remedial Solutions, 2022, In Press.

Aresta, M., Karimi, I., Kawi, S., 2020. An Economy Based on Carbon Dioxide and Water: Potential of Large-Scale Carbon Dioxide Utilization. Springer Nature, p. 632.

Arizona Oil, Gas Conversation Commission, 2021. Current Operators j Arizona Oil and Gas Conservation Commission. az.gov.

Armor, J.N., 2005, Catalysis and the hydrogen economy. Catalysis letters, 101(3), pp.131-135.

Artemieva, I.M., Mooney, W.D., 2001. Thermal thickness and evolution of Precambrian lithosphere: a global study. Journal of Geophysical Research 106 (B8), 387 - 414.

Arzamendi, G., P. M. Die, and L. M. Gandi, 2013, Renewable hydrogen technologies: Renewable hydrogen energy - An overview: 452 p.

Asaeda, M.; Yamasaki, S., 2001, Separation of inorganic/organic gas mixtures by porous silica membranes. Sep. Purif. Technol. 2001, 25, p. 151–159

Ashfield, J., and A. Kapadia, 2021, Helium - US $275/MCFG: Equity Research, no. December 2020, p. 75.

Astakhova, Olesya , 2021, Russia makes progress on shale oil output but hurdles remain. Reuters. Retrieved 1 May 2022.

Attanasi, E. D., and P. A. Freeman, 2020, Growth Drivers of Bakken Oil Well Productivity: Natural Resources Research, v. 29, no. 3, p. 1471–1486, doi:10.1007/s11053-019-09559-5.

Austerweil, G., 1914. Die angewandte Chemiein der Luftahart, Munchen and Berlin, pp. 8 - 9.

Avis, L.E., 1982. Left-handed field. In: Crouch III, M.A., et al. (Eds.), Oil and Gas Fields of Colorado-Nebraska and Adjacent Areas. Rocky Mountain Association of Geologist, pp. 286 - 299.

Ayad, M. A., N. A. El-Emam, and T. M. Aboul-Fotouh, 2018, A study on the different reforming techniques in gas to liquid technology: Petroleum and Coal, v. 60, no. 5, p. 822–831.

Ayhan, O., 2016, Depositional Environment, Diagenesis and Reservoir Quality of the Middle Bakken Member in the Williston Basin, North Dakota: University of Texas at Austin, 334 p.

Ayodele, B.V., Alsaffar, M.A., Mustapa, S.I., Adesina, A., Kanthasamy, R., Witoon, T. and Abdullah, S., 2021, Process intensification of hydrogen production by catalytic steam methane reforming: Performance analysis of multilayer perceptron-artificial neural networks and nonlinear response surface techniques. Process Safety and Environmental Protection, 156, pp.315-329.

Azimi, G., Leion, H., Rydén, M., Mattisson, T. and Lyngfelt, A., 2013, Investigation of different Mn–Fe oxides as oxygen carrier for chemical-looping with oxygen uncoupling (CLOU). Energy & Fuels, 27(1), pp.367-377.

AZO Nano, 2007, Hydrogen Production Using Environmentally Friendly Nanotechnology Based Techniques: p. 1–2. Accessed 09-2021, https://www.azonano.com/article.aspx?ArticleID=1841 P

B. M. P. Americas, 2021, Bakken Energy, Mitsubishi in blue hydrogen deal: no. June.

Baars, D.L., 1983. Rattlesnake Mississippian. In: Fassett, J.E., Thomaidis, N.D., Matheny, M.L. (Eds.), Oil and Gas Fields of the Four Corners Area, vol. III. Four Corners Geological Society, pp. 1006-1007.

Baars, D.L., Stevenson, G.M., 1981. Tectonic evolution of the Paradox Basin Utah & Colorado. In: Geology of Paradox Basin. RMAG, Rocky Mountain Association of Geologist, pp. 23 - 31.

Bach, W., Naumann, D., Erzinger, J., 1999. A helium, argon, and nitrogen record of upper continental crust (KTB drill holes, Oberpfalz): Germany: implications for crustal degassing. Chem. Geol. 160, 81 - 101.

Bagley, M.E., Ouckette, J., Boardman, D., Watney, W.L., 2011. Lithofacies and Reservoir Assessment for the Thirteen Finger Limestone Hugoton Embayment, Kansas. American Association of Petroleum Geologists. Search and Discovery #50513.

Bahadori, A., 2014. Natural Gas Processing. Elsevier, p. 896.

Bahr, C.W., 1962, The Holbrook anticline, Navajo County, Arizona, in Weber, R.H and Peirce, HW., eds., Mogollon rim region: New Mexico Geological Society 13th Field Conference, p. 118-122.

Baines, S.J., Worden, R.H., 2004. The long-term fate of CO_2 in the subsurface: natural analogues for CO_2 storage. In: Baines, S.J., Worden, R.H. (Eds.), Geological Storage of Carbon Dioxide. Geological Society, pp. 59 - 85.

Bains, P., Psarras, P. and Wilcox, J., 2017, CO_2 capture from the industry sector. Progress in Energy and Combustion Science, 63, pp.146-172.

Baker, M., 2021, The Cost of Hydrogen Infrastructure: p. 7.

Bakey, K., 2015. The production of hydrogen gas: steam methane reforming. ENGL 202C–Process Description.

Bakhsh, M.S.A., Jaynes, S.E., Neu, B.T., Smolarek, J., Emley, T., 2007. Helium Recovery, US Patent No. 20040237789.

Bakhsh, MSA, 2010, Methods and systems for helium recovery, US patent no. 2010/0251892 A1.

Bakhsh, MSA, Jaynes, SE, Neu, BT, Smolarek, J and Emley, T, 2007, Helium Recovery.

Bakken Energy, 2021, Bakken Energy and Mitsubishi Power Establish Clean Hydrogen. Acquisition of the Great Plains Synfuels Plant in the works.

Bakken Energy, 2022, New Clean-Hydrogen Hub in North Dakota – to be developed by Mitsubishi Power and Bakken Energy: Energy Capital Media, p. 5–9.

Baksh, M.S.A., 2010. Methods and Systems for Helium Recovery, US Patent No. 2010/0251892 A1.

Ball, M., Basile, A., ed., 2015, Compendium of Hydrogen Energy, Volume 1: Woodhead Publishing, 551 p., doi:10.1016/c2014-0-02671-8.

Ball, M., Basile, A., ed., 2016, Compendium of Hydrogen Energy, Volume 4: Elsevier, 361 p., doi:10.1016/c2014-0-02671-8.

Ballentine, C., 2007, Earth holds its breath. Nature 449, 294–296 https://doi.org/10.1038/449294a

Ballentine, C. J. and B. Sherwood-Lollar, 2002, Regional groundwater focusing of nitrogen and noble gases into the Hugoton Panhandle giant gas field, USA: Geochimica et Cosmochimica Acta, v. 66, p. 2483-2497.

Ballentine, C. J., and P. G. Burnard, 2002, Production, release, and transport of noble gases in the continental crust: Reviews in Mineralogy and Geochemistry v. 47, p. 481-538.

Ballentine, C.J., Burgess, R., Marty, B., 2002. Tracing fluid origin, transport and interaction in the crust. Rev. Mineral. Geochem. 47 (1), 539 - 614.

Ballentine, C.J., Lollar, B.S., 2002. Regional groundwater focusing of nitrogen and noble gases into the Hugoton-Panhandle giant gas field, USA. Geochem. Cosmochim. Acta 66, 2483 2497.

Ballentine, C.J., O’Nions, R.K., Coleman, M.L., 1996. A Magnus opus: helium, neon, and argon isotopes in a North Sea oilfield. Geochem. Cosmochim. Acta 60 (5), 831 - 849.

Ballentine, C.J., O’Nions, R.K., Oxburgh, E.R., Horvath, F., Deak, J., 1991. Rare gas constraints on hydrocarbon accumulation, crustal degassing and groundwater flow in the Pannonian Basin. Earth Planet Sci. Lett. 105 (1 - 3), 229 - 246.

Ballentine, C.J., Sherwood-Lollar, B., 2002. Regional groundwater focusing of nitrogen and noble gases into the Hugoton Panhandle giant gas field. USA: Geochem. Cosmochim. Acta 66, 2483 - 2497.

Balloon artists, 2020, balloonartists.com.au/helium-dangers.html.

Baltrusaitis, J. and Luyben, W.L., 2015, Methane conversion to syngas for gas-to-liquids (GTL): is sustainable CO_2 reuse via dry methane reforming (DMR) cost competitive with SMR and ATR processes? ACS Sustainable Chemistry & Engineering, 3(9), pp. 2100-2111.

Barboiu, C., Mourgues, A., Sala, B., Julbe, A., Sanchez, J., de Perthuis, S., Hittner, D., 2006. Ultra-microporous silica membranes for He purification. Desalination 200 (1 - 3), 89 - 91.

Barnard, P.C., Cooper, B.S., 1983. A Review of Geochemical Data Related to the Northwest European Gas Province, vol. 12(1), pp. 19 - 33. Geological Society, London, Special Publications.

Barnes, C.G., W.M. Shannon, and H. Kargi, 1999, Diverse Mesoproterozoic Basaltic Magmatism in West Texas, *in* C.D. Frost (ed.), Proterozoic Magmatism of the Rocky Mountains and Environs (Part 1, Rocky Mountain Geology, v. 34/2, p. 263-273.

Barrett, W.J., Hubley, M.D., M.D., 1969. The Madden Field Fremont County, Wyoming Geological Association, Wyoming, 21st Symposium on Tertiary Rocks of Wyoming, pp. 115 - 120.

Barry, P.H., Hilton, D.R., Fischer, T.P., De Moor, J.M., Mangasini, F., Ramirez, C., 2013. Helium and carbon isotope systematics of cold “mazuku” CO_2 vents and hydrothermal gases and fluids from Rungwe Volcanic Province, southern Tanzania. Chem. Geol. 339, 141 - 156.

Bartholomew, C.H., 2001, Mechanisms of catalyst deactivation. Applied Catalysis A: General, 212(1-2), pp.17-60.

Barton, M., Ratchford, M.E., 2020. Executive Summary-Petroleum Geochemistry: Insights into the Origin of Natural Gases and Fluid Hydrocarbons from the Western Snake River Plain, Idaho, Idaho Geological Survey, USGS, Grant G15AC00284: Reservoir Characterization & Petroleum Assessment of Miocene Sedimentary Rocks, Southwestern Idaho, 17 p. Beams, R.J., 1982.

Baubron, J.C., Appard, P., Toutain, J.P., 1990. Diffuse volcanic emissions of carbon dioxide from Vulcano Island, Italy. Nature 344, 51 - 53.

Baumgarner, H., C. Ryden, and M. Bagajewicz, 2009, Use of Membranes in Gas Conditioning: no. May, p. 1–53.

Beacom, E., 2015, Gas, Roads, and Glory: North Dakota and MHA Nation's Struggle Over Flaring Regulation. Wm. & Mary Envtl. L. & Pol'y Rev., 40, p.235.

Beams, R.J., 1982. Greenwood Topeka trend. In: Crouch III, M.A., et al. (Eds.), Oil and Gas Fields of Colorado- Nebraska and Adjacent Areas. Rocky Mountain Association of Geologist, pp. 217-220.

Beaumont, E.C., 1959, Helium in southern Black Mesa Basin [abs.], in Anderson, R.Y., and Harshbarger, J.W., eds., Guidebook of the Black Mesa Basin, northeastern Arizona: New Mexico Geological Society 9th Field Conference Guidebook, p. 160.

Bebout, G.E., Lazzeri, K.E., Geiger, C.A., 2015. Pathways for nitrogen cycling in Earth’s crust and upper mantle: a review and new results for microporous beryl and cordierite. Am. Mineral. 61.

Beck, D., 2015, Pair NGL recovery with LNG production to improve processing economics: Audubon Companies, Denver, Colorado, p. 1–5.

Beck, H.V., 1959. Geology and Ground-Water Resources of Kansas River Valley Between Wamego and Topeka Vicinity: State Geological Survey of Kansas Bulletin 135, 88 p.

Becker, T.P., Lynds, R., 2012. A geologic deconstruction of one of the world’s largest natural accumulations of CO2, Moxa Arch, southwestern Wyoming. Am. Assoc. Pet. Geol. Bull. 96 (9), 1643-1664.

Beebeejaun, Y., 2019, Questioning the local: environmental regulation, shale gas extraction, and the politics of scale. Local Environment, 24(8), pp.777-789.

Beebe, R.R., Reppy, J.D., Goldman, A.M., Lander, H.R., Macauley, M.K., Miller, M.A., Rose, A.Z., Siewert, T.A., Weisskoff, R.M., Shapero, D.C., Ehrenreich, R.M., Aylesworth, K.D. and Beike, D., 2011. Lunar Helium-3 Value Chain: Investment and Funding. American Association of Petroleum Geologists. Search and Discovery Article #80154, 14 p.

Bellamy, W., 2021, Airlines Show Growing Interest in Electric and Hydrogen-Powered Aircraft: Aviation Today, p. 1–5.

Belov, S., 2021, 33 years of the first flight of Tu-155: Russian Aviation, p. 9–10.

Berdais, K.H., Wilhelm, H. and Ungricht, T., 2008, March. Improvements of helium liquefaction/refrigeration plants and applications. In AIP Conference Proceedings (Vol. 985, No. 1, pp. 825-829). American Institute of Physics.

Berendsen, P., Borcherding, R.M., Doveton, J., Hutchison, D.R., Lee, M., Mikereit, B., Agena, W., Spencer, C., 1988. Crustal structure and deep rift basin of the Midcontinent Rift System - results from GLIMPCE deep seismic reflection profile. Geology 16, 81 - 85.

Berganza, C.J., Zhang, J.H., 2013. The role of helium gas in medicine. Med. Gas Res. 3 (18), 7. Bossy, J., Pearce, J., Schober, H., Glyde, H., 2008. Phonon - Roton modes and localized Bose - Einstein Condensation in liquid helium under pressure in nanoporous media. Phys. Rev. Lett. 101 (2).

Bernardo, P., E. Drioli, and G. Golemme, 2009, Membrane gas separation: A review/state of the art: Industrial and Engineering Chemistry Research, v. 48, no. 10, p. 4638–4663, doi:10.1021/ie8019032.

Bhattacharya, S., and T. Carr, 2016, Integrated Petrofacies Characterization and Interpretation of Depositional Environment of the Bakken Shale in the Williston Basin, North America: Petrophysics, v. 57, no. 02, p. 95–110.

Bian, Z., Das, S., Wai, M.H., Hongmanorom, P. and Kawi, S., 2017, A review on bimetallic nickel-based catalysts for CO2 reforming of methane. ChemPhysChem, 18(22), pp.3117-3134.

BID, 2018. Prospeccion de helioenreservporios de gas, FDG Energia Eficiente. www.fdgsa.com.

Biggs, P., 1957. CO_2 at North and South McCallum. In: Munoz, R.R. (Ed.), Guidebook to the Geology of the North and Middle Parks Basin. Rocky Mountain Association of Geologist, pp. 115 - 118.

Bird, K.J., Seggie, R., February 12-14, 1990. Barikewa and Iehi fields revisited. In: Petroleum Exploration in Papua New Guinea: Proceedings of the First PNG Petroleum Convention, Port Moresby, p. 565.

Black, R., 2021, Helium - The Manufacturing Process: p. 4, doi:10.1007/978-1-349-13429-8_6.

Blaettler, K.G., 2019, Percentage of Water Vapor in the Atmosphere, Sciencing, https://sciencing.com/percentage-water-vapor-atmosphere-19385.html, accessed 09-2021.

Blamey, N., Boston, P.J. and Rosales-Lagarde, L., 2016, High-resolution signatures of oxygenation and microbiological activity in speleothem fluid inclusions. International Journal of Speleology, 45(3), p.4.

Bledsoe Ranch. In: Rogers, J.P., Milne, J.J., Cumella, S.P., Dubois, D.P., Lillis, P.G. (Eds.), Oil and Gas Fields of Colorado. Rocky Mountain Association of Geologist, pp. 44 - 46.

Bloch, H. and Soares, C., 2001, Turboexpanders and Process Applications. Gulf Professional Publishing. ISBN 0-88415-509-9.

BNP Media, 2004, AIA: Software Analyzes Cost of Hydrogen Production: Assembly, p. 6.

Boerner, D.E., Craven, J.A., Kurtz, R.D., Ross, G.M. and Jones, F.W., 1998, The Great Falls Tectonic Zone: suture or intracontinental shear zone? Canadian Journal of Earth Sciences, v.35, no. 2, p.175-183.

Bolyard, D.W., 1990. Upper Morrow “B” sandstone reservoir, flank field, Baca County, Colorado. In: Sonnenberg, S.A., Shannon, L.T., Rader, K., von Drehle, W.F., Martin, G.W. (Eds.), Morrow Sandstones. Rocky Mountain Association of Geologist, pp. 191-205.

Bon, R.L., 1999. Petroleum Geology of the Harley Dome Field, Grand County, Utah, Utah Geological Survey, OG-21.

Boone Jr., W.J., 1958. Helium-bearing natural gas of the United States analysis and analytical methods, Supplement to Bulletin 576. USBLM Bull. Can. Pet. Geol. 576, 129.

Boreham, C.J., Edwards, D.S., Poreda, R.J., Darrah, T.H., Zhu, R., Grosjean, E., Main, P., Waltenberg, K., Henson, P.A., 2018. Helium in Australian liquefied natural gas economy. AAPEA J. 58, 209 - 237.

Boudou, J., Espitalie, J., 1995. Molecular nitrogen from coal pyrolysis: kinetic modelling. Chem. Geol. 126, 319 - 333.

Boulevard, T., and L. Lane, 2018, New Hydrogen Study Results from University of Tehran Described, Process development and exergy cost sensitivity analysis of a novel hydrogen liquefaction process: Energy Weekly News+, p. 2.

Bowen, D.W., Talbott, J., Lageson, D.R., Jackson, F.D., Eby, D.E., DeVault, B., 2012, Montana Characterization Study - Comprehensive Report (Task 15). Montana State University, Bozeman, MT, p. 63.

Bowen, D.W., Weimer, P., 2003. Regional sequence stratigraphic setting and reservoir geology of Morrow incised valley sandstones (lower Pennsylvanian), eastern Colorado and eastern Kansas. Am. Assoc. Petrol. Geol. 87 (5), 781 - 815.

Bowersox, J.R., 2018, Assessing the Potential Helium Resources in Central Kentucky. American Association of Petroleum Geologists. Search and Discovery #51573, 22 p.

Bowman, K., 2016. The History of Central Mississippi's Naturally Occurring CO2 Fields. American Association of Petroleum Geologists, Explorer March. Bowersox, J.R., 2019.

Bradshaw, A.M., Hamacher, T., 2013. Nuclear fusion and helium supply problem. Fusion Eng. Des. 88 (9 - 10), 2694 - 2697.

Brandt, A.R., Yeskoo, T., McNally, M.S., Vafi, K., Yeh, S., Cai, H. and Wang, M.Q., 2016, Energy intensity and greenhouse gas emissions from tight oil production in the Bakken formation. Energy & Fuels, 30(11), pp.9613-9621.

Bräuer, K., Geissler, W.H., Kämpf, H., Niedermannn, S. and Rman, N., 2016. Helium and carbon isotope signatures of gas exhalations in the westernmost part of the Pannonian Basin (SE Austria/NE Slovenia): Evidence for active lithospheric mantle degassing. Chemical Geology, 422, pp.60-70.

Braziel, R., 2013, Tailgate Blues – Gas Processing Economics – Part 5 : Value: Gas Processing Economics, p. 6–11.

Breedlovestrout, R.L., 2017. Hydrocarbon Potential of Arkosic Sands in the Weiser-Payette Basin, Southwest Idaho: A Discussion on Basin Fill, Subsurface Structure, and Syndepositional Maturation and Migration History. American Association of Petroleum Geologists. Search and Discovery Article #10904, 35 p.

Brennan, S.T., East, J.A., Dennen, K.O., Jahediesfanjani, H., and Varela, B., 2021, Dataset of Helium Concentrations in United States Wells: U.S. Geological Survey data release, https://doi.org/10.5066/P92QL79J.

Brennan, S.T., Rivera, J.L., Varela, B.A., and Park, A.J., 2021, National assessment of helium resources within known natural gas reservoirs: U.S. Geological Survey Scientific Investigations Report 2021–5085, 5 p., https://doi.org/10.3133/sir20215085.

British Columbia Ministry of Energy, Mines and Petroleum Resources (BMEMPR), 2006. Conventional Gas Play Atlas Northeast British Columbia. Petroleum Geology Publication 2006-01, 50 p. https://www2.gov.bc.ca/assets/gov/farming-natural-resources-and-industry/natural-gas-oil/petroleum-geoscience/oil-gas-reports/og_report_2006-1_nebc_atlas_part1.pdf.

Broadhead, R.F., 1998. Natural accumulations of carbon dioxide in the New Mexico region - where are they, how do they occur and what are the uses for CO2. Geology 20, 2 - 6.

Broadhead, R., 2005, Helium in New Mexico-geologic distribution, resource demand, and exploration possibilities: New Mexico Geology, V 27 #4, p. 93- 100.

Broadhead, R.F., and L. Gillard, 2004, Helium in New Mexico: geologic distribution and exploration possibilities: New Mexico Bureau of Geology and Mineral Resources, OFR 483, 62 p.

Broadhead, R.F., Mansell, M., Jones, G., 2009. Carbon Dioxide in New Mexico: Geologic Distribution of Natural Occurrences, vol. 514. NMBGMR, OFR, p. 131.

Brown, A. A., 2002, Petroleum Charge to The Mill Creek Syncline and Adjacent Areas, Southern Oklahoma: Oklahoma Geological Survey Circular 107, p. 17-36.

Brown, A., 2010, Formation of high helium gases: a guide for explorationists; poster *presented at* American Association of Petroleum Geologists, AAPG Convention, April 11 to 14, 2010, New Orleans, Louisiana.

Brown, A., 2019, Origin of helium and nitrogen in the Panhandle-Hugoton field of Texas, Oklahoma, and Kansas, United States: American Association of Petroleum of Petroleum Geologists Bulletin, Vol. 103, No. 2, p.369-403.

Brown, A.A., 2005. Origin of High Helium Concentrations in Dry Gas Water Fractionation, vol. 89. AAPG, Annual Convention, Calgary, AB, Canada.

Brown, A.A., 2010. Formation of High Helium Gases a Guide for Explorationist. AAPG. New Orleans Convention Poster, Search and Discovery Article 80115.

Brown, A.A., 2014. Compositional gas migrating through water-saturated rock. In: AAPG. April 6 - 9, Annual Convention and Exhibition, Houston, Texas, Search and Discovery 41391, p. 5.

Brown, A.A., 2017. Possible Origins for Low Thermal Maturity, High Nitrogen Natural Gases. AAPG. Search and Discovery, p. 9. Article #42065. Butt, C.R.M., Gole, M.J., 1985. Helium in soil and overburden gas as an exploration pathfinder - an assessment. J. Geochem. Explor. 24, 141 - 173.

Brown, A.A., 2019. Origin of helium and nitrogen in the Panhandle-Hugoton field of Texas, Oklahoma, and Kansas, United States. Am. Assoc. Pet. Geol. Bull. 103 (2), 369 - 403.

Brown, H.H., 1978. Beautiful mountain Mississippian. In: Fassett, J.E. (Ed.), Oil and Gas Fields of the Four Corners Area, vol. III. Four Corners Geological Society, pp. 207-208.

Brunetti, A., F. Macedonio, G. Barbieri, and E. Drioli, 2019, Membrane condenser as emerging technology for water recovery and gas pre-treatment: current status and perspectives: BMC Chemical Engineering, v. 1, no. 1, p. 1–15, doi:10.1186/s42480-019-0020-x.

Bukaty M.B., Groundwater geology of the Western Siberian craton (implications for petroleum exploration) (In Russian.), Geologiya i geofizika = Russian Geology and Geophysics, 2009, V. 50, no. 11, pp. 1201–1217.

Burbidge, G. and Hoyle, F., 2000. The Origin of Helium and the Other Light Elements. The Universe: Visions and Perspectives, pp.69-76.

Burchett, R.R., K.V. Luza, O.J. Van Eck, and F.W. Wilson, 1985, Seismicity and Tectonic Relationships of the Nemaha Uplift and Midcontinent Geophysical Anomaly (Final Project Summary: Oklahoma Geological Survey, Special Publications 85-2, 33 p.

Burke, J.H., 2019. China's New Wealth Creation Scheme: Mining the Moon, Nation Review. https://www.nationalreview.com/2019/06/china-moon-mining-ambitious-space-plans/.

Burnard, P.G., Hu, R.Z., Turner, G., Bi, X.W., 1999. Mantle, crustal and atmospheric noble gases in Ailaoshan gold deposits, Yunnan Province, China. Geochim Cosmochim Acta 63 (10), 1595 - 1604.

Burwash, R. A., and G. L. Cumming, 1974, Helium Source-Rock in Southwestern Saskatchewan. Bulletin of Canadian Petroleum Geology 1974; 22 (4): 405–412. doi: https://doi.org/10.35767/gscpgbull.22.4.405

Burwash, R.A. and Cumming, G.L., 1976, Uranium and thorium in the Precambrian basement of western Canada. I. Abundance and distribution; Canadian Journal of Earth Sciences, v.13, no.2, p.284-293.

Burwash, R.A., McGregor, C.R. and Wilson, J.A., 1994, Precambrian basement beneath the Western Canada Sedimentary Basin; Chapter 5 *in* Geological Atlas of the Western Canada Sedimentary Basin, Mossop, G.D. and Shetson, I. (comps.), Canadian Society of Petroleum Geologists and Alberta Research Council, p.49-56.

Butler, Shane, Azenkeng, Alexander, Mibeck, Blaise, Kurz, Bethany, and Kurt Eylands, 2019, Unconventional Rock Requires Unconventional Analysis: Methods for Characterization. Paper presented at the SPE/AAPG/SEG Unconventional Resources Technology Conference, Denver, Colorado, USA. doi: doi.org/10.15530/urtec-2019-971

Butt, C.R.M., Gole, M.J., 1986. Groundwater Helium surveys in mineral exploration in Australia. J. Geochem. Explor. 25, 309 - 344.

Buzco-Guven, B. and Harriss, R., 2010, Gas flaring and venting: extent, impacts, and remedies.

Byrne, P.H.B., Lawson, M., Ballentine, C.J., 2017. Noble gases in conventional and unconventional petroleum systems. In: Lawson, M., Formolo, M.J., Eiler, J.M. (Eds.), Source to Seep: Geochemical Applications in Hydrocarbon Systems. Geological Society, London, Special Publications no. 468.

Byrne, P.H.B., Lawson, M., Ballentine, C.J., 2020. The use of noble gas isotopes to constrain subsurface fluid flow and hydrocarbon migration in the East Texas Basin. Geochem. Cosmochim. Acta 268, 186 - 208.

Caffee, M.W., Hudson, G.U., Velsko, C., Huss, G.R., Alexander, E.C., Chivas, A.R., 1999. Primordial noble cases from Earth's mantle: identification of a primitive volatile component. Science 285, 2115 - 2118.

Cady, H.P., McFarland, 1903. Helium in Kansas natural gas. Trans. Kans. Acad. Sci. 20 (December).

Cady, H.P., McFarland, 1906. Helium in natural gas. Science, New Series 24. September 14, December.

Cady, H.P., McFarland, 1907a. The occurrence of Helium in natural gas and the composition of natural gas. J. Am. Chem. Soc. 29 (November).

Cady, H.P., McFarland, 1907b. Neon and Argon in natural gas. Trans. Kans. Acad. Sci. 21 (December), 64 - 65.

Caffee, M.W., Hudson, G.U., Velsko, C., Huss, G.R., Alexander, E.C., Chivas, A.R., 1999. Primordial noble cases from Earth's mantle: identification of a primitive volatile component. Science 285, 2115-2118.

Cai X, Dong X, Lin W, 2006, Autothermal reforming of methane over Ni catalysts supported on CuO-ZrO2-CeO2-Al2O3. J Nat Gas Chem 15(2):122–126

Cai, Z., Clarke, R.H., Nuttall, W.J., 2012. Applications, prices and substitutions. In: Nuttall, W.J., Clarke, R.H., Glowacki, B.A. (Eds.), The Future of Helium as a Natural Resource, Chapter 9. Routledge, pp. 134 - 156, 376pp.

Callaghan, C., 2006, Kinetics and catalysis of the water-gas-shift reaction: A Microkinetic and Graph Theoretic Approach (PDF) (PhD). Worcester Polytechnic Institute.

Cameron, C., 2021, North Dakota sues the Biden administration over oil and gas leases: 2 p. 2021. From https://www.nytimes.com/2021/07/08/us/politics/north-dakota-sues-biden.html,

Campbell, J. M., 1998, Gas Conditioning and Processing, Vol. 2. Norman, OK: Campbell Petroleum Series Caro, J, M. Noack, P. Kölsch, R. Schäfer, 2000, Zeolite membranes – state of their development and perspective, Micropor. Mesopor. Mater. 38, p. 3–24

Cantor, K.L., Stearns, D.B., Geesaman, R.C., Wilson, J.L., 1993. Paleostructural and related paleokarst controls on reservoir development in the lower Ordovician Ellenburger group, val Verde Basin, Texas, in Paleokarst Related Hydrocarbon Reservoirs. Society of Sedimentary Geology, pp. 61 - 100. Core Workshop No. 18, Cao, S., 2014. Natural Gas Flare Reduction: Case Studies in Russia, Nigeria, and the United States (Doctoral dissertation, Department of Geology and Geophysics, Yale University).

Cappa, J., Rice, D., 1995. Carbon Dioxide in Mississippian Rocks of the Paradox Basin and Adjacent Areas, Colorado, Utah, New Mexico and Arizona. USGS, Bulletin No. 2000-H.

Caracausi, A., Paternoster, M., 2015. Radiogenic helium degassing and rock fracturing: a case study of the southern Apennines active tectonic region. J. Geophys. Res.: Solid Earth 120 (4), 2200 - 2211.

Cardwell, L.E., Benton, L.F., 1967. Analysis of Natural Gases, 1966. BM-IC-8356. USBM, p. 130.

Cardwell, L.E., Benton, L.F., 1968. Analysis of Natural Gases, 1967. BM-IC-8395. USBM, p. 187.

Cardwell, L.E., Benton, L.F., 1969. Analysis of Natural Gases, 1968. BM-IC-8443. USBM, p. 169.

Cardwell, L.E., Benton, L.F., 1970. Analysis of Natural Gases, 1969. BM-IC-8475. USBM, p. 134.

Cardwell, L.E., Benton, L.F., 1971. Analysis of Natural Gases, 1970. BM-IC-8475. USBM, p. 130.

Cardwell, L.E., Benton, L.F., 1972. Analysis of Natural Gases, 1971. BM-IC-8554. USBM, p. 130.

Cardwell, L.E., Benton, L.F., 1973. Analysis of Natural Gases, 1972. BM-IC-8607. USBM, p. 163.

Carpen, T.R., 1957. North McCallum field, Jackson County, Colorado. In: Guidebook to the Geology of the North and Middle Parks Basin. Rocky Mountain Association of Geologist, pp. 109 - 112.

Carr, C.J., 2017. The seismic threat to the Gibe III Dam: a disaster in the waiting. In: River Basin Development and Human Rights in Eastern Africa, - a Policy Crossroads, pp. 43 - 52. Creative Commons, Chap. 3. Carver Jr., H.S., 1956.

Carter, T., 2021. Helium-3 Is Scarce, This Navy Invention Stretches it for Radiation Detectors. Techlink. https:// techlinkcenter.org/news/helium-3-is-scarce-this-navy-invention-stretches-it-for-radiation-detectors.

Carver Jr., H.S., 1956. Keyes field. In: Guidebook Panhandle of Oklahoma, Northeastern New Mexico, South-Central Colorado. Oklahoma City Geological Society, pp. 130-135.

Casey, T.A., 1983, Helium potential of the Four Corners area, in Fassett, J.E., ed., Oil and gas fields of the Four Corners area, v. 3: Four Corners Geological Society, p. 749-754.

Cassidy, M., 2006. Occurrence and Origin of Free Carbon Dioxide Gas Deposits in the Earth's Continental Crust (Ph.D.). University of Houston, Texas.

Castro, M. C., A. Jambon, G. de Marsily, and P. Schlosser, 1998, Noble gases as natural tracers of water circulation in the Paris basin 1. Measurements and discussion of their origin and mechanisms of vertical transport in the basin: Water Resources Research v. 34, #10, p. 2443-2466.

Cavallaro, S., V. Chiodo, A. Vita, and S. Freni, 2003, Hydrogen production by auto-thermal reforming of ethanol on Rh/Al2O3 catalyst: Journal of Power Sources, v. 123, no. 1, p. 10–16, doi:10.1016/S0378-7753(03)00437-3.

Cecconi, B., and I. Easow, 2017, Helium Detection at Wellsite: A Powerful Geochemical Tool. Paper presented at the Offshore Mediterranean Conference and Exhibition, Ravenna, Italy, March 2017.

Charlton, T.R., Dalgliesh, R.M., Kirichek, O., Langridge, S., Ganshin, A., McClintock, P.V.E., 2008. Neutron reflection from a Liquid helium surface. Low Temp. Phys. 34 (4), 316 - 319.

Chaudhuri, H., K. Seal, C. Maji, S. Pal, and M. K. Mandal, 2019, The unrevealed facts on helium resources of India: Arabian Journal of Geosciences, v. 12, no. 6, doi:10.1007/s12517-019-4369-1.

Cheekatamarla, P.K. and Lane, A.M., 2005, Catalytic autothermal reforming of diesel fuel for hydrogen generation in fuel cells: I. Activity tests and sulfur poisoning. Journal of Power Sources, 152, pp.256-263.

Chemical Engineering World, 2021. Cryogenic Distillation of Air. Chemical Engineering World.

Chen, A., Shen, C., Byrne, T.B., Sano, Y., Takahata, N., Yang, T.F., Wang, Y., 2019. Mantlefluids associated with crustal-scale faulting in a continental subduction setting, Taiwan. Sci. Rep. 9, 10805. https://doi.org/10.1038/ s41598-019-47070-2.

Chen, S., 2020. China Opens First Large-Scale Helium Plants as it Tries to Reduce Reliance on US Imports, South China Morning Post, 2/7/2020, China Opens First Large-Scale Helium Plant as it Tries to Reduce Reliance on US Imports (msn.com).

Chen, W.H., Lin, M.R., Lu, J.J., Chao, Y. and Leu, T.S., 2010, Thermodynamic analysis of hydrogen production from methane via autothermal reforming and partial oxidation followed by water gas shift reaction. international journal of hydrogen energy, 35(21), pp.11787-11797.

Chen, W.H., Su, Y.Q., Lin, B.J., Kuo, J.K. and Kuo, P.C., 2021, Hydrogen production from partial oxidation and autothermal reforming of methanol from a cold start in sprays. Fuel, 287, p.119638.

Chen, Z., Li, Y., Martinelli, G., Lu, C., Zhao, X., 2020. Spatial and temporal variations of CO2 emissions from the active fault zones in the capital area of China. Appl. Geochem. 112, 10.

Cherniak, D.J., Amidon, W., Hobbs, D., Watson, E.B., 2015. Diffusion of helium in carbonates: effects of mineral structure and composition. Geochem. Cosmochim. Acta 165, 449 - 465.

Chodos, A., 2004, August / September 2004, This Month in Physics History: APS Physics, v. 13, no. 8, p. 8–11.

Choi, Y.B., 1993, Paradigms and conventions: Uncertainty, decision making, and entrepreneurship. University of Michigan Press.

Chowdhury, S., Shipman, T., Chao, D., Elvidge, C.D., Zhizhin, M. and Hsu, F.C., 2014, Daytime gas flare detection using Landsat-8 multispectral data. In 2014 IEEE Geoscience and Remote Sensing Symposium (pp. 258-261). IEEE.

Christiansen, R. L, 1992, Plate 7. Approximate distributions of major tectonic, sedimentary and igneous features in the US Cordilleran region during several post-Laramide time periods: in B. C. Burchfiel, et al. (eds.) The Cordilleran Orogen: conterminous US: The Geology of North America, v G-3, Geological Society of America.

Christopher, J.E., Kent, D.M. and Simpson, F., 1971, Hydrocarbon Potential of Saskatchewan; Saskatchewan Energy and Mines, Report 157, 47p.

Cinti, G., Baldinelli, A., Di Michele, A. and Desideri, U., 2016. Integration of Solid Oxide Electrolyzer and Fischer-Tropsch: A sustainable pathway for synthetic fuel. Applied Energy, 162, pp.308-320.

Clair, J.R., Bradish, B.B., 1956. Model Dome Gas Field. Las Animas Arch Co., CO, Rocky Mountain Association of Geologist, Guidebook to the Geology of the Raton Basin Guidebook, p. 80. Clark, C.R., 1978.

Clark, C.R., 1978. Lisbon field. In: Fassett, J.E. (Ed.), Oil and Gas Fields of the Four Corners Area, vol. II. Four Corners Geological Society, pp. 662-665.

Cloete, S., 2020, Green or Blue Hydrogen: cost analysis uncovers which is best for the Hydrogen Economy: p. 1–10.

Coburn, M., Maze, M., 2008. The neuroprotective effects of xenon and helium in an in vitro model of traumatic brain injury. Crit. Care Med. 36 (2), 588 - 595.

Coker, A. K., 2010, Volume 2: Distillation, Packed Towers, Petroleum Fractionation, Gas Processing and Dehydration, in A. K. Coker, ed., Ludwig's Applied Process Design for Chemical and Petrochemical Plants: Boston, Gulf Professional Publishing, p. 483–678, doi: https://doi.org/10.1016/B978-0-7506-8366-1.10023-4.

Collerson, K.D., Van Schmus, R.W., Lewry, J.F. and Bickford, M.E., 1988, Buried Precambrian basement in south-central Saskatchewan: provisional results from Sm-Nd model ages and U-Pb zircon geochronology; *in* Summary of Investigations 1988, Saskatchewan Geological Survey, Saskatchewan Energy and Mines, Miscellaneous Report 88-4, p.142-150.

Collerson, K.D., Van Schmus, R.W., Lewry, J.F. and Bickford, M.E. (1989, Sm-Nd isotopic constraints on the age of the buried basement in central and southern Saskatchewan: implications for diamond exploration; *in* Summary of Investigations 1989.

Collodi, G., G. Azzaro, N. Ferrari, and S. Santos, 2017, Techno-economic Evaluation of Deploying CCS in SMR Based Merchant H_2 Production with NG as Feedstock and Fuel: Energy Procedia, v. 114, no. November 2016, p. 2690–2712, doi: 10.1016/j.egypro.2017.03.1533.

Colorado Oil and Gas Conservation Commission (COGCC), 2020. https://cogcc.state.co.us/maps.html#/gisonline.

Congress, U.S., 1924. Conservation of Helium Gas: Hearings before Committee on Military Affairs House of Representatives, 68th Congress, 1st Session, H.R, p. 5722.

Congress, U.S., 1937. Public-No. 411-75th Congress, Chapter 895, 1st Session, S. 1567, Sect. Post World War I.

Congress, U.S., 1960. Helium Act Amendments of 1960. Pub. L. 86-777, Sept, 13th, 1960 74 Stat 918.

Congressional Research Service, 2018, Natural Gas Liquids: The Unknown Hydrocarbons: CRS Report R45398, p. 21.

Conley, IN., 1974, Pinta Dome - Navajo Springs - East Navajo Springs helium gas pools, Apache County, Arizona, well location map: Arizona Oil and Gas Conservation Commission Pool Series Map P-1, scale 1:63,360 [now available as Arizona Geological Survey Publication OG-14]

Conley, J.N., 1977, Subsurface structure maps, eastern Mogollon slope region, east-central Arizona: Arizona Oil and Gas Conservation Commission Regional Maps G-6A, G-7, and G-8, scale 1:500,000 [now available as Arizona Geological Survey Publication OG-21]

Conley, J.N., and Giardina, S., Jr., 1979, Favorable and potentially favorable areas for hydrocarbon and geothermal energy sources in northeastern Arizona: Arizona Oil and Gas Conservation Commission Report of Investigation 7, 56 p. [now available as Arizona Geological Survey Publication OG-28]

Cook, E., 1979, The helium questions. Science, 206(4423), pp.1141-1147.

Cormos, A. M., S. Szima, S. Fogarasi, and C. C. Cormos, 2018, Economic assessments of hydrogen production processes based on natural gas reforming with carbon capture: Chemical Engineering Transactions, v. 70, p. 1231–1236, doi:10.3303/CET1870206.

Costa, J., 2021, Hydrogen Steam Methane Reformer Production Overview: p. 1–9. From: https://jefersoncosta.com/hydrogen-steam-methane-reformer-production-overview/, Accessed 09-2021.

Cox, 2008, Hydrogen: Its Technology and Implications. Volume 1: 208 p., doi:10.1201/9781351073301.

Cox, K., and K. Williamson, eds., 2018, Hydrogen: Its Technology and Implications: Hydrogen Properties Volume IV Utilization of Hydrogen: 256 p.

Cox, K., and Williamson, 2018, Hydrogen: Its Technology and Implications Vol II: Transmission and Storage of Hydrogen: 61 p.

Craddock, W.H., Blondes, M.S., DeVera, C.A., Hunt, A.G., 2017. Mantle and crustal gases of the Colorado Plateau Geochemistry, sources, and migration pathways. Geochem. Cosmochim. Acta 213, 346 - 374.

Craig, H., Clarke, W.B., Beg, M.A., 1975. Excess ^{3}He in deep water on the East Pacific Rise. Earth Planet Sci. Lett. 26 (2), 125 - 132.

Craig, H., Lupton, J.E., 1976. Primordial neon, helium, and hydrogen in oceanic basalts. Earth Planet Sci. Lett. 31, 369 - 385.

Crawford, D, Coyle, DA and Anantharaman, B, 2010, Method for nitrogen rejection and or helium recovery in a liquefaction plant. EPCM, https://epcmholdings.com/process-technologies-for-helium-recovery-from-natural-gas-a-review/. Accessed 10-2021,

Creedy, D.P., 1988. Geological controls on the formation and distribution of gas in British coal measure strata. Int. J. Coal Geol. 10 (1), 1 -31.

Crockett, A.H., Smith, K.C., Bartlett, N., 1973. The Chemistry of Monatomic Gases, Pergamon, p. 208.

Crovetto, R., R. Fernandez-Prima, and M. L. Japas, 1982, Solubilities of inert gases and methane in H_2O and D_2O in the temperature range of 300 - 600K.

Culberson, O. L., and J. J. McKetta, 1951, Phase equilibrium in hydrocarbon-water systems. III, The solubility of methane in water at pressures to 10,000 psia: AIME Petroleum Transactions, v. 192, p. 223-226.

Cunningham, K.I., 1987. Helium Concentration in Soil-gas Over Known Petroleum Accumulations. WaKeeney Area, Trego County, Kansas, USGS, OFR, 87 - 254, p. 26.

Currence, K. L., D. M. Rapavi, and M. J. Clifford, 2015, A new approach to NGL recovery from off-gases: Society of Petroleum Engineers - Abu Dhabi International Petroleum Exhibition and Conference, ADIPEC 2015, doi:10.2118/177784-ms.

Czapigo-Czapia, M., Brzezinski, D., 2020. The balance of mineral resources deposits in Poland as of 31 XII 2020. Polish Geological Institute National Research Institute. http://geoportal.pgi.gov.pl/surowce/energetyczne/hel/2020.

Dagle, R. A., V. Dagle, M. D. Bearden, J. D. Holladay, T. R. Krause, and S. Ahmed, 2017, An Overview of Natural Gas Conversion Technologies for Co-Production of Hydrogen and Value-Added Solid Carbon Products: (No. PNNL-26726; ANL-17/11). Pacific Northwest National Lab. (PNNL), Richland, WA (United States); Argonne National Lab. (ANL), Argonne, IL (United States)., p. 65.

Dasgupta, P. S., & Heal, G. M., 1979, Economic theory and exhaustible resources, 501 p. Cambridge: Cambridge University Press.

Dai, J., Ni, Y., Qin, S., Huang, S., Gong, D., Liu, D., Feng, Z., Peng, W., Han, W., Fang, C., 2017. Geochemical characteristics of He and CO2 from the Ordos (cratonic) and Bohaibay (rift basins). Chem. Geol. 468, 192 - 213.

Dai, J., Song, Y., Dai, C., Wang, D., 1996. Geochemistry and accumulation of carbon dioxide gases in China. Am. Assoc. Pet. Geol. Bull. 80 (10), 1615-1626.

Dai, Z., J. Deng, X. He, C. A. Scholes, X. Jiang, B. Wang, H. Guo, Y. Ma, and L. Deng, 2021, Helium separation using membrane technology: Recent advances and perspectives: Separation and Purification Technology, v. 274, no. February, p. 119044, doi:10.1016/j.seppur.2021.119044.

Daly, JW, 2005, Helium recovery from LNG. International Petroleum Technology Conference, American Association of Petroleum Geologists, AAPG; the European Association of Geoscientists and Engineers, EAGE; the Society of Exploration Geophysicists, SEG; and the Society of Petroleum Engineers, SPE, Doha, Qatar, 1–4.

Damak, Cyrine & Leducq, Denis & Hoang, Hong & Negro, Daniele & Delahaye, Anthony, 2019, Liquid Air Energy Storage (LAES) as a large-scale storage technology for renewable energy integration - A review of investigation studies and near perspectives of LAES. International Journal of Refrigeration. 110. 10.1016/j.ijrefrig.2019.11.009.

Danabalan, D., 2017. Helium: Exploration Methodology for a Strategic Resource (Ph.D.). Durham University, United Kingdom, 296 p. Danie, T.C., 1978. Dinah-Bi-Keyah. In: Fassett, J.E., Thomaidis, N.D., Matheny, M.L. (Eds.), Oil and Gas Fields of the Four Corners Area, Four Corners Geological Society, vol. 1, pp. 73 - 76.

Danie, T.C., 1978. Dinah-Bi-Keyah. In: Fassett, J.E., Thomaidis, N.D., Matheny, M.L. (Eds.), Oil and Gas Fields of the Four Corners Area, Four Corners Geological Society, vol. 1, pp. 73-76.

Das, N.K., Chaudhuri, H., Bhandari, R.K., Ghose, D., Sen, P., Binha, B., 2008. Purification of helium from natural gas by pressure swing adsorption. Curr. Sci. 95 (12), 1684 - 1687.

Das, Nisith & Kumar, Pradeep & Mallik, C. & Bhandari, Ratan, 2012, Development of a helium purification system using pressure swing adsorption. Current Science. 103. 631-634.

Davidson, M.J., July 1963. Geochemistry Can Help Find Oil If Properly Used. World Oil, pp. 94 - 106.

Davis, J.B., 1967. Petroleum Microbiology. Elsevier Publishing, Co., New York, p. 604.

Davis, T.S., 2016. Anthropocene Insecurities: Extraction, Aesthetics, and the Bakken Oilfields. English Language Notes, 54(2), pp.41-48.

Davison, I., Steel, I., Taylor, M., Beirne, E.O., Faull, T., 2014. Exploration in the East African Rift system. GeoExPro 11 (5), 8 p.

Day, D., Evans, R.J., Lee, J.W. and Reicosky, D., 2005, Economical CO2, SOx, and NOx capture from fossil-fuel utilization with combined renewable hydrogen production and large-scale carbon sequestration. Energy, 30(14), pp.2558-2579.

De Bruin, R.H., 1991. Wyoming's Carbon Dioxide Resources. Wyoming Geological Survey, OFR 91-6, 23 p.

De Bruin, R.H., 1995. Helium resources of Wyoming. In: Resources of Southwestern Wyoming: Field Conference Guidebook. Wyoming Geological Association, pp. 191-201.

De Castro, J., R. Rivera-Tinoco, and C. Bouallou, 2010, Hydrogen production from natural gas: Auto-Thermal Reforming and CO 2 capture: Chemical Engineering Transactions, v. 21, no. August, p. 163–168, doi:10.3303/CET1021028.

Devarajan, S., & Fisher, A. C., 1981, Hotelling's ''Economics of Exhaustible Resources'': Fifty years later. Journal of Economic Literature, 19(1), 65–73.

De Voto, R.H., 1980a. Mississippian stratigraphy and history of Colorado. In: Kent, H.C., Porter, K.W. (Eds.), Colorado Geology. Rocky Mountain Association of Geologist, pp. 57 - 70.

De Voto, R.H., 1980b. Pennsylvanian stratigraphy and history of Colorado. In: Kent, H.C., Porter, K.W. (Eds.), Colorado Geology. Rocky Mountain Association of Geologist, pp. 71 - 102.

de Vries, K., Erumban, A. and van Ark, B., 2021, Productivity and the pandemic: short-term disruptions and long-term implications. International Economics and Economic Policy, 18(3), pp.541-570.

Dean, J. W., 1960, Helium potential of the Navajo-Chambers area, Apache County, Arizona: Interstate Oil Compact Commission Committee Bulletin, December, v. 2, no. 2, p. 33-48.

Dean, J.W., and Lauth, R.E., 1961, Four Comers keeps lead in production of helium gas: Oil & Gas Journal, v. 59, no. 8, p. 194-199.

Demirel, Y., 2015, Technoeconomics and Sustainability of Renewable Methanol and Ammonia Productions Using Wind Power-based Hydrogen: Journal of Advanced Chemical Engineering, v. 5, no. 3, doi:10.4172/2090-4568.1000128.

Dengel, U., 2020, Membrane Units for Fuel Gas Conditioning Heavy Hydrocarbon and Water Removal from Natural Gas: 2 p.

Dengel, U., S. Karode, and Y. Ding, 2019, Streamlined natural gas treatment by membranes only: Proceedings of the Annual Offshore Technology Conference, v. 2019-May, no. May, p. 6–9, doi:10.4043/29489-ms.

Denning, S., Lucero, J., Koh, C.A. and Carreon, M.A., 2019, Chabazite Zeolite SAPO-34 Membranes for He/CH_4 Separation. ACS Materials Letters, 1(6), pp.655-659.

Desert Mountain Energy, 2021. http://desertmountainenergy.com/wp-content/uploads/2021/06/DME-InvestorPresentation-06282021-FINAL-.pdf .

Deshpande, R.D., Gupta, S.K., 2013. Groundwater helium: an indicator of active tectonic regions along Narmada River, central India. Chem. Geol. 344, 42 - 49.

Deusner, C., Bigalke, N., Kossel, E. and Haeckel, M., 2012, Methane production from gas hydrate deposits through injection of supercritical CO2. Energies, 5(7), pp.2112-2140.

Deyin, A., 2021, Overview of Gas Sweetening Methods / Processes Chemical Reaction Process (Continuous) for Gas Sweetening: p. 1–11. From https://whatispiping.com/gas-sweetening-methods/. Accessed 09-2021.

Dibrov, G., M. Ivanov, M. Semyashkin, V. Sudin, and G. Kagramanov, 2018, High-pressure aging of asymmetric Torlon® hollow fibers for helium separation from natural gas: Fibers, v. 6, no. 4, doi:10.3390/fib6040083.

Dilmare, D., 2004. Mining the Moon (October 2004). Popular Mechanics (October).

Directors, C. E. C., 2021, Mitsubishi Power moves into Bakken Shale on blue hydrogen infrastructure deal: Power Engineering, p. 3.

Dixon, J., 2007, Correlations in Cambrian and Lower Ordovician strata of Saskatchewan; Geological Survey of Canada, Open File 5523, 18p. (CD-ROM).

Dixon, J., 2008, Stratigraphy and facies of Cambrian to Lower Ordovician strata in Saskatchewan; Bulletin of Canadian Petroleum Geology, v.56, no.2, p.93-117.

Dobbin, C.E., 1935. Geology of Natural Gas, Rich in Helium, Nitrogen, Carbon Dioxide and Hydrogen Sulfide. American Association of Petroleum Geologists, pp. 1053-1072. Special Volume 7.

Dockrill, B., Shipton, Z.K., 2010. Structural controls from a natural gas CO_2 geologic storage site, Central Utah, U.S.A. J. Struct. Geol. 32 (11), 1768 - 1782.

DOE, 2019, North Dakota Natural Gas Flaring and Venting Regulations: US Department of Energy, p. 3.

Doering, W.P., Friedman, I., 1983. Survey of Helium in Natural Water Wells and Springs in Southwest Montana and Imperial Valley, California, Part V - Jan. 1 - Dec. 31, 1982. USGS. OFR 83-500, 32pp.

Dorrington, G. E., Baxter, G., Bil, C., Subic, A., & Trivailo, P.M., 2013, Prospects for Liquefied Natural Gas and other Alternative Fuels for Future Civil Air Transportation (http://researchbank.rmit.edu.au/view/rmit:20100/n2006040078.pdf) (PDF). Proceedings of the 15th Australian International Aerospace Congress (AIAC15). Melbourne, Australia: Royal Aeronautical Society, Australia Division: 116–125.

Dorrington, G. E., G. Baxter, C. Bil, A. Subic, and P. M. Trivailo, 2013, Tupolev Tu-155: Proceedings of the 15th Australian International Aerospace Congress, v. 154, p. 116–125.

Dotzenrod, A. N., S. Fong, V. Kenny, M. Leung, M. Nathal, J. Plaxco, S. Saldaña, M. Zuckerman, and E. Zuehlke, 2015, Natural Gas to Hydrogen, H: p. 15.

Drehle, W.F., 1990. Barrel Springs Field, Prowers County, Colorado. In: Sonnenberg, S.A., Shannon, L.T., Rader, K., von Drehle, W.F., Martin, G.W. (Eds.), Morrow Sandstones, Rocky Mountain Association of Geologist, pp. 183 - 189.

Drioli, E., and G. Barbieri, 2011, Gas-separation Problems with Membranes: 1–4 p.

Driskill, D.L., 2008, Analyses of natural gases, 2005–2007: Bureau of Land Management, Technical Note 427, 199 p., accessed May 14, 2021

Du, F., and B. Nojabaei, 2019, A review of gas injection in shale reservoirs: Enhanced Oil/Gas recovery approaches and greenhouse gas control: Energies, v. 12, no. 12, doi:10.3390/en12122355.

Dubois, M.K., Byrnes, A.P., Bhattacharya, S., Bohling, G.C., Doveton, J.H., Barba, R.E., 2007. Hugoton Geomodel Final Report, Kansas Geological Survey 2007-06-1.

Duke, M.C., Pas, S.J., Hill, A.J., Lin, Y.S. and Da Costa, J.C.D., 2008, Exposing the molecular sieving architecture of amorphous silica using positron annihilation spectroscopy. Advanced Functional Materials, 18(23), pp.3818-3826.

Dunlap, R.E., 1969, The geology of the Pinta Dome - Navajo Springs helium fields, Apache County, Arizona: Tucson, University of Arizona, M.S. thesis, 73 p.

Dunn, S.S., 1978, Boundary Butte, East: *in* Oil and Gas Fields of the Four Corners Area, Vol. 1, Four Corners Geological Society, p. 70-72.

Dutton, S.P., Garrett Jr., C.M., 1989. PN-13, Pennsylvanian fan-delta sandstone, Anadarko basin. In: Kosters, E.C., Bebout, D.G., Seni, S.J., Garrett Jr., C.M., Brown Jr., L.F., Hamlin, H.S.,

Dutton, S.P., Ruppel, S.C., Finley, R.J., Tyler, N. (Eds.), 2006, Atlas of Major Texas Gas Reservoirs. Gas Research Institute, pp. 146-147.

Dybkjær, I. and Aasberg-Petersen, K., 2016, Synthesis gas technology large-scale applications. The Canadian Journal of Chemical Engineering, 94(4), pp.607-612.

Dyck, W., 1976. The use of helium in mineral exploration. J. Geochem. Explor. 5 (1 - 2), 3 - 20.

Echt, W. I., and M. Singh, 2008, Integration of membranes into natural gas process schemes: GPA Annual Convention Proceedings, v. 2, p. 761–775.

Edison Investment Research, 2020. Helium - Macro View, 21. www.edisongroup.com/wp-content/uploads/2019/ 02/HeliumMacroUpdate2019.pdf .

EERC, 2020, Reduced Gas Flaring: Beyond the Boom, no. 24665, p. 14–15.

Ehinger, R., 2009. High Nitrogen Gas Wells - a Mid-continent Mystery. AAPG, Search and Discovery. Article 90097, Abstract.

Ehrman, M.U., 2014, Lights out in the Bakken: A review and analysis of flaring regulation and its potential effect on North Dakota shale oil production. W. Va. L. Rev., 117, p.549.

Einsele, G., 1991. Sedimentary Basins: Evolution, Facies, and Sediments Budget. Springer-Verlag, p. 792.

Elliot, D., W. R. Qualls, S. Huang, J. J. Chen, R. J. Lee, J. Yao, and Y. Zhang, 2005, Benefits of integrating NGL extraction and LNG liquefaction technology: 2005 AIChE Spring National Meeting, Conference Proceedings, p. 1943–1958.

Elschenbroich, C., 2016, Organometallics. John Wiley & Sons.

Emam, E.A., 2015, Gas flaring in industry: an overview. Petroleum & coal, 57(5).

Emam, E. A., 2015, Gas flaring in industry: An overview: Petroleum and Coal, v. 57, no. 5, p. 532–555.

Emsley, J., 2001. Nature’s Building Blocks. Oxford University Press, Oxford, pp. 175 - 179.

Energy and Environment, Volume 11, no 2, pages 90–95.

Energy Weekly News, 2016, Researchers' Work from University of Tehran Focuses on Energy Research, Advanced exergy analysis of novel flash-based Helium recovery from natural gas processes. 9 Dec. 2016, p. 538. Gale OneFile: News, link.gale.com/apps/doc/A472588587/STND?u=ndacad_58202zund&sid=bookmark-STND&xid=ab69db36. Accessed 11 July 2021.

Energy Weekly News., 2018, New Energy Data Have Been Reported Investigators at University of Tehran, Process development and sensitivity analysis of novel integrated helium recovery from natural gas processes: Energy Weekly News, p. 4.

Energy, B., 2021, Bakken Energy and Mitsubishi Power Establish Clean Hydrogen. Acquisition of the Great Plains Synfuels Plant in the works.

Energy, B., and N. Dakota, 2021, Bakken Energy plans North Dakota Hydrogen Hub: p. 2–5.

Energy, B., M. P. Americas, B. Energy, B. Energy, and N. D. The, 2021, Bakken Energy, Mitsubishi in blue hydrogen deal: no. 6, June.

Energy, H., 2016, Compendium of Hydrogen Energy, Volume 3: Woodhead Publishing Limited, 238 p., doi:10.1016/c2014-0-02673-1.

Energy, U. D. of, 2019, Hydrogen Production: Natural Gas Reforming How Does It Work? Fuel Cell Technologies Office, p. 1–5.

Engineering, C., 2020, Design and Techno-economic Evaluation of Multi-stage Membrane Processes for Helium Recovery from Natural Gas.

Engineering, N. A. of, 2004, The Hydrogen Economy: The National Academies Press, 256 p., doi:10.17226/10922.

Enrico Drioli, G. B., 2011, Membrane Engineering for the Treatment of Gases: Gas-Separation Problems ... - Google Books: 132 p.

Environmental Defense Fund, 2021, Methane: A Crucial Opportunity in the Climate Fight, www.edf.org/climate/methane-crucial-opportunity-climate-fight

EPA, 1999, Economic Impact Analysis of the Oil and Natural Gas Production Neshap and the Natural Gas Transmission and Storage Neshap: 1–160 p.

EPCM, 2021. https://epcmholdings.com/process-technologies-for-helium-recovery-from-natural-gas-a-review/

Eppink, J., Heidrick, T.L., Alvarado, R., Marquis, M., 2014. Subsurface Sources of CO_2 in the Contiguous United States. National Energy Technology Laboratory. DOE/NETL-2014/1637, 90 p.

Etherington, J.R. and Ritter, J.E., 2007, The 2007 SPE/AAPG/WPC/SPEE Reserves and Resources Classification, Definitions and Guidelines. Defining the Standard! In Hydrocarbon Economics and Evaluation Symposium. OnePetro.

Etiope, G., 2018, Natural gas: Encyclopedia of Earth Sciences Series, p. 961–965, doi:10.1002/14356007.a17_073.pub2.

Everett, M.A., 2012. The Precambrian Petroleum Systems of Eastern Siberia: Evidence from Oil Geochemistry and Basin Modeling. American Association of Petroleum Geologists. Search and Discovery Article 10433, 19 p.

Evonik, 2011, SEPURAN® Noble Membrane technology for helium and hydrogen generation: 1–6 p.

Exterran, 2015, C200 Cryogenic Gas Processing System: 4 p.

Faheem, H.H., Tanveer, H.U., Abbas, S.Z. and Maqbool, F., 2021, Comparative study of conventional steam-methane-reforming (SMR) and auto-thermal-reforming (ATR) with their hybrid sorption enhanced (SE-SMR & SE-ATR) and environmentally benign process models for the hydrogen production. Fuel, 297, p.120769.

Fahim, M. A., T. A. Alsahhaf, and A. Elkilani, 2010, Acid Gas Processing and Mercaptans Removal, in M. A. Fahim, T. A. Alsahhaf, and A. Elkilani, eds., Fundamentals of Petroleum Refining: Amsterdam, Elsevier, p. 377–402, doi:10.1016/b978-0-444-52785-1.00015-2.

Fairhead, J.D., and C.M. Green, 1989, Controls on Rifting in Africa and the Regional Tectonic Model for the Nigeria and East Niger Rift Basins, *in* B. Rosendahl (ed.), African Rifting, Journal of African Earth Science, Special Publications, v. 8, p. 231-249.

Feda, 2021. Pressure Swing Adsorption: Gas Separation and Purification. In: https://fedanitrogen.com/wp-content/ uploads/2018/09/Pressure-Swing-Adsorption-A-Gas-Separation-Purification-Process.pdf.

Feng, H., H. Zhang, and L. Xu, 2007, Polymeric membranes for natural gas conditioning: Energy Sources, Part A: Recovery, Utilization and Environmental Effects, v. 29, no. 14, p. 1269–1278, doi:10.1080/00908310600623611.

Ferreira-Aparicio, P., M. J. Benito, and J. L. Sanz, 2005, New trends in reforming technologies: From hydrogen industrial plants to multifuel microreformers: Catalysis Reviews - Science and Engineering, v. 47, no. 4, p. 491–588, doi:10.1080/01614940500364958.

Ferri, F., Hickin, A.S. and Reyes, J., 2012, Horn River basin–equivalent strata in Besa River Formation shale, northeastern British Columbia (NTS 094K/15); in Geoscience Reports

Finn, A., 2007, Rejection strategies: Hydrocarbon Engineering, v. 12, no. 10, p. 49–52, doi:10.1007/978-3-319-24612-3_302215.

Fisher, K.S, et al. 1995, Glycol Dehydrator Emission Control Improved. Oil & Gas J. 93 (9): 40.

Fitch, G.J., 2019, System Dynamics Models for the Valuation of Real Options in Infrastructure Investments (Doctoral dissertation, Columbia University).

Fitzsimmons, l Paul, 1973, Tertiary igneous rocks of the Navajo County, Arizona, New Mexico and Utah, in James, HL., ed., Guidebook of Monument Valley and vicinity, Arizona and Utah: New Mexico Geological Society 24th Field Conference Guidebook, p. 106-109.

Foos, A., 1999. Geology of the Colorado Plateau. Geology Department, University of Akron, National Park Service.

Fortezzoi, C.M., Spudis, P.D., Harrel, S.L., 2020. Release of the Digital Unified Global Geologic Map of the Moon at 1:5,000,000- SCALE. USGS.

Foster, D.A., Mueller, P.A., Mogk, D.W., Wooden, J.L. and Vogl, J.L., 2006, Proterozoic evolution of the western margin of the Wyoming craton: implications for the tectonic and magmatic evolution of the northern Rocky Mountains; Canadian Journal of Earth Sciences, v.43, p.1601-1619.

Foster, R.W., Jensen, J.G., 1972. Carbon Dioxide in Northeastern New Mexico: New Mexico Geological Society, Guidebook to 23rd Field Conference, pp. 192 - 200.

Frangoul, A., 2020, World's First Hydrogen-Powered Passenger Plane Completes Maiden Flight: p. 21–26: <https://observer.com/2020/09/hydrogen-electric-plane-uk-zeroavia-complete-maiden-flight/>.

Franklin, M., Chau, K., Cushing, L.J. and Johnston, J.E., 2019, Characterizing flaring from unconventional oil and gas operations in south Texas using satellite observations. Environmental science & technology, 53(4), pp.2220-2228.

Franseen, E. K., Byrnes, A. P., Cansler, J. R., Steinhauff, D. M., and Carr, T. R., 2004, The Geology of Kansas--Arbuckle Group; in, Current Research inEarth Sciences: Kansas Geological Survey, Bulletin 250, part 2.

Freeman, B., Y. Yampolskii, and I. Pinnau, 2006, Materials Science of Membranes for Gas and Vapor Separation: Wiley, 445 p.

French, J., 2020. Alberta's New Helium Royalties Could See Rise of Extraction Industry, CBC. May 17th. https://www. cbc.ca/news/canada/edmonton/alberta-s-new-helium-royalties-could-see-rise-of-extraction-industry-1.5572451.

Friedrichs, J. and Inderwildi, O.R., 2013. The carbon curse: Are fuel rich countries doomed to high CO_2 intensities? Energy Policy, 62, pp.1356-1365.

Froehlich, P., and J. J. Clausen, 2008, Large scale helium liquefaction and considerations for site services for a plant located in Algeria: AIP Conference Proceedings, v. 985, p. 549–556, doi:10.1063/1.2908596.

Frye, J.C., Byron Leonard, A., 1952. Pleistocene Geology of Kansas. Bulletin 99. State Geological Survey of Kansas, Lawrence, 230 p.

Gadhamshetty, V., Shrestha, N., Chilkoor, G. and Bathi, J.R., 2015, Emerging environmental impacts of unconventional oil development in the Bakken formation in the Williston Basin of Western North Dakota. In Hydraulic Fracturing: Environmental Issues (pp. 151-180). American Chemical Society.

Gage, B.D., and Driskill, D.L., 1998, Analyses of Natural Gases, 1996–1997: Bureau of Land Management, Technical Note 404, 71 p., accessed May 14, 2021

Gage, B.D., and Driskill, D.L., 2003, Analyses of Natural Gases, 1998–2001: Bureau of Land Management, Technical Note 412, 173 p., accessed May 14, 2021

Gage, B.D., and Driskill, D.L., 2005, Analyses of Natural Gases, 2002–2004: Bureau of Land Management, Technical Note 418, 243 p., accessed May 14, 2021

Gage, B.D., and Driskill, D.L., 2019, Analyses of Natural Gases, 2002–2004: Bureau of Land Management, Technical Note 418, 243 p., accessed May 14, 2021

Gage, B.D., Driskill, D.L., 2003. Analysis of Natural Gas 1998 - 2001. Technical Note 412. USBLM, p. 179.

Gage, B.D., Driskill, D.L., 2004. Helium Resources of the United States - 2003. Technical Note 415. USBLM, p. 42.

Gage, B.D., and Driskill, D.L., 2005, Analyses of Natural Gases, 2002–2004: Bureau of Land Management, Technical Note 418, 243 p., accessed May 14, 2021

Gallant, C., 2021, Helium Industry Begins to Take off. Medicine Hat News. August 10th. https://medicinehatnews. com/news/local-news/2021/06/22/helium-industry-begins-to-take-off/.

Gao, D., Shumaker, R.C., 1996. Subsurface geology of the Warfield structures in southwestern West Virginia: Implications for tectonic deformation and hydrocarbon exploration in the Central Appalachian Basin. Am. Assoc. Petrol. Geol. Bull. 80 (8), 1242 - 1261.

Garbarino, G., F. Pugliese, T. Cavattoni, G. Busca, and P. Costamagna, 2020, A study on CO_2 methanation and steam methane reforming over commercial Ni/calcium aluminate catalysts: Energies, v. 13, no. 11, doi:10.3390/en13112792.

Garvey, M., 2012, Waiting for the light at the end of the tunnel: the worldwide helium market; CryoGas International, October 2012.

Garvin, R.F., 1978. Slick Rock Dakota. In: Fassett, J.E., Thomaidis, N.D., Matheny, M.L. (Eds.), Oil and Gas Fields of the Four Corners Area, Four Corners Geological Society, vol. III, pp. 497-499.

Gary, J.H., Handwerk, G.E., 1984. Petroleum Refining Technology and Economics. CRC Press, p. 488.

Gavshin, V. M.; Zakharov, V. A., 1996, "Geochemistry of the Upper Jurassic-Lower Cretaceous Bazhenov Formation, West Siberia. Economic Geology. **91** (1, 122–133. doi:10.2113/gsecongeo.91.1.122. Retrieved April 1, 2013.

Geldon, A.L., 2003. Geology of Paleozoic rocks in the upper Colorado River Basin. In: Arizona, Colorado, New Mexico, Utah and Wyoming, Excluding the San Juan Basin, USGS, Professional Paper (1114A), p. 112.

Gendler, I., 2018, Isaac's science blog: Natural Gas Reforming: p. 22–23.

Geoscience Australia, 2021a, www.ga.gov.au/scientific-topics/energy/province-sedimentary-basin-geology/petroleum/offshore-southern-australia/otway .

Geoscience Australia, 2021b, www.ga.gov.au/scientific-topics/energy/province-sedimentary-basin-geology/petroleum/offshore-southern-australia/gippsland#heading-4.

Gerhard, L.C., 2004. A new look at an old petroleum province: Kansas Geological Survey, Current Research in Earth Sciences. Bulletin 250 (1), 27.

Gerling, C.R., 1983. McElmo Dome Leadville carbon dioxide field, Colorado. In: Fassett, J.E. (Ed.), Oil and Gas Fields of the Four Corners Area, vol. III. Four Corners Geological Society, pp. 735 - 739.

GeTech, 2002. The Basin Development of Arabia, Non-exclusive Study. Gilfillan, S.M., 2006. Deep Magmatic Degassing and the Colorado Plateau Uplift. University of Manchester (Ph.D. thesis), 141 p.

Gherabati, S. A., H. S. Hamlin, K. M. Smye, R. L. Eastwood, F. R. Male, and G. McDaid, 2019, Evaluating hydrocarbon-in-place and recovery factor in a hybrid petroleum system: Case of Bakken and three forks in North Dakota: Interpretation, v. 7, no. 3, p. T607–T624, doi:10.1190/int-2018-0213.1.

Ghorbani, B., and M. Amidpour, 2021, Energy, exergy, and sensitivity analyses of a new integrated system for generation of liquid methanol, liquefied natural gas, and crude helium using organic Rankine cycle, and solar collectors: Journal of Thermal Analysis and Calorimetry, doi:10.1007/s10973-021-10659-9.

Ghorbani, B., M. H. Hamedi, and M. Amidpour, 2016, Development and optimization of an integrated process configuration for natural gas liquefaction (LNG) and natural gas liquids (NGL) recovery with a nitrogen rejection unit (NRU): Journal of Natural Gas Science and Engineering, v. 34, p. 590–603, doi: 10.1016/j.jngse.2016.07.037.

Ghori, K.A.R., Craig, J., Thusu, B., Lüning, S. and Geiger, M., 2009, Global Infracambrian petroleum systems: a review. Geological Society, London, Special Publications, 326(1), pp.109-136.

Gibson, R.I., 1995, Basement tectonics and hydrocarbon production in the Williston Basin: An interpretive overview: 7th Int’l. Williston Basin Symposium, 1995 Guidebook, p. 3-11

Giggenbach, W.F., 1996. Chemical composition of volcanic gases. In: Scarpa, R., Tilling, R.I. (Eds.), Monitoring and Mitigation of Volcanic Hazards. Springer- Verlag, Berlin, pp. 221 - 256.

Giggenbach, W.F., Sano, Y., Schminke, H.U., 1991, CO_2-rich gases from Lakes Nyos and Monoun, Cameroon, Laacher See, Germany: Dieng, Indonesia; and Mt. Gambier, Australia - variations on a common theme. J. Volcanol. Geoth. Res. 45 (3 - 4), 311 - 323.

Gilat, A. and Vol, A., 2005, Primordial hydrogen-helium degassing, an overlooked major energy source for internal terrestrial processes. HAIT Journal of Science and Engineering B, 2(1-2), pp.125-167.

Gilfillan, S.M., 2006, Deep Magmatic Degassing and the Colorado Plateau Uplift. University of Manchester (Ph.D. thesis), 141 p.

Gilfillan, S.M.V., Ballentine, C.J., Holland, G., Blagburn, D., Lollar, B.S., Stevens, S., Schoell, M., Cassidy, M., 2008. The noble gas geochemistry of natural CO_2 gas reservoirs from the Colorado Plateau and Rocky Mountain provinces, USA. Geochim. Cosmochim. Acta 72, 1174-1198.

Go, KS, Son, SR, Kim, SD, Kang, KS, Park, CS., 2009, Hydrogen production from two-step steam methane reforming in a fluidized bed reactor. International journal of hydrogen energy. Feb 1;34(3):1301-9.

Goff, W.T., Hundley-Goff, E., 2014. Spelunker Field. In: Rogers, J.P., Milne, J.J., Cumella, S.P., Dubois, D.P., Lillis, P.G. (Eds.), Oil and Gas Fields of Colorado. Rocky Mountain Association of Geologists, pp. 335-338.

Gold, T., and M. Held, 1987, Helium-nitrogen-methane systematics in natural gases of Texas and Kansas: Journal of Petroleum Geology, v. 10, no. 4, p.415- 424.

Gomes, V.G. and Yee, K.W., 2002, Pressure swing adsorption for carbon dioxide sequestration from exhaust gases. Separation and purification technology, 28(2), pp.161-171.

Gorham, F.D., 1975. Tectogenesis of the central Colorado Plateau Aulacogen. In: Four Corners Geological Society - Canyonlands Country, Eighth Field Conference, 1975, Four Corners Geological Society, 8th Field Conference, pp. 211 - 216.

Grande, C. A., 2012, Advances in Pressure Swing Adsorption for Gas Separation: ISRN Chemical Engineering, v. 2012, p. 1–13, doi:10.5402/2012/982934.

Grandinetti, F., 2018, Noble Gas Chemistry: Structure, Bonding, and Gas-Phase Chemistry. John Wiley & Sons.

Grassberger, M., Krauskpf, A., 2007. Suicidal asphyxiation with helium: report of three cases. Wien Klin Wochenschr v 119, 323 - 325.

Graupner, T., Niedermann, S., Kempe, U., Klemd, R., Bechtel, A., A., 2006. Origin of ore fluids in the Muruntau gold system: constraints from noble gas, carbon isotope and halogen data. Geochem. Cosmochim. Acta 70 (21), 5356 - 5370.

Greenwood, N.N., Earnshaw, A., 1997. Chemistry of the Elements. Butterworth-Heinemann, p. 1364.

Grilly, E.R., 1973. Pressure-volume-temperature relations in liquid and solid ^{4}He. J. Low Temp. Phys. 11 (1 - 2), 33 - 52.

Greggs, D.H. (2000, The stratigraphy, sedimentology, and structure of the lower Paleozoic Deadwood Formation of western Canada; M.Sc. thesis, University of Calgary, Calgary, Alberta, 349p.

Groat, C.G., Richardson, R.C., Beebe, R.R., Campbell, J.R., Chan, M.H., Chermak, J.M., Dahl, C.A., Elam, T., Goldman, A.M., Hartness, N.E. and Lee, W.J., 2010. Selling the Nation's Helium Reserve.

Grynia, E., and P. J. Griffin, 2017, Helium in Natural Gas - Occurrence and Production: Journal of Natural Gas Engineering, v. 1, no. 2, p. 163–215, doi:10.7569/jnge.2016.692506.

GTI, 2021, Micro-Scale High Efficiency Steam Methane Reformer (SMR): p. 10–12.

Guangya, J., 2019. Tectonic Evolution and Hydrocarbon Distribution of Basins in Africa. American Association of Petroleum Geologists. Search and Discovery Article #30602.

Guerra, M., Lombardi, S., 2001. Soil-gas Method for Tracing Neotectonic Faults in Clay Basins: The Pisticci Field (Southern Italy).

Guilford, M.C., Hall, C.A., O'Connor, P. and Cleveland, C.J., 2011, A new long-term assessment of energy return on investment (EROI) for US oil and gas discovery and production. Sustainability, 3(10), pp.1866-1887.

Gupta, R. B., ed., 2009, Hydrogen fuel. Production, Transport, Storage: CRC Press - Taylor and Francis, 626 p.

Gupta, S.K., Gupta, A.B., Gupta, R., 2017. Pathophysiology of nitrate toxicity in humans in view of the changing trends of the global nitrogen cycle with special reference to India. In: The Indian Nitrogen Assessment, Sources of Reactive Nitrogen, Environmental and Climate Effects, Management Options, and Policies, pp. 459 - 468.

Haab, T., 2013, Env-Econ 101: Hotelling's Rule Part 1, Environmental Economics, https://www.env-econ.net/2013/12/env-econ-101-hotellings-rule-.html, accessed April 12, 2022.

Hadden, R., 2003, Hydrogen production: p. 71–72, doi:10.1002/9781119707875.ch12. From https://www.e-education.psu.edu/fsc432/content/hydrogen-production, Accessed 09-2021.

Haider, S., M. Saeed, A. Lindbråthen, and M. B. Hägg, 2019, Techno-economic evaluation of helium recovery from natural gas; A comparison between inorganic and polymeric membrane technology: Journal of Membrane Science and Research, v. 5, no. 2, p. 126–136, doi:10.22079/JMSR.2018.87998.1196.

Haines, P.W., and Allen, H.J., 2019, Hydrocarbon and helium prospectivity of the Amadeus and Murraba basins in Western Australia. In: Keep, M., Moss, S.J. (Eds.), The Sedimentary Basins of Western Australia V: Proceedings of the Petroleum Exploration Society of Australia Symposium, Perth, WA, 2019, 17 p.

Halabi, M. H., M. H. J. M. de Croon, J. van der Schaaf, P. D. Cobden, and J. C. Schouten, 2008, Modelling and analysis of autothermal reforming of methane to hydrogen in a fixed bed reformer: Chemical Engineering Journal, v. 137, no. 3, p. 568–578, doi:10.1016/j.cej.2007.05.019.

Halbertsma, H.L., Mossop, G.D. and Shetsen, I., 1994. Devonian Wabamun Group of the western Canada sedimentary basin. Geological Atlas of the Western Canada Sedimentary Basin, 4, pp.203-220.

Hale, P., and K. Lokhandwala, 2020, Advances in Membrane Materials Provide New Gas Processing Solutions: p. 1–27: <https://www.mtrinc.com/wp-content/uploads/2018/08/GPA2004FinalPres.pdf>.

Halford, D.T., 2018. Isotopic Analysis of Helium from Wells Located in the Four Corners Area, Southwestern US, Colorado School of Mines PHD Dissertation, 376 p.

Hall, G. L., 2011, Helium recovery: Hydrocarbon Engineering, v. 16, no. 1, p. 55–58, doi:10.1016/0958-2118,93,90075-w.

Hall, G. L., 2016, Nitrogen Rejection with Integrated High NGL Extraction: p. 1: http://www.bloomberg.com/energy, accessed 10-2021.

Hall, M., 2003, Nitrogen rejection: Hydrocarbon Engineering, v. 8, no. 5, p. 52–57, doi:10.1201/b14397-20.

Halford, D.T., 2018, Isotopic analyses of helium from wells located in the Four Corners area, Southwestern, US. Colorado School of Mines. p.89

Hamak, J.E., 2020. Helium, USGS, Minerals Yearbook. https://prd-wret.s3-us-west-2.amazonaws.com/assets/palladium/production/atoms/files/myb1-2016-helium.pdf .

Hamak, J.E., and Sigler, S.M., 1991, Analyses of Natural Gases, 1986–1990: U.S. Bureau of Mines, Information Circular 9301, 315 p., accessed May 14, 2021

Hamak, J.E., and Gage, B.D., 1992, Analyses of Natural Gases, 1991: U.S. Bureau of Mines, Information Circular 9318, 97 p.

Hamak, J.E., and Sigler, S.M., 1993, Analyses of Natural Gases, 1992: U.S. Bureau of Mines, Information Circular 9356, 62 p., accessed May 14, 2021

Hamak, J.E., and Driskill, D.L., 1996, Analyses of Natural Gases, 1994–1995: U.S. Bureau of Land Management, Technical Note 399, 70 p., accessed May 14, 2021

Hamak, J.E., Gage, B.D., 1992. Analyses of Natural Gases, 1991. IC9318, p. 97.

Hamak, J.E., Sigler, S., 1989. Analyses of Natural Gases, 1988. IC 9225. USBM, p. 66.

Hamak, J.E., Sigler, S., 1990. Analyses of Natural Gases, 1989. IC 9256. USBM, p. 60.

Hamak, J.E., Sigler, S., 1991a. Analyses of Natural Gases, 1990. IC 9290. USBM, p. 56.

Hamak, J.E., Sigler, S., 1991b. Analyses of Natural Gases, 1991. IC 9301. USBM, p. 315.

Hamak, J.E., Sigler, S.M., 1993. Analyses of Natural Gases, 1992. IC 9356. USBM, p. 62.

Hamal, J.E., Driskill, D.L., 1996. Analysis of Natural Gases - 1994 - 1995. USBLM Technical Note 399, 76 p.

Hamedi, H., Karimi, I.A. and Gundersen, T., 2019, A novel cost-effective silica membrane-based process for helium extraction from natural gas. Computers & Chemical Engineering, 121, pp.633-638.

Hamid, U.; Rauf, A.; Ahmed, U.; Shah, M.S.A.S.; Ahmad, N., 2020, Techno-economic assessment of process integration models for boosting hydrogen production potential from coal and natural gas feedstocks. Fuel https://doi.org/10.1016/j.fuel.2020.117111

Hamlin, H. Scott, Smye, Katie, Dommisse, Robin, Eastwood, Ray, Lemons, Casee R., and Guinevere McDaid, 2017, Geology and Petrophysics of the Bakken Unconventional Petroleum System. Paper presented at the SPE/AAPG/SEG Unconventional Resources Technology Conference, Austin, Texas, USA, July 2017. doi: https://doi.org/10.15530/URTEC-2017-2670679

Hammond, C.R., 2000. The Elements. In: Handbook of Chemistry and Physics, 81st ed. CRC

Hampel, C.A., 1968. The Encyclopaedia of the Chemical Elements. New York: Van Nostrand

Han, G., Han, W.S., Kim, K.-Y., Park, J.G., Piao, J., Yun, T.K., 2019. Role of fault structures and regional formations on CO_2 migration and distribution in shallow saline aquifer in Green River, Utah. J. Hydrol. 570, 786 - 801.

Handley, J.R., and W.C. Miller, 1992, Process Requirements and Enhanced Economics of Helium Recovery from Natural Gas." Paper presented at the SPE Mid-Continent Gas Symposium, Amarillo, Texas, April 1992. doi: https://doi.org/10.2118/24292-MS

Hanson, M.C., Oze, C., Horton, T.W., 2014. Identifying blind geothermal systems with soil CO2 surveys. Appl. Geochem. 50, 106 - 114.

Harris, S., and H.S. Bailey, Jr., 1977, What's So Funny About Science? Cartoons from American Scientist, Wm. Kaufman, 120 p., ISBN 0913232394

Hatfield, J.L., Follett, R.F., 2008. Nitrogen in the Environment. Academic Press, p. 720.

Hausfather, Z., 2008, The Water Vapor Feedback: Yale Climate Connections, p. 1–3.

Häussinger, P, Glatthaar, R, Rhode, W, Kick, H, Benkmann, C, Weber, J, Wunschel, HJ, Stenke, V, Leicht, E and Stenger, H, 2005, Noble gases, in: Ullmann's Encyclopedia of Industrial Chemistry, G. Walter, editor, Wiley-VCH Weinheim, Baden-Wärttemberg, Germany.

Hawkins, C.M., Baugh, R.A., 2006. Madden Field: a growing giant in the Wind River Basin, Wyoming, Rocky Mountain Association of Geologist. Mt. Geol. 43 (3), 177-180.

Haynes, A., 2019, The difference between green hydrogen and blue hydrogen: Petrofac, p. 3.

Heath, J.E., Lachmar, T.E., Evans, J.P., Kolesar, P.T., Williams, A.P., 2009. Hydrogeochemical characterization of leaking, carbon dioxide-charged fault zones in East-Central Utah, with implications for geologic carbon storage. Geophys. Monogr. 183, 147 - 158.

Heaton, T.H.E., 1984. Rates and sources of 4He accumulation in groundwater. Hydrol. Sci. J. 29 (1), 29 - 47.

Hector, S., Conrad, G., Blake, K.E., April 19 - 25, 2013. Robbins gas field: a low BTU, nitrogen rich gas accumulation. In: 2013 Pacific Section AAPG, SPE and SEPM Joint Technical Conference, Monterey, California. AAPG, Search and Discovery. Article #90162.

Hedman, E.R., 2006. A Fascinating Hour with Gerald Kulcinski, the Space Review.

Heindl, L.A., 1952, Occurrence of helium in northeastern Arizona: Geological Society of America Bulletin, v. 63, no. 12, pt. 2, p. 1331.

Helium One, 2017, Technical Presentation, June 2017.

Helmenstine, A., 2020, What is the most abundant element in the earth's crust? Science Notes, p. 10–16.

Henderson, L.B., 1985. Rudyard field. In: Montana Geological Society Oil and Gas Fields Symposium, vol. 2, pp. 995-998.

Hendry, M.J., Kotzer, T.G., Solomon, D.K., 2005. Sources of radiogenic helium in a clay till aquitard and its use to evaluate the timing geologic events. Geochimica et Cosmochimica Acta 69 (2), 475 - 483.

Henshaw, D.B., 1958. Structure of solid helium by neutron diffraction. Phys. Rev. Lett. 109 (2), 328 - 330.

Herbaly, E., 1973. Petroleum Geology Sweetgrass Arch, Alberta, Wyoming Geological Association, Earth Science Bulletin March, 21 p.

Hernandez-Valencia, V. N., M.W. Hlavinka, and J.A. Bullin, 1992, Design Glycol Units for Maximum Efficiency. Proceedings of the Seventy-First Gas Processors Association Annual Convention. Tulsa, OK: 310–317

Herrera, H., 2013, a Petroleum System Study of the Cratonic Williston Basin in North Dakota, USA.: The Role of the Laramide Orogeny: University of Houston, 177 p.

Hertweck Jr., F.R., Fox, D.D., 1984. Analyses of Natural Gases, 1983. IC 8993. USBM, p. 127.

Heyer, L., 2021, Live at 2 PM: A hydrogen hub is a big deal for North Dakota; Listen to the discussion: p. 7.

Hill, C.A., 1990, Sulfuric Acid Speleogenenesis of Carlsbad Cavern and its Relationship to Hydrocarbons, Delaware Basin, New Mexico and Texas, vol. 74. AAPG, Bull v, pp. 1685 - 1694 (11).

Hills, J.M., 1968. Gas in Delaware and Val Verde Basin, West Texas and Southeastern New Mexico, Association of Petroleum Geologists, Natural Gases of North America, Volume Two, M9, pp. 1394 - 1432.

Himmelstein, S., 2021, A more efficient SMR method for hydrogen production: Engineering 360, p. 1–2.

Hinze, W.J., D.J. Allen, L.W. Braile, and J. Mariano, 1997, The Mid-Continent Rift System: A Major Proterozoic Continental Rift, *in* R.W. Ojakangas, A.B. Dickas, and J.C. Green (eds.), Middle Proterozoic to Cambrian Rifting, Central North America: Geological Society of America Special Paper 312, p. 7-35.

Hitchon, B., 1963, Geochemical Studies of Natural Gas: Technology, v. No. 226, no. 226, p. 100–117.

Hiyagon, H., Kennedy, B.M., 1992. Noble gases in CH_4-rich gas fields, Alberta, Canada. Geochem. Cosmochim. Acta 56 (4), 1569 - 1589.

Hodgin, J. and Harrell, D.R., 2007, Assessment of World Petroleum Supply Enhanced by New Industry Resources Definitions. In Offshore Technology Conference. OnePetro.

Hoefs, J., 2004. Stable Isotope Geochemistry. Springer Verlag, pp. 1 - 244.

Holland, G., Gilfillan, S.M.V., 2013. Application of noble gases to the viability of CO_2 storage. In: Burnard, P. (Ed.), The Noble Gases as Geochemical Tracers, Advances in Isotopic Geochemistry. Springer-Verlag, pp. 177 - 223.

Holland, H.D., Turekian, K.K., 2011. Radioactivity Geochronometry: from the Treatise on Geochemistry. Academic Press, pp. 1 - 267.

Holland, P.W., Emerson, D.E., 1979. Helium in Ground Water and Soil Gas in the Vicinity of Bush Dome reservoir, Cliffside Field, Potter County, Texas, US Bureau of Mines, 22p.

Holling, Bernd & Kandziora, Christine & Ritter, Roland, 2013, CO2 Recovery from Industrial Hydrogen Facilities and Steel Production to Comply with Future European Emission Regulations. Energy Procedia. 37. 7221-7230. 10.1016/j.egypro.2013.06.660.

Holloway, J.M., Dahlgren, R.A., 2002. Nitrogen in rock: occurrences and biochemical implications. Glob. Biochem. Cycl. 16 (14), 17p.

Holmquest, H.J., 1965. Deep Pays in Delaware-Val Verde Basins, AAPG, Memoir, Fluids in Subsurface Environments, M4, pp. 257 - 279.

Holzner, C.P., McGinnis, D.F., Schubert, C.J., Kipfer, R., Imboden, D.M., 2008. Noble gas anomalies related to high-intensity methane gas seeps in the Black Sea. Earth Planet Sci. Lett. 265 (3), 396 - 409.

Honda, M., McDougall, I., Patterson, D.B., Doulgeris, A., Clague, D.A., 1991. Possible Solar Noble-gas Component in Hawaiian Basalts, vol. 349, pp. 149 - 151.

Hoppe, W.F., 1978. Table Mesa Mississippian (Gas), Table Mesa Pennsylvanian “C”. In: Fassett, J.E. (Ed.), Four Corners Geological Society, Oil and Gas Fields of the Four Corners Area, vol. III, pp. 1,046-1049.

Hosseini, S.S., 2009, Membranes and Materials for Separation and Purification Hydrogen and Natural Gas, Department of Chemical engineering and Biomolecular Engineering, National University of Singapore. https://transtextreating.com/equipments/amine-plants/, 2021, webpage accessed 09-2021.

Hotelling, H., 1931, The economics of exhaustible resources. The Journal of Political Economy, 39(2), 137–175.

Huang, B., Tian, H., Huang, H., Yang, J., Xiao, X., Li, L., 2015. Origin and accumulations of CO2 and its natural displacement oils in the continental margin basins, northern South China Sea. Am. Assoc. Petrol. Geol. 99 (7), 1349 - 1369.

Huang, B., Xiao, X., Zhu, W., 2004. Geochemistry, Origin, and Accumulations of CO2 in Natural Gases of the Yinggehai Basin, Offshore S. China Sea, vol. 88. AAPG, pp. 1277 - 1293 (9).

Hulston, J.R., Hilton, D.R., Kaplan, I.R., 2001. Helium and carbon isotope systematics of natural gases from Taranaki Basin, New Zealand. Appl. Geochem. 16, 419 - 436.

Hunt, J.M., 1996, Petroleum Geochemistry and Geology, Second Edition; W.H. Freeman and Company, New York, 743p.

Hurst, A., 2017. Light Gas Supports Heavy Mission. AMRDEC Public Affairs. October 17th. https://www.army.mil/ article/195211/light_gas_supports_heavy_mission .

Hutcheon, I., 1999. Controls on the distribution of non-hydrocarbon gases in the Alberta basin. Can. Petrol. Soc. Bull. 47 (4), 573 - 593.

Hydrogen Energy, 2006, Hydrogen stations: p. 1–6: <http://hydrogen-navi.jp/en/station/index.html>.

Hydrogen Energy, 2016, Compendium of Hydrogen Energy, Volume 3: Woodhead Publishing Limited, 238 p., doi:10.1016/c2014-0-02673-1.

Ibsen, K., 2015, Equipment design and cost estimation for small modular biomass systems, synthesis gas cleanup and oxygen separation equipment Title: NERL subcontract report, no. May.

Ikpeze, O.V., Osaro, E. and Ikpeze, N.G., 2016, Analysis of Energy Sources, Impact on Environment and Sustainable Development Referencing Landmark Cases in the USA, South Africa and Nigeria. Journal of Environment and Earth Science, 5(18).

Iledare, O.O., 2014, Upstream petroleum economic analysis: balancing geologic prospectivity with progressive, stable fiscal terms and instruments. The Way Ahead, 10(01), pp.28-30.

Inhabitat, 2010, https://inhabitat.com/worlds-first-solar-powered-blimp-set-to-cross-the-english-channel/.

Integrated Flow Solutions, 2016, Benefits of Membrane Element vs. Amines for Conditioning Natural Gas - Integrated Flow Solutions: 4 p.

Integrated Flow Solutions, I., 2021, Fuel Gas Conditioning Membrane Package: p. 5.

International Energy Agency, 2021, Pathway to Critical and Formidable Goal of Net-Zero Emissions by 2050 is Narrow but Brings Huge Benefits, according to IEA Special Report. www.iea.org/news/pathway-to-critical-and-formidable-goal-of-net-zero-emissions-by-2050-is-narrow-but-brings-huge-benefits

Irwin, J.S., 1923. Oil and Gas Possibilities of Eastern Alberta, American Association of Petroleum Geologists. Bulletin 7 (2), 147 - 158.

Ismail, A. F., K. C. Khulbe, and T. Matsuura, 2015, Gas separation membranes: Polymeric and inorganic: 1–331 p., doi:10.1007/978-3-319-01095-3.

Iulianelli, A. and Drioli, E., 2020, Membrane engineering: Latest advancements in gas separation and pre-treatment processes, petrochemical industry and refinery, and future perspectives in emerging applications. Fuel Processing Technology, 206, p.106464.

Jack, J., Lo, J., Maness, P.C. and Ren, Z.J., 2019, Directing *Clostridium ljungdahlii* fermentation products via hydrogen to carbon monoxide ratio in syngas. Biomass and Bioenergy, 124, pp.95-101.

Jacobs, E.K., 1998. Non-hydrocarbon and Hydrocarbon Gas Association with Hydrocarbon Associations with Hydrocarbon Reservoirs along the Las Animas Arch, Southeastern Colorado. Colorado School of Mines (MS thesis), 206 p.

Jadhao, J.S. and Thombare, D.G., 2013, Review on exhaust gas heat recovery for IC engine. International Journal of Engineering and Innovative Technology (IJEIT) Volume, 2.

Jahn, F., Cook, M. and Graham, M., 2008, Petroleum economics. Developments in Petroleum Science, 55, pp.337-364.

Jahn, J., W. A. P. Van Den Bos, and L. J. P. Van Den Broeke, 2012, Evaluation of membrane processes for acid gas treatment: SPE Production and Operations Symposium, Proceedings, v. 2, p. 1063–1070, doi:10.2118/157281-ms.

Jakobsen, D., and V. Atland, 2017, Concepts for Large Scale Hydrogen Liquefaction Plants: Norwegian University of Science and Technology, 156 p.

Jamasmie, C., June 11, 2019. India Unveils Spacecraft that Will Look for Energy Sources on the Moon, Education Energy Asia Canada Europe Gold Rare Earth. https://www.mining.com/india-unveils-spacecraft-that-will-lookfor-water-energy-sources-in-the-moon/ .

James, B. D., D. A. DeSantis, and G. Saur, 2016, Final Report: Hydrogen Production Pathways Cost Analysis (2013 – 2016): DOE-StrategicAnalysis-6231-1, no. September, p. 55.

James, T.C., 1967. Thermal springs in Tanzania. Trans. Appl. Earth Sci. 76 (section B), B1 - B18.

Janssen, J., 2018, Steam Methane Reforming, MR for Hydrogen Production: 2 p.

Jaremko, G., 2020. Albert’s Helium Industry Ballooning as Prices Soar Far Above Natural Gas, Natural Gas Intel, May 20th. https://www.naturalgasintel.com/albertas-helium-industry-ballooning-as-prices-soar-far-above-naturalgas/.

Jean, E., 2021, North Dakota could be largest, lowest cost producer of blue hydrogen in North America: p. 4.

Jenden, P. D., K. D. Newell, I. R. Kaplan, and W. L. Watney, 1988, Composition and stable-isotope geochemistry of natural gases from Kansas, Midcontinent, USA: Chemical Geology, v. 71, p. 117-147.

Jenden, P.D., Kaplan, I.R., 1989, Analysis of Gases in the Earth's Crust. Global Geochemistry Corp (Chapter 9), 44pp.

Jenden, P.D., Kaplan, I.R., Poreda, R.J., Craig, H., 1988, Origin of nitrogen-rich natural gases in the California Great Valley, evidence from helium, carbon and nitrogen isotope ratios. Geochem. Cosmochim. Acta 52 (4), 851 - 861.

Jenden, P.D., Newell, K.D., Kaplan, I.R., Watney, W.L., 1988. Composition and stable-isotope geochemistry of natural gases from Kansas, Midcontinent, U.S.A. Chem. Geol. 71, 117 - 147.

Jenkins, S., 2015, Hydrogen production from natural gas: Chemical Engineering, v. 122, no. 5, p. 48.

Jensen, G.K.S., 2015, Trace element and other analyses of Paleozoic-aged brines in southeastern Saskatchewan (Townships 1 to 13, Ranges 5 to 21 W2M); Saskatchewan Ministry of the Economy, Saskatchewan Geological Survey, Data File Report 37.

Jin, H., and S. A. Sonnenberg, 2013, Characterization for source rock potential of the Bakken shales in the Williston Basin, North Dakota and Montana: Unconventional Resources Technology Conference 2013, URTC 2013, v. 80356, doi:10.1190/urtec2013-013.

Jin, Hui, Sonnenberg, Stephen A., and J. Frederick Sarg, 2015, Source Rock Potential and Sequence Stratigraphy of Bakken Shales in the Williston Basin. Paper presented at the SPE/AAPG/SEG Unconventional Resources Technology Conference, San Antonio, Texas, USA, July 2015. doi: https://doi.org/10.15530/URTEC-2015-2169797

JLENS, 2009. Big Tactical Aerostat Flies for First Time, AMRDEC Public Affairs, April 2nd. https://www.army.mil/ article/19141/big_tactical_aerostat_flies_for_first_time.

Johnson, E.G., 2012. Helium in northeastern British Columbia. In: Geoscience Reports 2013, BC Ministry of Natural Gas Development, pp. 45 - 52.

Johnson, K.S., 1989. Geologic evolution of the Anadarko Basin. In: Johnson, K.S. (Ed.), Anadarko Basin Symposium. Circular 90. Oklahoma Geological Survey, Norman, pp. 3-12.

Joseph, I., E. Anankina, A. Prabhu, G. Grosberg, S. Redmond, and G. Lu, 2020, COVID-19 Dents Demand for Gas and Undermines its Role as a Bridge Fuel in the Energy Transition: S&P Global, p. 1–28.

Joshi, S., K. Lokhandwala, and M. Park, n.d., Reduce Emissions for Compressor Stations in Condensate-rich Shale Gas Plays by Reducing Heavy Hydrocarbons in Fuel Gas: p. 1–17.

Jurisch, A., Kross, B.M., Littke, R., Plessen, B., Lüders, V., Hoth, P., 2007. Concepts and models for the formation of N_2-rich natural gas reservoirs. In: AAPG Hedberg Conference: Basin Modeling Perspectives: Innovative Developments and Novel Applications, May 6 - 9, Search and Discovery, p. 90066.

Kajjumba, S., Emik, A., Ongen, H., Ozcan, K., Aydin, S., 2018. Modelling of Adsorption Kinetic Processes - Errors, Theory and Application. https://doi.org/10.5772/intechopen.80495 (Modelling of Adsorption Kinetic Processes d Errors, Theory and Application | IntechOpen).

Kalamaras, C. M., and A. M. Efstathiou, 2013, Hydrogen Production Technologies: Current State and Future Developments: Conference Papers in Energy, v. 2013, p. 1–9, doi:10.1155/2013/690627.

Kamaruddin, Abd Hamid, M., N. Ibrahim, A. Ibrahim, and A. Ahmad, 2006, Simulation of hydrogen production for mobile fuel cell applications via autothermal reforming of methane: no. July, p. 540–548.

Karol, P.J., 2019. The Legacy of Carbon Dioxide: Past and Present Impacts. Taylor & Francis Group, CRC Press, p. 241.

Katz, D. L., 1969, Source of helium in natural gases: USBM information circular 8417, P.242-255.

Keith, R., 2013. Helium critical supply to Army research, AMRDEC Public Affairs. August, 16th. https://www.army. mil/article/108491/Helium_supply_critical_to_Army_research/ .

Keller, A. B., 2012, NGL 101 - The Basics: NGL 101 - The Basics, Midstream Energy Group. https://www.eia.gov/conference/ngl_virtual/eia-ngl_workshop-anne-keller.pdf. Accessed 10-2021.

Kendrick, F.E., McLaughlin, H.C., 1929. Relation of petroleum accumulation to structure, Petrolia Field, Clay County, Texas. In: American Association of Petroleum Geologists, Structure of Typical American Oil Fields, vol. 2. Special Publication 4, pp. 543 - 555.

Kent, D.M. and Christopher, J.E., 1994, Geological history of the Williston Basin and Sweetgrass Arch; Chapter 27 *in* Geological Atlas of the Western Canada Sedimentary Basin,

Kent, D.M. and Haidl, F.M., 1993, The distribution of Ashern and Winnipegosis strata (Middle Devonian) on the Swift Current Platform, southern Saskatchewan; *in* Summary of Investigations 1993, Saskatchewan Geological Survey, Saskatchewan Energy and Mines, Miscellaneous Report 93-4, p.201-206.

Khalili-Garakani, A., M. Iravaninia, and M. Nezhadfard, 2021, A review on the potentials of flare gas recovery applications in Iran: Journal of Cleaner Production, v. 279, p. 123345, doi:https://doi.org/10.1016/j.jclepro.2020.123345.

Kidnay, A.J., Parrish, W.R., McCartney, D.G., 2019. Fundamentals of Natural Gas Processing. CRC Press, p. 498. Kim, D., 2014. Helium Extraction Form LNG End Flash. MS Thesis. Department of Energy and Process Engineering, Norwegian University of Science and Technology.

Kim, D, 2014, Helium Extraction form LNG End Flash, Department of Energy and Process Engineering, Norwegian University of Science and Technology, 292 p.

Kim, D., and T. Gundersen, 2015, Helium extraction from LNG end-flash: Chemical Engineering Transactions, v. 45, p. 595–600, doi:10.3303/CET1545100.

Kim, J., J. Park, M. Qi, I. Lee, and I. Moon, 2021, Process Integration of an Autothermal Reforming Hydrogen Production System with Cryogenic Air Separation and Carbon Dioxide Capture Using Liquefied Natural Gas Cold Energy: Industrial & Engineering Chemistry Research, v. 60, no. 19, p. 7257–7274, doi:10.1021/acs.iecr.0c06265.

Kipfer, R., Aeschbach-Hertig, W., Peeters, F., Stute, M., 2002. Noble gases in lakes and ground waters. Rev. Mineral. Geochem. 47 (1), 615 - 700.

Kiryukhin V.A., Regional'naya gidrogeologiya (Regional hydrogeology), St. Petersburg: Publ. of St. Peters-burg State Mining Institute (Technical University), 2005, 344 p.

Kita, H., K. Tanaka, and T. Koga, 2008, Gas Separation Membranes: Kobunshi, v. 57, no. 11, p. 894–897, doi:10.1295/kobunshi.57.894.

Klasner, J.S. and King, E.R., 1986, Precambrian basement geology of North and South Dakota. Canadian Journal of Earth Sciences, 23(8), pp.1083-1102.

Kleinspehn, K.L., Paola, C., 1988. New Perspectives in Basin Analysis. Springer-Verlag, p. 453.

Klesman, A., 2019, How did the first element form after the Big Bang? Astronomy, p. 2.

Knapik, E., Kosowski, P. and Stopa, J., 2018, Cryogenic liquefaction and separation of CO_2 using nitrogen removal unit cold energy. Chemical Engineering Research and Design, 131, pp.66-79.

Kohl, A., Nielson, R., 1997. Gas Purification. Gulf Publishing, p. 1408.

Kokorev, V.I.; Darischev, V.I.; Ahmadeyshin, I.A.; Schekoldin, K.A.; Bokserman, A.A. 2013, The Impact of Thermogas Technologies on the Bazhenov Formation Studies Results. Society of Petroleum Engineers. doi:10.2118/166890-MS.

Komissarov, D., 2007, Tupolev Tu-154, the USSR's Medium-Range Jet Airliner, (Hinckley, UK, 2007), 48–50. ISBN 1-85780-241-1.

Konecki, N. Casey, 1967, Natural Gas–A Review of its Occurrence and Potential in Australia and Papua. Paper presented at the 7th World Petroleum Congress, Mexico City, Mexico, April 1967.

Konert, G., Afifi, A.M., Al-Hajri, S.A., Droste, H.J., 2001. Paleozoic stratigraphy and hydrocarbon habitat of the Arabian plate. GeoArabia 6, 407 - 442.

Kontorovich A.A., Kontorovich A.E., Krinin V.A. et al., 1988, Yurubcheno-Tokhomskaya zone of gas and oil accumulation as an important object for concentration of regional investigation and exploration operations in Upper Proterozoic of Lena-Tunguska oil and gas province (In Russ.), Geologiya i geofizika, no. 11, pp. 45–55.

Kontorovich A.E., Izosimova A.N., Kontorovich A.A. et al., 1996, Geological structure and conditions of the formation of the the Yurubcheno-Tokhoma zone of oil and gas accumulation in the Upper Proterozoic of the Siberian platform (In Russ.), Geologiya i geofizika, no. 8 (37), pp. 166–195.

Kornbluth, P., 2015, Evolution of the global helium business— 1990–2015. Cornwall, UK: CryoGas International, September (pp. 34–36). Retrieved January 12, 2016, from http://www.kornbluthheliumconsulting.com/images/CryoGasArticle-Final.pdf.

Kornbluth, P., 2016, Helium—A market update. Cornwall, UK: gasworld.com Ltd., January 6 (pp. 38–41). Retrieved January 12, 2016, from http://www.kornbluthheliumconsulting.com/images/HeUpJan16.pdf.

Kornbluth, P., 2017a, Helium Extraction Act of 2017 aims to ease the path to new US sources. Cornwall, UK: gasworld.com Ltd., June 22. Retrieved July 27, 2017, from https://www.gasworld.com/helium-extraction-act-of-2017-aims-to-boost-sourcing/2013006.article.

Kornbluth, P., 2017b, Helium supply chain disrupted as Qatar blockade continues to challenge exports. Lexington, Massachusetts. Gasworld US Edition, 55(8), 6–7.

Kornbluth, P., 2017c, Praxair-Linde merger—Major new helium competitor. Lexington, Massachusetts. Gasworld US Edition, 56(11), 40–41.

Kotarba, M.J., Sumino, H., Nagao, K., 2020. Origin of hydrocarbon and noble gases, carbon dioxide and molecular nitrogen in the Miocene strata of the eastern part of the Polish Carpathian Foredeep: isotopic and geologic approach. Appl. Geochem. 122, 21p.

Kozarek, R.J., 1990. Frontera Field, Cheyenne County, Colorado. In: Sonnenberg, S.A., Shannon, L.T., Rader, K., von Drehle, W.F., Martin, G.W. (Eds.), Morrow Sandstones, Rocky Mountain Association of Geologist, pp. 153 - 156.

Kreis, L.K., Haidl, F.M., Nimegeers, A.R., Ashton, K.E., Maxeiner, R.O. and Coolican, J., 2004, Lower Paleozoic map series – Saskatchewan; Saskatchewan Industry and Resources, Miscellaneous Report 2004-8, CD-ROM.

Kringstad, J., B. A. Kurz, B. G. Stevens, and J. A. Sorensen, 2020, Assessment of Bakken Petroleum: Energy & Environmental Research Center (EERC), no. September, p. 68.

Krivanek, C.M., 1978. Elmo Field. In: Oil and Gas Fields of the Four Corners Are: Four Corners Geological Society, pp. 148 - 1951.

Krivanek, C.M., 1981. Newfields and exploration drilling Paradox Basin Utah and Colorado. In: Geology of the Paradox Basin - Field Conference. RMAG, pp. 77 - 81.

Krooss, B.M., Jurisch, A., Plessen, B., 2006. Investigation of the fate of nitrogen in Paleozoic Shales of Central European Basin. J. Geochem. Explor. 89, 191 - 194.

Kulcinski, G.L., 1989. Importance of Helium-3 for the Future. NASA, pp. 150 - 171. Nas_techdoc_19000006527.

Kulongoski, J.T., Hilton, D.R., 2011. Chapter 15: applications of groundwater helium. In: Baskaran, M. (Ed.), Handbook of Environmental Isotope Geochemistry, Advances in Isotope Geochemistry. Springer-Verlag Berlin Heidelberg, pp. 285 - 304.

Kulongoski, J.T., Hilton, D.R., Izbicki, J.A., 2005. Source and movement of helium in the eastern Morongo groundwater basin: the influence of regional tectonics on crustal and mantle helium fluxes. Geochem. Cosmochim. Acta 69 (15), 3857 - 3872.

Kundaliya, D., 2019. European Union Considers Mining Mission to Launch in 2025. https://www.computing.co.uk/news/3069703/european-union-considers-moon-mining-mission-to-launch-in-2025.

Kuo, J. C., K. H. Wang, and C. Chen, 2012, Pros and cons of different Nitrogen Removal Unit (NRU) technology: Journal of Natural Gas Science and Engineering, v. 7, p. 52–59, doi:10.1016/j.jngse.2012.02.004.

Kurz, D., Warren, J. M., Joshua Curtice, 2008, Mantle deformation and noble gases: helium and neon in oceanic mylonites. Chem. Geol. 266, 10 - 18.

Kurz, M.D., Jenkins, W.J., 1981. The distribution of helium in oceanic basalt glasses. Earth Planet Sci. Lett. 53, 41 - 54. Kurz, M.D., Warren, J.M., Curtice, J., 2009.

Kynett, K., 2012, What goes up must come down: Congress deadline looms: is helium doomed? AAPG Explorer, December 2012, pages 10–12.

Kyser, T.K., Rison, W., 1982. Systematics of rare gases in basaltic lavas and ultramafic xenoliths. J. Geophys. Res. 87, 5611 - 5630.

Lade, G.E. and Rudik, I., 2020, Costs of inefficient regulation: Evidence from the Bakken. Journal of Environmental Economics and Management, 102, p.102336.

Lake, J., Whittaker, S., 2006. Occurrences of CO_2 within southwest Saskatchewan - Natural analogues to Weyburn CO_2 injection site. In: Summary of Investigations 2006, Saskatchewan Geological Survey, Miscellaneous Reports 2006-4.1, 14 p.

Lake, L.W., 2007. Petroleum Engineering Handbook, vol. V. Society of Petroleum Engineers, 643. 1.

Lane, D.M., 1987, Subsurface carbon dioxide in Saskatchewan: sources and potential use in enhanced oil recovery; Saskatchewan Energy and Mines, Open File Report 87-2, 40p.

Lang, M., Afanasyev, I., Slutskiy, B., Schmid, F., 2017. Monetizing Gas of a Giant High Helium and Nitrogen Gas Reservoir - Amur Gas Processing Plant, F13-Sustainable Value Chains for Unconventional Gas, 22nd World Petroleum Congress, Istanbul, 10 p.

Lange, J.K., Wellborn, R.E., 1985. Seismic profile: North Park Basin, RMAG. In: Greis, R., Dyer, R.C. (Eds.), Seismic Exploration of the Rocky Mountain Region. Rocky Mountain Association of Geologist, pp. 239 - 246.

Laughery, C.H., 2017. Origin of Non-hydrocarbon Gases in Petroleum Systems - a Review. AAPG, Search and Discovery. #90308.

Laughrey, C., 2019, Stable isotope and noble gas geochemistry of a high-nitrogen Permian sandstone reservoir, Northern Denver-Julesburg (D-J) Basin, Southeastern Wyoming, U.S.A. In: 2019 AAPG Annual Convention and Exhibition, San Antonio, Texas. AAPG.

Lauth, R.E., 1978, Table Mesa Dakota. In: Fassett, J.E. (Ed.), Oil and Gas Fields of the Four Corners Area, Four Corners Geological Society, vol. III, pp. 507 - 509.

Lavenant, H., 2021, Unconditional convergence for discretizations of dynamical optimal transport. Mathematics of Computation, 90(328), pp.739-786.

Lawrence Journal-World, 1984, Gas well blowout longest in Kansas, p. 18. June 20.

Lee, H., 1962. Technical and Economic Aspects of Helium Production in Saskatchewan, Saskatchewan Department of Mineral Resources. 39041-Report-72, 41 p.

Lee, H., 1963, The Technical and Economic Aspects of Helium Production in Saskatchewan, in Journal of Canadian Petroleum Technology: p. 16–27, doi:10.2118/63-01-04.

LeFever, J.A., 1991, History of oil production from the Bakken Formation, North Dakota, in Hansen, W.B., ed., Geology and horizontal drilling of the Bakken Formation: Montana Geological Society, Guidebook, p. 3–17.

Lengyel, T., 2013, Geothermics of the Phanerozoic strata of Saskatchewan; M.Sc. thesis, University of Alberta, Department of Earth and Atmospheric Sciences, Edmonton, Alberta, 248p. https://era.library.ualberta.ca/downloads/vt150k31t.

Lerche, L., 1989. Basin Analysis Quantitative Methods, vol. 1. Elsevier Publishing, p. 576.

Lesniak, P.M., Sakai, H., Ishibashi, J.I. and Wakita, H., 1997. Mantle helium signal in the West Carpathians, Poland. Geochemical Journal, 31(6), pp.383-394.

Lewars, E.G., 2008. Helium Compounds, Chapter 5, Modeling Marvels. Springer, Dordrecht, pp. 67 - 80.

Li, C., L. Kong, M. Ostadhassan, and T. Gentzis, 2019, Nanoscale Pore Structure Characterization of Tight Oil Formation: A Case Study of the Bakken Formation: Energy and Fuels, v. 33, no. 7, p. 6008–6019, doi:10.1021/acs.energyfuels.9b00514.

Li, M., Wang, T., Liu, J., Lu, H., Wu, W., Gao, L., 2008. Occurrence and origin of carbon dioxide in the Fushan Depression, Beibuwan Basin, South China Sea. Mar. Petrol. Geol. 25 (6), 500-513.

Li, X, Zhou, C, Lin, Z, Rocha, J, Lito, PF, Santiago, AS and Silva, CM, 2011, Microporous Mesoporous Matter. 137, 43.

Li, X., Zhou, C., Lin, Z., Rocha, J., Lito, P.F., Santiago, A.S., Silva, C.M., 2011. Titanosilicate AM-3 membrane: a new potential candidate for H_2 separation. Microporous Mesoporous Matter. 137 (1 - 3), 43 - 48.

Liang, G., Y. Yu, and X. Peng, 2016, Standardized surface engineering design of shale gas reservoirs: Natural Gas Industry B, v. 3, no. 1, p. 90–98, doi: 10.1016/j.ngib.2016.02.009.

Lide, D.R., 2005. CRC Handbook of Chemistry and Physics, 86th ed. CRC Press, Boca Raton (FL), p. 2544.

Liemberger, W., M. Miltner, and M. Harasek, 2018, Efficient extraction of helium from natural gas by using hydrogen extraction technology: Chemical Engineering Transactions, v. 70, no. September, p. 865–870, doi:10.3303/CET1870145.

Lillie, R.J., 2015, Beauty from the Beast: Plate Tectonics and the Landscapes of the Pacific Northwest, Wells Creek Publishers, pp. 92

Lind, S.C., 1925. The origin of terrestrial helium and its association with other gases. Proceedings of the National Academy of Sciences, 11(12), pp.772-779.

Linde Air, 2012, Carbon Monoxide: p. 1–26: https://www.linde-gas.com/en/products_and_supply/packaged_chemicals/product_range/carbon_monoxide.html, Accessed 10-2021

Linde Engineering, 2021, Autothermal Reforming Syngas Generation.

Linde Engineering, 2021, Helium recovery and liquefaction plants: p. 6: <http://www.lindeus-engineering.com/en/plant_components/plate_fin_heat_exchangers/structure_and_technical_data/index.html>.

Lindemann, U., Boeck, S., Blum, L., Kurtcuoglu, K., 2010. Turnkey helium purification and liquefaction plant for Darwin, Australia. AIP Conf. Proc. 1218, 271.

Lindsey, R., 2020, Climate Change: Atmospheric Carbon Dioxide, https://www.climate.gov/news-features/understanding-climate/climate-change-atmospheric-carbon-dioxide, accessed 09-2021.

Lisbonfield. In: Fassett, J.E. (Ed.), Oil and Gas Fields of the Four Corners Area, vol. II. Four Corners Geological Society, pp. 662 - 665.

Litvinova I.V., Surnin A.I., 2016, Geothermal field of the sedimentary cover in the Lena-Tunguska Petroleum Province (In Russ.), Neftegazovaya geologiya, no. 2(26), pp. 41–49.

Liu, X., Jin, Z., Bai, G., Liu, J., Guan, M., Pan, Q., & Li, T., 2017, A comparative study of salient petroleum features of the Proterozoic–Lower Paleozoic succession in major petroliferous basins in the world. Energy Exploration & Exploitation, 35(1), 54–74. https://doi.org/10.1177/0144598716680308

Liu, Y., Li, J., Wang, Z., Wang, S. and Dong, Y., 2015. The role of surface and subsurface integration in the development of a high-pressure and low-production gas field. Environmental Earth Sciences, 73(10), pp. 5891-5904.

Loe, J.S. and Ladehaug, O., 2012. Reducing gas flaring in Russia: Gloomy outlook in times of economic insecurity. Energy Policy, 50, pp.507-517.

Lokhandwala, K., And M. Jacobs, 2000, Membranes for fuel gas conditioning: Hydrocarbon Engineering, v. 5, no. 5, p. 81–84.

Lollar, B.S., Frappe, S.K., Fritz, P., Macko, S.A., Welhan, J.A., Blomvist, R., Lahermo, P.W., 1993. Evidence for bacterially generated hydrocarbon gas in Canadian Shield and Fennoscandian rocks. Geochem. Cosmochim. Acta 57, 5073 - 5085.

Lollar, B.S., Weise, S.M., Frape, S.K., Barker, J.F., 1994. Isotopic constraints on the migration of hydrocarbon and helium gases of southwestern Ontario. Bull. Can. Pet. Geol. 42 (3), 283 - 295.

Lopatin, N.V.; Zubairaev, S.L.; Kos, I.M.; Emets, T.P.; Romanov, E.A.; Malchikhina, O.V., 2003, "Unconventional Oil Accumulations in the Upper Jurassic Bazhenov Black Shale Formation, West Siberian Basin: A Self-sourced Reservoir System". Journal of Petroleum Geology. AAPG. **26** (2, 225–244. Retrieved 2017-11-11.

Lopes, F. V. S., C. A. Grande, A. M. Ribeiro, J. M. Loureiro, O. Evaggelos, V. Nikolakis, and A. E. Rodrigues, 2009, Adsorption of H_2, CO_2, CH4, CO, N_2 and H_2O in Activated Carbon and Zeolite for Hydrogen Production: Separation Science and Technology, v. 44, no. 5, p. 1045–1073, doi:10.1080/01496390902729130.

Loukou, A., Mendes, M.A.A., Frenzel, I., Pereira, J.M.C., Ray, S., Pereira, J.C.F. and Trimis, D., 2017, Experimental and numerical investigation of methane thermal partial oxidation in a small-scale porous media reformer. International Journal of Hydrogen Energy, 42(1), pp.652-663.

Lowenstern, J.B., Bergfeld, D., Evans, W.C., Hunt, A.G., 2015. Origins of geothermal gases at Yellowstone. J. Volcanol. Geoth. Res. 302, 87 - 101.

Ludvigson, G.A., McKay, R.M., Anderson, R.R., 1990. Petrology of Keweenawan sedimentary rocks in the M.G. Eischeid #1 drillhole. In: Wilson, L.J., The Amoco, M.G. (Eds.), Eisheid #1, Deep Petroleum Test Carroll County, Iowa, Special Report Series, No. 2, pp. 77 - 112.

Lutey, T., 2021, Helium prospecting picking up in north- central Montana Helium prospecting picking up in north- central Montana.: www.greatfallstribune.com, p. 12–14.

Ma, F., Al-Asam, I. and Yang, J., 2006, Numerical modeling of hydrothermal fluid flow coupled with mass transport: an example from the Devonian Wabamun Group, northeast British Columbia, Canada; Journal of Geochemical Exploration, Volume 90, no 3, page 216.

Ma, L., 2009. Noble Gases Dissolved in Groundwaters of the Michigan Basin: Implications for Paleoclimatology, Hydrogeology, Tectonics and Mantle Geochemistry (Ph.D. Dissertation). University of Michigan, 229 p.

Ma, Y.Z. and La Pointe, P.R. eds., 2011, Uncertainty Analysis and Reservoir Modeling: Developing and Managing Assets in an Uncertain World, AAPG Memoir 96 (Vol. 96). AAPG.

MacDonald, G.A., 1972. Volcanoes. Prentice-hall, Englewood Cliffs NJ, p. 510.

MacDonald, G.J., 1983. The many origins of natural gas. J. Petrol. Geol. 5 (4), 341 - 362.

Macintosh, S.J., Ballentine, C.J., 2012. Using 3H 3 /4He isotope ratios to identify the source of deep reservoir contributions to shallow fluids and soil gas. Chem. Geol. 304 - 305, 142 - 150.

Macpherson, J., 2021, Companies aim to build 'clean hydrogen' hub in North Dakota: p. 1–8.

Madhusha, 2017, Main Difference – Helium vs Hydrogen: p. 1–5: https://pediaa.com/difference-between-helium-and-hydrogen/#:~:text=plants as wells. -Similarities Between Helium and Hydrogen, block of the periodic table.

Madi, A.J., Damte, A. and Hayes, M., 2003, Fault-associated hydrothermally- dolomitized reservoirs (HTD) in Devonian strata of northeastern British Columbia—a large-scale geological exploration concept; 2003 CSPG/CSEG Joint Convention: Partners in a New Environment, Canadian Society of Petroleum Geologists, Calgary, Alberta.

Madrid, P.J., 2012, Mineral commodity summaries: Helium; US Geological Survey, Amarillo, Texas, URL <http://minerals. usgs.gov/minerals/pubs/commodity/helium/mcs-2012-heliu.pdf>.

Maffly, B., 2021. Judge Rejects Last-Ditch Move to Block Helium Drilling in Utah Wilderness, Salt Lake Tribune, January 13th. https://www.sltrib.com/news/environment/2021/01/13/judge-rejects-last-ditch/ .

Magloire, P.R., 1970. Triassic gas field of Hassi er R'Mel, Algeria, American Association of Petroleum Geologists. In: Geology of Giant Petroleum Fields, Memoir, vol. 14, pp. 489 - 502.

Mahant, B., Linga, P. and Kumar, R., 2021, Hydrogen Economy and Role of Hythane as a Bridging Solution: A Perspective Review. Energy & Fuels, 35(19), pp.15424-15454.

Maione, S. J., 2004, Helium exploration- a 21st century challenge: Houston Geological Society, 23 February 2004, http://www.hgs.org/en/articles/printview.asp?162

Mamyrin, B.A., Tolstikhin, I.N., 1984. Helium Isotopes in Nature. Elsevier, p. 289. Manning, V.,H., 1919. Petroleum Investigations and Production of Helium. U.S. Bureau of Mines, Bulletin, 178C.

Manning, D.A., 2008, Where does all the helium that we use come from? Rapid Communications in Mass Spectrometry: An International Journal Devoted to the Rapid Dissemination of Up-to-the-Minute Research in Mass Spectrometry, 22(11), pp.1640-1642.

Marcoberardino, G.D., Vitali, D., Spinelli, F., Binotti, M. and Manzolini, G., 2018, Green hydrogen production from raw biogas: A techno-economic investigation of conventional processes using pressure swing adsorption unit. Processes, 6(3), p.19.

Mark, A., 1961. South McCallum Field. In: Oil and Gas Field Volume, Colorado-Nebraska. Rocky Mountain Association of Geologist, p. 186.

Market Insider, 2021, Natural Gas (Henry Hub), https://markets.businessinsider.com/commodities/natural-gas-price, accessed 09-2021.

Markiewicz, G. S., M. S. Losin, and K. M. Campbell, 1988, The membrane alternative for natural gas treating: two case studies, *in* 63rd Annual Technical Conference and Exhibition of the Society of Petroleum Engineers: p. 513–520, doi:10.2523/18230-ms.

Marsh, A. and Heinemann, K., 2006, Report on the Regional Stratigraphic Framework of Western Saskatchewan – Phase 1; Petroleum Technology Research Centre, publications, 18p. http://ptrc.ca/+pub/document/WSP%20Final%20Report.pdf.

Marsh, A. and Love, M., 2014, Regional stratigraphic framework of the Phanerozoic in Saskatchewan: Saskatchewan Phanerozoic Fluids and Petroleum Systems Project; Saskatchewan Ministry of the Economy, Saskatchewan Geological Survey, Open File 2014-1, set of 156 maps. http://www.economy.gov.sk.ca/OF2014-1.

Martin, M., A. Di Paola, Y. G. El-din, and V. Ratcliffe, 2021, Saudi Aramco Bets on Blue Hydrogen Exports Ramping Up From 2030: p. 3.

Martınez-Merino, V., Jose, M. and Gil, A.C., 2013, Biomass sources for hydrogen production. Renewable Hydrogen Technologies: Production, Purification, Storage, Applications and Safety, 87.

Martiniuk, C. D., 1988, Regional Geology and Petroleum Potential of Bakken Formation, Southwestern Manitoba: ABSTRACT: AAPG Bulletin, v. 72, doi:10.1306/703c906e-1707-11d7-8645000102c1865d.

Marty, B., Torgersen, T., Meynier, V., O'Nions, R.K., Marsily, G., 1993. Helium isotope fluxes and groundwater ages in the Dogger Aquifer. Paris Basin, Water Res. Res. 29 (4), 1025 - 1035.

Mason, J.W., 1968. Hugoton Panhandle Field, Kansas, Oklahoma and Texas. American Association of Petroleum Geologists, pp. 1539 - 1547. Natural Gases of North America, Memoir, Chapter 9.

Mast, R. F., D. H. Root, L. P. Williams, W. R. Beeman, and D. L. Barnett, 1998, Areas of historical oil and gas exploration and production in the conterminous United States: USGS Geologic Investigations map I-2582, one sheet.

Masters, John, 1960, Pinta Dome helium gas reserves: Interstate Oil Compact Commission Committee Bulletin, December, v. 2, no. 2, p. 33-48. 10

Matthey, J., R. J., 2021, Blue hydrogen Low Carbon Hydrogen: paving the way to net zero: p. 7.

Maung, T.A., Ripplinger, D.G., McKee, G.J. and Saxowsky, D.M., 2012, Economics of using flared vs. conventional natural gas to produce nitrogen fertilizer: a feasibility analysis (No. 1187-2016-93827).

Maynard, J., 1978b. Hogback Pennsylvanian. In: Fassett, J.E., Thomaidis, N.D., Matheny, M.L. (Eds.), Oil and Gas Fields of the Four Corners Area, Four Corners Geological Society, vol. 1, p. 334.

Mazor, E., Bosch, A., 1987. Noble gases in formational fluids from deep sedimentary basins: a review. Appl. Chem. 2, 621 - 627. MHS, 2020. https://www.renergen.co.za/sproule-evaluation-of-certain-helium-prospective-resources-on-the-tetra4virgina-gas-project-july-2020/ .

Mazumder, M., and Q. Xu, 2020, Modeling and Optimization for a Comprehensive Gas Processing Plant with Sensitivity Analysis and Economic Evaluation: Chemical Engineering and Technology, v. 43, no. 11, p. 2198–2207, doi:10.1002/ceat.202000216.

Mba, Kenechukwu, and Manika Prasad, 2010, Mineralogy and Its Contribution to Anisotropy and Kerogen Stiffness Variations with Maturity in the Bakken Shales. Paper presented at the 2010 SEG Annual Meeting, Denver, Colorado, October 2010.

McCarthy, R. D., 1975, Hydrogen: its Technology and Implications. Volume III.: CRC Press - Taylor and Francis, 336 p.

McCool, J. H., 1905, High on helium: KU History, p. 3.

McDowell, B.P., Milkov, A.V., Anderson, D.S., 2017. The He System - a Modification of the Petroleum System for Inert Gases. AAPG. Search and Discovery, p. 42098.

McKenny, J.W., Masters, J.A., 1968. Dineh-Bi-Keyah Field, Apache County, Arizona, American Association of Petroleum Geologists. Bulletin 52 (10), 2045-2057.

McMahon, P.B., Caldwell, R.R., Galloway, J.M., Valder, J.F. and Hunt, A.G., 2015. Quality and age of shallow groundwater in the Bakken Formation production area, Williston Basin, Montana and North Dakota. Groundwater, 53(S1), pp.81-94.

McMurty, R.P., 1982. Brown-Bassett. In: Selected Oil and Gas Fields in West Texas Symposium, West Texas Geological Society, Symposium V. 1, II and III, pp. 111 - 124.

McPhail, S., Walsh, W., Lee, C. and Monahan, P.A., 2008, Shale units of the Horn River Formation, Horn River Basin and Cordova Embayment, northeastern British Columbia; Petroleum Geology Open File 2008-1, British Columbia Ministry of Energy, Mines and Natural Gas, page 14.

Mehrpooya M., Zaitsev A. V., Lisovtsov A. O. Application of new external cooling cycles in technological scheme of helium extraction and natural gas liquefaction [Внедрение Новых Технологических Решений В Циклы Внешнего Охлаждения Процессов Извлечения Гелия И Ожижения Природного Газа] Omsk Scientific Bulletin. Series Aviation-Rocket and Power Engineering. 2020. Vol. 4, no. 2. P. 37–47. DOI: 10.25206/ 2588-0373-2020-4-2-37-47.

Mehrpooya, M and Shafaei, A, 2016, Advanced exergy analysis of novel flash-based helium recovery from natural gas processes, Energy, 114, 2016, 64-83.

Mehrpooya, M., M. Hossieni, and A. Vatani, 2014, Novel LNG-based integrated process configuration alternatives for coproduction of LNG and NGL: Industrial and Engineering Chemistry Research, v. 53, no. 45, p. 17705–17721, doi:10.1021/ie502370p.

Mehrpooya, M., Shafaei, A., 2016. Advanced exergy analysis of novel flash-based helium recovery from natural gas processes. Energy 114, 64 - 83.

Mehrpuya, M., A. V. Zaitsev, and A. O. Lisovtsov, Мехрпуйя, М., А. В. Зайцев, and А. О. Лисовцов, 2020, Implementation Of New Technological Solutions In The Cycles Of External Cooling Of The Processes Of Helium Extraction And Liquidation Of Natural Gas: Omsk Scientific Bulletin. Series Aviation-Rocket and Power Engineering., v. 4, no. 2, p. 11.

Meier, W.M., D.H. Olson, C. Baerlocher, 1996, Atlas of Zeolite Structure Types, fourth ed., Elsevier, London.

Melnik, A., 2012, Regional hydrogeology of southwestern Saskatchewan; M.Sc. thesis, University of Alberta, Department of Earth and Atmospheric Sciences, Edmonton, Alberta, 142p.

Mel'nikov N.V., Isaev A.V., 2004, Seismogeological models and perspective oil and gas objects of the Vendian complex in the Baikit oil and gas region (In Russ.), Geologiya i geofizika, no. 1(45), pp. 134–143.

Mel'nikov N.V., Smirnov E.V., Maslennikov M.A. et al., 2017, Geologic prerequisites for increment of the mineral resources base of the Yurubchen-Kuyumba petroleum production center, Russian Geology and Geophysics, V. 58, no. 3–4, pp. 479–492.

Mendeleev, D. I., 1869, Draft of system of elements: based on their atomic masses and chemical characteristics. Osnovy khimii [The Principles of Chemistry], University of St. Petersburg [now St. Petersburg State University], St. Petersburg, Russia. 816 p.

Merewether, E.A., 1987. Oil and Gas Plays of the Las Animas Arch, Southeastern Colorado: U.S. Geological Survey Open-File Report 87-450D, 22 p.

Merriam, D. F., 1963, The geologic history of Kansas: Kansas Geological Survey, Bulletin 162, 317 p.

Merriam, D.F., ed., 1964, Symposium on cyclic sedimentation: Kansas Geological Survey, Bulletin 169.

Merrill, M.D., Hunt, A., 2017. Updated Regional and Field Scale He Accumulation Geochemistry, La Barge Platform, WY. American Association of Petroleum Geologists. Search and Discovery 90301. MHS, 2019, https://www.renergen.co.za/mha-final-report/ .

Merrill, M.D., Hunt, A.G., Lohr, C.D., 2014. Noble gas geochemistry investigation of high CO2 natural gas at the La Barge Platform, Wyoming, USA. Energy Proc. 63, 4186-4190.

Metz, H. C., ed. Persian Gulf States: A Country Study. "Qatar" Washington: GPO for the Library of Congress, 1993.

MHS, 2019, https://www.renergen.co.za/mha-final-report/.

MHS, 2020, https://www.renergen.co.za/sproule-evaluation-of-certain-helium-prospective-resources-on-the-tetra4virgina-gas-project-july-2020/.

MHS, 2020, https://www.renergen.co.za/sproule-evaluation-of-certain-helium-prospective-resources-on-the-tetra4virgina-gas-project-july-2020/.

Miall, A.D., 1990. Principles of Sedimentary Basin Analysis. Springer-Verlag, p. 668.

Miller, L.N., Zawacki, T.S., 1978. Process for Acid Gas Removal from Gaseous Mixtures. Institute of Gas Technology.

Miller, M.H. and Upton, C.W., 1976, Leasing, buying, and the cost of capital services. The Journal of Finance, 31(3), pp.761-786.

Miller, R.D., Hertweck Jr., F.R., 1982. Analyses of Natural Gases, 1981. IC 8890. USBM, p. 84.

Miller, R.D., Hertweck Jr., F.R., 1983. Analyses of Natural Gases. IC 8942. USBM, p. 100.

Miller, R.D., Norrell, G.P., 1964a. Analyses of Natural Gases of the United States, 1961. IC 8221. USBM, p. 148.

Miller, R.D., Norrell, G.P., 1964b. Analyses of Natural Gases of the United States, 1962. IC 8239. USBM, p. 120.

Miller, R.D., Norrell, G.P., 1965. Analyses of Natural Gases of the United States, 1963. IC 8241. USBM, p. 102.

Miller, R.R., 1968, Geology of Otis-Albert Field, Rush and Barton Counties., Kansas, AAPG. In: Memoir 9 Natural Gases of North America, Volume Two, Chapter G, pp. 1588 - 1615.

Miller, S. J., D. Q. Vu, and W. J. Koros, 2007, Enhancing Natural Gas Purification with Advanced Polymer / Molecular Sieve Composite Membranes, *in* International Petroleum Technology Conference held in Dubai, U.A.E., 4–6 December 2007: p. 1–6.

Mills, R., and B. Y. Antoine, 2021, Having It Both Ways: GCC Oil Faces Peak Demand: Colombia Center on Global Energy Policy, no. September, p. 62.

Ministry of Natural Resources, 1983a. Gobles Pool, Structure on Top of the Shadow Lake, Fig D-5, Petroleum Section, Map.

Ministry of Natural Resources, 1983b. Gobles Pool, Cambrian Isopach, Fig D-6, Petroleum Section, Map.

Ministry of Natural Resources, 1983c. Innerkip and Innerkip East Pools, Cambrian Isopach, Fig D-9, Petroleum Section, Map.

Minkel, J., 2009, Strange but True: Superfluid Helium Can Climb Walls - Scientific American: Scientific American, p. 1–6.

Mjachina, K.V., Baynard, C.W., Chibilyev, A.A. and Richardson, R.D., 2018, Landscape disturbance caused by non-renewable energy production in a semi-arid region: a case study on the Russian steppe. International Journal of Sustainable Development & World Ecology, 25(6), pp.541-553.

Mohtada Sadrzadeh, T. M. (Ed.), 2020, Nanocomposite Membranes for Water and Gas Separation: Elsevier B.V, 509 P.

Mokhatab, S., and M. Mitariten, 2018, Efficient acid gas removal using membrane systems—Part 1: Gas Processing & LNG, p. 1–4.

Mokhatab, S., J. Y. Mak, J. V. Valappil, and D. A. Wood, 2013, Handbook of Liquefied Natural Gas: 1–589 p., doi:10.1016/C2011-0-07476-8.

Montgomery, S.L., 1996. Val Verde Basin: Thrusted Strawn (Pennsylvanian) carbonate reservoirs, Pakenham area. Am. Assoc. Pet. Geol. Bull. 80 (7), 987 - 998.

Moore, B.J., 1973. Analyses of Natural Gases, 1973. IC 8658. USBM, p. 96.

Moore, B.J., 1975. Analyses of Natural Gases, 1974. IC 8684. USBM, p. 122.

Moore, B.J., 1976a. Analyses of Natural Gases, 1917 - 74. CP 1-76. USBM, p. 889.

Moore, B.J., 1976b. Analyses of Natural Gases, 1975. IC 8717. USBM, p. 82.

Moore, B.J., 1977. Analyses of Natural Gases, 1976. IC 8749. USBM, p. 94.

Moore, B.J., 1978. Analysis of Natural Gas. USBM Info Circular 8810, 136 p.

Moore, B.J., 1978a. Analyses of Natural Gases, 1977. IC 8780. USBM, p. 95.

Moore, B.J., 1978b. Analysis of Natural Gas, 1978. Info Circular 8810. USBM, p. 136.

Moore, B.J., 1979. Analyses of Natural Gases, 1978. IC 8810. USBM, p. 113.

Moore, B.J., 1980. Analyses of Natural Gases, 1979. IC 8833. USBM, p. 100.

Moore, B.J., 1981. Analyses of Natural Gases, 1980. IC 8856. USBM, p. 236.

Moore, B.J., 1982. Analysis of Natural Gas, 1917 - 80. Info Circular 8870. USBM, p. 1074.

Moore, B.J., and Sigler, S.M., 1987, Analyses of Natural Gases, 1917–1985: U.S. Bureau of Mines, Information Circular 9129, 1197 p., accessed May 14, 2021

Moore, B.J., Miller, R.D., Shrewsbury, R.D., 1964. Analyses of Natural Gases of the United States, 1964. IC 8302, 1966. USBM, p. 144.

Moore, B.J., Shrewsbury, R.D., 1966. Analyses of Natural Gases of the United States, 1965. IC 8316. USBM, p. 181.

Moore, B.J., Sigler, S., 1985. Analysis of Natural Gas. USBM, Info Cir, 9096, 200 p.

Moore, C.A., 1981. Geologic factors which may affect the occurrence of natural gas in the Oklahoma Panhandle. In: Reckamp, J.U. (Ed.), Shale Shaker Digest Volumes XVIII - XX, 1967-1970. Oklahoma City Geological Society, pp. 203 - 210.

Moore, Hamak, 1985. Analyses of Natural Gases, 1984. IC9046. USBM, p. 102.

Moore, J.P., Dinterman, P.A., McDowell, R.R., Sminchak, J.R., Daft, G.W., 2018. From the Tuscarora Sandstone to the Bubbles in Your Beverage: Naturally - Occurring CO_2 in the Indian Creek Field, Kanawha Country, West Virginia. American Association of Petroleum Geologists. Eastern Section Joint Meeting, Abstract, October 7 to 11.

Moore, R.B., 1926. Commercial production of radium, Meso-thorium, and Helium. Ind. Eng. Chem. 18 (2), 203.

Morgan, C.D., 1994. Exploring for New Oil in Old Field, Salt Wash Field: A Case Study. Utah Geological Survey, OFR 307, 128 p.

Morgan, C.D., 2007. Structure, reservoir and characterization, and carbon dioxide resources of Farnham Dome Field. Carbon County, Utah, In Central Utah - Diverse geology of dynamic landscape, Utah Geological Association, p. 295 - 310.

Morgan, C.D., Chidsey Jr., T.C., 1991. Gordon Creek, Farnham Dome, and Woodside fields, Carbon and Emery counties, Utah. In: Chidsey Jr., T.C. (Ed.), Geology of East-Central Utah, UGS, pp. 301 - 309.

Morgan, D.F., 2000, The Impact of Selling the Federal Helium Reserve; The National Academies Press, Washington, DC, 80 pages.

Morley, C.K., Ngenoh, D.K., Ego, J.K., 1999. In: Morley, C.K. (Ed.), Geoscience of Rift Systems - Evolution of East Africa, American Association of Petroleum Geologists Studies in Geology, No. 44, pp. 1 - 18.

Mossop, G.D. and Shetsen, I. (comps.), Canadian Society of Petroleum Geologists and Alberta Research Council, p. 421-429.

Mottern, M.L.; Shi, J.Y.; Shqau, K.; Yu, D., Verweij, H., 2008, Microstructural Optimization of Thin Supported Inorganic Membranes for Gas and Water Purification. In Advanced Membrane Technology and Applications; Li, N.N., Fane, A.G., Ho, W.S.W., Matsuura, T., Eds.; Wiley: Hoboken, NJ, USA, 2008; pp. 899–928.

Mount Joy, E.W. and Halim-Dihardja, M.K., 1991, Multiple phase fracture and fault-controlled burial dolomitization, Upper Devonian Wabamun Group, Alberta; Journal of Sedimentary Petrology, Volume 61, no 4, pages 590–612.

Mtili, K.M., Byrne, D.J., Tyne, R.L., Kazimoto, E.O., Kimani, C.N., Kasanzu, C.H., Hillegonds, D.J., Ballentine, C.J. and Barry, P.H., 2021. The origin of high helium concentrations in the gas fields of southwestern Tanzania. Chemical Geology, 585, p.120542.

Mtili, K.M., Kazimoto, E.O., Barry, P., 2019. In: Helium Gas Seeps and Processes Involved in the Formation of the Helium Gas Field within the Rukwa Rift Basin Tanzania, Abs. Tanzania Geological Society, 2019 Annual Meeting and Workshop, Dar Es Salaam, September 25th to 27th, p. 18.

MTR, 2007, Field Demonstration of a Membrane Process to Separate Nitrogen from Natural Gas: Membrane Technology and Research Inc.

MTR, 2020, Natural Gas Conditioning Using Membranes: 1–18 p.

Mueller, M., 2020, “It’s a Gas” – A Unique Investment Opportunity in an Emerging Industry: Cormark Securities Inc., no. 403.

Muffler, P., White, D., 1968. Origin of CO2 in the Salton Sea Geothermal System, pp. 185 - 194. Southeastern California, U.S.A., XXIII International Geologic Congress, 1968, V. 17.

Munnerlyn, R.D., Miller, R.D., 1963. Helium-bearing Natural Gases of the United States: Analyses, Second Supplement to Bulletin 486. USBM Bull., p. 617 93

Myers, D.B., Ariff, G.D., James, B.D., Lettow, J.S., Thomas, C.E. and Kuhn, R.C., 2002, Cost and performance comparison of stationary hydrogen fueling appliances. The Hydrogen Program Office.

Naderi, M. and Khamehchi, E., 2019, Fuzzy logic coupled with exhaustive search algorithm for forecasting of petroleum economic parameters. Journal of Petroleum Science and Engineering, 176, pp.291-298.

NASA, 2006. Space Shuttle Use of Propellants and Fluids. NASA. https://www.nasa.gov/centers/kennedy/pdf/ 167433main_Propellants08.pdf .

NASA, 2019, NASA Awards Two Contracts for Supply of Gaseous, Liquid Hydrogen: 1–2 p.

NASA, 2020, NASA awards helium contract: 2–4 p.

Naterer, G. F., O. Jaber, and I. Dincer, 2010, Environmental Impact Comparison of Steam Methane Reformation and Thermochemical Processes of Hydrogen Production Environmental Impact Comparison of Steam Methane Reformation and Thermochemical Processes of Hydrogen Production: Essen Schriften des Forschungszentrums Jülich / Energy & Environment, v. 78.

Naterer, G. F., O. Jaber, and I. Dincer, 2010, Environmental Impact Comparison of Steam, National Energy Technology Laboratory / U.S. Department of Energy, 2004, Technologies for Hydrogen Production: Gasifipedia, p. 7.3.

National Energy Technology Laboratory / U.S. Department of Energy, 2004, Technologies for Hydrogen Production: Gasifipedia, p. 7.3.

National Research Council, 2000, The Impact of Selling the Federal Helium Reserve. Washington, DC: The National Academies Press. https://doi.org/10.17226/9860.

National Research Council, 2010, Selling the Nation's Helium Reserve: Washington, D.C.: The National Academies Press, 156 p., accessed May 14, 2021

Nationalgrid, 2021, The hydrogen colour spectrum: National Grid Group, p. 13–16.

Nave, K., 2016. Space Mining Will Take a Giant Leap. https://www.wired.co.uk/article/space-mining-a-reality-in2016 .

Nazir, S. M., J. H. Cloete, S. Cloete, and S. Amini, 2019, Efficient hydrogen production with CO_2 capture using gas switching reforming (GSR): Techno-economic assessment: ECOS 2019 - Proceedings of the 32nd International Conference on Efficiency, Cost, Optimization, Simulation and Environmental Impact of Energy Systems, no. June, p. 625–634, doi:10.5281/zenodo.3350172.

Nealey, L.D., and Sheridan, M.F., 1989, Post-Laramide volcanic rocks of Arizona and northern Sonora, Mexico, and their inclusions, in Jenney, J.P., and Reynolds, SJ., eds., Geologic evolution of Arizona: Arizona Geological Society Digest 17, p. 609-647.

Nelson, D.L., Cox, M.M., 2017. Lehninger Principles of Biochemistry, vol. 1. W.H. Freeman and Company, p. 130. Newell, K.D., 2021. Stratigraphic and Regional Trends in Chemistry and Quality of Natural Gas in Central and Western Kansas. Mid-Continent, USA, KGS (in press).

Nesheim, T.O., Kruger, N.W., 2019. Helium Trends in North Dakota, GI 223. North Dakota Geological Survey, 12 p.

Neuendorf, K.K., 2005, Glossary of geology. Springer Science & Business Media.

Newell, K. David, W. Lynn Watney, Stephen W. L. Cheng, and Richard L. Brownrigg, 1987, Stratigraphic and Spatial Distribution of Oil and Gas Production in Kansas: Kansas Geological Survey Subsurface Geology Series 9. http://www.kgs.ku.edu/Publications/Bulletins/Sub9/index.html

Newell, K.D., 2017. Compositional and Isotopic Analysis of Natural Gas from a Shallow Water Well in Southeastern Cowley County, Kansas, KGS, OFR 2017-9. www.kgs.ku.edu/Publications/OFR/2017/OFR17_9/index.html.

Newell, K.D., 2021. Stratigraphic and Regional Trends in Chemistry and Quality of Natural Gas in Central and Western Kansas, Mid-continent, USA, Kansas Geological Survey (in press).

Newell, K.D., Corsair, S., Chafin, S., Pennybaker, K., 2003. Low-BTU Gas in the Permian Chase Group in the Ryersee Field in Western Kansas: A Case History where Technology Creates a Marketable Commodity. Kansas Geological Survey, OFR 2003-57, Poster.

News, A. N. R.-S. N. E. at E. W., 2016, Researchers' Work from University of Tehran Focuses on Energy Research, Advanced exergy analysis of novel flash-based Helium recovery from natural gas processes: Energy Weekly News, no. July, p. 2.

Nguyen, T.V. and Clausen, L.R., 2018, Thermodynamic analysis of polygeneration systems based on catalytic hydropyrolysis for the production of bio-oil and fuels. Energy Conversion and Management, 171, pp.1617-1638.

Nicolas, M.P.B., 2018, Summary of helium occurrences in southwestern Manitoba; in Report of Activities 2016, Manitoba Growth, Enterprise and Trade, Manitoba Geological Survey, p. 110–118

Nightingale, S., 2019, Hydrogen Fuel is Getting Buzz, But Here's Why It Hasn't Gone Mainstream.: Fueling Change, p. 3.

Nikolaidis, P., and A. Poullikkas, 2017, A comparative overview of hydrogen production processes: Renewable and Sustainable Energy Reviews, v. 67, no. January 2018, p. 597–611, doi:10.1016/j.rser.2016.09.044.

Nikonov, V. F., 1973, Formation of helium-bearing gases and trends in prospecting for them: International Geology Review, v. 15 #5, p. 534-541.

Noelker, K. and Johanning, J., 2010, Autothermal reforming: a flexible syngas route with future potential. Nitrogen and Syngas.

Nordquist, J.W., 1953, Mississippian stratigraphy of northern Montana, Billings Geological Society, 4th Annual Field Conference Guidebook, pp. 68–82, 1953

Nordquist, J.W., Leskela, W., 1968. Natural gas in Sweetgrass arch area, Northwestern Montana, American Association of Petroleum Geologists. In: Natural Gas of North America, vol. 1, pp. 736 - 759. Chapter M9.

North Dakota Industrial Commission (NDIC), Oil and Gas Division (2021). Well stimulation dump file data: Spreadsheet available from North Dakota Industrial Commission, delivered 30 October, 2021.

Norton, J.A., 1978. Salt Wash. In: Fassett, J.E. (Ed.), Oil and Gas Fields of the Four Corners Area, Volume II: Four Corners Geological Society, pp. 697-699.

Norton, K., 2019. NASA Awards Two Contracts for Supply of Gaseous, Liquid Helium. NASA Kennedy. September 27th. https://www.nasa.gov/press-release/nasa-awards-two-contracts-for-supply-of-gaseous-liquid-helium .

Noureldin, M.M., Elbashir, N.O., Gabriel, K.J. and El-Halwagi, M.M., 2015, A process integration approach to the assessment of CO2 fixation through dry reforming. ACS Sustainable Chemistry & Engineering, 3(4), pp.625-636.

Novak Mavar, K.; Gaurina-Međimurec, N.; Hrnčević, L., 2019, Carbon Capture, Utilization and Storage (CCUS)—The Environmental Impact Rom Project Start to Closure. In Proceedings of the 7th International Symposium Mining and Environmental Protection, Vrdnik, Serbia, 25–28 September 2019; Ristović, I., Ed.; Faculty of Mining and Geology: Belgrade, Serbia, pp. 63–68.

Novikov D.A., Trifonov N.S., Hydrogeologic implications of industrial effluent disposal of the Yurubcheno-Tokhomo field (Siberian Craton, Russia), Arabian Journal of Geosciences, 2016, V. 9, no. 1, pp. 1–14.

Nuccio, P.M., Caracausi, A. and Costa, M., 2014. Mantle-derived fluids discharged at the Bradanic foredeep/Apulian foreland boundary: the Maschito geothermal gas emissions (southern Italy). Marine and petroleum geology, 55, pp.309-314.

Nuttall, W. J., R. H. Clarke, and B. A. Glowacki, 2012, Resources: Stop squandering helium: Nature, v. 485, no. 7400, p. 573–575, doi:10.1038/485573a.

Nuttall, W.J., Clarke, R.C., Glowacki, D.G., 2012. The Future of Helium as a Natural Resource. Routledge Publishing, p. 376.

O'Leary, J.R., Kunz, R.G. and von Alten, T.R., 2004, Selective catalytic reduction performance in steam–Methane reformer service: The chromium problem. Environmental progress, 23(3), pp.194-205.

O'Nions, R.K., Oxburgh, E.R., 1988. Helium, volatile fluxes and the development of continental crust. Earth Planet Sci. Lett. 90 (3), 331 - 347.

Oh, S. and Song, H.H., 2018, Exergy analysis on non-catalyzed partial oxidation reforming using homogeneous charge compression ignition engine in a solid oxide fuel cell system. International Journal of Hydrogen Energy, 43(5), pp.2943-2960.

Ohlrogge, K., J. Wind, and T. Brinkmann, 2002, Membrane Technology for Natural Gas Processing: SPE Gas Technology Symposium Proceedings, p. 1–6, doi:10.2523/75505-ms.

Oil & Gas 360, 2017, Growth in the Bakken is Coming from Gas Production: 2–5 p.

Ojijiagwo, E., C. F. Oduoza, and N. Emekwuru, 2016, Economics of gas to wire technology applied in gas flare management: Engineering Science and Technology, an International Journal, v. 19, no. 4, p. 2109–2118, doi:https://doi.org/10.1016/j.jestch.2016.09.012.

Okken, PA, 1992, Costs of Reducing CO_2 Emissions by Means of Hydrogen Energy. International Journal of Hydrogen Energy. 18(4): 319-323.

O'Neill, J.M. and Lopez, D.A., 1985, Character and regional significance of Great Falls tectonic zone, east-central Idaho and west-central Montana; American Association of Petroleum Geologists Bulletin, v.69, no.3, p.437-447.

Ortiz, M., Abad, A., Luis, F., García-Labiano, F., Gayán, P. and Adánez, J., 2011, Optimization of hydrogen production by chemical-looping auto-thermal reforming working with Ni-based oxygen-carriers. International Journal of Hydrogen Energy, 36(16), pp.9663-9672.

Othmer, K., 1998, Hydrogen. Encyclopedia of Chemical Technology. 13:759-807

Oty, J.W., 2014. Clyde field. In: Rogers, J.P., Milne, J.J., Cumella, S.P., Dubois, D.P., Lillis, P.G. (Eds.), Oil and Gas Fields of Colorado, Rocky Mountain Association of Geologist, pp. 68-73.

Oxburgh, E.R., O'Nions, R.K., Hill, R.I., 1986. Helium isotopes in sedimentary basins. Nature 324, 632 - 635.

Ozcan, H., & Dincer, I., 2015, Thermodynamic and environmental impact assessment of steam methane reforming and magnesium-chlorine cycle-based multigeneration systems: Comparative exergy-based environmental impact assessment. International Journal of Energy Research. 39. 10.1002/er.3317.

Ozima, M., 1994. Noble gas state in the mantle. Rev. Geophys. 32 (4), 405 - 426.

Ozima, M., Podosek, F., 1983. Noble Gas Geochemistry. Cambridge University Press, p. 367.

Ozimic, S., 2016. Non-petroleum gas accumulations, Gippsland, Bass and Otway basins. In:

Glenie, R.C. (Ed.), Second South-Eastern Australia Oil Exploration Symposium, November 14 - 15, Melbourne, pp. 375 - 382.

Pacheco, Norbert, 2003, Helium: US. Geological Survey, Mineral Commodity Summaries, p. 80-81.

Padappayil, R.P., Borger, J., 2021. Ammonia Toxicity. https://pubmed.ncbi.nlm.nih.gov/31536283/ .

Pakzad, P., M. Mehrpooya, and A. Zaitsev, 2021, Investigation of a new energy-efficient cryogenic process configuration for helium extraction and liquefaction: International Journal of Energy Research, v. 45, no. 7, p. 10355–10377, doi:10.1002/er.6525.

Palacas, J.G., J.W. Smoker, T.A. Davis, M.J. Pawlewicz, and R.R. Anderson, 1999, Petroleum source rock assessment of Middle Proterozoic (Keweenawan) sedimentary rocks, Eischeid #1 well, Carroll county, Iowa, in eds. L.J. Wilson, The Amoco M.G. Eischeid #1, Deep Petroleum Test Carroll County, Iowa, Special Report Series, No. 2, p. 119 - 134.

Palmer, C., Tarazkar, M., Gordon, M.J., Metiu, H. and McFarland, E.W., 2021, Methane pyrolysis in low-cost, alkali-halide molten salts at high temperatures. Sustainable Energy & Fuels, 5(23), pp.6107-6123.

Palmer, N., and Ambrose, G., 2012, Mount Kitty Prospect, Southern Amadeus Basin. In: Keep, M., Moss, S.J. (Eds.), The Sedimentary Basins of Western Australia V, Proceedings of Petroleum Exploration Society of Australia Symposium, Perth, WA, 10 p. Pan American, 1964.

Pan American, 1964. Well Files for Suniland State Unit A1, State of Utah. https://oilgas.ogm.utah.gov/oilgasweb/live-data-search/lds-files/files-lu.xhtml.

Pandey, G.N., Tek, M.R., Katz, D.L., 1974. Diffusion of fluids through porous media with implications in petroleum geology. AAPG 58 (2), 291 - 303.

Park, H.B., Kamcev, J., Robeson, L.M., Elimelech, M. and Freeman, B.D., 2017, Maximizing the right stuff: The trade-off between membrane permeability and selectivity. Science, 356(6343).

Parker, J.M., 1981. Lisbon Field Area, San Juan County, Utah, Rocky Mountain Association of Geologist. Geology of Paradox Basin Field Conference, pp. 89 - 100.

Pashchenko, D., 2019, Thermochemical waste-heat recuperation by steam methane reforming with flue gas addition. International Journal of Energy Research, 43(6), pp.2216-2226.

Pashchenko, D., 2020, A heat recovery rate of the thermochemical waste-heat recuperation systems based on experimental prediction: Energy, v. 198, p. 117395, doi:https://doi.org/10.1016/j.energy.2020.117395.

Paterson, D.F., 1971, The Stratigraphy of the Winnipeg Formation (Ordovician) of Saskatchewan; Saskatchewan Department of Mineral Resources, Report 140, 57p.

Paul, D. R., 2018, Polymeric Gas Separation Membranes: doi:10.1201/9781351075886.

Pearson, B. and Gupta, M., 2005, The CANiCAP Program.

Peirce, HW., Keith, S.B., and Wilt, J.C., eds., 1970, Coal, oil, natural gas, helium, and uranium in Arizona: Arizona Bureau of Mines Bulletin 182, 289 p.

Penrose, O., Onsager, L., 1956. Bose-Einstein condensation and liquid helium. Phys. Rev. 104 (3), 576.

People’s Gas, 2020, Top 5 Everyday Uses for Natural Gas: 1–4 p.

Peretti, S.W., Shepherd, R.D., Clayton, R.K. and Proffitt, D.E., 2005, Membrane-Mediated Extraction and Biodegradation of Volatile Organic Compounds from Air. North Carolina State Univ. at Raleigh.

Peterson, J. and Madrid, P., 2012, 2010 Minerals Yearbook: Helium; US Geological Survey, Amarillo, Texas, URL <http:// minerals.usgs.gov/minerals/pubs/commodity/helium/myb1-

Peterson, J.A.,1989, Geology and petroleum resources, Paradox basin province: United States Department of the Interior Geological Survey OFR 88-450 U, 69 p.

Petrel Robertson Consulting Ltd., 2003, Exploration assessment of deep Devonian gas plays, northeastern British Columbia; British Columbia Ministry of Energy, Mines and Natural Gas, Petroleum Agency SA, 2012, Petroleum Agency SA, 2012, http://info.matchdeck.com/hubfs/Petroleum_Potential_of_the_Karoo_Basins5.pdf .

Pettke, T., Frei, R., Kramers, J.D., Villa, I.M., 1997. Isotope systematics in vein gold from Brusson, Val d'Ayas (NW Italy) (U þ Th) He and K-Ar in native Au and its fluid inclusions. Chem. Geol. 135 (3 - 4), 173 - 187.

Pfaff, I. and Kather, A., 2009, Comparative thermodynamic analysis and integration issues of CCS steam power plants based on oxy-combustion with cryogenic or membrane-based air separation. Energy Procedia, 1(1), pp.495-502.

Pfeiffer, L., Wanner, C., Lweicki, J., 2018. Unraveling the dynamics of magmatic CO2 degassing at Mammoth Mountain, California. Earth Planet Sci. Lett. 484, 318-328.

Pierce, A. P., G. B. Gott, and J. W. Mytton, 1964, Uranium and helium in the Panhandle gas field, Texas, and adjacent areas: U.S. Geological Survey Professional Paper 454-G, 57 p.

Pimentel, B.R., A. Parulkar, E.-K. Zhou, N.A. Brunelli, R.P. Lively, 2014, Zeolitic imidazolate frameworks: next-generation materials for energy-efficient gas separations, ChemSusChem 7, p. 3202–3240

Pinceaux, J.P., Maury, J.P., Besson, J.M., 1979. Solidification of helium, at room temperature under high pressure. J. Phys., Lett. 40 (13), 307 - 308.

Pinti, D.L., B. Marty, B., 1998. The origin of helium in deep sedimentary aquifers and the problem of dating very old groundwaters. Geol. Soc. 144 (1), 53 - 68. London, Special Publications.

Pinti, D.L., Marty, B., 1995. Noble gases in crude oils from the Paris Basin, France: Implications for the origin of fluids and constraints on oil-water-gas interactions.

Pinti, D.L., Marty, B., 2000. Chapter 7: noble gases in oil and gas fields: origins and processes. Minera. Assoc. Canada Short Course 28, 160 - 169.

Piping Designer, 2021, Water knockout: *in* Piping Designer, p. 1. From https://www.piping-designer.com/index.php/disciplines/mechanical/stationary-equipment/vessel/1507-free-water-knockout, Accessed 09-2021.

Pippin, L., 1970, Panhandle-Hugoton field, Texas-Oklahoma-Kansas- The first fifty years, in M. T. Halbouty, ed., Geology of giant petroleum fields: AAPG Memoir 14, p. 204- 222.

Pironon, J., Grishina, S., 1995, Hydrocarbon and non-hydrocarbon gas in salt environments, a contribution to gas genesis understanding. In: 1995 International Convention and Exposition Meeting, Nice, France. AAPG, Search and Discovery. Article #90956.

Pitman, J., L. Price, and J. LeFever, 2001, Diagenesis and Fracture Development in the Bakken Formation, Williston Basin: Implications for Reservoir Quality in the Middle Member.: USGS Professional Paper 1653, p. 24.

Plessen, B., Hoth, P., Lüders, V., 2007. Formation of nitrogen-rich gas accumulations in the Central European Basin. I. The significance of fixed ammonium in Palaeozoic Rocks. In: Annual Convention, Long Beach, California. AAPG Search and Discover. Article #90063.

Plug Power, 2016, Plug Power and HyGear partner to provide small-scale SMR hydrogen production technology to fuel cell system customers: Green Car Congress, v. 2016, no. June, p. 1–14.

Plumer, B., 2012, Congress turns its attention to... America’s helium crisis; The Washington Post, Washington, DC, May 13, 2012.

Polish Geological Institute National Research Institute, 2017. Oil and Gas Fields in Poland as of 2019-12-31, Map.

Poole, F.G.; Stewart, J.H.; Palmer, A.R.; Sandberg, C.A.; Madrid, Raul; Ross, R.J., Jr.; Hintze, L.F.; Miller, M.M.; Wrucke, C.T., 1992, Latest Precambrian to latest Devonian time—Development of a continental margin. In Burchfiel, B.C.; Lipman, P.W.; Zoback, M.L. (eds.). The Cordilleran Orogen—Conterminous U.S. The Geology of North America, Decade of North American Geology. G-3. Boulder, Colo.: Geological Society of America. pp. 9–56.

Poreda, R.J., Hunt, A.G., Lyons, W.B., Welch, K.A., 2004. The helium isotopic chemistry of Lake Bonney, Taylor Valley, Antarctica: timing of late Holocene climate change in Antarctica. Aquat. Geochem. 10 (3 - 4), 353 - 371.

Poreda, R.J., Jeffrey, A.W.A., Kaplan, I.R., Craig, H., 1988. Magmatic helium in subduction-zone natural gases. Chem. Geol. 71 (1 - 3), 199 - 210.

Potter, D., 2010. Relationships of Cambro-Ordovician Stratigraphy to Paleotopography on the Precambrian Basement, Williston Basin, Saskatchewan Geological Society, Saskatchewan and Northern Plains Oil & Gas Symposium, 2006, pp. 63 - 73.

Potter, R. W. and M. A. Clynne, 1978, The solubility of the noble gases He, Ne, Ar, Kr, and Xe in water up to the critical point: Journal of Solution Chemistry, v. 7 #11, p. 837-844.

Power, M.J., Hattori, K., Pinti, D.L., Potter, E.G., 2013. Anomalous Abundance of He and Mobile Metals in Surface Media over the Deeply Buried Millennium U Deposit, Athabasca Basin, Canada, Goldschmidt Conference Abstracts, p. 1993.

Prasolov, E.M., Kamenskiy, I.L., Meshik, A.P., Subbotin, Y.S., Surovtseva, L.N., Yakovkev, O.N., 1982. Formation of gas fields of the North of West Siberia from isotope data. Petrol. Geol. 20 (7), 316 - 319.

Prats, M., Reinoehl, J.B., Sekachev, I., Siewert, T.A. and Thiemens, M.H., 2010, Selling the Nation’s Helium Reserve; The National Academies Press, Washington, DC, 140 pages.

Pratt, T.L., E.C. Hauser, and K.D. Nelson, 1992, Widespread Buried Precambrian Layered Sequences in the U.S. Mid-Continent: Evidence for Large Proterozoic Depositional Basins: American Association of Petroleum Geologists Bulletin, v. 76/9, p. 1384-1401.

Price, B. and M. Mahaley, 2013, Optimize small-scale LNG production with modular SMR technology: Gas Processing, no. April 2014, p. 1–8.

Price, L. C., 1981, Methane solubility in brines with application to the geopressured resource: in Proceedings of the fifth geopressured-geothermal energy conference, p. 205-214.

Prinzhofer, A., 2013, Noble gases in oil and gas accumulations: Adv. Isot. Geochemistry, p. 225–247, doi:10.1007/978-3-642-28836-4_9.

Priyatkina, N., Khudoley, A.K., Collins, W.J., Kuznetsov, N.B. and Huang, H.Q., 2016. Detrital zircon record of Meso-and Neoproterozoic sedimentary basins in northern part of the Siberian Craton: characterizing buried crust of the basement. Precambrian Research, 285, pp.21-38.

Protin, M., Blard, P.-H., Marrocchi, Y., Mathon, F., 2016. Irreversible adsorption of atmospheric helium on olivine: a lobster pot analogy. Geochem. Cosmochim. Acta 179, 76 - 88.

Qatargas, 2021, Setting higher standard of excellence: p. 44–46. From: https://www.qatargas.com/english/aboutus/directiors-statement., Accessed 10-2021.

Quader, M. A., T. E. Rufford, and S. Smart, 2020, Modeling and cost analysis of helium recovery using combined-membrane process configurations: Separation and Purification Technology, v. 236, no. February 2020, p. 116269, doi: 10.1016/j.seppur.2019.116269.

Quader, M. A., T. E. Rufford, and S. Smart, 2021, Evaluation of flowsheet design approaches to improve energy efficiency in multistage membrane processes to recover helium: Industrial and Engineering Chemistry Research, v. 60, no. 6, p. 2588–2599, doi:10.1021/acs.iecr.0c05871.

Quader, M. A., T. E. Rufford, and S. Smart, 2021, Integration of hybrid membrane-distillation processes to recover helium from pre-treated natural gas in liquefied natural gas plants: Separation and Purification Technology, v. 263, no. May, doi:10.1016/j.seppur.2021.118355.

R.M., Shapero, D.C. and Ehrenreich, R.M., 2000, The Impact of Selling the Federal Helium Reserve; National Academy Press, Washington D.C., 81p.

Rabe, B., Kaliban, C. and Englehart, I., 2020, Taxing flaring and the politics of state methane release policy. Review of Policy Research, 37(1), pp.6-38.

Rahimi, A. N., M. F. Mustafa, M. Z. Zaine, N. Ibrahim, K. A. Ibrahim, N. Yusoff, E. M. Al-Mutairi, and M. K. A. Hamid, 2015, Energy efficiency improvement in the natural gas liquids fractionation unit: Chemical Engineering Transactions, v. 45, no. December, p. 1873–1878, doi:10.3303/CET1545313.

Rahimpour-Bonab, H., 2007. A procedure for appraisal of a hydrocarbon reservoir continuity and quantification of its heterogeneity. J. Petrol. Sci. Eng. 58 (1), 1 - 12.

Rahimpour-Bonab, H., Esrafili-Dizaji, B., Tavakoli, V., 2010. Dolomitization and anhydrite precipitation in PermoTriassic carbonates at the South Pars Gas Field, offshore Iran: controls on reservoir quality. J. Petrol. Geol. 33 (1), 43 - 66.

Raissi, A., and D. Block, 2004, Hydrogen Basics - Production: IEEE Power & Energy, v. 2, no. 6.

Raitt, W.J., Schunk, R.W., Banks, P.M., 1978. Helium ion outflow from terrestrial ionosphere. Planet. Space Sci. 26, 255 - 268.

Randolph, K. et al., 2017, Hydrogen Production Tech Team Roadmap: US DOE, no. November, p. 55.

Ranjbar, H., Ahmadi, H., Sheshdeh, R.K. and Ranjbar, H., 2015, Application of relative sensitivity function in parametric optimization of a tri-ethylene glycol dehydration plant. Journal of Natural Gas Science and Engineering, 25, pp.39-45.

Rao, A.B. and Rubin, E.S., 2002, A technical, economic, and environmental assessment of amine-based CO2 capture technology for power plant greenhouse gas control. Environmental science & technology, 36(20), pp.4467-4475.

Rapatskaya, L.A., Tonikh, M.E., Ustyuzhanin, A.O., 2020. Natural reservoir as a geological body for storing helium reserves. IOP Conf. Ser. Earth Environ. Sci. 408, 5 p.

Rapier, R., 2020, Estimating the Carbon Footprint of Hydrogen Production: OilPrice.com, p. 1–6.

Rascoe Jr., B., 1968. Permian System in Western Mid-Continent, vol. 5 (3), pp. 127e138. Rocky Mountain Association of Geologists. The Mountain Geologists.

Rascoe Jr., B., Adler, F.J., 1983. Permo-Carboniferous hydrocarbon accumulations, mid-continent, U.S.A. Am. Assoc. Pet. Geol. Bull. 67 (6), 979-1001.

Rassenfoss, S., 2014, Revolutionary, evolutionary: Ideas for lowering the cost of gas separation: JPT, Journal of Petroleum Technology, v. 66, no. 9, p. 54–59, doi:10.2118/0914-0054-jpt.

Rauzi, S.L., 1999. Carbon Dioxide in the St. John’s - Springerville Area, Apache County, Arizona. Arizona Geological Survey, OFR 99-2.

Rauzi, S.L., 2003, Arizona Well Location Map and Report: Arizona Geological Survey Oil & Gas Publication OG-12, 27 p., scale 1:675,000.

Rauzi, S.L., 2003. Review of Helium Production and Potential in Arizona. Arizona Geological Survey, OFR 03-05, 30p.

Rauzi, S.L., 2005, Review of helium production and potential in Arizona: Arizona Geological Survey OFR 03-05, 30 p.

Ravindran, S., Ruffer, C. and Sneary, L., 2016, August. Bakken Flare Mitigation Field Trial. In Unconventional Resources Technology Conference, San Antonio, Texas, 1-3 August 2016 (pp. 2061-2068). Society of Exploration Geophysicists, American Association of Petroleum Geologists, Society of Petroleum Engineers.

Ray, M.C., Hilton, D.R., Muñoz, J., Fischer, T.P., Shaw, A.M., 2009. The effects of volatile recycling, degassing and crustal contamination on the helium and carbon geochemistry of hydrothermal fluids from the Southern Volcanic Zone of Chile. Chem. Geol. 266 (1), 38 - 49.

Reddy, G. K., and P. G. Smirniotis, 2015, Water gas shift reaction: Elsevier, 269 p., doi:10.1016/c2013-0-09821-0.

Reid, J., Hunt, A.G., Ellis, G.S., Taylor, K.B., Patterson III, O.F., 2015. Noble Gas Isotopes, Major Element Isotopes, and Gas Composition from the Cumnock Formation: Sanford Sub-Basin, Deep River Basin, Lee County, North Carolina, U.S.A. American Association of Petroleum Geologists. Search and Discovery Article #80492, 4 p.

Reimer, G.M., Denton, E.H., Freidman, I., Otton, J.K., 1979. Recent developments in uranium exploration using the U.S. Geological Surveys mobile helium detector. J. Geochem. Explor. 11, 1 - 12.

Reiners, P. W., 2005, Zircon (U-Th)/He thermochronometry: Reviews in Mineralogy and Geochemistry v. 58, p. 151-179.

Reinhold, pp. 256 - 268. Haussmann, R., 1994. Properties of a fermi liquid at the superfluid transition in the crossover region between BCS superconductivity and Bose-Einstein Condensation. Phys. Rev. B 49 (18), 12975 - 12983.

Renee, J., 2021, Flaring solutions are circling the Bakken, thanks in part to state’s new tax credit: p. 21–23.

Resources and International Petroleum Conference, 19–21 October 2010, Society of Petroleum Engineers, Calgary, Alberta.

Reutinger, C.A., 1968. Natural gas in Permian and Cisco Beds of Red River and Electra Arch, American Association of Petroleum Geologists. In: Memoir 9, Natural Gas of North America, vol. 2, pp. 1455-1458.

Rezakazemi, M., Sadrzadeh, M. and Matsuura, T., 2018. Thermally stable polymers for advanced high-performance gas separation membranes. Progress in Energy and Combustion Science, 66, pp.1-41.

Rice, D. D., 1983, Relation of natural gas composition to thermal maturity and source rock type in San Juan basin, Northwestern New Mexico and southwestern Colorado: AAPG Bulletin, v. 67, p.1199-1218.

Riggs, E.A., 1978. Tocito Dome Mississippian North. In: Fassett, J.E. (Ed.), Oil and Gas Fields of the Four Corners Area, Volume II Four Corners Geological Society, pp. 519e530.

Rinkesh, 2008, What Is Hydrogen? p. 24: From” <http://www.conserve-energy-future.com/advantages_disadvantages_hydrogenenergy.php>. Accessed 05-2021.

Rithauddeen, M., A. Faadzil, E. Al-Helal, and S. Al-Mudaibegh, 2021, Process selection for deep COS removal from feed gas: Gas Processing & LNG, p. 1–10.

Ritter, J.A., Ebner, A.D., 2007. State-of-the-art adsorption and membrane separation processes for hydrogen production in the chemical and petrochemical industries. Separ. Sci. Technol. 42 (6), 1123 - 1193.

RMAG, 1972, Geologic Atlas of the Rocky Mountain Region, Rocky Mountain Association of Geologists, Denver, CO, 1972: p. 81-85, 88-89, 94-97, 168, 184

Robbins, S.L., and G.R. Keller, 1992, Complete Bouguer and Isostatic Residual Gravity Maps of the Anadarko Basin, Wichita Mountains, and Surrounding Areas, Oklahoma, Kansas, Texas, and Colorado: U.S. Geological Survey Bulletin 1866-G, 11 p.

Roberts, A.A., 1981. Helium manometry for exploring for hydrocarbons: Part II. In: Unconventional Methods in Exploration for Petroleum and Natural Gas, Symposium II. Southern Methodist University Press, Dallas, TX, pp. 136 - 149.

Robertson, J.O., Chilingarian Jr, G.V. and Mazzullo, S.J., 1996, Appendix B Petroleum engineering glossary. In Developments in Petroleum Science (Vol. 44, pp. 921-937). Elsevier.

Robitski, D., 2019, Toyota is Selling a Hydrogen Fuel Cell Car for $50,000: Earth & Energy, v. 3, p. 3.

Rodrigue, J.-P., 1998, Energy Content of some Combustibles, in MJ/kg: Geography of transport systems.

Rodrigue, J.-P., C. Comtois, and B. Slack, 2019, Transport, energy and environment: 432 p., doi:10.4324/9781315618159-8.

Rogers, D., and Y. He, 2020, A global oil price war and COVID-19: How will NGL markets adapt and react to these unprecedented disruptions? Energy & Natural Resources Research & Analysis, p. 1–5.

Rogers, G.S., 1921. Helium-Bearing Natural Gas, Kansas Geological Survey Professional Paper 121, 107 p.

Rogers, J.P., 2014. Arrowhead gas field. In: Rogers, J.P., Milne, J.J., Cumella, S.P., Dubois, D.P., Lillis, P.G. (Eds.), Oil and Gas Fields of Colorado. Rocky Mountain Association of Geologist, pp. 20-23.

Romano, M.C., Cassotti, E.N., Chiesa, P., Meyer, J. and Mastin, J., 2011, Application of the sorption enhanced-steam reforming process in combined cycle-based power plants. Energy Procedia, 4, pp.1125-1132.

Romsom, E. and McPhail, K., 2021, Capturing economic and social value from hydrocarbon gas flaring and venting: evaluation of the issues (No. 2021/5). WIDER Working Paper.

Ross Jr., R.J., Tweto, O., 1980. Lower Paleozoic sediments and tectonics in Colorado, in Geology of Colorado Symposium. RMAG, pp. 47-56.

Roth, G., 1983. Sheep Mountain and Dike Mountain fields, Huerfano County, Colorado. In: Fassett, J.E. (Ed.), Oil and Gas Fields of the Four Corners Area, Volume II: Four Corners Geological Society, pp. 740-744.

Roy, C.D., Chakraborty, N. and Sarkar, S.C., 2019, Thermodynamic efficiency evaluation of a low-pressure turbo expander cryogenic cycle based on exergy analysis. Thermal Science, 23(3 Part B), pp.2097-2106.

Royston, M.K., Wheeler, H.P., 1956. Helium, Minerals Yearbook. USGS, p. 444.

Rudyardfield. In: Montana Geological Society Oil and Gas Fields Symposium, vol. 2, pp. 995 - 998.

Ruedemann, P. and L. M. Oles, 1929, Helium-its probable origin and concentration in the Amarillo Fold, Texas: AAPG Bulletin v13 #7, p.799-810.

Rufford, T. E., K. I. Chan, S. H. Huang, and E. F. May, 2014, A review of conventional and emerging process technologies for the recovery of helium from natural gas: Adsorption Science and Technology, v. 32, no. 1, p. 49–72, doi:10.1260/0263-6174.32.1.49.

Rumble, J.R., 2020. Handbook of Chemistry and Physics, 101st ed. CRC Press, p. 1572.

Ryan, S.G., Norton, A.J., 2010. Stellar Evolution and Nucleosynthesis. Cambridge University Press, p. 135.

S. Khatibi, M. Ostadhassan, R. A. Mohammed, and A. Aghajanpour, 2018, NMR T1-T2 Map of Different Hydrogen Contents of Bakken Formation: International Journal of Chemical Engineering and Applications, v. 9, no. 3, p. 93–96, doi:10.18178/ijcea.2018.9.3.705.

Saberimoghaddam, A. and Khebri, V., 2018, Design and construction of a helium purification system using cryogenic adsorption process. Iranian Journal of Chemical Engineering (IJChE), 15(1), pp.89-101.

Sadeghbeigi, R., 2020, Fluid catalytic cracking handbook: An expert guide to the practical operation, design, and optimization of FCC units. Butterworth-Heinemann.

SahleDemessie, E, U R. Pillai, S. Junsophonsri, & K. L. Levien, 2003, Solubility of Organic Biocides in Supercritical CO_2 And CO_2+ Cosolvent Mixtures. Marsh, K.N. (ed.), Chemical & Engineering Data. American Chemical Society, Washington, DC, 48(3):541-547

Salkuyeh, Y.K., Saville, B.A. and MacLean, H.L., 2017, Techno-economic analysis and life cycle assessment of hydrogen production from natural gas using current and emerging technologies. International Journal of hydrogen energy, 42(30), pp.18894-18909.

Sano, Y., Takahata, N., Igarashi, G., Koizumi, N., Sturchio, N.C., 1998. Helium degassing related to the Kobe earthquake. Chem. Geol. 150 (1 - 2), 171 - 179.

Sano, Y., Takahata, N., Kagoshima, T., Shibata, T., Onoue, T., Zhao, D., 2016. Groundwater helium anomaly reflects strain change during the 2016 Kumamoto earthquake in Southwest Japan. Sci. Rep. 6, 37939. https://doi.org/ 10.1038/srep37939, 2016.

Sartbaeva, A., V. L. Kuznetsov, S. A. Wells, and P. P. Edwards, 2008, Hydrogen nexus in a sustainable energy future: Energy and Environmental Science, v. 1, no. 1, p. 79–85, doi:10.1039/b810104n.

Saskatchewan Geological Survey, Saskatchewan Energy and Mines, Miscellaneous Report 89-4, p.168-171. Gas Development, p.45-52. file:///C:/Users/amarsh/Downloads/helium_johnson.pdf

Saskatchewan Ministry of the Economy, 2014, Stratigraphic Correlation Chart; Saskatchewan Ministry of Energy and Resources. http://www.economy.gov.sk.ca/stratigraphiccorrelationchart [accessed 14 March 2016].

Sawatzky, H., Agarwal, R.G. and Wilson, W. ,1960, Helium Prospects in Southwest Saskatchewan; Saskatchewan Department of Mineral Resources, Geological Sciences Branch, Report 49, 28p.

Sawatzky, H.B., 1967a, Composite seismic map, Regina, Saskatchewan; Saskatchewan Department of Mineral Resources, Geophysical Division, Geological Sciences Branch, Drawing No. N-1, scale 1 inch to 4 miles. http://www.economy.gov.sk.ca/N1.

Sawatzky, H.B., 1967b, Composite seismic map, Swift Current, Saskatchewan; Saskatchewan Department of Mineral Resources, Geophysical Division, Geological Sciences Branch, Drawing No. N-2, scale 1 inch to 4 miles. http://www.economy.gov.sk.ca/N2.

Sawatzky, H.B., 1967c, Composite seismic map, Yorkton, Saskatchewan; Saskatchewan Department of Mineral Resources, Geophysical Division, Geological Sciences Branch, Drawing No. N-3, scale 1 inch to 4 miles. http://www.economy.gov.sk.ca/N3.

Sawatzky, H.B., 1967d, Composite seismic map, Saskatoon, Saskatchewan; Saskatchewan Department of Mineral Resources, Geophysical Division, Geological Sciences Branch, Drawing No. N-4, scale 1 inch to 4 miles. http://www.economy.gov.sk.ca/N4.

Sazali, N., 2020, A review of the application of carbon-based membranes to hydrogen separation. Journal of Materials Science, 55, pp.11052-11070.

SBH4.de, 2021, SMR, ATR and POX processes for syngas production, from https://www.sbh4.de/assets/smr-atr-and-pox-processes.pdf, accessed 11-2021

Scharlin, P., Battino, R., Silla, E., Tuñón, I., Pascual-Ahuir, J.L., 1998. Solubility of gases in water: correlation between solubility and the number of water molecules in the first solvation shell. Pure Appl. Chem. 70 (10), 1895 - 1904.

Schimmelmann, A., 2019. Isotopes of Unconventional Systems, Part I, the Society for Organic Petrology, Annual Meeting, Bloomington, Indiana, p. 56.

Schmitt, H.H., 2013. Lunar Helium-3 energy resources. In: Ambrose, W.A., Reilly, J.F., Peters, D.C. (Eds.), Energy Resources for Human Settlement in the Solar System and Earth's Future in Space, American Association of Petroleum Geologists Memoir 101., pp. 33 - 51.

Schmitt, H.H., 2014. Synthesis of Current Data on Helium and Hydrogen Concentration in Lunar Regolith. American Association of Petroleum Geologists. Search and Discovery #70162, 26 p.

Schoell, M., and J. A. Lefever, 2011, Carbon and hydrogen isotope systematics in gases from horizontal Bakken Shale wells: Search and Discovery, no. 110149, p. 22pp, doi:10.13140/RG.2.1.2711.1528.

Scholes, C. A., and U. K. Ghosh, 2017, Review of membranes for helium separation and purification: Membranes, v. 7, no. 1, p. 1–13, doi:10.3390/membranes7010009.

Scholes, C. A., G. W. Stevens, and S. E. Kentish, 2012, Membrane gas separation applications in natural gas processing: Fuel, v. 96, p. 15–28, doi: 10.1016/j.fuel.2011.12.074.

Scholes, C.A., 2018, Helium recovery through inorganic membranes incorporated with a nitrogen rejection unit. Industrial & Engineering Chemistry Research, 57(10), pp.3792-3799.

Scholes, C.A., Ghosh UK, U.K., Ho, M.T., 2017. Ind. Eng. Chem. Res. 56, 335 - 383. Schrier, J., 2010. Helium separation using porous graphene membranes. J. Phys. Chem. Lett. 1 (15), 2284 - 2287.

Scholes, C.A., Ghosh, U.K., 2017. Review of membranes for helium separation and purification. Membranes 7 (9). https://doi.org/10.3390/membranes7010009 .

Scholes, CA and Ghosh, UK, 2016, Helium separation through polymeric membranes: Selectivity targets, J. Membr. Sci. 520, 2016, 221–230.

Scholes, CA, Ghosh UK and Ho, MT, 2017, Indust. Eng. Chem. Res. 56, 2017, 335-383.

Schrier, J., 2010, J. Phys. Chem. Lett., 1, 2284.

Schroth, H.A., 1953, Bowdoin dome, Montana; *in* Billings Geological Society, Guidebook: Fourth Annual Field Conference, September 10 to 12, 1953, p.137-141.

Schulze, G. and J. M. Prausnitz, 1981, Solubilities of gases in water at high temperature: Ind. Eng. Chem. Fundam. v. 20, p. 177-180.

Science alert, 2021, Plasma-record . www.sciencealert.com/china-s-nuclear-fusion-machine-just-smashed-germany-s-hydrogen

Sclierf, M., and T. E. Rufford, 2016, A Technical Evaluation of Hybrid Membrane-Absorption Processes for Acid Gas Removal, *in* International Petroleum Technology Conference held in Bangkok, Thailand, 14-16 November 2016: p. 5, doi:10.2523/iptc-18732-ms.

Seader, J.D., Henley, E.J., 2006. Separation Process Principles. John Wiley and Sons, Hoboken, NJ.

Sears, W.M., 2015. Helium the Disappearing Element. Springer International Publishing, p. 138.

Seibel, C.W., Kennedy, H.S., 1934. Helium. USGS Minerals Yearbook, pp. 757 - 764, 1934.

Sellars, R.T., 2014. Bledsoe Ranch. In: Rogers, J.P., Milne, J.J., Cumella, S.P., Dubois, D.P., Lillis, P.G. (Eds.), Oil and Gas Fields of Colorado. Rocky Mountain Association of Geologists, pp. 44-46.

Senn, E., 2016, DDG 1000 Zumwalt Class – Multi-mission Destroyer: Naval Technology, no. Ddg 1000, p. 1–12.

Sesack, S. A, 2011, Sequence Stratigraphy, Depositional Environments, and Regional Mapping of the Late Devonian Interval, Upper Three Forks Formation, Sanish Member, and Lower Bakken Shale, U.S. Portion of the Williston Basin: West Virginia University, 226 p.

Seth Stein, S., S. van der Lee, D. Jurdy, C. Stein, D. Wiens, M. Wysession, J. Revenaugh, A. Frederiksen, F. Darbyshire, T. Bollmann, J. Lodewyk, E. Wolin, M. Merino, and K. Tekverk, 2011, Learning from failure: The SPREE Mid-Continent Rift Experiment: GSA Today, v. 21/9, p. 5-7.

Settar, A., S. Abboudi, B. Madani, and R. Nebbali, 2018, Estimation of transient heat flux density during the heat supply of a catalytic wall steam methane reformer: Heat and Mass Transfer/Waerme- und Stoffuebertragung, v. 54, no. 2, p. 385–391, doi:10.1007/s00231-017-2131-3.

Shahab-Deljoo, M., Medi, B., Kazi, M.K. and Jafari, M., 2023, A Techno-Economic Review of Gas Flaring and Its Human and Environmental Impacts. Process Safety and Environmental Protection.

Shahan, Z., 2016, Why Hydrogen Fuel Cell Cars Are Not Competitive: Clean Technica, p. 1–15.

Shannon, C.W., 1962. Oil and gas developments in Utah and Nevada in 1961. Am. Assoc. Pet. Geol. Bull. 46 (6), 975.

Sharland, P.R., Archer, R., Casey, D.M., Davies, R.B., Hall, S.H., Heward, A.P., Horbury, A.D., Simmons, M.D., 2001.

Sharp, Z., 2006. Principles of Stable Isotope Geochemistry. Prentice Hall, pp. 1 - 344. Sherr, J., 2016. Neon. Saltire Books, Glasgow, Scotland, pp. 1 - 228.

Shemin G.G., 2007, Geologiya i perspektivy neftegazonosnosti venda i nizhnego kembriya tsentral’nykh rayonov Sibirskoy platformy (Nepsko-Botuobinskaya, Baykitskaya anteklizy i Katangskaya sedlovina) (Geology and oil and gas potential Vendian and Lower Cambrian deposits of central regions of the Siberian Platform (Nepa-Botuoba, Baikit anteclise and Katanga saddle)): edited by Kashirtsev V.A., Novosibirsk: Publ. of SB RAS, 2007, 467 p.

Sherif, S. A., D. Y. Goswami, E. K. Stefanakos, and A. Steinfeld, eds., 2014, Handbook of Hydrogen Energy, in Handbook of Hydrogen Energy: CRC Press, p. 1042.

Shi, W., Yang, H., Shen, Y., & Fu, Q., & Zhang, D., & Fu, B., 2018, Two-stage PSA/VSA to produce H_2 with CO_2 capture via steam methane reforming (SMR). International Journal of Hydrogen Energy. 43. 10.1016/j.ijhydene.2018.08.077.

Shindo, R., and K. Nagai, 2021, Gas Separation Membranes BT - Encyclopedia of Polymeric Nanomaterials, *in* S. Kobayashi, and K. Müllen, eds.: Berlin, Heidelberg, Springer Berlin Heidelberg, p. 1–8, doi:10.1007/978-3-642-36199-9_134-1.

Shipton, Z.K., Evans, J.P., Kirschner, D., Kolesar, P.T., Williams, A.P. and Heath, J., 2004, Analysis of CO2 leakage through ‘low-permeability’ faults from natural reservoirs in the Colorado Plateau, east-central Utah. Geological Society, London, Special Publications, 233(1), pp.43-58.

Sigler, S.M., 1994, Analyses of Natural Gases, 1993: U.S. Bureau of Mines, Information Circular 9400, 58 p., accessed May 14, 2021

Simmons, M.D., 2001. Arabian Plate Sequence Stratigraphy: GeoArabia Special Publication No. 2, Gulf PetroLink, Bahrain, 371 p.

Sims, P.K., Bankey, V., Finn, C.A., 2001. Preliminary Precambrian Basement Map of Colorado - a Geologic Interpretation of an Aeromagnetic Anomaly Map, USGS, OFR 01-0364.

Sinaei Nobandegani, M., M. R. Sardashti Birjandi, T. Darbandi, M. M. Khalilipour, F. Shahraki, and D. Mohebbi-Kalhori, 2016, An industrial Steam Methane Reformer optimization using response surface methodology: Journal of Natural Gas Science and Engineering, v. 36, no. October, p. 540–549, doi:10.1016/j.jngse.2016.10.031.

Singh, A., Rokosh, C.D., Branscombe, P., Filewich, C., 2020. Helium Concentrations of Natural Gas Analysis Tests in Alberta (Tabular Data, Tab-Delimited Format). Alberta Geological Survey. https://ags.aer.ca/publication/dig2020-0033 .

Singh, G., Singh, E.J., Singh, E.J. and Singh, A., 2017, Cryogenics (Helium Liquefaction). Int. Res. Jour. of Eng. and Tech, 4, pp. 867-873.

Sittig, M., 1980. Geophysical and Geochemical Techniques for Exploration of Hydrocarbons and Minerals. Noyes Data Corp, Newark, NJ.

Sivals, C.R., 1995, U.S. Will Require Glycol Dehydrator Emission Control. World Oil (November): 75.

Sloss, L. L., 1964, Tectonic Cycles of the North American Craton: Kansas Geological Survey, Bulletin, v. 169, p. 449–459.

Slyuta, E.N., Abdrakhimov, A.M., Galimov, E.M., 2007. Lunar and Planetary Science XXXVIII (1338), 2175.

Smith, M, and Bustin, R., 2000, Late Devonian and early Mississippian Bakken and Exshaw black shale source rocks, Western Canada Sedimentary Basin–a sequence stratigraphic interpretation: American Association of Petroleum Geologists Bulletin, 84, no. 7, p. 940–960.

Smith, P.K., and Pylant, H.S., 1962, Helium plant in commercial operation: Oil & Gas Journal, v. 60, no. 44 (October 29), p. 136-139.

Smith, R.B., 1970, Regional gravity survey of western and central Montana; American Association of Petroleum Geologists Bulletin, v.54, no.7, p.1172-1183.

Smouse, 1993. Salt Wash. In: Hill, B.G., Bereskin, S.R. (Eds.), Oil and Gas Fields of Utah, Utah Geological Association Publication 22, Unpaginated.

Society of Petroleum Engineers, World Petroleum Council, and American Association of Petroleum Geologists, 1997, Glossary of terms used: 287–288 p., doi:10.1515/9781618111128-009.

Soleimany, A., Hosseini, S.S., Gallucci, F., 2017. Recent Progress in Developments of Membrane Materials and Modification Techniques for High-Performance Helium Separation and Recovery: A Review, Chemical Engineering and Processing: Process Intensification. https://doi.org/10.1016/j.cep.2017.06.001 . June 2017, URL: South-tek Systems, 2021. Carbon Molecular Sieve (CMS). https://www.southteksystems.com/psa-technology/.

Soltani, R., M. A. Rosen, and I. Dincer, 2014, Assessment of CO_2 capture options from various points in steam methane reforming for hydrogen production: International Journal of Hydrogen Energy, v. 39, no. 35, p. 20266–20275, doi:10.1016/j.ijhydene.2014.09.161.

Soltanieh, M., Zohrabian, A., Gholipour, M.J. and Kalnay, E., 2016, A review of global gas flaring and venting and impact on the environment. International Journal of Greenhouse Gas Control, 49, pp.488-509.

Solutions, I. F., 2008, Fuel Gas Conditioning - Membrane Packages Fuel Gas Conditioning - Membrane Package: 4 p.

Song, Chunfeng & Kansha, Yasuki & Ishizuka, Masanori & Fu, Qian & Tsutsumi, Atsushi, 2014, Design of a Low-cost CO_2 Capture Process Based on Heat Integration Technology. Energy Procedia. 61. 365-368. 10.1016/j.egypro.2014.11.1126.

Song, P., R. Wang, Y. Sui, T. Shan, J. Hou, and X. Wang, 2021, Small Scale Skid-Mounted Natural Gas to Hydrogen Production System Provides Competitive Hydrogen for China, *in* International Petroleum Technology Conference held virtually on 23 March - 1 April 2021: p. 2–11, doi:10.2523/iptc-21365-ms.

Sonnenberg, S. A., 2019, Sequence Stratigraphy of the Bakken and Three Forks Formations, Williston Basin, USA: Sequence Stratigraphy: The Future Defined, v. 10990, doi:10.5724/gcs.17.121.

Sonnenberg, S. a., H. Jin, and J. F. Sarg, 2011, Bakken mudrocks of the Williston Basin, world class source rocks: Search and Discovery, v. 80171, no. 80171, p. 5pp, doi:10.13140/RG.2.1.3628.8406.

Sonnenberg, S.A., van Drehle, W.F., 1990. Morrow gas composition in southeast Colorado. In: Sonnenberg, S.A., Shannon, L.T., Rader, K., von Drehle, W.F., Martin, G.W. (Eds.), Morrow Sandstones, Rocky Mountain Association of Geologist, pp. 233 - 235.

Sönnichsen, N., 2021, Natural gas production in Qatar 1998-2020 Natural gas production in Qatar from 1989 to 2020 (in billion cubic meters): Stastica, p. 1–2. From: https://www.statista.com/statistics/265336/natural-gas-production-in-qatar/, accessed 10-2021.

Sorenson, R.P., 2005. A dynamic model for the Permian Panhandle and Hugoton fields, western Anadarko Basin. Am. Assoc. Petrol. Geol. 89 (7), 921 - 938.

Sorey, M.L., Evans, W.C., Kennedy, B.M., Farrar, C.D., Hainsworth, L.J., Hausback, B., 1998. Carbon dioxide and helium emissions from a reservoir of magmatic gas beneath Mammoth Mountain, California. J. Geophys. Res. Solid Earth 103 (87), 15 p.

Spacenews, 2021. Google to Shut Down Loon. https://spacenews.com/google-to-shut-down-loon/.

Spatolisano, E. and Pellegrini, L.A., 2021, CO_2-Tolerant Cryogenic Nitrogen Rejection Schemes: Analysis of Their Performances. Industrial & Engineering Chemistry Research, 60(11), pp.4420-4429.

Speer, R., and J. Stroeder, 2021, Government of Saskatchewan Launches Helium Action Plan: Saskatchewan Petroleum, p. 1–4.

Speight, J. G., 2014, Gasification of Unconventional Feedstocks: 1–191 p., doi:10.1016/C2013-0-14152-9.

Speight, J. G., 2016, Deep Shale Oil and Gas: Elsevier, 1–481 p.

Speight, J.G., 2015. Heavy hydrocarbon gasification for synthetic fuel production. In Gasification for Synthetic Fuel Production (pp. 221-239). Woodhead Publishing.

Speight, J.G., 2019, Glossary, in J. G. Speight, ed., Natural Gas (Second Edition): Boston, Gulf Professional Publishing, p. 397–432, doi:10.1016/b978-0-12-809570-6.00026-6.

Spencer, C.W., 1978a. Tohache Wash Area. In: Fassett, J.E., Thomaidis, N.D., Matheny, M.L. (Eds.), Oil and Gas Fields of the Four Corners Area, Four Corners Geological Society, vol. 1, pp. 92 - 93.

Spencer, C.W., 1978b. Tocito Dome Pennsylvanian "D". In: Fassett, J.E., Thomaidis, N.D., Matheny, M.L. (Eds.), Oil and Gas Fields of the Four Corners Area, Four Corners Geological Society, vol. 1, pp. 522 - 527.

Spencer, J.E., 1983, Helium resources and production in Arizona: Arizona Bureau of Geology and Mineral Technology Fieldnotes, v. 13, no. 2, p. 6-7,15-16.

Staffell, I., D. Scamman, A. Velazquez Abad, P. Balcombe, P. E. Dodds, P. Ekins, N. Shah, and K. R. Ward, 2019, The role of hydrogen and fuel cells in the global energy system: Energy and Environmental Science, v. 12, no. 2, p. 463–491, doi:10.1039/c8ee01157e.

Standard & Poors, 2021, Mitsubishi, Bakken Energy aim to develop Blue Hydrogen hub in North Dakota, S&P Global Market Intelligence, p. 3.

State Historical Society Of North Dakota (SHSND), 2020, Part 1: Geology Section 4: Bakken Formation: p. 2.

Stein, S., van der Lee, S., Jurdy, D., Stein, C., Wiens, D., Wyesession, M., Revenaugh, J., Frederiksen, A., Darbyshire, F., Bollmann, T., Lodewyk, J., Wolin, E., Merino, M., Tekverk, K., 2011. Learning from failure: the SPREE Mid-Continent Rift experiment. GSA Today (Geol. Soc. Am.) 21 (Issue 9), 4p.

Stell, J., 2020, The Bakken shale's good news for gas processors: Gas Processing & LNG, p. 2.

Stern, S.A., Sinclair, P.J., Hareis, N.P.V., Mohr, P.H., 1965. Ind. Eng. Chem. 57, 49.

Stern, S.A.; Sinclair, T.F.; Gareis, P.J.; Vahldieck, N.P.; Mohr, P.H., 1965, Helium recovery by permeation. Ind. Eng. Chem. 57, 49–60.

Stewart, M., 2014, Surface Production Operations, Volume Two: Elsevier, 685 p.

Stiglbauer, G.C., 2015. North Dakota natural gas: the decision to flare (Doctoral dissertation, Montana State University-Bozeman, College of Agriculture).

Stilwell, D.P., 1989. CO_2 Resources of the Moxa Arch and the Madison Reservoir: Gas Resources of Wyoming 40th Annual Field Conference Guidebook. Wyoming Geological Association (1989), pp. 105 - 115.

Stoddard, J.N., 1982. Brandon Field - Pennsylvanian, Morrow Formation and Lansing-Kansas City Group. In: Crouch III, M.C., et al. (Eds.), Oil and Gas Fields of Colorado and Nebraska and Adjacent Areas, Rocky Mountain Association of Geologist, p. 7881.

Stone, J.A., Stejskal, A., 2004. Using helium as a standard of refractive index: correcting errors in a gas refractometer. Metrologia 41 (3), 189 - 197.

Stratistics Market Research Consulting (MRC), 2020. Helium - Global Market Outlook (2019-2027), Research and Markets, Dublin, Ireland, p. 173. https://www.strategymrc.com

Stroncik, N.A., Niedermann, S., Haase, K.M., 2007. Neon and helium isotopes as tracers of mantle reservoirs and mantle dynamics. Earth Planet Sci. Lett. 258 (1), 334 - 344.

Strutt, R.J., 1908. On the accumulation of helium in geological time. Proceedings of the Royal Society of London. Series A, Containing Papers of a Mathematical and Physical Character, 81(547), pp.272-277.

Strutt, R.J., 1909. The accumulation of helium in geological time.-II. Proceedings of the Royal Society of London. Series A, Containing Papers of a Mathematical and Physical Character, 83(560), pp.96-99.

Stuart, F.M., Burnard, P.G., Taylor, R.E.A., Turner, G., 1995. Resolving mantle and crustal contributions to ancient hydrothermal fluids: He-Ar isotopes in fluid inclusions from Dae Hwa W-Mo mineralization, South Korea. Geochem. Cosmochim. Acta 59 (22), 4663 - 4673.

Studlick, J.R.J., Shaw, R.D., Basye, G.L., Ray, J.R., 1987. Carbon Dioxide Source Development, Northeast Jackson Dome, Mississippi. American Association of Petroleum Geologists. Search and Discovery Article #91038.

Sturmer, B, 2021, Gas conditioning using membrane technology: p. 1.

Stute, M., Sonntag, C., Déak, J., Schlosser, P., 1992. Helium in deep circulating groundwater in the Great Hungarian Plain: flow dynamics and crustal and mantle helium luxes. Geochem. Cosmochim. Acta 56 (5), 2051 - 2067.

Sunarso, J., Hashim, S.S., Lin, Y.S., Liu, S.M., 2016. Membranes for helium recovery: an overview on the context, materials and future directions. Separ. Purif. Technol. 176, 335 - 383.

Sunarso, J., S. S. Hashim, Y. S. Lin, and S. M. Liu, 2017, Membranes for helium recovery: An overview on the context, materials and future directions: Separation and Purification Technology, v. 176, p. 335–383, doi:10.1016/j.seppur.2016.12.020.

Superior Oil Company, 1982. Grey Ranch, in Selected Oil and Gas Fields in West Texas Symposium, West Texas Geological Society, Symposium V. 1, II and III, pp. 276 - 287.

Swee Leong, L., 2003, Study on the effect of lowering steam to carbon ratio in combined reforming of natural gas to the synthesis gas.

Szamalelek, K., Szuflicki, M., Malon, A., Tyminski, 2017. Mineral Resources of Poland. Polish Geological Institute National Research Institute, 191 p.

Tagliabue, M., Farrusseng, D., Valencia, S., Aguado, S., Ravon, U., Rizzo, C., Corma, A., Mirodatos, C., 2009. Natural gas treating by selective adsorption: material science and chemical engineering interplay. Chem. Eng. J. 155 (3), 553.

Takahashi, P. K., M. Cooney, J. Yu, and J. R. Benemann, 2021, Blue Hydrogen: p. 1–8.

Tamidi, A. M., and N. H. Yasin, 2020, CO2 and H2S co-removal from natural gas using membrane contactor technology: Society of Petroleum Engineers - SPE Asia Pacific Oil and Gas Conference and Exhibition 2020, APOG 2020, doi:10.2118/202269-ms.

Tamvakis, M., 2013, Energy Economics and Trade (pp. 147-202). Informa Law from Routledge.

Tanh, H.B., C. Jeazet, C. Staudt, Janiak, 2012, Metal-organic frameworks in mixed matrix membranes for gas separation, Dalton Trans. 41, 14003–14027.

Tanzania Geological Society, 2019 Annual Meeting and Workshop, Dar Es Salaam, September 25th to 27th, p. 18.

Tarbet, L.A., 1971. Petroleum Potential of Imperial Valley, California, American Association of Petroleum Geologists, Memoir: Future Petroleum Provinces of the United States - Their Geology and Potential, pp. 384 - 391.

Tardani, D., Reich, M., Roulleau, E., Takahata, N., Sano, Y., Perez-Flores, P., Sanchez-Alfaro, P., Cembrano, J., Arancibia, G., 2016. Exploring the structural controls on helium, nitrogen and carbon isotope signatures in hydrothermal fluids along an intra-arc fault system. Geochem. Cosmochim. Acta 184, 193 - 211.

Tavakoli, V., Rahimpour-Bonab, H., Esrafili-Dizaji, B., 2011. Diagenetic controlled reservoir quality of South Pars gas field, an integrated approach. Comptes Rendes Geosci. 343, 55-71.

Tedesco, S.A., 1994. Surface Geochemistry in Petroleum Exploration. Chapman and Hall.

Tedesco, S.A., 2017. The use of aeromagnetics and micromagnetics to identify potential areas of hydrocarbons in the Midcontinental United States. In: Gaci, S., Hachay, O. (Eds.), Oil and Gas Exploration: Methods and Application. John Wiley & Sons, pp. 237 - 259.

Tedesco, S.A., 2020. The Pennsylvanian Desmoinesian Mudstone and Carbonate Reservoirs in Southern Denver Basin. American Association of Petroleum Geologists. Search and Discovery Article 11340, 44 p.

Tedesco, S.A., 2021. Evaluation of the pilot waterflood at Arikaree Creek Field Case Study for enhancing oil recovery from a low temperature hydrothermal unconventional carbonate reservoir. In: Gaci, S., Olga, H., Nicolis, O. (Eds.), Methods and Applications in Petroleum and Mineral Exploration and Engineering Geology.

Tedesco, S.A., 2021. Microseeps as pathfinder and regional filtering tool in petroleum exploration. In: Methods and Applications in Petroleum and Mineral Exploration and Engineering Geology. Elsevier (Chapter 2).

Tedesco, S. A., 2022, Geology and Production of Helium and Associated Gases. Amsterdam, Netherlands: Elsevier. https://search-ebscohost-com.ezproxy.library.und.edu/login.aspx?direct=true&db=nlebk&AN=3051788&site=ehost-live&scope=site.

Theloy, C., 2014, Integration of geological and technological factors influencing production in the Bakken play, Williston Basin: PhD Thesis, Colorado School of Mines, Golden, Colorado, 223 p.

Thomas, E., 2017, Capping the Flame Solving North Dakota's Natural Gas Flaring Problem through Cap and Trade. Geo. Wash. J. Energy & Envtl. L., 8, p.137.

Thompson, J.A., 1964. The occurrence of helium in the Cambrian near Swift Current, Saskatchewan. In: North Dakota Geological Survey and Saskatchewan Geological Survey, Third Williston Basin Symposium, pp. 179 - 185.

Tobin J., et al., 2006, The Crucial Link between Natural Gas Production and its Transportation to Market In: Stages in the production of pipeline-quality natural gas and NGLs. 13.07.11, Available from: http://lba.legis.state.ak.us/sga/doc_log/2006-01-01_eia_publication_natural_gas_processing.pdf

Tolstikhin, I.N., Verchovsky, A.B., Kamensky, I.L., Skiba, V.I., Gannibal, M.A., Vetrin, V.R., V Tarakanov, S., 2016. Amphibole: a major carrier of helium isotopes in crustal rocks. Chem. Geol. 444, 187 - 198.

Tomonaga, Y., Marzocchi, R., Pera, S., Pfeifer, H.R., Kipfer, R., Decrouy, L., Vennemann, T., 2017. Using noble-gas and stable-isotope data to determine groundwater origin and flow regimes: application to the Ceneri Base Tunnel (Switzerland). J. Hydrol. 545, 395 - 409.

Tongish, Claude A., 1980, Helium -: Its Relationship to Geologic Systems and Its Occurrence with the Natural Gases, Nitrogen, Carbon Dioxide, and Argon. United States: Department of the Interior, Bureau of Mines, pp. 138.

Torgersen, T., 1989. Terrestrial helium degassing fluxes and the atmospheric helium budget: implications with respect to the degassing processes of continental crust. Chem. Geol. Isot. Geosci. 79 (1), 1 - 14.

Torgersen, T., & Clarke, W.B., 1985. Helium accumulation in groundwater, I: an evaluation of sources and the continental flux of crustal 4 He in the Great Artesian Basin, Australia. Geochem. Cosmochim. Acta 49 (5), 1211 - 1218.

Torgersen, T., & Ivey, G.N., 1985. Helium accumulation in groundwater, II: a model for the accumulation of the crustal 4 He degassing flux. Geochem. Cosmochim. Acta 49 (11), 2445 - 2452.

TransTexTreating, 2021, Amine Plants: p. 2. From: https://transtextreating.com/ equipments/amine-plants/, Accessed 11-2021.

Treptau, K.L., 1999, Sub-Phanerozoic Precambrian of southwest Saskatchewan: lithological, geochemical and geophysical interpretations; B.Sc. thesis, University of Regina, Regina, Saskatchewan, 47p.

Trop, P. and Goricanec, D., 2016. Comparisons between energy carriers' productions for exploiting renewable energy sources. Energy, 108, pp.155-161.

Truswell, J.F., 1977. The Geological Evolution of South Africa, Cape Town, Purnell.

Truswell, J.F., 1977. The Geological Evolution of South Africa, Cape Town, Purnell.

Tugnoli, A., Landucci, G., & Cozzani, V., 2008, Sustainability assessment of hydrogen production by steam reforming. International Journal of Hydrogen Energy. 33. 4345-4357. 10.1016/j.ijhydene.2008.06.011.

Turekian, K. and K. H. Wedepohl, 1961, Distribution of the elements in some major units of the earth's crust: Geological Society of America Bulletin v. 72, p. 175-192.

Turner, Daniel S., 1968, Natural gas in Black Mesa Basin, northeastern Arizona, in Beebe, B.W., ed., Natural gases of North America: AAPG Memoir 9, v. 2, p. 1357-1370.

Turner, M.G., 1989, Landscape ecology: the effect of pattern on process. Annual review of ecology and systematics, 20(1), pp.171-197.

Ulmishek, Gregory F., 2003, Petroleum Geology and Resources of the West Siberian Basin, Russia (PDF).

U.S. Geological Survey Bulletin (2201-G, 49. Retrieved 14 October 2012.

U.S. Congress, 2013, Helium Stewardship Act of 2013—Public Law 110–40: U.S. Government Printing Office, 15 p., accessed May 14, 2021

U.S. Department of Energy. Office of Oil and Natural Gas, 2019, Natural Gas Flaring and Venting: State and Federal Regulatory Overview, Trends, and Impacts: U.S. Department of Energy, no. June, p. 72.

U.S. Energy Information Administration, 2018, Petroleum and Other Liquids: Supply and Disposition, and Product Supplied, https://www.eia.gov/petroleum/data.php

U.S. Environmental Protection Agency, 2021, Global Greenhouse Gas Emissions Data, www.epa.gov/ghgemissions/global-greenhouse-gas-emissions-data

U.S. Geological Survey, 2015, Geochemistry Database: U.S. Geological Survey, Provisional Database, accessed May 14, 2021

U.S. Geological Survey, 2021, Mineral Commodity Summaries, Helium Data Sheet - Mineral Commodity Summaries 2021.

United States Department of Energy, 2019, Hydrogen Production: Natural Gas Reforming How Does It Work? Fuel Cell Technologies Office, p. 1–5.

Universal Royalty Company, 2020, History of the Bakken Shale: no. April, p. 9–11.

Urban, P., Schmoranzer, D., Hanzelka, P., Sreenivasan, R., Srbek, L., 2013. Anomalous heat and transport and condensation in convection of cryogenic helium. Proc. Natl. Acad. Sci. U.S.A. 10 (20), 8036 - 8039.

Urquhart, A.S.M., 2011. Structural Controls on CO2 and Diagenesis in a Natural Long-Term Carbon Sequestration-Analogue: Little Grand Wash Fault. University of Texas A & M, Utah (MS thesis), 461 p.

Urry, W.D., 1933. Helium and the Problem of Geological Time. Chemical Reviews, 13(2), pp.305-343.

US Department of Energy, 2019, Hydrogen Production: Natural Gas Reforming How Does It Work? Fuel Cell Technologies Office, p. 1–5.

US Energy Information Administration 2021, Production of hydrogen: 3 p.

USGS gas geochemistry dataset. Downloaded October 2008 from http://energy.cr.usgs.gov/prov/og/data2.htm.

USGS, 2020. Helium - Fact Sheet, 2. USGS msc2020. https://www.usgs.gov/centers/nmic/helium-statistics-andinformation .

USGS, 2021. Helium - Fact Sheet, 2. USGS msc2021. https://www.usgs.gov/centers/nmic/helium-statistics-andinformation .

U.S. Government Accountability Office, 2015, Bureau of Land Management—More information needed to implement the Helium Stewardship Act of 2013, GAO-15-394, April 16, 36 p. Retrieved October 23, 2022, from http://www.gao.gov/assets/670/69709.pdf.

Vakhromeev A.G., 2014, Fields of industrial multicomponent brines of Siberian platform hydromineral province deep horizons (In Russ.), Vestnik IrGTU = Proceedings of Irkutsk State Technical University, no. 9(92), pp. 73–78.

Valenti, G., 2016, Compendium of Hydrogen Energy. Volume 1: Introduction to hydrogen storage.

van Buchem, F.S.P., Svandsen, N., Hoch, E., Pedersen-Tatalovic, R., Habib, K., 2014. Depositional history and petroleum habitat of Qatar. In: Petroleum Systems of the Tethyan Region, American Association of Petroleum Geologists, Memoir 106, pp. 641 - 677.

Van Hull, K., 2017, Good to Be a Gas Processor - The Rejuvenation of Natural Gas Processing Economics, Part 2: The Rejuvenation of Natural Gas Processing Economics, p. 1–2.

Van Hull, K., 2018, Good to Be a Gas Processor - The Rejuvenation of Natural Gas Processing Economics, Part 3: The Rejuvenation of Natural Gas Processing Economics, Part 3|, v. 2018, p. 2–3.

Van Hull, K., 2018, Good to Be a Gas Processor - The Rejuvenation of Natural Gas Processing Economics, Part 4: The Rejuvenation of Natural Gas Processing Economics, v. 2, p. 1–2.

Van Hull, K., 2021, Industry Infrastructure: New Modeling Approach Improves Economic Analyses of Gas Processing: The American Oil & Gas Reporter, no. March 2018, p. 1–7.

Van Hull, K., 2021, Industry Infrastructure: New Modeling Approach Improves Economic Analyses of Gas Processing: The American Oil & Gas Reporter, no. March 2018, p. 1–7.

Van Schmus, W. R., M. E. Bickford, (eds.) et al., 1993, Chapter 4, Transcontinental Proterozoic provinces: in: J. C. Reed et al., eds., Precambrian: Conterminous US: Geological Society of America, The Geology of North America, v. C-2, p. 171-334.

Van Schmus, W.R., M.E. Bickford, and A. Turek, 1996, Proterozoic Geology of the East-Central Mid-Continent Basement, *in* B.A. van der Pluijm and P. Catacosinos (eds.), Basement and Basins of Eastern North America: Geological Society of America Special Paper 308, p. 7-32.

Velazquez Abad, A., and P. E. Dodds, 2017, Production of Hydrogen, *in* M. A. B. T.-E. of S. T. Abraham, ed., Encyclopedia of Sustainable Technologies: Oxford, Elsevier, p. 293–304, doi:10.1016/B978-0-12-409548-9.10117-4.

Verdon, M., 2021, The World's First Hydrogen-Powered Helicopter Could Soon Land on a Helipad Near You: Motors/Aviation, p. 15.

Vergis, M., 2007, Economics of Steam Methane Reformation and Coal Gasification for Hydrogen Production: University of Florida, 50 p.

Victory, D., Miles, M.W., Oelfke, R.H., 2009. Helium Recovery from Natural Gas Integrated with NGL Recovery. Google Patents. West, J.E., 2009. Helium Extraction and Production Techniques. URL: (Accessed: January 17, 2023).

Voelcker, J., 2020, Why We Still Can't Deliver on the Promise of Hydrogen Cars: p. 1–19.

von Drehle, W.F., 1990. Barrel Springs Field, Prowers County, Colorado. In: Sonnenberg, S.A., Shannon, L.T., Rader, K., von Drehle, W.F., Martin, G.W. (Eds.), Morrow Sandstones, Rocky Mountain Association of Geologist, pp. 183-189.

Vozhov V.I., 2006, Podzemnye vody i gidromineral'noe syr'e Leno-Tungusskoy neftegazonosnoy provintsii (Groundwater and hydromineral raw materials of Leno-Tunguska oil and gas province), Novosibirsk: Publ. of SNIIGGiMS, 209 p.

Wackerlig, J. and Schirhagl, R., 2016, Applications of molecularly imprinted polymer nanoparticles and their advances toward industrial use: a review. Analytical chemistry, 88(1), pp.250-261.

Wagner, C.R., 1961. Keyes Field. In: Oil and Gas Fields of Texas and Oklahoma Panhandles. Panhandle Texas Geological Society, pp. 239 - 243. Wiseman, T., Eckels, M.T., 2020. Proven and Hypothetical Helium Resources in Utah, SITLA and Utah DNR, vol. 174. Misc Pub, p. 43.

Wakita, H., Fuiji, N., Matsuo, S., Notsu, K., Nagao, K., Takoka, N., 1978. Helium spots caused by a diapiric magma from the upper mantle. Science 200 (4340), 430 - 431.

Wakita, H., Nakamura, Y., Kita, I., Fuiji, N., Notsu, K., 1980. Hydrogen release, new indicator of fault activity. Science 210 (4466), 188 - 189.

Walker, R. N., 1978. Big Gap Pennsylvanian. In: Fassett, J.E., Thomaidis, N.D., Matheny, M.L. (Eds.), Oil and Gas Fields of the Four Corners Area, Four Corners Geological Society, vol. III, pp. 936-937.

Wallace, K., Robinson, S., Heinz, J., 1990. Nee Noshe Field, Kiowa County, Colorado. In: Sonnenberg, S.A., Shannon, L.T., Rader, K., von Drehle, W.F., Martin, G.W. (Eds.), Morrow Sandstones, Rocky Mountain Association of Geologist, pp. 175-182.

Walters, R. F., 1958, Differential entrapment of oil and gas in Arbuckle Dolomite of Central Kansas: AAPG Bulletin, v. 42, p. 2133-2173.

Wang, X., and M. Economides, 2013, Advanced natural gas engineering: Advanced Natural Gas Engineering, p. 1–368, doi:10.1016/C2013-0-15532-8.

Wang, X., Liu, W., Li, X., Li, Q., Tao, C., Xu, Y., 2020. Radiogenic helium concentration and isotopic variations in crustal pools from Sichuan Basin, China. Appl. Geochem. 117, 9. Weiss, R.F., 1971. Solubility of helium and neon in water and seawater. J. Chem. Eng. Data 16 (2), 235 - 241.

Weaver, B.D., 2021. Keyes Helium Extraction Facility," the Encyclopedia of Oklahoma History and Culture. https:// www.okhistory.org/publications/enc/entry.php?entry ¼ KE018.

Webster, R.L., 2011. Petroleum source rocks and stratigraphy of the Bakken Formation in North Dakota.

Weinlich, F.H., Bräuer, K., Kämpf, H., Strauch, G., Tesa r, J., Weise, S.M., 1999. An active subcontinental mantle volatile system in the western Eger rift, Central Europe: Gasflux, isotopic (He, C, and N) and compositional fingerprints. Geochem. Cosmochim. Acta 63 (21), 3653 - 3671.

Weismann, T.J., 1971. Stable carbon isotope investigation of natural gases from Sacramento and Delaware-Val Verde Basins - Possible igneous origin. Am. Assoc. Pet. Geol. Bull. 55 (2), 369.

Well Files for Suniland State Unit A1, State of Utah. https://oilgas.ogm.utah.gov/oilgasweb/ live-data-search/lds-files/files-lu.xhtml

Wells, B., 2013, Please give us one more oil boom-I promise not to screw it up this time: The broken promise of casinghead gas flaring in the Eagle Ford Shale. Tex. J. Oil Gas & Energy L., 9, p.319.

Wendte, J. C. et al., 2007, Isotopic and fluid inclusion analysis of diagenetic mineral phases of the Upper Devonian Jean Marie Member (Redknife Formation) in the July Lake area of northeastern British Columbia.

Wescott, P., 1989. Analysis of Gases in Earth's Crust, January 1982 - May 31, 1988, Final Report. Gas Research Institute, 88-262, 571 p.

West, J E, 2009, Helium extraction and production techniques. URL: Accessed: January 27, 2011.

What, A. M., 2020, What can be manufactured from natural gas: Informatorium, p. 1–3.

White, M., Goff, S., Deduck, S. and Gohlke, O., 2009, January. New process for achieving very low NOx. In North American Waste-to-Energy Conference (Vol. 48807, pp. 83-87).

Whiticar, M.J., 1994. Correlation of natural gases with their sources. In: Magoon, L.B., Dow, W.G. (Eds.), The Petroleum System from Source to Trap: American Association of Petroleum Geologists, Memoir, vol. 60, pp. 261 - 283.

Wierzbicki, R. and Todorovic-Maranic, D., 2010, Exploiting natural fracture and fault fairways in the Jean Marie Carbonate Platform, N.E. British Columbia; Canadian Unconventional

Wijaya, N. and Sheng, J.J., 2020, Probabilistic forecasting and economic evaluation of pressure-drawdown effect in unconventional oil reservoirs under uncertainty of water blockage severity. Journal of Petroleum Science and Engineering, 185, p.106646.

Wikipedia, 2021, https://en.wikipedia.org/wiki/Helium.

Wikipedia, 2021. https://en.wikipedia.org/wiki/Carbon_dioxide.

Wilcox, A., 2019, Flaring Issues, Solutions & Technologies, U.S. Department of Energy National Energy Technology Laboratory, DE-FE0031691

Wilhelm, E., R. Battino, and R. Wilcock, 1977, Low pressure solubility of gases in liquid water: Chemical reviews, v. 77, p. 219-262.

Wilhelms, D.E., 1987. The Geologic History of the Moon. USGS. Professional Paper 1348, 309 p.

Williams, A.G., 2020, The products of American shale development, Internal Publication, 1–2 p.

Williams, A.E., McKibben, M.A., Eldridge, C.S., 1991. An Overview of Fluid Geochemistry and Ore Genesis in the Salton Sea Geothermal System and Comparison with the Gulf of California Hydrothermal Systems, AAPG, Memoir 47, The Gulf and Peninsular Province of California, Chapter 37, pp. 781 - 792.

Williams, M., 2007. Mining the Moon: Lab Experiments Suggest that Future Fusion Reactors Could Use Helium-3 Gathered from the Moon. MIT Technology Review. August 23rd.

Willis, A., 2021, Company execs boast future 'hydrogen hub' in North Dakota, Grand Forks Herald, 2 Jun 2021, 1.p

Williston Basin Petroleum Conference 2022, 2021, *in* Energy from the Earth: p. 1–6, https://wbpc.ca/

Willyard, K.A., 2019, An historical political economy analysis and review of Texas oil and gas well flaring laws and policy. Energy Policy, 128, pp.639-647.

Wilson, M.S., Grove, K.W., Wilson, A.B., 2003. Exploration of the Mississippian Leadville Limestone in the Piceance Basin, western Colorado, Chapter 15. In: Piceance Basin Guidebook, Rocky Mountain Association of Geologist, pp. 252 - 270.

Winckler, G., Severinghaus, J.P., 2013. Noble gases in ice cores: indicators of the earth's climate history. In: The Noble Gases as Geochemical Tracers. Springer, pp. 33 - 53.

Winckler, G., Suess, E., Wallmann, K., de Lange, G.J., Westbrook, G.K., Bayer, R., R., 1997. Excess helium and argon of radiogenic origin in Mediterranean brine basins. Earth Planet Sci. Lett. 151 (3 - 4), 225 - 231.

Wingerter, H.R., 1968. Greenwood Gas Field, Kansas, Colorado and Oklahoma, American Association of Petroleum Geologists Memoir 14, Geology of Giant Petroleum Fields, pp. 1557 - 1566.

Winterbone, D. E., and A. Turan, 2015, Advanced Thermodynamics for Engineers: Second Edition: 1–551 p., doi:10.1016/C2013-0-13437-X.

Wirojanagud, P., C. W. Kreitler, and D. A. Smith, 1985, Numerical modeling of regional groundwater flow in the deep-basin brine aquifer of the Palo Duro Basin, Texas Panhandle: Texas Bureau of Economic Geology Report of Investigations No. 159, 68 p.

Wiseman, T., 2019. Personal Communication, Helium Production at Harley Dome. SITLA, Grand County, Utah.

Wiseman, T., Eckels, M.T., 2020. Proven and hypothetical helium resources in Utah, 174. SITLA and Utah Department of Natural Resources, Misc. Pub, 43 p.

Wishart, J., 2019, Fuel Cells vs Batteries in the Automotive Sector: Intertek Transportation Technologies, no. August 2014, p. 1–18, doi:10.13140/RG.2.2.24357.70882.

Wittenberg, L.J., Santarius, J.F., Kulcinski, G.L., 1986. Lunar source of $^{+3}$He for commercial fusion power. Fusion Technol. 10, 167 - 178.

Wolfe, R. A., K. A. Farley, and L. T. Silver, 1996, Helium diffusion and low-temperature thermochronometry of apatite: Geochimica et Cosmochimica Acta v. 60

Woods, A.D.B., Cowley, R.A., 1973. Structure and excitations of liquid Helium. Rep. Prog. Phys. 36 (9), 1135 - 1231. Yang, S., Ellis, A.M., 2012. Helium droplets: a chemistry perspective. Chem. Soc. Rev. 42 (2), 472 - 484.

Worrall, J., 2004. Preliminary Geology of Oakdale Field, Northwest Raton Basin, Huerfano County, Colorado, American Association of Petroleum Geologists, Search and Discovery Article 20017.

Worrell, G., 2019, Helium researcher interested in more than party balloons: p. 1–5. From https://chemeng.uq.edu.au/article/2019/09/helium-researcher-interested-more-than-party-balloons Accessed 10-2021.

Wright, G.N., McMechan, M.E. and Potter, D.E.G., 1994, Structure and architecture of the Western Canada Sedimentary Basin; Chapter 3 *in* Geological Atlas of the Western Canada Sedimentary Basin, Mossop, G.D. and Shetsen, I. (comps.), Canadian Society of Petroleum Geologists and Alberta Research Council, p.24-40.

Wu, W., and P. C. Kuo, 2015, Conceptual designs of hydrogen production, purification, compression and carbon dioxide capture: Energy Conversion and Management, v. 103, p. 73–81, doi:10.1016/j.enconman.2015.06.046.

Wycherly, H., Fleet, A., Shaw, H., 1999. Some observations on the origins of large volumes of carbon dioxide accumulations in sedimentary basins. Mar. Petrol. Geol. 16, 489 - 494.

Xu, D., Dong, L. and Ren, J., 2017, Introduction of hydrogen routines. In Hydrogen Economy (pp. 35-54). Academic Press.

Yampolskii, Y., and B. Freeman (eds.), 2020, Membrane Gas Separation: Wiley, 370 p., doi:10.1557/S0883769400039506.

Yancheshmeh, M.S., Radfarnia, H.R. and Iliuta, M.C., 2016, High temperature CO_2 sorbents and their application for hydrogen production by sorption enhanced steam reforming process. Chemical Engineering Journal, 283, pp.420-444.

Yang, J.H., Wu, F.Y., Wilde, S.A., 2003. A review of the geodynamic setting of large scale Late Mesozoic gold mineralization in the North China Craton: an association with lithospheric thinning. Ore Geol. Rev. 23 (3), 125 - 152.

York, A.P., Xiao, T. and Green, M.L., 2003, Brief overview of the partial oxidation of methane to synthesis gas. Topics in Catalysis, 22(3), pp.345-358.

Yurkowski, M.M., 2016, Helium in southwestern Saskatchewan: accumulation and geological setting; Saskatchewan Ministry of the Economy, Saskatchewan Geological Survey, Open File Report 2016-1, 20p.

Yurkowski, M.M., 2021. Helium in Southern Saskatchewan: Geological Setting and Prospectivity; Saskatchewan Ministry of Energy and Resources, Saskatchewan Geological Survey, Open File Report 2021-2, 77p. and two Microsoft Excel files. https://publications.saskatchewan.ca/#/products/115248 .

Zaitsev, A., M. Mehrpooya, B. Ghorbani, R. Sanavbarov, F. Naumov, and F. Shermatova, 2020, Novel integrated helium extraction and natural gas liquefaction process configurations using absorption refrigeration and waste heat: International Journal of Energy Research, v. 44, no. 8, p. 6430–6451, doi:10.1002/er.5377.

Zaręba, J.K., 2017, Tetraphenylmethane and tetraphenylsilane as building units of coordination polymers and supramolecular networks–A focus on tetraphosphonates. Inorganic Chemistry Communications, 86, pp.172-186.

Zarei, E., K. Shooli, M. N. Kosari, A. Samadiafshar, and E. Mokarinezhad, 2012, Effect of Sodium Salts on Demercaptanization Process: International Journal of Science and Engineering Investigations, v. 1, no. 9, p. 57–60.

Zartman, R. E., G. J. Wasserburg, and J. H. Reynolds, 1963, Helium, argon, and carbon in some natural gases: Journal of Geophysical Research, v. 66, p

Zartman, R.E., Wasserburg, G.J., 1961. Helium, argon, and carbon in some natural gases. J. Geophys. Res. 66 (1), 277 - 306.

Zeitler, P.K., Enkelmann, E., Thomas, J.B., Watson, E.B., Ancuta, L.D., Idleman, B.D., 2017. Solubility and trapping of helium in apatite. Geochem. Cosmochim. Acta 209, 1 - 8.

Zephyr solutions, 2015, https://zephyrsolutions.com/power-your-house-with-solar-helium-balloons/ .

Zhang, J., Wei, Y., Haiyong, Y., Wuren, X., Zengye, X., Fuying, Z., Yongjing, C., 2015. Feasibility of high-helium natural gas exploration in the Presinian strata, Sichuan Basin. Nat. Gas. Ind. B 2, 88 - 94.

Zhang, M., Guo, Z., Zhang, L., Sun, Y., Cheng, Z., 2017. Geochemical constraints on origin of hydrothermal volatiles from understanding the degassing sys in the India-Asia continental subduction zone. Chem. Geol. 469, 19 - 33.

Zhang, T., Zhang, M., Bai, B., Wang, X., Li, L., 2008. Origin and accumulation of carbon dioxide in the Huanghua depression, Bohai Bay Basin, China. Am. Assoc. Pet. Geol. Bull. 92 (3), 341 - 358.

Zhang, W., Li, Y., Zhao, F., Han, W., Li, Y., Wang, Y., Holland, G., Zhou, Z., 2019a, Using noble gases to trace groundwater evolution and assess helium accumulation in Weihe Basin, central China. Geochem. Cosmochim. Acta 251, 229 - 246.

Zhang, W., Li, Y., Zhao, F., Han, W., Zhou, J., Holland, G., Zhou, Z., 2019b. Quantifying the helium and hydrocarbon accumulation processes using noble gases in the North Qaidam Basin, China. Chem. Geol. 525, 368 - 379.

Zhou, Z., Ballentine, C.J., Schoell, M., Stevens, S.H., 2012. Identifying and quantifying natural CO_2 sequestration processes over geological timescales: the Jackson Dome CO_2 Deposit, USA. Geochem. Cosmochim. Acta 86, 257 - 275.

Zhu, Y., Shi, B., Fang, C., 2000. The isotopic compositions of molecular: nitrogen implications on their origins in natural gas accumulations. Chem. Geol. 164 (3 - 4), 321 - 330.

Zona, 2010, NASA - Liquid Hydrogen--the Fuel of Choice for Space Exploration: p. 10–12: http://www.nasa.gov/topics/technology/hydrogen/hydrogen_fuel_of_choice.html

Zornoza, B., C. Tellez, J. Coronas, J. Gascon, F. Kapteijn, 2013, Metal organic framework based mixed matrix membranes: an increasingly important field of research with a large application potential, Micropor. Mesopor. Mater. 166, 67–78